

RAI Responses 56-63

**RESPONSE TO RAI COMMENT 56
ROADMAP TO REFERENCES**

REFERENCED DOCUMENT	*EXCERPT LOCATION	REMARK
Baes et al. 1984	Excerpt enclosed following response.	This pdf file is password protected, so entire document is provided.
Baes et al. 1984	Excerpt enclosed following response.	Figure 2.1 in enclosed entire document.
Cook et al. 2005 Sections 7.5.3 and 7.5.4	Excerpt enclosed following response.	
Hamby 1992	Excerpt enclosed following response.	
Lee 2004 Table 2.2-1	Excerpt included in response.	
Phifer and Nelson 2003 Appendix K	Excerpt enclosed following response.	

***Excerpt Locations:**

1. Excerpt included in response: The excerpt is included within the text of the response or is appended to the response.
2. Excerpt enclosed following response: The excerpt is enclosed on a separate sheet or sheets following the response.
3. Representative excerpt(s) enclosed following response: Representative excerpts from a document that is wholly or largely applicable are enclosed following the response.
4. Other

APPROVED for Release for
Unlimited (Release to Public)

7/14/2005

ornl

ORNL-5786

OAK RIDGE
NATIONAL
LABORATORY

MARTIN MARIETTA

A Review and Analysis of Parameters for Assessing Transport of Environmentally Released Radionuclides through Agriculture



C. F. Baes III
R. D. Sharp
A. L. Sjoreen
R. W. Shor

MANAGED BY
MARTIN MARIETTA ENERGY SYSTEMS, INC.
FOR THE UNITED STATES
DEPARTMENT OF ENERGY

Health and Safety Research Division

**A Review and Analysis of Parameters for Assessing Transport
of Environmentally Released Radionuclides through
Agriculture**

C. F. Baes III

Environmental Sciences Division

R. D. Sharp

Computer Sciences

A. L. Sjoreen

Computer Sciences

R. W. Shor

Health and Safety Research Division

Date Published: September 1984

Research Sponsored by the Office of Radiation Programs, U. S.
Environmental Protection Agency under Interagency Agreement
AD-89-F-2-A106 (formerly EPA-78-D-X0394)

Prepared by the

Oak Ridge National Laboratory

Oak Ridge, Tennessee 37831

operated by

Martin Marietta Energy Systems, Inc.

for the

U. S. DEPARTMENT OF ENERGY

under contract No. DE-AC05-84OR21400

DISCLAIMER

Although the research described in this report has been funded by the United States Environmental Protection Agency through Interagency Agreement Number AD-89-F-2-A106 (formerly EPA-78-D-X0394) with Oak Ridge National Laboratory, it has not been subjected to the Agency's required peer and policy review and therefore does not necessarily reflect the views of the Agency and no official endorsement should be inferred.

CONTENTS

	Page
DISCLAIMER	ii
LIST OF FIGURES	v
LIST OF TABLES	xi
PARAMETER SYMBOLS AND DEFINITIONS	xiii
ACKNOWLEDGMENT	xvii
HIGHLIGHTS	xvii
1. INTRODUCTION	1
2. ELEMENT-SPECIFIC TRANSPORT PARAMETERS	4
2.1 Soil-to-Plant Uptake Parameters B_s and B_r	4
2.1.1 Protocols for determination of parameter values	5
2.1.2 Group IA and IIA elements	9
2.1.3 Group IIIA, IVA, and VA elements	20
2.1.4 Group VIA and VIIA elements	24
2.1.5 Group IIIB and the rare earth elements	26
2.1.6 Period IV transition elements	27
2.1.7 Period V transition elements	30
2.1.8 Period VI transition elements	40
2.1.9 The actinide elements	45
2.1.10 Comparison of default estimates with previously published values	47
2.2 Ingestion-to-Milk Parameter, F_m	47
2.3 Ingestion-to-Beef Parameter, F_m	49
2.4 The Distribution Coefficient, K_d	53
2.4.1 Variability in K_d	53
2.4.2 Estimates of K_d based on default B_s values	63
3. INTERCEPTION FRACTION FOR VEGETATION	65
3.1 Pasture Grasses and Hay	65
3.2 Leafy Vegetables	65
3.3 Silage	71
3.4 Exposed Produce	73
3.5 Correlation Between Interception Fraction and Standing Crop Biomass	75
4. SITE-SPECIFIC PARAMETERS	80
4.1 Agricultural Parameters	84
4.2 Climatological Parameters	109
4.3 Demographic and Miscellaneous SITE Parameters	114
5. MISCELLANEOUS PARAMETERS	124
5.1 The Weathering Removal Loss Constant, λ_w	124
5.2 The Metabolic Turnover Constant For Milk, λ_m	124
5.3 The Metabolic Turnover Constant For Beef, λ_f	125
5.4 Lifetime Grain and Forage Requirements For Cattle On Feed, Q_s^{fc} and Q_f^{fc} Respectively	127
5.5 The Carbon and Water Content of Foods	127
5.6 Coarse (2.5 - 15 μ m) Suspended Particulate Matter	128
6. SUMMARY	133
7. REFERENCES	134

LIST OF FIGURES

Figure	Page
1.1. The categorization of all vegetable crops and animal feeds in the TERRA code based on radionuclide transport and agricultural pathway characteristics	2
2.1. Values of the soil-to-plant concentration factor B_v , adopted as default estimates in the computer code TERRA	10
2.2. Values of the soil-to-plant concentration factor B_r , adopted as default estimates in the computer code TERRA	11
2.3. Lognormal probability plot of geometric means of B_v for cesium (calculated from references 26, 34, and 55-71), including one geometric standard deviation of the mean	12
2.4. Assumed systematic trends in for Group IA and IIA elements. Solid dots and error bars represent geometric means and standard deviations determined from available references	15
2.5. Correlation between soil potassium concentration and the soil-to-plant concentration factor, B_v , for potassium based on references 16 and 65	16
2.6. Assumed systematic trends in (B_r/B_v) ratio for Group IA and IIA elements. Solid dots and error bars represent geometric means and standard deviations determined from available references	17
2.7. Lognormal probability plot of geometric means of B_v for strontium (calculated from references 11, 16, 17, 21, 31, 33, 59, 60, 62-70, 72, 74-76, 78, 81-83, 85, and 86), including one geometric standard deviation of the mean	18
2.8. Correlation between soil boron concentration and the soil-to-plant concentration factor, B_v , for boron based on references 16, 65, and 76	21
2.9. Correlation between soil phosphorus concentration and the soil-to-plant concentration factor, B_v , for phosphorus based on reference 16	23
2.10. Assumed systematic trends in and (B_r/B_v) ratio for aluminum, scandium, and yttrium. Solid dots and error bars represent geometric means and standard deviations of the mean determined from available references	28
2.11. Correlation between soil chromium concentration and the soil-to-plant concentration factor, B_v , for chromium based on references 16 and 65	31

LIST OF FIGURES (continued)

Figure	Page
2.12. Correlation between soil manganese concentration and the soil-to-plant concentration factor, B_v , for manganese based on references 16, 36, 37, 104, 112, and 113	32
2.13. Correlation between soil iron concentration and the soil-to-plant concentration factor, B_v , for iron based on references 16, 65, and 104	33
2.14. Correlation between soil cobalt concentration and the soil-to-plant concentration factor, B_v , for cobalt based on references 16 and 65	34
2.15. Correlation between soil copper concentration and the soil-to-plant concentration factor, B_v , for copper based on references 16, 104, and 115	35
2.16. Correlation between soil zinc concentration and the soil-to-plant concentration factor, B_v , for zinc based on references 16, 35, 37, 67, 97, 104, 114, 115, and 119	36
2.17. Assumed systematic trend in B_v for Period IV elements based on default estimates. Solid dots and error bars represent geometric means and standard deviations determined from available references	37
2.18. Assumed systematic trend in (B_v / B_v) ratio for Period IV elements. Solid dots and error bars represent geometric means and standard deviations of the mean determined from available references	38
2.19. Assumed systematic trends in the ratio of for Period V and IV elements (Nb/V, Rh/Co, Pd/Ni, and Ag/Cu) based on the ratios of default B_v estimates for other elements in the periods	41
2.20. Assumed systematic trend in B_v for Period V transition elements based on default B_v estimates. Solid dots and error bars represent geometric means and standard deviations determined from available references	42
2.21. Assumed systematic trend in for Period VI elements based on assumed systematic trends in Period IV and V elements	44
2.22. Lognormal probability plot of geometric means of B_v for plutonium (calculated from references 8-10, 30, 59, 101, 129, 131, 132, and 134-138), including one geometric standard deviation of the mean	46

LIST OF FIGURES (continued)

Figure	Page
2.23. Comparison of soil-to-plant concentration factor default values reported in this report and derived from reference 15. The "+" and "-" signs indicate whether our estimates are greater or less than, respectively, those derived from reference 15. The values indicated are the difference factor, and circled elements indicate a difference of at least an order of magnitude	48
2.24. Values of the ingestion-to-milk transfer coefficient F_m adopted as default estimates in the computer code TERRA	50
2.24. Values of the ingestion-to-beef transfer coefficient F_f adopted as default estimates in the computer code TERRA	51
2.25. Systematic trends in the ratio of default estimates for B_v and F_m for successive elements and corresponding assumed ratios for F_f for successive elements used to determine default F_f estimates	52
2.26. Systematic variations in default estimates for Period II, III, IV, and V elements	54
2.27. Systematic variations in default estimates for Period VI and VII elements	55
2.28. Systematic variations in default and F_f estimates for Period II, III, IV, and V elements	56
2.29. Systematic variations in default and F_f estimates for Period VI and VII elements	57
2.30. Values of the soil-water distribution coefficient K_d adopted as default estimates in the computer code TERRA	58
2.31. Percent error in K_d estimation from one to five percent overestimates of soil concentration or underestimates of water concentration in a 10g-100mL batch-type K_d experiment	60
2.32. Lognormal probability plots of for cesium and strontium in soils of pH 4.5 to 9 based on available references	62
2.33. Correlation between and based on geometric means of available reference geometric means	64
3.1. Relationship between interception fraction and productivity for forage grasses (pasture and hay)	66
3.2. Model of field geometry of leafy vegetable spacings	67

LIST OF FIGURES (continued)

Figure	Page
3.3. Hypothetical growth curve for plants. Leafy vegetables are harvested at the time of maximum growth, and silage is harvested at grain maturity	70
3.4. Model of field geometry of silage plant spacings	72
3.5. Three plots of equal area containing hypothetical crops of varying size and planting density	77
3.6. Assumed relationships between interception fraction and fresh weight productivity for exposed produce and leafy vegetables and between interception fraction and dry weight productivity for silage	78
3.7. The ratio of interception fraction to productivity (r^i/Y_i) as a function of interception fraction dependent on (A) and independent of (B) productivity of silage, exposed produce, and leafy vegetables. The ranges of productivity found in the U.S., based on reference 7, are shown at the bottom of the figure	79
4.1. Map of the conterminous United States showing county delineations	81
4.2. Map of the conterminous United States with half degree longitude-latitude grid indicated	82
4.3. Geographic distribution of SITE parameter leafy vegetable production, P_{lv}	86
4.4. Geographic distribution of SITE parameter leafy vegetable productivity, Y_{lv}	87
4.5. Geographic distribution of SITE parameter exposed produce production, P_e	88
4.6. Geographic distribution of SITE parameter exposed produce productivity, Y_e	89
4.7. Geographic distribution of SITE parameter protected produce production, P_{pp}	90
4.8. Geographic distribution of SITE parameter protected produce productivity, Y_{pp}	91
4.9. Geographic distribution of SITE parameter grain food production, P_{gh}	92

LIST OF FIGURES (continued)

Figure	Page
4.10. Geographic distribution of SITE parameter grain food productivity, Y_{gh}	93
4.11. Geographic distribution of SITE parameter grain feed production, P_{gf}	94
4.12. Geographic distribution of SITE parameter grain feed productivity, Y_{gf}	95
4.13. Geographic distribution of SITE parameter silage feed production, P_s	96
4.14. Geographic distribution of SITE parameter silage feed productivity, Y_s	97
4.15. Geographic distribution of SITE parameter hay feed production, P_h	98
4.16. Geographic distribution of SITE parameter hay feed areal yield, Y_h^a	99
4.17. Geographic distribution of SITE parameter number of frost-free days, d_{ff}	101
4.18. Geographic distribution of SITE parameter cattle and calves inventory, n_{cc}	102
4.19. Geographic distribution of SITE parameter milk cow inventory, n_m	103
4.20. Geographic distribution of SITE parameter annual number of cattle on feed sold, s_g	104
4.21. Geographic distribution of SITE parameter sheep inventory, n_s	105
4.22. Geographic distribution of SITE parameter pasture area, A_p , shown as a fraction of total cell area	106
4.23. Geographic distribution of SITE parameter beef cows inventory, n_b	108
4.24. Geographic distribution of SITE parameter estimated annual average evapotranspiration, E	111
4.25. Geographic distribution of SITE parameter estimated annual average irrigation, I	112

LIST OF FIGURES (continued)

Figure	Page
4.26. Geographic distribution of SITE parameter estimated annual average precipitation, P	113
4.27. Geographic distribution of SITE parameter estimated annual average morning mixing height, M_{am}	115
4.28. Geographic distribution of SITE parameter estimated annual average afternoon (evening) mixing height, M_{pm}	116
4.29. Geographic distribution of SITE parameter estimated annual average absolute humidity, H	117
4.30. Geographic distribution of SITE parameter (estimated 1980) U.S. Population, pop_t	118
4.31. Geographic distribution of SITE parameter fraction of (1970) population classified as urban, pop_u	119
4.32. Geographic distribution of SITE parameter fraction of (1970) population classified as rural-farm, pop_{rf}	120
4.33. Geographic distribution of SITE parameter fraction of (1970) population classified as rural-nonfarm, pop_{nf}	121
4.34. Geographic distribution of SITE parameter dominant land feature, L_{df}	122
5.1. Metabolic half-times for the elements in milk (days), based on reference 145	126
5.2. Lognormal probability plot of coarse suspended particulate Matter (2.5 - 15 μm)	131

LIST OF TABLES

Table	Page
2.1. Examples of non-uniform elemental distribution in plants	6
2.2. Relative importance of food crop categories in selected states and the conterminous U. S.	7
2.3. Dry-to-wet weight conversion factors for exposed produce, protected produce, and grains	8
2.4. Comparison of observed and predicted concentrations of Group IA and IIA elements in produce and plants	14
2.5. Literature values of B_v , B_r , and the (C_r/C_v) ratio for radium	19
2.6. Comparison of observed and predicted concentrations of Group IIIA, IVA, and VA elements in produce and plants	22
2.7. Comparison of observed and predicted concentrations of Group VIA and VIIA elements in produce and plants	25
2.8. Comparison of observed and predicted concentrations of Group IIIB and the rare earth elements in produce and plants	27
2.9. Comparison of observed and predicted concentrations of Period IV transition elements in produce and plants	30
2.10. Comparison of observed and predicted concentrations of Period V transition elements in produce and plants	40
2.11. Comparison of observed and predicted concentrations of Period VI transition elements in produce and plants	43
2.12. Comparison of observed and predicted concentrations of actinide elements in produce and plants	47
2.13. Estimates of distribution of K_d for various elements in agricultural soils of pH 4.5 to 9.0	61
3.1. Weighting factors for leafy vegetable interception fraction model simulation	69
3.2. Relative importance of various exposed produce in the U.S.	74
3.3. Values of interception fraction for five important crops in the exposed produce category	76
4.1. Example derivation of agricultural parameters for SITE cell #3284 from county-averaged parameters	83

LIST OF TABLES (continued)

Table	Page
4.2. Derivation of number of frost-free days for half degree cells from values for the three nearest weather stations to the centroid of the cell	85
4.3. Agricultural and climatological parameters for seven selected SITE cells and parameters derived from them in TERRA	109
5.1. Water content of produce, beef, and cow's milk	129
5.2. Carbon content of produce, beef, and cow's milk	130

PARAMETER SYMBOLS AND DEFINITIONS

Symbol	Definition
A_{hi}	The area allocated to crop i which is harvested or harvest area (m^2).
A_i	The inventory area allocated to crop i (m^2).
A_p	The area of pasture (m^2).
B_r	Soil-to-plant concentration factor which is the ratio of activity concentration in plant parts usually associated with reproductive or storage functions (fruits, seeds, tubers, etc.) in dry weight to the dry weight activity concentration in root zone soil at edible maturity or time of harvest (unitless).
B_v	Soil-to-plant concentration factor which is the ratio of activity concentration in plant parts usually associated with vegetative functions (leaves, stems, straw, etc.) in dry weight to the dry weight activity concentration in root zone soil at edible maturity or time of harvest (unitless).
C_a^{C14}	Carbon-14 activity concentration in air (Bq or Ci/ m^3).
C_a^{H3}	Tritium activity concentration in air (Bq or Ci/ m^3).
C_a^r	Resuspension air concentration (Bq or Ci/ m^3).
C_{cd}^{C14}	Carbon-14 activity concentration in atmospheric carbon dioxide (Bq or Ci/kg).
C_{food}^{H3}	Tritium activity concentration in food (Bq or Ci/ m^3).
C_p	The annual consumption of pasture by livestock (kg/yr).
C_r	Activity concentration in plant parts usually associated with reproductive or storage functions (fruits, seeds, tubers, etc.) in dry weight (Bq or Ci/kg).
C_s	Activity concentration in dry weight in root zone soil (Bq or Ci/kg).
C_s^t	Activity concentration in dry weight in average or typical root zone soil (Bq or Ci/kg).
C_v	Activity concentration in plant parts usually associated with vegetative functions (leaves, stems, straw, etc.) in dry weight (Bq or Ci/kg).
C_{wv}^{H3}	Tritium activity concentration in atmospheric water vapor (Bq or Ci/kg).
C^{ps}	The activity concentration on the surfaces of plants (Bq or Ci/kg).
D_r^t	The deposition rate of resuspended material (Bq or Ci/ m^2/s).
d	Depth of the soil layer of interest, e.g., root zone (cm).
d_{ff}	Average annual number of frost-free days (d).
d_l	The linear distance between a weather station and the centroid of the SITE cell (km).
d_p	The distance between plants in a row in a field of row crops (cm).
d_r	The distance between rows of plants in a field of row crops (cm).
E	Average annual evapotranspiration (cm).
F_f	The fraction of daily ingested activity concentration (from feeding) which is transferred to and remains in a kilogram of muscle at equilibrium (d/kg).
f_{gi}	The fraction of grain which is imported from outside of the assessment area (unitless).
F_m	The fraction of daily ingested activity concentration (from feeding) which is transferred to and remains in a kilogram of milk at equilibrium (d/kg).
f_{ff}	The fractional transfer of ingested activity to beef (unitless).

PARAMETER SYMBOLS AND DEFINITIONS (Continued)

Symbol	Definition
f_{tm}	The fractional transfer of ingested activity to milk (unitless).
f_w^a	The fraction of water in vegetation derived from atmospheric sources (unitless).
f^m	The fraction of maximum growth attained by plants (unitless).
g_{pg}	The number of successive grazings of pasture by cattle (yr^{-1}).
H	Average annual absolute humidity (g/m^3).
h_h	The number of hay harvests in a year (yr^{-1}).
I	Average annual irrigation (cm).
i	Identification number for each SITE cell based on the longitude and latitude of the southeastern corner of the cell (unitless).
K_d	The soil-water distribution coefficient which is the ratio of activity or elemental concentration in soil to that in water at equilibrium (mL/g).
L_{df}	Dominant land feature of the assessment area (unitless).
l	The length of a unit area (cm).
M_{am}	Average annual morning mixing height (m).
M_{pm}	Average annual afternoon mixing height (m).
m_m	The muscle mass of a cow (kg).
m_p	The quantity of milk produced from a milk cow per milking (kg).
n	The number of fruit per plant or tree (unitless).
n_a	The inventory of "all other cattle" (head).
n_b	The inventory of "beef cattle" (head).
n_{cc}	The inventory of cattle and calves (head).
n_g	The inventory of grain-fattened cattle (head).
n_m	The inventory of milk cows (head).
n_r	The number of plants in a row in a field of row crops (unitless).
n_s	The inventory of sheep (head).
P	Average annual total precipitation (cm).
P_{ai}	The annual yield or production of crop i (kg/yr).
P_e	The annual production of exposed produce (kg).
P_{gf}	The annual production of grain feed (kg).
P_{gh}	The annual production of grain food (kg).
P_h	The annual production of hay (kg).
P_{hf}	The annual production of harvested forage or hay + silage (kg).
P_{hi}	The harvest yield or production of crop i per harvest (kg).
P_{lv}	The annual production of leafy vegetables (kg).
P_{pg}	The annual production (equal to consumption by livestock inventory) of pasture grass (kg).
P_{pp}	The annual production of protected produce (kg).
P_s	The annual production of silage (kg).
P_{sl}	Pressure corrected to sea level (mb).

PARAMETER SYMBOLS AND DEFINITIONS (Continued)

Symbol	Definition
P_{sus}	Suspended particulate matter in the range of 2.0-15 μm from resuspension processes ($\mu\text{g}/\text{m}^3$).
p_c	The parameter value for a SITE cell (variable).
p_1	The parameter value for the nearest weather station to the centroid of a SITE cell (variable).
p_2	The parameter value for the second nearest weather station to the centroid of a SITE cell (variable).
p_3	The parameter value for the third nearest weather station to the centroid of a SITE cell (variable).
pop_{rf}	The fraction of the population classified as "rural-non-farm" (unitless).
pop_{rf}	The fraction of the population classified as "rural-farm" (unitless).
pop_t	The total population of the assessment area (unitless).
pop_u	The fraction of the population classified as "urban" (unitless).
Q_f^{fc}	The lifetime forage requirement of grain-fed cattle (kg/yr).
Q_{feed}	Feed ingestion rate by cattle used in meat and milk concentration calculations (k/s).
Q_g^{fc}	The lifetime grain requirement of grain-fed cattle (kg/yr).
R_f	The collective forage requirement by livestock (kg/yr).
R_g	The collective grain requirement by livestock (kg/yr).
r_f	The radius of an individual fruit or plant (cm).
r_n	The number of rows of plants in a field of row crops (unitless).
r^e	The average interception fraction for exposed produce (unitless).
r^{ef}	The average interception fraction for exposed fruit (unitless).
r^h	The interception fraction for hay (unitless).
r^i	The interception fraction for plant i (unitless).
r^{lv}	The interception fraction for leafy vegetables (unitless).
r^{mf}	The interception fraction for mature tree fruit (unitless).
r^{mh}	The interception fraction for mature leafy vegetables (unitless).
r^{ms}	The interception fraction for mature silage (unitless).
r^{msb}	The interception fraction for mature snap beans (unitless).
r^{mt}	The interception fraction for mature tomatoes (unitless).
r^{pg}	The interception fraction for pasture grass (unitless).
r^s	The interception fraction for silage (unitless).
s_g	The annual sales of grain-fattened cattle (head/yr).
T_f	The metabolic half-time for material in beef (s).
T_m	The metabolic half-time for material in milk (s).
T_w	The weathering removal half-time for material deposited on plant surfaces (s).
t_i	The time of interest (d).
t_m	The time at which milk is sampled (s).

PARAMETER SYMBOLS AND DEFINITIONS (Continued)

Symbol	Definition
t_{\max}	The time at which maximum plant growth occurs (d).
t_s	The time at which cattle are slaughtered (s).
V_d^r	The deposition velocity of resuspended material (cm/s).
V_i	The velocity of a migrating material in a soil column (cm/s).
V_w	The velocity of water in a soil column (cm/s).
w	The width of a unit area (cm).
w_1	The weighting factor (inversely proportional to distance) used with the nearest weather station to the centroid of a SITE cell (unitless).
w_2	The weighting factor (inversely proportional to distance) used with the second nearest weather station to the centroid of a SITE cell (unitless).
w_3	The weighting factor (inversely proportional to distance) used with the third nearest weather station to the centroid of a SITE cell (unitless).
X	Longitude ($^{\circ}$ W)
Y	Latitude ($^{\circ}$ N)
Y_e	The productivity of exposed produce (kg/m ²).
Y_{gf}	The productivity of grain feed (kg/m ²).
Y_{gh}	The productivity of grain food (kg/m ²).
Y_h	The productivity of hay (kg/m ²).
Y_i	The productivity of plant i based on the ratio of production to area harvested (kg/m ²).
Y_i^a	The areal yield of crop i (kg/yr/m ²).
Y_{lv}	The productivity of leafy vegetables (kg/m ²).
Y_{pg}	The productivity of pasture grass (kg/m ²).
Y_{pg}^a	The areal yield of pasture grass (kg/yr/m ²).
Y_{pp}	The productivity of protected produce (kg/m ²).
Y_s	The productivity of silage (kg/m ²).
z	Altitude (m).
λ_R	The turnover rate of cattle in the "cattle on feed" category (yr ⁻¹).
λ_f	The metabolic removal rate constant for beef (s ⁻¹).
λ_m	The metabolic removal rate constant for milk (s ⁻¹).
λ_w	The weathering removal constant for plant surfaces (s ⁻¹).
ρ	Soil bulk density (g/cm ³).
θ	Volumetric water content of the soil [mL (equal to cm ³ H ₂ O) /cm ³].

ACKNOWLEDGMENT

We wish to express our deepest gratitude to C. B. Nelson, C. W. Miller, S. Y. Ohr, B. D. Murphy, O. W. Hermann, and C. L. Begovich for their cooperation, suggestions, help, and encouragement in producing the TERRA computer code. We also wish to acknowledge G. G. Killough for his assistance in the Monte Carlo simulations which were essential to some of our analyses and P. E. Johnson and R. C. Durfec for their assistance in creating the SITE data base. Finally, we wish to recognize Y. C. Ng, C. A. Little, D. E. Fields, A. P. Watson, and R. J. Raridon for their time and effort in reviewing this manuscript.

HIGHLIGHTS

Assessment models of radionuclide transport through terrestrial agricultural systems rely on input parameters to describe transport behavior and define interrelationships among the agricultural ecosystem compartments. Often a single set of default parameters, such as those given in the USNRC Reg. Guide I. 109, is recommended for use in generic assessments in lieu of site specific information. These parameters are often based on an incomplete knowledge of transport processes, on readily available literature references, and on generalized or idealized conceptualizations of common agricultural practice. Usually, in lieu of solid experimental, observational, or theoretical support, parameters are chosen to provide conservative results. Further, inconsistencies may occur between experimental determination of the parameter and its use in the assessment model.

The above-mentioned limitations in model input parameters are usually unavoidable and seem to be inherent in the assessment modeling process, but are usually acceptable (in many applications) within the context of overall uncertainty in assessment methodology. However, in some assessment applications, including comparisons among various facilities and source terms in a variety of geographical locations, many of these limitations are not acceptable. This report describes an evaluation of terrestrial transport parameters designed to address many of the above-mentioned limitations and provides documentation of default parameters incorporated into the food-chain-transport assessment code TERRA.

The parameters discussed in this report are divided into five categories: agricultural, climatological, demographic, element-specific, and miscellaneous. The climatological, demographic, and many of the agricultural parameters have been determined on a location-specific basis for the conterminous United States with a resolution of $\frac{1}{2} \times \frac{1}{2}$ degree longitude-latitude. These parameters include various land use and geographic information, population and its distribution in rural and urban settings, agricultural production and productivity, precipitation, and estimates of evapotranspiration, morning and afternoon mixing heights, absolute humidity, and number of frost-free days. These location-specific parameters have been stored in computer readable format and are collectively referred to as the Specific-Information on the Terrestrial Environment (SITE) data base. This report describes the SITE data base and the protocols used in its generation.

The element-specific parameters include soil-to-plant concentration factors, B_v , and B_f , ingestion-to-milk and ingestion-to-beef transfer parameters, F_m and F_f , respectively, and the soil-water distribution coefficient, K_d . The report describes the available literature references, the protocols and assumptions made, and correlations between parameters used to determine these default parameters and compares concentrations predicted using them with experimentally measured concentrations.

1. INTRODUCTION

Under Task I of contract EPA-AD-89-F-2-A106 (formerly EPA-78-D-X0394), the Health and Safety Research Division (HASRD) of the Oak Ridge National Laboratory (ORNL) prepared the AIRDOS-EPA¹ and DARTAB² computer codes to provide the Environmental Protection Agency (EPA) with an integrated set of codes and data bases to simulate atmospheric and terrestrial transport of radionuclides routinely released to the atmosphere and to calculate resulting health impacts to man consequent from these releases. Under Task II of the project an integrated set of computer codes and data bases is being designed to replace the AIRDOS-EPA and DARTAB system. This report describes the Specific Information on the Terrestrial Environment (SITE) computerized data base, element-specific transport parameters, and other parameters used in lieu of user input in the terrestrial transport code TERRA³ or accessed by the atmospheric transport code ANEMOS⁴ and/or the dose and risk code ANDROS.⁵

The terrestrial transport and agricultural parameters reviewed and documented by Moore et al.¹ represented an attempt to update and reevaluate parameters previously recommended in USNRC Regulatory Guide 1.109.⁶ Experience with the AIRDOS-EPA computer code has highlighted several problems in the modeling approach and certain limitations in the assessment methodology which are addressed under Task II. One problem occurs in the protocols used in reviewing literature values for soil-to-plant concentration factors. Other limitations apparent in the AIRDOS-EPA computer code are the absence of transport parameters for many elements and the incorporation of a single set of default agricultural parameters to describe a highly diverse agricultural system in the United States.

Much of the effort under Task II has been directed towards resolution of these problems or inconsistencies and construction of a location-specific data base of default agricultural, meteorological, and demographic parameters for use in generic assessments. Element-specific transport parameters have been reevaluated with regard to their use in the model TERRA, literature references given by Moore et al.¹ have been reevaluated, and new references have been added. For those elements for which experimental experience has been slight, systematic assumptions based on their location in the periodic table of the elements have been used to estimate default values. Theoretical models based on two- and three-dimensional geometries of food and feed crops have been used to suggest default values of the interception fraction, r .

It is beyond the scope of this report to detail the TERRA computer code, but a general understanding of the simulation of transport in vegetable and feed crops is prerequisite to interpretation of our analyses. All vegetable and feed crops have been assigned to seven categories based on their phenotypic and agricultural transport characteristics.⁷ These categories are leafy vegetables, exposed produce, protected produce, grains, pasture, hay, and silage (Fig. 1.1). The first three are classed as human foods and the last three as livestock feeds. Grains are classed as both. Leafy vegetables present a broad flat leaf surface for direct interception of atmospherically depositing material. Furthermore, the edible portion of the plant is primarily concerned with vegetative growth (leaves and stems). Exposed produce (snap beans, tomatoes, apples, etc.) intercept atmospherically depositing material on edible surfaces, but surface areas for exposure are relatively small compared to leafy vegetables. Additionally, edible portions are typically concerned with reproductive functions (fruits and seeds). Protected produce (potatoes, peanuts, citrus fruits, etc.) are not directly exposed to atmospherically depositing material because their growth habit is underground, or if aboveground, the edible portions are protected by pods, shells, or nonedible skins or peels. Typically, edible portions are reproductive or storage organs.

Grains are similar to protected produce, but their use as both livestock feeds and food for man necessitates a separate category. The other three categories of livestock feeds are pasture, hay, and (corn and sorghum) silage. All of these feeds are composed, primarily, of vegetative growth. Silage is categorized separately from hay and pasture based on its interception characteristics. Hay and pasture are separated because their residence times in the field are significantly different, and therefore, parent nuclide decay and ingrowth of daughters calculated in TERRA for these two

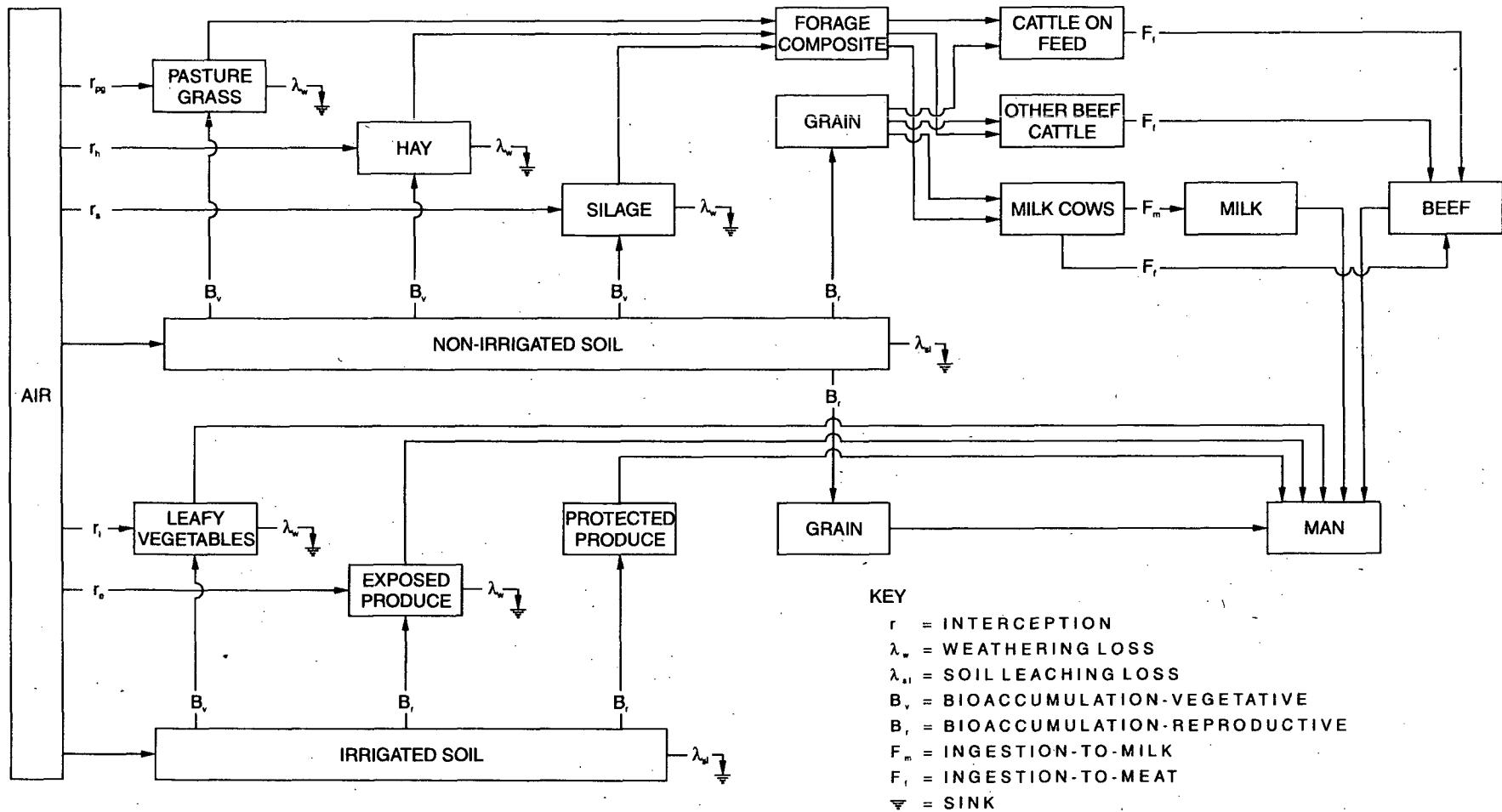


Figure 1.1. The categorization of all vegetable crops and animal feeds in the TERRA code based on radionuclide transport and agricultural pathway characteristics.

categories may be significantly different. Furthermore, hay is easily imported and exported from a location and pasture is not. This difference between the two is important in the calculation of location-specific estimates of pasture productivity and feed fractions based on livestock inventories (Section 4.1).

The elaboration of vegetation into seven categories has been determined chiefly by the protocols necessary in analyzing transport behavior, allowing for location-specific variability in agricultural practice, and simulating radiological decay in the TERRA code. Similarly, for all parameters the following analyses reflect our intent towards "reasonable estimates" based on unbiased approaches, parameter correlations, and theoretical or systematic models when available information is limited. We will attempt to estimate distributions of these parameters whenever possible to allow the reader to select more or less conservative parameter estimates than those used as default in TERRA. Finally, any changes in parameter definitions from those given by Moore et al.,¹ or listed in the USNRC Regulatory Guide 1.109,⁶ have not been made capriciously; but reflect responses to limitations or inconsistencies of past approaches.

2. ELEMENT-SPECIFIC TRANSPORT PARAMETERS

Quantification of nuclide transport through agricultural systems in TERRA involves the parameters describing soil-to-plant uptake for vegetative growth (leaves and stems), B_v ; and nonvegetative growth (fruits, seeds, and tubers), B_r ; ingestion-to-milk transfer, F_m ; ingestion-to-meat transfer for beef cattle, F_f ; and the soil-water distribution coefficient, K_d . Ideally, these transport parameters should be nuclide-specific. For example, isotopic differences in plant availability have been shown for plutonium.⁸⁻¹⁰ However, available information for other elements and the lack of compelling theory for a nuclide-specific approach necessitates an element-specific determination for these parameters. Thus, it is assumed here that variability among isotopes of the same element is insignificant compared to variability among different elements and the overall variability inherent in the parameters themselves. For soil-plant uptake of strontium, available information supports this assumption.¹¹

2.1 Soil-to-Plant Uptake Parameters B_v and B_r

Root uptake of radionuclides incorporated into surface horizons of soil is parameterized by the transfer coefficients B_v and B_r , representing the ratio of elemental concentrations in plant and soil at harvestable maturity. The parameters B_v and B_r are given by

$$B_v = \frac{C_v}{C_s} \text{ and} \quad (1)$$

$$B_r = \frac{C_r}{C_s} \quad (2)$$

where

- B_v = soil-to-plant elemental transfer coefficient for vegetative portions of food crops and feed plants,
- B_r = soil-to-plant elemental transfer coefficient for nonvegetative (reproductive) portions of food crops and feed plants,
- C_v = elemental concentration in vegetative portions of food crops and feed plants (dry weight) at edible maturity,
- C_r = elemental concentration in nonvegetative (reproductive) portions of food crops and feed plants (dry weight) at edible maturity, and
- C_s = elemental concentration in root zone soil (dry weight).

This approach to concentration ratios is significantly different from the B_{iv1} and B_{iv2} approach used by Moore et al.¹ and is in response to some inconsistencies and inadequacies experienced with the AIRDOS-EPA approach.¹² In Moore et al.,¹ B_{iv1} values were calculated from dry plant/dry soil concentration ratios for livestock feeds, and B_{iv2} values were calculated from fresh weight plant/dry soil concentration ratios for food crops. This approach was used because information on feed and food crops is customarily reported in dry and fresh weights, respectively. In analysis of available literature for these concentration ratios, all data in a reference were divided into "animal feeds" and "direct consumption by man" categories, corresponding to B_{iv1} and B_{iv2} , respectively. A literature reference could be used for B_{iv1} or B_{iv2} or both. Conversely, B_{iv1} and B_{iv2} for an element might be derived from two sets of data and references which could be equal, share common elements, or be disjointed. For most elements, $B_{iv2} \leq B_{iv1}$ was observed. This result is logical because the concentration of a finite quantity of material in a plant decreases as plant weight increases. However, if two disjointed sets of references were used, $B_{iv2} \geq B_{iv1}$ for an element could occur. The resultant

values of B_{iv1} and B_{iv2} were appropriate with respect to the references used to generate them, but were not directly comparable with each other. In the approach used here, classification of references is based on physiologic plant characteristics, and not upon ultimate fate of the plant in the human food chain.

Also, in the Moore et al.¹ approach, any statistical analysis of B_{iv2} would have to be based on "converted" parameter values because they are usually reported in dry weight. Because very few references include dry-to-wet weight conversion factors, general references such as Morrison (1959)¹³ and Spector (1959)¹⁴ were used for generation of B_{iv2} . In some cases a value of 25% dry matter^{1,6,15} was used to convert to wet weight. These transformations of reported data added unnecessary uncertainty to parameter estimates, and statistical analysis would be less precise than analysis of original data. Thus, the adoption of dry weight concentration ratios here reduces additional imprecision in parameter estimates and facilitates a more direct comparison between the two concentration factors (B_v and B_r).

Adoption of B_v and B_r over B_{iv1} and B_{iv2} is based on an evaluation of literature references for root uptake and distribution of elements in plants. Nonuniform elemental distributions in food and feed crops has been widely observed (Table 2.1). Typically, nonnutritional elemental concentrations in agricultural plants are generally ordered as roots > leaves \geq stems > tubers \geq fruits \geq seeds.^{10,17,31-37} Variations in the relative distribution of elements among plant parts occur with species, variety, growth conditions, and element, but in general for most elements, $C_v > C_r$.

Analysis of food and feed production in the conterminous United States suggests that B_v and B_r are analogous to B_{iv1} and B_{iv2} , respectively. Leafy vegetables are the only group of food crops for which B_v is the appropriate transfer parameter. Nationally, leafy vegetables comprise a relatively small portion of food crop production (Table 2.2). Thus, major portions of food crops in the United States are associated with the transport parameter B_r . For feed crops, grains are the only category associated with B_r . Although the relative importance of grain feeds varies considerably by state and county, in most areas nongrain feeds dominate. Therefore, the use of default soil-to-plant transport parameters (reviewed in the following sections) in the computer code AIRDOS-EPA merely requires substitution of B_v for B_{iv1} and substitution of a B_r , converted from dry weight to wet weight, for B_{iv2} . Appropriate generic factors for conversion of B_r to B_{iv2} , based on relative importance of various nonleafy vegetables in the United States, are 0.126, 0.222, and 0.888 for exposed produce, protected produce, and grains, respectively (Table 2.3). Weighting these conversion factors by the relative importance (based on production in kilograms) of each category in the United States (Table 2.2) yields an overall average value of 0.428. However, regional differences in the relative importance of the food categories and assessment requirements may require the selection of more appropriate conversion factors from Tables 2.2 and 2.3.

2.1.1 Protocols for determination of parameter values

All estimates of B_v and B_r are based on any combination of 1) analysis of literature references, 2) correlations with other parameters, 3) elemental systematics, or 4) comparisons of observed and predicted elemental concentrations in foods. In general, no *a priori* biases or protocols were used to produce conservative values.

Analysis of literature references required subjective evaluation of the experimental techniques, reliability of reported data, and appropriateness of reported values to the parameters. Practically, when many references were available for an element, subjective standards were relatively high; when only one or a few references were available, standards were less rigorous, and alternative approaches became increasingly important. Occasionally, reported data was not amenable for direct calculation of B_v or B_r based on Eqs. (1) and (2). If such corollary information such as soil bulk density, crop yield, background concentration, counting efficiency, and specific activities were not reported or easily available from other references, estimates of them were made for indirect

Table 2.1. Examples of nonuniform elemental distribution in plants

Element	$(C/C_v)^a$	Plant	Reference
Li	1.6×10^{-1}	pumpkin	16
Be	1.4×10^{-1}	pumpkin	16
B	3.1×10^{-1}	various vegetables	17
Na	6.8×10^{-1}	pumpkin	16
Mg	6.6×10^{-1}	grain and root crops	18
Ca	1.6×10^{-1}	grain and root crops	18
Ti	5.3×10^{-1}	sedge and nut grasses	19
Cr	5.7×10^{-1}	pumpkin	16
Mn	2.0×10^{-1}	various vegetables	17
Fe	1.1×10^{-1}	pumpkin	16
Co	2.7×10^{-1}	sedge and nut grasses	19
Zn	3.5×10^{-1}	corn	20
Sr	8.7×10^{-2}	oats	21
Y	1.3×10^{-1}	beans	22
Mo	1.2×10^{-1}	various vegetables	17
Tc	1.9×10^{-2}	wheat	23
Cd	7.0×10^{-2}	various vegetables	24
I	4.9×10^{-1}	various vegetables	25
Cs	2.6×10^{-1}	wheat	26
Ba	9.6×10^{-2}	pumpkin	16
Ce	3.4×10^{-1}	beans	22
Pb	4.2×10^{-2}	various vegetables	27
Po	1.5×10^{-1}	various vegetables	28
U	5.0×10^{-1}	various grain and root crops	29
Np	3.5×10^{-2}	wheat	30
Pu	1.2×10^{-2}	various vegetables	10
Am	4.2×10^{-3}	various vegetables	10
Cm	6.7×10^{-3}	various vegetables	10

^a (C/C_v) ratios were determined when pairs of observations were reported for a plant type. values in the table are the geometric mean of these ratios for the given reference.

calculation of B_v or B_s . Acceptance or rejection of such references was subjective, depending on the number and quality of other available references and comparison of indirect estimates with direct estimates from reliable sources. Often reported data were presented graphically. When such references were used, some error from visual interpretation of the graphs is inherent in resultant parameter estimates.

Although past estimates of plant uptake parameters have been based on the assumption of equilibrium,^{39,40} studies in which the concentration of polonium,⁴¹ radium,⁴² cesium,⁴³ a mixture of fission products,⁴⁴ or strontium^{43,45-51} in assorted plants has been repeatedly measured indicate that concentration factors for radionuclides change with time. If equilibrium or near-equilibrium conditions are achieved, they occur late in plant ontogeny. Because the transport parameters are used to generate plant concentrations at edible maturity for all vegetative categories, except pasture, an attempt was made to use references in which plant and soil concentrations were measured at edible maturity of the plant. In a majority of references, soil concentrations are given for the beginning of the experiment and plant concentrations are usually measured several weeks or months later. Because for most elements concentration factors are small and removal mechanisms from soil are controlled, only slight error is introduced in using such references. Also, concentration factors determined before edible maturity were used if subjective evaluation of the experiment suggested only slight error would be introduced from using these references. However, most references in which concentration factors were measured within three weeks of seed germination were rejected. For experimental determination of concentration factors for technetium, the above considerations severely limited the available data base.

Table 2.2. Relative importance of food crop categories in selected states and the conterminous U.S.^a

	Percent of total			
	Leafy vegetables	Exposed produce	Protected produce	Grains
California				
Area harvested	8.1	32.7	42.6	16.5
Production	14.4	52.3	29.7	3.5
Florida				
Area harvested	2.8	6.8	87.0	3.5
Production	4.9	7.2	87.4	0.6
Maine				
Area harvested	0.1	14.9	83.1	2.0
Production	0.1	3.1	96.6	0.2
Minnesota				
Area harvested	<0.1	0.4	25.2	74.3
Production	0.2	1.3	46.6	51.9
Montana				
Area harvested	<0.1	<0.1	4.1	95.9
Production	<0.1	0.1	12.0	87.9
Texas				
Area harvested	1.4	1.8	33.1	63.7
Production	10.3	5.2	55.1	29.4
Virginia				
Area harvested	1.5	14.6	32.1	51.8
Production	4.7	31.7	34.9	28.6
Conterminous U.S.				
Area harvested	1.2	6.1	23.3	69.4
Production	5.8	20.0	42.2	32.0

^aReference: Shor, Baes, and Sharp⁷, Appendix B.

If a reference was judged appropriate, analysis of the reported values was done in a manner similar to that of Moore et al.¹ with several modifications. First, all reported values were divided into those for vegetative growth (leaves, stems, straws) or nonvegetative growth (reproductive and storage parts such as fruits, seeds, and tubers). Plant concentrations for the former were used in calculation of B_v and the latter for B_r . Also, if C_v and C_r were reported for a single plant type (e.g., wheat straw and grain or carrot top and root), the ratio (C_r/C_v) was calculated. The geometric mean of all reported values applied to B_v , B_r , or (C_r/C_v) ratio was calculated for each reference. For some references the (C_r/C_v) ratio could be calculated, but B_v and B_r could not because hydroponic solutions were used to grow plants or C_v was not reported. Finally, the geometric means for each reference were used to construct a distribution for B_v , B_r , or (C_r/C_v) ratio. The geometric means of these (inter-reference) distributions were taken to be the best unbiased estimates of the parameters, because reported values often spanned more than an order of magnitude, and because the distributions for elements strontium, cesium, and plutonium (for which there were numerous references) appeared to be lognormally distributed.

Table 2.3. Dry-to-wet weight conversion factors for exposed produce, protected produce, and grains

Vegetable	Conversion factor ^a	Weighting factor ^b	Reference	Vegetable	Conversion factor	Weighting factor	Reference
Exposed produce				Protected produce			
Apple	0.159	15.4	14	Onion	0.125	3.6	14
Asparagus	0.070	0.6	14	Orange	0.128	22.8	14
Bushberries	0.151	1.6	14	Peanut	0.920	3.4	38
Cherry	0.170	0.7	14	Peas	0.257	0.4	14
Cucumber	0.039	4.0	14	Potato	0.222	33.7	14
Eggplant	0.073	0.1	14	Sugarbeet	0.164	6.5	13
Grape	0.181	20.2	14	Sugarcane	0.232	5.5	13
Peach	0.131	6.9	14	Sweet corn	0.261	6.0	14
Pear	0.173	3.5	14	Sweet potato	0.315	1.5	14
Plums and prunes	0.540	3.1	14	Tree nuts	0.967	0.4	14
Sweet pepper	0.074	1.3	14	Watermelon	0.079	2.6	14
Snap bean	0.111	0.7	14	Weighted average	0.222		
Squash	0.082	1.8	14	Grains			
Strawberry	0.101	1.3	14	Barley	0.889	10.1	14
Tomato	0.059	38.8	14	Corn (for meal)	0.895	37.7	38
Weighted average	0.126			Oats	0.917	2.3	14
Protected produce				Rye	0.890	0.5	14
Bean (dry)	0.878	2.2	14	Soybean	0.925	5.3	14
Cantaloupe	0.060	1.1	14	Wheat	0.875	44.0	14
Carrot	0.118	2.4	14	Weighted average	0.888		
Grapefruit	0.112	5.5	14				
Lemon	0.107	2.4	14				

^aConversion factor = grams dry/grams wet.

^bRelative importance based on production in kilograms (percent of total) in the United States based on reference 7.

When only a few literature references were available, alternatives or supplements to the geometric means of distributions method were employed. For example, it was found that B_v was correlated with C_s for several elements, e.g., B, P, Cu, and Zn. That is, entry of the element into the plant appeared to be regulated rather than a constant fraction of the soil concentration. Therefore, studies employing highly enriched soil concentrations might yield inappropriate concentration factors for model calculations. Such correlations were combined with average or typical observed soil concentrations⁵² to generate appropriate concentration factors.

Another approach to determination of concentration factors was to compare plant concentrations surveyed in the literature^{53,54} with those generated by the equations

$$C_v = B_v C'_s \text{ and} \quad (3)$$

$$C_r = B_r C'_s, \quad (4)$$

where C'_s is an average or typical soil concentration reported in the literature.⁵² If predicted plant concentrations were clearly atypical of reported values, the concentration factors were revised accordingly. In general, this method served as a critique of, or supplement to, other methods because of the uncertainties in values for "average" soil and plant concentrations. Typically, these values ranged over two orders of magnitude.

Finally, for rare elements and elements with little or no experimental information available, elemental systematics were used to derive best estimates when no other method or information was available. That is, relationships established between concentration factors for an element and those for other elements of the same or adjacent periods or groups were examined for trends. Such trends were extrapolated to the element in question, with the implication that chemically similar elements act similarly in the soil-plant environment. This elemental analog approach was extremely useful when support information for B_r was unavailable or meager. Systematic trends in observed (C_r/C_v) ratios were often used to predict B_r from B_v when the support data for the former was lacking, but relatively good for the latter.

Selection of values used as default in the TERRA code involved all of the above procedures. The final value selected as default was estimated to two significant digits rounded off to the nearest 0.5 decimal place (Figs. 2.1 and 2.2). That is, if a value of 1.3 was determined from the various above-outlined procedures a value of 1.5 was adopted. A determined value of 1.2 was rounded off to 1.0. The values of B_v and B_r in Figures 2.1 and 2.2 are further discussed in the following sections (2.1.2 through 2.1.10).

2.1.2 Group IA and IIA elements

The Group IA or alkali metals (Li, Na, K, Rb, Cs, and Fr) and the Group IIA or alkaline earth metals (Be, Mg, Ca, Sr, Ba, and Ra) are, generally, relatively easily taken up from soil by plants. Many of the lighter of these elements are essential plant nutrients and some, including isotopes of cesium, strontium, and radium, are extremely important radiologically. Literature references for calculation of B_r and B_v for cesium^{26,34,55-71} and strontium^{11,16-19,21,31-33,59-86} are quite abundant. Available references for the rest of the elements in these two groups are less numerous. References were available for lithium,¹⁶ sodium,^{16,17,65} potassium,^{16-18,65,71,84} rubidium,⁶⁵ beryllium,¹⁶ magnesium,^{16,18,65,71} calcium,^{16,18,65,71,72,84,85} and radium.⁸⁷⁻⁹³ No references were found for francium.

Cesium is the best documented of the Group IA elements. Analysis of the 18 references from which B_v estimates were taken suggests that the distribution of geometric means is lognormal (Fig. 2.3). The geometric means established for each of the 18 references ranged from 0.018 to 0.52 with a geometric mean of the means = 0.078. This value was rounded off to 0.08 for use in TERRA. Half of the B_v references included information pertinent to B_r , yielding a geometric mean of 0.018 for B_r . Ten of the references yielded (C_r/C_v) ratios, suggesting a value of 0.49 for this ratio. Using this ratio value with the B_v estimate previously mentioned yields a second estimate of B_r of 0.038 by the equation

$$B_r = B_v \left[\frac{C_r}{C_v} \right] \quad (5)$$

Thus, an estimate of $B_r = 0.03$, which is near the midpoint of the range (0.018 to 0.038), was adopted. The ratio of default values of B_r and B_v (B_r/B_v) is within one standard deviation of the (C_r/C_v) ratio distribution determined from the 10 references. Comparison of observed concentrations of cesium in plant foods with those predicted using the default estimate for B_r (Fig. 2.2) suggests that the default value is not unreasonable (Table 2.4). No information on naturally occurring cesium in vegetation applicable to B_v was available, but a radiological survey of the Marshall Islands⁹⁴ indicates that predicted Cs-137 concentrations in plants using the default estimate of B_v and measured soil concentrations are less than observed concentrations (which include resuspended material).

The B_v and B_r values chosen for lithium are derived from an unpublished study by Baes and Katz of natural variations in elemental concentrations in associated pumpkins and soils.¹⁶

	IA	IIA											IIIA	IVA	V A	VI A	VII A
II	Li 0.025	Be 0.010											B 4.0		N 30		F 0.060
III	Na 0.075	Mg 1.0	IIIB	IVB	VB	VIB	VII B	VIII		IB	IIB		Al 4.0×10^{-3}	Si 0.35	P 3.5	S 1.5	Cl 70
IV	K 1.0	Ca 3.5	Sc 6.0×10^{-3}	Ti 5.5×10^{-3}	V 5.5×10^{-3}	Cr 7.5×10^{-3}	Mn 0.25	Fe 4.0×10^{-3}	Co 0.020	Ni 0.060	Cu 0.40	Zn 1.5	Ga 4.0×10^{-3}	Ge 0.40	As 0.040	Se 0.025	Br 1.5
V	Rb 0.15	Sr 2.5	Y 0.015	Zr 2.0×10^{-3}	Nb 0.020	Mo 0.25	Tc 9.5	Ru 0.075	Rh 0.15	Pd 0.15	Ag 0.40	Cd 0.55	In 4.0×10^{-3}	Sn 0.030	Sb 0.20	Te 0.025	I 0.15
VI	Cs 0.080	Ba 0.15		Hf 3.5×10^{-3}	Ta 0.010	W 0.045	Re 1.5	Os 0.015	Ir 0.055	Pt 0.095	Au 0.40	Hg 0.90	Tl 4.0×10^{-3}	Pb 0.045	Bi 0.035	Po 2.5×10^{-3}	At 1.0
VII	Fr 0.030	Ra 0.015															

Lanthanides	La 0.010	Ce 0.010	Pr 0.010	Nd 0.010	Pm 0.010	Sm 0.010	Eu 0.010	Gd 0.010	Tb 0.010	Dy 0.010	Ho 0.010	Er 0.010	Tm 0.010	Yb 0.010	Lu 0.010
Actinides	Ac 3.5×10^{-3}	Th 8.5×10^{-4}	Pa 2.5×10^{-3}	U 8.5×10^{-3}	Np 0.10	Pu 4.5×10^{-4}	Am 5.5×10^{-3}	Cm 8.5×10^{-4}							

Key:

Li 0.025

 — Symbol
— Transfer Coefficient, B_v

Figure 2.1. Values of the soil-to-plant concentration factor B_v , adopted as default estimates in the computer code TERRA.

	I A	II A											III A	IV A	V A	VI A	VII A
II	Li 4.0×10^{-3}	Be 1.5×10^{-3}											B 2.0		N 30		F 6.0×10^{-3}
III	Na 0.055	Mg 0.55	III B	IV B	V B	VI B	VII B	VIII		IB	II B		Al 6.5×10^{-4}	Si 0.070	P 3.5	S 1.5	Cl 70
IV	K 0.55	Ca 0.35	Sc 1.0×10^{-3}	Ti 3.0×10^{-3}	V 3.0×10^{-3}	Cr 4.5×10^{-3}	Mn 0.050	Fe 1.0×10^{-3}	Co 7.0×10^{-3}	Ni 0.060	Cu 0.25	Zn 0.90	Ga 4.0×10^{-4}	Ge 0.080	As 6.0×10^{-3}	Se 0.025	Br 1.5
V	Rb 0.070	Sr 0.25	Y 6.0×10^{-3}	Zr 5.0×10^{-4}	Nb 5.0×10^{-3}	Mo 0.060	Tc 1.5	Ru 0.020	Rh 0.040	Pd 0.040	Ag 0.10	Cd 0.15	In 4.0×10^{-4}	Sn 6.0×10^{-3}	Sb 0.030	Te 4.0×10^{-3}	I 0.050
VI	Cs 0.030	Ba 0.015		Hf 8.5×10^{-4}	Ta 2.5×10^{-3}	W 0.010	Re 0.35	Os 3.5×10^{-3}	Ir 0.015	Pt 0.025	Au 0.10	Hg 0.20	Tl 4.0×10^{-4}	Pb 9.0×10^{-3}	Bi 5.0×10^{-3}	Po 4.0×10^{-4}	At 0.15
VII	Fr 0.030	Ra 0.015															

Lanthanides	La 4.0×10^{-3}	Ce 4.0×10^{-3}	Pr 4.0×10^{-3}	Nd 4.0×10^{-3}	Pm 4.0×10^{-3}	Sm 4.0×10^{-3}	Eu 4.0×10^{-3}	Gd 4.0×10^{-3}	Tb 4.0×10^{-3}	Dy 4.0×10^{-3}	Ho 4.0×10^{-3}	Er 4.0×10^{-3}	Tm 4.0×10^{-3}	Yb 4.0×10^{-3}	Lu 4.0×10^{-3}
Actinides	Ac 3.5×10^{-4}	Th 8.5×10^{-5}	Pa 2.5×10^{-4}	U 4.0×10^{-3}	Np 0.010	Pu 4.5×10^{-5}	Am 2.5×10^{-4}	Cm 1.5×10^{-5}							

Key:

Li	—	Symbol
4.0×10^{-3}	—	Transfer Coefficient, B,

Figure 2.2. Values of the soil-to-plant concentration factor B , adopted as default estimates in the computer code TERRA.

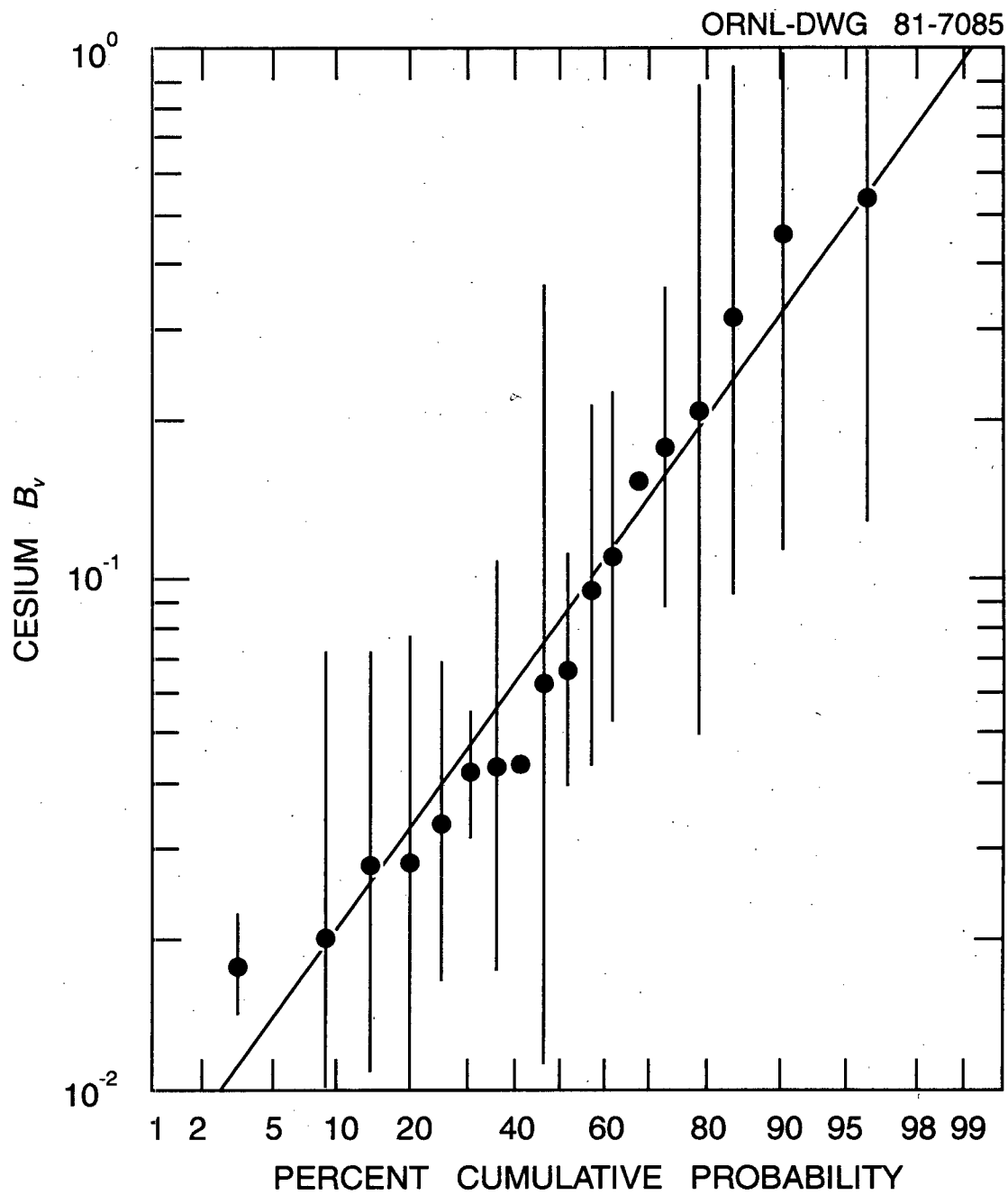


Figure 2.3. Lognormal probability plot of geometric means of B_v for cesium (calculated from references 26, 34, and 55-71), including one geometric standard deviation of the mean.

Comparison of observed and predicted plant concentrations in Table 2.4 indicates that both default B_p and B_r predict plant concentrations which are within observed ranges.

The B_p for sodium (0.075) was also derived from reference 16. Reference 65 reported soil and plant concentrations from which a lower estimate of B_p for sodium was derived, but systematic trends observed by plotting B_p against atomic number for Group IA and IIA elements (Fig. 2.4), suggest the rejection of this lower value. Comparison of observed and predicted plant sodium using the higher value supports its selection, because the predicted value is slightly below the reported range.

An estimate of the (C_r/C_p) ratio for sodium of 0.74 was derived from references 16 and 17. One and two standard deviations of the data reported in references 17 and 16, respectively, include the value 1.0. Thus, $B_p = B_r$ for sodium is quite likely for many plants. However, reported values of C_r for sodium are generally less than C_p . Thus, the derived ratio of 0.74 was judged acceptable, yielding a default value of 0.055 for sodium B_r using Eq. (5). This estimate of B_r appears reasonable (Table 2.4).

The default value of B_p for potassium was determined to be 1.0. This value is based on the geometric mean of values determined for two references (16 and 65), the correlation between B_p and C_r for potassium observed from these references (Fig. 2.5), and the assumption that typical agricultural practice includes soil fertilization with potassium.

The (C_r/C_p) ratio based on literature references is quite variable for potassium. Values at or near 1.0 were found for pumpkin¹⁶ and many common vegetables,¹⁷ including root crops.⁷¹ Lower ratios near 0.4 have been observed for grains.^{18,71,84} From Table 2.4, $C_r < C_p$ appears to apply to potassium, and thus the geometric mean of values determined for references 16-18, 71, and 84 was used to generate a value of $B_r = 0.55$. This estimate yields predicted C_r for potassium which agrees well with the observed range (Table 2.4).

One reference was found for rubidium B_p , but both default B_p and B_r values were derived by assuming systematic trends in B_p (Fig. 2.4) and (B_r/B_p) ratio (Fig. 2.6) for Group IA and IIA elements and comparing observed and predicted C_p and C_r . No references were found for francium B_p , B_r , C_p , or C_r ; and therefore, assumed systematic trends in B_p and (B_r/B_p) ratio were used exclusively for default estimates of the concentration factors. The B_p of 0.03 determined here for francium compares well with the value of 0.04 derived from Ng et al.¹⁵ (assuming 25% dry matter).

Strontium is perhaps the best studied of all elements in the periodic table with respect to plant uptake. As for cesium, analysis of the references for B_p indicates that this parameter is lognormally distributed (Fig. 2.7). The range of reference mean values, 0.077 to 17, is larger than the range for cesium, but the number of references is also greater. The geometric mean of the reference means = 2.7, and it was rounded off to 2.5 for use in TERRA. Fifteen references applicable to B_p yielded a value of 0.25. Twenty-five references yielded estimates of (C_r/C_p) , which when multiplied by the default value of B_p also gave a $B_r = 0.25$.

A $B_p = 0.01$ for beryllium was derived from reference 16. That reference also yielded a $B_r = 0.0028$ for pumpkin, but examination of Figs. 2.4 and 2.6 suggest that a value of 0.0015 is more reasonable. Adoption of this value yields a predicted C_r value which is approximately an order of magnitude higher than reported values (Table 2.4). However, as noted by Shacklette et al.,⁵³ toxicity to plants is severe and measurable amounts are rarely observed in plants.

The B_p for magnesium (1.0) was determined from references 16 and 65. The geometric mean of values of (C_r/C_p) ratio for references 16, 18, and 71 was used to derive a $B_r = 0.55$. Predicted and observed C_p and C_r for magnesium agree well (Table 2.4).

Calcium B_p (3.5) was derived from references 16, 65, 71, and 72. Comparison of predicted and observed C_p values using this B_p value (Table 2.4) and comparison among other Group IIA elements for B_p in Fig. 2.4 support the reasonableness of this value. Calculated mean (C_r/C_p) ratios for calcium, strontium, barium, and radium, 0.081, 0.13, 0.18, and 0.095, respectively, suggested the adoption of a value of 0.1 for all Group IIA elements below magnesium. Thus, $B_r = 0.35$ for calcium is used in TERRA. Comparison of predicted and observed C_r values using this B_r (Table 2.4) is good.

Table 2.4. Comparison of observed and predicted concentrations of Group I A and II A elements in produce and plants (ppm, dry wt.)

Element	Average concentration in soil (C_s) ^a	Vegetative growth (C_v)		Fruits and tubers (C_f)	
		Observed range ^b	Predicted ^c	Observed range ^b	Predicted ^d
Group IA					
Li	30	0.15 to 55	0.75	0.010 to 9.8	0.12
Na	6,300	700 to 20,000	470	15 to 3,500	350
K	14,000	1,000 to 77,000 ^{e,f}	14,000	7,800 to 28,000 ^e	7,500
Rb	100	18 to 400	15	1.0 to 50	7.0
Cs	5.0		0.40	2.0×10^{-3} to 0.35	0.15
Fr					
Group IIA					
Be	6.0	0.090	0.060	1.0×10^{-3}	9.0×10^{-3}
Mg	6,300	110 to 14,000 ^{f,g}	6,300	200 to 11,000 ^{f,g}	3,500
Ca	14,000	1,000 to 78,000 ^f	48,000	71 to 6,400 ^{f,g}	4,800
Sr	300	13 to 1,900	750	0.060 to 40	75
Ba	500	28 to 80	75	0.30 to 86	7.5
Ra	8.0×10^{-7}	2.6×10^{-9}	1.2×10^{-8}	1.1×10^{-9}	1.2×10^{-9}

^aReference 52.

^bTaken or calculated from values in reference 53 assuming ash wt./dry wt. = .128 and .057 for vegetative growth and fruits and tubers, respectively

^cThe product, $B_v \times C_s$.

^dThe product, $B_f \times C_s$.

^eReference 13.

^fReference 14.

^gReference 54.

The B_v for barium (0.15) was determined from references 16, 59, and 65. The default B_v value was calculated in a manner similar to that for calcium using Eq. (5). Observed and predicted C_v and C_f agree well (Table 2.4).

Because of its importance radiologically, the concentration factors for radium used in AIRDOS-EPA have been both highly scrutinized and criticized.⁹⁵ Reevaluations of the B_{iv1} and B_{iv2} values listed in Moore et al.¹ have been based on corrections of values reported in the literature¹² and subjective evaluation of the quality of the references.⁹⁵ Unfortunately, available references for calculation of soil-to-plant concentration factors for radium must all be judged subjectively (Table 2.5). However, separation of plants into the two categories in association with B_v and B_f eliminates inconsistencies in the B_{iv1} and B_{iv2} approach and suggests that only one available reference reports questionable results. The earliest reference found for radium soil-plant concentration factors, reported by Kirchmann and Boulenger in 1968,⁸⁷ has not been used in support of B_v and B_f here because their analytical technique is questionable⁹⁵ and yields extremely high values. Furthermore, the experimental technique for determination of radium used by Kirchmann and Boulenger has been questioned.⁹⁵ However, reference 87 does yield a (B_v/B_f) ratio consistent with those for calcium, strontium, and barium. Insufficient criteria have been found for rejection of any of the remaining references.

ORNL-DWG 81-7093R

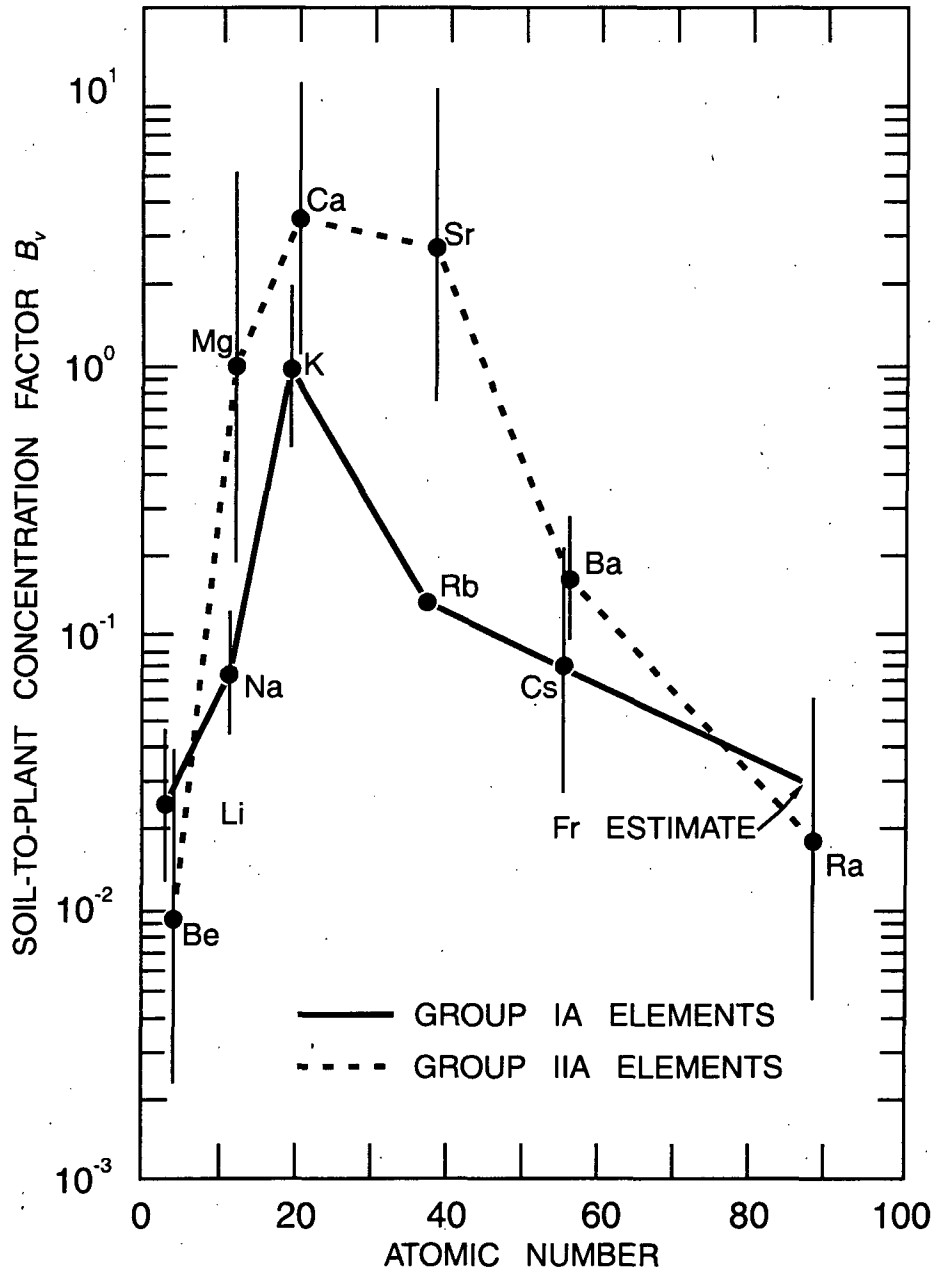


Figure 2.4. Assumed systematic trends in B_v for Group IA and IIA elements. Solid dots and error bars represent geometric means and standard deviations determined from available references.

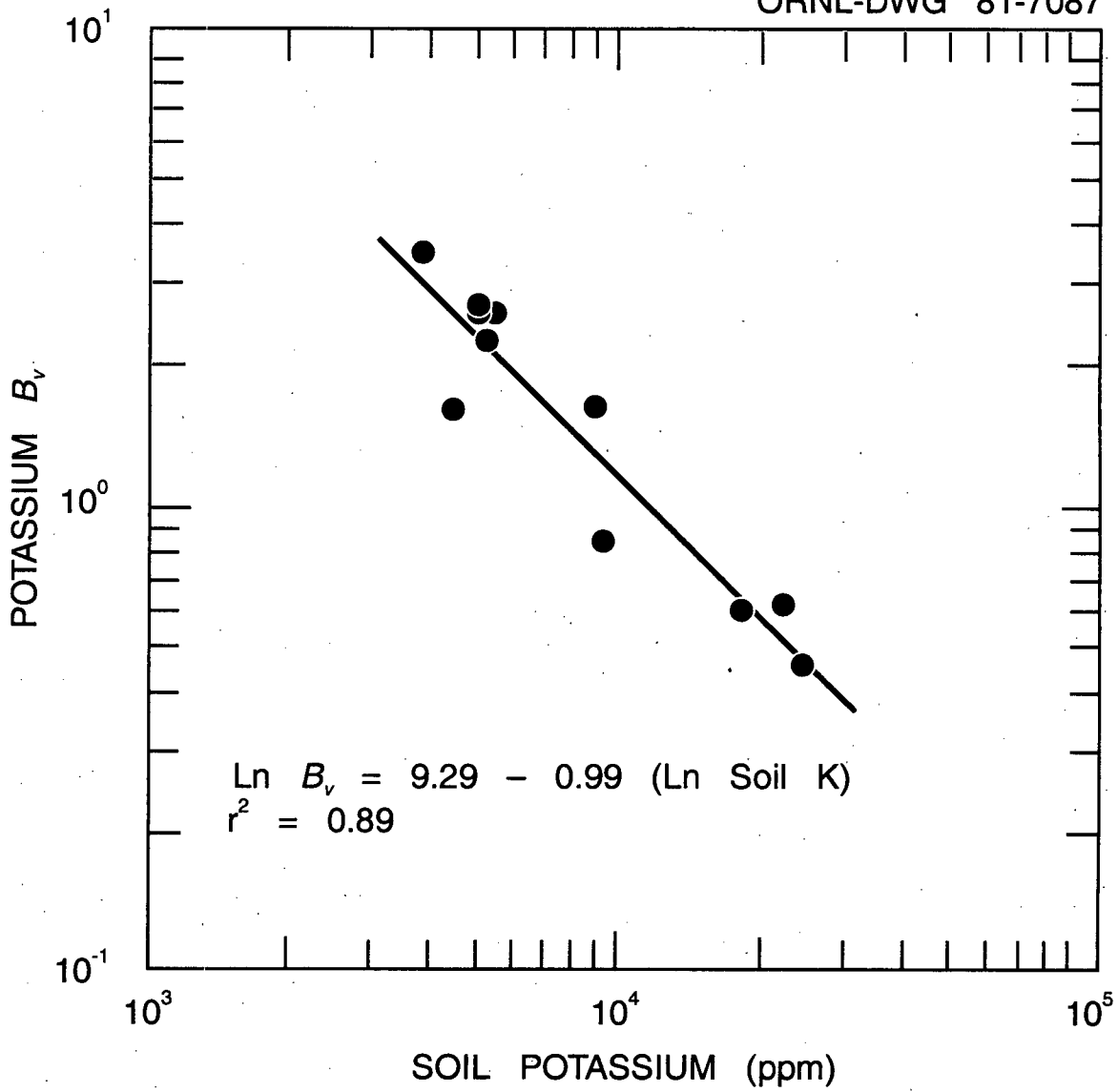


Figure 2.5. Correlation between soil potassium concentration and the soil-to-plant concentration factor, B_v , for potassium based on references 16 and 65.

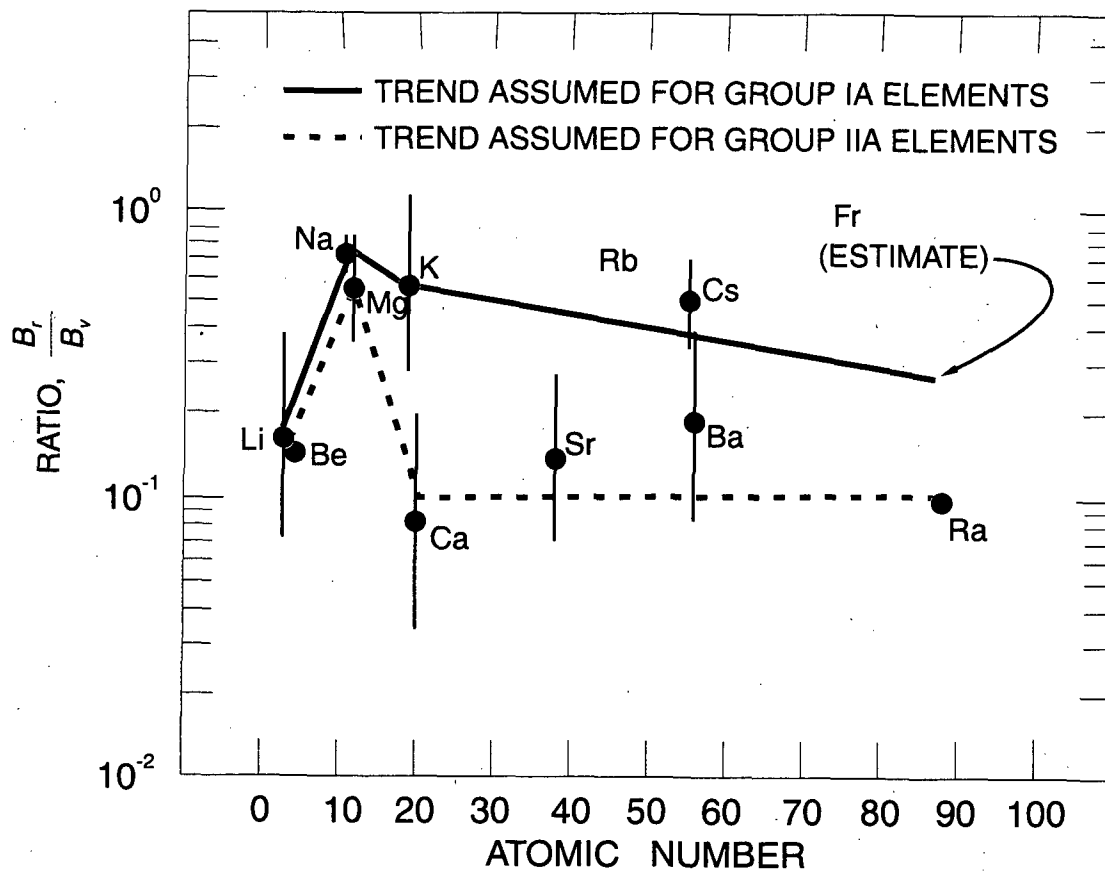


Figure 2.5. Assumed systematic trends in (B_r/B_v) ratio for Group IA and IIA elements. Solid dots and error bars represent geometric means and standard deviations determined from available references.

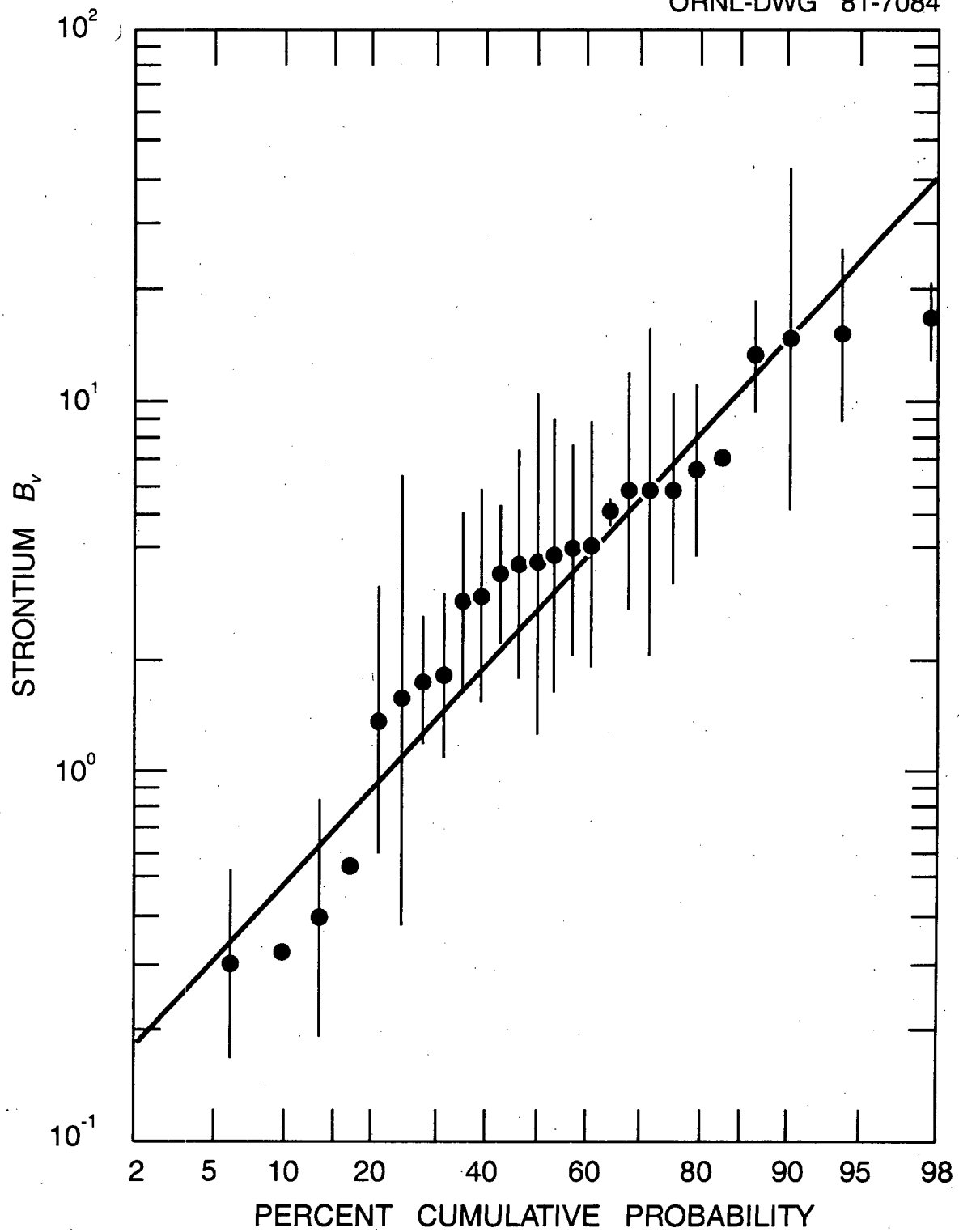


Figure 2.7. Lognormal probability plot of geometric means of B_v for strontium (calculated from references 11, 16, 17, 21, 31, 33, 59, 60, 62-70, 72, 74-76, 78, 81-83, 85, and 86), including one geometric standard deviation of the mean.

Table 2.5. Literature values of B_v , B_f , and the (C_v/C_f) ratio for radium^a

B_v	B_f	(C_v/C_f)	Reference	Comments
0.71	0.10	0.95	87	Ra-226 measurement technique questionable. Estimates of B_v and B_f not used in present analysis.
	5.0×10^{-4}		90	Reported wet weight plant concentrations converted to dry weight using reference 13.
0.045	3.2×10^{-3}		88	Values reported for "herbage and fruit" required assumptions as to exact makeup. Wet weight plant concentrations converted to dry weight using reference 14.
0.060		1.8	93	Vegetation sampled inappropriate to human pathways. Resuspension of soil onto plant surfaces suspected.
0.012			89	Pot geometry and soil bulk density assumed in order to estimate soil radium concentrations. Ash weight plant concentrations converted to dry weight using reference 13.
0.020			91	
2.4×10^{-3}	8.2×10^{-4}		92	"Salad" was assumed to be lettuce. Ash weight plant concentrations converted to dry weight using reference 14.

^aGeometric means of all values reported.

In a review of Ra-226 transport by McDowell-Boyer, Watson, and Travis,⁹⁶ a value of 0.09 was recommended for a radium forage and hay concentration factor. The authors recommended a value of 0.02 for vegetables, fruit, and grain. The dry weight equivalent of this value would be a factor of 4 to 10 higher, depending on the assumed water content of vegetables, fruit, and grains. The value for B_v derived from five references listed in Table 2.5 is 0.017, which is roughly a factor of 5 lower than the value recommended in reference 96. This value has been rounded off to 0.015. The B_f value derived from three references listed in Table 2.5 is 0.0011, which is much lower than the value recommended in reference 96. The (B_f/B_v) ratio obtained from reference 87 and similar ratios found for calcium, strontium, and barium suggest that a $B_f = 0.0015$ is reasonable. These default B_v and B_f values appear to be acceptable based on systematic trends (Figs. 2.4 and 2.6) for Group IIA elements and comparison of observed and predicted C_v and C_f values (Table 2.4).

Much work has been done on the effect of available soil calcium on the uptake of strontium by plants,^{18,21,33,71,78,79,81,82} and this subject has been thoroughly reviewed by Francis;²³³ in general, plant uptake of strontium is inversely proportional to the amount of exchangeable calcium in the soil. The same effect of soil calcium on plant uptake of radium has also been suggested.⁸⁸ Therefore, it is likely that plant uptake of all Group IIA elements will be negatively affected by increasing soil calcium. The exact relationships between calcium and other IIA elements will be affected by plant type, plant part, and soil characteristics; therefore, in the TERRA computer code, soil calcium influence on B_v and B_f for Group IIA elements is not considered. However, a user of the code may wish to select higher B_v and B_f values than the defaults (Figs. 2.1 and 2.2) for Group IIA elements for pasture pathways and lower values for food crop pathways, assuming that in the latter case soils are more intensively prepared and amended (including liming).

2.1.3 Group IIIA, IVA, and VA elements

Groups IIIA, IVA, and VA contain elements which are essential plant nutrients, elements for which some isotopes are important radiologically, and elements for which experimental evidence for B_v and B_r is scanty. By far, the best documented element of these groups for B_v and B_r is lead,^{16,20,27,91,99-105} followed by arsenic,^{16,19,98} boron,^{16,17,65,76} aluminum,^{16,17,19,65} phosphorus,^{16,17,97} indium,⁶⁵ tin,⁶⁵ and antimony.⁶⁵ No references were readily obtainable for nitrogen, silicon, gallium, germanium, thallium, and bismuth. Corollary information was used to estimate transfer parameters for these elements.

The B_v value of 4.0 adopted for boron is based on the relationship between soil boron concentration and boron B_v determined from references 16, 65, and 76 (Fig. 2.8), and an assumed average soil boron concentration of 10 ppm (Table 2.6).⁵² The (B_r/B_v) ratio as determined from references 16 and 17 is approximately 0.5, and a B_r value of 2.0 was adopted. Comparison of observed and predicted boron food concentrations (Table 2.6) indicates that the default B_v and B_r values are reasonable.

The B_r estimate of 0.004 for aluminum is based on references 16 and 65. The (B_r/B_v) ratio of 0.167 determined from reference 17 was used to generate a default value for B_r of 6.5×10^{-4} . This value is a factor of 2.5 greater than the single value of 2.6×10^{-4} found by Baes and Katz,¹⁶ but comparison of observed and predicted aluminum concentrations in produce (Table 2.6) indicates the default B_v and B_r estimates give reasonable predictions which are near the low end of reported ranges.

The B_v for indium was taken from a single value determined from reference 65. Because the default B_v estimate for indium equals the default B_v estimate for aluminum, a gallium B_v of 0.004 was also assumed for this Period IV element. Since no data were available for thallium B_v , its value was set equal to that for aluminum, gallium, and indium. A (B_r/B_v) ratio of 0.1 was assumed for gallium, indium, and thallium, yielding a B_r of 4.0×10^{-4} for these elements. Unfortunately, elemental concentrations of gallium, indium, and thallium in soils and a variety of produce are not well-documented. However, the values assumed here are consistent with the fragmentary information of observed plant concentrations of these elements.

Of the Group IVA elements, lead is the best documented with respect to B_v and B_r . The default B_v value of 0.045 is the geometric mean of values determined for nine references. A (B_r/B_v) ratio of 0.2 based on references 16, 20, 27, 99 and 102 yields a B_r estimate of 0.009. Table 2.6 shows that these B_v and B_r default values yield appropriate estimates of lead concentrations in produce.

No references for the direct measurement of B_v or B_r for silicon were found. Ng et al.¹⁵ provide data from which a dry weight transfer factor of 6.1×10^{-4} can be derived. Menzel,¹⁰⁶ however, reported that the transfer coefficient for soluble forms of silicon ranged between 0.1 and 1.0. Using the 330,000 ppm (33%) value for silicon in soil reported by Vinogradov⁵² and the C_v range reported by Shacklette et al.,⁵³ the Ng et al. value is approximately an order of magnitude too low and the range reported by Menzel is too high. Therefore, for a B_v estimate, the C_v value reported for grasses of 110,000 ppm silicon (plant concentrations for other produce or vegetables were reported in wet or ash weight) was combined with the reported average soil concentration according to Eq. (3) to give a $B_v = 0.35$ for silicon. The (B_r/B_v) ratio for silicon was assumed to be the same as for lead, generating a B_r estimate of 0.07.

Reference 15 yields a dry weight transfer factor of 0.4 for germanium. This value appears to be slightly low when predicted and measured C_v values are compared (Table 2.6). However, in the absence of experimental evidence and because the value agrees well with the default B_v estimate for silicon, it is used for germanium B_v also. The (B_r/B_v) ratio is also assumed to be 0.2 as for lead and silicon, yielding a B_r estimate of 0.08.

The B_v for tin of 0.03 is based on reference 65, and the B_r value of 0.006 is based on an assumed (B_r/B_v) ratio of 0.2. Comparison of observed and predicted C_v and C_r values in Table 2.6 indicates that the default B_v and B_r values are reasonable.

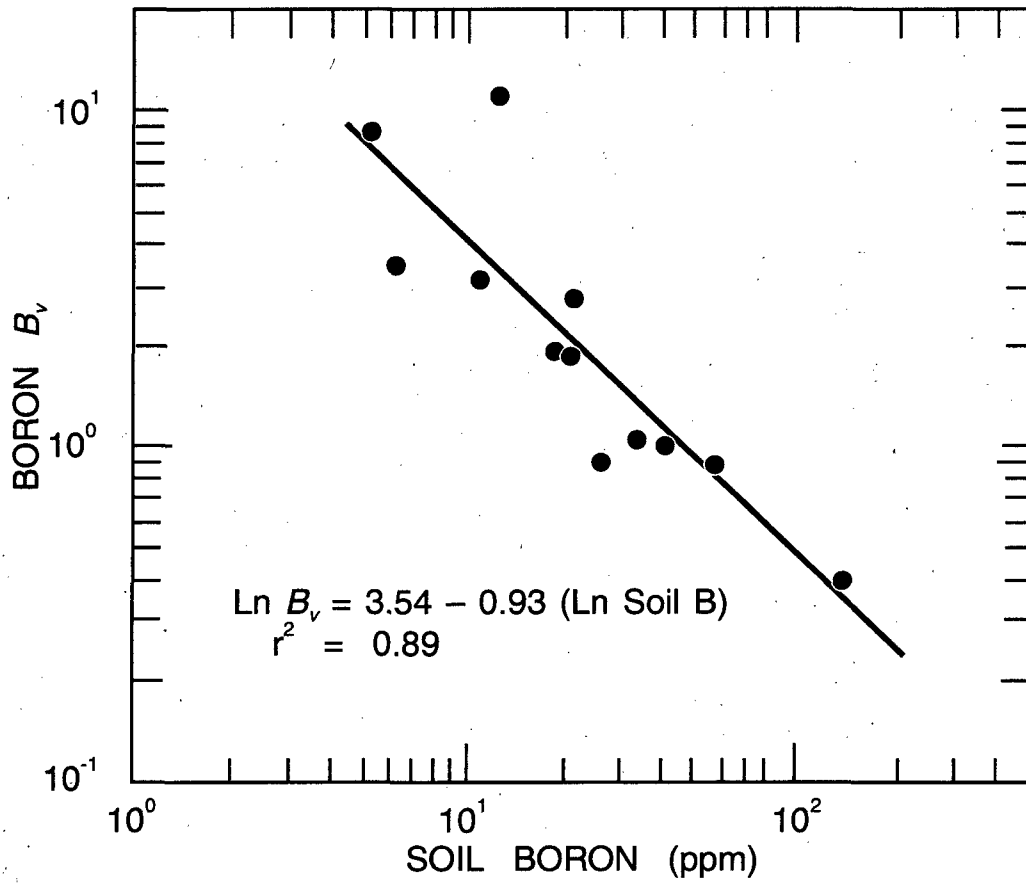


Figure 2.8. Correlation between soil boron concentration and the soil-to-plant concentration factor, B_v , for boron based on references 16, 65, and 76.

Table 2.6. Comparison of observed and predicted concentrations of Group III A, IV A, and V A elements in produce and plants (ppm, dry wt.)

Element	Average concentration in soil (C_s) ^a	Vegetative growth (C_v)		Fruits and tubers (C_r)	
		Observed range ^b	Predicted ^c	Observed range ^b	Predicted ^d
Group III A					
B	10	4.0 to 2,100	40	66 to 520	20
Al	71,000	900	280	11 to 86	46
Ga	30	0.13	0.12		0.012
In					
Tl		0.26 to 0.90			
Group IV A					
Si	330,000	24,000 to 110,000	120,000		23,000
Ge	1.0	0.64 to 13	0.40		0.080
Sn	10	0.13	0.30	0.10 to 1.8	0.060
Pb	10	0.13 to 9.0	0.45	0.015 to 1.0	0.090
Group V A					
N	1,000	16,000 to 43,000 ^e	30,000	4,500 to 29,000 ^{e,f}	30,000
P	800	600 to 9,800 ^e	2,800	630 to 52,000 ^f	2,800
As	5.0	<0.05 to 0.25	0.20	<0.05 to 3.9	0.030
Sb	0.10	<0.056 ^g	0.020	1.3×10^{-4} to 0.039 ^g	3.0×10^{-3}
Bi	1.0	0.15	0.035	0.068	5.0×10^{-3}

^aReference 52.

^bTaken or calculated from values in reference 53 assuming ash wt./dry wt. = .128 and .057 for vegetative growth and fruits and tubers, respectively

^cThe product, $B_v \times C_s$.

^dThe product, $B_r \times C_s$.

^eReference 14.

^fReference 13.

^gReference 54.

No references for experimental determination of B_v for the essential plant nutrient nitrogen were readily available. The review reference 15 yields a default value of 30, which gives a predicted C_v in the midrange of reported values (Table 2.6). Thus, this value was adopted for use in TERRA. Comparison of observed C_v and C_r ranges indicates that nitrogen uptake in vegetative and reproductive plant parts is approximately the same. In the absence of evidence to the contrary, $B_v = B_r$ was assumed.

The B_v for phosphorus is based on the relationship between soil phosphorus concentration and B_v found from data in reference 16 (Fig. 2.9), assuming an average soil concentration of phosphorus of 800 ppm.⁵² Three references yield estimates of (B_v/B_s) ratio. Two references (16 and 97) yield estimates greater than 1.0. Reference 17 yields a value of 0.78, but one standard deviation of the mean includes 1.0. Thus as for nitrogen, $B_v = B_s$ was adopted. Comparison of observed and predicted C_v and C_r indicates that default values of B_v and B_r for phosphorus are reasonable.

The B_v for arsenic of 0.04 was determined from references 16 and 98. References 16 and 19 both indicate that, unlike the lighter members of Group VA elements, the accumulation of arsenic in nonvegetative plant parts is less than for vegetative parts. A (B_v/B_s) ratio for arsenic of 0.15 was used to calculate a default $B_v = 0.006$. Comparison of observed and predicted C_v and C_r values (Table 2.6) shows that the default B_v predicts C_v values near the high end of the observed range and the B_r predicts C_r values near the low end of the observed range.

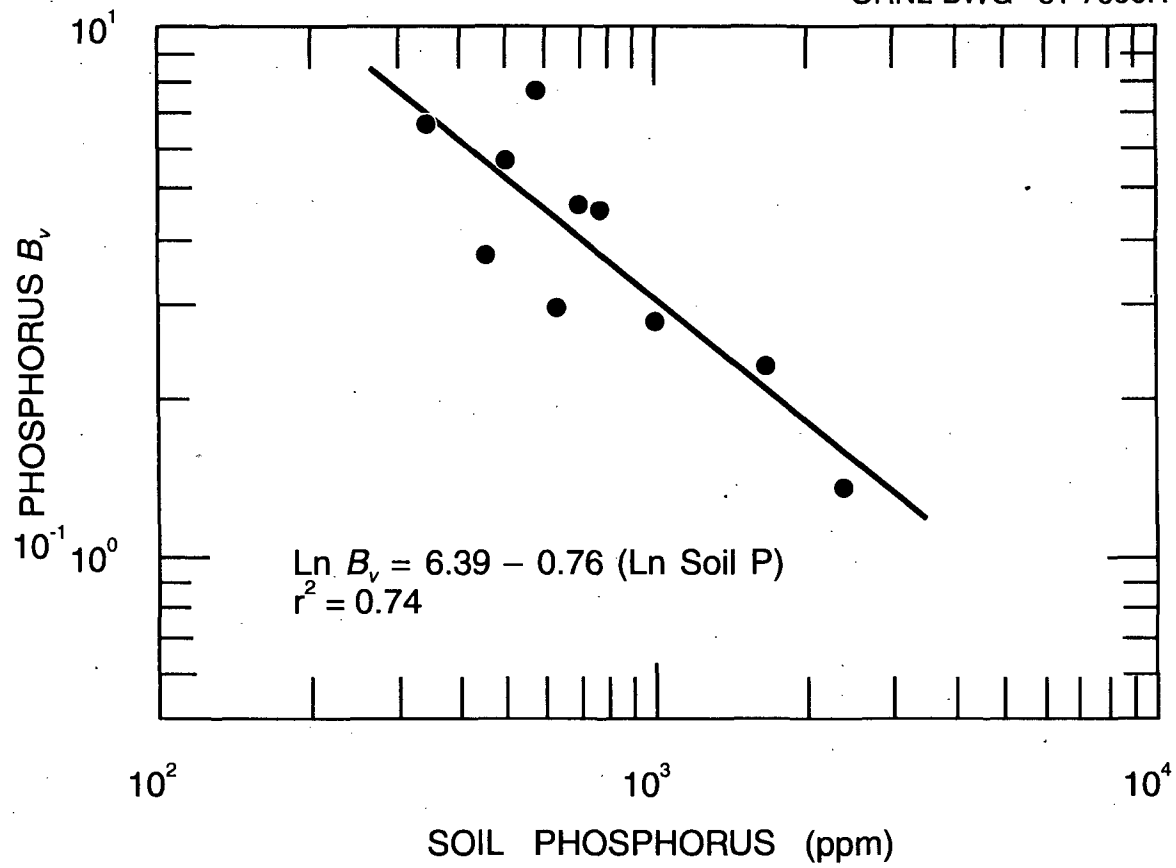


Figure 2.9. Correlation between soil phosphorus concentration and the soil-to-plant concentration factor, B_v , for phosphorus based on reference 16.

The B_v for antimony was taken from reference 65. The (B_p/B_v) ratio for arsenic was also used for antimony. Comparisons of observed and predicted C_v and C_r for arsenic (Table 2.6) are reasonably good.

The B_v for bismuth was determined from the B_v estimates for lead and polonium (discussed in Sec. 2.1.4). The B_v estimate was generated from the default B_v of 0.035 and the (B_p/B_v) ratio used for arsenic and antimony. Comparison of observed and predicted C_v and C_r , although not definitive, are relatively good (Table 2.6).

2.1.4 Group VIA and VIIA elements

The Group VIA and VIIA elements include the relatively mobile anions and the radiologically important elements polonium and iodine. Of these elements the best documented are iodine,^{25,59,65,107,234,235} selenium,^{19,65,76} and polonium.^{28,91} Single references were available for fluorine,¹⁰⁸ chlorine,⁶⁵ and bromine,⁶⁵ and no references were readily available for sulfur, tellurium, and astatine.

No references on direct determination of soil-to-plant transfer coefficients for sulfur were readily available. However, assuming an average sulfur concentration of 1400 ppm in vegetative portions of plants¹⁴ and 850 ppm in soil,⁵² a B_v of 1.5 results. Comparison of observed C_v and C_r for sulfur indicate that $B_v = B_r$ for this element (Table 2.7).

The default B_v value for selenium of 0.025 was determined via several approaches. The value obtained from references 65 and 76 (0.032) was compared with values given by Ng et al.¹⁵ and Menzel.¹⁰⁶ The latter two estimates were several orders of magnitude higher than the value obtained from references 65 and 76. Although B_v for plant-fly ash relationships^{19,65,76} is comparable to B_v estimates given by Ng et al.¹⁵ and Menzel,¹⁰⁶ their estimates, when combined with an average selenium soil concentration of 1 ppm, tend to over-predict observed C_v values (Table 2.7). Therefore, as a model for selenium the As/P and Br/Cl B_r ratios were used as analogs for the Se/S B_r ratio. If such ratios are assumed to change systematically, then the Se/S ratio may be assumed to be 0.016. This value, multiplied by the B_v for sulfur, yields a default selenium B_v estimate of 0.025. Comparison of observed and predicted selenium C_v using this default value (Table 2.7) suggests that the default value is reasonable. Although the (B_p/B_v) ratio for selenium taken from reference 19 is less than 1.0, comparison of observed C_v and C_r ranges suggest that $B_v = B_r$ for selenium also.

The B_v for polonium based on references 28 and 91 is 2.5×10^{-3} . The (B_p/B_v) ratio taken from reference 28 is 0.15. This ratio generates a default B_v value of 4.0×10^{-4} . Unfortunately, no references for comparison of observed C_v and C_r were immediately available for comparison with predicted values.

No references were found for tellurium. The default B_v values determined for selenium and polonium suggest that a reasonable assumption for tellurium B_v is also a value of 0.025. Correspondingly, the (B_p/B_v) ratio of 0.15 for polonium was used to predict a B_v for tellurium of 0.004. As for polonium, no observed C_v and C_r values were available. Furthermore, no average tellurium soil concentrations were available either.

The B_v for fluorine is based on reference 108. The value of 0.06 generates a predicted C_v value which falls within the range of observed values (Table 2.7). Comparison of observed C_v and C_r ranges suggest a discrimination factor of approximately an order of magnitude. Thus, a (B_p/B_v) ratio of 0.1 was assumed and $B_r = 0.006$.

The B_v and B_r for chlorine were determined through comparison of observed C_v and C_r and average C_v for chlorine (Table 2.7). Both the resulting B_v and $B_r = 70$, the highest concentration factors for any element reviewed here. Reference 65 yielded a B_v of 2.1 and a value of 20 was obtained from reference 15, but the C_v predicted with these factors are well below the reported range. Thus the more indirect method was deemed more appropriate for chlorine.

Table 2.7. Comparison of observed and predicted concentrations of Group VI A
VII A elements in produce and plants (ppm, dry wt.)

Element	Average concentration in soil (C_s) ^a	Vegetative growth (C_v)		Fruits and tubers (C_f)	
		Observed range ^b	Predicted ^c	Observed range ^b	Predicted ^d
Group VI A					
S	850	100 to 17,000 ^e	1,300	200 to 450 ^e	1,300
Se	1.0 ^f	<0.01 to 0.35	0.025	<0.01 to 0.50	0.025
Te					
Po	1.0×10^{-11}		2.5×10^{-14}		4.0×10^{-15}
Group VII A					
F	200	1.3 to 28	12	0.020 to 8.4	1.2
Cl	100	2,000 to 23,000	7,000	300 to 8,500	7,000
Br	5.0	0.31 to 4.9	7.5	0.20 to 260	7.5
I	5.0	4.3 to 10	0.75	2.8 to 10	0.25
At					

^aReference 52.

^bTaken or calculated from values in reference 53 assuming ash wt./dry wt. = .128 and .057 for vegetative growth and fruits and tubers, respectively

^cThe product, $B_v \times C_s$.

^dThe product, $B_f \times C_s$.

^eReference 14.

^fBased on values given in references 65 and 76.

The B_v for bromine is based on reference 65. Although the corresponding predicted C_v is slightly high with respect to the observed C_v range, comparison of observed C_v and C_f ranges suggest that the reported C_v range may be low (the upper end of the C_v range is higher than that for the C_f range and a discrimination factor of greater than 1.0 for C_v appears unlikely). In lieu of contrary information, a (B_v / B_f) ratio of 1.0 was assumed for bromine, and thus $B_v = B_f$ was assumed.

The B_v for iodine (0.15) is the geometric mean of values determined for references 25, 59, 65, 107, 234, and 235. References 59 and 107 indicate that B_v for iodine ranges between 1.0 to 2.0. However, references 65, 234, and 235 indicate a much lower B_v for iodine (0.04 to 0.10). Menzel¹⁰⁶ reports that the concentration factor for bromine is greater than that for iodine, and examination of Table 2.7 shows that the adopted B_v for iodine does not predict a C_v value greater than observed. Thus, the default value adopted in the TERRA code seems reasonable.

The B_v value of 0.050, adopted as a default in TERRA, is based on a compromise between the value of 0.02 derived from reference 234 and the product of the B_v/B_f ratio (0.5) derived from references 25 and 234 and the default B_v of 0.15. Examination of Table 2.7 shows that the default B_v value does not over-predict observed C_v values reported in the literature.

No references were found for astatine. A value of 1.0 for B_v is derived from Ng et al.,¹⁵ and this value is adopted as a default value for TERRA. Using polonium as an analog, the assumed (B_v/B_f) ratio is 0.15, producing a $B_v = 0.15$.

2.1.5 Group IIIB and the rare earth elements

The Group IIIB and the rare earth or lanthanide series elements are generally not important for plant nutrition, nor do they accumulate to any large extent in plants. Radiologically, isotopes of cerium are important. In our analysis, we found yttrium^{16,22,59,60,67} and cerium^{22,59,60,65} to be the best documented of these elements, followed by scandium,⁶⁵ lanthanum,⁶⁵ promethium,^{22,59} samarium,⁶⁵ and ytterbium.⁶⁵ No references were obtained for praseodymium, neodymium, europium, gadolinium, terbium, dysprosium, holmium, erbium, and thulium. However, because of the similarity of chemical behavior of all the lanthanides,^{110,111} soil-to-plant concentration factors for these undocumented elements are based on our analysis of cerium. The B_v for yttrium of 0.015 was derived from references 16, 22, 59, 60, and 67. A (C_v/C_s) ratio of 0.29 was determined from references 16, 22, and 60 and compared with a (B_r/B_v) ratio of 0.46 which was based on a B_r derived from these same references. A (B_r/B_v) ratio midway between these two estimates (0.36) was used to derive a default $B_r = 0.006$. Comparison of observed and predicted C_v and C_r for yttrium (Table 2.8) indicate that the default B_v and B_r values are perhaps slightly low, but not unreasonable.

The B_v for scandium of 0.006 is based on the observation by Baes and Mesmer¹¹⁰ that the chemistry of scandium is between that for aluminum (Sect. 2.1.3) and that for yttrium, but surprisingly more like that for aluminum. A value of 0.0078 was taken from reference 65, and data from Ng et al.¹⁵ yields a value of 0.0043. The mean of these two values corresponds well with the value of 0.006 determined through systematic interpretation of Baes and Mesmer's observation (Fig. 2.10). The (B_r/B_v) ratio was determined in a similar manner to B_v , assuming a systematic variation in this parameter. The ratio value of 0.2 was used to calculate a default $B_r = 0.001$. Comparison of observed and predicted scandium food concentrations (Table 2.8) are difficult because of the uncertainty in the observed range values. However, if the observed C_r range reported is reasonable, then both predicted C_v and C_r values are not unreasonable.

The B_v for cerium of 0.01 was derived from references 22, 59, 60, and 65. Because of the similarity in the lanthanide elements, the B_v values from references 22, 59, and 65 for other members of the series were pooled with and without those for cerium to estimate B_v for all of the lanthanides. Both sets of pooled references yielded a $B_v = 0.01$. Thus, this value was adopted for elements 57 through 71. Pooling of references for (B_r/B_v) ratio^{22,60} yielded a value of 0.4. This value was also used for elements 57 through 71.

Comparisons of observed and predicted lanthanide concentrations in produce and plants is difficult because of the paucity of good experimental information. However, examination of Table 2.8 shows that for elements in which comparisons can be made, our soil-to-plant transfer coefficients tend to slightly underpredict reported food concentrations. Although some underpredictions are by more than an order of magnitude, the uncertainty involved in a typical soil concentration or the applicability of a few measurements to the true range of food concentrations does not warrant revision of the estimates.

Table 2.8. Comparison of observed and predicted concentrations of Group IIIB and the rare earth elements in produce and plants (ppm, dry wt.)

Element	Average concentration in soil (C_s) ^a	Vegetative growth (C_v)		Fruits and tubers (C_r)	
		Observed range ^b	Predicted ^c	Observed range ^b	Predicted ^d
Sc	7.0	1.0×10^{-4e}	0.042	5.0×10^{-5} to $0.10^{b,e}$	7.0×10^{-3}
Y	50	2.7 to 9.1	0.75	0.40 to 4.5	0.30
La	40	<0.074	0.40	0.052 to 0.31^e	0.16
Ce	50	0.084	0.50	0.033 to $0.10^{b,e}$	0.20
Pr	4.5		0.045		0.18
Nd	18		0.18	0.080	0.072
Pm				0.080	
Sm	4.9		0.049	0.080	0.020
Eu	0.39	$<5.3 \times 10^{-3e}$	3.9×10^{-3}	0.080	1.6×10^{-3}
Gd	5.5		0.055	0.080	0.022
Tb	0.85		8.5×10^{-3}	0.080	3.4×10^{-3}
Dy	6.0		0.060	0.080	0.024
Ho	0.95		9.5×10^{-3}	0.080	3.8×10^{-3}
Er	4.5		0.045	0.080	0.018
Tm	0.45		4.5×10^{-3}	0.080	1.8×10^{-3}
Yb	4.6	0.53 to 3.2	0.046	0.080 to 13	0.018
Lu	1.2		0.012	0.080	4.8×10^{-3}

^aSc-Ce from reference 52; Pr-Lu estimated from ranges reported by Gibson et al.¹¹¹

^bTaken or calculated from values in reference 53 assuming ash wt./dry wt. = .128 and .057 for vegetative growth and fruits and tubers, respectively

^cThe product, $B_v \times C_v$.

^dThe product, $B_r \times C_r$.

^eReference 54.

2.1.6 Period IV transition elements

Elements of atomic number 22 through 30 (titanium through zinc) are perhaps the best documented for plant uptake from soil. Several of these elements, including manganese, iron, and zinc are generally accepted as essential plant micronutrients.⁵³ Others, including chromium and cobalt, are recognized as essential for animal nutrition and are suspected as plant nutrients, although their essentiality has not been established. Stable isotopes of these elements have been extensively studied because most are toxic to plants and animals at sufficient concentrations, although radiologically they are relatively unimportant. As the following discussion will show, the concept of a single equilibrium concentration factor for many of these elements can be questioned. For those elements which are essential to plant nutrition, and thus are likely to be regulated by the plant, correlations between soil concentrations and B_v have been established in a manner similar to those for potassium, phosphorus, and nitrogen.

Available references for B_v , B_r , and (B_r/B_v) ratio numbered 16 for zinc,^{16,17,19,20,35,37,65,67,97,104,114-119} nine for manganese,^{16,17,19,36,37,65,104,112,113} eight for copper,^{16,17,19,20,65,104,114,115} five for nickel,^{16,20,102,104,114} iron,^{16,17,19,65,104} and cobalt,^{16,17,19,65,104} four for chromium,^{16,19,65,102} three for titanium,^{16,19,65} and two for vanadium.^{16,65} Correlations between soil concentrations and B_v were found for all but vanadium, titanium, and nickel. These correlations were often used in lieu of the geometric means approach to define default B_v values.

ORNL-DWG 81-11749

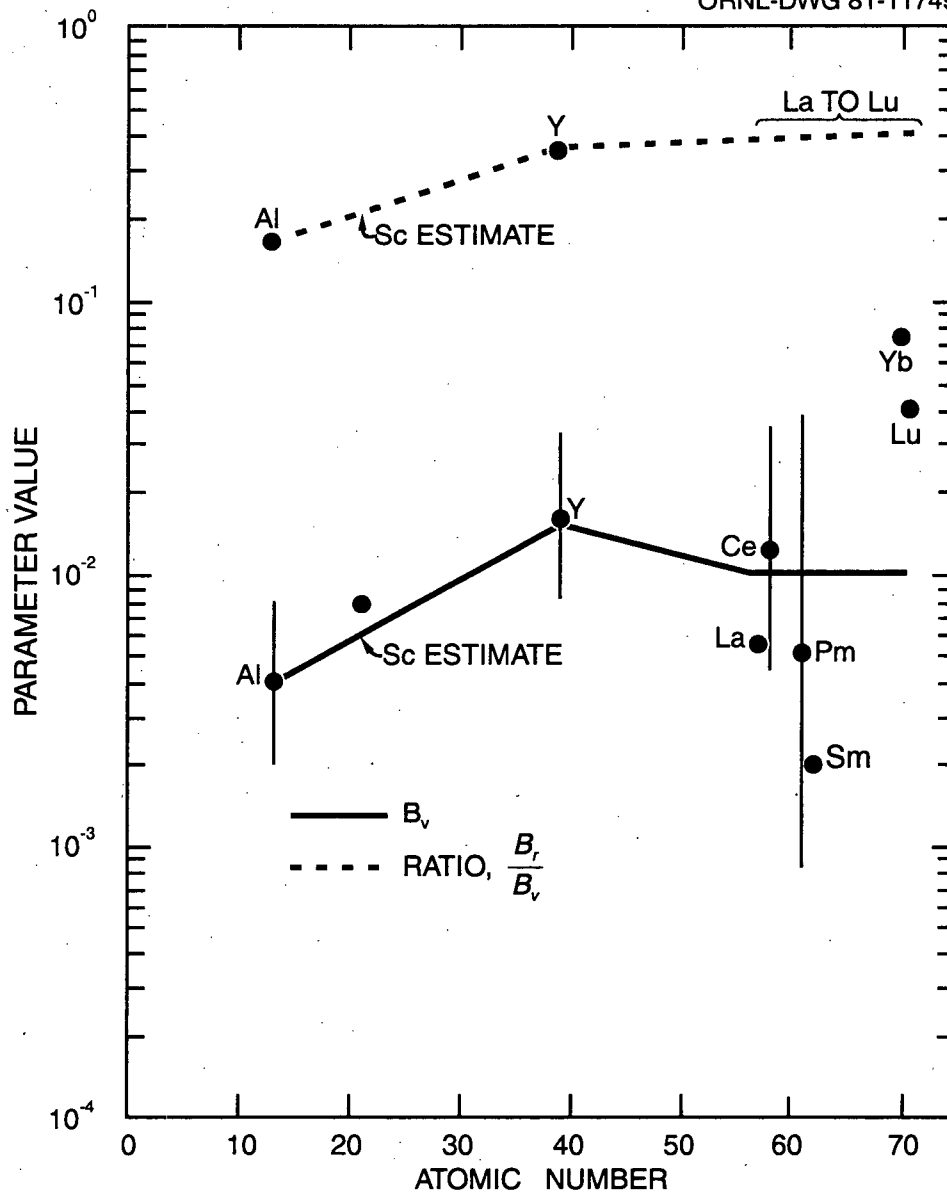


Figure 2.10. Assumed systematic trends in B_v and (B_r/B_v) ratio for aluminum, scandium, and yttrium. Solid dots and error bars represent geometric means and standard deviations of the mean determined from available references.

As before, predicted plant concentrations were compared with observed values in order to assure reasonable B_v and B_r estimates. These approaches were used in lieu of elemental systematics because subsequent analyses (see Sec. 2.1.7 and 2.1.8) depended heavily on the values obtained for these Period IV elements.

The B_v for titanium of 0.0055 is the geometric mean derived from references 16 and 65. The B_r value was generated from a (B_r/B_v) ratio derived from reference 19. Both soil-to-plant concentration factors predict plant concentrations from typical soil titanium concentrations which agree well with observed plant concentrations (Table 2.9).

The B_v for vanadium was also derived from references 16 and 65, and it is numerically equal to the B_v for titanium. No information was available on the (B_r/B_v) ratio for vanadium, and therefore, it was assumed equal to that for titanium, yielding a $B_r = 0.003$. Comparison of observed and predicted C_v and C_r for vanadium (Table 2.9) is also good.

References 16 and 65 yield a B_v by the geometric means method of 0.03 for chromium. However, a correlation between soil chromium concentration and chromium B_v was observed from the data in these two references (Fig. 2.11). Although this correlation is weak, the B_v determined by geometric means predicts C_v for chromium greater than the observed range. Therefore, the relationship in Fig. 2.11 was used to predict a chromium B_v of 0.0075 at a soil chromium concentration of 200 ppm.⁵² This value of B_v does predict a reasonable C_v , (Table 2.9).

A (B_r/B_v) ratio of 0.6 for chromium was determined from references 16, 19, and 102. This value generates a $B_r = 0.0045$, which predicts a C_r within the reported range of observed C_r values (Table 2.9).

The B_v for manganese generated by the geometric means method is 0.41. However, from data in references 16, 36, 37, 104, 112, and 113 a strong correlation between B_v and soil manganese concentration was observed (Fig. 2.12). At a typical soil manganese concentration of 850 ppm,⁵² the corresponding $B_v = 0.25$. This latter value was adopted for TERRA. Although this latter B_v value for manganese overpredicts C_v with respect to the reported observed range, the former value overpredicts C_v by an even larger factor.

The (B_r/B_v) ratio for manganese of 0.2 was determined from references 16, 17, and 19. This ratio generates a $B_r = 0.05$. Comparison of observed and predicted C_r using this B_r value (Table 2.9) indicates that the default B_r is reasonable.

Iron is an essential plant nutrient, and therefore, root uptake is probably regulated by the plant. It is not surprising that the relationship between soil iron concentration and B_v shown in Fig. 2.13 was found. At a typical soil iron concentration of 3.8%,⁵² the corresponding $B_v = 0.004$. The (B_r/B_v) ratio based on references 16, 17, and 19 = 0.25, yielding a B_r of 0.001. Comparison of observed and predicted C_v and C_r (Table 2.9) for iron indicates the reasonableness of the default B_v , and B_r .

The B_v for cobalt of 0.02 is based on the weak correlation between soil cobalt concentration and B_v (Fig. 2.14) and a typical soil cobalt concentration of 8 ppm.⁵² A (B_r/B_v) ratio of 0.35 was derived from references 16, 17, and 19. This ratio generates a $B_r = 0.007$. Predicted C_v and C_r using these default concentration factors for cobalt agree well with observed C_v and C_r ranges (Table 2.9).

The B_v for nickel is based on references 16 and 104. Unlike chromium, manganese, iron, and cobalt, no clear relationship between soil nickel concentration and B_v was indicated from the available data. Also, unlike the other Period IV transition elements no discrimination factor between vegetative and nonvegetative plant parts was found. In fact, the geometric mean of references 16, 20, 102, and 114 for (B_r/B_v) ratio was 1.2. Therefore, a (B_r/B_v) ratio of 1.0 was assumed and $B_v = B_r$ for nickel. Examination of Table 2.9 indicates that the observed C_r range includes the C_v range, supporting this assumption. Predicted C_v and C_r values agree well with reported observed ranges.

The B_v for copper is based on the strong correlation between soil copper concentration and B_v shown in Fig. 2.15 and an average soil copper concentration of 20 ppm.⁵² The (B_r/B_v) ratio, as

Table 2.9. Comparison of observed and predicted concentrations of Group IV transition elements in produce and plants (ppm, dry wt.)

Element	Average concentration in soil (C_s) ^a	Vegetative growth (C_v)		Fruits and tubers (C_f)	
		Observed range ^b	Predicted ^c	Observed range ^b	Predicted ^d
Ti	4,600	1.6 to 160	25	0.087 to 80	14
V	100	<0.091 to 21	0.55	4.60×10^{-4} to 47	0.30
Cr	200	0.18 to 2.9	1.5	0.030 to 8.0	0.90
Mn	850	1.9 to 16	210	8.0 to 80	43
Fe	38,000	6.5 to 410 ^e	150	10 to 160 ^e	38
Co	8.0	0.010 to 0.54	0.16	6.0×10^{-3} to 0.36	0.056
Ni	40	0.23 to 5.2 ^{b,f}	2.4	0.028 to 10	2.4
Cu	20	1.7 to 11	8.0	0.80 to 27	5.0
Zn	50	2.5 to 630	75	0.50 to 110	45

^aReference 52.

^bTaken or calculated from values in reference 53 assuming ash wt./dry wt. = .128 and .057 for vegetative growth and fruits and tubers, respectively

^cThe product, $B_v \times C_s$.

^dThe product, $B_f \times C_s$.

^eReference 14.

^fReference 54.

determined from references 16, 17, 19, 20, and 114, equals 0.63. This ratio yields a $B_v = 0.25$. Both soil-to-plant concentration factors yield reasonable predicted plant copper concentrations (Table 2.9).

The B_v for zinc was determined from the strong correlation between soil zinc concentration and B_v determined from references 16, 35, 37, 67, 97, 104, 114, 115, 117, and 119 (Fig. 2.16) and an average zinc soil concentration of 50 ppm.⁵² The (B_v/B_v) ratio of 0.6 was determined from references 16, 17, 19, 20, 67, 97, 114, and 116. Combining this ratio with the default B_v value generates a $B_v = 0.9$. Examination of Table 2.9 shows that predicted plant concentrations using these default concentration factors fall well within observed ranges.

Figures 2.17 and 2.18 show the default B_v and (B_v/B_v) ratios, respectively, for Period IV transition elements used in the TERRA computer code. The solid lines in the figures show the systematic trends in these parameters defined by the default estimates. The dots represent the parameter values as determined from the geometric means method. The error bars represent one geometric standard deviation. With the exception of chromium, all B_v default values fall within one standard deviation of the mean. For all elements except nickel, the (B_v/B_v) ratio is the geometric mean of the reference values.

2.1.7 Period V transition elements

The Period V transition elements contain the controversial and radiologically important element technetium and the toxic metal cadmium. Additionally, this period includes the element ruthenium which is also important radiologically. For concentration factors, cadmium,^{16,17,19,20,24,65,97,102,104,105,114,116,124-126} molybdenum,^{16,17,19,65,76,120,121} technetium^{23,107,122,123,127} and are the best documented, followed by ruthenium^{22,59,60,63} and zirconium.¹⁶ No references were found for niobium, rhodium, palladium, and silver.

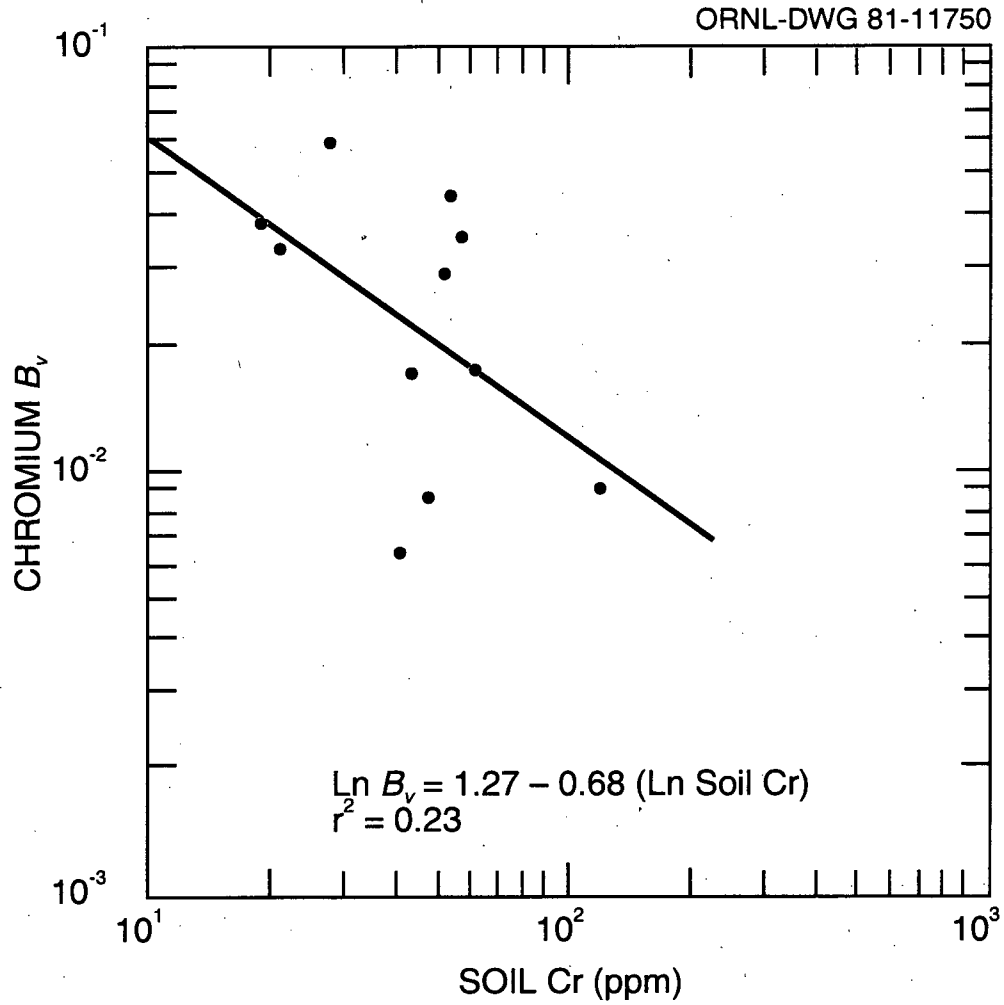


Figure 2.11. Correlation between soil chromium concentration and the soil-to-plant concentration factor, B_v , for chromium based on references 16 and 65.

ORNL-DWG 81-11753

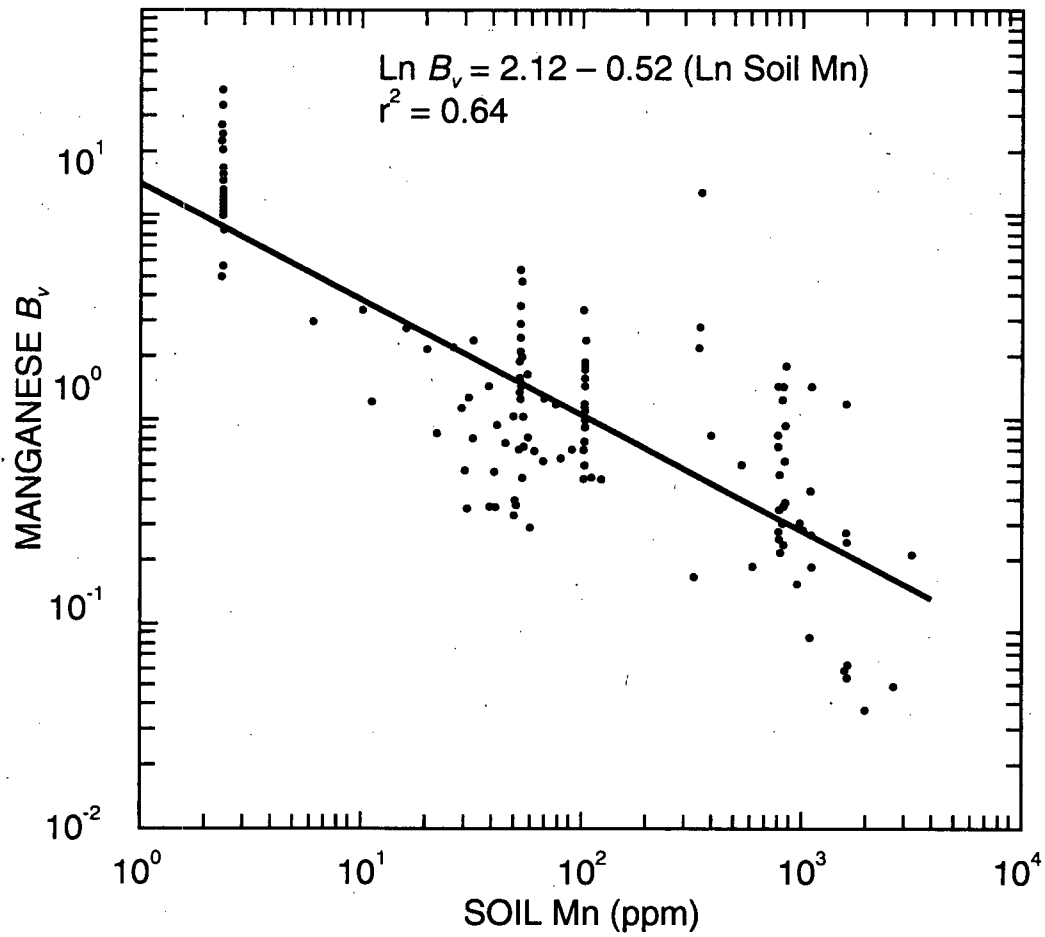


Figure 2.12. Correlation between soil manganese concentration and the soil-to-plant concentration factor, B_v , for manganese based on references 16, 36, 37, 104, 112, and 113.

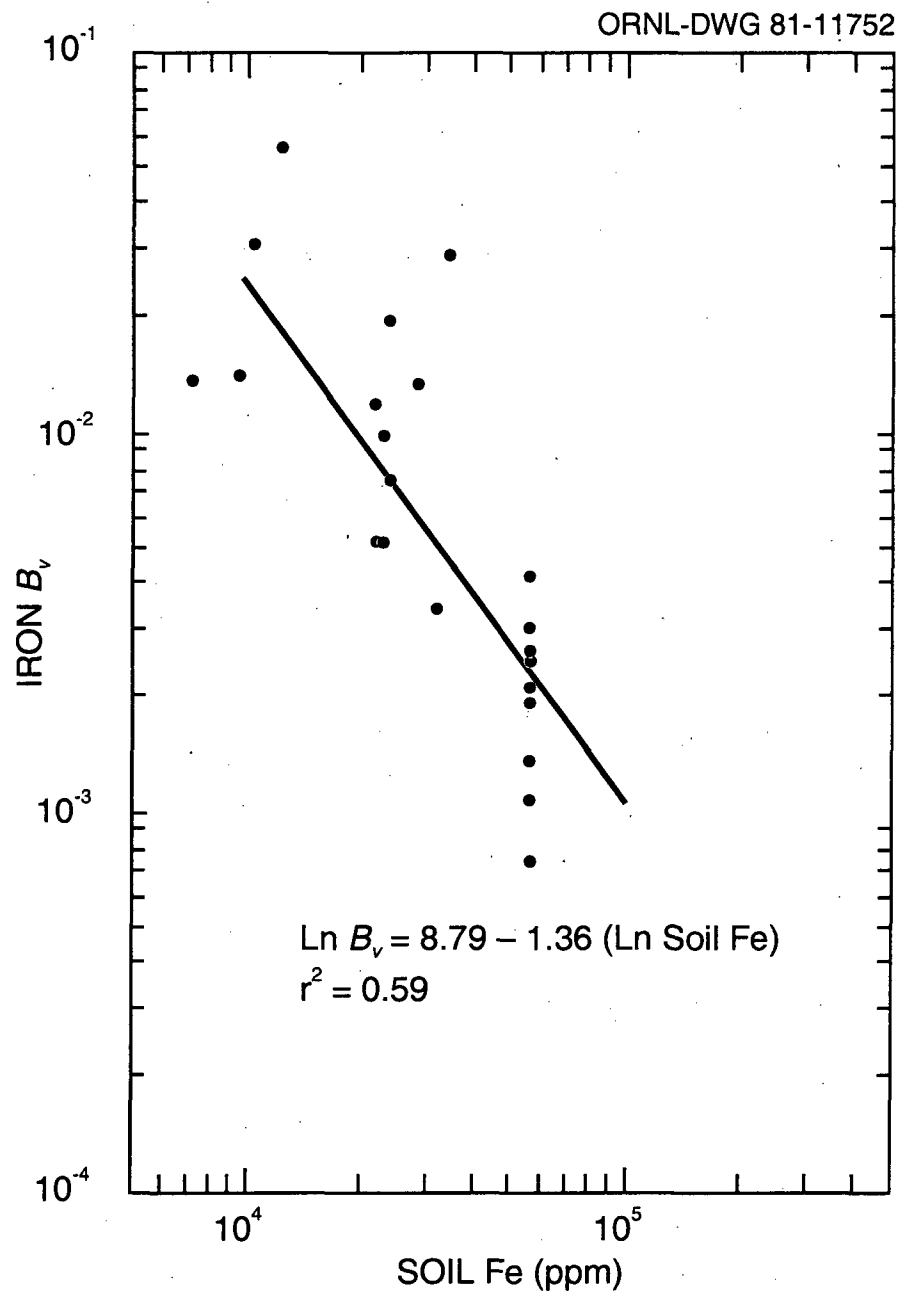


Figure 2.13. Correlation between soil iron concentration and the soil-to-plant concentration factor, B_v , for iron based on references 16, 65, and 104.

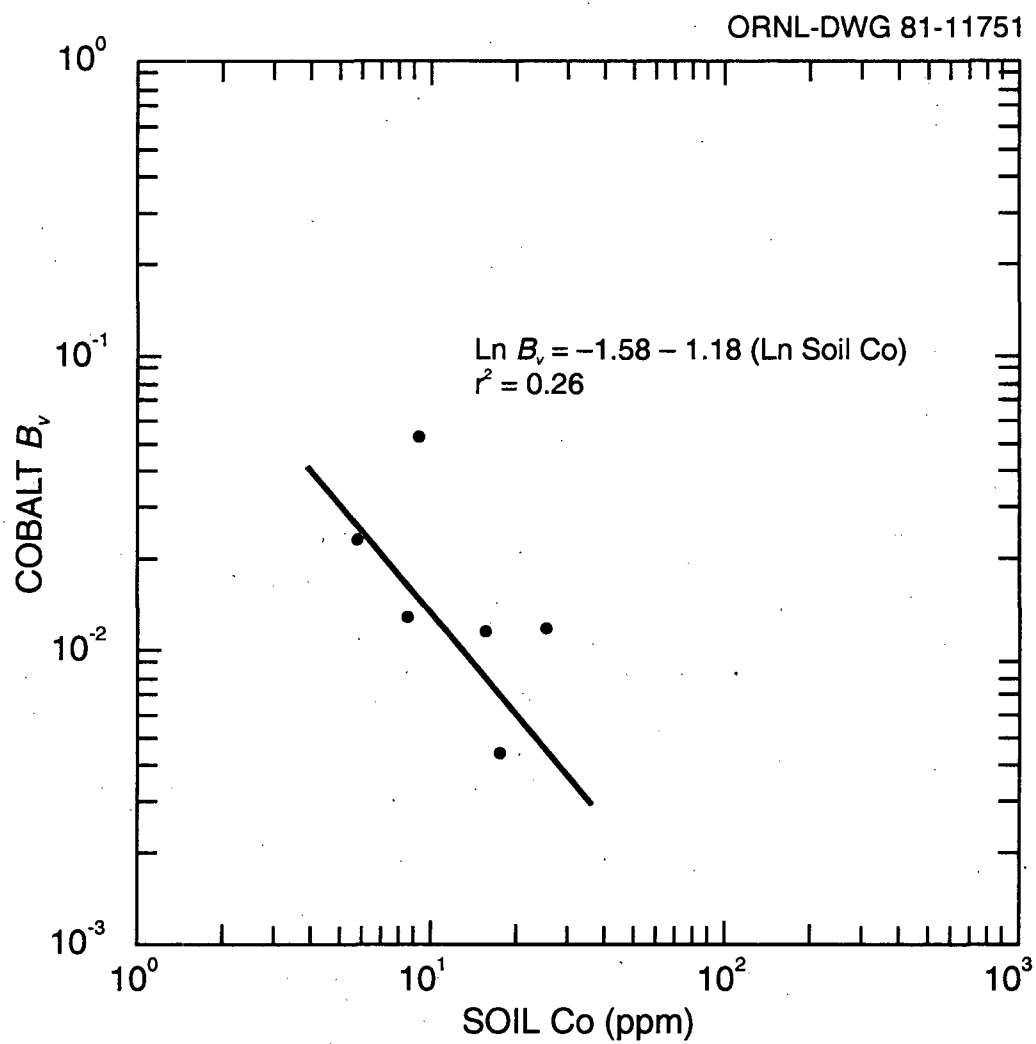


Figure 2.14. Correlation between soil cobalt concentration and the soil-to-plant concentration factor, B_v , for cobalt based on references 16 and 65.

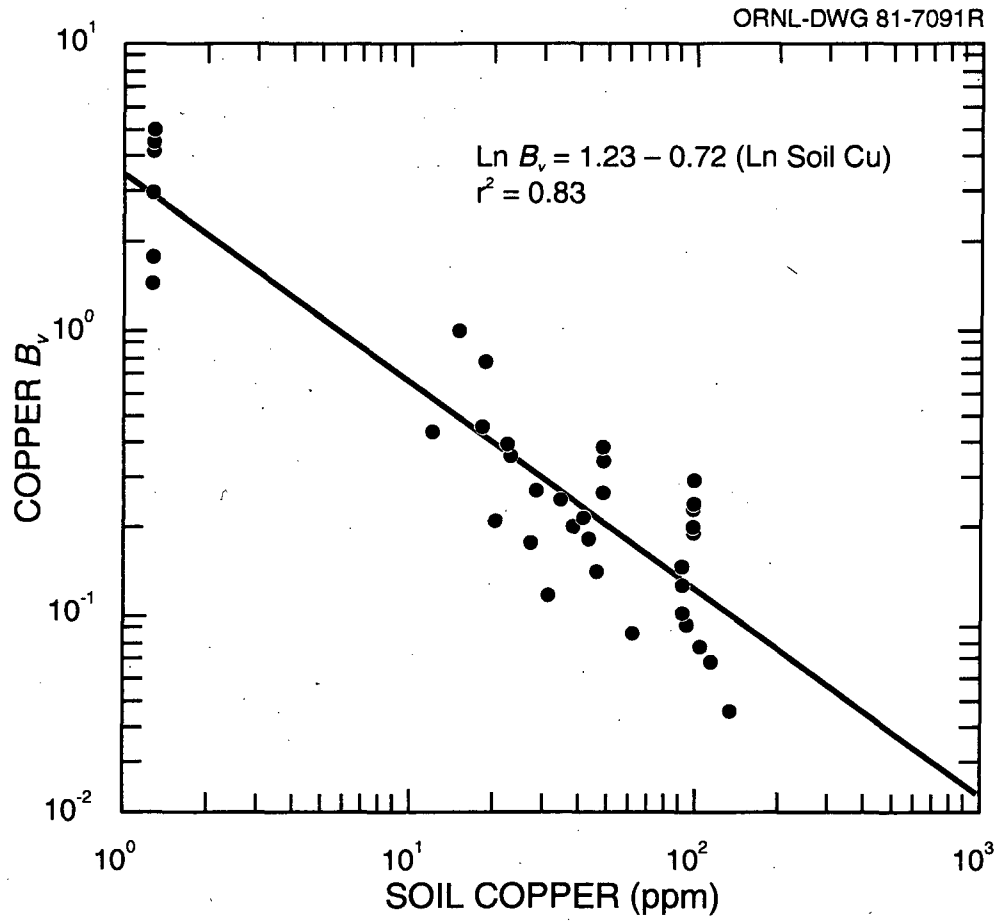


Figure 2.15. Correlation between soil copper concentration and the soil-to-plant concentration factor, B_v , for copper based on references 16, 104, and 115.

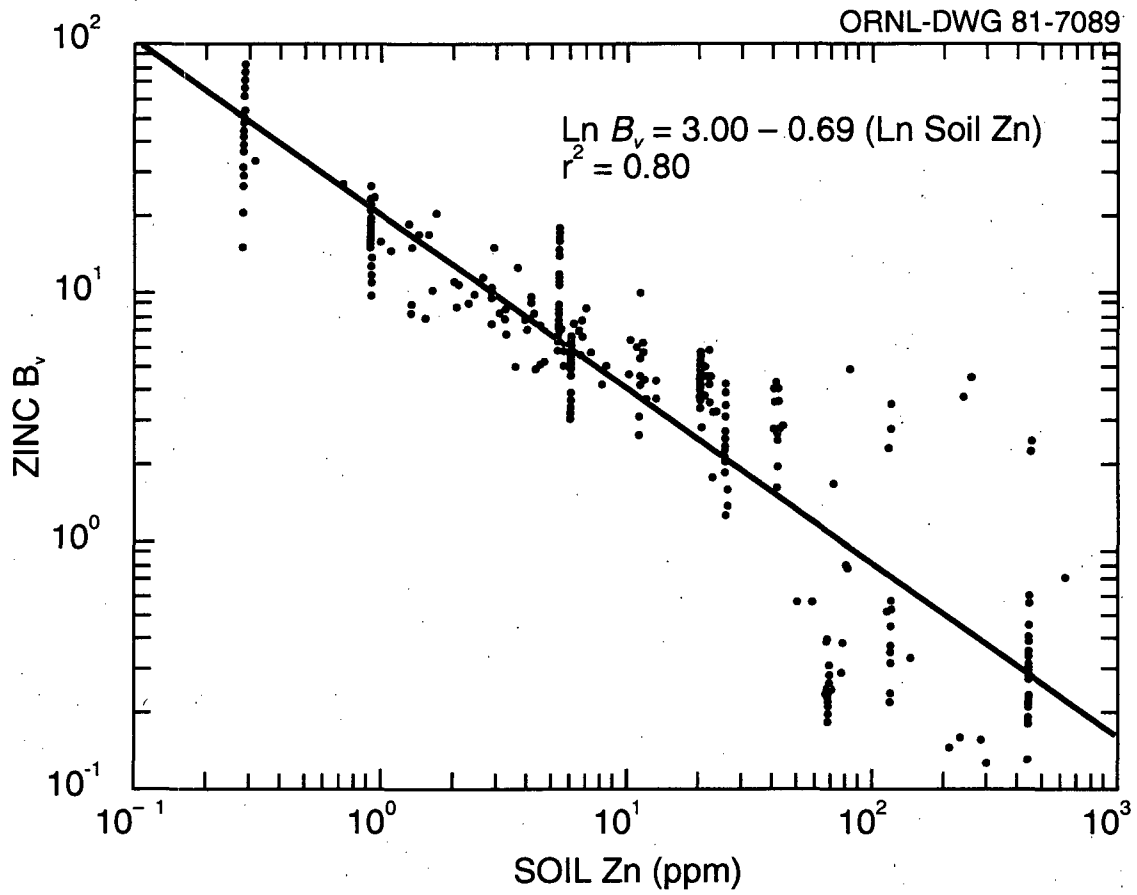


Figure 2.16. Correlation between soil zinc concentration and the soil-to-plant concentration factor, B_v , for zinc based on references 16, 35, 37, 67, 97, 104, 114, 115, and 119.

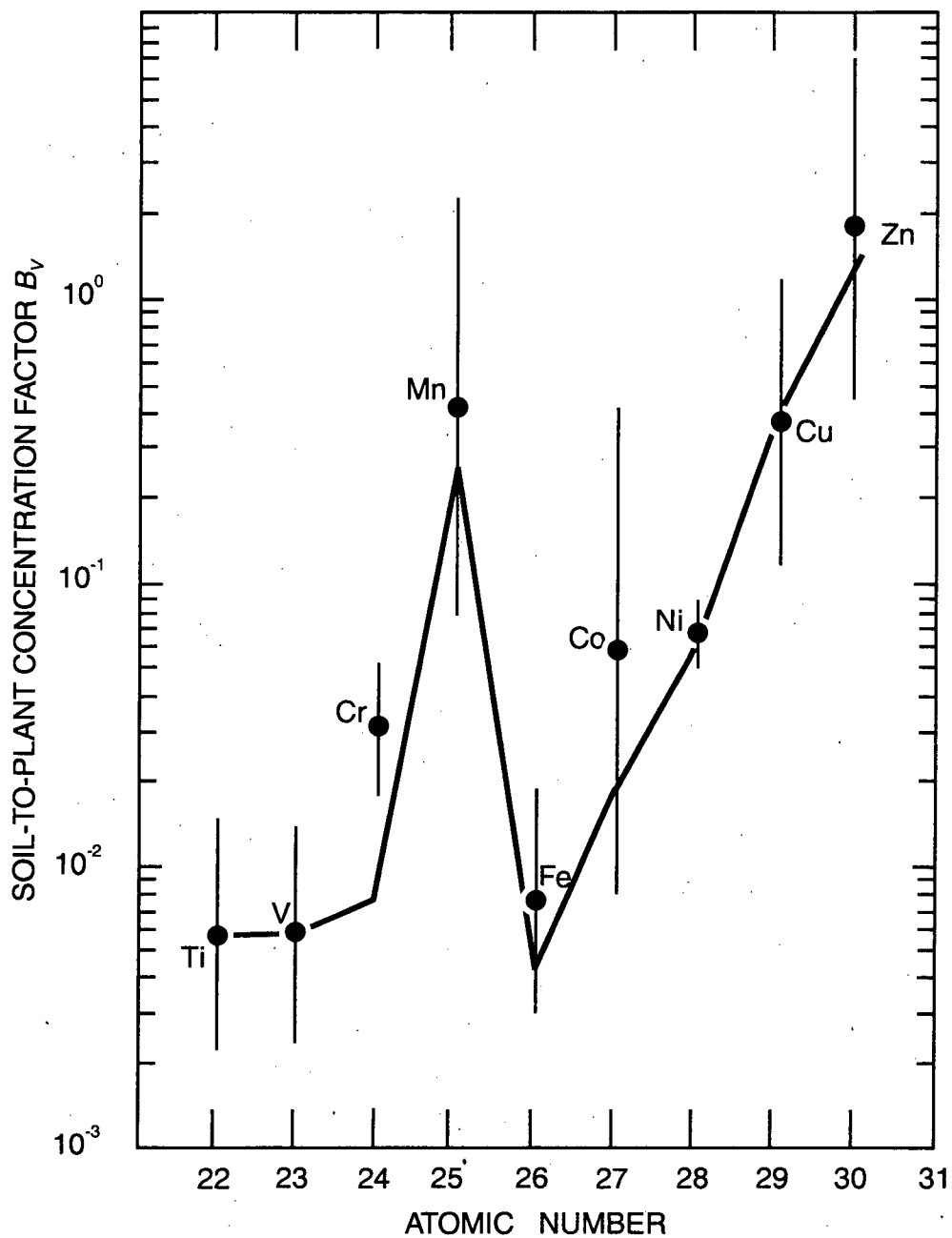


Figure 2.17. Assumed systematic trends in B_v for Period IV elements based on default B_v estimates. Solid dots and error bars represent geometric means and standard deviations determined from available references.

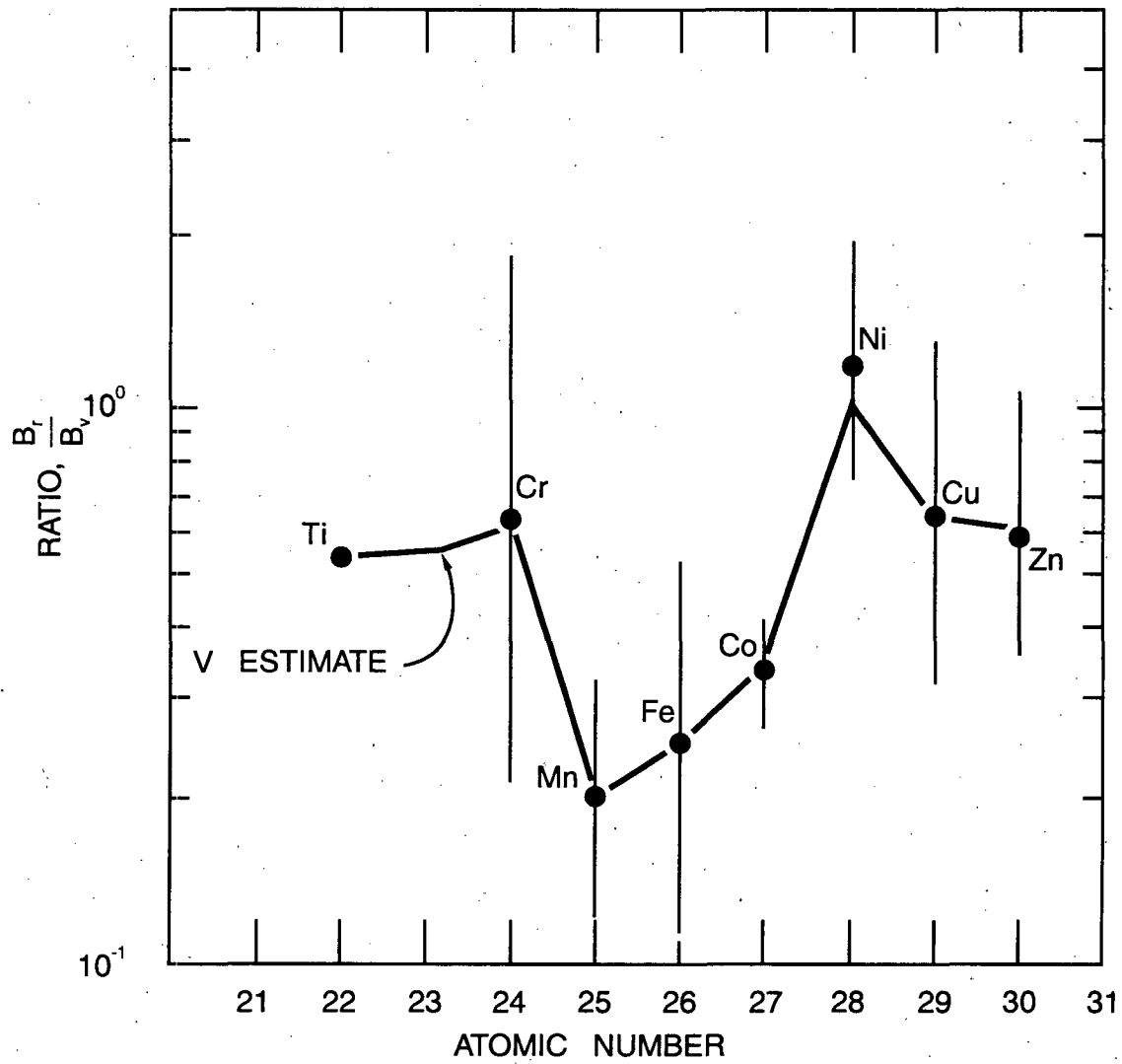


Figure 2.18. Assumed systematic trends in (B_r/B_v) ratio for Period IV elements. Solid dots and error bars represent geometric means and standard deviations of the mean determined from available references.

Because of its importance radiologically and because of the high concentration factors previously reported for technetium,^{23,107,122} it will be given special attention. Hoffman et al.¹²³ critiqued past studies of technetium uptake using the pertechnetate anion (TcO_4^-) and concluded that the concentration factors of 100-1000 derived from these studies were inappropriate because of the high levels of technetium added to the soils and the measurement of concentration factors before plant maturity. Evidence further suggests that technetium in soil becomes increasingly sorbed and thus is less available for plant uptake with time.^{23,128} Aging of soils over 100 days decreased observed concentration ratios by factors of 1.5 to 5.1 in one study by Cataldo.¹⁰⁷ Thus, the application of short-term pot studies to long-term assessments is clearly inappropriate for technetium. Therefore, the concentration factors representing field measurements of long-term technetium uptake in plants reported by Hoffman et al.¹²³ were adopted for the TERRA code, and references 23, 107, and 122 were used only for calculation of B_p or were excluded from our analyses.

The geometric mean of the B_p values reported by Hoffman et al.¹²³ is 9.5. The geometric mean for B_p derived from references 23 and 122 is 1.3. This value was rounded to 1.5 for use as a default value in TERRA. The (B_p/B_v) ratio generated by the two default values is 0.16 which compares favorably with the observed (B_p/B_v) ratios for molybdenum and ruthenium. It is interesting that a $B_{p/2}$ generated from B_p (see Sect. 2.1) is roughly an order of magnitude less than the value suggested in Moore et al.¹ which takes into account successive harvesting of food crops. No information is available on average technetium concentrations in typical soils and vegetation. Until such information becomes available the B_p and B_v for technetium remain suspect.

The B_p for molybdenum of 0.25 is based on references 16, 65, 76, and 120. Although Singh and Kumar¹²¹ reported soybean grain and leaf molybdenum concentrations from which a (B_p/B_v) ratio of 2.2 was derived, the (B_p/B_v) ratio for determination of B_p was derived from references 16, 17, and 19. This (B_p/B_v) ratio is 0.25 and yields a B_p estimate of 0.06. These B_p and B_v estimates predict vegetable and produce concentrations which agree well with observed concentrations (Table 2.10).

The B_p estimate of 0.002 for zirconium is based on the data on pumpkin leaves and vines by Baes & Katz.¹⁶ A value of 0.25 was chosen for the default (B_p/B_v) ratio for zirconium based on the above analysis for molybdenum. The resultant B_p estimate of 5.0×10^{-4} yields predicted plant concentrations which are consistent with observed concentrations (Table 2.10). Observed zirconium concentrations in vegetative growth in Table 2.10 are based on a range of values reported for cabbage. Shacklette et al.⁵³ report that zirconium is "infrequently detected in food plants." Thus, the "observed" plant concentrations in Table 2.10 for zirconium may not be entirely representative of actual produce concentration. Therefore, agreement of observed and predicted concentrations in Table 2.10 was not considered essential to acceptance or rejection of B_p and B_v values. Thus, although the predicted C_p is below the reported C_p for zirconium the default B_p for zirconium based on reference 16 is used as default in TERRA.

The B_p for ruthenium of 0.075 is based on references 22, 59, 60, and 63. The (B_p/B_v) ratio from references 22, 60, and 63 is 0.26, yielding a B_p estimate of 0.02. Unfortunately, no estimate of ruthenium in typical soils was available for comparison of observed and predicted plant concentrations.

The occurrence of cadmium in soils and plants has been well studied. The B_p for cadmium was determined from eleven references (16, 17, 24, 65, 97, 104, 105, 114, and 124-126). The geometric mean of the eleven geometric means is 0.55. A (B_p/B_v) ratio of 0.26 was derived from references 16, 19, 20, 24, 97, 102, 105, 114, 116, 125, and 126, yielding an estimate of $B_p = 0.15$. Agreement between observed and predicted cadmium concentrations in plants is excellent (Table 2.10).

Default values of B_p and B_v for niobium, rhodium, palladium, and silver were determined primarily through elemental systematic approaches, because no references on direct determination of B_p or B_v for these elements were available. The assumption that Period V transition elements

Table 2.10. Comparison of observed and predicted concentrations of Period V transition elements in produce and plants (ppm, dry wt.)

Element	Average concentration in soil (C_s) ^a	Vegetative growth (C_v)		Fruits and tubers (C_f)	
		Observed range ^b	Predicted ^c	Observed range ^b	Predicted ^d
Zr	300	53 to 74	0.60	5.0×10^{-3} to 11	0.15
Nb		0.038		0.017	
Mo	2.0	0.35 to 2.9	0.50	0.060 to 13	0.12
Tc					
Ru				1.0×10^{-4} to 4.0×10^{-3}	
Rh					
Pd					
Ag	0.10	0.13	0.040	0.057	0.010
Cd	0.50	0.13 to 2.4	0.28	0.013 to 0.82	0.075

^aReference 52.

^bTaken or calculated from values in reference 53 assuming ash wt./dry wt. = .128 and .057 for vegetative growth and fruits and tubers, respectively

^cThe product, $B_v \times C_s$.

^dThe product, $B_f \times C_s$.

are natural analogs of Period IV transition elements suggested that the ratio of B_v estimates for these periods might vary systematically from Group IVB to Group IIB. Examination of these ratios for which B_v estimates had been made via other approaches (Fig. 2.19) yielded estimates of B_v ratio for Nb/V by linear extrapolation between the Zr/Ti ratio and the Mo/Cr ratio. Likewise the Rh/Co, Pd/Ni, and Ag/Cu ratios were extrapolated from the Ru/Fe and Cd/Zn ratios. These estimated ratios, when multiplied by default B_v estimates for Period IV elements (Sect. 2.1.6), yielded B_v estimates for the Period V elements niobium, rhodium, cobalt, palladium, and silver. Plotting of the resultant Period V transition element B_v estimates by atomic number (Fig. 2.20) yields results somewhat similar to the same plot for Period IV transition elements (Fig. 2.17). Unfortunately, comparison of observed and predicted C_v and C_f for niobium, rhodium, and palladium is not possible until more information is available. Some comparison for silver is possible (Table 2.10), although typical silver concentrations in plants are only approximates. The systematics approach seems to underpredict B_v for silver, but by less than an order of magnitude. The default B_v estimates for niobium, rhodium, palladium, and silver used in Fig. 2.2 were derived from an assumed (B_v/B_s) value of 0.25, which is consistent with observations for molybdenum and cadmium.

2.1.8 Period VI transition elements

Very few references for plant uptake of the Period VI transition elements were available. Also, comparisons between observed and predicted produce and plant concentrations were difficult to make because of the uncertainty in typical soil and plant concentrations (Table 2.11). Therefore, B_v and B_f default estimates for Period VI transition elements are mostly based on their Period IV and V analogs.

Single measurements of associated soil and plant concentrations applicable to B_v were found in reference 65 for hafnium, tantalum, and tungsten. Three additional measurements were found in reference 101 for tungsten. The geometric means approach for tungsten indicates a B_v which is

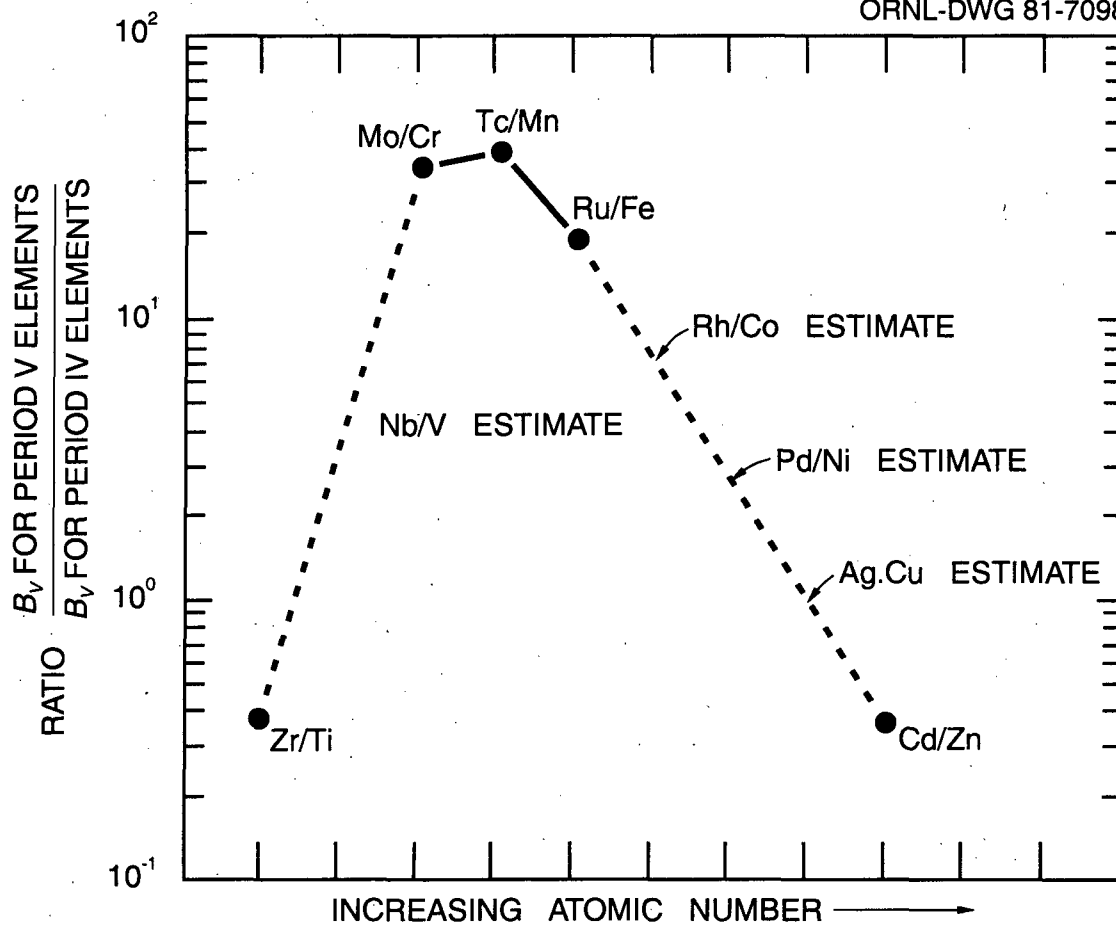


Figure 2.19. Assumed systematic trends in the ratio of B_V for Period V and IV elements (Nb/V, Rh/Co, Pd/Ni, and Ag/Cu) based on the ratios of default B_V estimates for other elements in the periods.

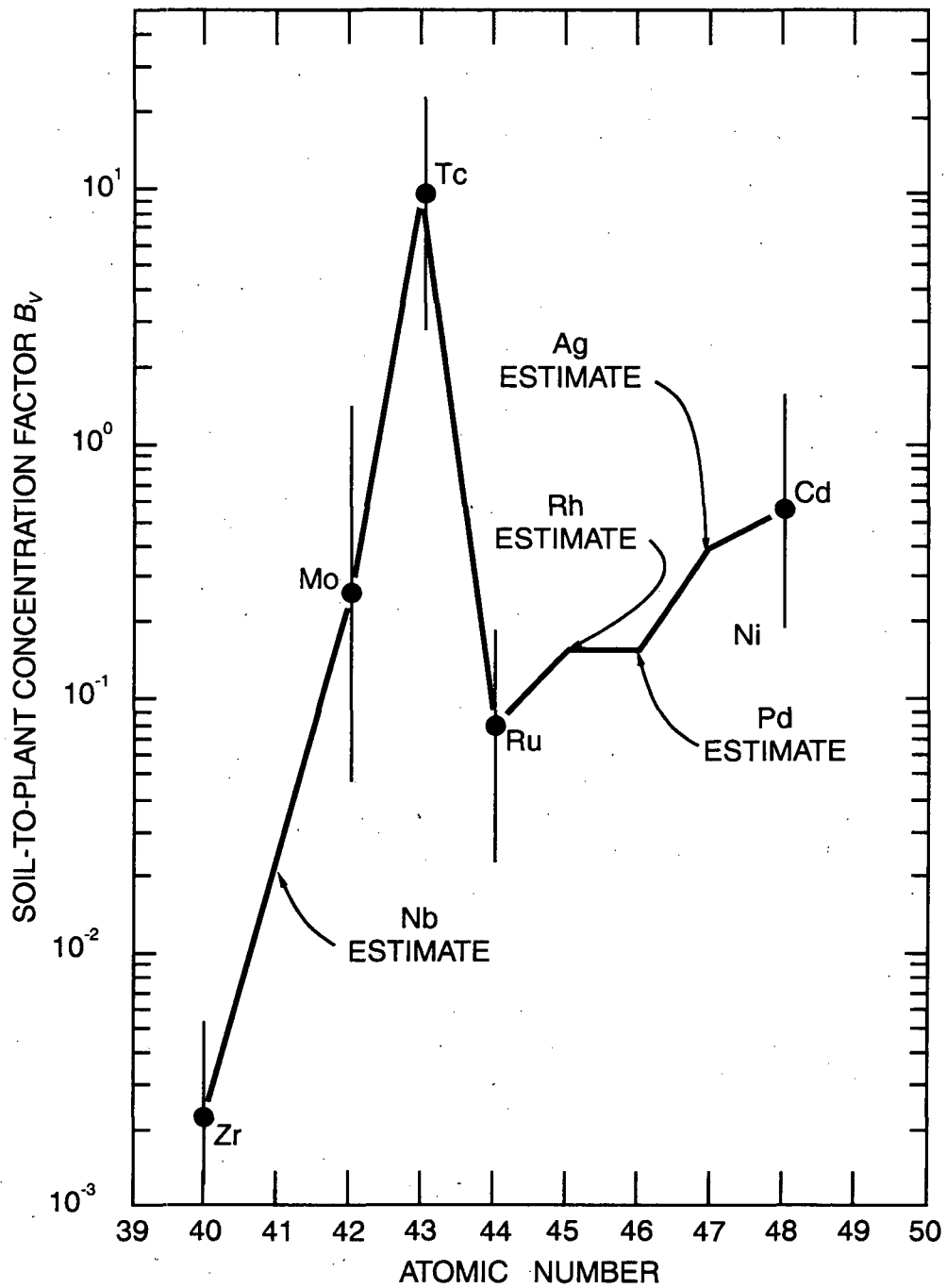


Figure 2.20. Assumed systematic trend in B_v for Period V transition elements based on default B_v estimates. Solid dots and error bars represent geometric means and standard deviations determined from available references.

Table 2.11. Comparison of observed and predicted concentrations of Period VI transition elements in produce and plants (ppm, dry wt.)

Element	Average concentration in soil (C_s) ^a	Vegetative growth (C_v)		Fruits and tubers (C_f)	
		Observed range ^b	Predicted ^c	Observed range ^b	Predicted ^d
Hf	6.0	<6.3×10 ^{-3e}	0.021	2.3×10 ⁻³ to 2.0 ^e	5.1×10 ⁻³
Ta					
W		0.064		0.029	
Re		6.4×10 ⁻⁴		2.9×10 ⁻⁴	
Os					
Ir					
Pt					
Au		<1.1×10 ⁻⁴ to 5.3×10 ^{-3e}		1.0×10 ⁻⁵ to 1.1×10 ^{-3e}	
Hg	0.010	<0.01 to 0.020	9.0×10 ⁻³	<0.010 to 0.020	2.0×10 ⁻³

^aReference 52.

^bTaken or calculated from values in reference 53 assuming ash wt./dry wt. = .128 and .057 for vegetative growth and fruits and tubers, respectively

^cThe product, $B_v \times C_s$.

^dThe product, $B_f \times C_s$.

^eReference 54.

much greater than that for chromium and more nearly equal to that for molybdenum, although in reference 65 the derived molybdenum B_v exceeds the derived tungsten B_v by a factor of approximately three. Comparison of B_v values derived from reference 65 for hafnium and tantalum with their respective Period IV and V analogs indicates that if the single derived values are appropriate, the Period VI transition element concentration factors exceed those for their Period IV analogs, but are less than their Period V analogs.

While the above observations lend insight into the concentration factors for some Period VI transition elements, concentration factors for the rest must rely on supposition until further experimental evidence is available. Figure 2.21 represents the methodology used in determination of default B_v estimates for Period VI transition elements. To derive these, B_v default estimates for Period IV transition elements (Sect. 2.1.6) and Period V transition elements (Sect. 2.1.7) were plotted by increasing atomic number. The default B_v estimate for the Period VI elements were simply the log-averages of the two other elements within each group rounded to the nearest 0.5 decimal place. This method insures that trends observed in Periods IV and V are generally repeated in Period VI (increasing B_v for the first four members of the period, decrease in the fifth, etc.). While such repetition of trends may be acceptable if general chemical properties are assumed to be an important basis for B_v behavior, our method has serious limitations. Our procedure implies that, except for Groups IVB and IIB, Period VI element B_v values exceed those for Period IV and are exceeded by those for Period V. Such an implication is unfounded and may be a serious limitation to our approach. However, determination of the most appropriate default estimates of B_v for Period VI transition elements will require direct experimental measurement of them.

There were no available references for the (B_v/B_s) ratio or for B_v for the Period VI elements. Therefore, a value of 0.25 for the (B_v/B_s) ratio was assumed, based on analysis of Period V transition elements. This value was used with the default B_v estimates to generate default B_s estimates.

ORNL-DWG 81-7097R

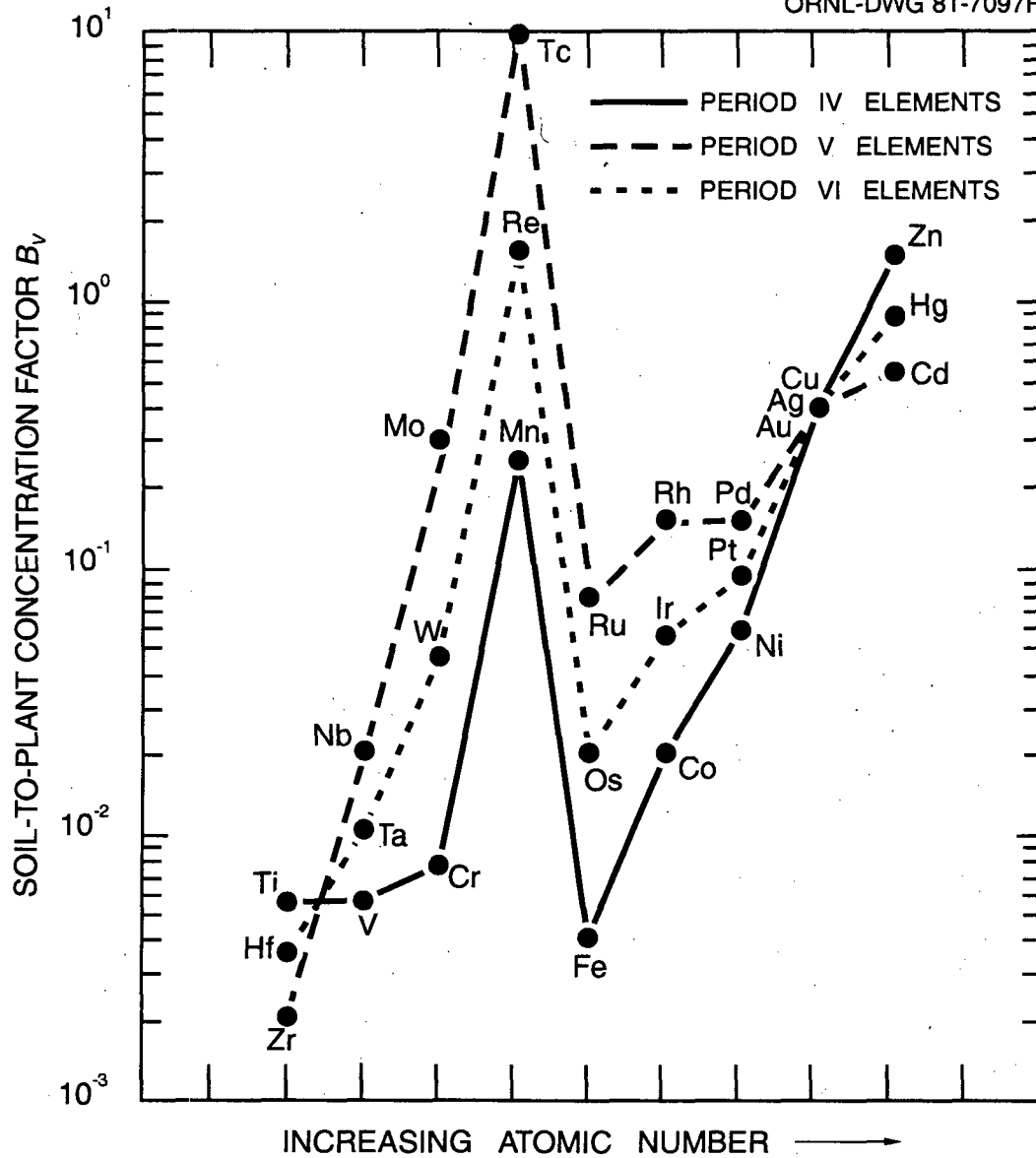


Figure 2.21. Assumed systematic trend in B_v for Period VI elements based on assumed systematic trends in Period IV and V elements.

Comparisons of observed and predicted plant concentrations were possible only for hafnium and mercury. For these elements predicted values were always within an order of magnitude of the observed ranges. However, observed ranges were usually bounded on the low sides by detection limits of the analysis procedures.⁵⁴

2.1.9 The actinide elements

The actinide elements have been extensively studied with respect to plant uptake from soil. The greatest number of references were found for plutonium^{8-10,30,59,101,129-138} and americium,^{10,30,129,131,133,136,137,139-142} with fewer references for uranium,^{29,65,90,91,143} thorium,^{65,90,91} neptunium, and curium.^{10,30,131} No literature references were found for actinium, protactinium, or any elements of atomic number greater than 96.

The B_v for plutonium appears to be lognormally distributed and reported values range from 10^{-6} to 10^{-2} (Fig. 2.22). The fourteen references used to determine B_v for plutonium yielded a geometric mean of 4.5×10^{-4} . The (B_p/B_v) ratio of 0.1 was calculated from references 8, 10, 30, 129, 130, 134, and 136. This value produces a $B_p = 4.5 \times 10^{-5}$ which agrees well with the geometric mean of B_p derived from references 8, 10, 30, 129, 133, 134, 136, and 138. No measurements of typical or average concentrations of plutonium in soils or vegetable produce were available for comparison between predicted and observed concentrations. Comparisons of predicted and observed actinide concentrations were only possible for thorium and uranium (Table 2.12).

The B_v for americium of 0.0055 was derived from references 10, 30, 129, 131, 136, 137, and 139-142. A B_p of 2.5×10^{-4} was derived from references 10, 30, 129, and 136 by selecting a value midway between the range defined by the geometric mean of B_p and the product of the default B_v estimate and the geometric mean for (B_p/B_v) ratio.

The B_v for uranium of 0.0085 was determined from references 29, 65, and 91. The (B_p/B_v) ratios derived from data reported by Prister²⁹ and Fedorov and Romanov¹⁴³ both equaled a value of 0.5, and this value was used to determine a default B_p estimate of 0.004. Comparison of predicted and observed vegetable concentrations supports the default concentration factors, although typical uranium concentrations in vegetative portions of produce are unavailable.

The B_v for thorium of 8.5×10^{-4} was determined from references 65 and 91. No references were available for a thorium (B_p/B_v) ratio, and thus the value of 0.1 used for radium was assumed, yielding a default B_p estimate of 8.5×10^{-5} . Comparisons of observed and predicted vegetation concentrations are hampered by the uncertainty in thorium concentrations in vegetation. In the food surveys carried out by Oakes et al.⁵⁴ and Monford et al.¹⁴⁴ most thorium concentrations in food items were at or below detection limits. However, it may be concluded that the default B_v and B_p estimates assumed here do not overpredict observed food concentrations.

The default B_v estimates for actinium and protactinium were determined from those of radium and thorium and thorium and uranium, respectively, by assuming systematic variation in B_v with atomic number in a manner similar to that used for radium and francium (see Sect. 2.1.2). Such a procedure implies that thorium has the lowest B_v of the actinides of atomic number 89 through 92. This implication has yet to be tested, but examination of our default estimates of the ingestion-to-cow's milk (F_m) transfer coefficient shows that it is less than or equal to those for actinium, protactinium, and uranium (see Sect. 2.2 for the milk transfer coefficient). The B_p for actinium and protactinium was determined by assumption of a (B_p/B_v) ratio of 0.1 as for radium and thorium.

The B_v for neptunium of 0.1 is based on references 10, 30, and 131. The B_p default estimate of 0.01 is based on the geometric means of B_p values from references 10 and 30. This value suggests that a (B_p/B_v) ratio of 0.1 is appropriate for neptunium also.

The B_v for curium of 8.5×10^{-4} is based on references 10, 30, and 141. The B_p estimate of 1.5×10^{-3} is based on the geometric means of B_p from references 10 and 30, suggesting an appropriate (B_p/B_v) ratio of less than 0.1. In the TERRA code B_v and B_p estimates for elements of atomic number greater than 96 are set equal to those for curium (element 96).

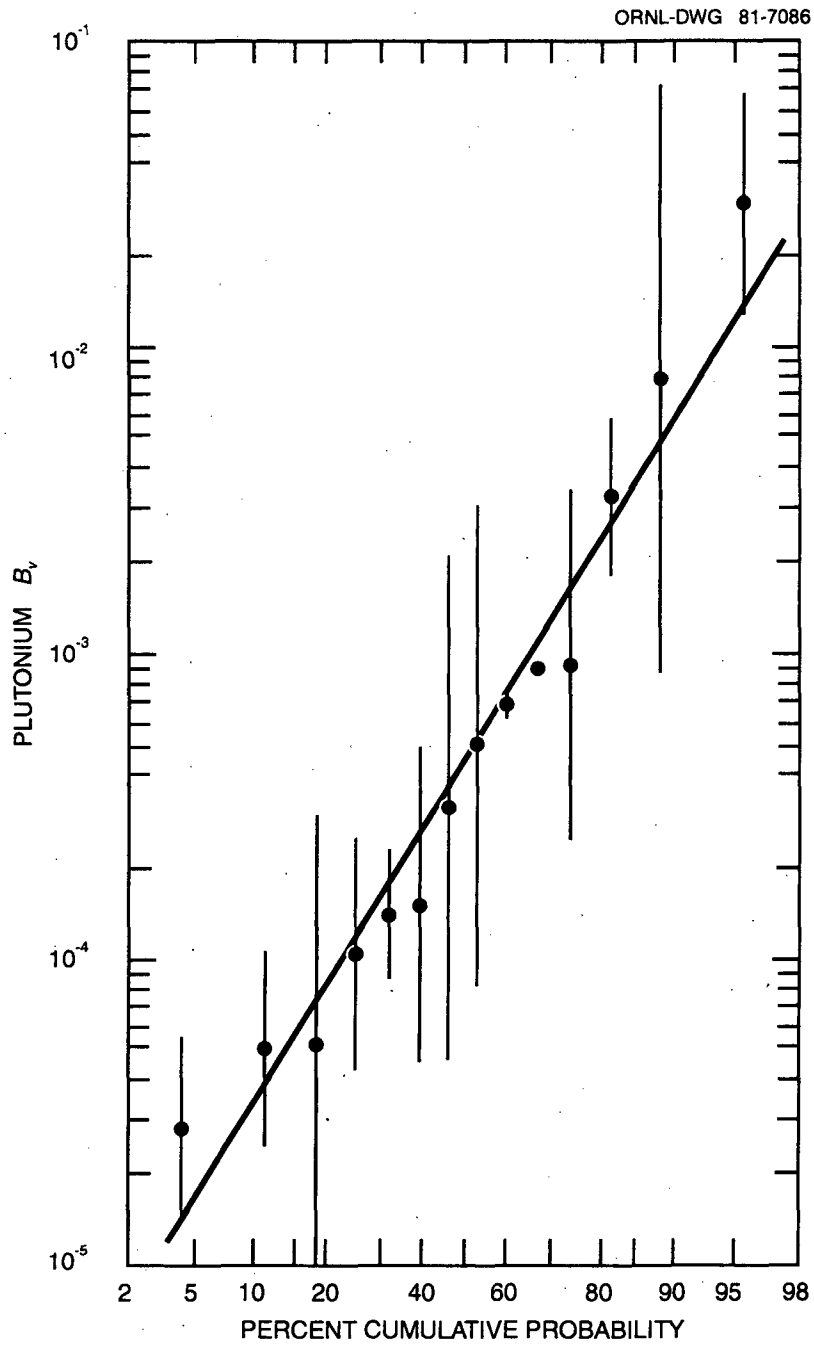


Figure 2.22. Lognormal probability plot of geometric means of B_v for plutonium (calculated from references 8-10, 30, 59, 101, 129, 131, 132, and 134-138), including one geometric standard deviation of the mean.

Table 2.12. Comparison of observed and predicted concentrations of actinide elements in produce and plants (ppm, dry wt.)

Element	Average concentration in soil (C_s) ^a	Vegetative growth (C_v)		Fruits and tubers (C_f)	
		Observed range ^b	Predicted ^c	Observed range ^b	Predicted ^d
Actinide elements					
Ac					
Th	6.0	<0.032	5.1×10^{-3}	$<2.5 \times 10^{-3}$ to 0.12	5.1×10^{-4}
Pa					
U	1.0		8.5×10^{-3}	3.8×10^{-4} to 0.020	4.0×10^{-3}
Np					
Pu					
Am					
Cm					

^aReference 52.

^bTaken or calculated from values reported in reference 144.

^cThe product, $B_v \times C_s$.

^dThe product, $B_f \times C_s$.

2.1.10 Comparison of default estimates with previously published values

Comparisons of our default estimates of B_v and B_f with previously used or reported values is difficult because the parameter definitions used here differ somewhat from past soil-plant uptake parameter definitions. However, general comparisons may be made. The most useful comparison is with the soil-to-plant uptake parameter B_{iv} in Table E-1 of the NRC Reg. Guide 1.109.⁶ Most of these values of B_{iv} were, in turn, taken from reference 15 by dividing the "concentration in terrestrial plants" (Table 10A) by the "elemental composition of typical agricultural soil" (Table 4). In reference 15 the plant concentrations were converted to a wet or fresh weight basis by assuming 25% dry matter in plants. Thus, the B_{iv} values generated from Tables 10A and 4 may be converted to a dry weight basis by multiplying by a factor of four. The resultant dry weight B_{iv} values may be directly compared with our B_v estimates (Fig. 2.23).

In comparing plant uptake parameters it should be remembered that the criteria for B_v and B_{iv} definition are comparable, but not equivalent. Also, as evidenced by figures 2.3, 2.7, and 2.22, each default estimate is representative of a distribution of values. Thus, a factor of 2 or 3 difference between B_v and B_{iv} should not be considered significant. Therefore, in Fig. 2.23 we have highlighted those elements for which an order of magnitude difference or greater occurs between our numbers and those in reference 15. These elements include fluorine, silicon, calcium, titanium, selenium, strontium, rhodium, palladium, indium, tellurium, osmium, iridium, platinum, gold, thallium, bismuth, polonium, radium, thorium, neptunium, and curium. Our approaches to determination of B_v estimates have led to lower estimates than those derived from reference 15 for more than half of these elements. For elements calcium, strontium, and neptunium, numerous experimental results indicate higher default values than those derived from reference 15.

2.2 Ingestion-to-Milk Parameter, F_m

The ingestion-to-milk transfer coefficients for milk cows used in TERRA are representative of the fraction of the daily elemental intake in feed which is transferred to a kilogram of milk. The

	I A	II A		III B	IV B	V B	VI B	VII B	VIII	IB	II B	III A	IV A	V A	VIA	VII A	
II	Li +8	Be +6										B +5		N		F +100	
III	Na -3	Mg										Al +5	Si +600	P	S	Cl +4	
IV	K	Ca +100	Sc	Ti +25	V	Cr +7.5	Mn	Fe	Co	Ni	Cu	Zn	Ga +4	Ge	As	Se -200	Br -2
V	Rb -3.5	Sr +38	Y	Zr +3	Nb	Mo -2	Tc +9.5	Ru -3	Rh -350	Pd -133	Ag	Cd -2	In -250	Sn +3	Sb +5	Te -200	I +2
VI	Cs +2	Ba +7.5		Hf +5	Ta +4	W	Re	Os -13	Ir -950	Pt -21	Au +40	Hg	Tl -250	Pb -6	Bi -17	Po -1600	At
VII	Fr	Ra +12															

Lanthanides	La	Ce	Pr	Nd	Pm	Sm	Eu	Gd	Tb	Dy	Ho	Er	Tm	Yb	Lu
Actinides	Ac -3	Th -20	Pa -4	U	Np +10	Pu -2	Am +5.5	Cm -12							

Figure 2.23. Comparison of soil-to-plant concentration factor default values reported in this report and derived from reference 15. The "+" and "-" signs indicate whether our estimates are greater or less than, respectively, those derived from reference 15. The values indicated are the difference factor, and circled elements indicate a difference factor of at least an order of magnitude.

elemental values for this parameter (Fig. 2.24) were taken from the extensive review in 1977 by Ng et al.,¹⁴⁵ except for the elements chromium, manganese, iron, nickel, zirconium, antimony, mercury, polonium, and americium which were taken from a later (1979) reference.⁴⁰ The protocol for rounding adopted for B_v and B_f was used also for F_m . The error introduced in defining the parameter in days/kilogram (here) rather than days/liter (as by Ng and his associates) is much less than that introduced by the rounding protocol, because the density of milk ranges from 1.028 to 1.035 kg/L.¹⁴⁶

2.3 Ingestion-to-Beef Parameter, F_f

The ingestion-to-beef parameters in TERRA are representative of the fraction of the daily elemental intake in feed which is transferred to and remains in a kilogram of beef until slaughter. The elemental values for this parameter (Fig. 2.25) were either taken from several reviews published by Ng and his coworkers^{15,39,40} or determined from elemental systematic assumptions. Estimates of F_f for 32 elements were available from the more recent reviews (references 39 and 40). Values for sodium, phosphorus, potassium, calcium, manganese, iron, zinc, strontium, niobium, antimony, and cerium were taken from reference 40, and values for chromium, cobalt, nickel, copper, rubidium, yttrium, zirconium, molybdenum, technetium, ruthenium, rhodium, silver, tellurium, iodine, cesium, barium, lanthanum, praseodymium, neodymium, tungsten, and americium were taken from reference 39. The F_f estimates for the remaining elements were derived from reference 15, except for those which exceeded a theoretical maximum value of 1.0 day/kg.

A theoretical maximum F_f value may be calculated by assuming a 1 unit/kg (wet) concentration of an element in feed. If an extremely conservative 100% efficiency in transfer from feed to muscle is assumed, and beef cattle consume 50 kg (wet) feed per day,¹⁵ and the average muscle mass per head of beef cattle is 200 kg,¹³ then the average daily increase in elemental concentration in beef muscle is given by

$$\frac{(1 \text{ unit / kg})(50 \text{ kg / head / day})}{200 \text{ kg beef / head}} = 0.25 \text{ unit / kg beef / day.} \quad (6)$$

Further, if a second extremely conservative assumption that there is no biological turnover of the element from the muscle is made, then assuming that the average beef cow is fed for 200 days before slaughter¹³ gives a value of 50 units/kg beef at slaughter. Relating this value to the daily consumption of feed yields a conservative maximum F_f of (50 units/kg)/(50 units/day) or 1.0 days/kg. Clearly, default estimates near or exceeding this value are highly suspect.

Review of the F_f values derived from reference 15 indicates that estimates for gallium, germanium, tantalum, polonium, astatine, francium, actinium, thorium, protactinium, neptunium, plutonium, and curium all exceed the above-calculated theoretical maximum. Because of the radiological importance of elements of atomic number greater than 82, a systematic approach based on elemental variation of B_v and F_m was used to determine default F_f estimates (Fig. 2.26). A similar approach using systematic trends observed in F_m for Period IV elements was used to determine F_f estimates for gallium and germanium.

The approach used for elements of atomic number greater than 82 was to observe ratios of default B_v (Fig. 2.1) and F_m (Fig. 2.24) values for successive elements (Fig. 2.26). The ratios determined for both parameters were log-transformed and averaged. The exponentials of these averages were used to define a default ratio value for successive F_f default estimates. The F_f value for americium was then used to determine the default F_f estimates for curium and plutonium. In turn, each default F_f estimate was calculated by multiplication with the proper ratio, i.e., $\text{Pu } F_f = (\text{Pu}/\text{Am})$ ratio \times (Am F_f), $\text{Np } F_f = (\text{Np}/\text{Pu})$ ratio \times (Pu F_f), and so on. Implicit in such an argument is the assumption that the availability of an element for plant uptake and transportability to milk is indicative of its availability or transportability to beef. Some support for this argument is

	IA	IIA										IIIA	IVA	VA	VIA	VIIA	
II	Li 0.020	Be 9.0×10^{-7}										B 1.5×10^{-3}		N 0.025		F 1.0×10^{-3}	
III	Na 0.035	Mg 4.0×10^{-3}	IIIB	IVB	VB	VIB	VII B	VIII			IB	II B	Al 2.0×10^{-4}	Si 2.0×10^{-5}	P 0.015	S 0.015	Cl 0.015
IV	K 7.0×10^{-3}	Ca 0.010	Sc 5.0×10^{-6}	Ti 0.010	V 2.0×10^{-5}	Cr 1.5×10^{-3}	Mn 3.5×10^{-4}	Fe 2.5×10^{-4}	Co 2.0×10^{-3}	Ni 1.0×10^{-3}	Cu 1.5×10^{-3}	Zn 0.010	Ga 5.0×10^{-5}	Ge 0.070	As 6.0×10^{-5}	Se 4.0×10^{-3}	Br 0.020
V	Rb 0.010	Sr 1.5×10^{-3}	Y 2.0×10^{-5}	Zr 3.0×10^{-5}	Nb 0.020	Mo 1.5×10^{-3}	Tc 0.010	Ru 6.0×10^{-7}	Rh 0.010	Pd 0.010	Ag 0.020	Cd 1.0×10^{-3}	In 1.0×10^{-4}	Sn 1.0×10^{-3}	Sb 1.0×10^{-4}	Te 2.0×10^{-4}	I 0.010
VI	Cs 7.0×10^{-3}	Ba 3.5×10^{-4}		Hf 5.0×10^{-6}	Ta 3.0×10^{-6}	W 3.0×10^{-4}	Re 1.5×10^{-3}	Os 5.0×10^{-3}	Ir 2.0×10^{-6}	Pt 5.0×10^{-3}	Au 5.5×10^{-6}	Hg 4.5×10^{-4}	Tl 2.0×10^{-3}	Pb 2.5×10^{-4}	Bi 5.0×10^{-4}	Po 3.5×10^{-4}	At 0.010
VII	Fr 0.020	Ra 4.5×10^{-4}															

Lanthanides	La 2.0×10^{-5}	Ce 2.0×10^{-5}	Pr 2.0×10^{-5}	Nd 2.0×10^{-5}	Pm 2.0×10^{-5}	Sm 2.0×10^{-5}	Eu 2.0×10^{-5}	Gd 2.0×10^{-5}	Tb 2.0×10^{-5}	Dy 2.0×10^{-5}	Ho 2.0×10^{-5}	Er 2.0×10^{-5}	Tm 2.0×10^{-5}	Yb 2.0×10^{-5}	Lu 2.0×10^{-5}
Actinides	Ac 2.0×10^{-5}	Th 5.0×10^{-6}	Pa 5.0×10^{-6}	U 6.0×10^{-4}	Np 5.0×10^{-6}	Pu 1.0×10^{-7}	Am 4.0×10^{-7}	Cm 2.0×10^{-5}							

Key:

Li
0.020

 — Symbol
— Transfer Coefficient, F_m

Figure 2.24. Values of the ingestion-to-milk transfer coefficient F_m adopted as default estimates in the computer code TERRA.

	I A	II A											III A	IV A	V A	VIA	VII A
II	Li 0.010	Be 1.0×10^{-3}											B 8.0×10^{-4}		N 0.075		F 0.15
III	Na 0.055	Mg 5.0×10^{-3}	III B	IV B	V B	VI B	VII B	VIII		I B	II B	Al 1.5×10^{-3}	Si 4.0×10^{-5}	P 0.055	S 0.10	Cl 0.080	
IV	K 0.020	Ca 7.0×10^{-4}	Sc 0.015	Ti 0.030	V 2.5×10^{-3}	Cr 5.5×10^{-3}	Mn 4.0×10^{-4}	Fe 0.020	Co 0.020	Ni 6.0×10^{-3}	Cu 0.010	Zn 0.10	Ga 5.0×10^{-4}	Ge 0.70	As 2.0×10^{-3}	Se 0.015	Br 0.025
V	Rb 0.015	Sr 3.0×10^{-4}	Y 3.0×10^{-4}	Zr 5.5×10^{-3}	Nb 0.25	Mo 6.0×10^{-3}	Tc 8.5×10^{-3}	Ru 2.0×10^{-3}	Rh 2.0×10^{-3}	Pd 4.0×10^{-3}	Ag 3.0×10^{-3}	Cd 5.5×10^{-4}	In 8.0×10^{-3}	Sn 0.080	Sb 1.0×10^{-3}	Te 0.015	I 7.0×10^{-3}
VI	Cs 0.020	Ba 1.5×10^{-4}		Hf 1.0×10^{-3}	Ta 6.0×10^{-4}	W 0.045	Re 8.0×10^{-3}	Os 0.40	Ir 1.5×10^{-3}	Pt 4.0×10^{-3}	Au 8.0×10^{-3}	Hg 0.25	Tl 0.040	Pb 3.0×10^{-4}	Bi 4.0×10^{-4}	Po 9.5×10^{-5}	At 0.010
VII	Fr 2.5×10^{-3}	Ra 2.5×10^{-4}															

Lanthanides	La 3.0×10^{-4}	Ce 7.5×10^{-4}	Pr 3.0×10^{-4}	Nd 3.0×10^{-4}	Pm 5.0×10^{-3}	Sm 5.0×10^{-3}	Eu 5.0×10^{-3}	Gd 3.5×10^{-3}	Tb 4.5×10^{-3}	Dy 5.5×10^{-3}	Ho 4.5×10^{-3}	Er 4.0×10^{-3}	Tm 4.5×10^{-3}	Yb 4.0×10^{-3}	Lu 4.5×10^{-3}
Actinides	Ac 2.5×10^{-5}	Th 6.0×10^{-6}	Pa 1.0×10^{-5}	U 2.0×10^{-4}	Np 5.5×10^{-5}	Pu 5.0×10^{-7}	Am 3.5×10^{-6}	Cm 3.5×10^{-6}							

Key:

Li	—	Symbol
0.010	—	Transfer Coefficient, F_i

Figure 2.25. Values of the ingestion-to-beef transfer coefficient F_i adopted as default estimates in the computer code TERRA.

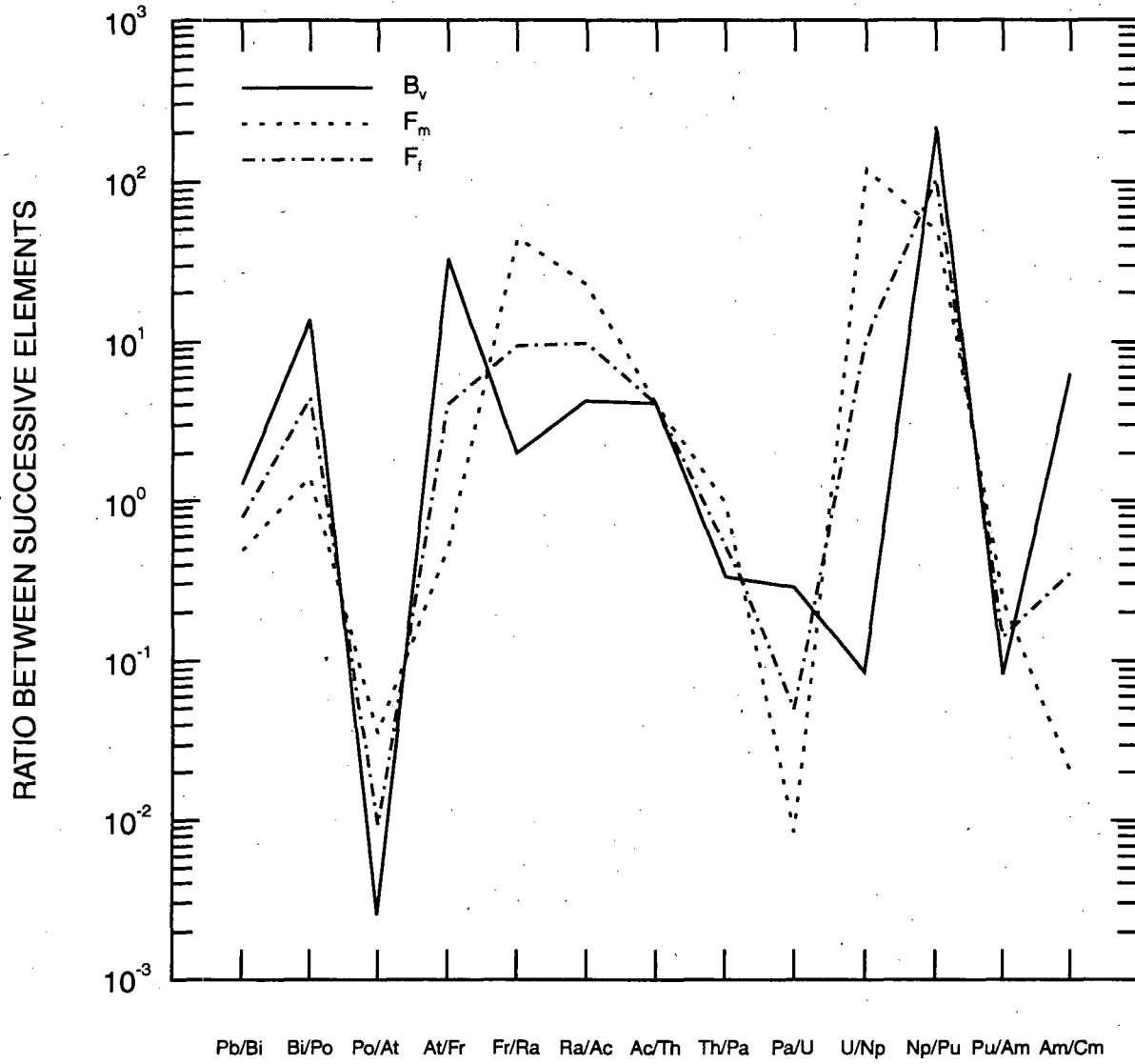


Figure 2.26. Systematic trends in the ratio of default estimates for B_v and F_m for successive elements and corresponding assumed ratios for F_r for successive elements used to determine default F_r estimates.

seen in the systematic variability of our B_v estimates (Figs. 2.27 and 2.28) and F_m estimates (Figs. 2.29 and 2.30). However, experimental determination of F_f for elements of atomic number greater than 82 would be preferable to our present approach, if available.

2.4 The Distribution Coefficient, K_d

The distribution coefficient, K_d is the ratio of elemental concentration in soil to that in water in a soil-water system at equilibrium. In general, K_d is measured in terms of gram weights of soil and milliliter volumes of water. In TERRA the distribution coefficient is used in the following equation to determine a location-specific leaching constant for elemental removal from a given soil depth,

$$\lambda_i = \frac{P + I - E}{\theta d [1 + (\frac{\rho}{\theta} K_d)]} \quad (7)$$

where

- P = annual average total precipitation (cm),
- E = annual average evapotranspiration (cm),
- I = annual average irrigation (cm),
- d = depth of soil layer from which leaching occurs (cm),
- ρ = soil bulk density (g/cm^3),
- θ = volumetric water content of the soil [$\text{mL}(=\text{cm}^3)/\text{cm}^3$], and
- K_d = the distribution coefficient (mL/g).

Default estimates of K_d used in the TERRA code are presented in Fig. 2.31. The mantissa of these values has been rounded off to the nearest 0.5 decimal place as for the other element specific transport parameters. The values for magnesium, potassium, calcium, manganese, iron, cobalt, copper, zinc, strontium, yttrium, molybdenum, technetium, ruthenium, cesium, lead, polonium, cerium, thorium, uranium, neptunium, plutonium, americium, and curium were determined through a review of the K_d literature. The estimates for the remaining elements were determined by a correlation of K_d with B_v . Because of the inherent uncertainties in estimates of K_d for various materials, a brief discussion of the parameter and its determination is appropriate.

2.4.1 Variability in K_d

The first source of variability in the parameter is associated with the laboratory methods used to determine K_d . Generally, the two most common techniques for determination of K_d are the column and batch methods, although other methods have been employed to measure distributions of chemical forms¹⁴⁷ or distribution among soil fractions.¹⁴⁸ In the column method a solution of material in water is applied to a column containing uniformly packed soil. The K_d of the material is determined from comparison of the 50% breakthrough curves for the water and material according to the equation

$$\frac{V_i}{V_w} = \frac{1}{1 + \frac{\rho}{\theta} K_d}, \quad (8)$$

where

- V_i = the velocity of the migrating material (determined from the 50% breakthrough curve) and
- V_w = the velocity of the water.

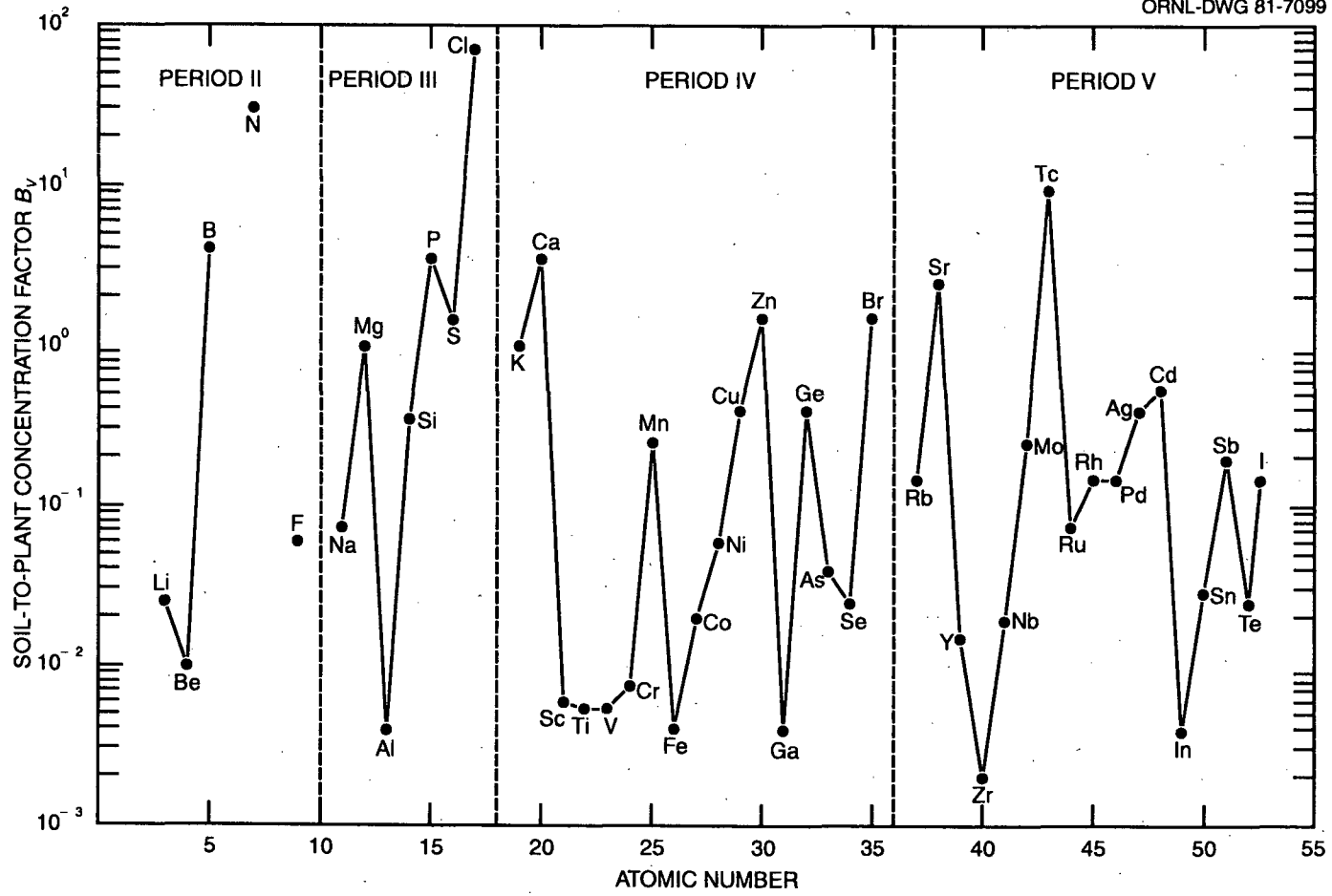


Figure 2.27. Systematic variations in default B_v estimates for Period II, III, IV, and V elements.

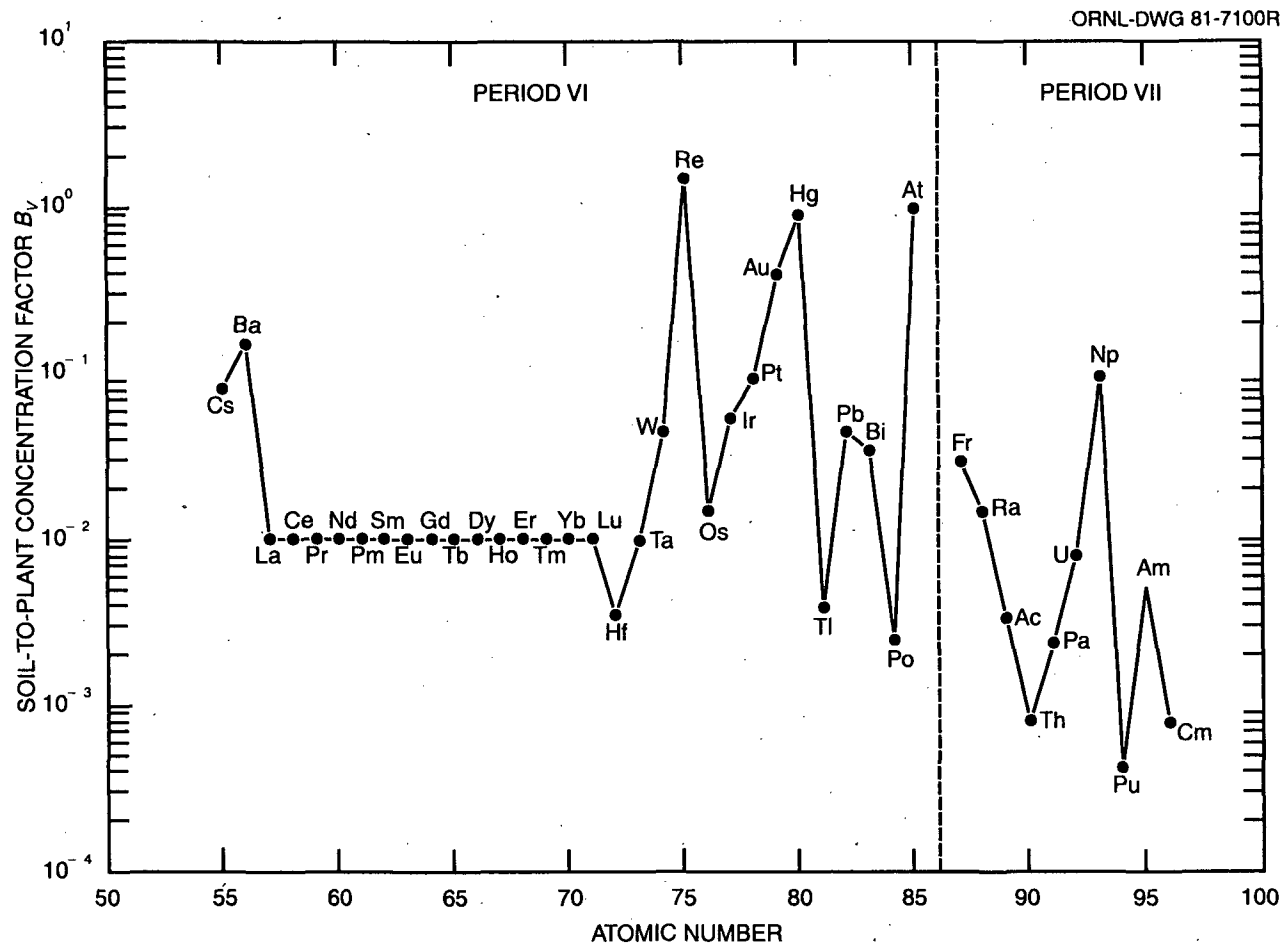


Figure 2.28. Systematic variations in default B_v estimates for Period VI and VII elements.

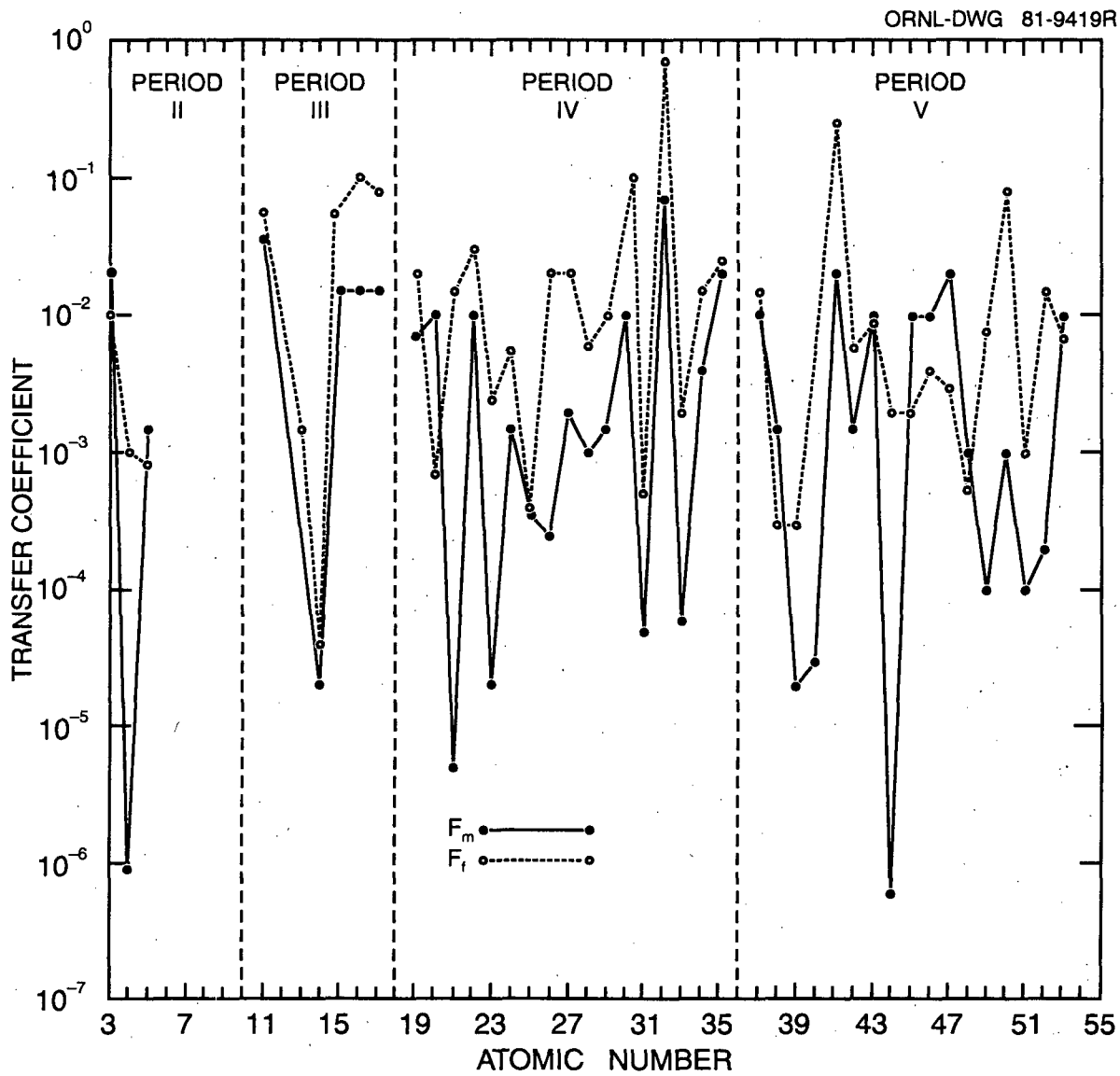


Figure 2.29. Systematic variations in default F_m and F_f estimates for Period II, III, IV, and V elements.

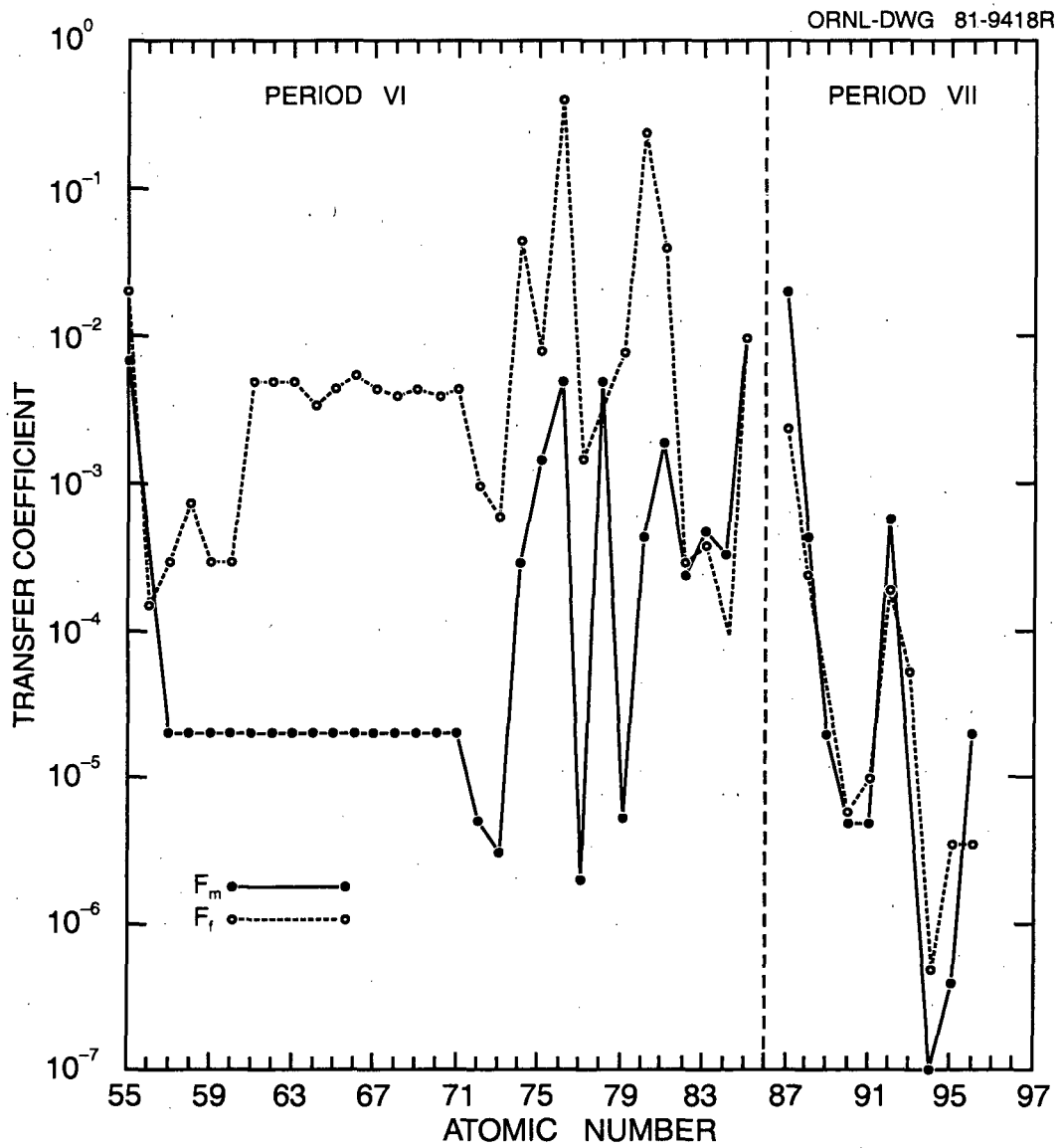


Figure 2.30. Systematic variations in default F_m and F_f estimates for Period VI and VII elements.

	I A	II A											III A	IV A	V A	VIA	VII A
II	Li 300	Be 650											B 3.0		N 0.50		F 150
III	Na 100	Mg 4.5	III B	IV B	V B	VI B	VII B	VIII		IB	II B	Al 1500	Si 30	P 3.5	S 7.5	Cl 0.25	
IV	K 5.5	Ca 4.0	Sc 1000	Ti 1000	V 1000	Cr 850	Mn 65	Fe 25	Co 45	Ni 150	Cu 35	Zn 40	Ga 1500	Ge 25	As 200	Se 300	Br 7.5
V	Rb 60	Sr 35	Y 500	Zr 3000	Nb 350	Mo 20	Tc 1.5	Ru 350	Rh 60	Pd 60	Ag 45	Cd 6.5	In 1500	Sn 250	Sb 45	Te 300	I 60
VI	Cs 1000	Ba 60		Hf 1500	Ta 650	W 150	Re 7.5	Os 450	Ir 150	Pt 90	Au 25	Hg 10	Tl 1500	Pb 900	Bi 200	Po 500	At 10
VII	Fr 250	Ra 450															

Lanthanides	La 650	Ce 850	Pr 650	Nd 650	Pm 650	Sm 650	Eu 650	Gd 650	Tb 650	Dy 650	Ho 650	Er 650	Tm 650	Yb 650	Lu 650
Actinides	Ac 1500	Th 1.5×10^5	Pa 2500	U 450	Np 30	Pu 4500	Am 700	Cm 2000							

Key:

Li 300

 — Symbol
— Transfer Coefficient, K_d

Figure 2.31. Values of the soil-water distribution coefficient K_d adopted as default estimates in the computer code TERRA.

In the batch method, soil and water are shaken with the material for a period of time until equilibrium distribution between soil and water is achieved or assumed. Because of nonequilibrium or the influences of convection and diffusion in the column method, these two techniques may give different results for nonionic elemental forms.¹⁴⁹ Thus, in searching the literature for K_d values, various biases and confounding factors inherent in the laboratory methods used to determine K_d are reflected in the values reported.

A second factor responsible for variation or imprecision in K_d measurement is a result of the parameter being a ratio of two concentrations. A small amount of error in measurement of either the soil or water concentration of material may produce a large amount of error in the resultant ratio. For example, in a batch-type experimental system of 10 g soil, 100 mL H₂O, and 100 µg of material for which the true K_d is 190 mL/g, a 1% overestimate of the soil concentration (95.95 µg in soil) yields a K_d of 237 mL/g, or approximately a 25% overestimate of K_d . The relative error in K_d estimate from a given percent error in measurement of soil concentration increases rapidly with increasing K_d (Fig. 2.32). The same is true with a given percent underestimate of the water concentration as the true K_d of the material decreases. Thus, if an investigator measures only one fraction of the soil-water system and determines the concentration of the other fraction by default, significant errors may be introduced into the K_d estimate from very small experimental errors of measurement. This magnification of experimental error undoubtedly contributes a significant amount of variability to K_d estimates for materials which are highly soluble or insoluble.

A third source of variability in K_d is its variation with soil type. Soils with different pH, clay content, organic matter content, free iron and manganous oxide contents, or particle size distributions will likely yield different K_d values. For example, in a study by Griffin and Shimp¹⁵⁰ of lead absorption by clay minerals, pH was shown to be an extremely important determinant of K_d . From their data, an exponential relationship between K_d and pH of the clays was found. At pH > 7.0, lead K_d is on the order of 10³, and below this pH, K_d ranges from 10¹ to 10². Soil pH has also been shown to influence K_d for plutonium and curium;¹⁵¹⁻¹⁵³ ruthenium, yttrium, zirconium, niobium, and cerium;¹⁵⁴ arsenic and selenium;^{155,156} and manganese, iron, zinc, cobalt, copper, cadmium, and calcium.¹⁵⁷⁻¹⁵⁹

Another source of variation in K_d is the time factor involved with its determination. Batch-type K_d determinations are usually made over a period of a few to several hours until equilibrium is achieved or assumed. If equilibrium does not occur within this short time period, some error is introduced. Errors from nonequilibrium K_d determinations made after 24 hours, however, are relatively insignificant.^{151,152,160} A more significant error may be introduced by using short term K_d determinations to simulate leaching over time periods of months or years. Gast et al.²³ found that sorption of Tc-99 by low organic soils tended to significantly increase over a 5-6 week period. Treatments of the soil with dextrose, H₂O₂, and steam sterilization, and sorption variation with temperature—all indicated that microbiota played either a direct or indirect role in sorption. Heterotrophic bacteria capable of solubilizing PbS, ZnS, and CdS have been reported by Cole,¹⁶¹ and microbial influences on the solubility of transuranics has also been suggested by Wildung and Garland.¹⁶² If microbial action is, indeed, important over the long term, then the applicability of K_d experiments carried out with oven dried and sieved soil to models of leaching in agricultural soils over long time periods must be questioned.

An analysis of the literature was performed to ascertain appropriate distributions of K_d for various elements (Table 2.13). Because of the variation of K_d with soil pH, an analysis of 222 agricultural soils^{163,164} was used to determine a typical range of pH for agricultural soils. In these soils, pH was found to be normally distributed with a mean pH of 6.7 and 95% of the values between a pH of 4.7 to 8.7. Thus, the criterion was adopted of discarding K_d values which were measured in soils outside of the pH range of 4.5 to 9. The K_d determinations used to generate Table 2.13 represent a diversity of soils, pure clays (pure minerals were excluded), extracting solutions (commonly H₂O, CaCl₂, or NaCl), laboratory techniques, and magnification of experimental error. Also, unavoidably, single measurements have been combined with replicates, means, and means of means to derive K_d distributions. When many references have been used to

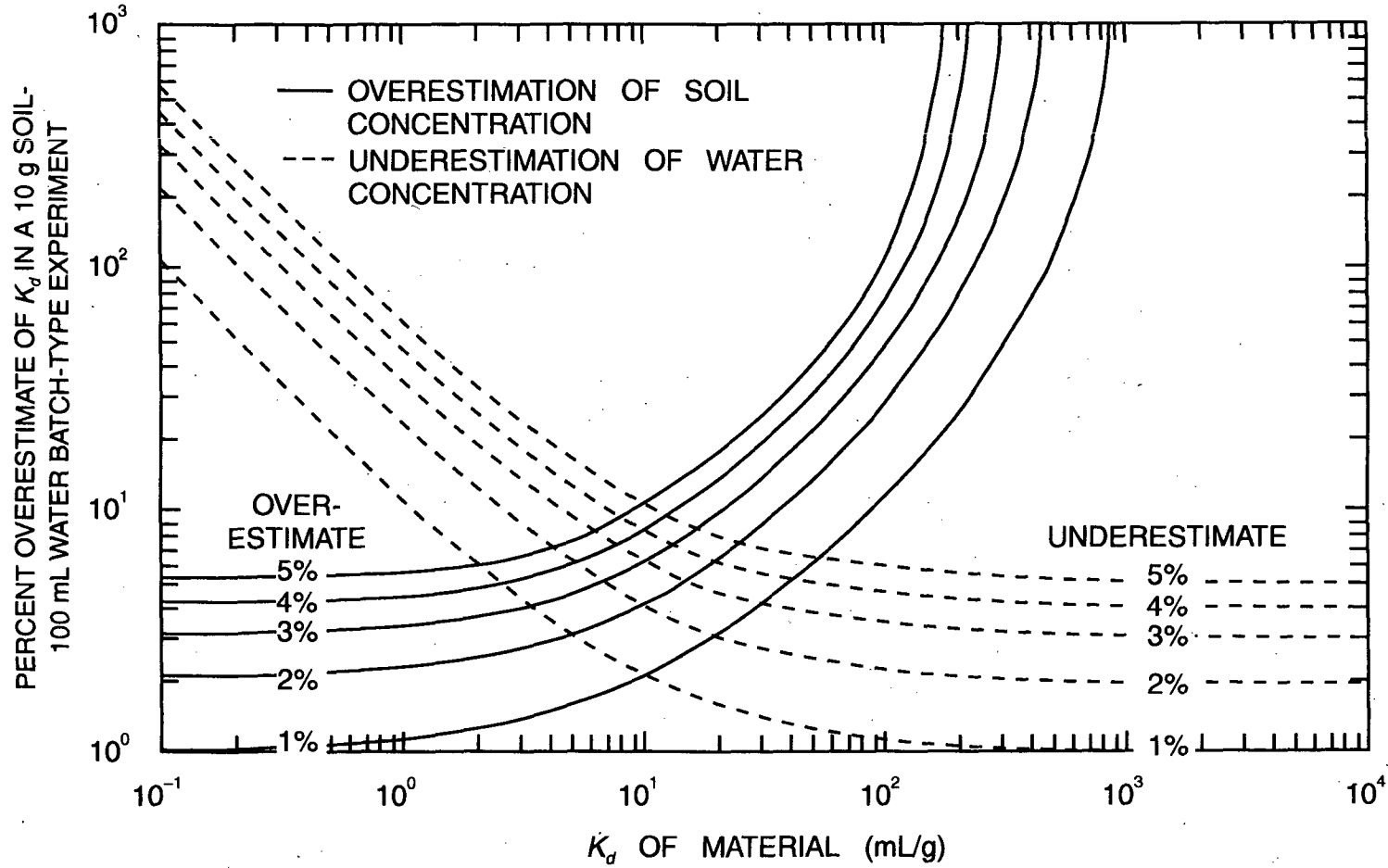


Figure 2.32. Percent error in K_d estimation from one to five percent overestimates of soil concentration or underestimates of water concentration in a 10 g-100 mL batch-type K_d experiment.

Table 2.13. Estimates of the distribution of K_d for various elements in agricultural soils of pH 4.5 to 9.0

Element	# Obs.	μ^a	σ^b	Exp(μ) ^c	Observed range ^b	References
					— mL/g —	
Mg	58	1.5	0.40	4.6	1.6 to 13.5	165, 166
K	10	1.7	0.49	5.6	2.0 to 9.0	165
Ca	10	1.4	0.78	4.1	1.2 to 9.8	165
Mn	45	4.2	2.5	65	0.2 to 10,000	149, 158, 167, 168
Fe	30	3.2	2.0	25	1.4 to 1,000	149, 158, 167, 169
Co	57	3.9	1.1	47	0.2 to 3,800	149, 158, 160, 167, 169-171
Cu	55	3.6	0.97	35	1.4 to 333	157, 158
Zn	146	3.6	1.8	38	0.1 to 8,000	149, 157-159, 167
Sr	218	3.6	1.6	37	0.15 to 3,300	149, 152, 154, 160, 167, 169, 171-180
Y	2	6.2	1.7	510	160 to 1,640	154
Mo	17	2.9	2.2	18	0.37 to 400	149
Tc	24	-3.4	1.1	0.033	0.0029 to 0.28	23
Ru	17	5.9	0.75	350	48 to 1,000	154, 160
Ag	16	3.8	1.5	46	10 to 1,000	149, 167
Cd	28	1.9	0.86	6.4	1.26 to 26.8	157
Cs	135	6.9	1.8	1,000	10 to 52,000	149, 160, 167, 169, 171, 173, 175, 177, 178, 180-183
Ce	16	6.7	0.54	840	58 to 6,000	154, 160
Pb	125	6.0	2.1	400	4.5 to 7,640	150, 184
Po	6	6.3	0.65	520	196 to 1,063	184
Th	17	12	0.57	150,000	2,000 to 510,000	185-187
U	24	6.1	2.5	450	10.5 to 4,400	185-187
Np	44	3.4	2.5	29	0.16 to 929	148, 186, 188, 189
Pu	40	8.4	2.4	4,500	11 to 300,000	151, 152-154, 177, 182, 186, 187, 189
Am	46	6.5	2.4	680	1.0 to 47,230	148, 188-190
Cm	31	7.6	1.6	1,900	99.3 to 51,900	148, 153, 189

^aThe mean of the logarithms of the observed values.

^bThe standard deviation of the logarithms of the observed values.

^cGeometric mean (50% cumulative probability).

generate the distribution, greater assurance can be given that the distribution is a representative distribution because it is not heavily biased by one or two experimental designs or techniques. Where a single or a few references were used, less assurance can be given.

On the basis of distributions computed for cesium and strontium (Fig. 2.33), a lognormal distribution for K_d has been assumed for all elements. Thus, the median value of the assumed lognormal distribution is used as a best estimate default K_d for TERRA (except for lead, and technetium where judgement was exercised). However, if the distribution of K_d computed for cesium and strontium are typical, then K_d may vary by as much as three orders of magnitude in soils of pH 4.5 to 9.0. Such variation in K_d is greater than or equal to the variation in B_v observed for cesium, strontium, and plutonium (Figs. 2.3, 2.7, and 2.22) and suggests the advisability of using site-specific values when available.

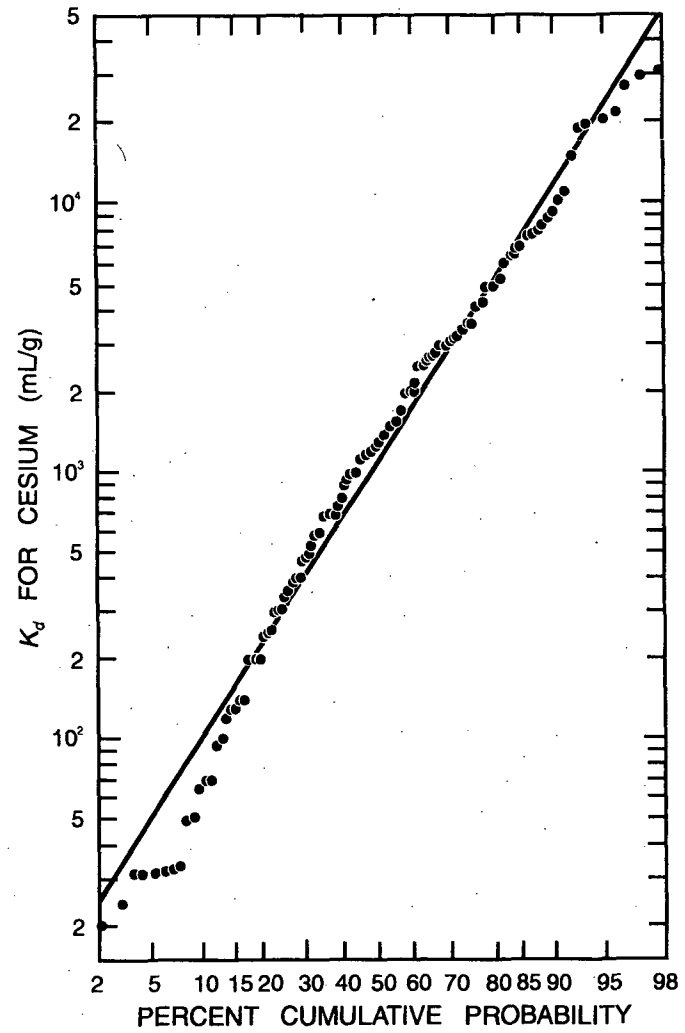
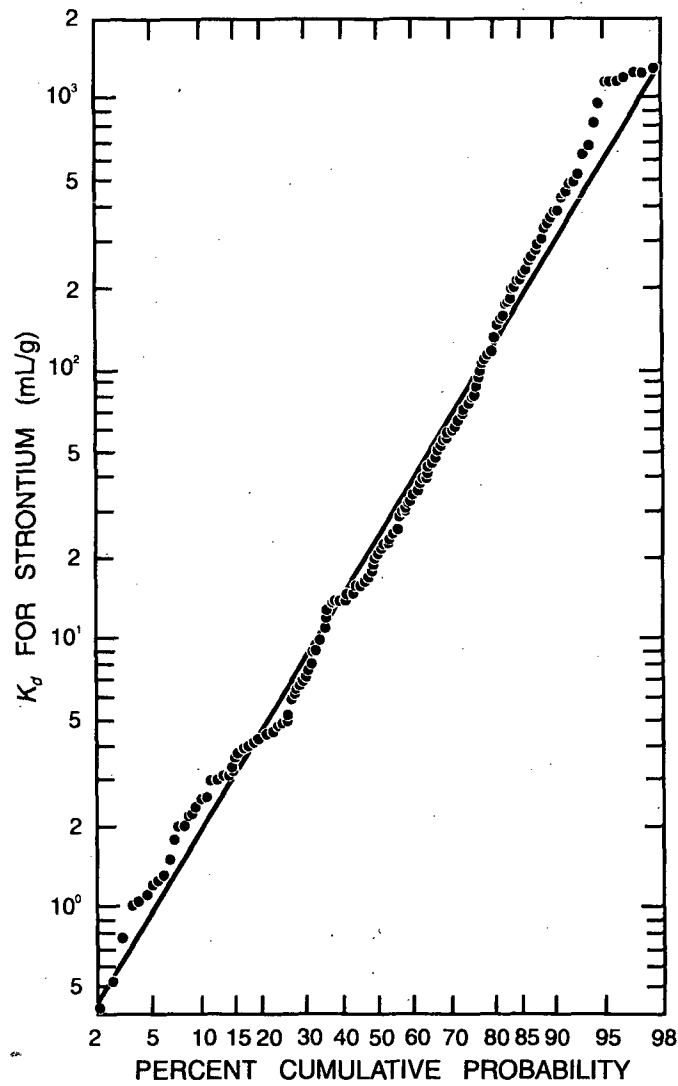


Figure 2.33. Lognormal probability plots of K_d for cesium and strontium in soils of pH 4.5 to 9 based on available references.

2.4.2 Estimates of K_d based on default B_v values

Although K_d estimates for the 23 above-mentioned elements are subject to great uncertainty, they are based on values reported in the literature. No references are immediately available for the remaining elements of the periodic table. In order to provide a default estimate for these elements, an alternative method is used. In 1979, Van Dorp, Eleveld, and Frissel¹⁹ proposed a model for estimation of the soil-plant concentration factor. Their approach was to calculate the solubility of a nuclide in soil water, its ability to transfer across root membranes, and its upward movement with the transpiration stream. They reasoned that measured values of K_d ; root selectivity coefficient (S), and transpiration coefficient (T_c) would allow them to predict the soil-plant concentration factor from soil-radionuclide concentration. Their model has not become generally used or accepted for dose calculations, but their implied dependency of B_v on K_d is the basis of our approach for estimating default K_d estimates in lieu of experimental determinations.

Our approach is to presume that the default K_d estimates for elements in Sect. 2.4.1 and their corresponding B_v estimates represent a wide variety of soils and plants. Therefore, a single default estimate for B_v and K_d will reflect soils, plants, and experimental conditions which are "averaged" or "generalized." Thus, any relationship observed between K_d and B_v may be used to predict "average" or "generalized" K_d estimates from our default B_v estimates.

Figure 2.34 shows the correlation found between B_v and K_d . It should be noted that the B_v estimates in Fig. 2.34 are the geometric means determined directly through analysis of reviewed literature, and not necessarily the default values from Fig. 2.1. Technetium is an example. The technetium B_v of 89 is the geometric mean of the geometric means of references 23, 107, 122, and 123. It was felt that although the short-term plant uptake studies represented in references 23, 107, and 122 were inappropriate for long-term B_v estimates, they were appropriately associated with the short-term K_d determinations for technetium (because B_v decreases and K_d increases with time). Thus, these two short-term parameters were used in the definition of the B_v - K_d relationship. However, in Fig. 2.31 we used our best estimate of technetium B_v and the regression equation

$$K_d = \exp(2.38 - 0.89(\ln B_v)) \quad (9)$$

to determine our best estimate of technetium K_d of 1.5. In addition to technetium the K_d default estimates for elements not mentioned in Sect. 2.4.1 were determined via Eq. (9) and the best estimate B_v default values in Fig. 2.1.

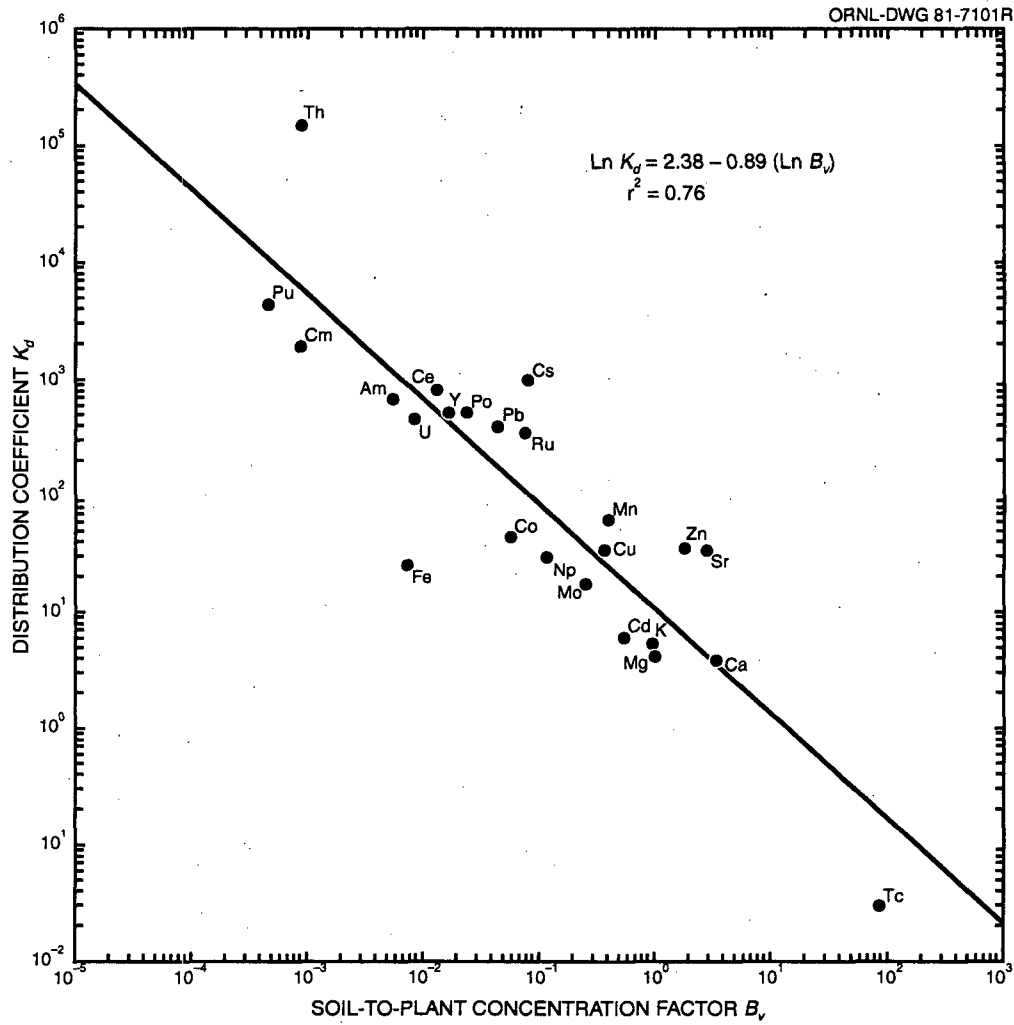


Figure 2.34. Correlation between B_v and K_d based on geometric means of available reference geometric means.

3. INTERCEPTION FRACTION FOR VEGETATION

The interception fraction for a given vegetation type, r^i , is a factor which accounts for the fact that not all of the airborne material depositing within a unit area will initially deposit on edible vegetation surfaces. The fraction of the total deposit which is initially intercepted by vegetation is the interception fraction, r^i , such that $0 \leq r^i \leq 1$. In the TERRA code, as in other food chain transport models,⁶ the processes of initial deposition and weathering removal with time are treated separately. In the NRC Regulatory Guide 1.109 model, separate interception fractions are suggested for iodines and other particulate types.⁶ The analysis of agricultural food and feed crops in the United States by Shor, Baes, and Sharp⁷ suggests that the diversity of growth forms necessitates vegetation-specific estimates of interception fraction as well. The following sections outline a theoretical approach to vegetation-specific interception fractions. The results of such approaches have been used as default estimates in lieu of user-input values in the TERRA computer code. Variation of interception fraction with element, chemical form, and deposition process (e.g., wet, dry) will require further research.

In Section 3 pasture, hay, and silage productivities are considered to be on an air-dry weight basis as reported in reference 7. Vegetable and produce productivities are in fresh weight as reported in reference 7.

3.1 Pasture Grasses and Hay

The interception fraction for pasture grasses and hay are modeled in a different manner than for other vegetation types because experimental determinations of interception fractions for grasses have been performed.¹⁹²⁻¹⁹⁸ In these studies a correlation between initial interception fraction and productivity (standing crop biomass) has been found. This relationship and an empirical fit of the available data (summarized in Table 3.5 of reference 199) is shown in Figure 3.1. The empirical relationship is given by

$$r^{pg} = 1 - \exp(-2.88Y_{pg}) \quad (10)$$

where

- r^{pg} = the interception fraction for pasture grass and
- Y_{pg} = the productivity of pasture grass (kg/m^2 , dry).

This relationship has been assumed to apply to hay as well as pasture grasses in the computer code TERRA.

3.2 Leafy Vegetables

There are no readily available literature references for the interception fraction for leafy vegetables. Therefore, the interception fraction for leafy vegetables is based on a theoretical model (Fig. 3.2). With this model a range of possible interception fractions may be generated if the following assumptions are made:

1. On a two-dimensional basis the fractional area represented by leafy vegetables is equal to the interception fraction;
2. leafy vegetables may be represented by circles on a two-dimensional basis (Fig. 3.2);
3. leafy vegetables are planted in rows;

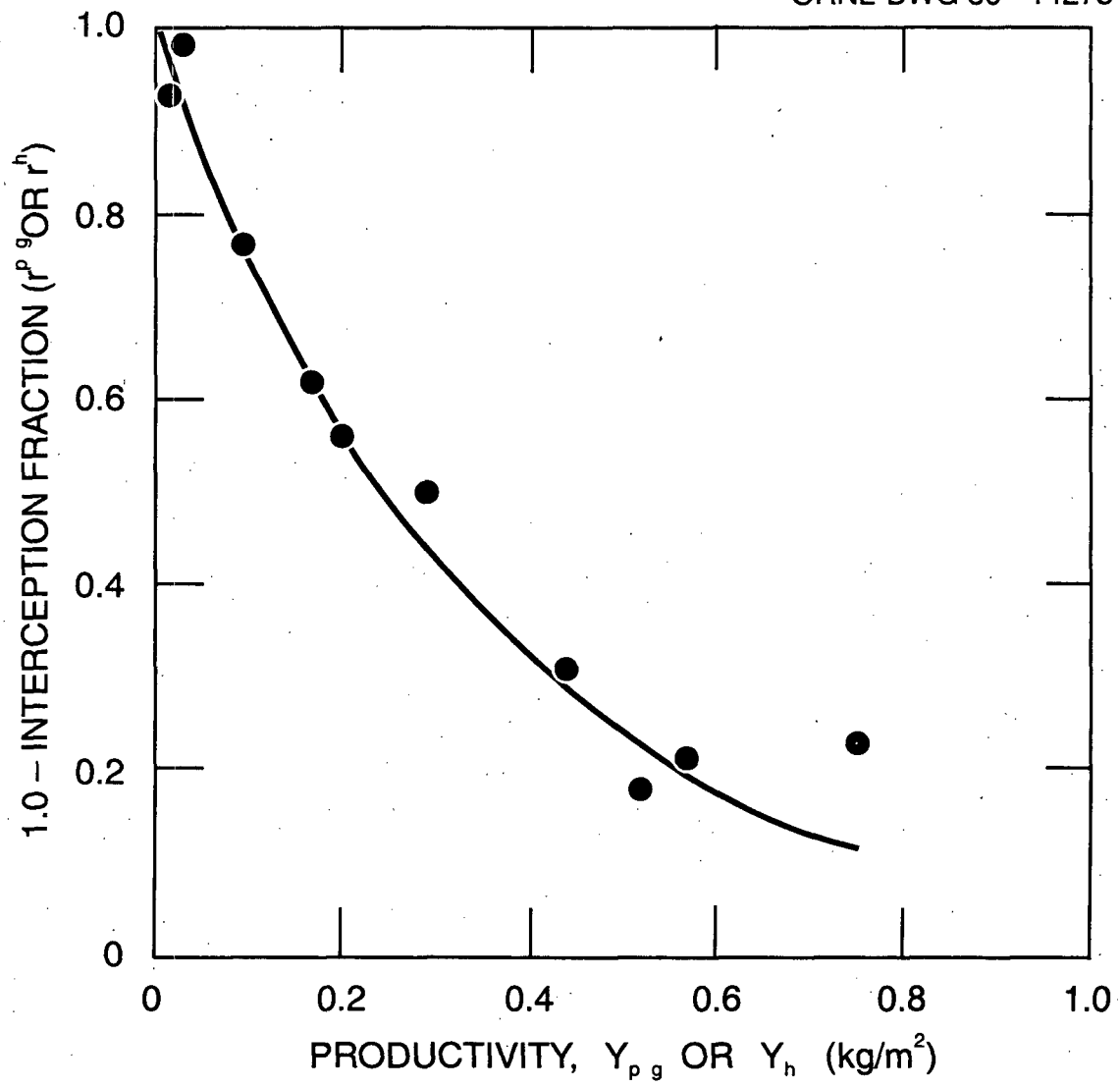
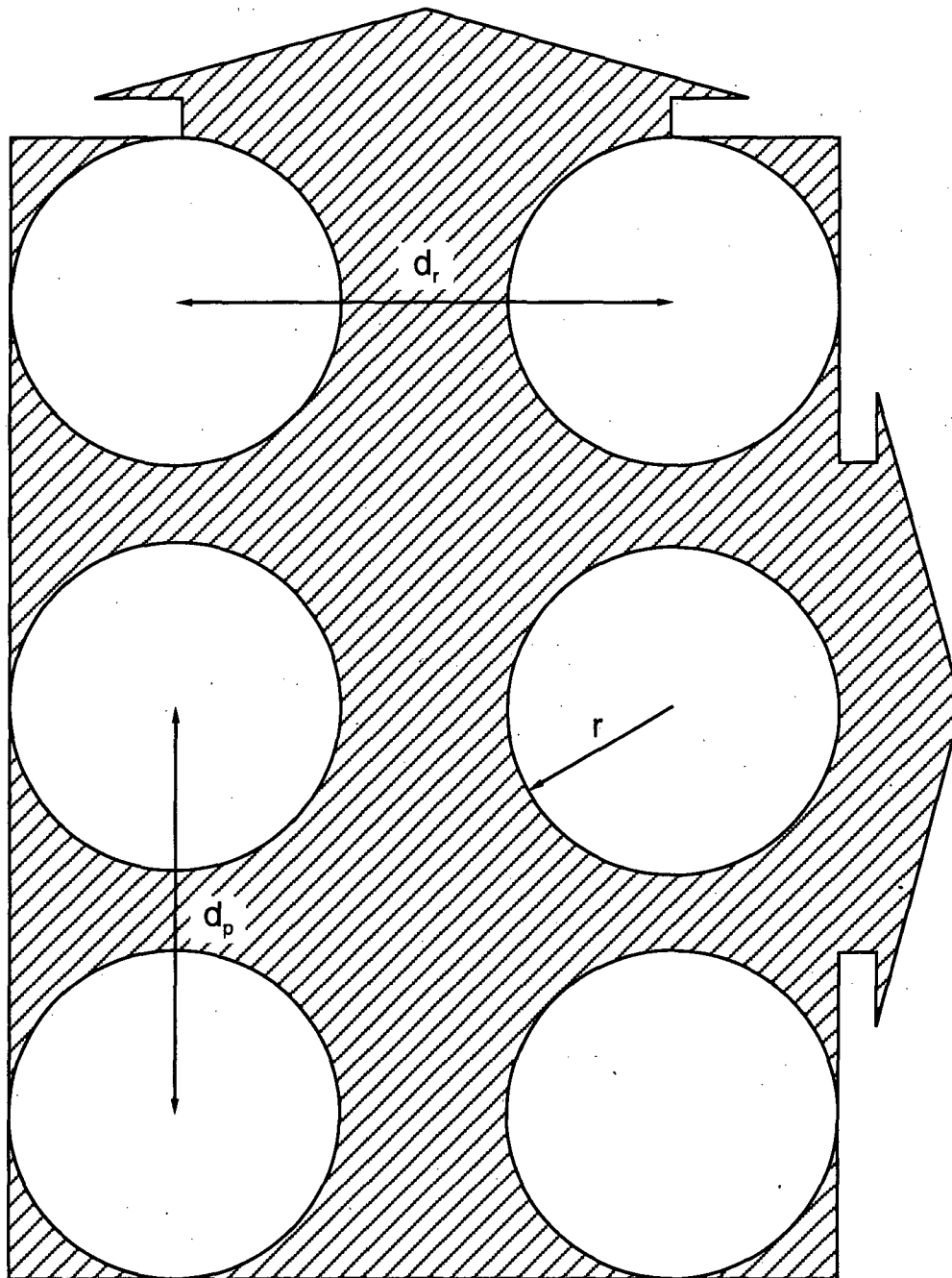


Figure 3.1. Relationship between interception fraction and productivity (in dry weight) for forage grasses (pasture and hay).



CONSTRAINTS: $2r \leq d_p \leq d_r$

Figure 3.2. Model of field geometry of leafy vegetable spacings.

4. the ranges of between-plant and between-row spacings in the United States are approximately equal to the minima and maxima recommended by Knott;²⁰⁰
5. a farmer will not plant individual leafy vegetables so close together that leaves from adjacent plants overlap (thereby decreasing yield);
6. rows will generally be spaced farther apart than individual plants in a row; and
7. harvest of leafy vegetables occurs at the time of maximum yield, and maximum yield corresponds to maximum plant diameter.

With the above assumptions, the model given by Fig. 3.2 predicts that the fraction of planted area occupied by leafy vegetables, equivalent to the interception fraction at harvestable maturity, is given by

$$r^{mv} = \frac{n_r r_n \pi r_f^2}{[(n_r - 1)d_p + 2r_f][(r_n - 1)d_r + 2r_f]}, \quad (11)$$

where

- r^{mv} = the interception fraction for mature leafy vegetables,
- n_r = the number of plants per row,
- r_n = the number of rows of plants,
- r_f = the radius of an individual fruit or plant,
- d_p = the distance between plants in a row, and
- d_r = the distance between rows of plants.

The constraints on the model are

$$2r_f \leq d_p \leq d_r. \quad (12)$$

As the land area planted becomes infinitely large, Eq. (11) becomes

$$r^{mv} = \frac{\pi r_f^2}{d_p d_r}. \quad (13)$$

If a farmer maximizes the number of plants per row such that $d_p = 2r_f$, then Eq. (13) becomes

$$r^{mv} = \frac{\pi r_f}{2d_r}. \quad (14)$$

When $2r_f = d_p = d_r$ (maximum utilization of planted land), then the interception fraction for mature leafy vegetables is 0.785.

In order to predict an average interception fraction for the mature leafy vegetable, recommended field spacings³⁰⁰ for leafy vegetables were assumed to represent typical spacings actually encountered in American agriculture. A distribution of field spacings was determined by obtaining a range of recommended spacings for each leafy vegetable and weighting each vegetable according to its importance (by area planted) in the United States (Table 3.1). By determining distributions of typical d_p spacings and values of r_f , a Monte Carlo technique was used to produce a distribution of solutions to Eq. (14). The mean value of this distribution is $r^{mv} = 0.30$. In this simulation the average d_r was 73.5 cm (28.7 inches).

Table 3.1. Weighting factors for leafy vegetable interception fraction model simulation

Leafy vegetable	Quantity planted (km ²)	Percent	Weight factor
Lettuce	948	42	
cos			14
head			14
leaf			14
Cabbage	367	16	
early			6
late			5
Chinese			5
Greens	246	11	
collards			3
kale			3
spinach			3
New Zealand spinach			2
Broccoli	176	8	
sprouting			4
raab			4
Mint	160	7	7
Celery	140	6	6
Cauliflower	113	5	5
Green onions	59.3	3	3
Escarole	33.6	2	
chicory			1
endive			1
Brussels sprouts	24.8	1	1
Total	2267.7	100	100

From the theoretical interception fraction for mature leafy vegetables of 0.30 it is possible to generate an average interception fraction over the time in the field by taking into account the logistic growth characteristics of plants (Fig. 3.3). It is commonly known that plants (and many living organisms) have growth patterns which follow a logistic growth pattern.²⁰¹⁻²⁰⁵ Logistic growth curves have been defined by various equations which yield the appropriate shape. For our analysis the following equation was used:

$$f^m = \frac{1 - \cos\left[180\left(\frac{t_i}{t_m}\right)\right]}{2}, \quad (15)$$

where

- f^m = the fraction of maximum growth,
- t_i = the time of interest, and
- t_m = the time at which maximum growth normally occurs

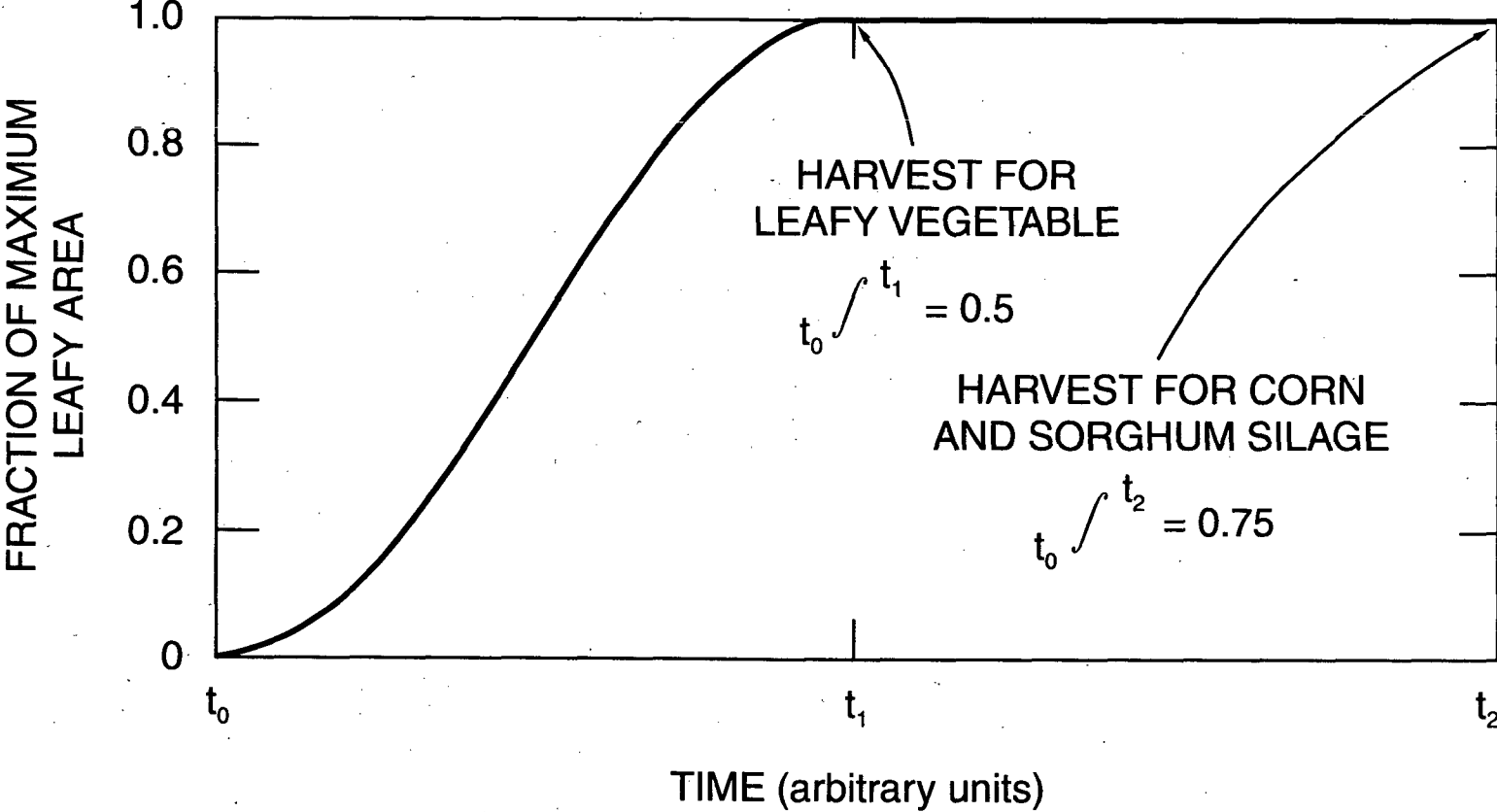


Figure 3.3. Hypothetical growth curve for plants. Leafy vegetables are harvested at the time of maximum growth, and silage is harvested at grain maturity.

Equation (15) was chosen because at time = $t_m/2$, $f^m = 0.5$ and integration of Eq. (15) from t_0 to t_m yields 0.5. Thus, an average interception fraction for leafy vegetables over the time in the field is equal to 0.5×0.30 or 0.15. It must be emphasized that the value of 0.15 represents a theoretical average over the United States for leafy vegetables. A corresponding theoretical maximum would be 0.5×0.785 or 0.39.

3.3 Silage

The analysis of silage interception fraction is based on an approach similar to that for leafy vegetables. A modification of the two-dimensional model was made to allow for overlap of leaves from adjacent plants (as seen in aerial views of corn and sorghum fields). However, no overlap was allowed between leaves from adjacent rows (Fig. 3.4). It was assumed in our analyses that the silage is not harvested until the grain has matured. This period of maturity corresponds to the period t_1 to t_2 in Fig. 3.3. According to descriptions of growth stages in corn by Hanaway²⁰⁶ and Norman,²⁰⁷ grain maturity occurs at a time approximately equal to twice the time to maximum plant growth (and thus maximum surface area). Accordingly, the integral of plant surface area from t_0 to t_2 in Fig. 3.3 is 0.75.

From Fig. 3.4, the fraction of total area occupied by the silage at maturity is given by

$$r^{ms} = \frac{r_f^2 \left[\frac{4\pi}{3} + (n_r - 1) \frac{\sqrt{3}}{2} + (n_r - 2) \frac{\pi}{3} \right] r_n}{[d_r(r_n - 1) + 2r_f][d_p(n_r + 1)]} \quad (16)$$

The model constraints are

$$r_f = d_p \leq \frac{d_r}{2} \quad (17)$$

As the planted area becomes infinitely large, Eq. (16) approaches

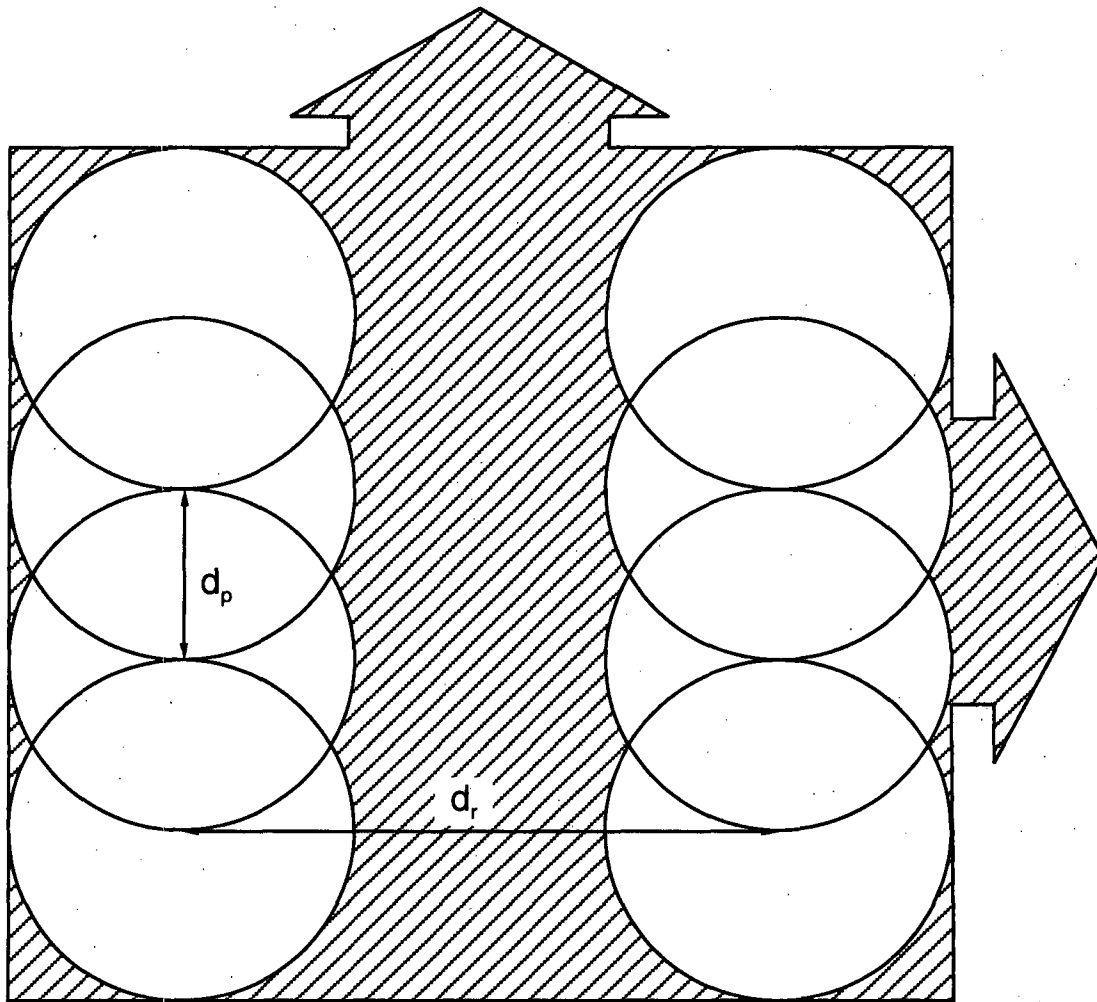
$$r^{ms} = \frac{r_f^2 \left[\frac{\pi}{3} + \frac{\sqrt{3}}{2} \right]}{d_r \cdot d_p} \quad (18)$$

Since $d_p = r_f$, Eq. (18) becomes

$$r^{ms} = \frac{d_p \left[\frac{\pi}{3} + \frac{\sqrt{3}}{2} \right]}{d_r} \quad (19)$$

At maximum silage density ($d_r = 2d_p$) Eq. (19) becomes a value of 0.96. Correspondingly, the maximum average interception fraction is equal to 0.72.

The average interception fraction was derived from average values of d_r and d_p for corn and sorghum plantings. An average d_p of 30.5 cm (12 inches) and d_r of 99 cm (39 inches) was taken from Knott²⁰⁰ and Rutledge.²⁰⁸ Using these values, an interception fraction at maturity of 0.59 was determined from Eq. (19). This value yields an average interception fraction of 0.44.



CONSTRAINT: $r = d_p \leq d_r$

Figure 3.4. Model of field geometry of silage plant spacings.

3.4 Exposed Produce

The exposed produce category includes 31 commercially important fruits and vegetables in the United States.⁷ These produce may be broadly classified as noncitrus fruits, berries, and important field crops. Because of the diversity of growth forms in the exposed produce category, our analysis is based on five of the most important noncitrus fruits and field crops in the category—apples, snap beans, tomatoes, peaches, and cherries. For this analysis, importance is defined in terms of area planted (see Table 3.2).

For noncitrus fruits and tomatoes, as with leafy vegetables and silage, it is assumed that the fruits can be represented by circles on a two-dimensional basis. The interception fraction is calculated by determining the total fruit cross-sectional area per square meter which is given by

$$r^{mf} = \frac{n\pi r_f^2}{lw}, \quad (20)$$

where

- r^{mf} = the interception fraction of the mature fruit,
- n = the number of fruit per square meter
- r_f = the radius of the fruit (mm),
- l = the length of the unit area (1000 mm), and
- w = the width of the unit area (1000 mm).

It is assumed that an average interception fraction over the lifetime of the fruit is provided for by the model of logistic growth and maturity used for silage. That is, half of the fruit's residence time in the tree or on the plant is assumed to be for growth and development, and one half of the time is assumed to be for maturing or ripening before harvest. Thus, Eq. (20) becomes

$$r^{\sigma} = \frac{0.75n\pi r_f^2}{lw}, \quad (21)$$

where

- r^{σ} = average interception fraction for exposed fruit.

For snap beans the same approach as for round fruits is used, except that the effective surface area of a snap bean is modeled in two dimensions as a rectangle—a two dimensional view of a cylinder on its side. For mature snap beans

$$r^{msb} = \frac{n2r_f l_f}{lw}, \quad (22)$$

where

- l_f = the length of the snap bean.

As with tree fruits and tomatoes, the average interception fraction over the time in the field is 0.75 times the value of the mature interception fraction.

A search of the literature was performed to determine values of n , r_f , r_i , and l_f or collateral information from which to deduce them. Empirical measurements of r_f and r_i were combined with literature values to determine default values. Fruit weights were compared with estimated weights of spheres of water of the same radius to check default estimates. Information from the 1974

Table 3.2. Relative importance of various exposed produce in the U.S.

Vegetable	Quantity planted (km ²)	Percent of category	Percent of sub- category
Non-citrus tree fruits			
Apple	1960	27.2	57.3
Apricot	6.00	0.1	0.2
Cherry	429	6.0	12.5
Date	0.101	≤0.1	≤0.1
Fig	0.0647	≤0.1	≤0.1
Mango	4.86	≤0.1	0.1
Nectarine	3.63	≤0.1	0.1
Peach	644	9.0	18.8
Pear	229	3.2	6.7
Hot Pepper	48.2	0.7	1.4
Plum	36.6	0.5	1.1
Prune	61.4	0.9	1.8
Total	3423	47.6	
Berries & vine fruits			
Blackberry	94.5	1.3	10.6
Blueberry	154	2.1	17.3
Boysenberry	4.75	≤0.1	0.5
Cranberry	91.2	1.3	10.2
Currant	1.12	≤0.1	0.1
Gooseberry	0.348	≤0.1	≤0.1
Grape	411	5.7	46.1
Pimento	1.64	≤0.1	0.2
Raspberry	29.9	0.4	3.4
Strawberry	104	1.5	11.7
Total	892	12.4	
Field crops			
Asparagus	269	3.7	9.3
Cucumber	380	5.3	13.2
Eggplant	16.0	0.2	0.6
Okra	16.7	0.2	0.6
Rhubarb	6.80	0.1	0.2
Sweet pepper	155	2.2	5.4
Snap bean	1250	17.4	43.4
Squash	133	1.9	4.6
Tomato	655	9.1	22.7
Total	2880	40.0	

Census of Agriculture²⁰⁹ was used to calculate values of n for each fruit or vegetable. Estimated interception fractions for mature apples, snap beans, tomatoes, peaches, and cherries were calculated according to Eqs. (21) and (22) and weighted to derive a default interception fraction estimate of 0.052 for exposed produce (Table 3.3). Surprisingly, the values for the noncitrus fruits (apples, peaches, and cherries) are within approximately a factor of 1.3 of each other, and the values for the field crops are approximately equal to each other.

3.5 Correlation Between Interception Fraction and Standing Crop Biomass

As mentioned in Sect. 3.1, Chamberlain found a relationship between standing crop biomass or productivity and the interception fraction for pasture grasses. This relationship [Eq. (10)] is used in the TERRA code to calculate the interception fraction for pasture grasses and hay. The analyses of interception fraction for leafy vegetables, silage, and exposed produce (Sect. 3.2, 3.3, and 3.4, respectively) are based on generalized or average crops. Use of the interception fraction values for these categories as default estimates independent of complementary values of productivity (Y_i) could result in unreasonable overestimates of surface plant concentrations, c^{ps} , because

$$c^{ps} \propto \frac{r^i}{Y_i}. \quad (23)$$

That is, low values of Y_i coupled with values of r^i for average crops (represented by average Y_i values) could produce high values of r^i/Y_i . As Y_i approaches zero, the r^i/Y_i ratio approaches infinity.

Figure 3.3 indicates that leaf (or edible produce) surface area increases with time as the plant grows. Clearly, since interception fraction is proportional to surface area, the interception fraction for very young plants is less than that for mature plants, and r^i is a function of Y_i for the individual plant. However, it is not clear whether r^i is a function of Y_i for the mature plant in the field. Figure 3.5 illustrates the problem.

Figure 3.5 presents three plots of equal area with hypothetical crops represented by spheres. The relative ordering of productivity is $A > B > C$. In plots A and B planting geometry (packing) has been maximized (without staggering) by planting individual plants within a row and rows of plants adjacent to one another. The difference between the two crops is that the crop in plot A is of greater size (radius, r_p) than the crop in plot B. In plots B and C the crop radii are equal, but planting geometry is less efficient in plot C. In all plots the interception characteristics of the individual crops are equal.

It can be shown mathematically that the total surface area of crops in plots A and B are equal. That is, the decrease in surface area per plant as plant radius is reduced is exactly counterbalanced by the increase in number of plants per unit area. Therefore, the interception fraction for crops A and B should be the same. The productivity, however, is dependent on the volume multiplied by the number of plants per unit area. Since volume is proportional to the cube of plant radius, the productivity of plot A is greater than that of plot B. In this example, regardless of plant size the interception fraction is a constant value which is independent of productivity.

In plots B and C the interception fraction is a function of productivity. The surface area per plant is constant, and as planting geometry becomes less efficient, both productivity and interception fraction decrease proportionately.

The above examples illustrate that interception fraction for nongrasslike plants may or may not be a function of productivity, depending on whether a difference in productivity reflects a difference in plant size or a difference in plant spacings. This dilemma has been addressed in TERRA. As mentioned in the introduction to this report (and as will be discussed later), the TERRA code allows input of location-specific agricultural parameters, including location-specific productivity

Table 3.3. Values of the interception fraction for five important crops in the exposed produce category

Produce	r_i	r_f	n	l_f	Interception fraction	Weighting factor ^a
Apples	4.2 m	38 mm	10/m ²		0.034 ^b	0.29
Snap beans		4 mm	220/m ²	55 mm	0.073 ^c	0.21
Tomatoes		38 mm	20/m ²		0.068 ^b	0.29
Peaches	1.8 m	31.8 mm	15/m ²		0.036 ^b	0.14
Cherries	5.3 m	8.5 mm	160/m ²		0.027 ^b	0.07
Weighted average					0.052	

^aBased on values in Table 3.2.

^bEq.(21).

^c0.75 × Eq. (22).

estimates. In TERRA the location-specific productivity estimate determines a corresponding interception fraction. In other words, it has been assumed that location-specific variations in productivity are more reflective of the differences in plots B and C than in A and B.

Since observed relationships between interception fraction and productivity are unavailable for nongrasslike plants, the relationship shown in Fig. 3.1 has been assumed to apply to nongrasslike plants also. The coefficients of the exponential terms for exposed produce, leafy vegetables, and silage have been determined by fitting an exponential regression equation, forced through the point $[(1-r^i = 0), (Y_i = 0)]$ to the points representing the United States average productivity-average interception fraction and maximum observed productivity-theoretical maximum interception fraction. The average and maximum productivities are taken from Appendices B and C of reference 7. The resulting relationships are (Fig. 3.6),

$$r^e = 1 - \exp(-0.0324Y_e), \quad (24)$$

$$r^{lv} = 1 - \exp(-0.0846Y_{lv}), \text{ and} \quad (25)$$

$$r^s = 1 - \exp(-0.769Y_s), \quad (26)$$

where the superscripts and subscripts "e," "lv," and "s" are for exposed produce, leafy vegetables, and silage, respectively.

Although this approach is at best *ad hoc*, the consequences of setting the interception fraction at a constant value and allowing productivity to vary over its reported range are serious. Figure 3.7 compares the method of using Eqs. (24)-(26), case A, and using a single interception fraction, case B, over the observed productivity range shown at the bottom of the figure. At the extremes of the ranges, especially at productivities less than 0.1 kg/m², the ratio of r^i/Y_i is particularly suspect.

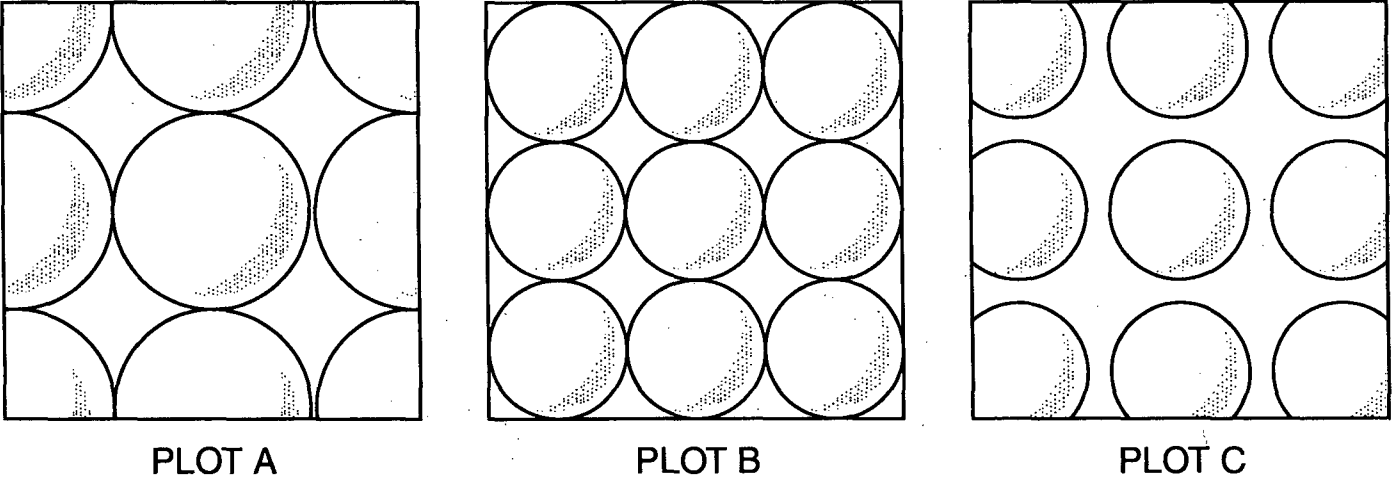


Figure 3.5. Three plots of equal area containing hypothetical crops of varying size and planting density.

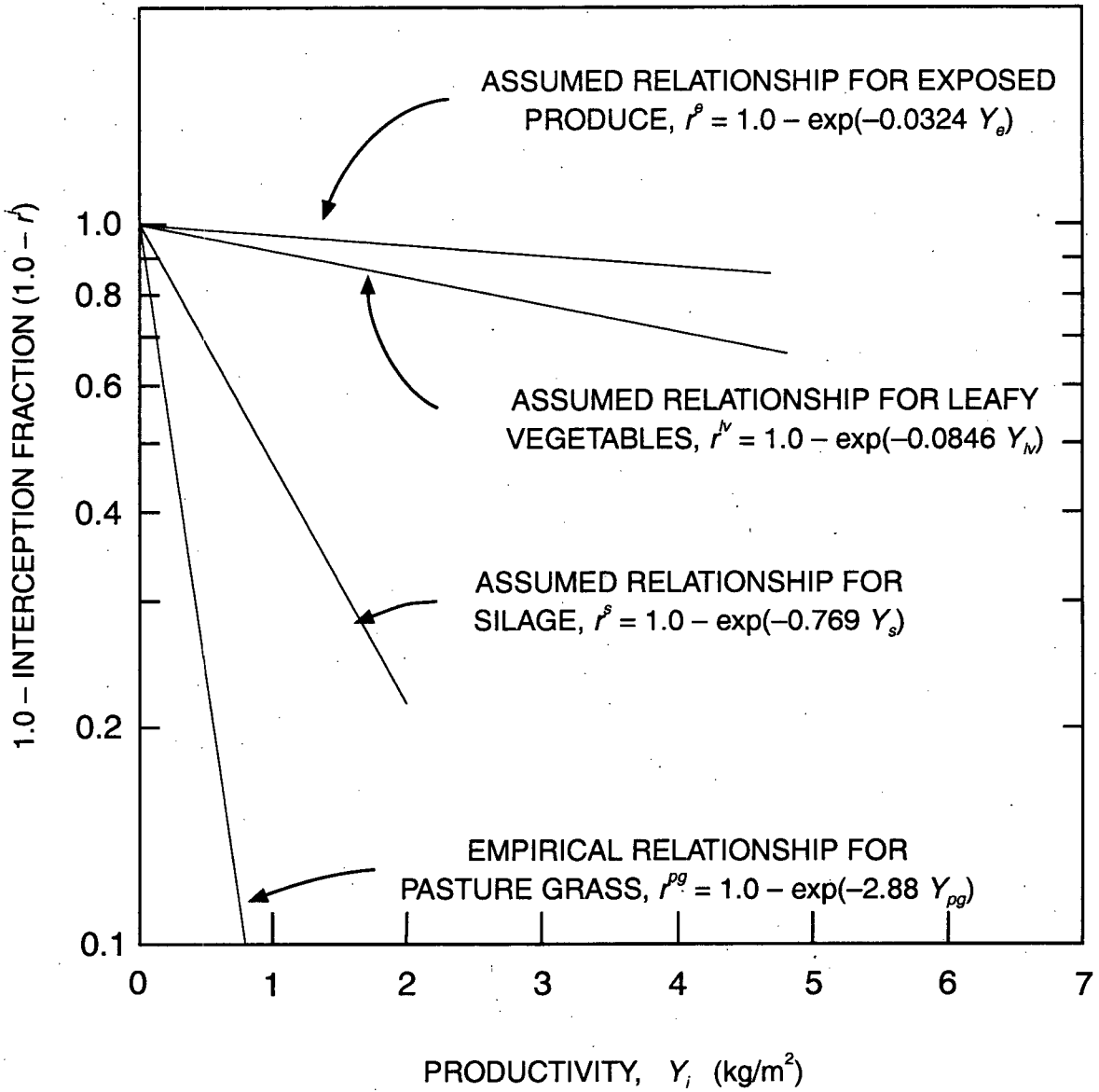


Figure 3.6. Assumed relationships between interception fraction and fresh weight productivity for exposed produce and leafy vegetables and between interception fraction and dry weight productivity for silage.

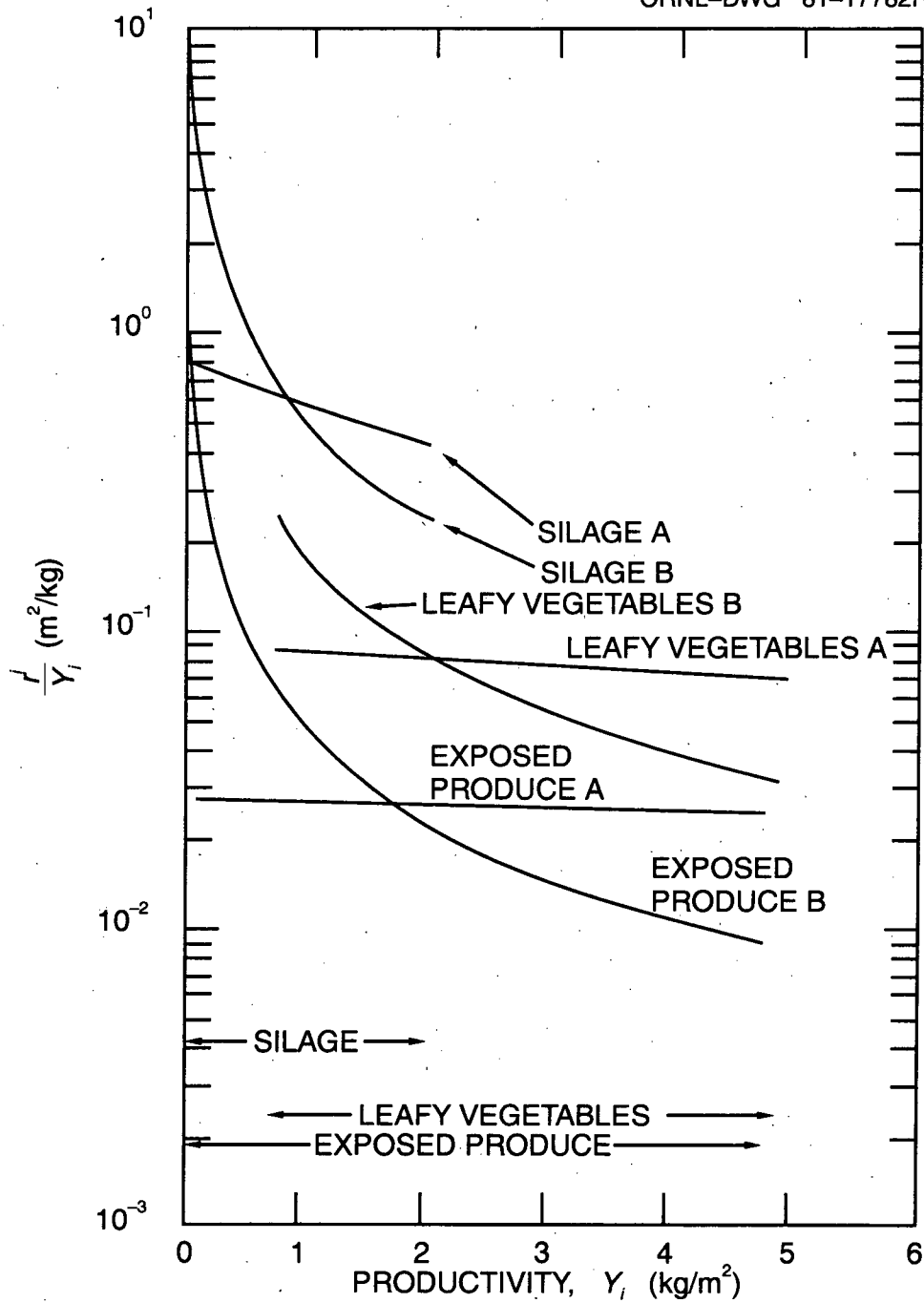


Figure 3.7. The ratio of interception fraction to productivity (r^i/Y_i) as a function of interception fraction dependent on (A) and independent of (B) productivity of silage, exposed produce, and leafy vegetables. The ranges of productivity found in the U.S., based on reference 7, are shown at the bottom of the figure.

4. SITE-SPECIFIC PARAMETERS

For a given location, as specified by a longitude-latitude coordinate (X, Y), TERRA simulates terrestrial transport by incorporating 21 site-specific agricultural and climatological parameters into its calculations. These parameters are available on a $\frac{1}{2} \times \frac{1}{2}$ degree longitude-latitude basis and are part of a data base, called SITE, which includes 36 agricultural, climatological, demographic, and other parameters. The remaining 15 parameters not used by the TERRA code are either used by or are available for use by the other codes of the CRRIS system. The agricultural parameters were derived from the report by Shor, Baes, and Sharp⁷, which analyzes the 1974 Census of Agriculture.²⁰⁹ Climatological parameters were interpolated from long-term averages recorded by United States weather stations as reported in several sources.²¹⁰⁻²¹² Demographic parameters describing the fraction of the population in various urbanization categories were available on a half-degree cell basis from the analyses of the 1970 U.S. Census by Haaland and Heath.^{213,214} Estimates of population were taken from the 1980 U.S. Census.

The half-degree cell grid was preferred over the United States county resolution because of the variation in county area (Fig. 4.1). Bristol county, Rhode Island, the smallest county, is 64.5 km², and San Bernardino county, California, the largest, is 52,100 km², a range of over 800 fold. Half-degree cells provide a more uniform grid (Fig. 4.2). The areas of the cells vary from 2,030 km² at 49°N latitude to 2,810 km² at 25°N latitude—a variation of less than 30% over the conterminous United States. Half-degree cell areas are comparable to the areas of counties in northeast Texas (Fig. 4.1).

Each SITE cell is defined by an identification number, i , such that

$$i = 2[(X - 66.5) + 116(Y - 24.5)], \quad (27)$$

where

- X = the longitude (in degrees W) of the southeast corner of the cell and
- Y = the latitude (in degrees N) of the southeast corner of the cell.

Equation (27) is based on the reference point 66.5°W, 24.5°N and the fact that the conterminous United States lies between 66.5°W and 125°W. One hundred and sixteen half-degree cells define this span, horizontally.

Two methods were needed to convert county data to half-degree cell data because some data were stored per unit area and others were stored as a total count. The data stored as a total count was distributed according to the fraction of each county included in the individual cell (method A). The data stored per unit area was distributed according to the fraction of each cell included in the appropriate counties (method B). Both of these transformation fractions were determined for each SITE cell and each United States county using the IUCALC program which calculates polygon-polygon intersections, unions, and relative differences.²¹⁵ Table 4.1 shows the derivation of the number of cattle and calves, n_c , and productivity of protected produce, Y_p , for SITE cell #3284, which has coordinates at the southeast corner of 84.5°W, 38.5°N. Three counties in Indiana and nine counties in Kentucky overlap this cell.

Method A is used for all parameters representing discrete entities, e.g., head of livestock, numbers of people, kilograms of produce. The assumption in effect is that number distribution is uniform throughout the county. The proportion of the county total within the cell is proportional to the area of the county within the cell. Method B is used for all parameters representing densities and representative averages, e.g., productivities and climatic variables. The effective assumption here is that the contribution from the county to the cell is proportional to the fraction of the cell which coincides with the county.

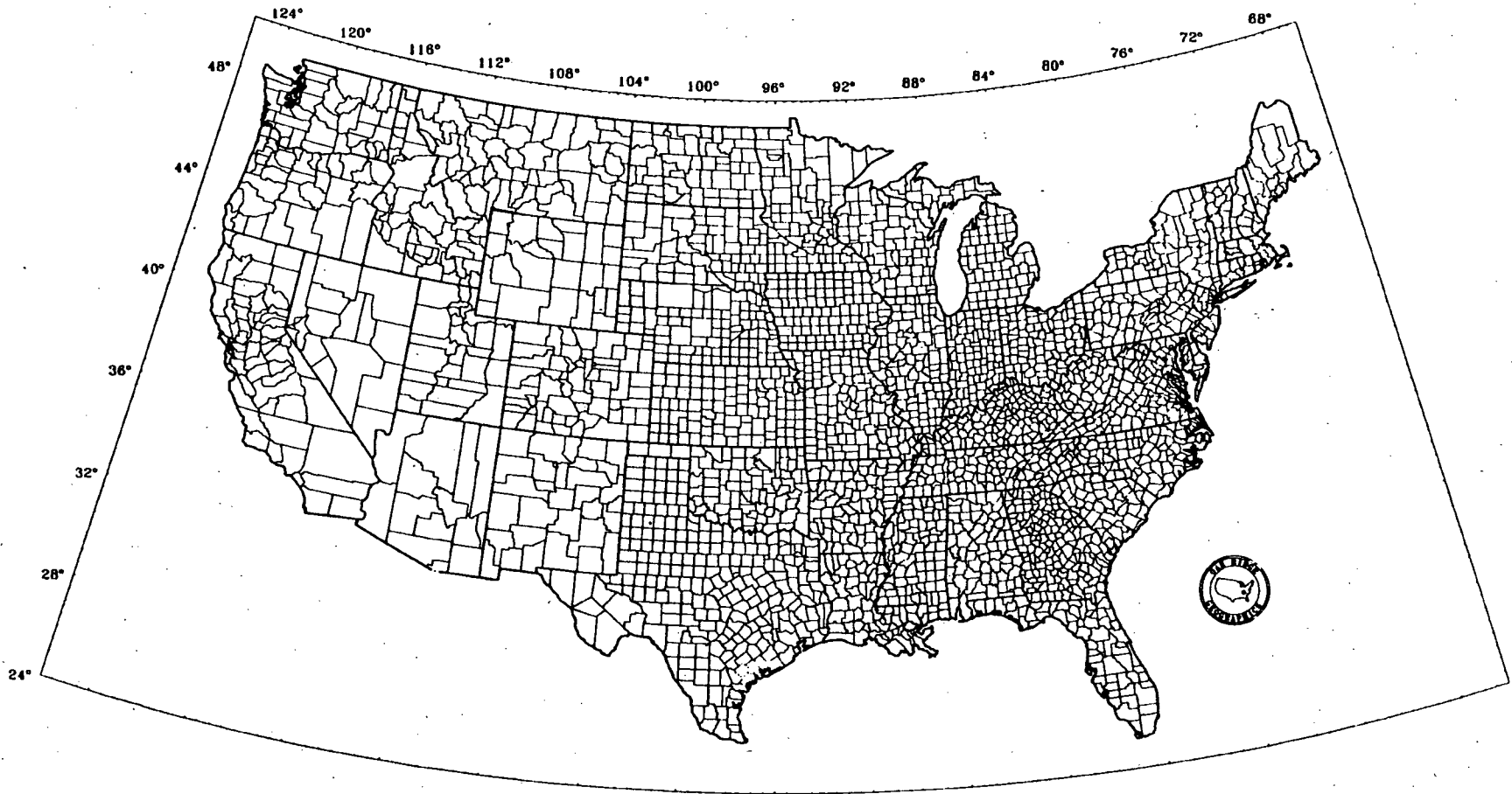


Figure 4.1. Map of the conterminous United States showing county delineations.

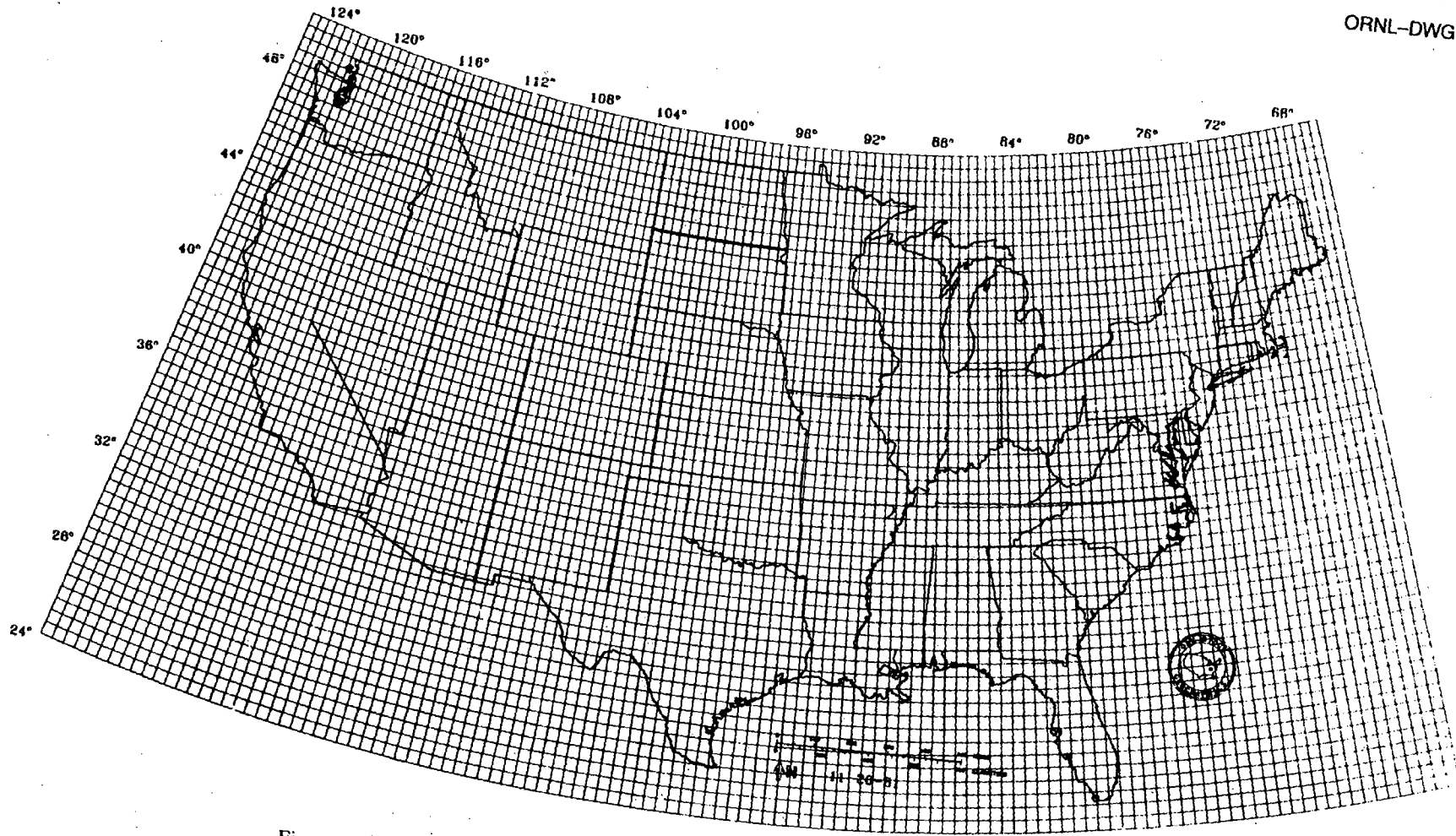


Figure 4.1. Map of the conterminous United States with half degree longitude-latitude grid indicated.

Table 4.1. Example derivation of agricultural parameters for SITE cell #3284 from county-averaged parameters

County, state ^a	— Transfer parameter ^b —		n_c^c (head)	Y_p^d (kg/m ²)
	Method A	Method B		
Dearborn, In	3.60×10^{-3}	1.25×10^{-3}	17288	1.52
Ohio, In	5.59×10^{-1}	5.51×10^{-2}	7111	0.060
Switzerland, In	3.74×10^{-1}	9.38×10^{-2}	12863	0.060
Boone, Ky	6.18×10^{-1}	1.75×10^{-1}	20926	1.42
Carroll, Ky	8.45×10^{-2}	1.25×10^{-2}	11370	0.040
Gallatin, Ky	9.71×10^{-1}	1.10×10^{-1}	7512	2.12
Grant, Ky	9.31×10^{-1}	2.63×10^{-1}	22148	0.61
Harrison, Ky	9.00×10^{-4}	3.14×10^{-4}	44345	1.22
Henry, Ky	2.60×10^{-3}	8.52×10^{-4}	36319	0.78
Kenton, Ky	4.74×10^{-1}	8.88×10^{-2}	10633	1.18
Owen, Ky	4.91×10^{-1}	1.96×10^{-1}	26555	0.75
Pendleton, Ky	1.32×10^{-2}	4.18×10^{-3}	24125	0.82
Total or average			69190	0.99

^aAll counties which share area with SITE cell #3284 which has coordinates of southeast corner of 84.5°W, 38.5°N.

^bFor method A parameter is fraction of each county within the cell. For method B parameter is fraction of cell within each county.

^cNumber of cattle and calves.

^dYield of protected produce.

Climatological parameters were determined on a half degree cell basis by selecting the three United States weather stations nearest the centroid of the cell. The three parameter values for the weather stations were weighted according to distance from the weather station to the cell centroid such that

$$p_c = w_1 p_1 + w_2 p_2 + w_3 p_3, \quad (28)$$

where

- p_c = the parameter value for the half degree cell,
 w_1, w_2, w_3 = the weighting factors for the first, second, and third nearest weather stations, respectively, and
 p_1, p_2, p_3 = the parameter values for the first, second, and third nearest weather stations, respectively.

The weighting factors were defined such that

$$w_1 + w_2 + w_3 = 1 \text{ and} \quad (29)$$

$$w = \frac{1}{d_i}, \quad (30)$$

where

d_i = the linear distance between the weather station and the centroid of the cell.

The linear distance between weather stations and the centroid of the cell was determined by

$$\frac{\text{kilometers}}{1.0^\circ \text{ longitude}} = A \cos Y + B + CY + DY^2 \text{ and} \quad (31)$$

$$\frac{\text{kilometers}}{1.0^\circ \text{ latitude}} = \frac{\text{Eq. (31)}}{\cos Y} + E + FY + GY^2. \quad (32)$$

where

$$\begin{aligned} A &= 1.113 \times 10^2, \\ B &= -9.855 \times 10^{-2}, \\ C &= 7.789 \times 10^{-3}, \\ D &= -5.894 \times 10^{-5}, \\ E &= -8.570 \times 10^{-1}, \\ F &= 7.927 \times 10^{-1}, \text{ and} \\ G &= 5.888 \times 10^{-5}. \end{aligned}$$

Table 4.2 shows example derivations of cell-averaged values of frost-free days from values from the three nearest United States weather stations.

4.1 Agricultural Parameters

The SITE data base contains 21 parameters describing location-specific agricultural practice, 14 of which are used by TERRA in simulating terrestrial transport of radionuclides. In addition, the climatic parameter, number of frost-free days, is used to estimate the number of harvests of hay and grazings of pasture by cattle. These parameters are described in detail in the report by Shor, Baes, and Sharp⁷. It is beyond the scope of this report to detail their derivation, but a brief description of their use in TERRA follows.

As discussed in Sect. 3., atmospheric deposition on edible portions of food and feed crops is inversely proportional to standing crop biomass. The best estimate of standing crop biomass at harvest is given by the productivity, defined as

$$Y_i = \frac{P_{hi}}{A_{hi}}, \quad (33)$$

where

$$\begin{aligned} Y_i &= \text{the productivity (yield) of crop } i \text{ (kg/m}^2\text{)}, \\ P_{hi} &= \text{the harvest yield (production) of crop } i \text{ (kg) per harvest, and} \\ A_{hi} &= \text{the area planted to crop } i \text{ which is harvested or harvest area (m}^2\text{)}. \end{aligned}$$

For leafy vegetables, exposed and protected produce, grains, and silage, harvest yields and areas were obtained directly from the 1974 Census of Agriculture. However, for hay and pasture only, annual yields (summed over all harvests) and areas allocated for hay and pasture (not necessarily

Table 4.2. Derivation of number of frost-free days for half-degree cells from values for the three nearest weather stations to the centroid of the cell^a

Cell#	Longitude ^b	Latitude ^c	Stations	Weighting factors ^d			Frost-free days
				w ₁	w ₂	w ₃	
3615	76.0	40.0	B, A, C	0.462	0.287	0.251	203
3616	75.5	40.0	B, F, E	0.858	0.074	0.067	201
3617	77.0	40.0	B, F, E	0.612	0.225	0.163	201
3618	77.5	40.0	B, F, E	0.436	0.342	0.222	200
3731	76.0	40.5	A, B, D	0.372	0.334	0.294	185
3732	76.5	40.5	B, A, D	0.489	0.262	0.249	189
3733	77.0	40.5	B, F, D	0.525	0.241	0.234	189
3847	76.0	41.0	D, A, B	0.508	0.279	0.213	181

^aThe following weather station values were used:

- A = Allentown, Pa: 180 frost-free days
- B = Harrisburg, Pa: 201 frost-free days
- C = Philadelphia, Pa: 232 frost-free days
- D = Scranton, Pa: 174 frost-free days
- E = Baltimore, Md: 234 frost-free days
- F = Frederick, Md: 176 frost-free days.

^bSoutheast corner of cell.

^cFirst, second, and third nearest weather station, respectively.

^dGiven by Eqs. (30) and (31).

areas actually harvested) were given or derived from census information. Thus, for hay and pasture Shor, Baes, and Sharp⁷ calculated "areal yields" defined by

$$Y_i^a = \frac{P_{ai}}{A_i}, \quad (34)$$

where

- Y_i^a = the areal yield of crop i (kg/yr/m²),
- P_{ai} = the annual yield of crop i (kg/yr), and
- A_i = the inventory area for crop i (m²).

The sum of all harvest yields (production) and productivity estimates for leafy vegetables (Figs. 4.3 and 4.4), exposed produce (Figs. 4.5 and 4.6), protected produce (Figs. 4.7 and 4.8), grain for food (Figs. 4.9 and 4.10), grain for feed (Figs. 4.11 and 4.12), and silage (Figs. 4.13 and 4.14) are included in the SITE data base. Also included are the annual yield (production) of hay (Fig. 4.15) and areal yield estimate for hay (Fig. 4.16). The areal yield of pasture estimate is not included in the SITE data base, but is calculated in TERRA from information contained in SITE (as discussed below). The productivity estimates for hay and pasture are calculated by dividing areal yields by the estimated numbers of hay harvests and successive pasture grazings by cattle, respectively.

Number of harvests per year for hay is initially estimated by

$$h_h = \frac{d_{ff}}{60 \text{ days}}, \quad (35)$$

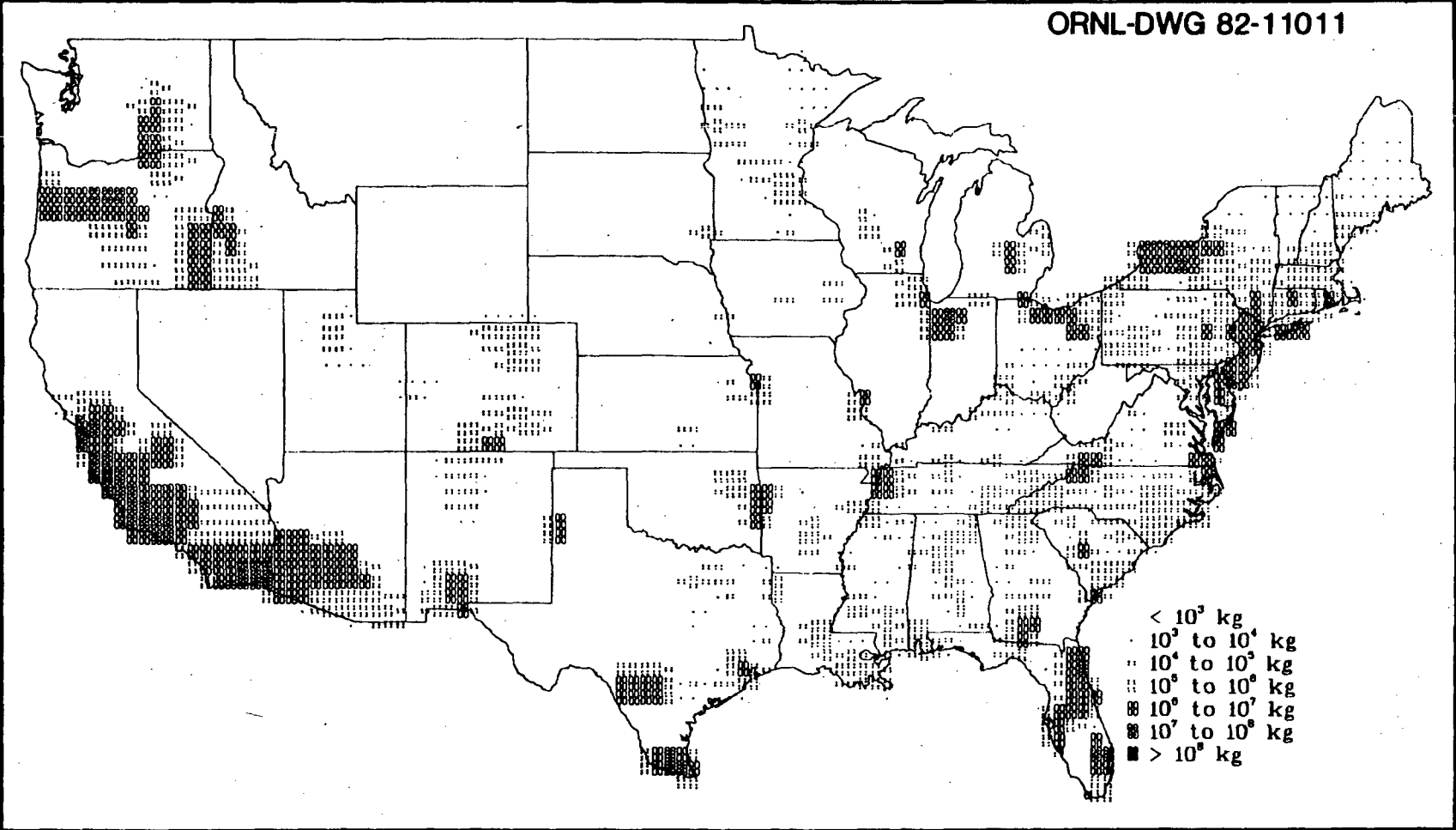


Figure 4.3. Geographic distribution of SITE parameter leafy vegetable production, P_v .

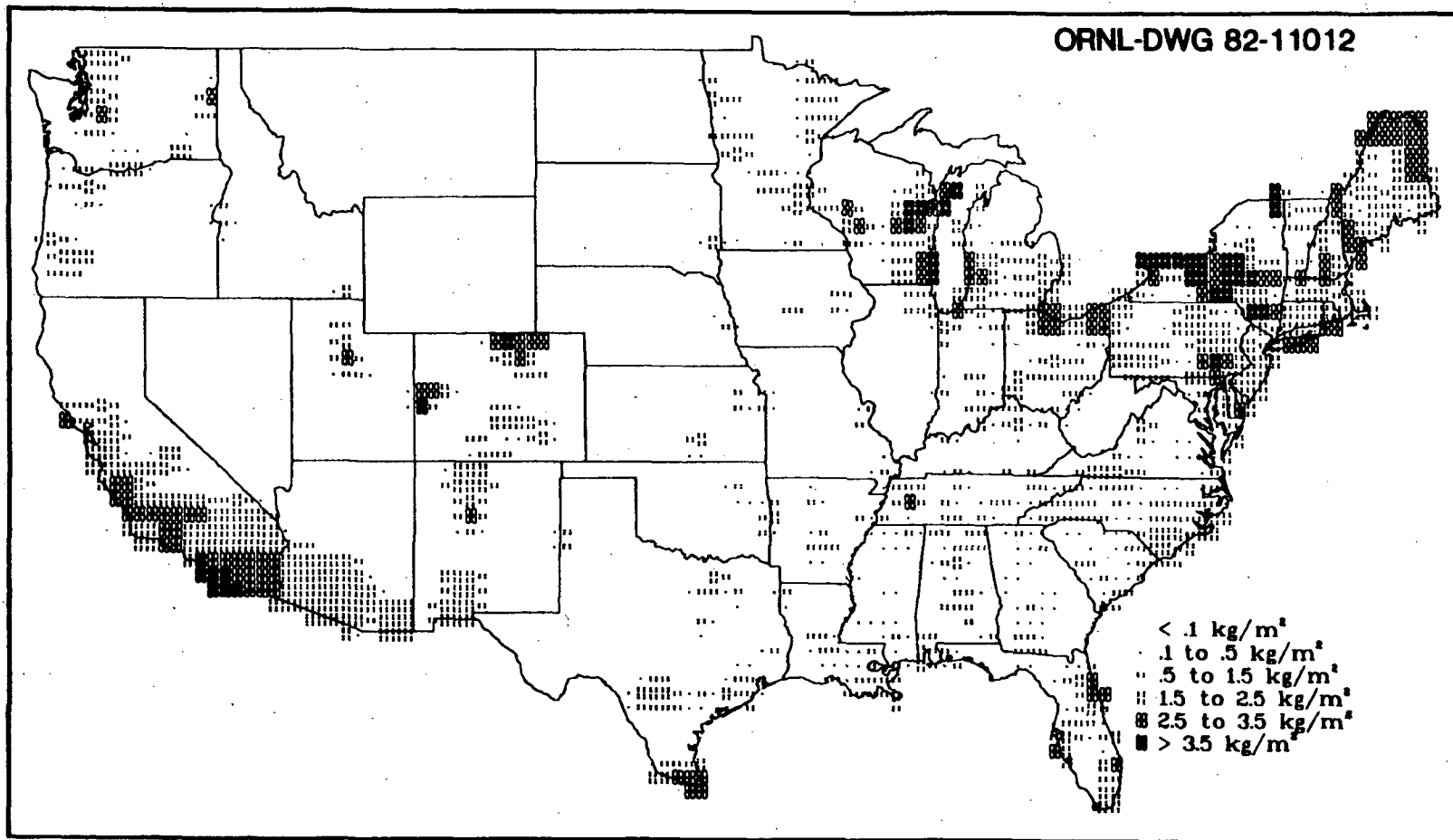


Figure 4.4. Geographic distribution of SITE parameter leafy vegetable productivity, Y_v

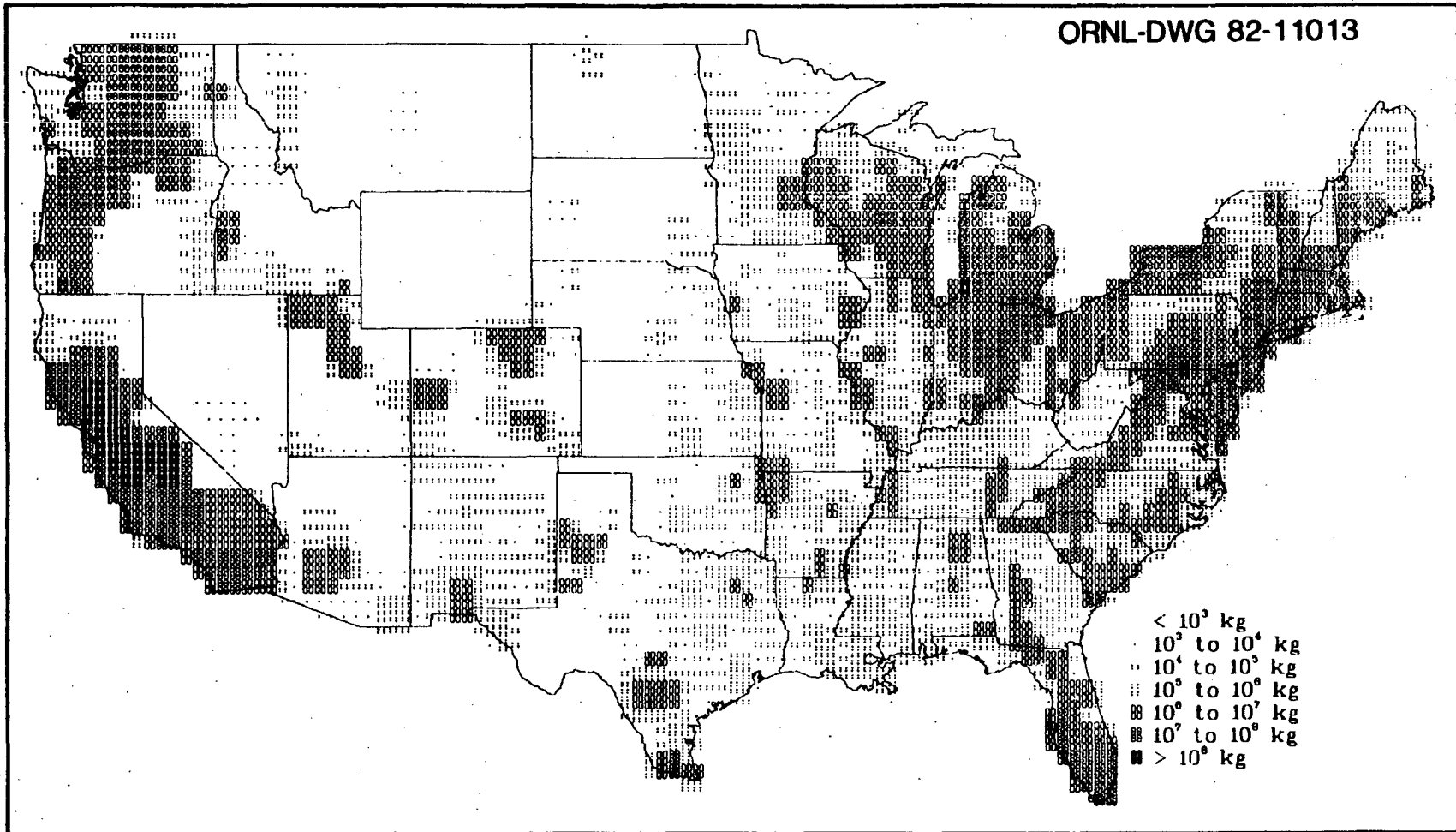


Figure 4.5. Geographic distribution of SITE parameter exposed produce production, P_e .

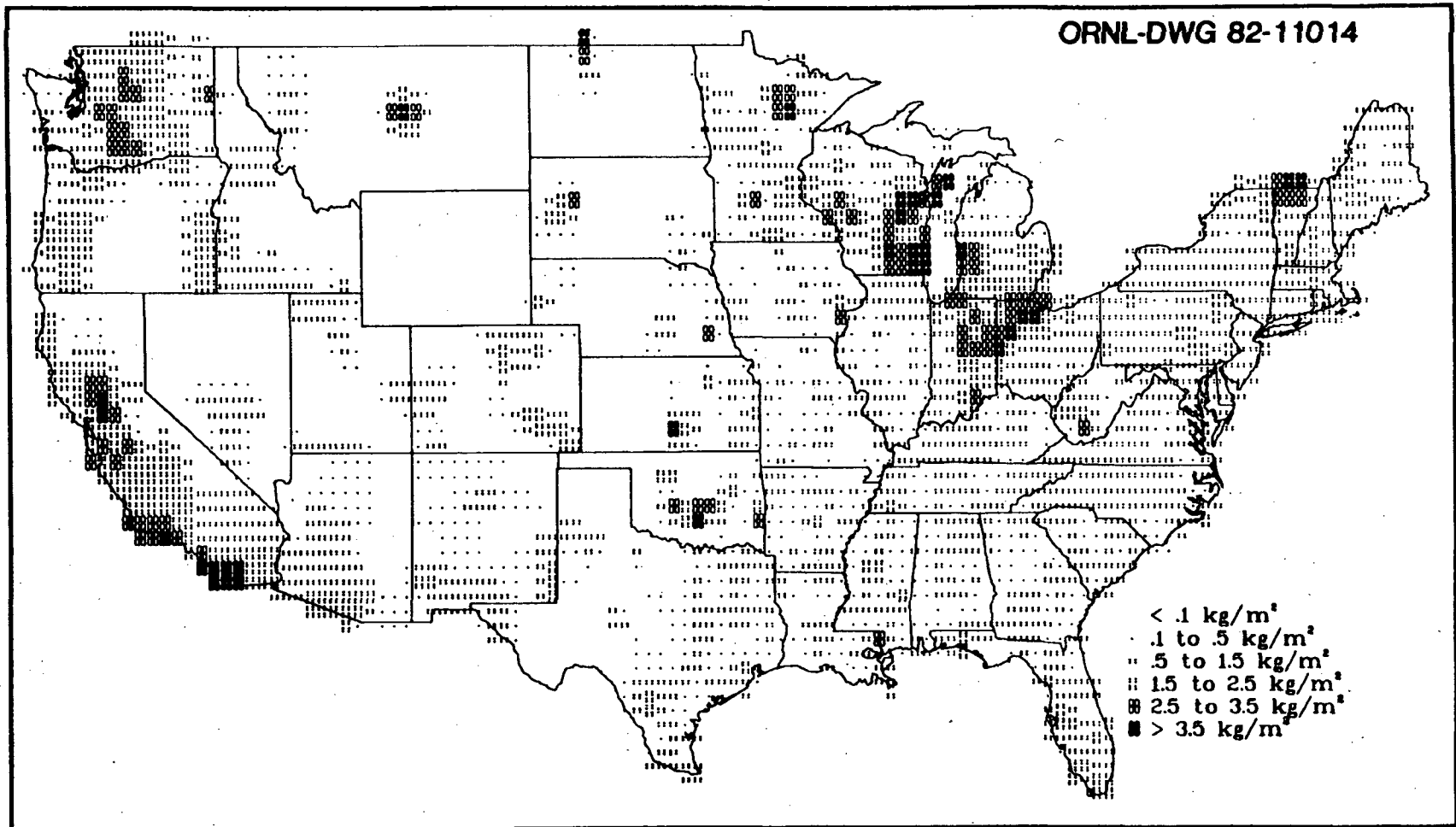


Figure 4.6. Geographic distribution of SITE parameter exposed produce productivity, Y_e

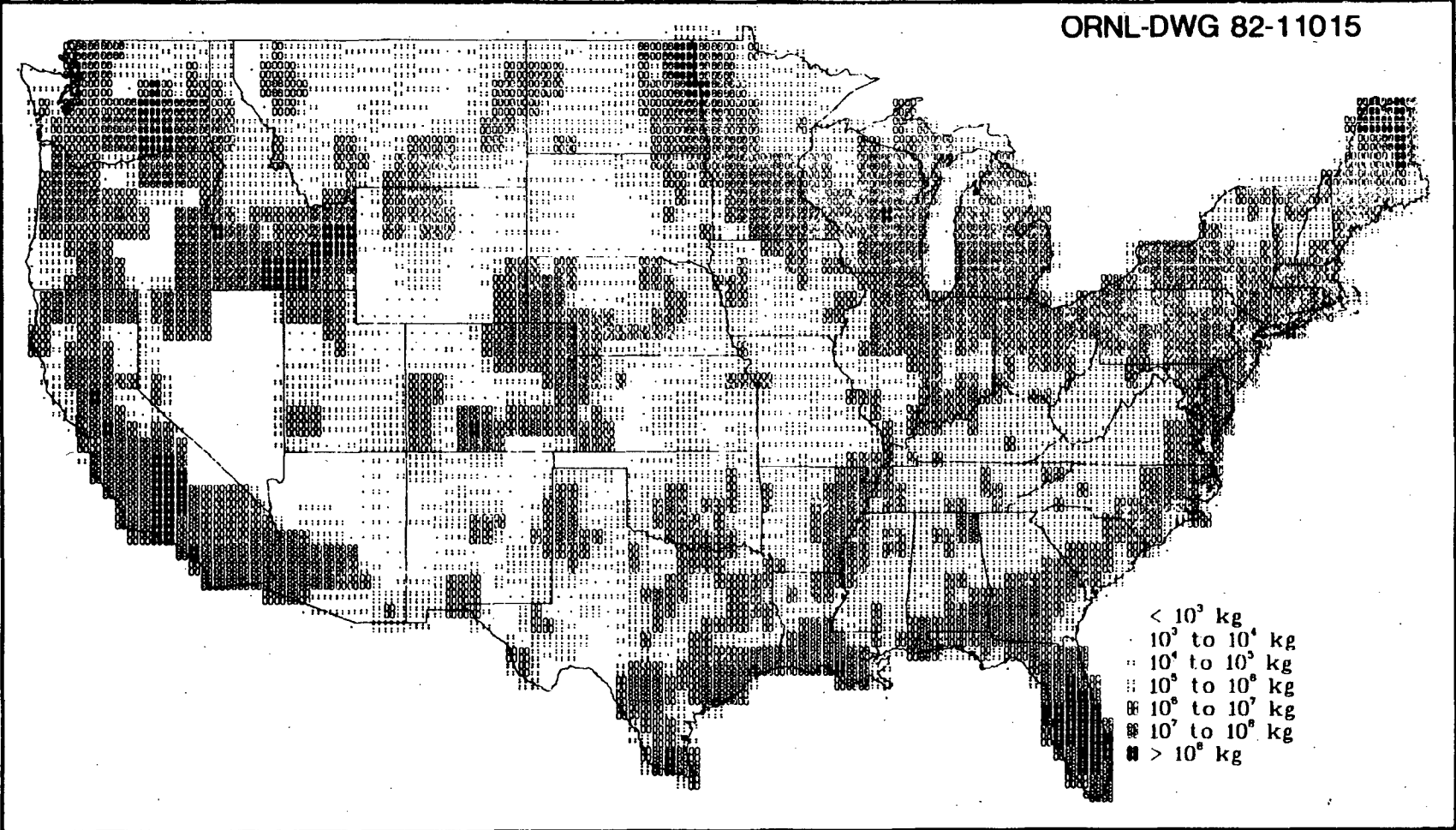


Figure 4.7. Geographic distribution of SITE parameter protected produce production, P_{pp}

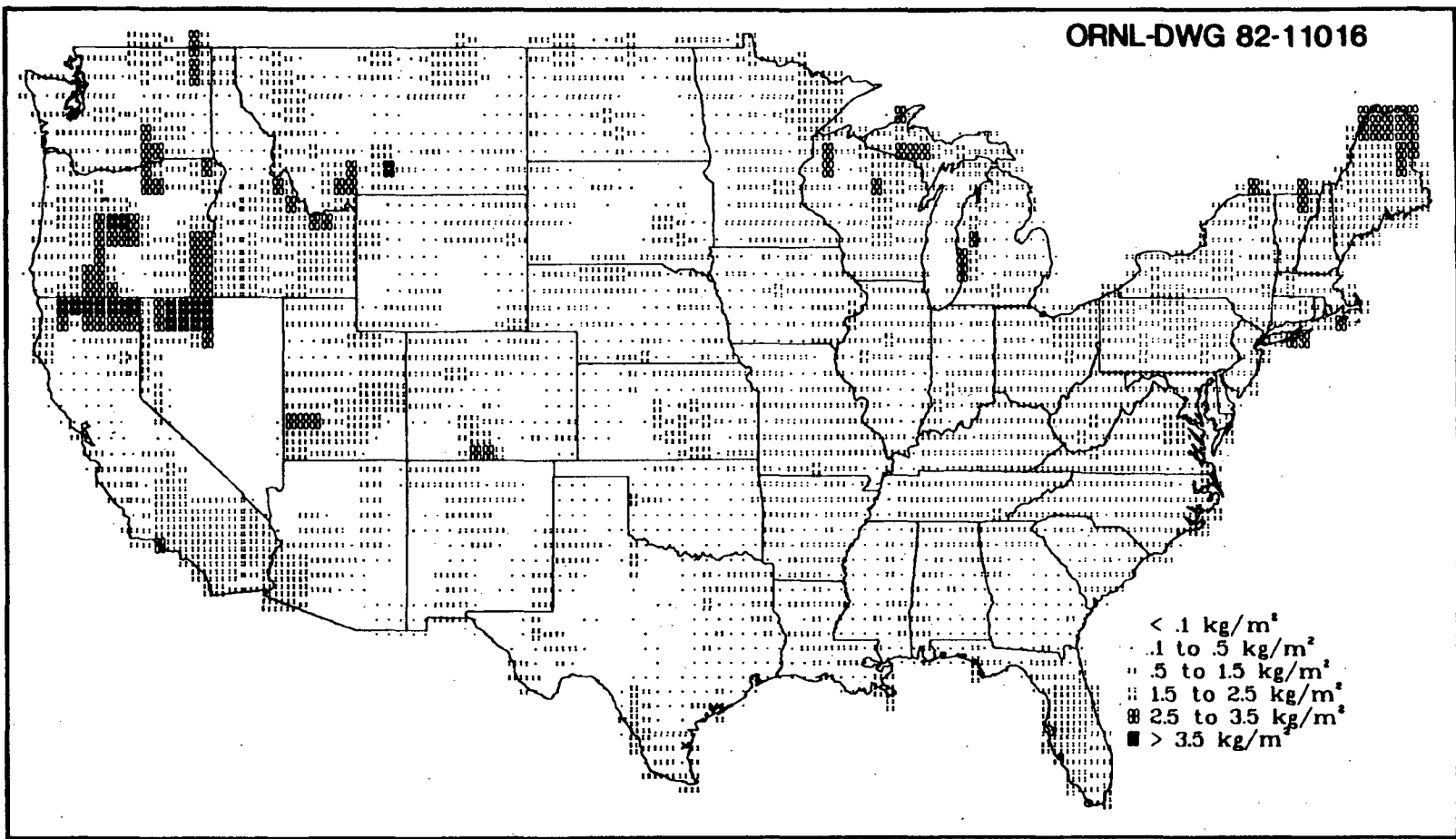


Figure 4.8. Geographic distribution of SITE parameter protected produce productivity, Y_{pp}

ORNL-DWG 82-11017

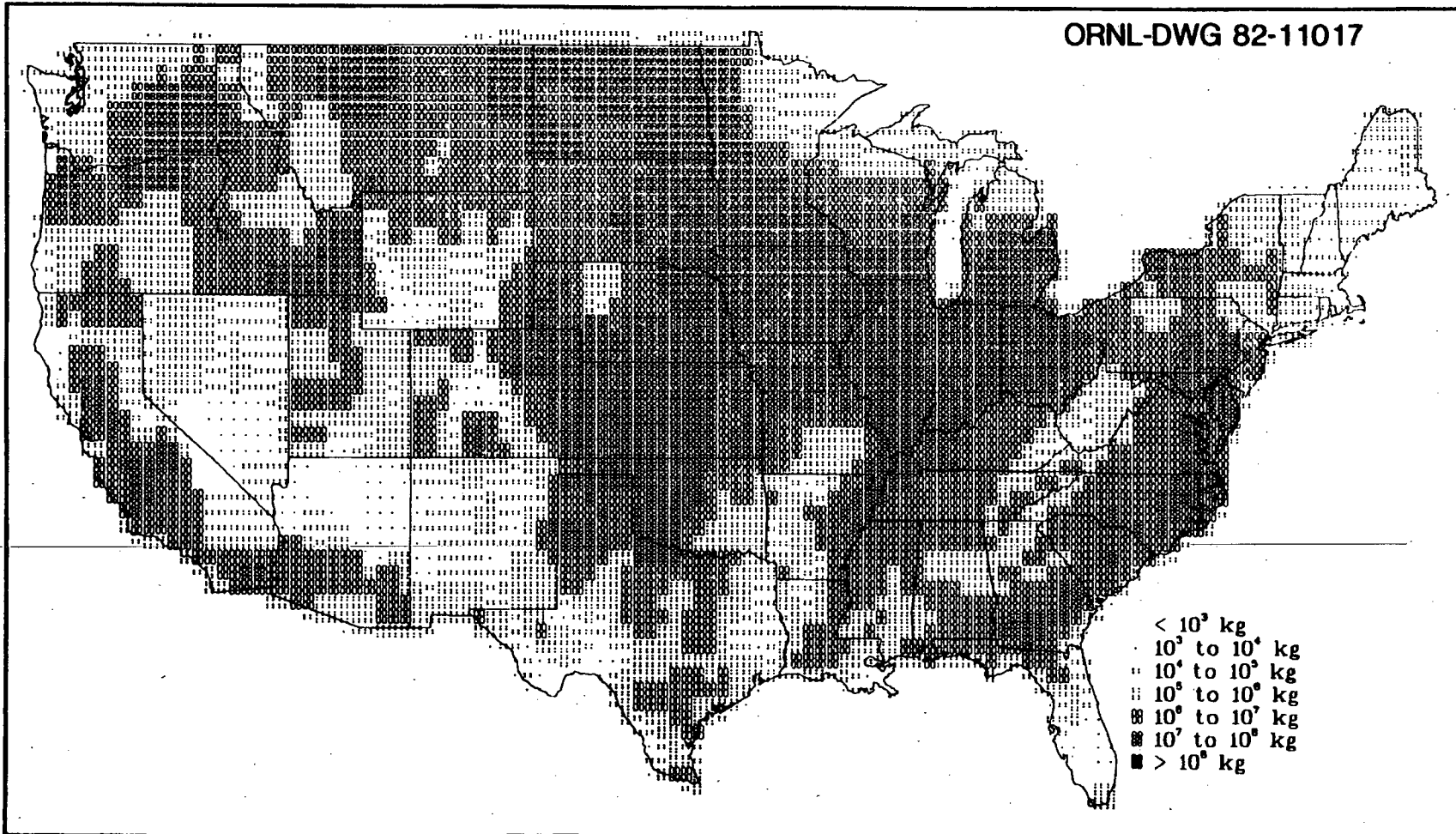


Figure 4.9. Geographic distribution of SITE parameter grain food production, P_{gh}

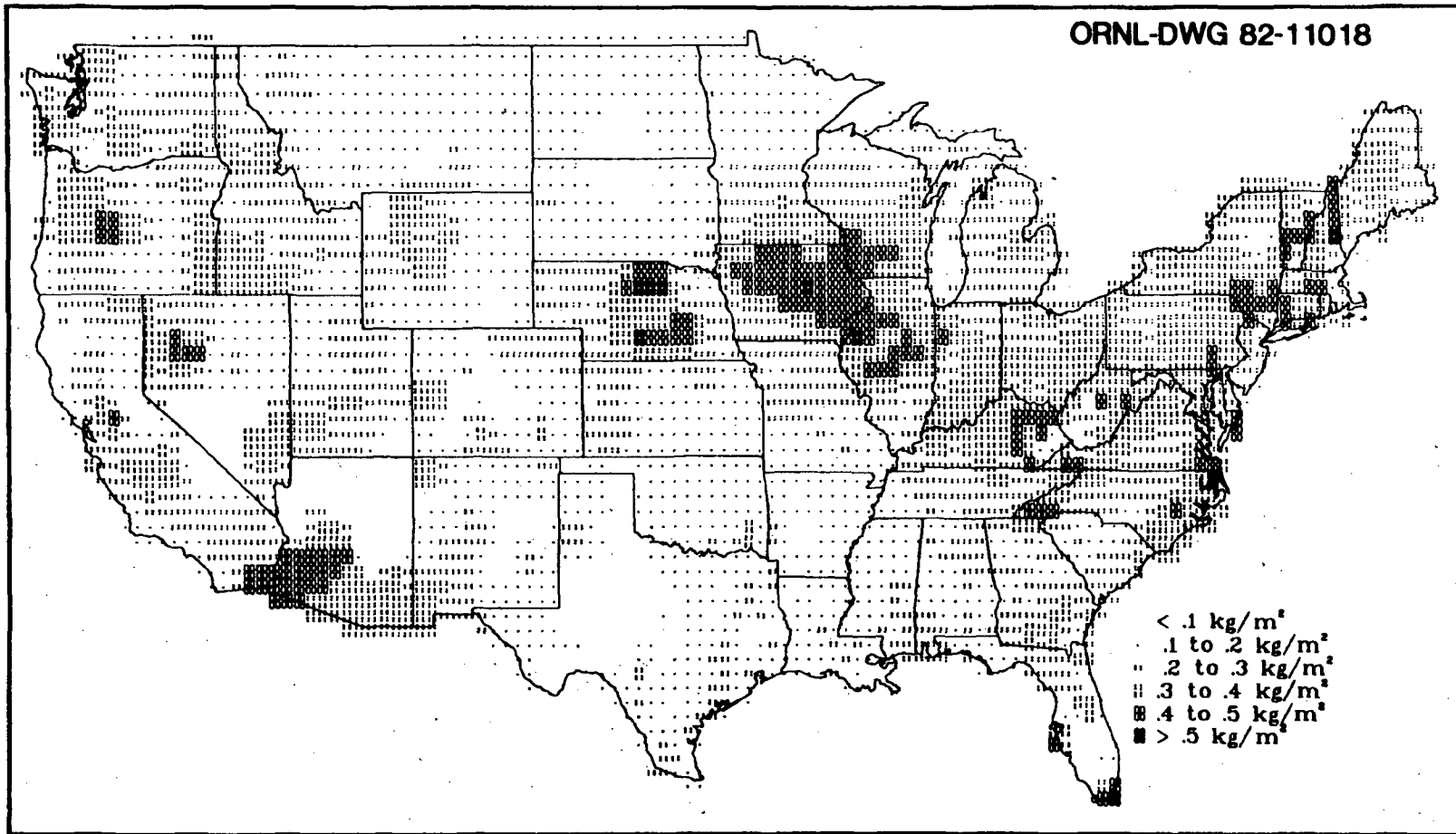


Figure 4.10. Geographic distribution of SITE parameter grain food productivity, $Y_{g,h}$

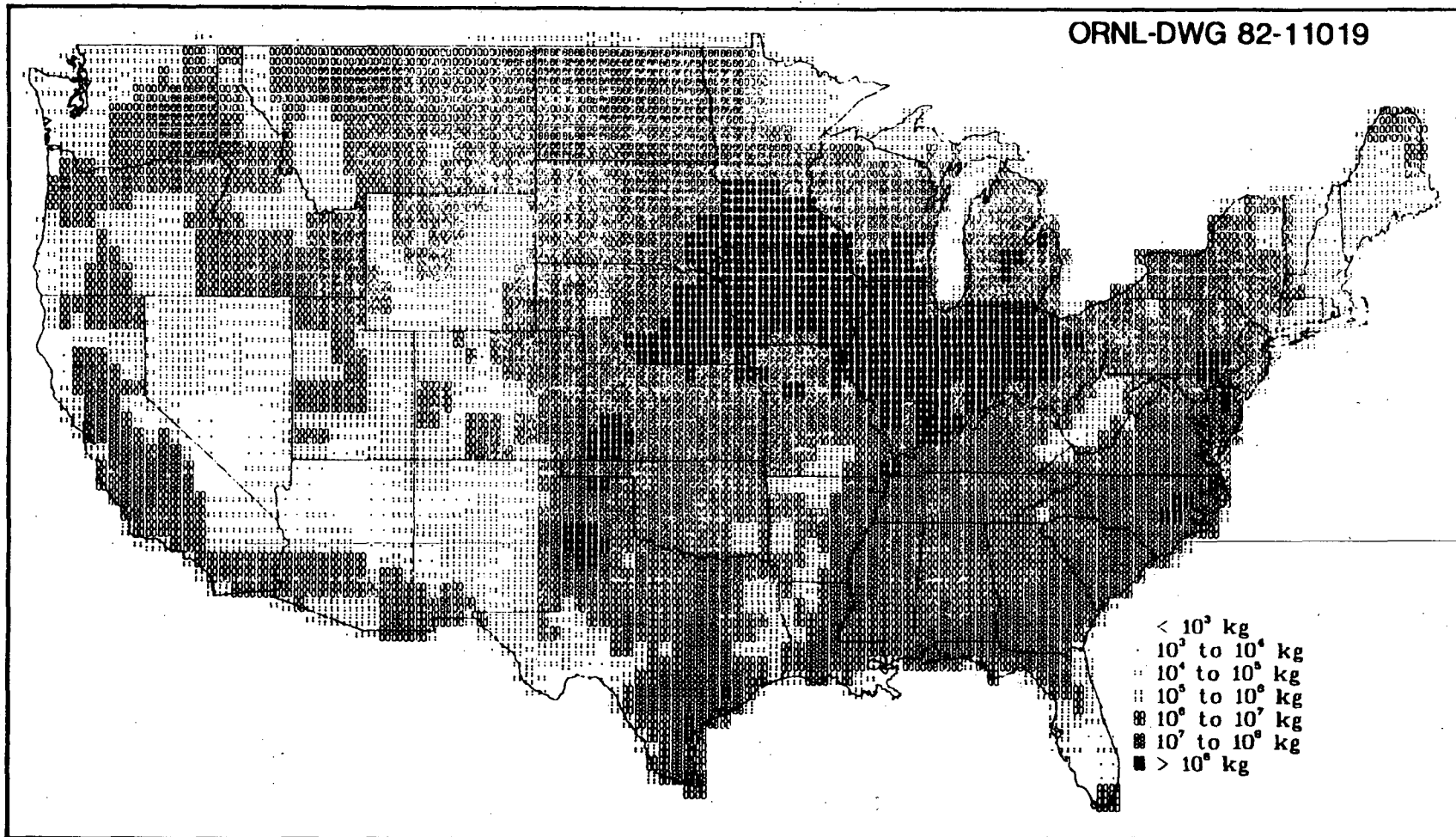


Figure 4.11. Geographic distribution of SITE parameter grain feed production, P_{gf}

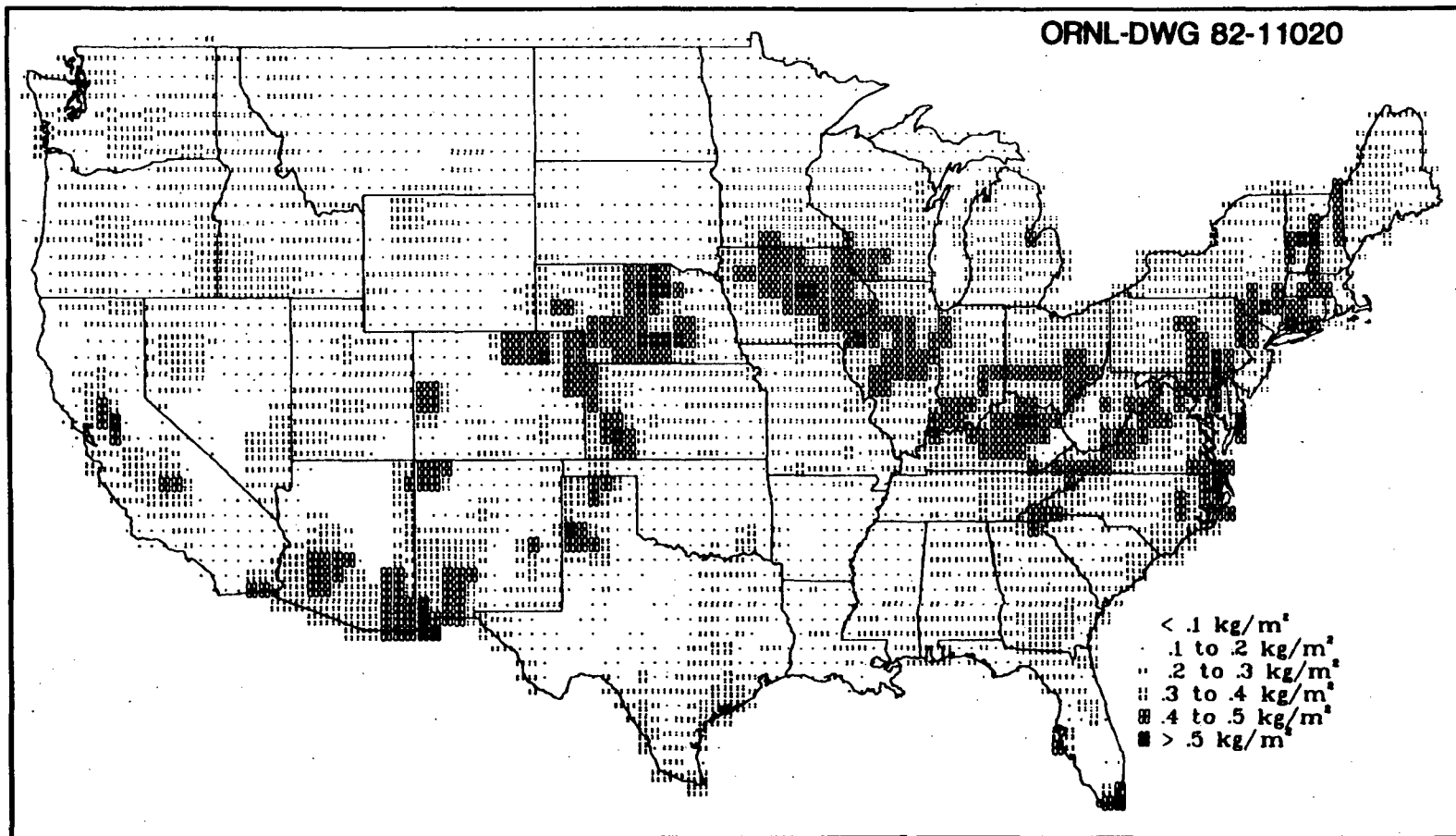


Figure 4.12. Geographic distribution of SITE parameter grain feed productivity, Y_{gf}

ORNL-DWG 82-11023

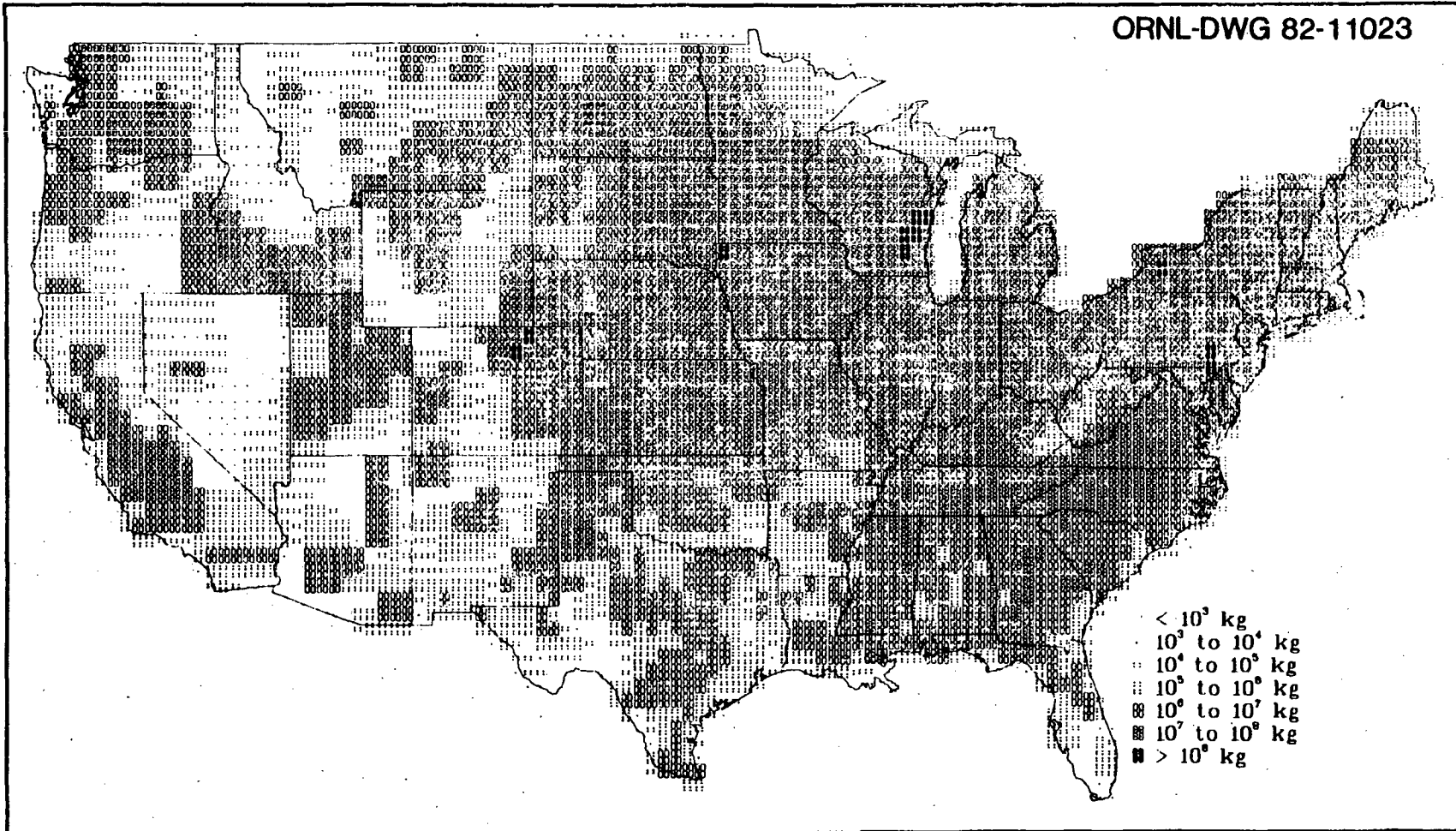


Figure 4.13. Geographic distribution of SITE parameter silage feed production, P_s .

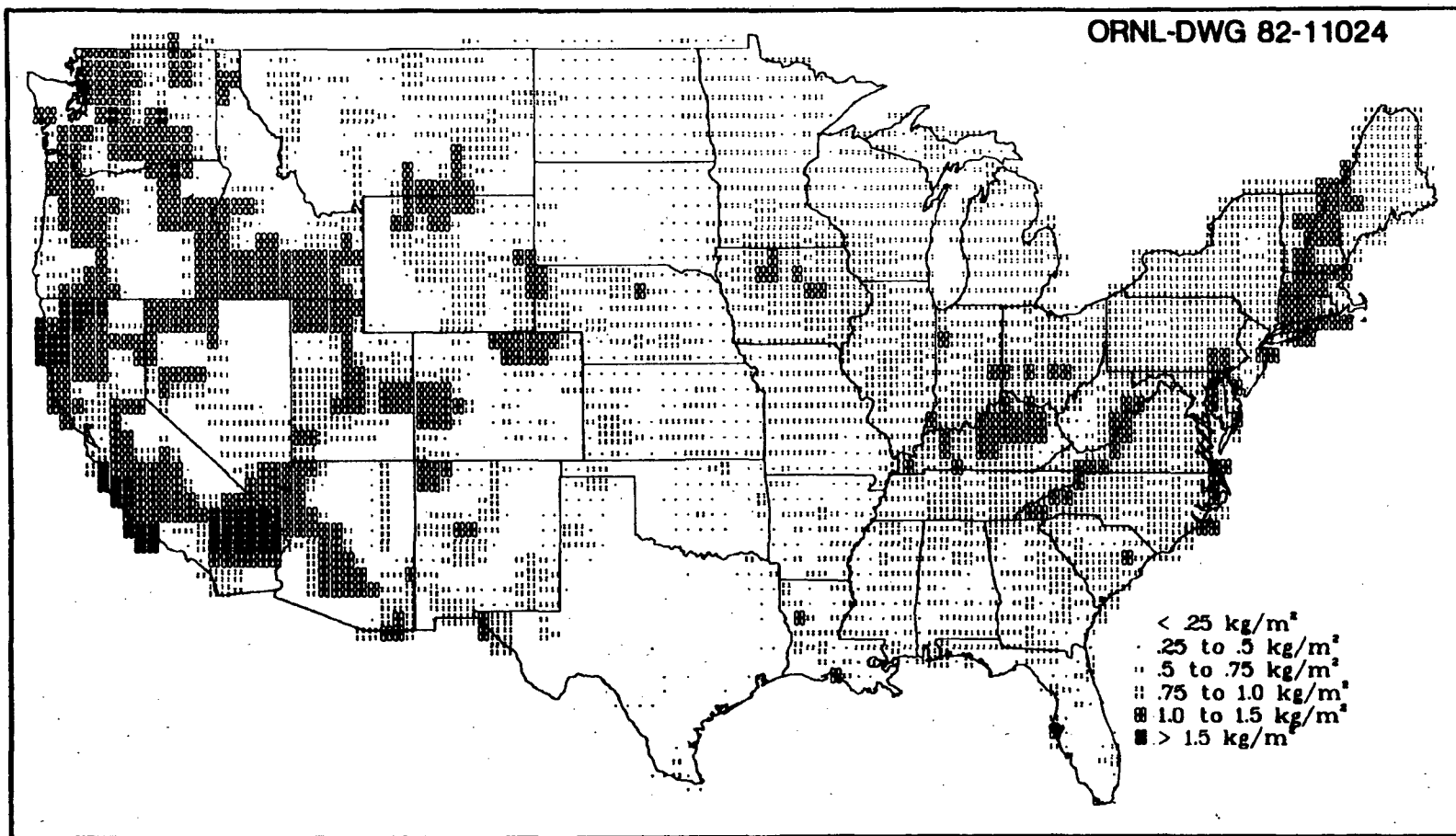


Figure 4.14. Geographic distribution of SITE parameter silage feed productivity, Y_s

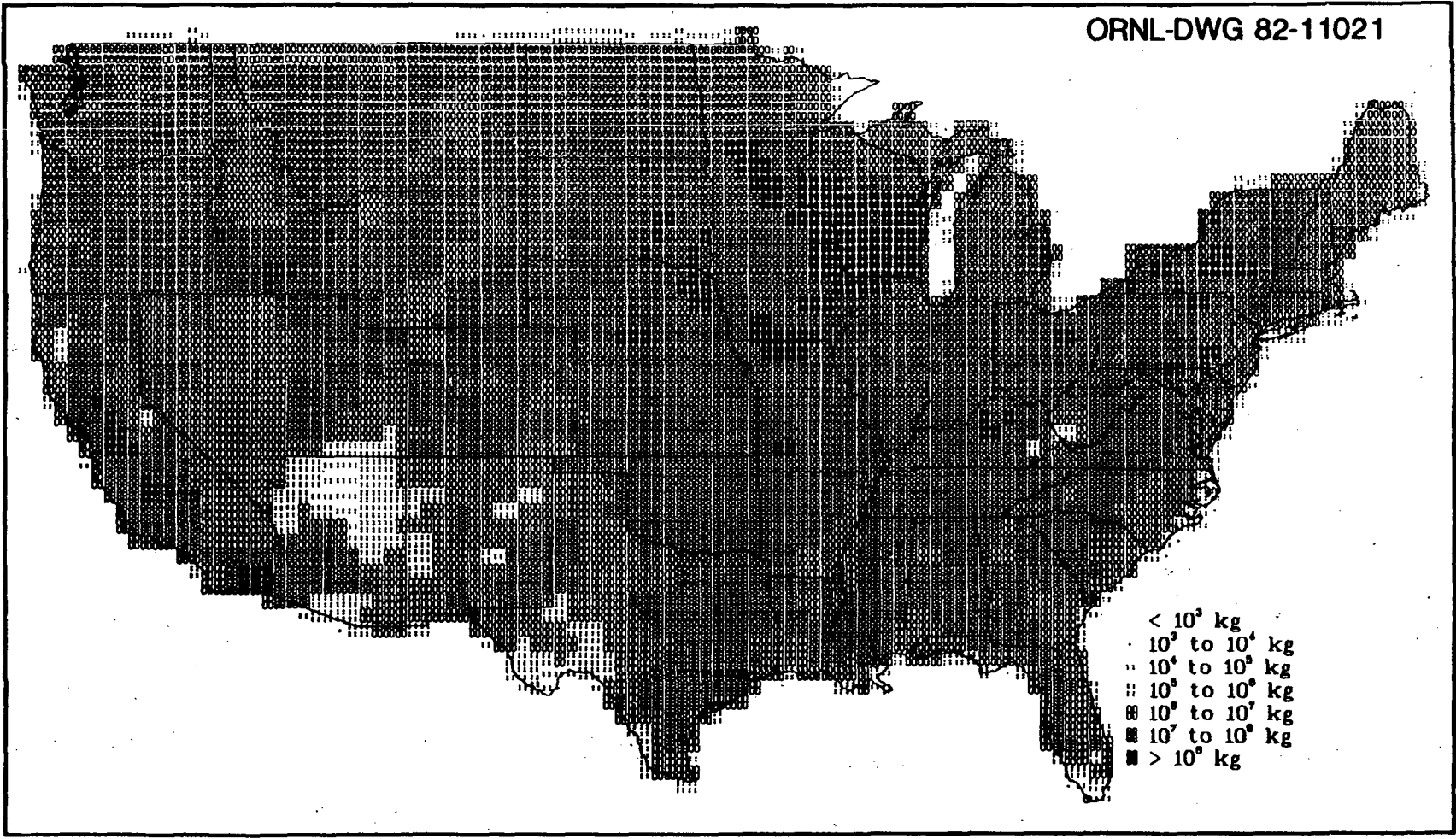


Figure 4.15. Geographic distribution of SITE parameter hay feed production, P_h

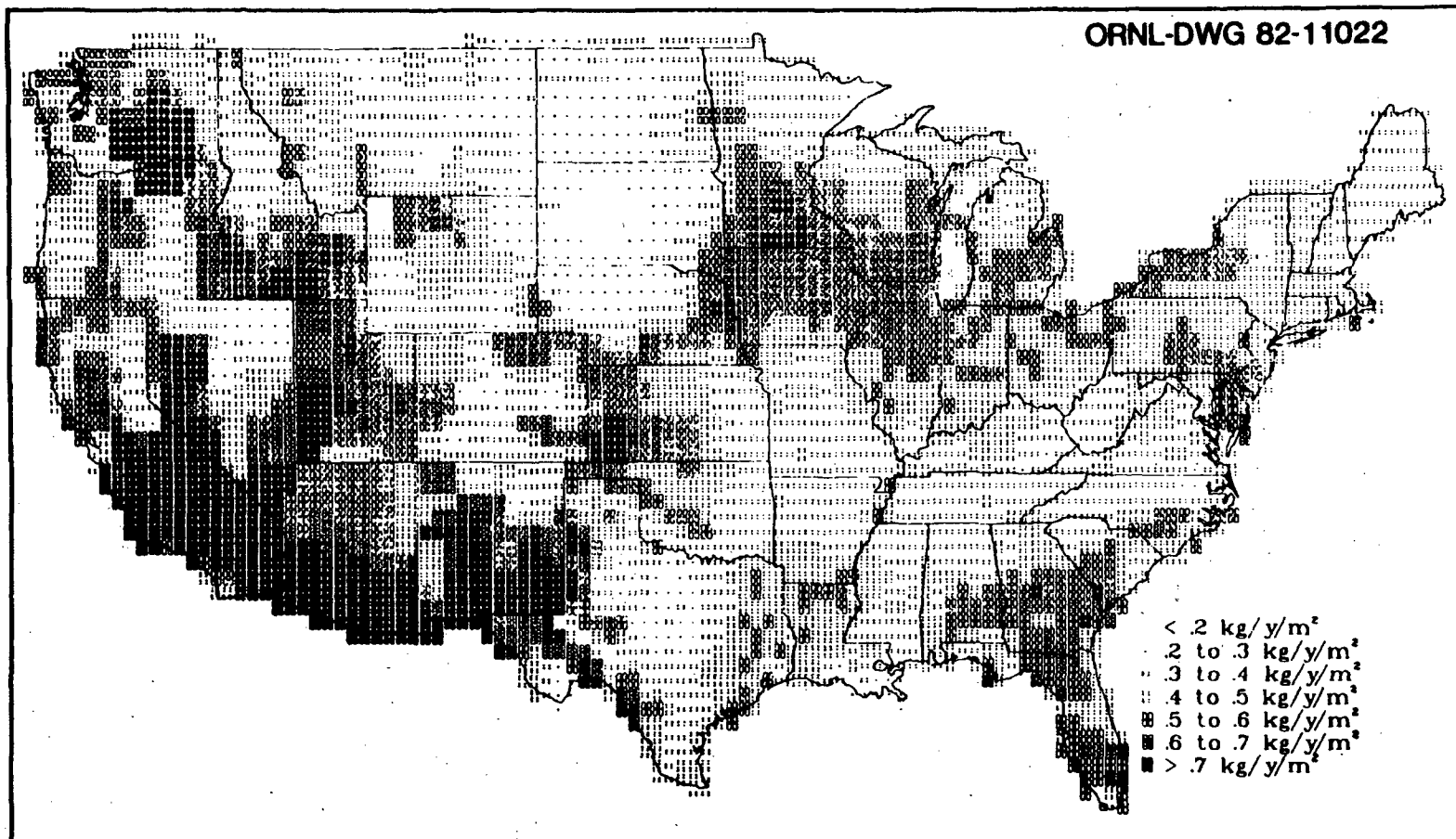


Figure 4.16. Geographic distribution of SITE parameter hay feed areal yield, Y_h^a

where

- h_h = the number of hay harvests (yr^{-1}),
 d_{ff} = the number of frost-free days (day/yr), and
 60 days = the average time between successive hay harvests.⁷

The initial estimate of h_h is rounded off to the nearest integer and hay productivity, Y_h , is calculated according to

$$Y_h = \frac{P_h}{h_h} \quad (36)$$

If $Y_h < 0.10 \text{ kg/m}^2$, then the initial estimate of h_h is reduced to the largest integer for which $Y_h > 0.10 \text{ kg/m}^2$. The value of 0.10 kg/m^2 is considered the minimum productivity at which hay harvesting is economically feasible.⁷ The same general procedure is followed for calculation of pasture grass productivity, Y_{pg} , except that the initial estimate of successive grazings (harvests) by cattle, g_{pg} , is given by

$$g_{pg} = \frac{d_{ff}}{30 \text{ days}}, \quad (37)$$

where

30 days = the average time between successive grazings by cattle.⁶

and the minimum productivity is 0.005 kg/m^2 .⁷ The SITE data base includes estimated number of frost-free days in a year (Fig. 4.17).

In TERRA the areal yield of pasture grass, from which pasture grass productivity is calculated, is estimated from the cattle and calf inventory, n_{cc} (Fig. 4.18), the inventory of milk cows, n_m (Fig. 4.19), the annual sales of cattle on grain, s_g (Fig. 4.20), and the inventory of sheep, n_s (Fig. 4.21), in the manner described in Section 5.1 of the report by Shor, Baes, and Sharp.⁷ Briefly, annual consumption of pasture grass is defined by a mass balance of livestock forage requirement or need and harvested supply. The difference between need and supply is assumed to be pasture consumption. The harvested supply is defined as 75% of hay and silage production, and need is defined according to the numbers and types of forage consuming livestock. The following equations are used to calculate pasture grass areal yield Y_{pg}^a in TERRA:

$$Y_{pg}^a = \frac{C_p}{A_p}, \quad (38)$$

where

- C_p = the annual consumption of pasture in a half-degree cell by livestock (kg/yr) and
 A_p = the area of pasture (Fig. 4.22) in the cell (m^2).

Pasture consumption is calculated according to

$$C_p = R_f - 0.75P_{hf}, \text{ and} \quad (39)$$

$$P_{hf} = P_s + P_h,$$

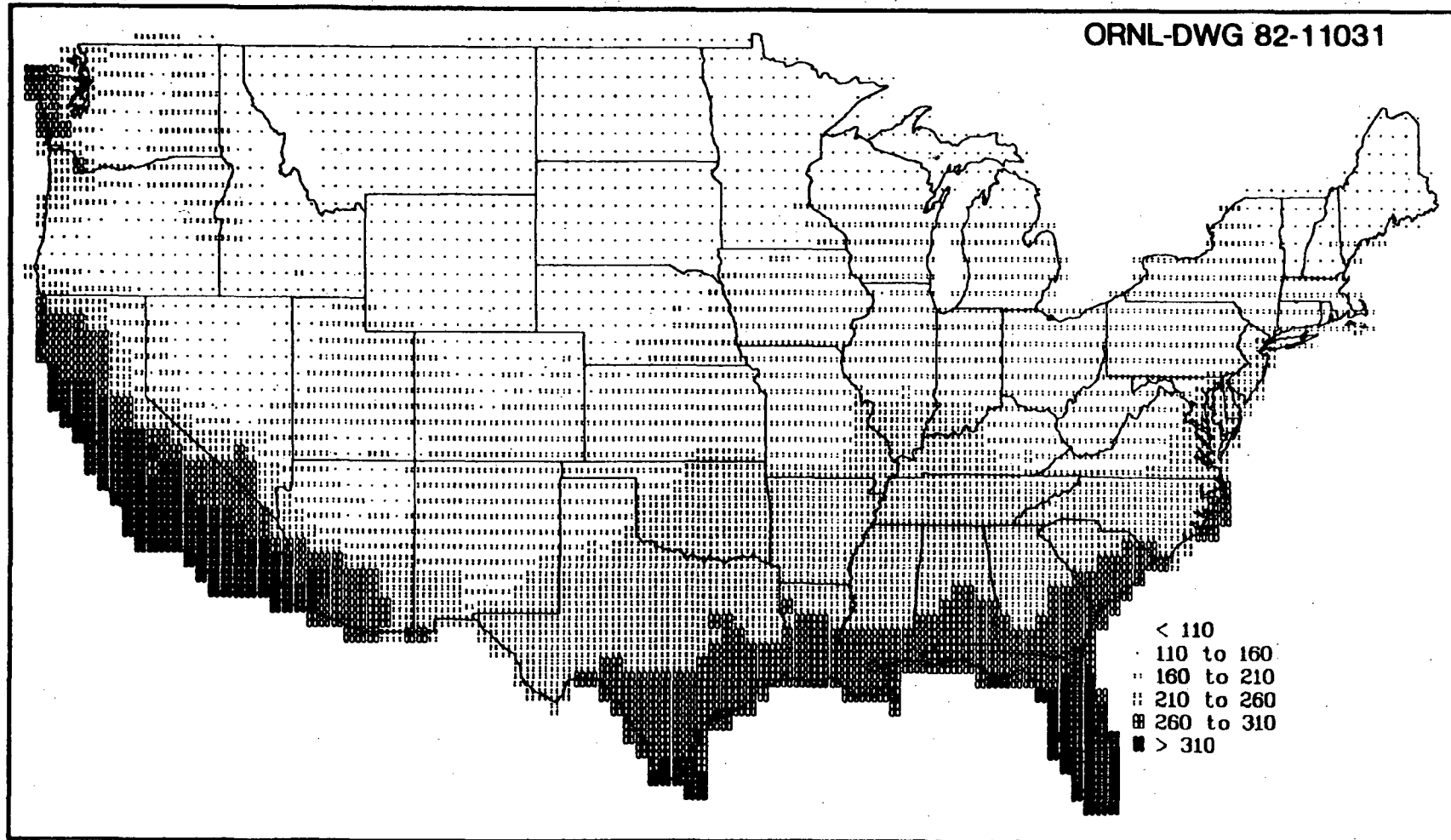


Figure 4.17. Geographic distribution of SITE parameter number of frost-free days, d_f

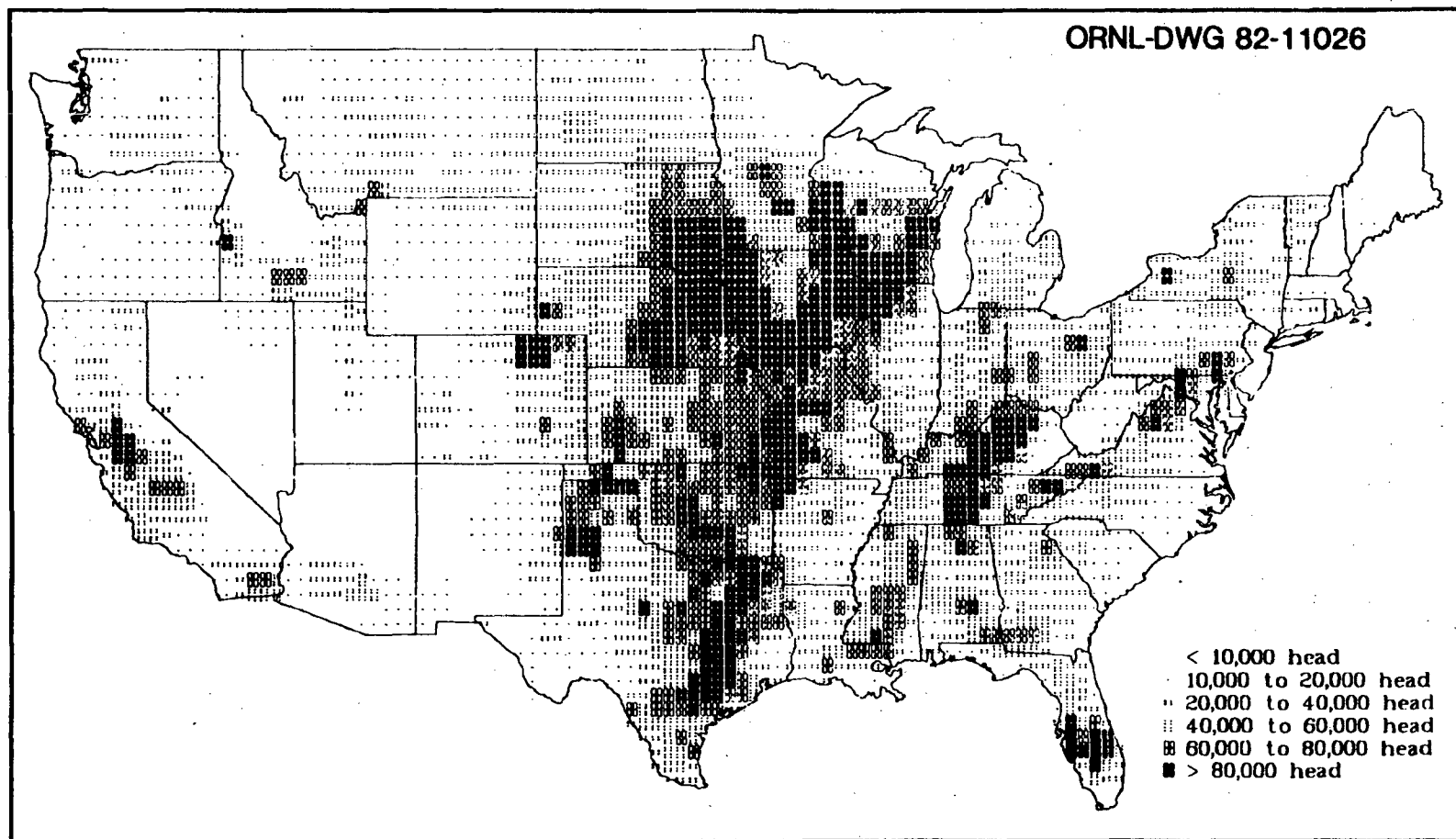


Figure 4.18. Geographic distribution of SITE parameter number cattle and calves inventory, n_{cc}

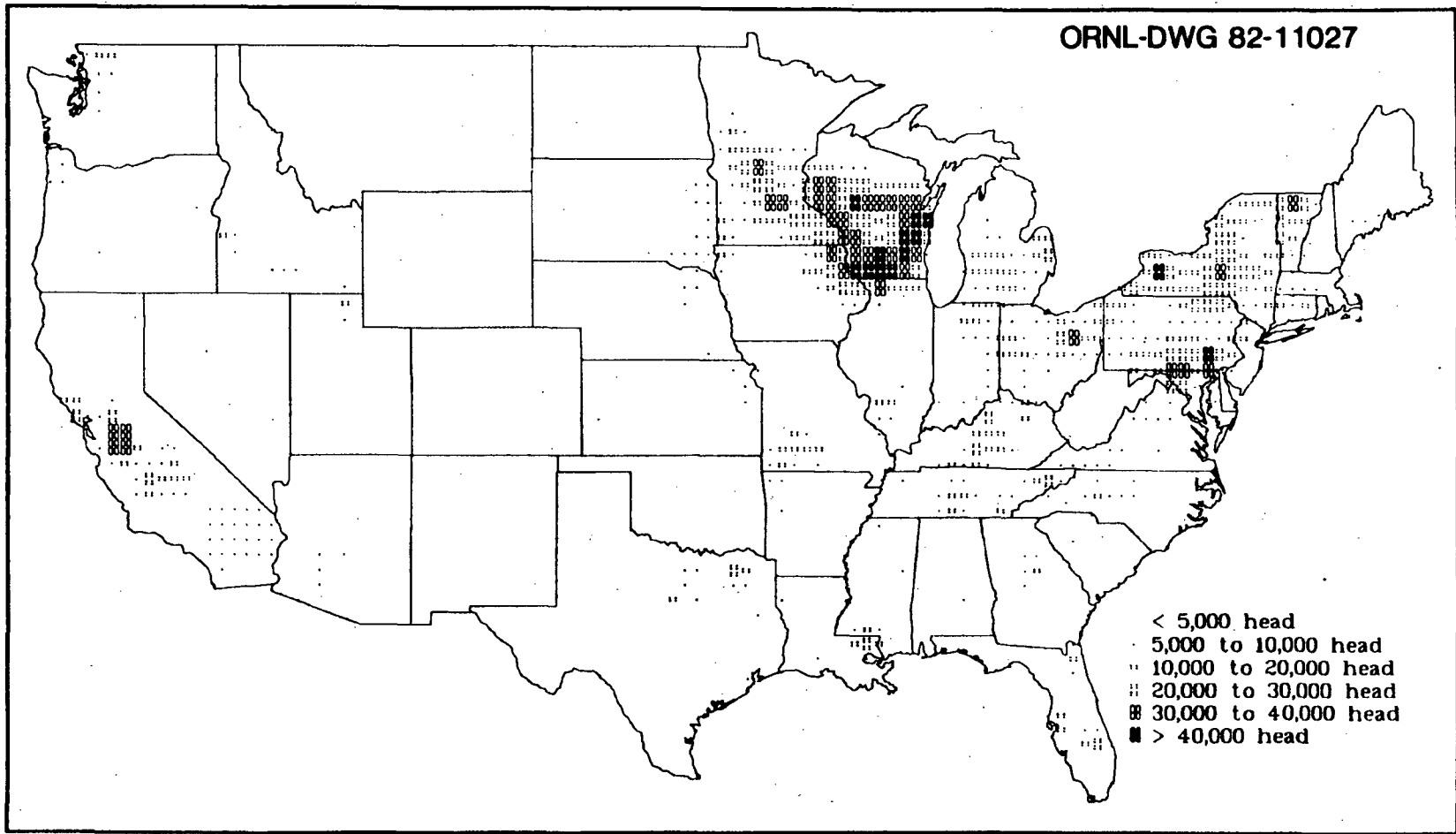


Figure 4.19. Geographic distribution of SITE parameter milk cow inventory, n_m

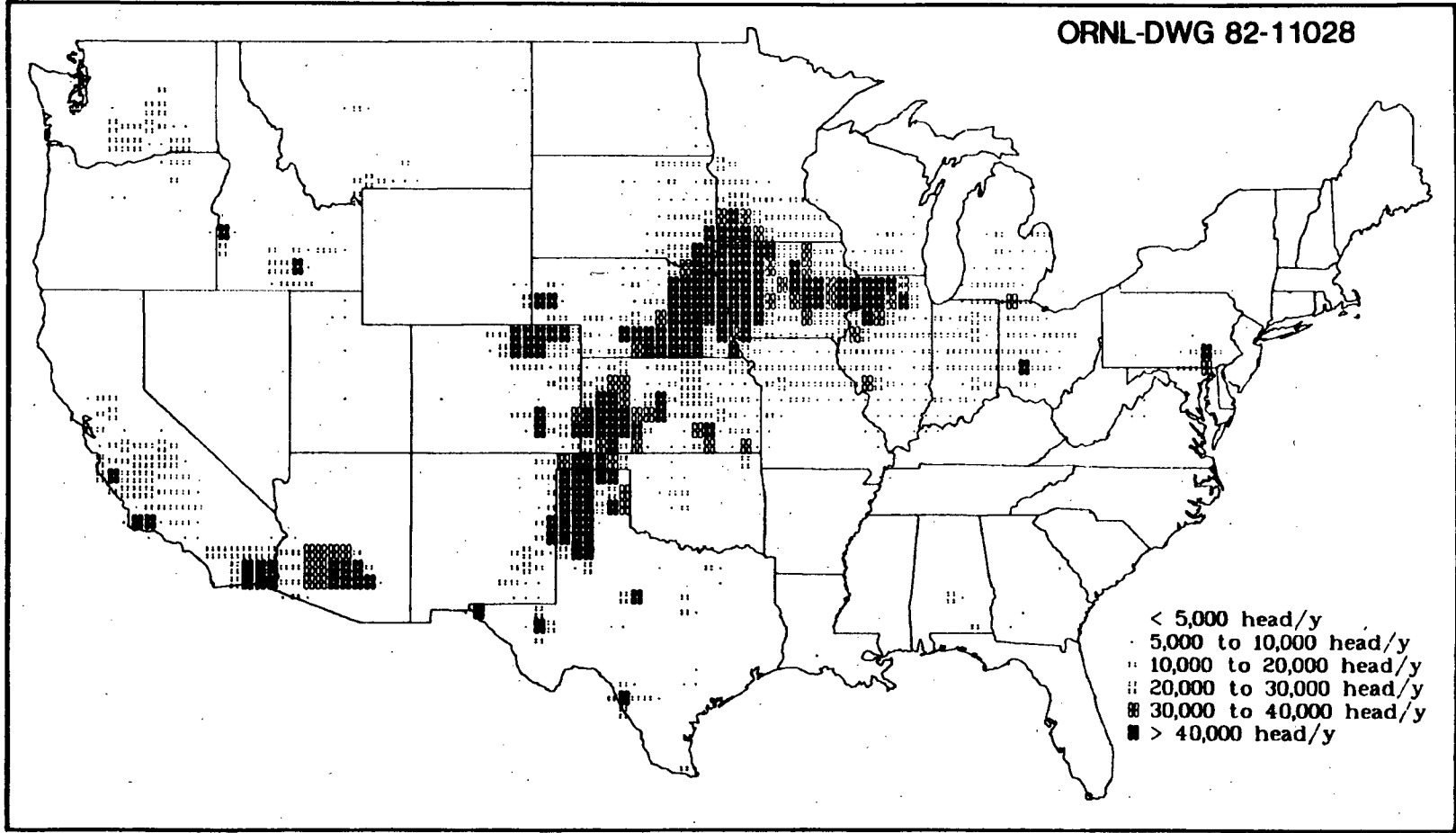


Figure 4.20. Geographic distribution of SITE parameter annual number of cattle on feed sold, s_g .

ORNL-DWG 82-11029

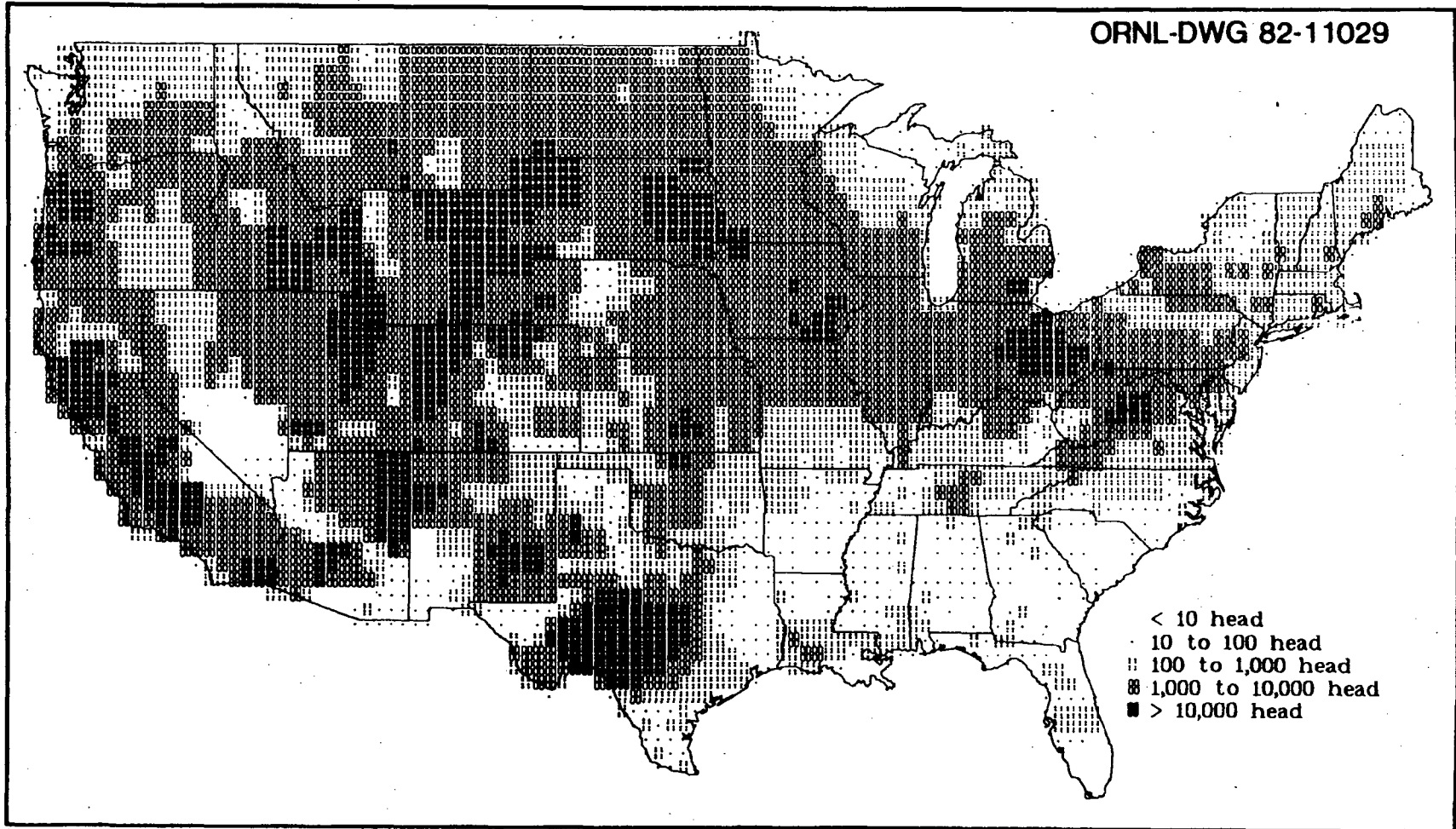


Figure 4.21. Geographic distribution of SITE parameter sheep inventory, n_s

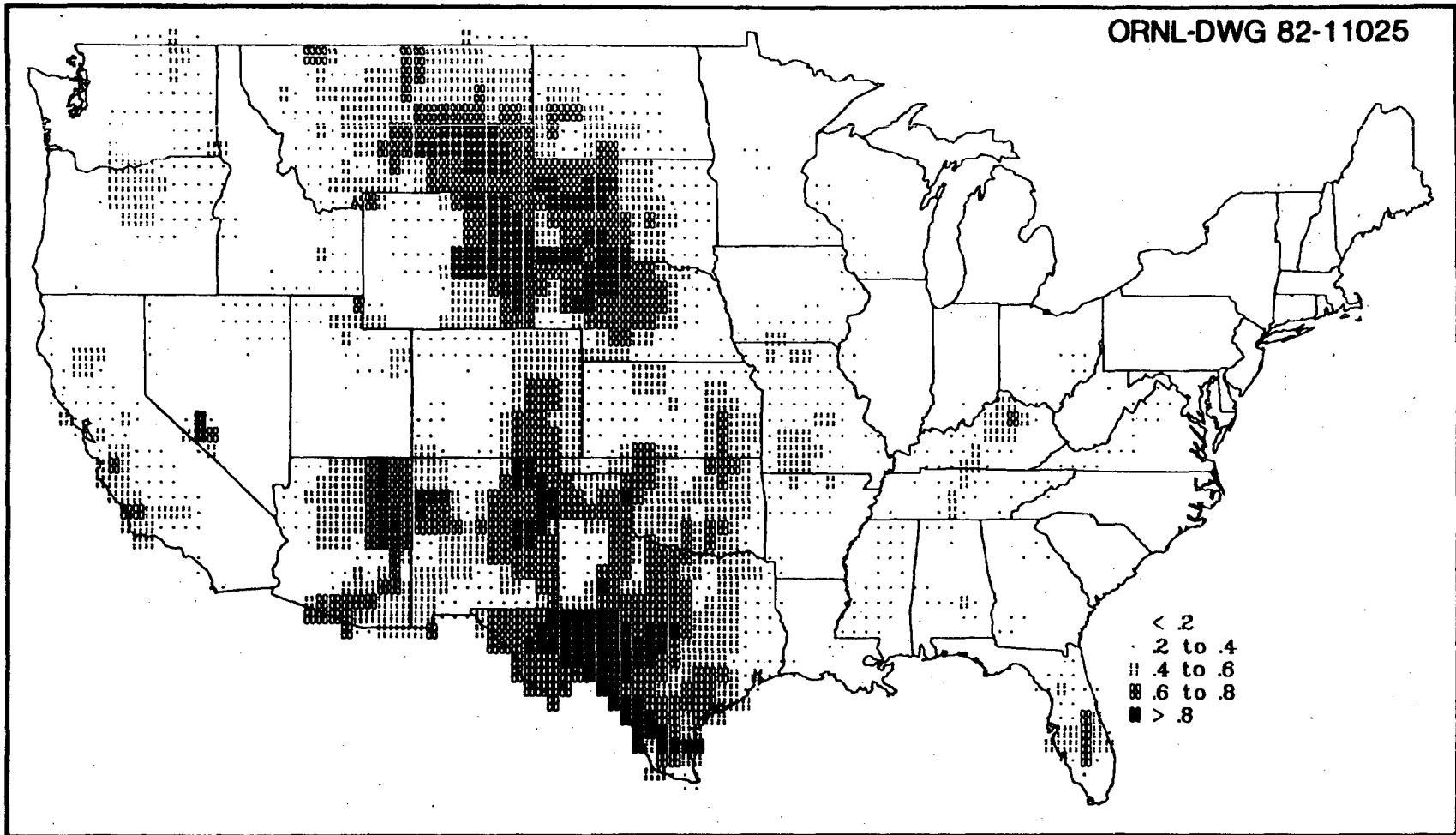


Figure 4.22. Geographic distribution of SITE parameter pasture area, A_p , shown as a fraction of total cell area.

where

- R_f = the collective forage requirement by forage-consuming livestock in the cell (kg/yr),
 P_{hf} = annual production of harvested forage in the cell (kg/yr),
 P_s = the annual production of silage in the cell (kg/yr), and
 P_h = the annual production of hay in the cell (kg/yr).

The collective livestock forage requirement is given by

$$R_f = 4010n_m + 970n_g + 3030n_a + 600n_s, \quad (41)$$

where

- n_g = the inventory of cattle on grain (head) in the cell,
 n_a = the average annual inventory of "all other cattle" (neither milk cows or cattle on feed) in the cell (head), and

the coefficients are annual forage requirements for each livestock category (kg/head/yr).⁷ Inventory numbers of milk cows, n_m , and sheep, n_s , are given in SITE, and n_g and n_a are calculated by

$$n_g = \frac{s_g}{\lambda_g}, \text{ and} \quad (42)$$

$$n_a = n_{cc} - n_m - \frac{3}{2}n_g, \quad (43)$$

where

- λ_g = the turnover rate of cattle on feed grain (1/yr).

The number of cattle and calves in the cell, n_{cc} , is given in SITE. The turnover rate λ_g is assumed to be 2.0/yr.⁷

In some states, notably Texas, Oklahoma, Nebraska, and Kansas, large numbers of cattle are imported and placed on feedlots for fattening. In these areas Eq. (43) may produce a negative value due to the high value of n_g . This possibility is tested for in the TERRA code, and when Eq. (43) is negative the value of n_a is set equal to the SITE parameter beef cow inventory, n_b (Fig. 4.23).

As shown in Eq. (39), all forage consumed by livestock in a cell is assumed to be produced locally within the cell in TERRA. This type of assumption is not applied to grain. That is, a grain requirement for all livestock in the cell is calculated according to

$$R_g = 2600n_m + 1820n_g + 150n_a, \quad (44)$$

where

- R_g = the collective grain requirement of all grain-consuming livestock in the cell (kg/yr)
 and

the coefficients are the annual grain requirements for each livestock category (kg/head/yr).⁷ Sheep are assumed to consume forage only. The grain requirement is compared to the SITE parameter, annual harvest yield or production of grain feed, P_{gf} (kg), and the fraction of grain imported from outside of the cell, f_{gi} , is calculated according to

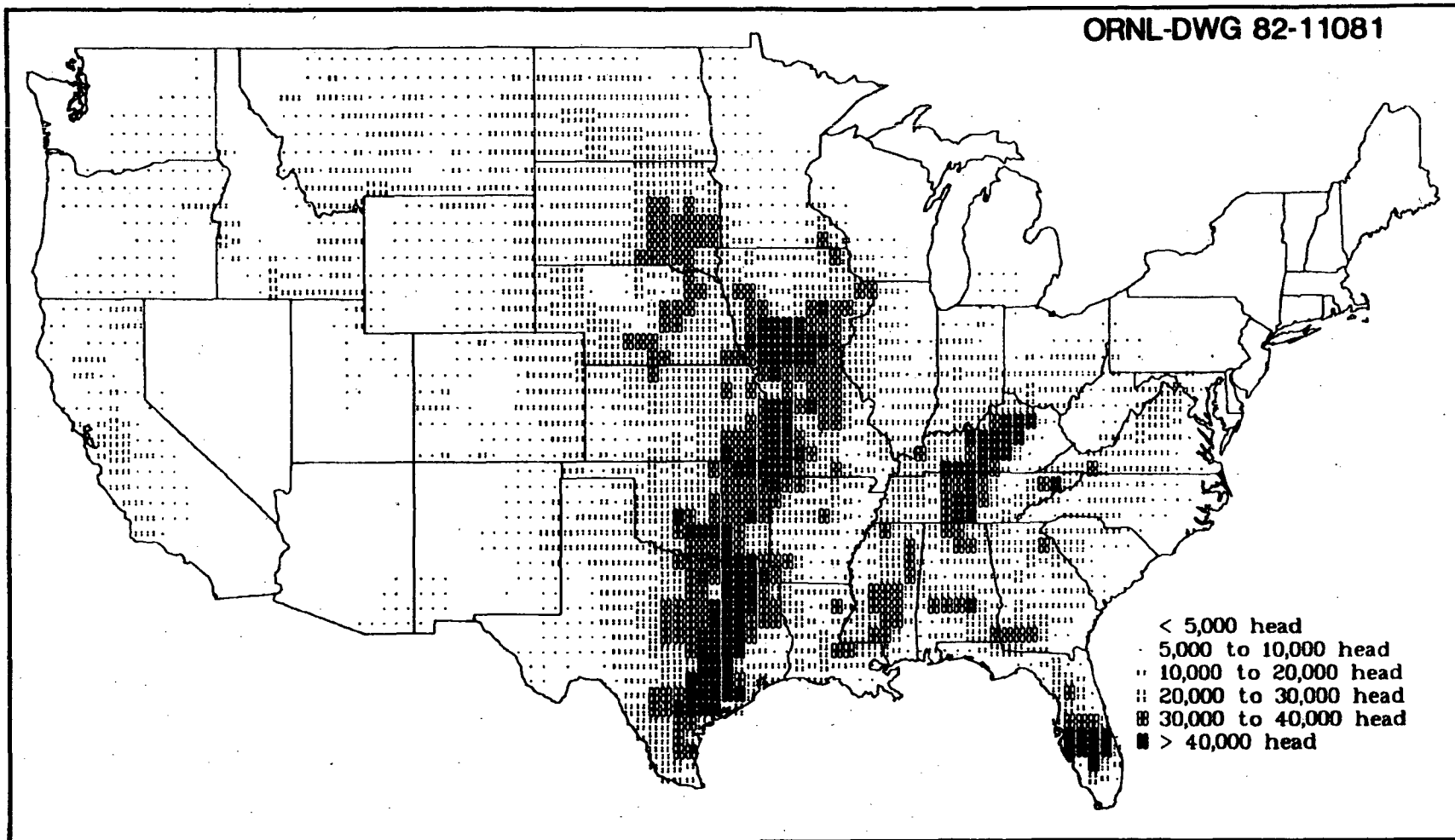


Figure 4.23. Geographic distribution of SITE parameter beef cows inventory, n_b .

Table 4.3. Agricultural and climatological parameters for seven selected SITE cells and parameters derived from them in TERRA

Parameter	Cell number; (X,Y); state						
	#1655 (82,31.5) GA	#2069 (115,33) CA	#2273 (101,34) TX	#3051 (84,37.5) KY	#3182 (91.5,38) MO	#3628 (82.5,40) OH	#4541 (75,44) NY
SITE Parameter							
Y_v (kg/m ²)	0.536	2.28	0.577	0.721	0.154	1.13	1.29
Y_{lv} (kg/m ²)	0.0	2.84	0.0	0.209	0.0	2.06	0.177
Y_s (kg/m ²)	0.843	0.187	0.391	1.04	0.591	0.847	0.917
Y_{sa}^a (kg/m ²)	0.540	1.40	0.365	0.397	0.394	0.495	0.441
d_{ff} (day/yr)	287	357	209	201	206	191	162
A_p (m ²)	2.73×10^8	4.00×10^7	9.18×10^8	1.28×10^9	1.06×10^9	3.10×10^8	2.24×10^8
P_v (kg/yr)	6.42×10^6	2.36×10^5	4.43×10^6	1.75×10^7	5.52×10^6	1.88×10^7	3.38×10^7
P_h (kg/yr)	8.54×10^6	1.61×10^8	4.01×10^6	6.97×10^7	5.70×10^7	5.97×10^7	7.22×10^7
n_{cc}	29,536	72,784	35,451	124,414	67,263	42,645	27,564
n_m (head)	2,446	1,460	40	3,504	2,250	8,907	15,125
n_s (head)	1	34,385	1,776	3,184	444	22,226	280
n_b (head)	12,543	2,334	13,265	52,694	32,797	10,748	817
s_g (head)	2,117	136,978	1,391	3,856	2,437	6,279	127
P_{gf} (kg)	8.64×10^7	9.32×10^6	1.05×10^8	2.23×10^7	1.47×10^7	1.24×10^8	1.83×10^6
Parameters calculated in TERRA							
h_h (1/yr)	5	6	3	3	3	3	3
Y_h (kg/m ²)	0.108	0.233	0.122	0.132	0.131	0.165	0.147
n_e (head)	1,059	68,489	696	1,592	1,219	3,140	64
n_a (head)	25,502	2334 ^a	34,367	119,522	63,184	29,028	12,343
R_f (kg/yr)	8.81×10^7	1.00×10^8	1.06×10^8	3.80×10^8	2.02×10^8	1.40×10^8	9.83×10^7
C_p (kg/yr)	7.69×10^7	0	9.97×10^7	3.15×10^8	1.55×10^8	8.11×10^7	1.88×10^7
Y_{ps}^a (kg/yr/m ²)	0.282	0	0.109	0.246	0.146	0.262	0.084
g_{pe} (1/yr)	10	0	7	7	7	6	5
Y_{ps} (kg/m ²)	0.028	0	0.016	0.035	0.021	0.044	0.017

^aSet equal to inventory of beef cattle in this SITE cell.

$$f_{gi} = 1 - \frac{P_{gf}}{R_g}, \quad (45)$$

unless $P_{gf}/R_g > 1.0$, in which case f_{gi} is set to 1.0.

Table 4.3 lists 13 of the 14 agricultural parameters in SITE and number of frost-free days, which is used by TERRA for selected SITE cells in the United States. The 14th agricultural parameter, irrigation, is discussed in Sect. 4.2. The other seven parameters—annual yields (production) of leafy vegetables, P_v , exposed produce, P_e , protected produce, P_{pp} , grains consumed by man, P_{gh} , and productivity estimates for protected produce, Y_{pp} , grain feeds, Y_{gf} , and grain foods consumed by man, Y_{gh} ,—are not currently used by TERRA.

4.2 Climatological Parameters

The SITE data base contains six climatological parameters—precipitation, evapotranspiration, absolute humidity, morning mixing height, afternoon mixing height, and number of frost-free days. All except evapotranspiration have been calculated according to the method described in Sect. 4 for climatological parameters (interpolation among the three nearest weather stations).

Evapotranspiration was calculated by United States county and converted to SITE cell basis according to Method B. Of the six, only precipitation, evapotranspiration, absolute humidity, and frost-free days are used by TERRA. Frost-free days has been discussed in Sect. 4.1. The following discussion will detail the derivation and use of the remaining five climatological parameters and the agricultural parameter irrigation.

Evapotranspiration (Fig. 4.24), irrigation (Fig. 4.25) and precipitation (Fig. 4.26) are used in the calculation of leaching constants [Eq. (7)] as described in Sect. 2.4. Leaching constants are calculated for both irrigated and nonirrigated soils in TERRA. Food crops (except grains) are assumed to be grown on irrigated soils and all livestock feeds are assumed to be grown on nonirrigated soils. The numerator of Eq. (7), $(P + I - E)$, is assumed to be a mass balance of water inputs and outputs for a given agricultural area. Surface runoff and storage of water in surface agricultural soils is not considered in TERRA.

Evapotranspiration was calculated according to a model proposed by Morton.²¹⁶ The model requires as input annual precipitation, sea level pressure (or altitude), monthly dew point, monthly ambient air temperatures, and monthly fraction of maximum possible sunshine. Annual precipitation was taken from Olson, Emerson, and Nungesser²¹⁷ by county in eastern states and by state climatic division in western states. Conversion of precipitation by state climatic division to a county basis was achieved using the IUCALC code.²¹⁵ The altitude of each county centroid in meters was estimated using the TERGHT code.²¹⁸ Each altitude was converted to sea level pressure in millibars using²¹⁹

$$P_{st} = \left[\frac{z - 44308}{-11876.94} \right]^{5.25679} \quad (46)$$

where

$$\begin{aligned} P_{st} &= \text{sea level pressure (mb) and} \\ z &= \text{altitude (m).} \end{aligned}$$

Monthly dew point and ambient air temperatures were taken from references 210, 211, and 212 for various United States weather stations. The monthly fractions of maximum possible sunshine were taken from references 211 and 212 for various weather stations. All parameters derived from weather station data were interpolated to county centroids and finally to the half degree cells using methods previously described.

Annual irrigation in centimeters was taken from information reported in the 1974 Census of Agriculture. For each county the 1974 Census reports total land irrigated in acres and the estimated quantity of irrigation water applied in acre-feet. The latter was divided by the former and the quotient was converted to centimeters.

Irrigation was not included with precipitation in the model input parameters, although it is considered in Eq. (7). This discrepancy will add a small amount of error to the evapotranspiration by county calculation. Because the Morton model is designed for large land areas and does not provide for local discontinuities, it was assumed that irrigation water is an insignificant fraction of total precipitation over the entire county or cell. This assumption is supported by the observation that nationally only 3-4% of all farmland is irrigated. However, in some counties irrigated land may be a significant fraction of the total land area and our calculations inappropriate.

According to Morton, the evapotranspiration model has been verified over a wide range of environments and compares satisfactorily with annual precipitation less runoff for 81 river basins in Canada, 36 river basins in the southern United States, three river basins in Ireland, and two river basins in Kenya. Wallace²²⁰ compared the model with the Thornthwaite-Mather²²¹ and Penman²²² approaches to modeling evapotranspiration and found the Morton model to be superior in modeling arid environments. Morton, however, warns against use of the model near sharp environmental discontinuities. Therefore, estimates of evapotranspiration near coast-lines and mountain ranges are suspect.

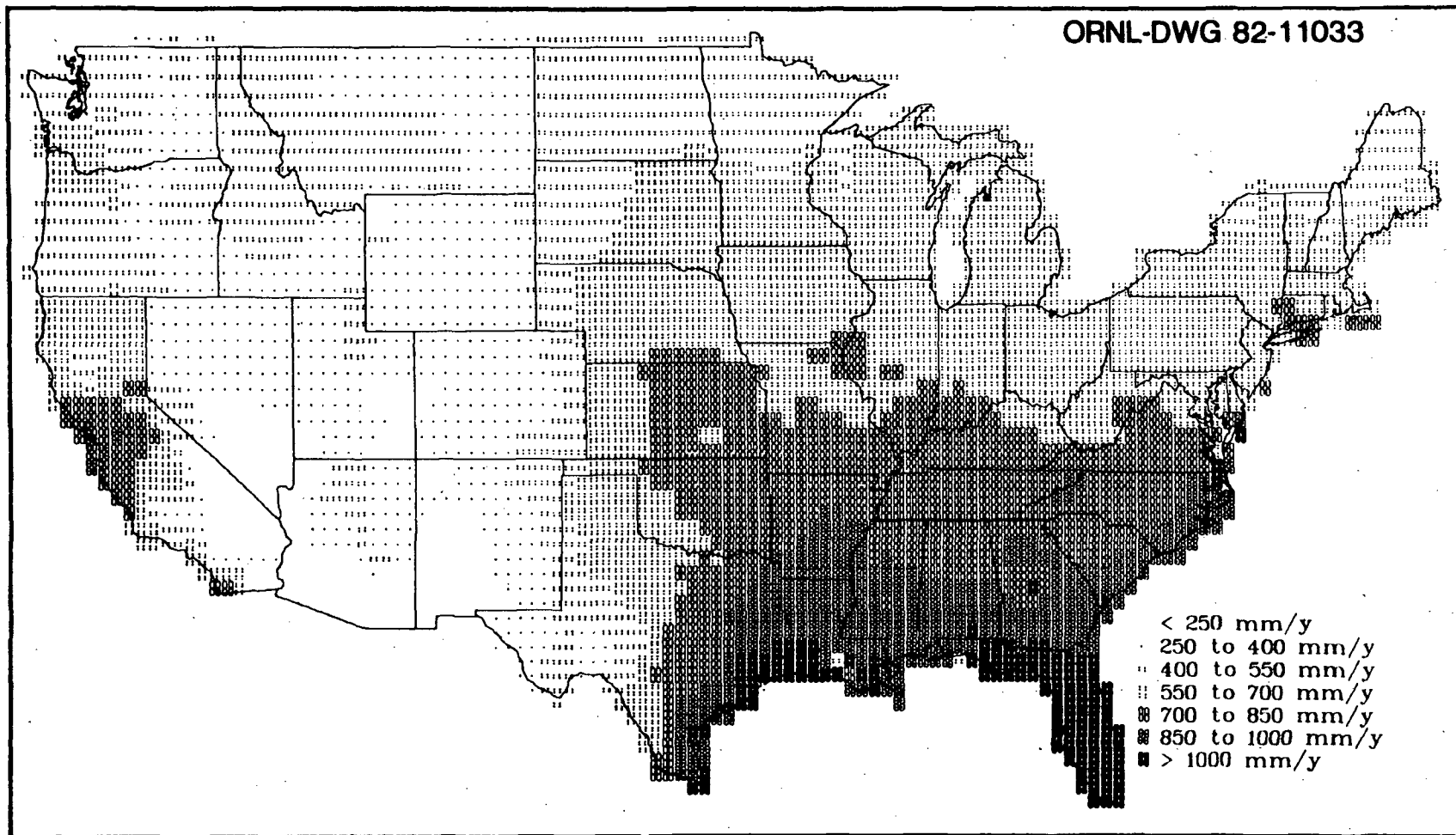


Figure 4.24. Geographic distribution of SITE parameter estimated annual average evapotranspiration, E .

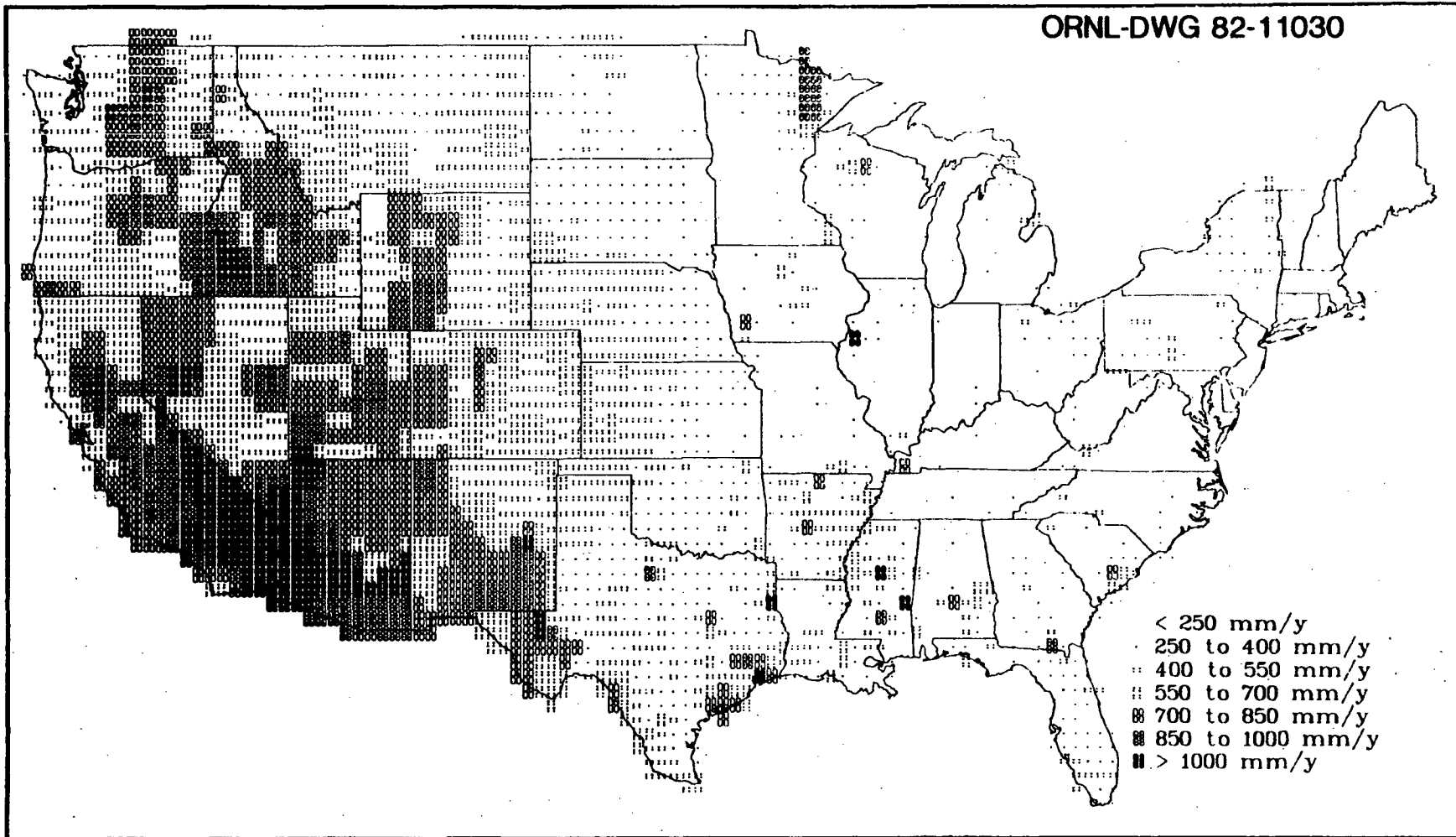


Figure 4.25. Geographic distribution of SITE parameter estimated annual average irrigation, *I*.

ORNL-DWG 82-11032

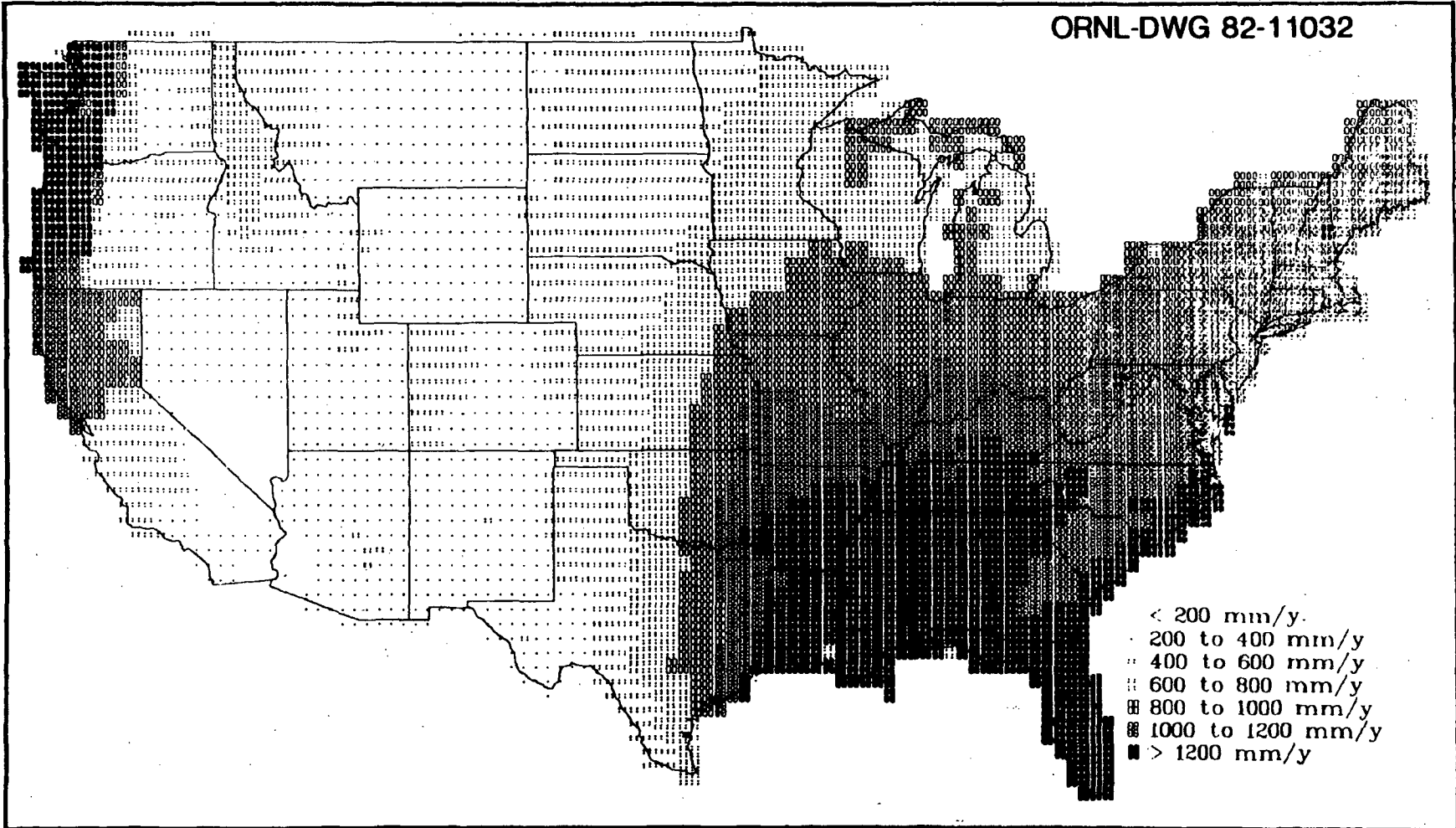


Figure 4.26. Geographic distribution of SITE parameter estimated annual average precipitation, P .

Morning and afternoon mixing heights in meters (Figs. 4.27 and 4.28, respectively) were taken from the annual average tabulation for 62 United States weather stations reported by Holzworth²²³ under both precipitation and nonprecipitation conditions. Cell values are interpolations among the three nearest weather stations. Currently, morning and afternoon mixing height estimations are not used in TERRA. However, they may be of use to atmospheric dispersion computer codes and models which calculate dispersion of elevated releases.

The estimates of absolute humidity (Fig. 4.29) were taken from the annual averages for 218 United States weather stations calculated by Etnier²²⁴ from annual-average temperature and relative humidity data. The cell-averaged values were interpolated from the three nearest weather stations as previously described.

4.3 Demographic and Miscellaneous SITE Parameters

In addition to the 29 parameters previously discussed, SITE includes seven parameters describing the population of the cell and cell characteristics. These parameters include the estimated 1980 population and fractions (based on the 1970 Census) which are classified as urban, rural-farm, and rural-nonfarm, the actual land area of the cell, the dominant land feature in the cell, and the coarse suspended particulate matter due to resuspension.

The 1980 population estimate for half degree cells (Fig. 4.30) was determined from data by enumeration district as described in references 213 and 214. The definitions of "urban," "rural-farm," and "rural-nonfarm" are as follows. The urban population (Fig. 4.31) comprises all persons living in (1) places of 2,500 inhabitants or more incorporated as cities, boroughs, villages, and towns (except towns in New England, New York, and Wisconsin); (2) the densely settled urban fringe, whether incorporated or unincorporated, of urbanized areas; (3) towns in New England and townships in New Jersey and Pennsylvania which contain no incorporated municipalities as subdivisions and have either 25,000 inhabitants or more or a population of 2,500 to 25,000 and a density of 580 persons or more per square kilometer (1,500 persons per square mile); (4) counties in states other than the New England States, New Jersey, and Pennsylvania that have no incorporated municipalities within their boundaries and have a density of 580 persons or more per square kilometer (1,500 persons per square mile); and (5) unincorporated places of 2,500 inhabitants or more. The rural population is divided into "rural-farm," (Fig. 4.32) comprising all persons living on farms, and "rural-nonfarm," (Fig. 4.33) comprising the remainder. According to the 1970 Census definition, the farm population consists of all persons living in rural territory on places of less than 0.04 km² yielding agricultural products which sold for \$250 or more in the previous year, or on places of 0.04 km² (10 acres) or more yielding agricultural products which sold for \$50 or more in the previous year.

The land area of the cell in square meters is less than or equal to the theoretical area of the cell, depending on the area of surface waters in the cell. The actual area of the cell was determined from the county areas reported in the 1974 Census of Agriculture. "Land areas" includes land temporarily or partially covered by water (marshlands, swamps, etc); canals under 201 m (one eighth statute mile) wide; and lakes, reservoirs, and ponds under 0.16 km² (40 acres).

The SITE data base contains a coded number which describes the dominant land feature of the cell (Fig. 4.34). The dominant land feature may be useful to atmospheric dispersion calculations requiring location-specific surface roughness correction factors. The dominant land features considered are

- 1) Tall row crops,
- 2) Short row crops,
- 3) Hay or tall grass,
- 4) Urban areas,
- 5) Small lakes,
- 6) Short grass, and
- 7) Forest.

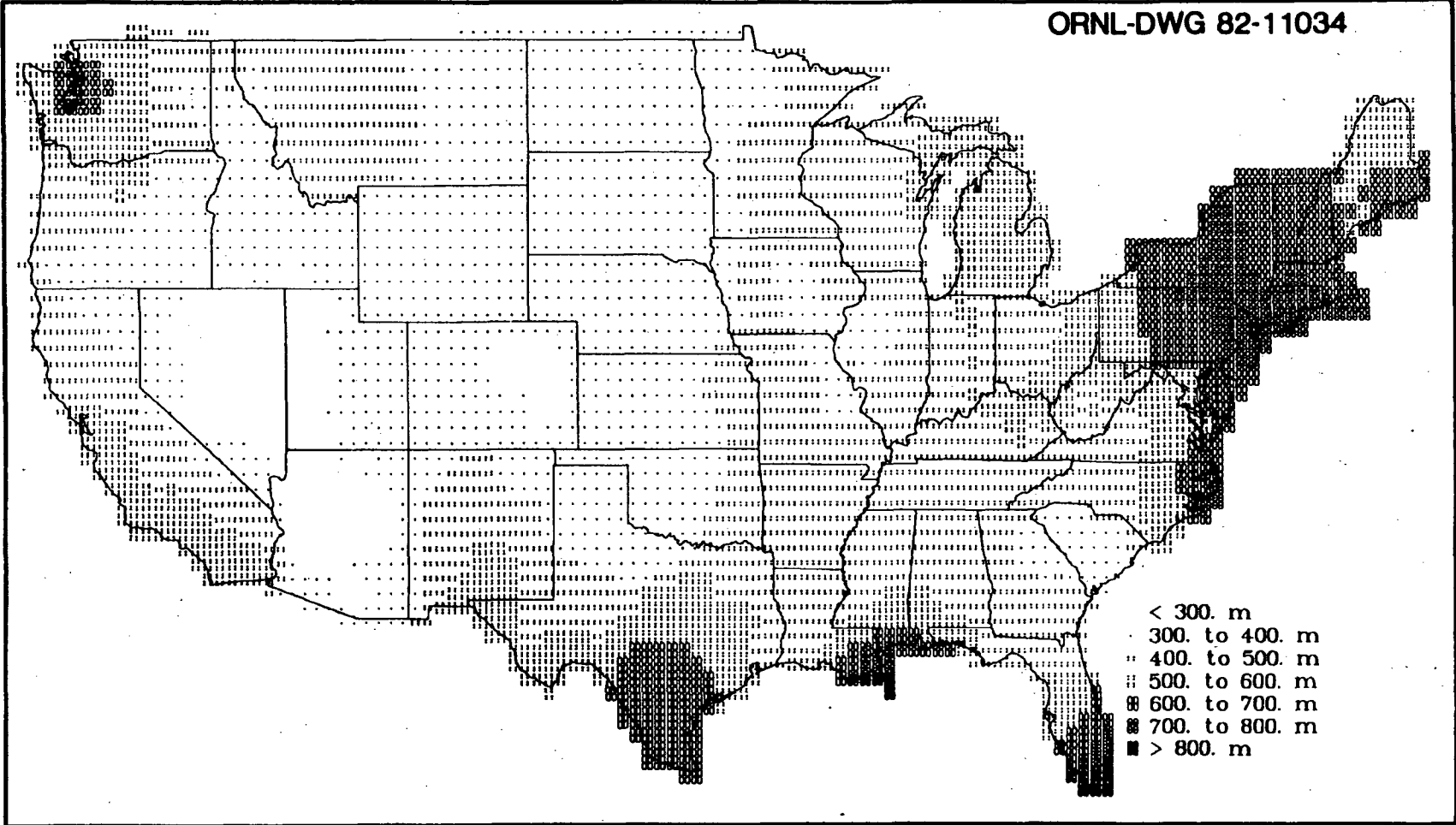


Figure 4.27. Geographic distribution of SITE parameter estimated annual average morning mixing height, $M_{a,m}$

ORNL-DWG 82-11035

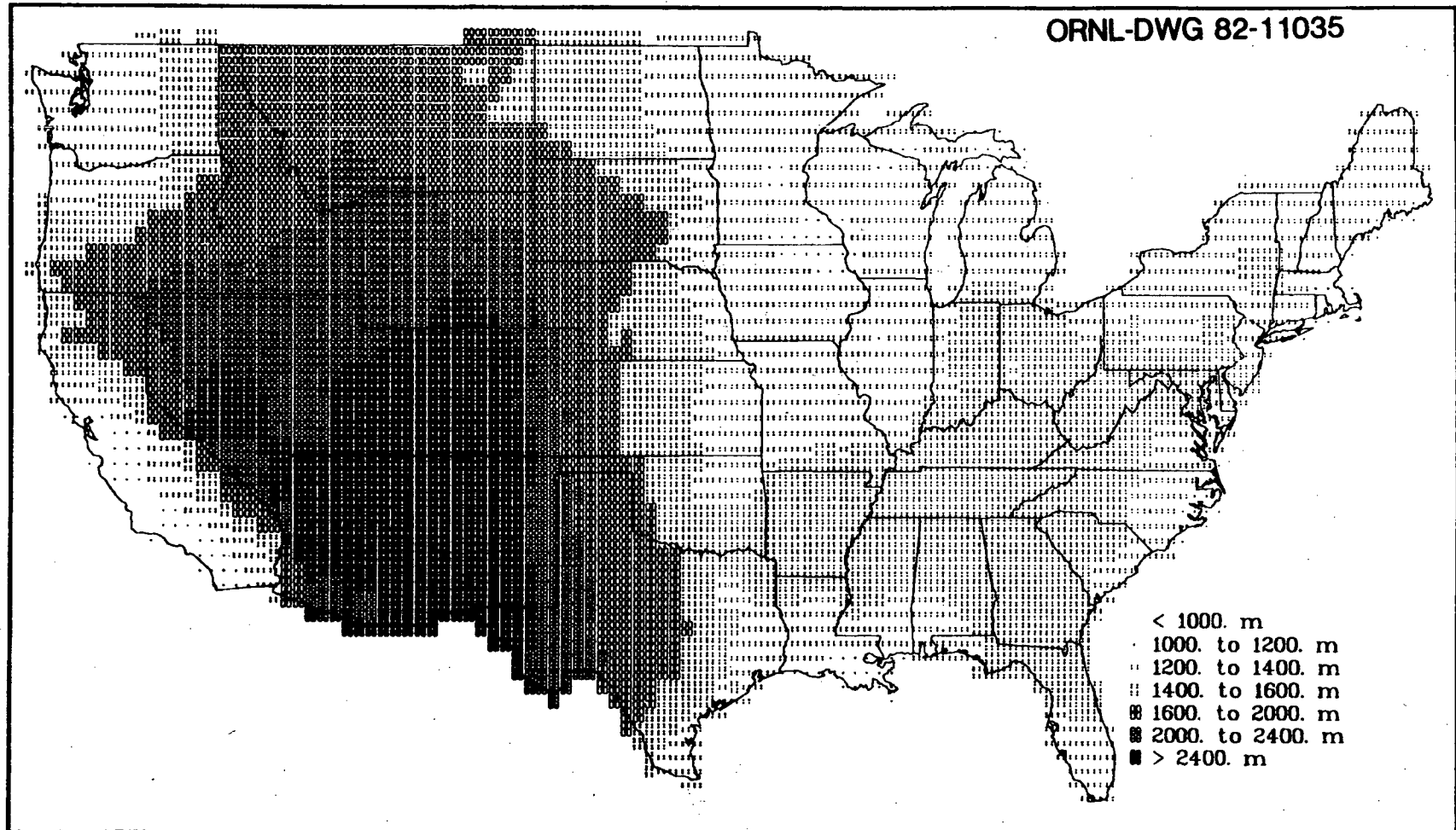


Figure 4.28. Geographic distribution of SITE parameter estimated annual average afternoon (evening) mixing height, $M_{p,m}$

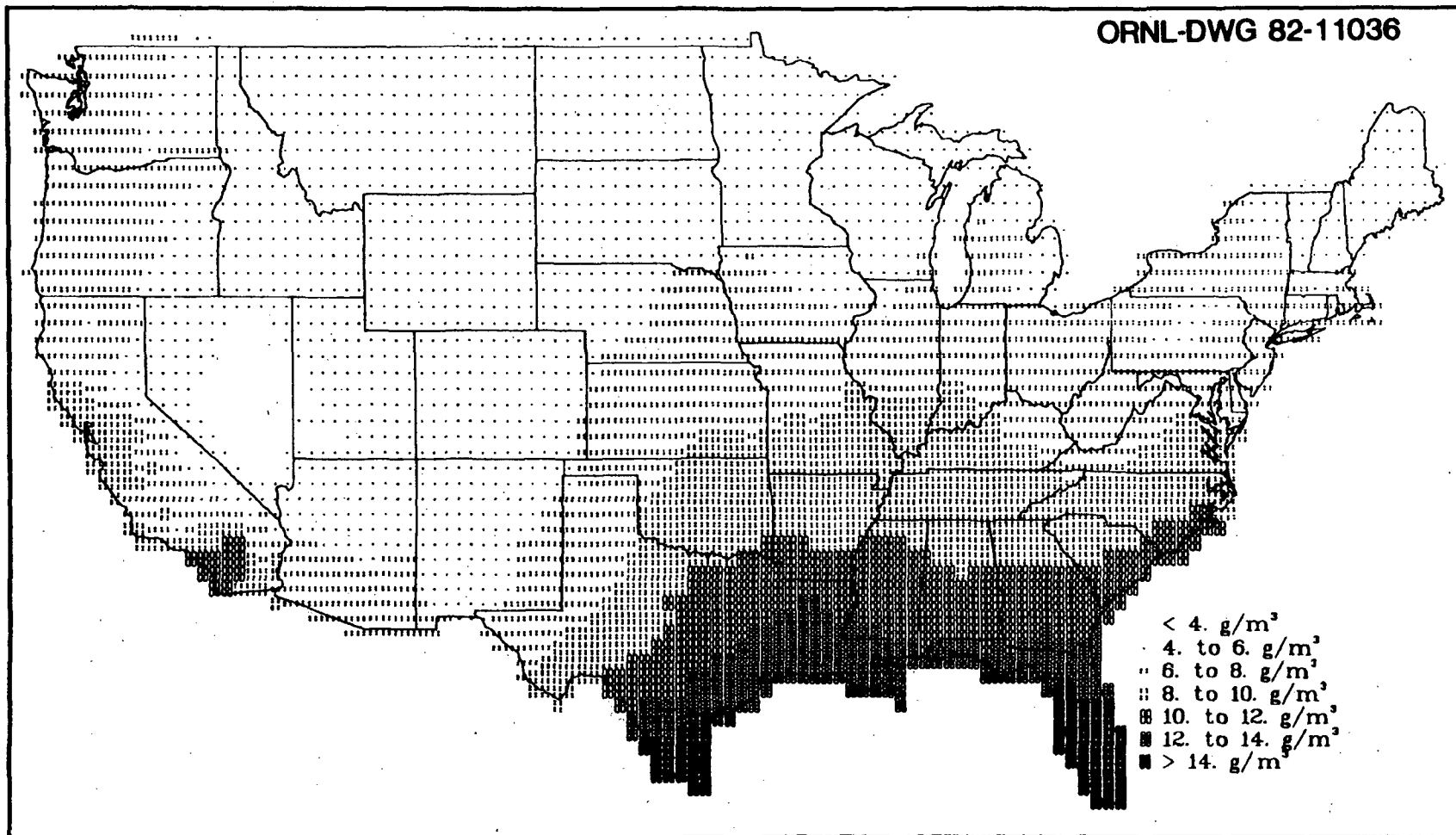


Figure 4.29. Geographic distribution of SITE parameter estimated annual average absolute humidity, H .

ORNL-DWG 82-11038

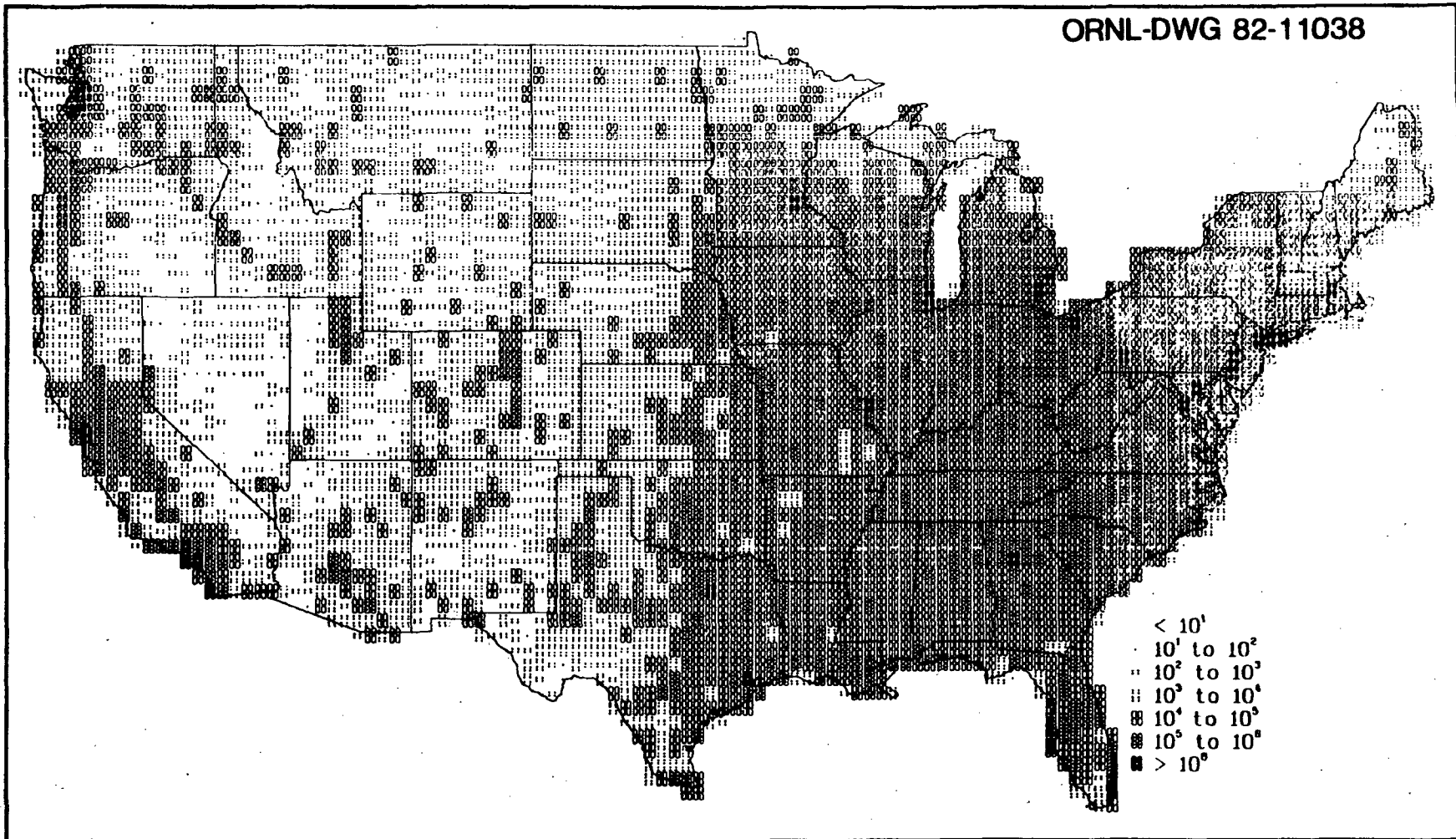


Figure 4.30. Geographic distribution of SITE parameter (estimated 1980) U.S. population, pop_i .

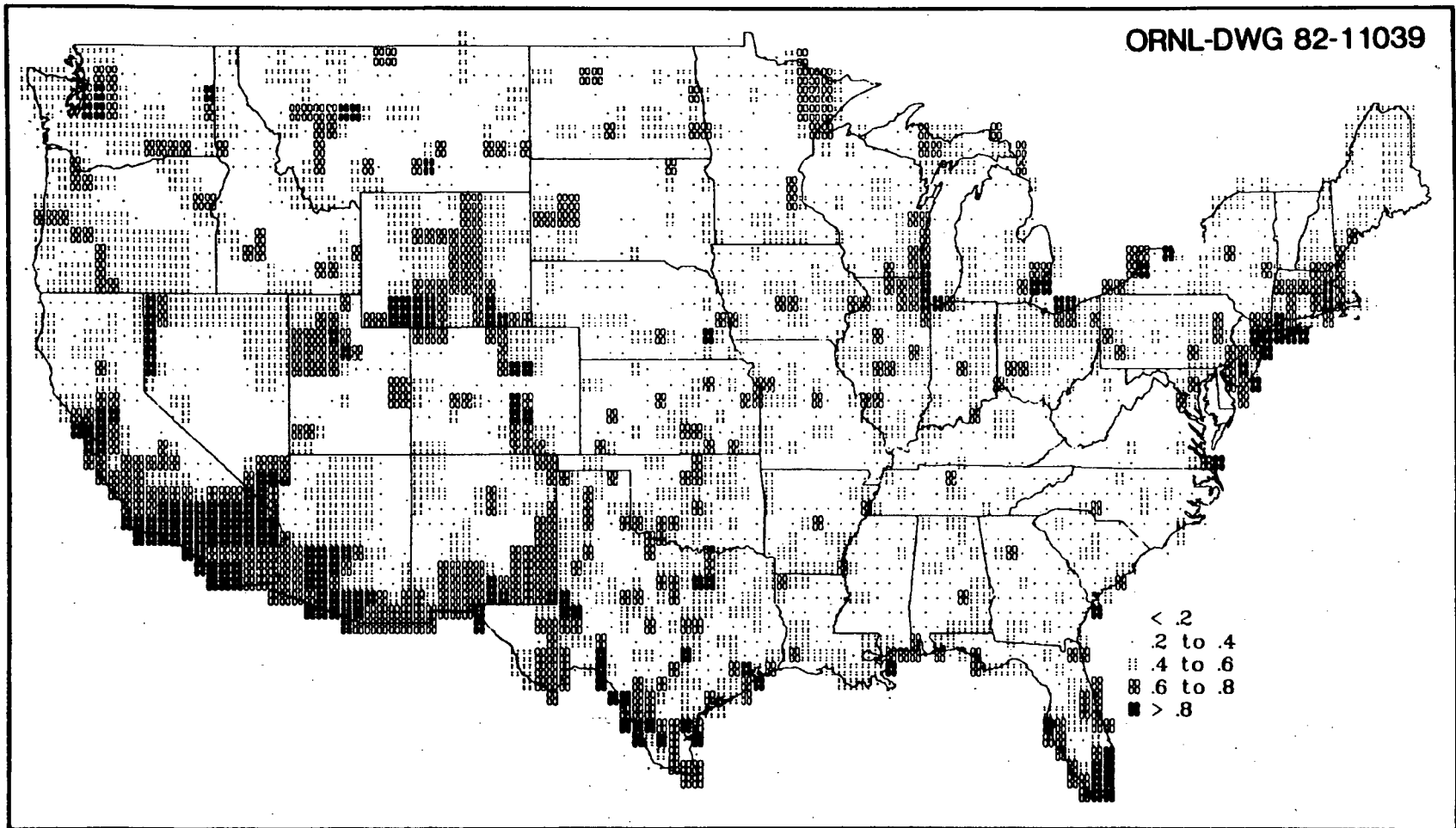


Figure 4.31. Geographic distribution of SITE parameter fraction of (1970) population classified as urban, pop_u .

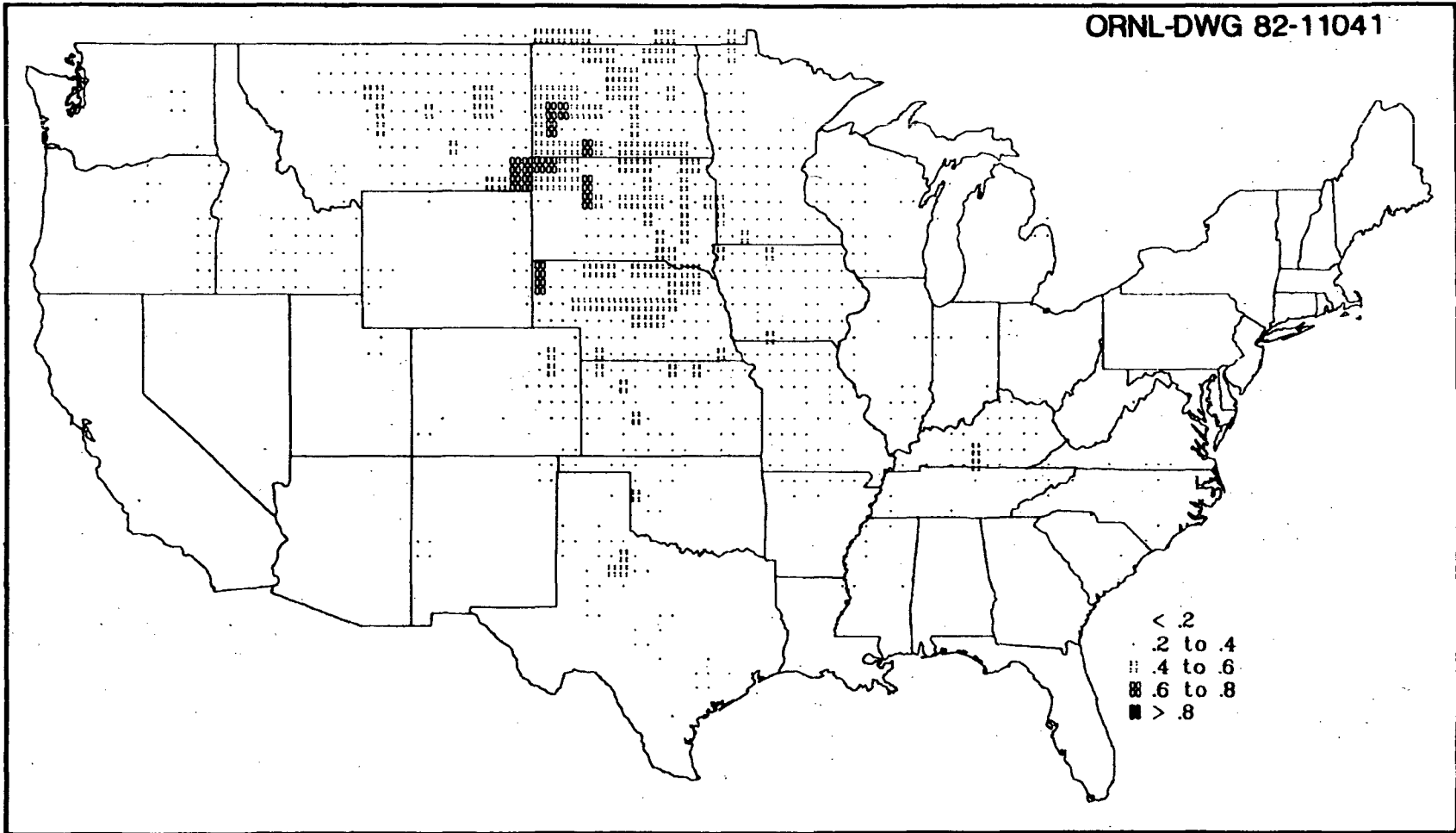


Figure 4.32. Geographic distribution of SITE parameter fraction of (1970) population classified as rural-farm, pop_r

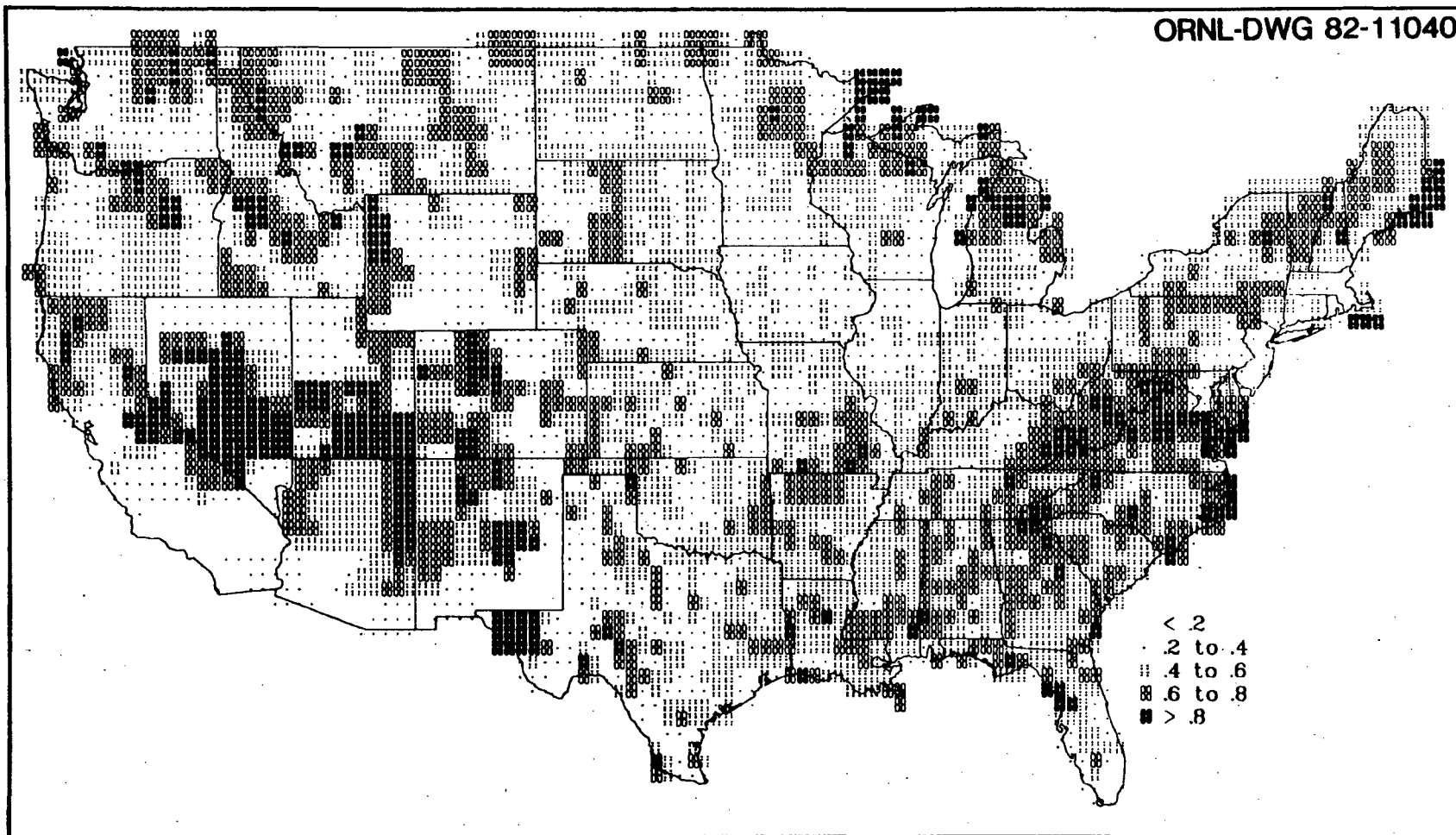


Figure 4.33. Geographic distribution of SITE parameter fraction of (1970) population classified as rural-nonfarm, $pop_{n,r}$

ORNL-DWG 82-11037

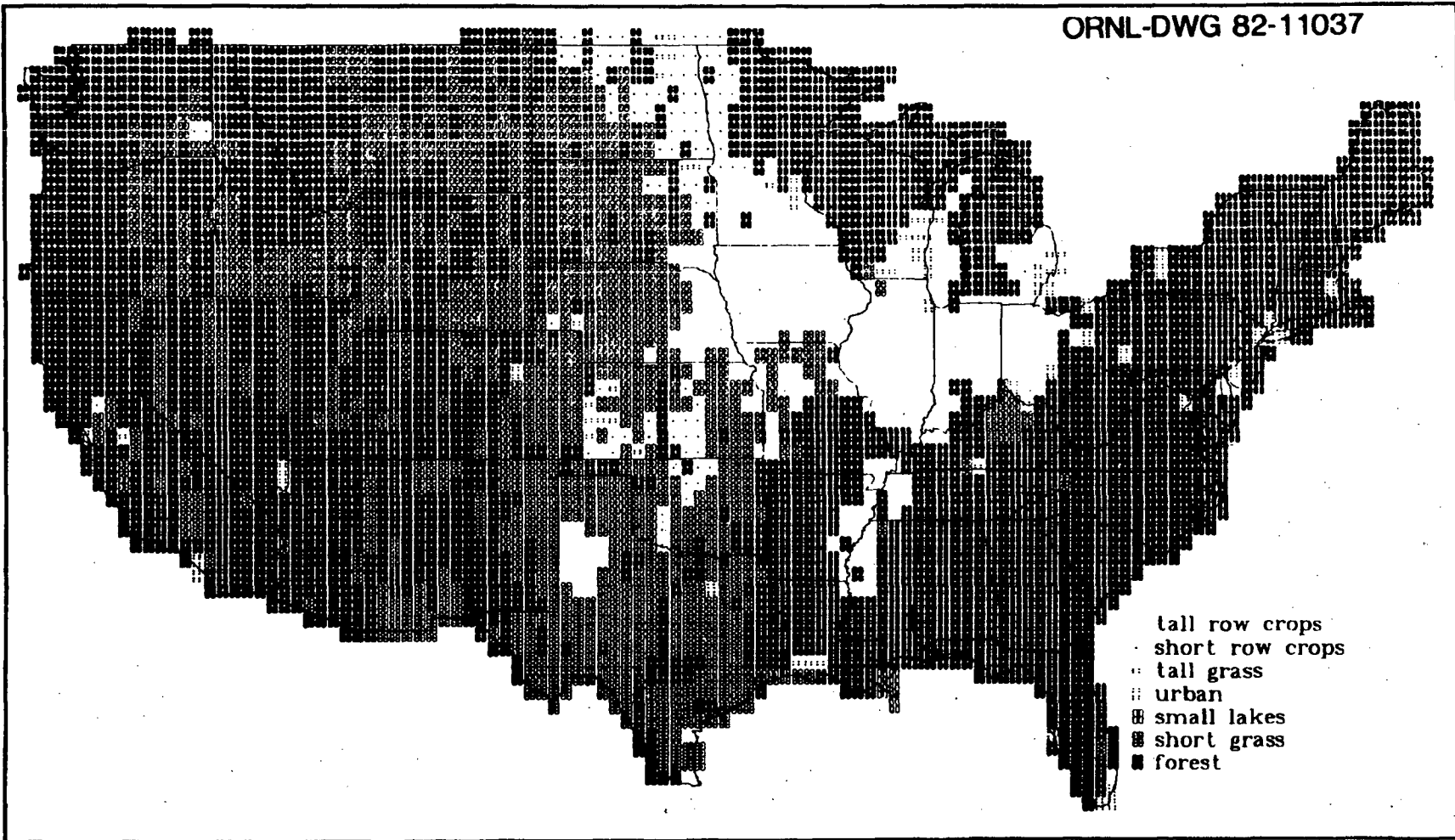


Figure 4.34. Geographic distribution of SITE parameter dominant land feature, L_{df} .

The dominant land features were determined from data gathered by Olson, Emerson, and Nungesser.²¹⁷ They reported areas for each land feature by county. The county areas were converted to cell areas by methods previously described. The land feature with the largest area is considered the dominant land feature.

The dominant land feature is expressed as a code of the form FLPPP. The "F" value is either "0" or "1," for less than or more than 50% of the total area in the cell classified as Federal land, respectively. Federal land was not subclassified as to land use in data gathered by Olson, Emerson, and Nungesser.²¹⁷ Therefore, an assumption inherent in our estimation of dominant land feature is that Federal and privately owned lands are similar in land feature make up. This assumption may be incorrect, especially when Federal lands are protected forest or wildlife areas. The "L" value corresponds to the seven land features previously given. The "PPP" value indicates the percentage of the total area of the cell corresponding to the "L" category.

5. MISCELLANEOUS PARAMETERS

Other default parameters included in the TERRA code are the weathering removal constant, λ_w , the metabolic removal rate constants from milk and beef, λ_m and λ_f , respectively, and the lifetime grain and forage requirements of cattle on feed, Q_g^{fc} and Q_f^{fc} , respectively. The weathering removal constant is extremely important in calculating surface plant concentrations due to direct deposition processes, and the latter four parameters are utilized in calculating beef and milk concentrations.

5.1 The Weathering Removal Loss Constant, λ_w

After radionuclides are initially deposited on vegetation surfaces environmental processes (in addition to radiological decay) will begin to remove the deposited material. Miller and Hoffman²²⁵ have reviewed the literature on weathering removal of radionuclides from vegetation. They classify the environmental removal processes as wind removal, water removal, growth dilution, and herbivorous grazing. Wind removal may be very effective in removal of freshly deposited large particles ($> 1 \mu\text{m}$ diameter), but not nearly as effective after the first few days. Submicron particles may be released from plant surfaces during periods of rapid growth and high transpiration rates. Also, surface abrasion from wind action may dislodge salt particles, wax, and other surface fragments. Radioactivity associated with these components would also be removed from the vegetation.

Precipitation, fog, dew, and mist—all may remove surface-deposited radionuclides via direct washoff and leaching. Leaching, in addition, may remove radionuclides incorporated into plants through root uptake. Wash-off, like wind removal, seems to be most effective on freshly deposited material. Precipitation falling as a light, continuous drizzle is more efficient than a large quantity of precipitation falling over a much shorter period.²²⁵

Removal due to growth dilution and grazing by herbivores may vary considerably by plant and location. Produce growth characteristics may be quite varied. Slow-growing varieties may be expected to be less affected by growth dilution than faster growing varieties. Grazing by herbivores may be particularly hard to predict. Weathering removal tends to occur in an exponential manner with a characteristic half-time, T_w .²²⁵ From this half-time a weathering removal constant, λ_w , may be derived according to

$$\lambda_w = \frac{\ln 2}{T_w} \quad (47)$$

In the TERRA code the value of λ_w adopted by the USNRC⁶ of 5.73×10^{-7} (equal to a T_w of 14 d) is used for all radionuclides (except for iodine) on all plant surfaces. This value is somewhat arbitrary, but is within the range of reported values in the literature. In their literature review Miller and Hoffman²²⁵ found measured values of T_w to range between 2.8 to 34 days with a geometric mean of all reported values of 10 days. For I_2 vapor, iodine particulates, and other particulates on herbaceous vegetation the geometric means of reported values of T_w are 7.2, 8.8, and 17 days, respectively. The value of T_w used in TERRA is $1.0 \times 10^{-6} \text{ s}^{-1}$, which corresponds to a T_w of 8 days.

5.2 The Metabolic Turnover Constant For Milk, λ_m

In the TERRA code radionuclide transfers to beef and milk are modeled via a single compartment model whereby the radionuclide is transferred from feed directly to milk and beef. This approach differs from the approach taken by the USNRC⁶ in that isotopes of the same

element with significantly different half-lives may yield different milk and beef concentrations, even though the milk and beef transfer coefficients (F_m and F_f , respectively) are the same for the isotopes. Such one-compartment models require quantification of all inputs and outputs from the compartment. For milk and beef the metabolic removal constants must be known.

The model for radionuclide transfer to milk is given by

$$C_m = \frac{C_{feed} Q_{feed} f_{im} (1 - \exp(-\lambda_m t_m))}{m_p \lambda_m} \quad (48)$$

where

- C_m = the radionuclide concentration in milk (Bq or Ci/kg),
- C_{feed} = the radionuclide concentration in feed (Bq or Ci/kg),
- Q_{feed} = the ingestion rate of feed (kg/s),
- f_{im} = the fractional transfer from ingested feed to milk (unitless),
- λ_m = the metabolic turnover constant for milk (s^{-1}),
- t_m = the time at which milk is sampled (s), and
- m_p = the quantity of milk collected per milking (kg).

At equilibrium Eq. (48) reduces to

$$C_m = \frac{C_{feed} Q_{feed} f_{im}}{m_p \lambda_m} \quad (49)$$

Since by the USNRC⁶ approach,

$$C_m = 86,400 C_{feed} Q_{feed} F_m \quad (50)$$

where 86,400 = the number of seconds in a day, then

$$f_{im} = 86,400 F_m m_p \lambda_m \quad (51)$$

Since F_m and m_p are already known (from reference 7 $m_p = 13.4$ kg), then the only parameter which needs to be defined is λ_m .

Ng and his associates¹⁴⁵ have determined values of metabolic halftimes, T_m , for various elements in milk (Fig. 5.1: note that these values of T_m are in terms of days rather than seconds). They consider a value of T_m of 0.693 d (equal to $\ln 2$) to be conservative. Such a value of T_m is equivalent to a λ_m of 1.0/d or $1.16 \times 10^{-5}/s$. This latter value is adopted for calculation of milk concentrations in the TERRA code. Using this value in Eqs. (49) and (51) allows for an equilibrium milk concentration to be achieved within approximately seven days.

5.3 The Metabolic Turnover Constant For Beef, X,

The metabolic turnover constant for beef is determined in a manner similar to that for milk by substituting the fractional transfer to beef, f_f , the time to slaughter, t_s , the muscle mass of beef cattle, m_m , the metabolic turnover constant for beef, λ_f , and the beef transfer coefficient, F_f for the respective parameters f_m , t_m , m_p , λ_m , and F_m in Eqs. (49)-(51). However, estimates of λ_f do not appear to be available in the literature. In fact, the question of whether equilibrium beef concentration ever occurs for some radionuclides has never been completely resolved. As default in

	I A	II A											III A	IV A	V A	VIA	VII A	
II	Li 0.693	Be 0.80											B 0.693		N 0.693		F 0.693	
III	Na 17	Mg 0.693	III B	IV B	V B	VI B	VII B	VIII				IB	II B	Al 0.693	Si 0.693	P 1.97	S 0.693	Cl 0.693
IV	K 5.3	Ca 1.01	Sc 0.693	Ti 0.693	V 0.693	Cr 0.693	Mn 0.693	Fe 0.693	Co 0.693	Ni 0.693	Cu 0.693	Zn 2.71	Ga 0.693	Ge 0.693	As 0.693	Se 2.21	Br 0.693	
V	Rb 0.54	Sr 2.11	Y 0.693	Zr 0.693	Nb 0.693	Mo 0.89	Tc 0.693	Ru 0.693	Rh 0.693	Pd 0.693	Ag 0.693	Cd 0.693	In 0.693	Sn 0.693	Sb 0.693	Te 1.35	I 1.01	
VI	Cs 0.93	Ba 1.58		Hf 0.693	Ta 0.693	W 0.863	Re 0.67	Os 0.693	Ir 0.693	Pt 0.693	Au 0.693	Hg 0.693	Tl 2.19	Pb 3.33	Bi 0.693	Po 1.15	At 0.693	
VII	Fr 0.693	Ra 1.97																

Lanthanides	La 0.693	Ce 0.693	Pr 0.693	Nd 0.693	Pm 0.693	Sm 0.693	Eu 0.693	Gd 0.693	Tb 0.693	Dy 0.693	Ho 0.693	Er 0.693	Tm 0.693	Yb 0.693	Lu 0.693
Actinides	Ac 0.693	Th 0.693	Pa 0.693	U 0.693	Np 0.693	Pu 0.693	Am 0.693	Cm 0.693							

Key:

Li
0.693

 ——— Symbol
 ——— Transfer Coefficient, T_m

Figure 5.1. Metabolic half-times for the elements in milk (days), based on reference 145.

TERRA we have assumed that equilibrium does, indeed, occur, and a λ_f of $5.73 \times 10^{-7}/s$ (equal to a T_f of 14 d) is reasonable. Such a turnover rate constant allows for equilibrium to be achieved after approximately 90 days.

5.4 Lifetime Grain and Forage Requirements For Cattle On Feed, Q_g^{fc} and Q_f^{fc} , Respectively

In calculating radionuclide transport into beef the average annual lifetime feeding schedule of the cattle is combined with the predicted radionuclide concentrations in the feed to predict average annual intake of radionuclides by the cattle. For milk cows and "all other" cattle the inventory feeding schedules may be used in the calculation because slaughtered individuals from these categories may be assumed to have always resided in their respective category. However, lifetime grain and forage requirements for cattle on feed are different from the inventory grain and forage requirements (discussed in the report by Shor, Baes, and Sharp⁷) which are used in the calculation of pasture production (Sect. 4.1) because they take into account the movement of the individuals from one inventory category to another. These lifetime average feeding rates are used in the calculation of beef concentrations in the TERRA code.

Since the cattle in feedlots are slaughtered after an average occupancy of six months, and since they enter and leave the feedlot throughout the year, the lifetime feeding rate of grain and forage is a mix of the feeding schedules in the inventory categories "all other cattle" and "cattle on feed." For example, an animal entering the feedlot at the beginning of the year would have been fed on the feedlot schedule only before slaughter, but those entering thereafter until the end of the year would have been fed a combination of the feedlot and "all other cattle" schedules before slaughter. In determining the lifetime feeding schedule of slaughtered cattle from feedlots, we assume that entry and exit from the feedlot is at a constant rate equal to $s_g/365$ or $n_g/182.5$. The ideal animal entering the lot is 9 months old and is fed for 6 months or 182.5 days. In order to find an average feeding rate for this animal, his feed is added over the last 13.5 months of his life (the first 1.5 months is assumed to be on milk) and $12/13.5$ of this amount is his annual rate of feeding. From Table 17 of reference 7 the daily grain consumption rate for cattle on grain is 5.0 kg/d (equal to 1820/365). The comparable rate for forage is 2.7 kg/d. The respective rates for the "all other cattle" category are 0.4 kg/d for grain and 8.3 kg/d for forage. Therefore the totals for grain and forage for the last 13.5 months of life are 910 kg and 1003 kg, respectively. The annual rates are 891 kg and 2108 kg for grain and forage, respectively. These rates are used in the TERRA code in the calculation of radionuclide concentrations in beef from slaughtered feedlot cattle.

5.5 The Carbon and Water Content of Foods

In the TERRA code concentrations of tritium (H-3) and carbon-14 in foods are calculated according to a model which assumes that the specific activities of tritium and carbon-14 in foods at a given location are the same as the specific activities of H-3 and C-14 in atmospheric H_2O and CO_2 , respectively (equilibrium is assumed). Thus, the first step in calculating activity concentrations of tritium and carbon-14 in food is calculating their respective activity concentrations in atmospheric water vapor and carbon dioxide. For tritium, this calculation is made by utilizing the SITE parameter, absolute humidity, H , by the equation

$$C_{ww}^{H3} = 1000 \frac{C_a^{H3}}{H}, \quad (52)$$

where

- C_{ww}^{H3} = the activity concentration of tritium in atmospheric water vapor (Bq or Ci/kg),
- C_a^{H3} = the activity concentration of tritium in air based on the atmospheric dispersion calculation (Bq or Ci/m³), and
- H = the absolute humidity (g/m³).

Once the specific activity of H-3 in atmospheric water vapor is calculated, then the same activity in the atmospherically derived water of vegetable produce, beef, and milk is assumed. That is

$$C_{food}^{H3} = C_a^{H3} \cdot f_w^a, \quad (53)$$

where

$$\begin{aligned} C_{food}^{H3} &= \text{The tritium activity concentration in food (Bq or Ci/kg) and} \\ f_w^a &= \text{the fraction of water in food derived from atmospheric sources (unitless).} \end{aligned}$$

Traditionally, the tritium concentration in food has been assumed to be 50% of tritium concentration in air ($f_w^a = 0.5$) based on a model by Anspaugh, et al.²²⁶ However, recent empirical evidence suggests that tritium concentration in vegetation under chronic exposure conditions is nearly equal to the tritium air concentration ($f_w^a = 1.0$).²²⁷ In the TERRA code the default is the latter assumption.

The water content of the produce categories may be derived from the dry-to-wet weight conversion factors presented in Table 2.3. The value (1.0 – the listed conversion factor) gives the kilograms of H₂O per kilogram fresh produce. For beef and milk, reference 14 yields 0.615 and 0.87 kilograms of water per kilogram of fresh, uncooked food, respectively. The water content of leafy vegetables is assumed to be 0.934 (Table 5.1).

A specific activity approach, analogous to that for tritium, is used for carbon-14. The specific activity of C-14 in atmospheric CO₂ is given by

$$C_{cd}^{C14} = 1000 \frac{C_a^{C14}}{0.18}, \quad (54)$$

where

$$\begin{aligned} C_{cd}^{C14} &= \text{the activity concentration of carbon-14 in atmospheric CO}_2 \text{ (Bq or Ci/kg),} \\ C_a^{C14} &= \text{the activity concentration of carbon-14 in air based on the atmospheric dispersion} \\ &\quad \text{calculation (Bq or Ci/m}^3\text{), and} \\ 0.18 &= \text{the average concentration of CO}_2 \text{ in the atmosphere (g/m}^3\text{), corresponding to 330} \\ &\quad \text{ppm by volume.}^{228} \end{aligned}$$

The carbon content of the food categories in TERRA, based on a recent review by Killough²²⁹ and supplemental information from reference 14, is given in Table 5.2.

5.6 Coarse (2.5 - 15 m) Suspended Particulate Matter

Resuspension of material deposited on surface soils is calculated in TERRA via a mass loading approach.²³⁰ In such an approach the specific activity of a radionuclide in resuspended material is assumed to be the same as the specific activity of surface soil. Thus, the calculation of surface soil concentration is used together with the quantity of resuspended material in the air (mass loading) to calculate an air concentration due to resuspension. This air concentration is given by

$$C_a^r = \frac{C_s^s P_{sus}}{1 \times 10^9}, \quad (55)$$

Table 5.1. Water content of produce, beef, and cow's milk

Food	Water content ^a	Weighting factor ^b	Food	Water content
Leafy vegetables			Beef	
Broccoli	0.899	3.7	Chuck	0.65
Brussel sprouts	0.849	0.6	Flank	0.61
Cabbage	0.924	22.0	Hamburger	0.55
Cauliflower	0.917	2.8	Liver	0.697
Celery	0.937	15.5	Porterhouse	0.58
Escarole	0.866	1.1	Rib roast	0.59
Green onions	0.876	2.6	Round	0.69
Lettuce	0.948	46.0	Rump	0.55
Spinach greens	0.927	5.7	Sirloin	0.62
Weighted average	0.934		Average	0.615
Exposed produce ^c	0.874		Whole cow's milk	0.870
Protected produce ^c	0.778			
Grain foods ^c	0.112			

^aKilograms of water per kilograms fresh, unprepared produce or edible portions of uncooked food (reference 14)

^bRelative importance based on production in kilograms (% of total) in the conterminous United States.

^cBased on values given in Table 2.3.

where

- C_s^s = surface soil (depth = 1 cm) concentration (Bq or Ci/kg),
- 1×10^9 = the number of micrograms per kilogram ($\mu\text{g}/\text{kg}$),
- C_a^r = resuspension air concentration (Bq or Ci/ m^3), and
- P_{sm} = suspended particulate matter ($\mu\text{g}/\text{m}^3$).

In TERRA the mass loading value P_{sm} is based on data reported by the EPA.²³¹ This parameter represents the 2.5-15 μm diameter particle fraction collected by either the Size-Selective Inlet (SSI) hi vol or the dichotomous samplers operated as part of the Inhalable Particulate Network (IPN) operated by EPA's Environmental Monitoring and Support Laboratory, Research Triangle Park. Inhalable suspended particulate matter appears to be bimodally distributed into fine and coarse particle sizes. The fine fraction (<0.1-2 μm) are mostly generated by fossil fuel combustion and atmospheric photochemistry processes. The coarse fraction (2.5-15 μm) is primarily a result of windblown dusts, mechanical processes, and pollen.

The value of P_{sm} of 15.5 $\mu\text{g}/\text{m}^3$ used as default in TERRA is the geometric mean of values taken from the April 1979-June 1980 IPN summary (Fig. 5.2). The data are reported for 46 sampling locations in the conterminous United States, and represent annual arithmetic averages for each station. As shown in Fig. 5.2, the parameter P_{sm} is lognormally distributed. The range of measured values is from 3.2 to 52.4 $\mu\text{g}/\text{m}^3$.

Table 5.2. Water content of produce, beef, and cow's milk

Food	Carbon content ^a	Weighting factor ^b	Reference	Food	Carbon content	Weighting factor	Reference
Leafy vegetables				Protected produce			
Broccoli	0.042	3.7	229	Bean (dry)	0.198	2.2	229
Brussel sprouts	0.065	0.6	229	Cantaloupe	0.025	1.1	229
Cabbage	0.032	22.0	229	Carrot	0.049	2.4	229
Cauliflower	0.035	2.8	229	Grapefruit	0.048	5.5	14
Celery	0.024	15.5	229	Lemon	0.047	2.4	14
Escarole	0.056	1.1	14	Onion	0.054	3.6	14
Green onions	0.053	2.6	14	Orange	0.055	22.8	229
Lettuce	0.020	46.0	229	Peanut	0.574	3.4	229
Spinach greens	0.028	5.7	229	Peas	0.114	0.4	14
Weighted average	0.026			Potato	0.095	33.7	229
Exposed produce ^c				Sugarbeet	0.051	6.5	14
Apple	0.070	15.4	229	Sugarcane	0.438	5.5	229
Asparagus	0.030	0.6	229	Sweet corn	0.118	6.0	229
Bushberries	0.070	1.6	229	Sweet potato	0.137	1.5	229
Cherry	0.074	0.7	14	Tree nuts	0.659	0.4	229
Cucumber	0.016	4.0	14	Watermelon	0.034	2.6	14
Eggplant	0.031	0.1	14	Weighted average	0.116		
Grape	0.083	20.2	229	Grains			
Peach	0.056	6.9	229	Barley	0.395	10.1	229
Pear	0.076	3.5	229	Corn (for meal)	0.118	37.7	229
Plums and prunes	0.062	3.1	229	Oats	0.431	2.3	229
Sweet pepper	0.033	1.3	14	Rye	0.396	0.5	229
Snap bean	0.047	0.7	229	Soybean	0.465	5.3	229
Squash	0.021	1.8	229	Wheat	0.391	44.0	229
Strawberry	0.044	1.3	229	Weighted average	0.293		
Tomato	0.025	38.8	229	Whole cow's milk			
Weighted average	0.050				0.069		14
Beef	0.228		229				

^aKilograms of carbon per kilograms fresh, unprepared produce. Based on protein, fat, and carbohydrate content of 50, 76, and 44%, respectively.

^bRelative importance based on production in kilograms (% of total) in the conterminous United States.

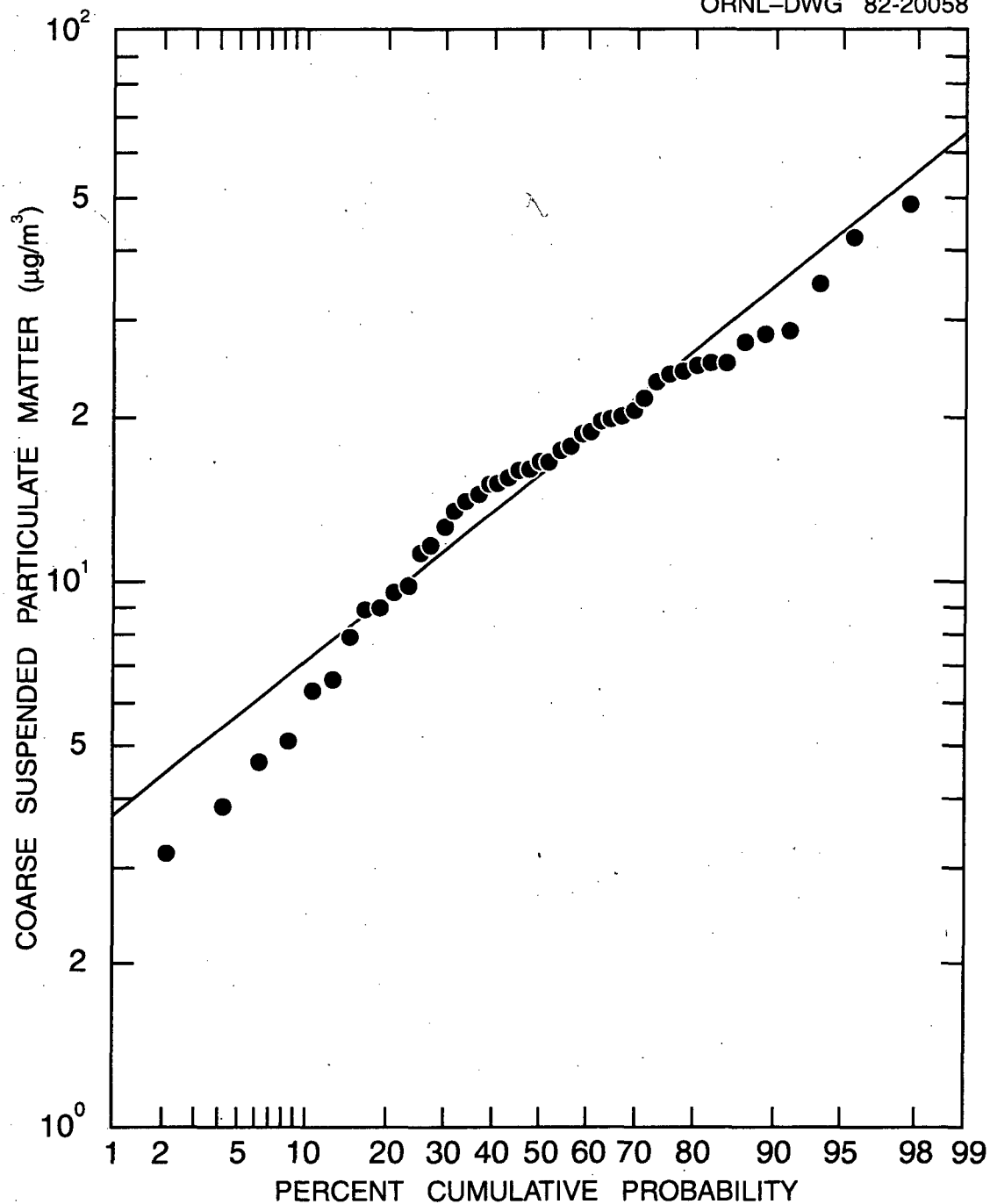


Figure 5.23. Lognormal probability plot of coarse suspended particulate matter (2.5 – 15 μm).

Resuspended material may contribute to plant surface concentrations before and after termination of the atmospheric source term. In TERRA a deposition rate of the resuspended activity is calculated according to

$$D_r' = \frac{C_a' V_d'}{100}, \quad (56)$$

where

- D_r' = the deposition rate of resuspended material (Bq or Ci/m²/s),
- V_d' = deposition velocity of the resuspended material (cm/s), and
- 100 = the number of centimeters in a meter (cm/m).

The value of V_d' used in TERRA is 0.1 cm/s, which is a reasonable estimate for particle diameters between 2 and 15 μm , a friction velocity of 30 cm/s, and particle densities $>1 \text{ g/cm}^3$ as shown by Sehmel²³² (Figure 5 in reference 232).

6. SUMMARY

In this report we have documented most of the default parameters incorporated into the TERRA computer code. Especially, we have presented a literature review and systematic analysis of element-specific transfer parameters B_v , B_r , F_m , F_f , and K_d . This review and analysis merely suggests default values which are consistent with the modeling approaches taken in TERRA and may be acceptable for most assessment applications of the computer code. However, particular applications of the code and additional analysis of elemental transport may require alternative values to the default values in TERRA. Also, use of the values reported herein in other computer codes simulating terrestrial transport is not advised without careful interpretation of the limitations and scope of our analyses.

In addition to the default elemental transport parameters, we have discussed an approach to determination of vegetation-specific interception fractions. The limitations of this approach are many, and its use indicates the need for analysis of deposition, interception, and weathering processes. Judgement must be exercised in interpretation of plant surface concentrations generated through use of our approach.

Finally, we have documented the location-specific agricultural, climatological, and population parameters in the default SITE data base. These parameters are intended as alternatives to "average" values currently used in assessment models. Indeed, areas in the United States where intensive crop, milk, or beef production occurs will be reflected in the parameter values as will areas where little agricultural activity occurs. However, the original information sources contained some small error and the interpolation and conversion methods used will add more. Therefore, our values should be regarded as default best estimates, not absolute "correct" values. As with any assessment, site-specific information is recommended over default values.

Parameters used in TERRA not discussed herein are discussed in the companion report to this one—ORNL-5785.³ In the companion report the models employed in and the coding of TERRA are discussed. These reports together provide documentation of the TERRA code and its use in assessments.

7. REFERENCES

- [1] Moore, R. E., C. F. Baes, III, L. M. McDowell-Boyer, A. P. Watson, F. O. Hoffman, J. C. Pleasant, and C. W. Miller. 1979. *AIRDOS-EPA: A Computerized Methodology for Estimating Environmental Concentrations and Dose to Man from Airborne Releases of Radionuclides*. ORNL-5532. Oak Ridge National Laboratory.
- [2] Begovich, C. L., K. F. Eckerman, E. C. Schlatter, S. Y. Ohr, and R. O. Chester. 1981. *DARTAB: A Program to Combine Airborne Radionuclide Environmental Exposure Data with Dosimetric and Health Effects Data to Generate Tabulations of Predicted Impacts*. ORNL-5692. Oak Ridge National Laboratory.
- [3] Baes, C. F., III, R. D. Sharp, A. L. Sjoreen, and O. W. Hermann. In press. *TERRA: A Computer Code for Calculation of the Transport of Environmentally Released Radionuclides Through Agriculture*. ORNL-5785. Oak Ridge National Laboratory.
- [4] Miller, C. W., C. L. Begovich, O. W. Hermann and A. L. Sjoreen. In press. *ANEMOS: A Computer Code to Estimate Air Concentrations and Ground Deposition Rates for Atmospheric Nuclides Emitted from Multiple Operating Sources*. ORNL-5913. Oak Ridge National Laboratory.
- [5] Begovich, C. L., S. Y. Ohr, R. O. Chester, and A. L. Sjoreen. In press. *ANDROS: A Code for Assessment of Nuclide Doses and Risks with Option Selection*. ORNL-5889. Oak Ridge National Laboratory.
- [6] U.S. Nuclear Regulatory Commission. 1977. Regulatory Guide 1.109, *Calculation of Annual Doses to Man from Routine Releases of Reactor Effluents for the Purpose of Evaluating Compliance with 10 CFR Part 50 Appendix Z (Revision I)*. Office of Standards Development.
- [7] Shor, R. W., Baes, C. F., III, and R. D. Sharp. 1982. *Agricultural Production in the United States by County: A Compilation of Information from the 1974 Census of Agriculture for Use in Terrestrial Food Chain Transport and Assessment Models*. ORNL-5768. Oak Ridge National Laboratory.
- [8] Gibbons, J. W., D. C. Adriano, J. J. Alberts, and K. W. McLeod. 1978. *Critical Pathways of Radionuclides to Man from Agro-Ecosystems*. NUREG/CR-0536.
- [9] Herslöf, L. W. and J. C. Corey. 1978. "Uptake of three isotopes of plutonium from soil by sweet corn grown in a growth chamber." In Adriano, D. C. and I. L. Brisbin, Jr., (eds.) *Environmental Chemistry and Cycling Process*. Proceedings of a symposium held at Augusta, Ga. April 28-May 1, 1976. pp. 622-627.
- [10] Schreckhise, R. G. and J. F. Cline. 1980. "Comparative uptake and distribution of plutonium, americium, curium, and neptunium in four plant species." *Health Phys.* **38**: 817-824.
- [11] Morgan, A. 1959. "The uptake of ⁹⁰Sr by rye grass." *J. Nucl. Energy Part A: Reactor Sci.* **11**: 8-13.
- [12] Baes, C. F., III and R. D. Sharp. 1981. *A Directory of Parameters Used in a Series of Assessment Applications of the AIRDOS-EPA and DARTAB Computer Codes*. ORNL-5710. Oak Ridge National Laboratory.
- [13] Morrison, F. B. 1956. *Feeds and Feeding. A Handbook for the Student and Stockman*. 22nd ed. The Morrison Publishing Co., Ithaca, New York.
- [14] Spector, W. S. 1956. *Handbook of Biological Data*. W. B. Saunders Co., Philadelphia. p. 187.

- [15] Ng, Y. C., C. A. Burton, S. E. Thompson, R. K. Tandy, H. K. Kretner, and M. W. Pratt. 1968. "Prediction of the maximum dosage to man from the fallout of nuclear devices." In *Handbook for Estimating the Maximum Internal Dose from Radionuclides Released to the Biosphere*. UCRL-50163, Pt. IV. Lawrence Radiation Laboratory.
- [16] Baes, C. F., III and J. A. Katz. Unpublished analysis of East Tennessee pumpkins, vines, and soils.
- [17] Haghiri, F. 1964. "Strontium-90 accumulation by some vegetable crops." *Ohio J. Sci.* **64**(5): 371-374.
- [18] Fredriksson, L. and Å. Eriksson. 1970. "Plant uptake of fission products I. Uptake of ⁹⁰Sr in pot experiments in relation to uptake under field conditions." *Lantbrökogsk. Annlr.* **36**: 3-18.
- [19] Cherry, D. S. and R. K. Guthrie. 1979. "The uptake of chemical elements from coal ash and settling basin effluent by primary producers II. Relation between concentrations in ash deposits and tissues of grasses growing on the ash." *Sci. Tot. Environ.* **13**: 27-31.
- [20] Sheaffer, C. C., A. M. Decker, R. L. Chaney, and L. W. Douglass. 1979. "Soil temperature and sewage sludge effects on metals in crop tissue and soils." *J. Environ. Qual.* **8**(4): 455-459.
- [21] Andersen, A. J. 1971. "Influence of phosphorus and nitrogen nutrition on uptake and distribution of strontium and calcium in oat plants." *Soil Sci. Soc. Am. Proc.* **35**: 108-111.
- [22] Essington, E., H. Nishita, and A. Wallace. 1963. "Effect of chelating agents on the uptake of Y-91, Ru-106, Ce-144, and Pm-147 by beans grown in a calcareous soil." *Soil. Sci.* **95**: 331-337.
- [23] Gast, R. G., E. R. Landa, L. J. Thorvig, D. F. Grigal, and J. C. Balogh. 1979. *The behavior of technetium-99 in soils and plants: Final Report for the period April 1, 1974 to December 31, 1978*. COO-2447-6. National Technical Information Service, Springfield, Virginia.
- [24] Schroeder, H. A. and J. J. Balassa. 1963. "Cadmium: uptake by vegetables from superphosphate in soil." *Science* **140**: 819-820.
- [25] Orr, J. B., F. C. Kelly, and G. L. Stuart. 1978. "The effect of iodine maturing on the iodine content of plants." *J. Agri. Sci.* **18**: 159-161.
- [26] Haak, E. and Å. Eriksson. 1973. *Studies on Plant Accumulation of Fission Products under Swedish Conditions XIV Uptake of ¹³⁷Cs by Wheat and Timothy from Six Different Soils as Influenced by Rate of K-Fertilization and by Type and Rate of N-Fertilization in Pot Experiments*. FOA 4 Rapport. C4557-A3. October, 1973. 36 pp.
- [27] Ter Haar, G. 1970. "Air as a source of lead in edible crops." *Environ. Sci. Technol.* **4**(3): 226-30.
- [28] Watters, R. L., J. E. Johnson, and W. R. Hansen. 1969. *A Study of Unsupported Polonium-210 for Ion Exchange in Soil and Uptake in Vegetation*. Second Technical Progress Report of the Department of Radiology and Radiation Biology, Colorado State University, Fort Collins, Colorado. 8052 1. COO-1733-3.
- [29] Prister, B. S. 1970. "Behavior of uranium in the biologic chain." In *USSR Reports on Natural and Fallout Radioactivity*. pp. 194-207. AEC-tr-7128, USAEC/HSL.
- [30] Wallace, A., E. M. Romney, H. Nishita, and E. K. Schulz. 1979. *Preliminary Analysis of First Crop of Plants Grown in Seven Soils Uniformly Contaminated with Four Transuranic Elements Simultaneously*. University of California, L.A. NUREG/CR-0700.136

- [31] Romney, E. M., W. L. Ehrler, A. H. Lange, and K. H. Larson. 1960. "Some environmental factors influencing radiostrontium uptake by plants." *Plant and Soil* 12(1): 41-48.
- [32] Duckworth, R. B. and J. Hawthorn. 1960. "Uptake and distribution of strontium in vegetables and cereals." *J. Sci. Food Agric.* 11: 218-225.
- [33] Evans, E. J. and A. J. Dekker. 1962. "Comparative Sr-90 content of agricultural crops grown in a contaminated soil." *Can. J. Plant Sci.* 42: 252-258.
- [34] Evans, E. J. and A. J. Dekker. 1968. "Comparative Cs-137 content of agricultural crops grown in a contaminated soil." *Can. J. Plant Sci.* 48: 183-188.
- [35] Singh, B. R. and K. Steenberg. 1974. "Plant response to micronutrients I. Uptake, distribution and translocation of zinc in maize and barley plants." *Plant and Soil* 40: 637-646.
- [36] Singh, B. R. and K. Steenberg. 1974. "Plant response to micronutrients II. Uptake, distribution and translocation of manganese in maize and barley plants." *Plant and Soil* 40: 647-654.
- [37] Singh, B. R. and K. Steenberg. 1974. "Plant response to micronutrients III. Interaction between manganese and zinc in maize and barley plants." *Plant and Soil* 40: 655-667.
- [38] National Academy of Sciences. 1971. *Nutrient Requirements of Dairy Cattle* (fourth ed.). ISBN 0-309-01916-8.
- [39] Ng, Y. C., C. S. Colsher, and S. E. Thompson. 1979. "Transfer coefficients for terrestrial food chains — their derivation and limitations." In Kellermann, H. J. (ed.) *Radioaktivität und Umwelt*. Proceedings of the 12th Annual Conference of the Fachverband für Strahlenschutz, Norderney, West Germany, 2-6 October 1978. Band I. pp. 455-481.
- [40] Ng, Y. C., C. S. Colsher, and S. E. Thompson. 1979. "Transfer factors for assessing the dose from radionuclides in agricultural products." In *Biological Implications of Radionuclides Released from Nuclear Industries, Vol. II*. Proceedings of an International Symposium on Biological Implications of Radionuclides Released from Nuclear Industries, Vienna, 26-30 March 1979. pp. 295-318 (IAEA-SM-237/54).
- [41] Hansen, W. R. and R. L. Watters. 1970. "Plant uptake of ²¹⁰Po from soil." *Rad. Bot.* 10(4): 371-375.
- [42] Vavilov, P. P., I. N. Verkhovskaya, O. N. Popova, and R. P. Kodaneva. 1972. "Conditions of radium accumulation by plants from the soil." *Radioekologicheskie Issledovaniya v Prirodnykh Biogeotsenozakh* (Verkhovskaya, I. N., ed.) pp. 95-103. Moscow: Izdatel'stvo Nauka.
- [43] Routson, R. C. and D. A. Cataldo. 1978. "A growth chamber study of the effect of soil concentration and plant age on the uptake of Sr and Cs by tumbleweed." *Comm. Soil Sci. Pt. Anal.* 9(3): 215-30.
- [44] Il'ina, G. V. and S. G. Rydkii. 1965. "Uptake of radioactive fission products by field crops. Report 1: Accumulation of radioactive fission products by grain and oil-bearing crops." *Fed. Am. Soc. Exp. Bio. Proc.* 25: T123-T127.
- [45] Andersen, A. J. 1971. "The uptake and distribution of strontium in oat as influenced by the time of supply." *Soil Sci.* 111(6): 379-81.
- [46] Baranova, Z. A. and A. S. Frid. 1975. "Absorption of strontium-90, potassium and calcium by oat plants from soil during ontogenesis." *Soviet Ph. Phys. (tr.)* 22(6): 1173-1176.137

- [47] Myttenaere, C. 1965. "The influence of the strontium/calcium ratio of the nutrient solution on the translocation and chemical forms of strontium and calcium in *Pisum sativum*." *Rad. Bot.* 5: 1143-151.
- [48] Ringoet, A. and D. de Zeeuw. 1968. "Discrimination between calcium and strontium in oat plants. I. Influence of the growth stage of the plants and of the osmotic potential of the root medium." *Z. Phlan. Bd.* 59(3): 238-248.
- [49] Ringoet, A. and D. de Zeeuw. 1968. "Discrimination between calcium and strontium in oat plants. II. Relation to the differential chemical binding of both ions." *Z. Phlan. Bd.* 59(3): 249-257.
- [50] Soileau, J. M. 1973. "Activity of barley seedling roots as measured by strontium uptake." *Agron. J.* 65(4): 625-628.
- [51] Kodaira, K., A. Tsumura, and H. Kobayashi. 1973. "Uptake of radioactive strontium and cesium in rice plants. (1) Accumulation of Sr and Cs in rice grains through roots." *J. Radial. Res.* 14: 31-39.
- [52] Vinogradov, A. P. 1959. *The Geochemistry of Rare and Dispersed Elements in Soils*, 2nd ed. Consultants Bureau, Inc., New York.
- [53] Shacklette, H. T., J. A. Erdman, T. F. Harms, and C. S. E. Papp. 1978. "Trace elements in plant foodstuffs." In Dehme, F. W. (ed.). *Toxicity of Heavy Metals in the Environment* Part 1. Marcel Dekker, Inc., New York. pp. 25-68.
- [54] Oakes, T. W., K. E. Shank, C. E. Easterly, and L. R. Quintana. 1977. "Concentrations of radionuclides and selected stable elements in fruits and vegetables." In *Environmental Health, 11th Annual Conference on Trace Substances*.
- [55] Barber, D. A. 1964. "Influence of soil organic matter on the entry of cesium-137 into plants." *Nature* 204: 1326-1327. Schulz, R. K. 1965. "Soil chemistry of radionuclides." *Health Phys.* 11: 1317-1324.
- [56] Fredriksson, L., Å. Eriksson, and H. Lönsjö. 1966. *Studies on Plant Accumulation of Fission Products under Swedish Conditions. VIII. Uptake of ¹³⁷Cs in Agricultural Crops as Influenced by Soil Characteristics, and Rate of Potassium Fertilization in a Three Year Micro Plot Experiment*. Research Institute of National Defense, Stockholm, Sweden. FOA 4 Rapport A 4486-4623.
- [57] Fredriksson, L., H. Lönsjö and Å. Eriksson. 1969. *Studies on Plant Accumulation of Fission Products under Swedish Conditions. X. Absorption of ⁹⁰Sr and ¹³⁷Cs from Soil by Vegetable Crops*. Research Institute of National Defense, Stockholm, Sweden. FOA 4 Rapport C 4387-28.
- [58] Fredriksson, L., H. Lönsjö, and Å. Eriksson. 1969. *Studies on Plant Accumulation of Fission Products under Swedish Conditions. XII. Uptake of ¹³⁷Cs by Barley and Peas from 12 Different Top Soils Combined with 2 Sub-soils in a Long Term Micro Plot Experiment*. Research Institute of National Defense, Stockholm, Sweden. FOA 4 Rapport C 4405-4428.
- [59] Rediske, J. H., J. F. Cline, and A. A. Selders. 1955. *The Absorption of Fission Products by Plants*. HW-36734.
- [60] Romney, E. M., J. W. Neel, H. Nishita, J. H. Olafson, and K. H. Larson. 1957. "Plant uptake of ⁹⁰Sr, ⁹¹Y, ¹⁰⁶Ru, ¹³⁷Cs, and ¹⁴⁴Ce from soils." *Soil Sci.* 83: 369-376.
- [61] Fredriksson, L., H. Lönsjö, and Å. Eriksson. 1969. *Studies on Plant Accumulation of Fission Products Under Swedish Conditions. X. Absorption of ⁹⁰Sr and ¹³⁷Cs from Soil by Vegetable Crops*. Research Institute of National Defense, Stockholm, Sweden. FOA 4 Rapport C 4387-28.

- [62] Andersen, A. J. 1967. *Investigations on the Plant Uptake of Fission Products from Contaminated Soils. I. Influence of Plant Species and Soil Types on the Uptake of Radioactive Strontium and Caesium*. Danish Atomic Energy Commission, Research Establishment Risø. Risø Report No. 170. November, 1967.
- [63] Neel, J. W., J. H. Olafson, A. J. Steen, B. E. Gillooly, H. Nishita, and K. H. Larson. 1953. *Soil-Plant Interrelationships with Respect to the Uptake of Fission Products: I. The Uptake of Sr⁹⁰, Cs¹³⁷, Ru¹⁰⁶, Ce¹⁴⁴, and Y⁹⁰*. The University of California. UCLA-247.
- [64] Routson, R. C. 1975. *The Effect of Soil Concentration on the Tumbleweed Uptake of ⁹⁰Sr and ¹³⁷Cs from a Burbank Sand*. Battelle-Pacific Northwest Laboratories. BNWL-1905.
- [65] Furr, A. K., T. F. Parkinson, C. L. Heffron, J. T. Reid, W. M. Haschek, W. H. Gutenmann, C. A. Bathe, L. E. St. John, Jr., and D. J. Lisk. 1978. "Elemental content of tissues and excreta of lambs, goats, and kids fed white sweet clover growing on fly ash." *J. Agric. Food Chem.* **26**(4): 847-851.
- [66] Cataldo, D. A. 1979. *Comparative Availability of Cesium and Strontium for Plant Absorption from Amended Rupert Surface Soil and Associated Subsoil: Influence of Growth Conditions*. Pacific Northwest Laboratory PNL-2741.
- [67] Essington, E., H. Nishita, and A. Wallace. 1962. "Influence of chelates on availability of fission products to plants grown in a contaminated soil." *Soil Sci.* **94**: 96-105.
- [68] Nishita, H., A. J. Steen, and K. H. Larson. 1958. "Release of Sr⁹⁰ and Cs¹³⁷ from Vina loam upon prolonged cropping." *Soil Sci.* **86**: 195-201.
- [69] Nishita, H., R. M. Haug, and M. Hamilton. 1968. "Influence of minerals on Sr⁹⁰ and Cs¹³⁷ uptake by bean plants." *Soil Sci.* **105**: 237-243.
- [70] Nishita, H. and R. M. Haug. 1972. "Influence of clinoptilolite on Sr⁹⁰ and Cs¹³⁷ uptakes by plants." *Soil Sci.* **114**(2): 149-157.
- [71] Fredriksson, L., B. Eriksson, B. Rasmuson, B. Gahne, K. Edvarson, and K. Löw. 1958. "Plant uptake of Sr⁹⁰ and Cs¹³⁷ from soils." In *Proceedings of the Second United Nations International Conference on the Peaceful Uses of Atomic Energy Vol. 18*, held in Geneva 1-13, September, 1958. pp. 449-470.
- [72] Vose, P. B. and Koontz, H. V. 1959. "Uptake of strontium by pasture plants and its possible significance in relation to the fall-out of strontium." *Nature* **183**: 1447-1448.
- [73] Milbourn, G. M., F. B. Ellis, and R. S. Russell. 1959. "The absorption of radioactive strontium by plants under field conditions in the United Kingdom." *J. Nucl. Energy Part A: Reactor Sci.* **10**: 116-132.
- [74] Ralls, J. W., S. Primbsch, T. R. Guckeen, H. J. Maagdenberg, J. Rinehart, F. C. Lamb, and W. A. Mercer. 1967. "Distribution of strontium and calcium in major vegetable and fruit crops and criteria for use of fallout-contaminated foods." *Radiol. Health Data Rep.* **8**(7): 355-358.
- [75] Andersen, A. J. 1965. "Uptake by plants of radionuclides from contaminated soils." *Nature* **208**(5006): 195-196.
- [76] Furr, A. K., T. F. Parkinson, R. A. Hinrichs, D. R. Van Campen, C. A. Bathe, W. H. Gutenmann, L. E. St. John, Jr., I. S. Pakkala, and D. J. Lisk. 1977. "National survey of elements, and radioactivity in fly ashes and absorption of elements by cabbage grown in fly ash-soil mixtures." *Environ. Sci. Technol.* **11**(3): 1194-1201.
- [77] Arkhipov, N. P., Y. A. Fedorov, E. F. Bondar, R. M. Aleksakhin, G. N. Romanov, and L. T. Feuraleva. 1974. "Predicting ⁹⁰Sr accumulation in the crop harvest as a result of its uptake from the soil." *Soviet Soil Sci.* **6**(4): 412-419.

- [78] Fredriksson, L., Å. Eriksson, and E. Haak. 1961. *Studies on Plant Accumulation of Fission Products Under Swedish Conditions. II. Influence of Lime and Phosphate Fertilizer on the Accumulation of Sr-89 in Red Clover Grown in 29 Different Swedish Soils*. Research Institute of National Defense. Stockholm, Sweden. FOA 5 Rapport A4188-4626.
- [79] Fredriksson, L., E. Haak, and Å. Eriksson. 1969. *Studies on Plant Accumulation of Fission Products Under Swedish Conditions. XI. Uptake of ⁹⁰Sr by Different Crops as Influenced by Liming and Soil Tillage Operations*. Research Institute of National Defense. Stockholm, Sweden. FOA Rapport C 4395-28.
- [80] Haak, E. and H. Lönsjö. 1975. *Studies on Plant Accumulation of Fission Products Under Swedish Conditions. XVI. Uptake of ⁹⁰Sr by Barley and Peas from 12 Different Topsoils Combined with 2 Subsoils in a Long Term Microplot Experiment*. Department of Radiobiology, Agricultural College of Sweden. S-750 07 UPPSALA 7.
- [81] Romney, E. M., G. V. Alexander, G. M. LeRoy, and K. H. Larson. 1959. "Influence of stable Sr on plant uptake of Sr90 from soils." *Soil Sci.* **87**: 42-45.
- [82] Lee, C. C. 1961. "Effects of plant nutrients on uptake of radiostrontium by thatcher wheat." *Science* **133**: 1921-1922.
- [83] Andersen, A. J., G. Gissel-Nielsen, and G. Nielsen. 1967. "Effects of fertilization on the strontium-calcium and cesium-potassium relationships in plants. I. The uptake and distribution of radioactive strontium and calcium in oats." *Kgl. Vet.-og. Landbohøjskoles Arsskrift* **1967**: 154-167.
- [84] Shirshova, R. A. 1962. "Effect of potassium fertilizers on the uptake of radioactive strontium by plants." *Pochvovedenie* **1962**(3): 36-43.
- [85] Mel'nikova, M. K. and Z. A. Baranova. 1969. "The mechanism of radiostrontium intake in potato tubers." In *USSR Reports on Natural and Fallout Radioactivity*. U.S. Atomic Energy Commission, Health and Safety Laboratory. UNSCLEAR Number A/AC.82/G/L.-1288. pp. 127-142.
- [86] Wallace, A., R. K. Schulz, E. M. Romney, and H. Nishita. 1979. *Biological Transport of Radionuclides at Low Level Waste Storage Sites*. Laboratory of Nuclear Medicine and Radiation Biology, University of California. NUREG/CR-0701.
- [87] Kirchmann, R., R. Boulenger, and A. LaFontaine. 1968. "Absorption of ²²²Ra in cultivated plants." pp. 1045-1051. In W. S. Synder et al., eds.). *Proceedings of the IRPA Congress on Radiation Protection, Vol. II*. Rome, 1966. Pergamon Press.
- [88] DeBortoli, M. and P. Gaglione. 1972. "Radium-226 in environmental materials and foods." *Health Phys.* **22**(1): 43-48.
- [89] Grzybowska, D. 1974. "Uptake of ²²⁶Ra by plants from contaminated soils." *Nukleonika* **19**: 71-78.
- [90] Mordberg, E. L., V. M. Aliksandruk, G. F. Kovygin, I. I. Shevchenko, V. M. Blyumshtein, and G. F. Yushkevich. 1976. "Translocation of isotopes of the uranium-radium series into the grain of some agricultural crops." *Gig. Sanit.* **2**: 58-61.
- [91] Moffett, D. and M. Tellier. 1977. "Uptake of radioisotopes by vegetation growing on uranium tailings." *Can. J. Soil. Sci.* **56**: 417-424.
- [92] Khademi, B., A. Alemi, and A. Nasserli. 1980. "Transfer of radium from soil to plants in the area of high natural radioactivity in Iran (Ramsar)." In Gesell, T. F., W. M. Lowder, and J. E. McLaughlin. (eds.) *The Natural Radiation Environment III, Vol. I*. CONF-78422.

- [93] Marple, M. L. 1980. *Radium-224 in Vegetation and Substrates at Inactive Uranium Mill Sites*. Ph.D. Thesis. University of New Mexico, Albuquerque, New Mexico. LA-8183-T.
- [94] Nelson, V. A. 1979. *Radiological Survey of Plants, Animals, and Soil at Five Atolls in the Marshall Islands September - October 1976*. University of Washington, College of Fisheries, Laboratory of Radiation Ecology, Seattle, Washington. NVO-269-36.
- [95] Fowler, T. W. 1980. "Comments on Ra-226 edible plant/soil bioaccumulation factor recommended by ORNL in the AIRDOS-EPA manual." Letter to Christopher B. Nelson, May 21, 1980.
- [96] McDowell-Boyer, L. M., A. P. Watson, and C. C. Travis. 1979. *Review and Recommendations of Dose Conversion Factors and Environmental Transport Parameters for ²¹⁰Pb and ²²⁶Ra*. Final Report Oak Ridge National Laboratory. NUREG/CR-0574. ORNL/NUREG-56.
- [97] Mulla, D. J., A. L. Page, and T. J. Ganje. 1980. "Cadmium accumulations and bioavailability in soils from long-term phosphorus fertilization." *J. Environ. Qual.* 9(3): 408-412.
- [98] Isaac, R. A., S. R. Wilkinson, and J. A. Stuedemann. 1978. "Analysis and fate of arsenic in broiler litter applied to coastal Bermuda grass and Kentucky-31 tall fescue." In Adriano, D. C. and I. L. Brisbin, Jr. (eds.), *Environmental Chemistry and Cycling Processes*. Proceedings of a symposium held at Augusta, Georgia April 28-May 1, 1976. pp. 207-220.
- [99] Dedolph, R., Ter Haar, G., Holtzman, R., and Lucas, H., Jr. 1970. "Sources of Pb in perennial ryegrass and radishes." *Environ. Sci. Technol.* 4(3): 217-225.
- [100] Rabinowitz, M. 1972. "Plant uptake of soil and atmospheric lead in southern California." *Chemosphere* 1(4): 175-180.
- [101] Wilson, D. O. and J. F. Cline. 1966. "Removal of plutonium-239, tungsten-185, and lead-210 from soils." *Nature* 209: 941-942.
- [102] Keefer, R. F., R. M. Singh, D. J. Horvath, and A. R. Khawaja. 1979. "Heavy metal availability to plants from sludge application." *Compost. Sci.* 20(3): 31-34.
- [103] Karamanos, R. E., J. R. Bettany, and J. W. B. Stewart. 1976. "The uptake of native and applied lead by alfalfa and bromegrass from soil." *Can. J. Soil Sci.* 56: 485-494.
- [104] Okamoto, K., Y. Yamamoto, and K. Fuwa. 1978. "Accumulation of manganese, zinc, cobalt, nickel, and cadmium by *Clethra barbinervis*." *Agric. Biol. Chem.* 42(3): 663-664.
- [105] Preer, J. R., H. S. Sekhon, B. R. Stephens, and M. S. Collins. 1980. "Factors affecting heavy metal content of garden vegetables." *Environ. Pollut. B* 1: 95-104.
- [106] Menzel, R. G. 1965. "Soil-plant relationships of radioactive elements." *Health Phys.* 11: 1325-1332.
- [107] Cataldo, D. A. 1979. *Behavior of Technetium and Iodine in a Hanford Sand and Associated Subsoil: Influence of Soil Aging on Uptake by Cheatgrass and Tumbleweed*. Pacific Northwest Laboratory. PNL-2740. March 1979.
- [108] Davis, R. D. 1980. "Uptake of flouride by ryegrass grown in soil treated with sewage sludge." *Environ. Pollut. B* 1: 277-284.
- [109] Nishita, H., A. Wallace, and E. M. Romney. 1978. *Radionuclide Uptake by Plants*. Laboratory of Nuclear Medicine and Radiation Biology, University of California, Los Angeles. NUREG/CR-0336. UCLA 12-1 158.
- [110] Baes, C. F., Jr. and R. E. Mesmer. 1976. *The Hydrolysis of Cations*. John Wiley & Sons, New York. 489 pp.

- [111] Gibson, J. A., J. F. Miller, P. S. Kennedy, and G. W. P. Rengstorff. 1959. *The Properties of the Rare Earth Metals and Compounds*. Prepared for the Rare Earth Research Group. Battelle Memorial Institute.
- [112] Salcedo, I. H., B. G. Ellis, and R. E. Lucas. 1979. "Studies in soil manganese: II. Extractable manganese and plant uptake." *Soil Sci. Soc. Am. J.* **43**: 138-141.
- [113] Shuman, L. M. and O. E. Anderson. 1974. "Evaluation of six extractants for their ability to predict manganese concentrations in wheat and soybeans." *Soil. Sci. Amer. Proc.* **38**: 788-790.
- [114] Sommers, L. E. 1980. "Toxic metals in agricultural crops." In Britton, G., B. L. Damron, G. T. Edds, and J. M. Davidson (eds.) *Sludge - Health Risks of Land Application*. Ann Arbor, Michigan. pp. 105-140.
- [115] Safaya, N. M. 1976. "Phosphorus-zinc interaction in relation to absorption rates of phosphorus, zinc, copper, manganese, and iron in corn." *Soil Sci. Soc. Am. J.* **40**: 1976.
- [116] Giordano, P. M., D. A. Mays, and A. D. Behel, Jr. 1979. "Soil temperature effects on uptake of cadmium and zinc by vegetables grown on sludge-amended soil." *J. Environ. Qual.* **8**(2): 233-236.
- [117] Shukla, U. C. and H. Raj. 1974. "Influence of genetic variability on zinc response in wheat." *Soil Sci. Soc. Amer. Proc.* **38**: 477-479.
- [118] MacClean, A. J. 1974. "Effects of soil properties and amendments on the availability of zinc in soils." *Can. J. Soil. Sci.* **54**: 369-378.
- [119] Coffman, C. B. and J. R. Miller. 1973. "Response of corn in the greenhouse to soil applied zinc and a comparison of three chemical extractions for determining available zinc." *Soil. Sci. Soc. Amer. Proc.* **37**: 721-724.
- [120] Gammon, N., Jr., G. M. Volk, E. N. McCubbin, and A. H. Eddins. 1954. "Soil factors affecting molybdenum uptake by cauliflower." *Soil Sci. Soc. Amer. Proc.* **18**: 302-305.
- [121] Singh, M. and V. Kumar. 1979. "Sulfur, phosphorus, and molybdenum interactions on the concentration and uptake of molybdenum in soybean plants (*Glycine max*)." *Soil Sci.* **127**(5): 307-312.
- [122] Wildung, R. E., T. R. Garland, and D. A. Cataldo. 1977. "Accumulation of technetium by plants." *Health Phys.* **32**: 315-317.
- [123] Hoffman, F. O., J. W. Huckabee, D. M. Lucas, C. T. Garten, Jr., T. G. Scott, R. L. Walker, P. S. Gouge, and C. V. Holmes. 1980. *Sampling of Technetium-99 in Vegetation and Soils in the Vicinity of Operating Gaseous Diffusion Facilities*. ORNL/TM-7386. Oak Ridge National Laboratory. October, 1980.
- [124] Mahler, R. J., F. T. Bingham, G. Sposito, and A. L. Page. 1980. "Cadmium-enriched sewage sludge application to acid and calcareous soils: relation between treatment, cadmium in saturation extracts, and cadmium uptake." *J. Environ. Qual.* **9**(3): 359-364.
- [125] Peel, J. W., R. J. Vetter, J. E. Christian, W. V. Kessler, and W. W. McFee. 1978. "The uptake and distribution of cadmium in corn." In Adriano, D. C. and I. L. Brisbin, Jr., (eds.) *Environmental Chemistry and Cycling Processes*. Proceedings of a symposium held at Augusta, Georgia April 28-May 1, 1976. pp. 628-636.
- [126] Haghiri, F. 1973. "Cadmium uptake by plants." *J. Environ. Qual.* **2**(1):93-95.
- [127] Gast, R. G., E. R. Landa, and L. J. Thorvig. 1976. *The Behavior of Technetium-99 in Soils and Plants: Progress Report for the Period April 1, 1974-March 31, 1977*. COO-2447-5.

- [128] Landa, E. R., L. H. Thorvig, and R. G. Gast. 1977. "Effect of selective dissolution, electrolytes, aeration, and sterilization on technetium-99 sorption by soils." *J. Environ. Qual.* **6**: 181-187.
- [129] Romney, E. M., A. Wallace, and J. E. Kinnear. 1978. *Plant Uptake of Pu and Am Through Roots in Nevada Test Site Soils, Vol. I*. Laboratory of Nuclear Medicine and Radiation Biology, University of California, Los Angeles. NVO-192. June 1978.
- [130] Crawford, T. V. 1977. *Savannah River Laboratory Environmental Transport and Effects Research, Annual Report-1977*. Savannah River Laboratory, Aiken, South Carolina. DP-1489. pp. 25-28.
- [131] Price, K. R. 1972. *Uptake of ²³⁷Np, ²³⁹Pu, ²⁴¹Am, and ²⁴⁴Cm from Soil by Tumbleweed and Cheatgrass*. Battelle Pacific Northwest Laboratories, Richland, Washington. BNWL-1688.
- [132] Romney, E. M., H. M. Mork, and K. H. Larson. 1970. "Persistence of plutonium in soil, plants, and small mammals." *Health Phys.* **19**: 487-491.
- [133] Schulz, P. K., G. A. Tompkins, and K. J. Babcock. 1976. "Uptake of plutonium and americium by plants from soil: uptake by wheat from various soils and effect of oxidation of plutonium added to soil." In *Proc. Int. Symp. Transuranium Nuclides in the Environment*. San Francisco, 17-21 November 1975, Vienna. IAEA.
- [134] Gnevshva, G. I. 1971. "Uptake of plutonium-239 into agriculture plants from soil." *Biol. Nauki.* **14**: 60 (*Chemical Abstracts*) **76**: 1446f.
- [135] Lipton, W. V. and A. S. Goldin. 1976. "Some factors influencing the uptake of plutonium-239 by pea plants." *Health Phys.* **31**: 425-430.
- [136] Au, F. H. F., V. D. Leavitt, W. F. Becker, and J. C. McFarlane. 1977. "Incorporation of transuranics into vegetable and field crops grown at the Nevada Test Site." pp. 1-16. In White, M. G. and P. B. Dunaway (eds.) *Transuranics in Desert Ecosystems*. Nevada Applied Ecology Group. NVO-181. November, 1977.
- [137] Cline, J. F. 1968. "Uptake of ²⁴¹Am and ²³⁹Pu by plants." pp. 8.24-8.25. In Thompson, R. C., P. Teal, and E. G. Swazi (eds.) *Pacific Northwest Laboratory Annual Report for 1967 to the USAEC Division of Biology and Medicine, Vol. I*, Biological Sciences. BNWL-714. May 1968.
- [138] Dahlman, R. C., E. A. Bondietti, and L. D. Eyman. 1976. "Biological pathways and chemical behavior of plutonium and other actinides in the environment." pp. 47-80. In Friedman, A. M. (ed.) *Actinides in the Environment*. ACS Symposium Series, No. 35.
- [139] Wallace, A., R. T. Mueller, and E. M. Romney. 1978. "Variable ²⁴¹Am concentration in soil uptake and C. R. in barley plants." pp. 629-635. In White M. G. and P. B. Dunaway (eds.) *Selected Environmental Plutonium Research Reports of the NAEG*. Nevada Applied Ecology Group. NVO-192.
- [140] Wallace, A. 1972. "Effect of soil pH and chelating agent (DTPA) on uptake by and distributions of ²⁴¹Am in plant parts of bush beans." *Rad. Bot.* **12**: 433-435.
- [141] Wallace, A. 1972. "Increased uptake of ²⁴¹Am by plants caused by the chelating agent DTPA." *Health Phys.* **22**: 559-562.
- [142] Wallace, A., R. K. Schulz, E. M. Romney, and H. Nishita. 1979. *Biological Transport of Radionuclides at Low Level Waste Storage Sites, Annual Report, October 1, 1977-September 30, 1978*. Laboratory of Nuclear Medicine and Radiation Biology, University of California. NUREG 1 CR-0701.

- [143] Fedorov, Ye. A. and G. N. Romanov. 1969. "Quantitative characteristics of the relation between the environmental contamination levels and radioisotope concentrations in selected types of farm produce." pp. 112-126. In *USSR Reports on Natural and Fallout Radioactivity*. U.S. Atomic Energy Commission, Health and Safety Laboratory.
- [144] Montford, M. A., K. E. Shank, C. Hendricks, and T. W. Oakes. 1980. "Concentration of stable elements in food products." In *Proceedings of the 14th Annual Conference on Trace Substances in Environmental Health*. University of Missouri, June 3-6, 1980.
- [145] Ng, Y. C., C. S. Colsher, D. J. Quinn, and S. E. Thompson. 1977. *Transfer Coefficients for the Predictions of Dose to Man Via the Forage-Cow-Milk Pathway from Radionuclides Released to the Biosphere*. Lawrence Livermore Laboratory. UCRL-51939.
- [146] Weast, R. C. and M. J. Astle (eds.). 1979. *CRC Handbook of Chemistry and Physics 60th Ed.* CRC Press, Inc., Boca Raton, Florida. p. F-3.
- [147] Francis, C. W., M. Reeves III, R. S. Fisher, and B. A. Smith. 1977. "Soil chromatograph k_d values." In *Waste Isolation Safety Assessment Program, Task 4. Contractor Information Meeting Proceedings*. September 23-23, 1977. Battelle Memorial Institute. Human Affairs Research Centers, Seattle, Washington. PNL-SA-6957. pp. 403-431
- [148] Sheppard, J. C., J. A. Kittrick, M. J. Campbell, and T. L. Hardt. 1977. *Determination of Distribution Ratios and Diffusion Coefficients of Neptunium, Americium and Curium in Soil-Aquatic Environments*. Washington State University, Pullman, Washington. RLO-2221-T-12-3.
- [149] Inoue, Y. and S. Morisawa. 1976. "Distribution coefficient k_d of radionuclide between sample soil and water." *Nippon Genshiryoku Gakkai Shi* **18**(8): 525-534.
- [150] Griffin, R. A. and N. F. Shimp. 1976. "Effect of pH on exchange-adsorption or precipitation of lead from landfill leachates by clay minerals." *Environ. Sci. Technol.* **10**(13): 1256-1261.
- [151] Relyea, J. F. and D. A. Brown. 1978. "Adsorption and diffusion of plutonium in soil." In Adriano, D. C. and I. L. Brisbin, Jr. (eds.) *Environmental Chemistry and Cycling Processes*. Proceedings of a symposium held at Augusta, Georgia, April 28-May 1, 1976. Technical Information Center, U.S. Department of Energy. pp. 479-495.
- [152] Rhodes, D. W. 1957. "Adsorption of plutonium by soil." *Soil Sci.* **84**: 465-471.
- [153] Nishita, H. 1978. "Extractability of plutonium-238 and curium-242 from a contaminated soil as a function of pH and certain soil components. $\text{CH}_3\text{COOH-NH}_4\text{OH}$ " In Adriano, D. C. and I. L. Brisbin, Jr. (eds.) *Environmental Chemistry and Cycling Processes*. Proceedings of a symposium held at Augusta, Georgia, April 28-May 1, 1976. Technical Information Center, U.S. Department of Energy. pp. 403-416.
- [154] Rhodes, D. W. 1957. "The effect of pH on the uptake of radioactive isotopes from solution by a soil." *Soil Sci. Soc. Am. Proc.* **21**: 389-392.
- [155] Bishop, R. F. and D. Chisholm. 1962. "Arsenic accumulation in Annapolis Valley orchard soils." *Can. J. Soil Sci.* **42**: 77-80.
- [156] Frost, R. R. and R. A. Griffin. 1977. "Effect of pH on adsorption of arsenic and selenium from landfill leachate by clay minerals." *Soil Sci. Soc. Am. J.* **41**: 53-57.
- [157] Frost, R. R. and R. A. Griffin. 1977. "Effect of pH on adsorption of copper, zinc, and cadmium from landfill leachate by clay minerals." *J. Environ. Sci. Health.* **A12**(4&5): 139-156.
- [158] Graham, E. R. 1973. "Selective distribution and labile pools of micro-nutrient elements as factors affecting plant uptake." *Soil Sci. Soc. Am. Proc.* **37**: 70-74.

- [159] Reddy, M. R. and H. F. Perkins. 1974. "Fixation of zinc by clay minerals." *Soil Sci. Soc. Amer. Proc.* **38**: 229-231.
- [160] Wildung, M. W. and D. W. Rhodes. 1963. *Removal of Radioisotopes from Solution by Earth Materials from Eastern Idaho*. Phillips Petroleum Company, Atomic Energy Division. National Reactor Testing Station. U.S. Atomic Energy Commission. IDO-14624, November 1963.
- [161] Cole, M. A. 1979. "Solubilization of heavy metal sulfides by heterotrophic soil bacteria." *Soil Sci.* **127**(5): 313-317.
- [162] Wildung, R. E. and J. R. Garland. 1977. *The Relationship of Microbial Processes to the Fate and Behavior of Transuranic Elements in Soils, Plants, and Animals*. Battelle Pacific Northwest Laboratories. PNL-2416, October 1977. 45 pp.
- [163] Holtan, H. N., C. B. England, G. P. Lawless, and G. A. Schumaker. 1968. *Moisture-Tension Data for Selected Soils on Experimental Watersheds*. U.S. Department of Agriculture, Agricultural Research Service. ARS 41-144.
- [164] Free, G. R., G. M. Browning, and G. W. Musgrave. 1940. "Relative infiltration and related physical characteristics of certain soils." *U.S. Department of Agriculture Technical Bulletin 729*. U.S. Department of Agriculture. 52 pp.
- [165] Graham, E. R. and C. G. Silva. 1979. "Labile pools and distribution coefficients for soil calcium, magnesium, and potassium determined with exchange equilibria and radioisotopes." *Soil Sci.* **128**(1): 17-22.
- [166] Mokwunye, A. U. and S. W. Melsted. 1973. "Magnesium fixation and release in soils of temperate and tropical origins." *Soil Sci.* **116**(5): 349-362.
- [167] Inoue, Y. and S. Morisawa. 1976. "Migration of radionuclides in a model saturated zone, (1)." *Nippon Genshiryoku Gakkai Shi* **18**(5): 42-50.
- [168] Sims, J. L., P. Duangpatra, J. H. Ellis, and R. E. Phillips. 1979. "Distribution of available manganese in Kentucky soils." *Soil Sci.* **127**(5): 270-274.
- [169] Rancon, D. 1972. *Utilisation Pratique du Coefficient de Distribution pour la Mesure de la Contamination Radioactive des Mineraux, des Roches, du sol et des Eaux Souterraines*. Department de Surete Nucleaire, Centre d'Etudes Nucleaires de Cadarache, Saclay, France. Rapport CEA-R-4274. 35 pp.
- [170] Graham, E. R. and D. D. Killion. 1962. "Soil colloids as a factor in the uptake of cobalt, cesium, and strontium by plants." *Soil Sci. Soc. Am. Proc.* **26**: 545-547.
- [171] Schmalz, B. L. 1972. *Radionuclide Distribution in Soil Mantle of the Lithosphere as a Consequence of Waste Disposal at the National Reactor Testing Station*. Idaho Operations Office. U.S. Atomic Energy Commission. IDO-10049. 62 pp.
- [172] Inoue, Y., S. Morisawa, and Y. Mahara. 1975. "Radionuclide migration in aerated zones, (1). Migration characteristics of nuclides contained in percolating water." *Nippon Genshiryoku Gakkai Shi* **17**(7): 376-384.
- [173] Klechkovskii, V. M. 1957. *On the Behavior of Radioactive Fission Products in Soil, their Absorption by Plants and their Accumulation in Crops* (Translated from Russian). U.S. Atomic Energy Commission, Washington, DC.
- [174] Gailledreau, C. 1963. "Reactions physico-chimiques lors du mouvement souterrain des radioisotopes." In *The International Symposium on the Retention and Migration of Radioactive Ions in Soils*. Saclay, 16, 17, and 18 October, 1962. Center for Nuclear Studies, Saclay, The University Press of France. pp. 270-275.

- [175] Jacobs, D. G. 1963. "Ion exchange in the deep-well disposal of radioactive wastes." In *International Symposium on the Retention and Migration of Radioactive Ions in Soils*. Saclay, 16, 17, and 18 October, 1962. Center for Nuclear Studies, Saclay, The University Press of France. pp. 43-54.
- [176] McHenry, J. R. 1958. "Ion-exchange properties of strontium in a calcareous soil." *Soil Sci. Soc. Amer. Proc.* **22**: 514-518.
- [177] Tamura, T. 1972. "Sorptions phenomena significant in radioactive-waste-disposal." In Cook, T. D. (ed.) *Underground Waste Management and Environmental Implications*. Proceedings of a Symposium 6-9 December, 1971. Houston, Texas, American Association of Petroleum Geologists and United States Geological Survey. pp. 318-330.
- [178] Nishita, H., B. W. Kowalewsky, A. J. Steen, and K. H. Larson. 1956. "Fixation and extractability of fission products contaminating various soils and clays: I. Sr90, Y91, Ru106, Cs137, and Ce144." *Soil Sci.* **81**: 317-326.
- [179] Juo, A. S. R. and S. A. Barber. 1970. "The retention of strontium by soils as influenced by pH, organic matter and saturation cations." *Soil Sci.* **109**(3): 143-148.
- [180] Dames and Moore. 1977. *Assessment of the Levels, Potential Origins and Transport Routes of the Radioactivity Measured in the Vicinity of the Maxey Flat Low-Level Radioactive Waste Disposal Site*. March 1977 report.
- [181] Rogowski, A. S. and T. Tamura. 1965. "Movement of ¹³⁷Cs by runoff, erosion and infiltration on the alluvial captina silt loam." *Health Phys.* **11**: 1333-1340.
- [182] Prout, N. E. 1958. "Adsorption of radioactive wastes by Savannah River Plant soil." *Soil Sci.* **85**(1): 13-17.
- [183] Tamura, T. 1966. "Development and applications of minerals in radioactive waste disposal." In *Proceedings of the International Clay Conference*. Jerusalem, Israel. Vol. 1. pp. 425-439.
- [184] Tso, T. C. 1970. "Limited removal of Po²¹⁰ and Pb²¹⁰ from soil and fertilizer by leaching." *Agron. J.* **62**: 663-664.
- [185] Rancon, D. 1973. "Comportement dans les milieux souterrains de l'uranium et du thorium rejetes par l'industrie nucleaire." pp. 333-346. In *Environmental Behavior of Radionuclides Released in the Nuclear Industry*. Proceedings of a Symposium. Aix-en-Provence. 14-18 May 1973. IAEA-SM-172/55.
- [186] Dahlman, R. C., E. A. Bondiotti, and L. D. Eymän. 1976. "Biological pathways and chemical behavior of plutonium and other actinides in the environment." In A. M. Friedman (ed.) *Environmental Behavior of the Actinide Elements*. American Chemical Society Symposium Series 35. pp. 47-80.
- [187] Bondiotti, E. A., S. A. Reynolds, and M. H. Shanks. 1976. "Interaction of plutonium with complexing substances in soils and natural waters" (IAEA-SM-199/51). In *Transuranium Nuclides in the Environment*. Proceedings of the Symposium Held in San Francisco, 17-21 November 1975. International Atomic Energy Agency, Vienna, 1976. pp. 273-287.
- [188] Routson, R. C., G. Jansen, and A. V. Robinson. 1975. *Sorption of ⁹⁹Tc, ²³⁷Np and ²⁴¹Am on Two Subsoils from Differing Weathering Intensity Areas*. Battelle Pacific Northwest Laboratories. Richland, Washington. BNWL-1889. 13 pp.
- [189] Nishita, H., A. Wallace, E. M. Romney, and R. K. Schulz. 1979. *Effect of Soil Type on the Extractability of ²³⁷Pu, ²⁴¹Am and ²⁴⁴Cm as a Function of pH*. Laboratory of Nuclear Medicine and Radiation Biology, University of California at Los Angeles. UCLA 12-1192. 32 pp.

- [190] Nishita, H. and M. Hamilton. 1977. "Factors influencing the chemical extractability of ^{241}Am from a contaminated soil." In White, M. G. and P. B. Dunaway (eds.) *Transuranics in Natural Environments*. A Symposium at Gatlinburg, Tennessee, October 1976. Nevada Applied Ecology Group, U.S. Energy Research and Development Administration, Las Vegas, Nevada. NVO-178. pp. 77-96.
- [191] Van Dorp, F., R. Eleveld, and M. J. Frissel. 1979. "A new approach for soil-plant transfer calculations." In *International Symposium on Biological Implications of Radionuclides Released from Nuclear Industries*. Vienna, 26-30 March 1979. IAEA-SM-237134.
- [192] Chamberlain, A. C. 1967. "Transport of Lycopodium spores and other small particles to rough surfaces." *Proc. R. Soc. London A296*: 45-70.
- [193] Chamberlain, A. C. 1970. "Interception and retention of radioactive aerosols by vegetation." *Atmos. Environ.* **4**: 57-78.
- [194] Chamberlain, A. C. and R. C. Chadwick. 1966. "Transport of iodine from atmosphere to ground." *Tellus XVIII*(2): 226-237.
- [195] Chadwick, R. C. and A. C. Chamberlain. 1970. "Field loss of radionuclides from grass." *Atmos. Environ.* **4**: 51-56.
- [196] Mibourn, G. M. and R. Taylor. 1965. "The contamination of grassland with radioactive strontium. I. Initial retention and loss." *Radiat. Bot.* **5**: 337-47.
- [197] Peters, L. N. and J. P. Witherspoon. 1972. "Retention of 44-88 μ simulated fallout particles by grasses." *Health Phys.* **22**: 261-266.
- [198] Witherspoon, J. P. and F. G. Taylor, Jr. 1970. "Interception and retention of a simulated fallout by agricultural plants." *Health Phys.* **19**: 493-499.
- [199] Hoffman, F. O. and C. F. Baes, III (eds.). 1979. *A Statistical Analysis of Selected Parameters for Predicting Food Chain Transport and Internal Dose of Radionuclides. Final Report*. ORNL/NUREG/TM-282. Oak Ridge National Laboratory
- [200] Knott, J. E. 1957. *Handbook for Vegetable Growers*. J. Wiley and Sons, Inc., New York.
- [201] Brenchley, W. E. and V. G. Jackson. 1921. "Root development in barley and wheat under different conditions of growth." *Ann. Bot.* **XXXV**: 533-556.
- [202] Watson, D. J., G. N. Thorne, and S. A. W. French. 1958. "Physiological causes of differences in grain yield between varieties of barley." *Ann. Bot.* **22**: 321-352.
- [203] Thorne, G. N. 1961. "Effects of age and environment on net assimilation rate of barley." *Ann. Bot.* **25**: 29-38.
- [204] Crow, J. F. and M. Kimura. 1970. *An Introduction to Population Genetics Theory*. Harper and Row, publishers, New York.
- [205] Ryan, J. W., P. A. Garza, and S. L. Brown. 1974. *A Damage Assessment Model for Agricultural Crops*. Stanford Research Institute. AD/A-002.
- [206] Hanaway, J. J. 1963. "Growth stages of corn (*Zea mays*, L.)." *Agron. J.* **55**: 487-492.
- [207] Norman, A. G. 1956. *Advances in Agronomy*. Academic Press Inc., New York.
- [208] Rutledge, A. D. 1979. "Vegetable garden guide." Publication 447 (Revised) University of Tennessee Agricultural Extension Service, The University of Tennessee.
- [209] U.S. Department of Commerce, Bureau of the Census. 1977. *The 1974 Census of Agriculture, United States Summary and State Data*. Vol. 1, Part 51. U.S. Government Printing Office, Washington, D.C.

- [210] U.S. Department of Commerce. 1968. *Climatic Atlas of the United States*. Environmental Science Services Administration, Environmental Data Service. Reprinted by the National Oceanic and Atmospheric Administration. 1977.
- [211] U.S. Department of Commerce. 1979. *Comparative Climatic Data for the United States through 1978*. Environmental Data and Information Service, National Climatic Center, Asheville, N.C.
- [212] Ruffner, J. A. 1978. *Climates of the States*. Vols. 1&2. Gale Research Company. Book Tower, Detroit, Michigan.
- [213] Haaland, C. M. and M. T. Heath. 1973. *Mapping of Population Density*. ORNL-TM-4246. Oak Ridge National Laboratory.
- [214] Haaland, C. M. and M. T. Heath. 1974. "Mapping of population density." *Demography* 11(2): 321-336.
- [215] Edwards, R. G. and P. R. Coleman. 1976. *IUCALC-A FORTRAN Subroutine for Calculating Polygon-Line Intersections, and Polygon-Polygon Intersections, Unions, and Relative Differences*. ORNL/CSD/TM-12. Oak Ridge National Laboratory.
- [216] Morton, F. I. 1978. "Estimating evapotranspiration from potential evaporation: practicality of an iconoclastic approach." *J. Hydro.* 38: 1-32.
- [217] Olson, R. J., C. J. Emerson, and M. K. Nungesser. 1980. *GEOECOLOGY A County-Level Environmental Data Base for the Conterminous United States*. ORNL/TM-7351. Environmental Sciences Division Publication No. 1537. Oak Ridge National Laboratory.
- [218] Taylor, A. B. TERHGT program. Air Sources Laboratory, NOAA, Rockville, Md. 20852.
- [219] Haltiner, G. J. and F. L. Martin. 1957. *Dynamical and Physical Meteorology*. McGraw-Hill Book Co., Inc. New York.
- [220] Wallace, R. W. 1978. *A Comparison of Evapotranspiration Estimates Using DOE Hanford Climatological Data*. Pacific Northwest Laboratory. Richland, Washington. PNL-2698. 20 pp.
- [221] Thornthwaite, C. W. and J. R. Mather. 1955. "The water balance." *Climatol.* 8(1); Laboratory of Climatology, Drexel Institute. 104 pp.
- [222] Penman, H. L. 1948. "Natural evaporation from open water, bare soil and grass." *Proc. Royal Soc. London, Series A* 193: 120-145.
- [223] Holzworth, G. C. 1972. *Mixing Heights, Wind Speeds, and Potential for Urban Air Pollution Throughout the Contiguous United States*. PB-207 103. Environmental Protection Agency, Research Triangle Park, North Carolina. U.S. Department of Commerce. National Technical Information Service. January 1972.
- [224] Etnier E. L. 1980. "Regional and site-specific absolute humidity data for use in tritium dose calculations." *Health Phys.* 39: 318-320.
- [225] Miller, C. W. and F. O. Hoffman. (Submitted to *Health Phys.*) "An examination of the environmental half-time for radionuclides deposited on vegetation."
- [226] Anspaugh, L. R., J. J. Koranda, W. L. Robison, and J. R. Martin. 1972. *Dose to Man via the Food-Chain Transfer Resulting from Exposure to Tritiated Water Vapor*. USAEC Report UCRL-73195, Rev. 1.
- [227] Murphy, C. E., Jr. and M. M. Pendergast. 1979. "Environmental transport and cycling of tritium in the vicinity of atmospheric releases." pp. 361-371. In Freeman, S. (ed.) *Symposium on the Behavior of Tritium in the Environment*. IAEA, Vienna.

- [228] Baes, C. F., Jr., H. E. Goeller, J. S. Olson, and R. M. Rotty. 1976. *The Global Carbon Dioxide Problem*. ORNL-5194. Oak Ridge National Laboratory.
- [229] Killough, G. G., J. E. Till, E. L. Etnier, and B. D. Murphy. In press. "Dose equivalent due to atmospheric releases of carbon-14." In Miller, C. W. (ed.). *Models and Parameters for Environmental Radiological Assessments*. DOE/TIC-11468. Department of Energy Technical Information Center, Oak Ridge, Tennessee.
- [230] Linsley, G. S. 1978. *Resuspension of the Transuranium Elements - A Review of Existing Data*. NRPB-R75. National Radiological Protection Board. Harwell, Didcot, Oxon OX11 ORQ.
- [231] Suggs, J. C., C. E. Rodes, E. G. Evans, and R. E. Bumgardner. 1981. *Inhalable Particulate Network Annual Report: Operation and Data Summary (Mass Concentrations Only)* April 1979-June 1980. EPA-600/4-81-037. United States Environmental Protection Agency. May 1981.
- [232] Sehmel, G. A. 1980. "Particle and gas dry deposition: a review." *Atmos. Environ.* **14**: 983-1011
- [233] Francis, C. W. 1978. *Radiostrontium Movement in Soils and Uptake in Plants*. DOE Critical Review Series. Technical Information Center. U. S. Department of Energy.
- [234] Klepper, B., D. G. Watson, and J. F. Cline. 1976. "Iodine-129 concentration factors for food products." In *Pacific Northwest Laboratory Annual Report for 1975 to the USERDA Division of Biomedical and Environmental Research (Part 2 Ecological Sciences)*. BNWL-2000 PT2.
- [235] Johnson, J. M. and G. W. Butler. 1957. "Iodine content of pasture plants I. Method of determination and preliminary investigation of species and strain differences." *Physiol. Plant.* **10**: 100-111.

INTERNAL DISTRIBUTION

1. S. I. Auerbach
- 2-6. C. F. Baes III
7. L. W. Barnthouse
8. E. A. Bondietti
9. R. O. Chester
10. W. D. Cottrell
11. C. C. Coutant
12. K. E. Cowser
13. A. G. Croff
14. B. S. Ellis
15. W. R. Emanuel
16. J. T. Ensminger
17. W. Fulkerson
18. R. H. Gardner
19. W. R. Garrett
20. C. T. Garten, Jr.
21. H. B. Gerstner
22. S. G. Hildebrand
23. F. O. Hoffman, Jr.
24. S. V. Kaye
25. C. W. Miller
26. T. W. Oakes
27. D. C. Parzyck
28. H. A. Pfuderer
29. R. M. Reed
30. D. E. Reichle
31. C. R. Richmond
32. P. S. Rohwer
33. T. H. Row
34. R. D. Sharp
35. R. W. Shor
36. A. L. Sjoreen
37. S. H. Stow
38. G. W. Suter
39. C. C. Travis
40. R. I. Van Hook, Jr.
41. W. Van Winkle
42. P. J. Walsh
43. A. P. Watson
44. Central Research Library
45. Y-12 Technical Library
- 46-47. Laboratory Records
48. ORNL Patent Office

EXTERNAL DISTRIBUTION

49. L. R. Anspaugh, Lawrence Livermore Laboratory, P.O. Box 808, Livermore, California 94550
50. J. A. Auxier, Applied Science Laboratory, Inc., P.O. Box 549, Oak Ridge, Tennessee 37830
51. D. A. Baker, Battelle-Pacific Northwest Laboratories, P.O. Box 999, Richland, Washington 99352
52. P. Cho, HHAD/OHER/ER, U.S. Department of Energy, Washington, D.C. 20545
53. Hugh W. Church, Sandia Laboratory, Division 5333, Albuquerque, New Mexico 87115
54. Bernard L. Cohen, Department of Physics and Astronomy, University of Pittsburg, Pittsburg, Pennsylvania 15260
55. Frank J. Congel, U.S. Nuclear Regulatory Commission, Washington, D.C. 20555
56. T. V. Crawford, Savannah River Laboratory, Aiken, South Carolina 29801
57. R. G. Cuddihy, Inhalation Toxicology Research Institute, 5200 Gibson Blvd., SE., Albuquerque, New Mexico 87108

58. F. L. Culler, Electric Power Research Institute, P.O. Box 10412, Palo Alto, California 94303
59. Ray Dickson, National Oceanic and Atmospheric Administration, 550 Second Street, Idaho Falls, Idaho 93401
60. G. G. Eichholz, School of Nuclear Engineering, Georgia Institute of Technology, Atlanta, Georgia 30332
61. J. Falco, ORD, U.S. Environmental Protection Agency, 401 M Street, SW, Washington, D.C. 20460
62. Mike Smith, EERF, U.S. Environmental Protection Agency, P.O. Box 3009, Montgomery, Alabama 36193
63. Carl V. Gogolak, U. S. Department of Energy, Environmental Measurement Laboratory, 376 Hudson Street, New York, New York 10014
64. J. W. Healy, Health Physics Division, Los Alamos Scientific Laboratory, P.O. Box 1663, Los Alamos, New Mexico 97544
65. Bruce Hicks, Director, Air Resources Atmospheric Turbulence and Diffusion Laboratory, National Oceanic and Atmospheric Administration, Oak Ridge, Tennessee 37830
66. Wayne Lowder, U.S. Department of Energy, Washington, D.C. 20545
67. W. A. Mills, U.S. Nuclear Regulatory Commission, Washington, D.C. 20555
68. Dade Moeller, School of Public Health, Harvard University, 677 Huntington Ave., Boston, Massachusetts 02115
69. A. A. Moghissi, ORD, U.S. Environmental Protection Agency, 401 M Street, SW, Washington, D.C. 20460
70. Sam Morris, Brookhaven National Laboratory, Building 475, Upton, New York 11973
71. Paul Moskowitz, Brookhaven National Laboratory, Building 475, Upton, New York 11973
- 72.-76. Christopher B. Nelson, Office of Radiation Programs, U.S. Environmental Protection Agency, Washington, D.C. 20460
77. Yook C. Ng, Biomedical and Environmental Research Division, Lawrence Livermore Laboratory, P.O. Box 808, Livermore, California 94550
78. J. K. Soldat, Pacific Northwest Laboratories, Battelle Memorial Institute, Richland, Washington 99352
79. W. L. Templeton, Ecosystems Department, Battelle-Pacific Northwest Laboratories, Richland, Washington 99352
80. E. C. Watson, Battelle-Pacific Northwest Laboratories, P.O. Box 999, Richland, Washington 99352
81. F. W. Whicker, Department of Radiology and Radiation Biology, Colorado State University, Fort Collins, Colorado 80521
82. W. H. Wilkie, Tennessee Valley Authority, River Oaks Building, Muscle Shoals, Alabama 35660
83. Office of Assistant Manager, Energy Research and Development, Department of Energy, Oak Ridge Operations Office, Oak Ridge, Tennessee 37830
- 84-96. Technical Information Center, P.O. Box 62, Oak Ridge, Tennessee 37831

APPROVED for Release for
Unlimited (Release to Public)
6/6/2005

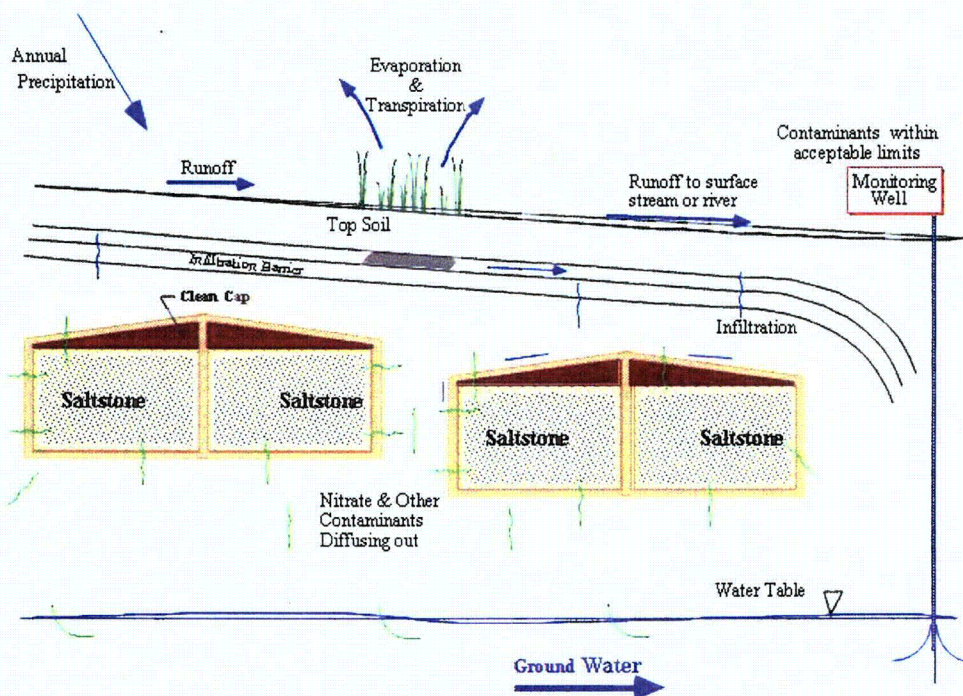
WSRC-TR-2005-00074 ←
Revision 0

KEY WORDS: Performance Assessment
Low-level Radioactive Waste Disposal

**SPECIAL ANALYSIS:
REVISION OF SALTSTONE VAULT 4 DISPOSAL LIMITS (U)**

PREPARED BY:
James R. Cook
Elmer L. Wilhite
Robert A. Hiergesell
Gregory P. Flach

MAY 26, 2005



Westinghouse Savannah River Company
Savannah River Site
Aiken, SC 29808

Prepared for the U.S. Department of Energy Under
Contract Number DE-AC09-96SR18500



The conclusion of this quick study is that there is no impact of plume interaction from Vault 1 for nitrate beyond the 100-ft point of assessment and the 1,000-year time of assessment. There appears to be an impact beyond the 100-m perimeter of Vault 4. However, the interaction only increases nitrate concentrations by about 25%. The Sum-of-Fractions of the 10,000-year groundwater limits is only 0.004. Applying a 25% reduction factor to all 10,000-year groundwater limits would only increase the Sum-of-Fractions to 0.005. The potential for plume interaction will be quantified in the upcoming Saltstone PA revision and will be included, as appropriate, in limits determined therein.

7.5.2 Peak Fractional Contaminant Flux of I-129 to the Water Table

The fractional contaminant flux of I-129 to the water table at 10,000 years is 1.29E-07 mole/yr/mole as shown in Table A-11. The flux is predominantly the diffusive component of the total flux and quickly rising beyond 10,000 years (Figure 7-16). To capture the peak of the flux, the simulation run time was extended to 70,000 years. As shown in Figure 7-17, the flux curve has an inflection point before 30,000 years and approaches a peak at 70,000 years. The peak fractional contaminant flux of I-129 to the water table at 70,000 years is 3.83E-06 mole/yr/mole which is a factor of 30 greater than the value at 10,000 years. This result is helpful in understanding the behavior of the SDF over extremely long times but results calculated over such time frames are not appropriate for establishing disposal limits. However, even if the 10,000-year disposal limit for ^{129}I based on the groundwater pathway were decreased by a factor of 30 (i.e., to 7.3 Ci), the projected Vault 4 inventory of ^{129}I would be only about 10% of that limit.

→ 7.5.3 Inadvertent Intruder Post-Drilling Scenario

In the inadvertent intruder analysis, which is presented in Section 3 and Appendix B, the long-term durability of the Saltstone waste form and the concrete vault are assumed to prevent drilling a well through a disposal vault. To explore the sensitivity of the analysis results to this assumption, an alternate scenario, termed the post-drilling scenario, was assessed.

The post-drilling scenario is based on the assumption that a person could drill a well through a disposal vault. For this sensitivity analysis, the assumption is that drilling through a vault first becomes credible at 1,000 years after closure. The post-drilling scenario is assessed from 1,000 years after closure to 10,000 years after closure. In the post-drilling scenario, the subsurface material exhumed during drilling includes some of the Saltstone waste. This material is assumed to be mixed with soil in a garden and the intruder is exposed to the waste through a variety of pathways (e.g. direct radiation, ingesting food stuffs grown in the garden). The limits derived from the post-drilling analysis are presented in Table B-5.

The post-drilling limits are generally smaller (i.e., more restrictive) than the resident limits, which are presented in Table 3-2. If the post-drilling scenario were to be considered credible, the sum-of-fractions of the 10,000-year limits would increase from 0.22 to 0.31. ←

→ 7.5.4 Agricultural Scenario Following Failure of Erosion Barrier

In the inadvertent intruder analysis, which is presented in Section 3 and Appendix B, the long-term persistence of the erosion barrier is assumed to preclude the Agricultural Scenario by maintaining a distance greater than that required to excavate a basement (10 ft.). To explore the sensitivity of the analysis results to this assumption, an alternate scenario in which the erosion barrier was assumed to erode at the same rate as the other cover material was assessed. The disposal limits derived from this study for a 10,000-year assessment period are shown in Table 7-9. Table 7-10 shows a comparison of these limits with the projected Vault 4 inventory.

→ The Sum-of-Fractions for these limits is 1.49, which, if the scenario were considered credible, would indicate non-compliance with the intruder performance measure. However, the erosion barrier is constructed of material sized to remain in place during a rainfall event with a 10,000-year recurrence interval calculated using an extreme-value distribution (i.e., 3.3 inches of rain in a 15 minute time span, [Weber 1998]). Thus, the scenario is not credible.

Table 7-9. Intruder-Based Radionuclide Disposal Limits for Vault 4 – Agriculture Scenario Following Failure of Erosion Barrier with Transient Calculation for 100 – 10,000 Years

Radionuclide	Time of Limit (Years)	Concentration Limit ($\mu\text{Ci}/\text{m}^3$)	Inventory Limit (Ci/Unit)
C-14	3275	1.64E+04	1.30E+03
Al-26	3275	4.37E+01	3.44E+00
Cl-36	3275	1.43E+02	1.13E+01
Ar-39	1132	1.63E+07	1.29E+06
K-40	3275	5.84E+02	4.60E+01
Ca-41	3275	6.90E+04	5.44E+03
Ni-59	3275	2.43E+06	1.91E+05
Ni-63	1280	8.72E+10	6.87E+09
Se-79	3275	1.33E+05	1.05E+04
Rb-87	3275	8.50E+04	6.70E+03
Sr-90	1132	2.11E+16	1.66E+15
Zr-93	3275	2.61E+06	2.06E+05
Nb-94	1132	8.18E+01	6.45E+00
Mo-93	1720	1.31E+06	1.03E+05
Tc-99	3275	1.39E+04	1.09E+03
Pd-107	3275	4.89E+06	3.85E+05
Ag-108m	1132	5.17E+02	4.07E+01
Sn-121m	1132	5.67E+11	4.47E+10
Sn-126	1132	6.48E+01	5.11E+00
I-129	3275	2.07E+03	1.63E+02
Cs-135	3275	1.37E+05	1.08E+04
Cs-137	1132	4.82E+13	3.79E+12
Sm-151	1132	9.51E+11	7.50E+10
Eu-152	3275	4.12E+17	3.25E+16
Pb-210	1150	---	9.56E+18
Bi-207	1132	5.15E+12	4.06E+11

SITE-SPECIFIC PARAMETER VALUES FOR THE NUCLEAR REGULATORY COMMISSION'S FOOD PATHWAY DOSE MODEL

D. M. Hamby* ←

Abstract—Routine operations at the Savannah River Site (SRS) in Western South Carolina result in radionuclide releases to the atmosphere and to the Savannah River. The resulting radiation doses to the off-site maximum individual and the off-site population within 80 km of the SRS are estimated on a yearly basis. These estimates are currently generated using dose models prescribed for the commercial nuclear power industry by the Nuclear Regulatory Commission (NRC). The NRC provides default values for dose-model parameters for facilities without resources to develop site-specific values. A survey of land- and water-use characteristics for the Savannah River area has been conducted to determine site-specific values for water recreation, consumption, and agricultural parameters used in the NRC Regulatory Guide 1.109 (1977) dosimetric models. These site parameters include local characteristics of meat, milk, and vegetable production; recreational and commercial activities on the Savannah River; and meat, milk, vegetable, and seafood consumption rates. This paper describes how parameter data were obtained at the Savannah River Site and the impacts of such data on off-site dose. Dose estimates using site-specific parameter values are compared to estimates using the NRC default values.

Health Phys. 62(2):136-143; 1992

Key words: environmental transport; food chain; health effects; nutrition pathways

INTRODUCTION

THE NUCLEAR Regulatory Commission (NRC) provides numerical data to estimate committed doses to individuals and populations from routine releases of radioactive materials. The data are furnished in Appendix E of NRC Regulatory Guide 1.109 (1977) for various models presented therein and are implemented in the NRC's GASPARG computer code (USNRC 1980). Approximately half of the NRC default values were derived using the HERMES code developed by the Hanford Engineering and Development Laboratory (Fletcher and Dotson 1971).

Most of the usage and consumption data accessed

* Westinghouse Savannah River Company, Savannah River Laboratory, Aiken, SC 29808.

(Manuscript received 11 July 1991; revised manuscript received 27 September 1991; accepted 3 October 1991)

0017-9078/92/\$3.00/0

Copyright © 1992 Health Physics Society

by HERMES originated in a 1965 U.S. Department of Agriculture survey of consumption habits of families living in North Central United States (Fletcher and Dotson 1971). One-third of the defaults are judgments of the NRC staff. The remaining parameters (agricultural and garden productivity) are national averages obtained from the U.S. Census Bureau (U.S. Bureau of the Census 1972). It is therefore appropriate that site-specific estimates of parameter values be determined for the NRC dose models since most default values are obtained from usage data that are nearly 20 y old, specific to the North Central U.S., or not adequately documented.

METHODOLOGY AND RESULTS

This report focuses on determining those parameters necessary for estimating radiation dose to humans via consumption of potentially contaminated foodstuffs and external gamma exposure from water immersion. The parameters include consumption rates of meat, milk, and vegetables contaminated by the deposition of radionuclides released to the atmosphere; the consumption of drinking water, fish, and invertebrates contaminated by liquid effluents reaching the Savannah River; and recreational river usage leading to external irradiation of humans engaged in activities either along or in the Savannah River. SRS-specific parameter values are compared to the NRC default values in Table 1.

Two state agencies and 21 county agencies within an 80-km radius of the SRS and along the downstream portion of the Savannah River provided much of the information for the land- and water-use survey. The majority of the information on livestock grazing habits, source of forage, vegetation production, etc., was obtained from a questionnaire distributed to county agricultural extension agents within the 80-km region. Information on beef and milk preparation was obtained from direct contact with several meat-packing and milk-processing plants in Georgia and South Carolina.

Meat and milk production

Farmers in the South rely on year-round grazing of fresh, coastal Bermuda grass.[†] Bermuda grass is the

[†] Personal communication (12 November 1990), T. Mathis, Aiken County Extension Service, Aiken, SC.

Table 1. SRS-specific and NRC Regulatory Guide 1.109 model parameter values for dose estimates.

Description	Units	NRC ^a	SRS
Cattle forage consumption (wet)	kg d ⁻¹	50	44
Fraction of time cattle on pasture	—	0.75	1
Fraction of milk-cow intake from pasture	—	1	0.56
Fraction of beef-cow intake from pasture	—	1	0.75
Feed-milk-man transport time	days	4	3
Time from slaughter to consumption	days	20	6
Crop exposure time	days	60	70
Pasture grass productivity	kg m ⁻²	0.7	1.8
Agricultural productivity (veg/produce)	kg m ⁻²	2	0.7
Sport fish harvest ^b	kg y ⁻¹	—	3.5 × 10 ⁴
Commercial fish harvest ^b	kg y ⁻¹	—	2.7 × 10 ³
Invertebrate harvest ^{b,c}	kg y ⁻¹	—	3.9 × 10 ⁵
Maximum shoreline usage	h y ⁻¹	12	23
Population shoreline usage	person-hours	—	9.6 × 10 ⁵
Maximum swimming usage	h y ⁻¹	—	8.9
Population swimming usage	person-hours	—	1.6 × 10 ⁵
Maximum boating usage	h y ⁻¹	—	21
Population boating usage	person-hours	—	1.1 × 10 ⁶
Effective population—Beaufort/Jasper	persons	—	5.0 × 10 ⁴
Effective population—Port Wentworth	persons	—	1.5 × 10 ⁴
Annual average absolute humidity	g m ⁻³	8.0	11.4
Bioaccumulation factor for cesium in fish	L kg ⁻¹	2000	3000
Average adult consumption rates			
Leafy vegetables	kg y ⁻¹	30	21
Other vegetables	kg y ⁻¹	190	163
Meat	kg y ⁻¹	95	43
Milk	L y ⁻¹	110	120
Fish	kg y ⁻¹	6.9	9.0
Seafood	kg y ⁻¹	1	2
Maximum adult consumption rates			
Leafy vegetables	kg y ⁻¹	64	43
Other vegetables	kg y ⁻¹	520	276
Meat	kg y ⁻¹	110	81
Milk	L y ⁻¹	310	230
Fish	kg y ⁻¹	21	19
Seafood	kg y ⁻¹	5	8

^a Taken from the U.S. NRC Regulatory Guide 1.109, Revision 1 (1977).

^b Only edible portions are considered.

^c Includes crabs, clams, oysters, and shrimp.

best hay plant for South Carolina; with adequate fertilization and frequent cuttings, yields of up to 1.8 kg m⁻² (8 tons per acre) are common (Clemson University 1988). Beef-cattle diets in this region generally consist of about 75% pasture grass and 25% stored grass, with total forage consumption averaging about 36 kg d⁻¹ (wet). Dairy cattle consume approximately 52 kg d⁻¹ (wet) of which 55% is pasture grass, 25% is silage, and 20% is commercial grain.

Bermuda grass that is not consumed is cut and baled every 30 d with storage times ranging from 1 mo to 1 y, or sometimes as long as 2 y. Silage may be stored for up to 1 y before consumption. Under these circumstances, the NRC stored-feed holdup time of 90 d is considered conservative and appropriate for the Savannah River Site.

Most beef-cattle farmers in this region of the U.S. operate on a cow-calf system: Calves are raised locally until weaned (6 mo) and then marketed to western feeder lots where their weights are increased before slaughter. These calves' average weight when sold is approximately 180 kg (400 lbs). Ideally, cows producing

calves each year remain with the farmer, whereas cows not producing calves are slaughtered locally. Those cows slaughtered locally average about 360 kg (800 lbs). For purposes of dose assessment, it is assumed that all calves are slaughtered at 180 kg and all calfless cows are slaughtered at 360 kg. All beef is assumed to be consumed locally. Approximately 40% of a beef cow is processed into retail cuts and sold for human consumption. Only about 1% of beef cattle in the Savannah River region are slaughtered and consumed on family farms.

Hogs and chickens are also raised on farms within 80 km of the SRS. Retail cuts of locally produced pork (7.7 × 10⁶ kg y⁻¹) are approximately half that of retail cuts of locally produced beef (1.5 × 10⁷ kg y⁻¹). Chicken production in 1989 reached approximately 2.7 × 10⁷ kg in Aiken County alone. Generally, commercially raised hogs do not graze; they are fed imported commercial feeds.

Similarly, chickens raised for profit are housed in covered shelters; they eat imported feed provided by the parent companies responsible for marketing the

**APPROVED for Release for
Unlimited (Release to Public)
3/19/2004**

WSRC-TR-2003-00436

Revision 0

KEY WORDS:

Saltstone Disposal Facility

Performance Assessment

Closure Cap

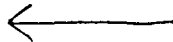
**SALTSTONE DISPOSAL FACILITY
CLOSURE CAP CONFIGURATION AND DEGRADATION
BASE CASE:
INSTITUTIONAL CONTROL TO PINE FOREST SCENARIO (U)**

SEPTEMBER 22, 2003

PREPARED BY:

Mark A. Phifer^a

Eric A. Nelson^a



Westinghouse Savannah River Company LLC^a

ADC and Reviewing Official

**M. K. Harris, Manager, Geo-Modeling
Environmental Restoration Technology Section**

**Westinghouse Savannah River Company LLC
Savannah River Site
Aiken, SC 29808**

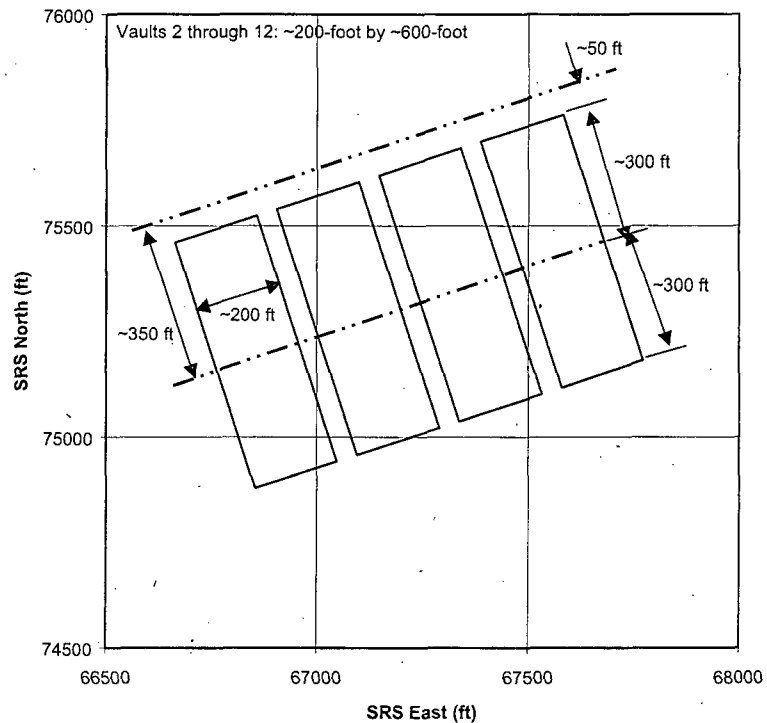


Prepared for the U.S. Department of Energy under Contract No. DE-AC09-96SR18500



Appendix K, Erosion Barrier Sizing and Material Properties

The erosion barrier has been sized based upon the maximum precipitation event for a 10,000-year return period. The maximum precipitation event for a 10,000-year return period is 3.3 inches over a 15-minute accumulation period (Table XIX from Weber et al. (1998)). The figure below shows that the maximum drainage length is 350 feet over a 200-foot wide vault.



Determine the maximum flow (Q in ft^3/s) resulting from the 3.3-inch over a 15-minute accumulation period rainfall event:

To be conservative it has been assumed that all rainfall results in runoff and that there is no lag period due to the 350-foot flow path (that is all the rainfall over the entire area immediately becomes discharge out the end of the area).

$$Q = \frac{(P/12 \text{ in/ft}) \times (350' \times 200')}{D \times 60 \text{ min/hr} \times 60 \text{ s/min}}, \text{ where } P = \text{precipitation in inches and } D = \text{duration in hours}$$

$$Q = 1.62 \frac{P}{D}, \text{ where } P = 3.3 \text{ inches and } D = 15 \text{ minutes} = 0.25 \text{ hours}$$

$$Q = 1.62 \frac{3.3}{0.25} \text{ ft}^3/\text{s}, \text{ over a 200-foot width}$$

$$Q = 21.4 \text{ ft}^3/\text{s}, \text{ over a 200-foot width}$$

Determine the approximate depth of flow using Manning's equation (Clark et al. 1977):

$$V = \frac{1.49}{n} R^{2/3} S^{1/2}, \text{ where } V = \text{velocity, fps; } n = \text{coefficient of roughness;}$$

R = hydraulic radius, ft; and S = slope

$$V = \frac{Q}{A}, \text{ where } V = \text{velocity, ft/s; } Q = \text{flow, ft}^3/\text{s; } A = \text{area, ft}^2$$

$$Q = 21.4 \text{ ft}^3/\text{s}, \text{ over a 200-foot width (i.e. } b)$$

$$A = bd, \text{ where } b = \text{width, ft; } d = \text{depth, ft}$$

$$A = 200d \text{ ft}^2$$

insert values:

$$V = \frac{21.4 \text{ ft}^3/\text{s}}{200d \text{ ft}^2}$$

Assume the use of 2-inch to 6-inch granite stone with a d_{50} (i.e. median size) of 4 inches. From Figure 7.29 of Goldman (1986): $n = 0.033$

$$R = A/\text{wetted perimeter} = A/(b + 2d)$$

$$R = 200d/(200 + 2d)$$

3% slope (see Section 2.0): $S = 0.03$

insert values:

$$\frac{21.4}{200d} = \frac{1.49}{0.033} \left(\frac{200d}{200 + 2d} \right)^{2/3} (0.03)^{1/2}$$

$$0.0137 = d \left(\frac{200d}{200 + 2d} \right)^{2/3}$$

Given d	0.0137
0.1	0.0215
0.08	0.0148
0.075	0.0133
0.076	0.0136

$$d \approx 0.076$$

Determine if the use of a 2-inch to 6-inch granite stone with a d_{50} (i.e. median size) of 4 inches is satisfactory to perform as an erosion barrier for a 10,000-year return period, maximum precipitation event:

$$b/d = 200'/0.076' = 2632, \text{ therefore } b/d > 50.$$

From Figure 7.30 of Goldman (1986): Since the $b/d > 50$ then the P/R is greater than 60.

From Figure 7.31 of Goldman (1986): With a slope (S) of 0.03, a flow (Q) of $21.4 \text{ ft}^3/\text{s}$, and a P/R > 60, the minimum d_{50} of the stone must be approximately 3 inches.

Therefore the use of a 2-inch to 6-inch granite stone with a d_{50} (i.e. median size) of 4 inches is satisfactory to perform as an erosion barrier for a 10,000-year return period, maximum precipitation event.

The selection of the 2-inch to 6-inch granite stone as an erosion barrier is also satisfactory versus Figure C-3 of Logan 1997.

Based upon NCSU 1991 the 2-inch to 6-inch granite stone is a common sized erosion control stone. NCSU 1991 also indicates the minimum thickness of the erosion control stone must be 1.5 times the maximum stone diameter. That is the thickness must be at least 9 inches for a maximum 6-inch stone. A 12-inch thickness of 2-inch to 6-inch granite stone with a d_{50} (i.e. median size) of 4 inches will be utilized as the erosion barrier.

Determine the combined soil material properties for the 2-inch to 6-inch granite stone filled with CLSM or Flowable Fill:

The porosity of the 2-inch to 6-inch granite stone with a d_{50} (i.e. median size) of 4 inches is taken as 0.397 based upon the porosity of poorly graded gravel from USEPA 1994a and USEPA 1994b.

Typical CLSM or Flowable Fill properties based upon a May 8, 2003 personal conversation with Christine A. Langton:

Typical CLSM consists of sand with a porosity of 30%, with the pore space filled with 50% porosity binder and has a saturated hydraulic conductivity of $1.0E-03$ cm/s.

Based upon this information the following are the assumed properties of the CLSM:

Property	Property Value
Saturated Hydraulic Conductivity	$1.0E-03$ cm/s
Porosity	$0.30 \times 0.50 = 0.15$
Field Capacity ¹	0.14
Wilting Point ¹	0.13

¹ Field capacity is assumed to be 0.01 less than the porosity, and the wilting point is assumed to be 0.01 less than the field capacity based upon the porosity-wilting point-field capacity relationship of the clean grout and concrete vault roof and floor, which like the CLSM uses cement as the binder.

The matrix of an individual granite stone itself is considered impermeable and non-porous. The porosity of a layer of granite stone is considered to be 0.397. When the granite stone porosity is filled with CLSM, the resultant hydraulic properties, which are area or volume based, become that of the CLSM times the granite stone porosity. The resultant hydraulic properties are shown below:

Property	Property Value
Saturated Hydraulic Conductivity	$1.0E-03$ cm/s \times 0.397 = $3.97E-04$ cm/s
Porosity	$0.15 \times 0.397 = 0.06$
Field Capacity ¹	$0.14 \times 0.397 = 0.056$
Wilting Point ¹	$0.13 \times 0.397 = 0.052$

APPROVED for Release for
 Unlimited (Release to Public)

**RESPONSE TO RAI COMMENT 57
 ROADMAP TO REFERENCES**

REFERENCED DOCUMENT	*EXCERPT LOCATION	REMARK
Cozzi 2004	Entire document enclosed following response.	Entire report documents testing performed. Section 3.11.3 discusses results of TCLP testing for mercury.
Cozzi and Zamecnik 2004	Entire document enclosed following response.	This document directs testing to be performed as documented in WSRC-TR-2005-00180 (interim report) for Tank 48 waste decomposition products.
Cozzi 2005	Entire document enclosed following response.	Task Technical & QA Plan documents plan for Isopar L testing requested in TTR.
Cozzi et al. 2005	Entire document enclosed following response.	Section 3.2.1 discussed results of benzene testing.
Delmau et al. 2002	Entire document enclosed following response.	Conclusions section 8.0 discusses solvent composition and the body of report discusses overall solvent performance.
Fowler 2005	Excerpt enclosed following response.	Summary attached to document TPB concentration.
Norato et al. 2002	Excerpt enclosed following response.	Section 2.0 attached to document trioctylamine function.
Norato 2005	Entire document enclosed following response.	Technical Task Request (TTR) documents work requested to determine Isoper L release rates from Saltstone.
Peterson et al. 2000	Entire document enclosed following response.	Entire document attached to document radiation stability testing of solvent.
Shah 2003	Excerpts enclosed following document.	Table of Contents and Attachment 5.1 provided.
Subosits 2003	Excerpt enclosed following response.	Page 5 enclosed to document MST

7/15/2005

		concentration in feed.
--	--	------------------------

***Excerpt Locations:**

1. **Excerpt included in response:** The excerpt is included within the text of the response or is appended to the response.
2. **Excerpt enclosed following response:** The excerpt is enclosed on a separate sheet or sheets following the response.
3. **Representative excerpt(s) enclosed following response:** Representative excerpts from a document that is wholly or largely applicable are enclosed following the response.
4. **Other**

APPROVED for Release for
Unlimited (Release to Public)
2/5/2003

Key Words: Cesium,
Waste processing

Retention: Permanent

**HIGH LEVEL WASTE DEMONSTRATION OF THE CAUSTIC-SIDE SOLVENT
EXTRACTION PROCESS WITH OPTIMIZED SOLVENT IN THE 2-CM
CENTRIFUGAL CONTACTOR APPARATUS USING TANK 37H/44F SUPERNATE**

**M. A. Norato, S. G. Campbell, M. L. Crowder, M. W. Geeting,
G. F. Kessinger, R. A. Pierce, and D. D. Walker**

November 1, 2002

Westinghouse Savannah River Company
Savannah River Site
Aiken, SC 29808



**Prepared for the U.S. Department of Energy Under
Contract Number DE-AC09-96SR18500**

2.0 INTRODUCTION

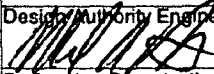
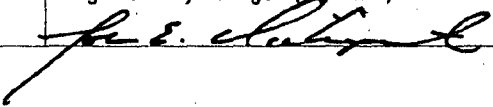
→ A solvent extraction process for removal of cesium from alkaline solutions has been developed utilizing a novel solvent invented at the Oak Ridge National Laboratory.^{1,2} This solvent consists of a calix[4]arene-crown-6 extractant (BOBCalix[®]) dissolved in an inert hydrocarbon matrix (Isopar[®] L). An alkylphenoxy alcohol modifier (1-(2,2,3,3-tetrafluoropropoxy)-3-(4-*sec*-butylphenoxy)-2-propanol, also known as Cs-7SB) added to the solvent enhances the extraction power of the calixarene and prevents the formation of a third phase. An additional additive, trioctylamine (TOA), improves stripping performance and mitigates the effects of any surfactants present in the feed stream.⁴ The solvent extraction process was successfully demonstrated with actual SRS high level waste supernate during testing performed at SRTC in FY-2001.¹ However, the solvent system has recently been optimized to enhance extractant solubility in the diluent and increase suppressor concentration. The original solvent mixture represented a metastable solution that thermodynamic analysis indicated could experience extractant precipitation during long-term use and storage. Also, radiolytic degradation of the TOA suppressor necessitated an increase in suppressor concentration. Therefore, the concentration of BOBCalix[®] in the optimized solvent mixture was decreased from 0.01 M in the initial formulation, to 0.007 M. The Cs-7SB modifier concentration was increased from 0.50 M in the initial formulation, to 0.75 M. The TOA suppressor concentration was increased from 0.001 M in the initial formulation, to 0.003 M.

The SRS tank farms store soluble high level waste in two forms, supernate and salt cake. Previous testing with actual waste¹ demonstrated the process chemistry for supernate solution using the original CSSX solvent formulation. However, it was necessary to verify that the new optimized solvent mixture could also effectively decontaminate waste supernate and allow for stable hydraulic operation of the contactor apparatus.

This report summarizes the results of tests at SRTC with radioactively spiked simulated Tank 37H/44F waste and actual Tank 37H/44F supernate composite waste. The spiked simulant tests demonstrated that stable hydraulic conditions could be maintained with the new solvent formulation and the radioactive feed could be decontaminated to background levels. The 24 hour actual Tank 37H/44F waste test demonstrated similar hydraulic stability and higher DFs.

Technical Task Request

Proc. Ref. E7, 2.02

Funding Source		Modification Traveler No. N/A	Technical Task Request No. SSF-TTR-2005-0004	Revision 1
Design Authority Engineer (Signature) 	Name (Print) Michael A. Norato	Phone 8-7157	Site Address 704-27S	Date 5/24/2005
Performing Organization SRNL/ITS		Design Authority Manager* (Signature) 		Date 5-24-05
Task Description Determine Isopar L Release Rates from Saltstone				Due Date 9/1/2005
Task Activity <input checked="" type="checkbox"/> All activities are to be performed and documented in accordance with Manual E7. Specific procedures are referenced with the associated tasks. <input checked="" type="checkbox"/> Task Specific QA Plan, Reference _____				
Definition of Scope of Modification <input checked="" type="checkbox"/> Not applicable to this request. <input type="checkbox"/> Provided, Reference _____ <input type="checkbox"/> To be developed as part of this request. Specific activities are: <input type="checkbox"/> Scoping Studies <input type="checkbox"/> Feasibility Studies <input type="checkbox"/> Technology Assessment <input type="checkbox"/> Technology Development <input type="checkbox"/> Other, Specify _____				
Functional Requirements and Basis <input checked="" type="checkbox"/> Not applicable to this request. <input type="checkbox"/> Provided, Reference _____ <input type="checkbox"/> To be developed as part of this request. Specific activities are: <input type="checkbox"/> Develop functional performance requirements to be included as part of the MT or Task Requirements and Criteria.				
Facility Hazard Category <input type="checkbox"/> Nuclear 2 <input type="checkbox"/> Radiological <input type="checkbox"/> Chemical (Low) <input type="checkbox"/> To be developed as part of this request (Manual 11Q) <input checked="" type="checkbox"/> Nuclear 3 <input type="checkbox"/> Chemical (High) <input type="checkbox"/> Other Industrial				
Functional Design Criteria <input checked="" type="checkbox"/> Not applicable to this request. <input type="checkbox"/> Provided, Reference _____ <input type="checkbox"/> To be developed as part of this request. Specific activities are: <input type="checkbox"/> Alternative Studies <input type="checkbox"/> Develop functional design criteria to be included as part of the MT or Task Requirements and Criteria.				
Functional Classification <input type="checkbox"/> Safety Class <input checked="" type="checkbox"/> Production Support <input type="checkbox"/> To be developed as part of this request. <input type="checkbox"/> Safety Significant <input type="checkbox"/> General Service				
Criteria Technical Review <input checked="" type="checkbox"/> Not applicable to this request. <input type="checkbox"/> To be performed as part of this request.				
Design and Analysis/Technical Baseline Development <input type="checkbox"/> Not applicable to this request. <input type="checkbox"/> Provided, Reference _____ <input checked="" type="checkbox"/> To be developed as part of this request. Specific activities are: <input type="checkbox"/> Calculations <input type="checkbox"/> FDD <input type="checkbox"/> Functional Acceptance Criteria <input type="checkbox"/> Drawings <input type="checkbox"/> SDD <input type="checkbox"/> Technical Specifications <input type="checkbox"/> Specifications <input type="checkbox"/> Design Process Hazard Review <input checked="" type="checkbox"/> Other, Specify <u>Technical Report</u> <input type="checkbox"/> DSA <input type="checkbox"/> Quality Inspection Plans				

* Design Authority Manager's signature required if request is not associated with an MT.

WSRC-TR-2000-00413
November 20, 2000
Rev. 0

APPROVED for Release for
Unlimited (Release to Public)
9/10/2003

SOLVENT EXTRACTION EXTERNAL RADIATION STABILITY TESTING

R. A. Peterson ←
T. L. White
S. Crump
L. H. Delmau

Publication Date: November 20, 2000

November 20, 2000

Rev. 0

SUMMARY

This study entailed exposing mixtures of calixarene-based solvent and simulants of the extraction, scrub and strip solutions to external gamma radiation. The primary results of these tests are:

1. No significant degradation of the primary solvent components was observed over doses typical of the proposed facility lifetime.
 - a. Less than 10% calixarene loss occurred at received doses up to 16 Mrad (a 160 year dose)
 - b. No statistically significant loss of Cs-7SB modifier occurred at doses up to 16 Mrad. A 10% loss occurred at a dose of 50 Mrad.
 - c. Less than 10% TOA loss occurred at received doses up to 6 Mrad (a 60 year dose)
2. The primary degradation product observed was 4-*sec*-butylphenol. However, additional testing indicated that, as expected based on the design of the modifier, this material would easily wash out during the process.
3. No significant degradation of either extraction or stripping performance occurred over the range of doses employed.

INTRODUCTION

During the technology selection process for Salt Processing Project (SPP), a systems engineering analysis identified caustic side solvent extraction (CSSX) as one of the leading candidates for removal of cesium from SRS high level waste.¹ Testing in 1998 demonstrated some susceptibility of the available solvent system to degradation due to irradiation.² Subsequent to these results, the ORNL developers changed the solvent system to improve its chemical and radiolytic stability.³ A number of limitations existed in the preliminary tests. Those tests did not continuously agitate the solutions, and exposure to radiation dose only occurred in the presence of simulated waste solution. The current tests were designed to eliminate both of these limitations.

Researchers at ORNL estimated that the solvent system will receive less than 100 krad/year of dose.⁴ The doses employed in this testing (i.e., 50 Mrad) far exceed the estimated annual dose that the solvent will receive. This testing attempted to determine the rate of loss of species of interest due to radiation damage, the impact of this degradation on solvent performance, and to identify any key degradation products. Irradiated samples shared with ORNL have also led to the generation of further analytical and performance data that will be reported by ORNL.

November 20, 2000

Rev. 0

MATERIALS AND METHODS

Researchers at ORNL prepared the four different solvents used in these tests. All of these solvents employ calix[4]arene-bis(*t*-octylbenzo-crown-6) (BOBCalixC6) as the extractant. Other components of the solvent included the modifier, trioctylamine as a suppressor and a diluent. Table 1 lists the other components present in these four solvents. Figure 1 provides additional detail pertaining to each of the key solvent components.

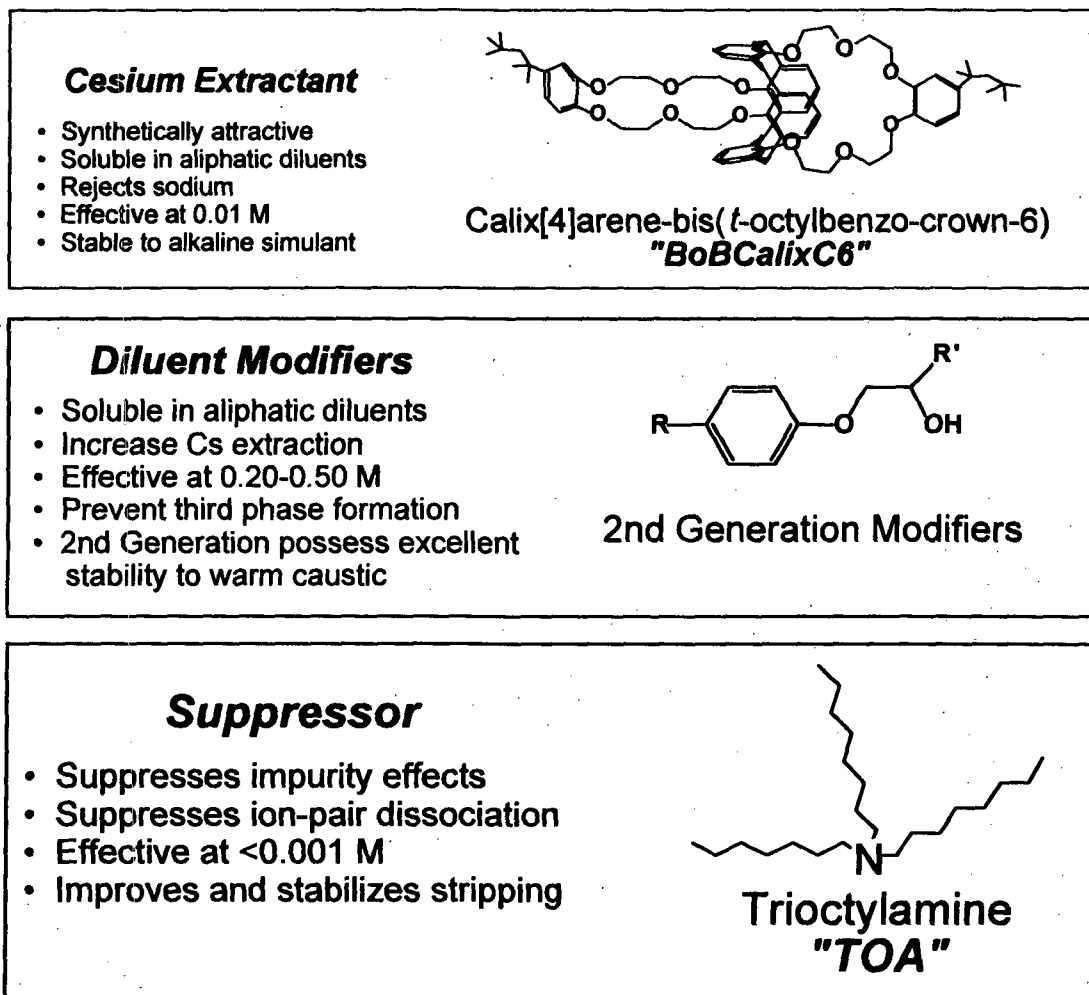


FIGURE 1. KEY SOLVENT COMPONENTS

Table 1, solvents employed

ORNL solvent batch ID	Modifier employed	Diluent employed
PVB B000718-110W	Cs-7SB	Isopar® L
PVB B000718-107W	Cs-7SBT	Isopar® L
PVB B000718-108W	Cs-6	Isopar® L
PVB B000718-109W	Cs-6	Norpar® 12

November 20, 2000

Rev. 0

However, approximately 1 month after receipt of the Cs-6 modified solvents -108W and -109W, the authors observed solids in some of the samples. Due to the formation of the solids, which in most samples involved the solidification of the entire sample, further analysis of these samples proved impossible. Further investigation at Oak Ridge National Laboratory indicated that the formation of solids in these samples reflected the limited solubility of a hydrated form of the Cs-6 modifier. Hence, the Cs-6 modifier is no longer a candidate for CSSX solvent development. No analogous problems with Cs-7SB modifier were observed, nor have attempts at ORNL to crystallize analogous hydrates with Cs-7SB been successful. Crystallization of Cs-7SB is considered to be unfavorable because this compound is a mixture of isomers. Note that for Cs-6, the aryl R group is a *tert*-octyl-benzyl group. For Cs-7SB, the aryl R group is a 4-*sec*-butyl benzyl group. Further note that Cs-7SB and Cs-7SBT were found to be indistinguishable in these studies and as such are treated as identical throughout the remainder of this report. The only difference between these two modifier designations is the source of the modifier precursor.

High Level Waste Salt Disposition Process Engineering developed a single simulated waste composition for all solvent extraction testing.⁵

The tests described herein involved exposure of the solvents listed in Table 1 to external radiation from a ⁶⁰Co gamma source with samples continuously agitated by magnetic stirring (Teflon® coated stir bar). During irradiation, sample temperatures ranged between 20 °C and 35 °C (some heating of the samples occurs during irradiation). Also note that the samples were loosely sealed in an air atmosphere during irradiation. Thus, minimal evaporation of the solvent occurred during evaporation. Table 2 contains a matrix of the test conditions. Each extraction test employed 25 mL of solvent, while the tests with the scrub and strip solutions employed 50 mL of solvent. For each exposure, the organic sample was used for two extractions with fresh simulant. For the scrub and strip exposures, the solvent was then contacted with the appropriate volume of 0.05 M nitric acid. For the strip exposures, the solvent was then contacted with the appropriate volume of 0.001 M nitric acid. Note that one additional sample of the Cs-7SB/Isopar® L solvent (with no aqueous phase) was exposed to a 50 Mrad dose.

Note that for all the samples that used the Cs-7SB/Isopar® L, cross-phase contamination with caustic occurred during the initial preparation of the scrub and strip samples. The cross-phase contamination was later detected at ORNL by the elevated pH values of the aqueous scrub solutions that had been contacted with the loaded solvent. These samples were irradiated before the problem was known, and the characterization of the irradiated solvent is reported. However, this cross-phase contamination likely compromised the D_{Cs} values for these samples. Therefore, D_{Cs} values for stripping are not reported for any samples with an aqueous phase pH more than 2 standard deviations removed from the average. However, additional samples were prepared for exposure under scrub and strip solutions using 1.5 and 6 Mrad for scrub and 2 and 8 Mrad for strip. Although the cross-phase contamination was reduced, it was not totally eliminated, as pH values in the scrub aqueous solutions were still high. The characterization and D_{Cs} values for these samples are reported. The result of the cross-phase contamination is thought to be increased

November 20, 2000

Rev. 0

scatter in the D_{Cs} values and elevated values of D_{Cs} on stripping, including at zero dose. However, within the total set of samples prepared for this study, the results may be considered self-consistent with regard to assessment of the effect of external irradiation.

Table 2. Test conditions

Aqueous Phase	Organic Phase	Exposure (Mrad)	O/A Ratio
Extraction	Cs-7SB/Isopar® L	0.5,1,2,4	0.33
Scrub	Cs-7SB/Isopar® L	1.5,3,6,12	5
Strip	Cs-7SB/Isopar® L	2,4,8,16	5
Extraction	Cs-7SBT/Isopar® L	0,2	0.33
Scrub	Cs-7SBT/Isopar® L	0,6	5
Strip	Cs-7SBT/Isopar® L	0,8	5

At the completion of each irradiation, SRTC personnel analyzed the samples. Analysis included determination of the D_{Cs} (distribution coefficient for Cs between the phases) after irradiation, measurement of the concentration of the various solvent species and determination of the concentrations of any detectable degradation products. Appendix B provides the methodology used for performing distribution coefficients.

BOBCalixC6, Cs-7SB, Cs-6, Norpar® 12 diluent and Isopar® L diluent were supplied by Oak Ridge National Laboratory. Personnel purchased 4-*tert*-octylphenol, 4-*sec*-butylphenol and trioctylamine from Aldrich. The HPLC analysis used HPLC-grade isopropanol (Acros) and ultrapure water obtained from a Waters Milli-Q system.

Analysts used two high performance liquid chromatography (HPLC) instruments for the analysis of the Isopar® L solvent to determine the concentration of Cs-7SB, BOBCalixC6, 4-*tert*-octylphenol, and 4-*sec*-butylphenol. (Note that since these two phenols are precursor compounds for the modifiers, they were anticipated to be primary degradation products of each modifier respectively. Also note that 4-*tert*-octylphenol is a potential fragment from BOBCalixC6.) One device consisted of a Hewlett-Packard 1090 HPLC with a diode array detector and a Polymer Laboratories evaporative light scattering detector (ELSD). The second arrangement included a Hewlett-Packard 1090 HPLC with a diode array detector enclosed in a radiological hood. Both systems used the HP ChemStation version 6.0 software. Note that all samples the analyst diluted samples with isopropanol until the analyte concentration fell within the range of the linear calibration curve and then completed the analysis.

The analysis of trioctylamine occurred on a Hewlett Packard 6890 gas chromatograph, equipped with a 30 m DB-5 column, with 0.25 mm diameter and 0.25 μ m film thickness. Quantitation occurred via a Hewlett Packard 5973 mass selective detector. Personnel

November 20, 2000

Rev. 0

confirmed the mass spectrometer tuning within 24 hours prior to each measurement using perfluorotributylamine.

STANDARDS AND PREPARATION

Personnel prepared stock solutions by weighing the analytes into volumetric flasks and diluting with isopropanol. They combined the stock solutions to form a single stock solution containing all three analytes at high concentrations. Final working standards were prepared by diluting the stock solution with isopropanol. The following describes an example preparation.

Personnel weighed 20 mg of Cs-7SB, 20 mg of BOBCalixC6 and 100 mg of 4-*sec*-butylphenol into separate 10 mL volumetric flasks. In order to replicate the dilution of the sample matrix (Norpar or Isopar) with isopropanol, flasks containing BOBCalixC6 and 4-*sec*-butylphenol were diluted with a solvent similar in polarity mainly isopropanol/hexane (9:1) solvent. Researchers then added 1.0 mL of the BOBCalixC6 solution and 0.05 mL of the 4-*sec*-butylphenol solution to the flask containing Cs-7SB and diluted to volume with isopropanol.. This stock solution was diluted to prepare the working standards.

The analyst diluted samples with isopropanol until the analyte concentration fell within the range of the linear calibration curve and then completed the analysis.

The reverse-phase HPLC gradient method resulted in separation of the compounds (Table A.1). The authors selected a wavelength of 226 nm for monitoring Cs-7SB, Cs-6, 4-*tert*-octylphenol and 4-*sec*-butylphenol, while 205 nm provided the best sensitivity for BOBCalixC6. The response for the analytes proved linear over the concentration ranges present in the solvent (Table A.2). Table A.3 provides the chromatographic resolution parameters for complete separation of the analyte peaks. This methodology typically provided an accuracy of $\pm 10\%$ for the analytes of interest.

Personnel used the gel permeation chromatography (GPC) method with a evaporative light scattering detector and diode array detector (280 nm) to separate, analyze, and estimate the molecular weight of unknown degradation products (Table A.4). Analysts correlated retention time to molecular weight using polystyrene standards in chloroform. For quantitation, the diode array detector proved better suited because of a wider linear range.

Triethylamine analysis used samples diluted 1:10 in isopropanol prior to analysis by GC/MS. A selective ion monitoring (SIM) method set to the molecular weight of TOA (MW = 354) was used to quantify the TOA. The calibration curve ($n = 4$) remained linear from 5 mg/L to 40 mg/L with a within-day RSD of <3%.

RESULTS

Figure 2 contains a plot of the modifier concentration as a function of dose received. Inspection of this figure indicates no significant loss of modifier at doses of 16 Mrad. This

November 20, 2000

Rev. 0

represents an exposure far in excess of that anticipated during the operational lifetime of the final facility. The authors irradiated an additional sample to 50 Mrad. This sample exhibited 10% loss of the modifier, which equates to a rate of modifier loss of 0.02% per year.

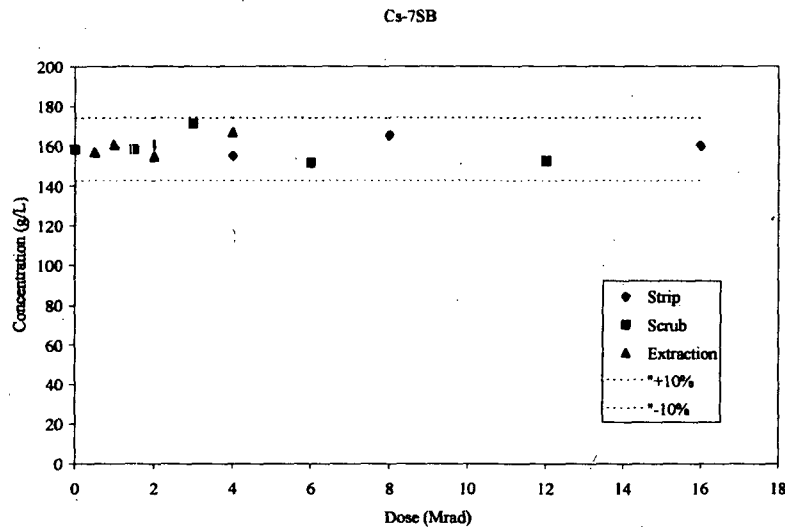


FIGURE 2. MODIFIER COMPOSITION AS A FUNCTION OF DOSE RECEIVED.

Figure 3 contains a plot of the calixarene concentration as a function of dose received. Inspection of this figure indicates approximately 10% loss of calixarene at doses of 16 Mrad. Note that the annual dose expected to be received by the solvent under plant operating conditions is estimated to be less than 100 krad/y.⁴ Hence this study indicates a loss of calixarene associated with radiation damage of less than 0.1%/y.

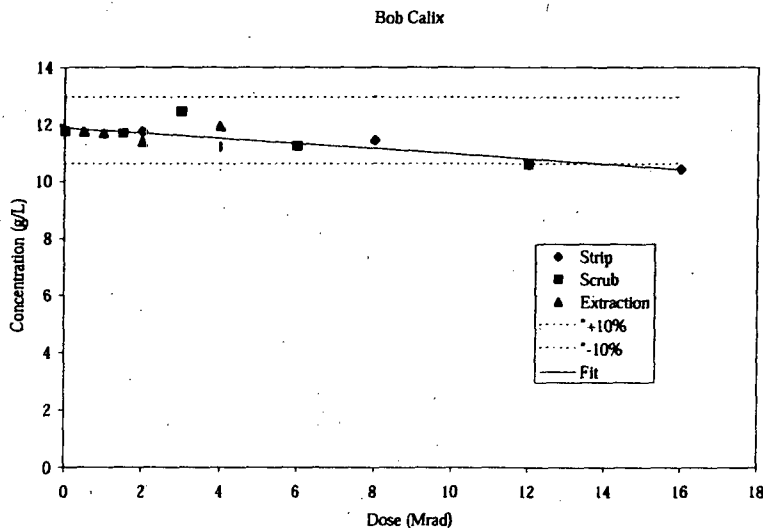


FIGURE 3. CALIXARENE COMPOSITION AS A FUNCTION OF DOSE RECEIVED.

November 20, 2000

Rev. 0

Figure 4 contains a plot of the TOA concentration as a function of dose received. Inspection of this figure indicates approximately 50% loss of TOA at doses of 16 Mrad, some scatter in the data notwithstanding. Since the annual dose to be received by the solvent is less than 100 krad/y, these data indicate a loss of TOA to irradiation damage of less than 0.5%/y.

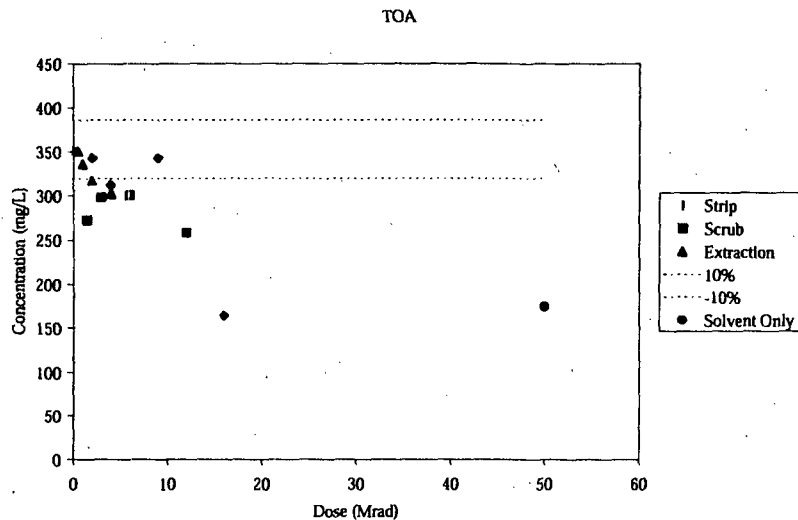


FIGURE 4. TOA COMPOSITION AS A FUNCTION OF DOSE RECEIVED.

Figure 5 contains a plot of the 4-*sec*-butylphenol concentration as a function of dose. Inspection of this figure indicates that the 4-*sec*-butylphenol concentration increases as dose increases. However, some of the 4-*sec*-butylphenol distributed to the aqueous phase (as indicated in the washing test discussed below). Thus, we will need additional testing to determine more precise total generation rates. However, since the partition coefficient should be near 1, these generation rates will likely be correct to within an order of magnitude. However, the authors performed an additional test to determine the ability to wash the phenol with 1 M NaOH solution. These tests indicated a partitioning coefficient of 0.75 for the phenol at a solvent-to-wash volume ratio of 1. Further, notice that the maximum concentration of 4-*sec*-butylphenol in the solvent equaled less than 0.4% of the total modifier concentration.

November 20, 2000

Rev. 0

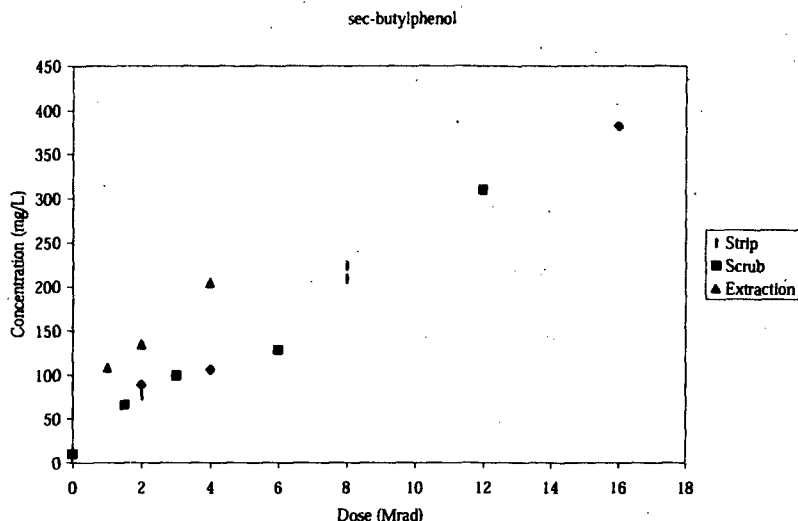


Figure 5. 4-sec-Butylphenol concentration in the solvent as a function of dose received. Analysis of unirradiated solvent and solvent exposed to 50 Mrad of external gamma radiation was examined by gel permeation chromatography (GPC) connected to a photo diode array detector (PDA) and an evaporative light scattering detector (ELSD). Molecules are separated in GPC according to molecular size, which roughly correlates, to their molecular weight. By analyzing standards within the molecular weight range of your unknowns, a molecular weight for unknowns can be estimated. The Table A.5 contains the information about the estimated molecular weight of unknown peaks in the chromatograms from Figures A.1 and A.2. Figure A.1 is the plot of molecular weight vs elution volume for the PDA and Figure A.2 is the plot of the molecular weight vs elution volume for the ELSD. The radiated sample yielded a distinctive chromatogram with the growth of a board peak at 6.2 mL (min). This peak eluted earlier (higher molecular weight) than the Cs-7SB the peak indicating it consists of decomposition products from the modified calix[4]arene molecule. It should be noted that trioctylamine (TOA) contained in the solvent would appear at 6.1 mL (min) but at 100 to 1 dilution (3.5 mg/L) it is not a significant peak by ELSD.

Table 3 contains the distribution coefficients measured for irradiated and unirradiated solvent. (Note: This table also identifies the other conditions employed in the preparation of these samples identified in Appendix B). These distribution coefficients were measured at both SRTC and at ORNL. Inspection of Table 3 indicates that the exposure of samples to doses to 8 Mrad did not have any significant impact on performance of the solvent in extraction, scrubbing and stripping relative to unirradiated solvent. The reader should compare data for irradiated and unirradiated samples at similar doses. These samples that were repeated with reduced cross contamination are indicated by an *.

Table 3.1. D_C data for extraction

November 20, 2000

Rev. 0

Dose (Mrad)	D _{Cs}	Lab	Measurement method	Equilibrium Temperature	Separation Method	Irradiation Point	Measurement Point
0	15.4	SRTC	ICP-MS	25 °C	Centrifuge	N/A	2nd Extraction
0.5	15.3	SRTC	gamma scan	Ambient	Gravity	2 nd E	2nd Extraction
1	14.5	SRTC	gamma scan	Ambient	Gravity	2 nd E	2nd Extraction
2	15.6	SRTC	gamma scan	Ambient	Gravity	2 nd E	2nd Extraction
4	15.6	SRTC	gamma scan	Ambient	Gravity	2 nd E	2nd Extraction
0.5	16.8	ORNL	gamma scan	25 °C	Centrifuge	2 nd E	2nd Extraction
1	15.8	ORNL	gamma scan	25 °C	Centrifuge	2 nd E	2nd Extraction
2	17.4	ORNL	gamma scan	25 °C	Centrifuge	2 nd E	2nd Extraction
4	16.2	ORNL	gamma scan	25 °C	Centrifuge	2 nd E	2nd Extraction

November 20, 2000

Rev. 0

Table 3.2. D_{Cs} data for scrubbing

Dose (Mrad)	D_{Cs}	Lab	Measurement method	Equilibrium Temperature	Separation Method	Irradiation Point	Measurement Point
0	1.6	SRTC	ICP-MS	25 °C	Centrifuge	N/A	Scrub*
0	1.3	SRTC	ICP-MS	25 °C	Centrifuge	N/A	Scrub
0	1.5	ORNL	Gamma Scan	25 °C	Centrifuge	N/A	Scrub*
1.5	1.7	SRTC	ICP-MS	25 °C	Centrifuge	Scrub	Scrub*
1.5	1.7	ORNL	Gamma Scan	25 °C	Centrifuge	Scrub	Scrub*
3	1.5	ORNL	Gamma Scan	25 °C	Centrifuge	Scrub	Scrub
6	1.7	SRTC	ICP-MS	25 °C	Centrifuge	Scrub	Scrub*
6	1.6	SRTC	ICP-MS	25 °C	Centrifuge	Scrub	Scrub*
6	1.3	ORNL	Gamma Scan	25 °C	Centrifuge	Scrub	Scrub
6	1.6	ORNL	Gamma Scan	25 °C	Centrifuge	Scrub	Scrub*
12	1.1	ORNL	Gamma Scan	25 °C	Centrifuge	Scrub	Scrub
0.5	1.5	ORNL	Gamma Scan	25 °C	Centrifuge	2 nd E	Scrub
1	1.5	ORNL	Gamma Scan	25 °C	Centrifuge	2 nd E	Scrub
2	1.5	ORNL	Gamma Scan	25 °C	Centrifuge	2 nd E	Scrub
4	1.5	ORNL	Gamma Scan	25 °C	Centrifuge	2 nd E	Scrub

Table 3.3. D_{Cs} data for 1st Strip

0	0.29	SRTC	ICP-MS	25 °C	Centrifuge	N/A	1st Strip*
0	0.20	SRTC	ICP-MS	25 °C	Centrifuge	N/A	1st Strip*
0	0.34	SRTC	ICP-MS	25 °C	Centrifuge	N/A	1st Strip*
0	0.29	ORNL	Gamma Scan	25 °C	Centrifuge	N/A	1 st Strip*
2	0.48	SRTC	ICP-MS	25 °C	Centrifuge	Strip	1st Strip*
2	0.31	ORNL	Gamma Scan	25 °C	Centrifuge	Strip	1 st Strip*
2	0.41	ORNL	Gamma Scan	25 °C	Centrifuge	Strip	1 st Strip*
4	0.28	ORNL	Gamma Scan	25 °C	Centrifuge	Strip	1 st Strip*
8	0.20	SRTC	ICP-MS	25 °C	Centrifuge	Strip	1st Strip*
8	0.35	SRTC	ICP-MS	25 °C	Centrifuge	Strip	1st Strip*
8	0.13	ORNL	Gamma Scan	25 °C	Centrifuge	Strip	1 st Strip
8	0.29	ORNL	Gamma Scan	25 °C	Centrifuge	Strip	1 st Strip*
1.5	0.24	SRTC	ICP-MS	25 °C	Centrifuge	Scrub	1st Strip*
1.5	0.19	ORNL	Gamma Scan	25 °C	Centrifuge	Scrub	1 st Strip*
3	0.17	ORNL	Gamma Scan	25 °C	Centrifuge	Scrub	1 st Strip
6	0.24	SRTC	ICP-MS	25 °C	Centrifuge	Scrub	1st Strip*
6	0.24	SRTC	ICP-MS	25 °C	Centrifuge	Scrub	1st Strip*
6	0.19	ORNL	Gamma Scan	25 °C	Centrifuge	Scrub	1 st Strip
6	0.21	ORNL	Gamma Scan	25 °C	Centrifuge	Scrub	1 st Strip*
12	0.18	ORNL	Gamma Scan	25 °C	Centrifuge	Scrub	1 st Strip
0.5	0.17	ORNL	Gamma Scan	25 °C	Centrifuge	2 nd E	1 st Strip
1	0.17	ORNL	Gamma Scan	25 °C	Centrifuge	2 nd E	1 st Strip
2	0.18	ORNL	Gamma Scan	25 °C	Centrifuge	2 nd E	1 st Strip
4	0.19	ORNL	Gamma Scan	25 °C	Centrifuge	2 nd E	1 st Strip

November 20, 2000

Rev. 0

Table 3.4. D_{Cs} data for 2nd Strip

0	0.18	SRTC	ICP-MS	25 °C	Centrifuge	N/A	2nd Strip*
0	0.25	SRTC	ICP-MS	25 °C	Centrifuge	N/A	2nd Strip*
0	0.12	ORNL	Gamma Scan	25 °C	Centrifuge	N/A	2nd Strip*
2	0.19	SRTC	ICP-MS	25 °C	Centrifuge	Strip	2nd Strip*
2	0.13	ORNL	Gamma Scan	25 °C	Centrifuge	Strip	2nd Strip*
4	0.10	ORNL	Gamma Scan	25 °C	Centrifuge	Strip	2nd Strip
8	0.23	SRTC	ICP-MS	25 °C	Centrifuge	Strip	2nd Strip*
8	0.22	SRTC	ICP-MS	25 °C	Centrifuge	Strip	2nd Strip*
8	0.08	ORNL	Gamma Scan	25 °C	Centrifuge	Strip	2nd Strip
8	0.12	ORNL	Gamma Scan	25 °C	Centrifuge	Strip	2nd Strip*
1.5	0.18	SRTC	ICP-MS	25 °C	Centrifuge	Scrub	2nd Strip*
1.5	0.12	ORNL	Gamma Scan	25 °C	Centrifuge	Scrub	2nd Strip*
3	0.11	ORNL	Gamma Scan	25 °C	Centrifuge	Scrub	2nd Strip
6	0.25	SRTC	ICP-MS	25 °C	Centrifuge	Scrub	2nd Strip*
6	0.15	SRTC	ICP-MS	25 °C	Centrifuge	Scrub	2nd Strip*
6	0.12	ORNL	Gamma Scan	25 °C	Centrifuge	Scrub	2nd Strip
6	0.12	ORNL	Gamma Scan	25 °C	Centrifuge	Scrub	2nd Strip*
12	0.11	ORNL	Gamma Scan	25 °C	Centrifuge	Scrub	2nd Strip
0.5	0.10	ORNL	Gamma Scan	25 °C	Centrifuge	2 nd E	2nd Strip
1	0.10	ORNL	Gamma Scan	25 °C	Centrifuge	2 nd E	2nd Strip
2	0.10	ORNL	Gamma Scan	25 °C	Centrifuge	2 nd E	2nd Strip
4	0.11	ORNL	Gamma Scan	25 °C	Centrifuge	2 nd E	2nd Strip

Table 3.5. D_{Cs} data for 3rd Strip

0	0.14	SRTC	ICP-MS	25 °C	Centrifuge	N/A	3rd Strip*
0	0.08	ORNL	Gamma Scan	25 °C	Centrifuge	N/A	3rd Strip*
2	0.09	ORNL	Gamma Scan	25 °C	Centrifuge	Strip	3rd Strip*
4	0.07	ORNL	Gamma Scan	25 °C	Centrifuge	Strip	3rd Strip
8	0.07	SRTC	ICP-MS	25 °C	Centrifuge	Strip	3rd Strip*
8	0.07	ORNL	Gamma Scan	25 °C	Centrifuge	Strip	3rd Strip
8	0.09	ORNL	Gamma Scan	25 °C	Centrifuge	Strip	3rd Strip*
1.5	0.08	ORNL	Gamma Scan	25 °C	Centrifuge	Scrub	3rd Strip*
3	0.08	ORNL	Gamma Scan	25 °C	Centrifuge	Scrub	3rd Strip
6	0.08	ORNL	Gamma Scan	25 °C	Centrifuge	Scrub	3rd Strip
6	0.09	ORNL	Gamma Scan	25 °C	Centrifuge	Scrub	3rd Strip*
12	0.08	ORNL	Gamma Scan	25 °C	Centrifuge	Scrub	3rd Strip
0.5	0.07	ORNL	Gamma Scan	25 °C	Centrifuge	2 nd E	3rd Strip
1	0.07	ORNL	Gamma Scan	25 °C	Centrifuge	2 nd E	3rd Strip
2	0.08	ORNL	Gamma Scan	25 °C	Centrifuge	2 nd E	3rd Strip
4	0.08	ORNL	Gamma Scan	25 °C	Centrifuge	2 nd E	3rd Strip

November 20, 2000

Rev. 0

CONCLUSIONS

Personnel irradiated a number of samples of calixarene-based solvent. Analysis of these samples indicated that measurable loss of the calixarene occurred at very high doses (~ 16 Mrad). No measurable loss of the Cs-7SB modifier occurred at equivalent doses. The primary degradation product, 4-*sec*-butylphenol, observed during analysis of the samples came from degradation of the modifier. Also, TOA proved more susceptible to damage than the other components of the solvent. The total degradation of the solvent proved relatively minor. The consistent solvent performance, as indicated by the measured D_{Cs} values, after exposure at high total doses serves as evidence of the relatively low degree of degradation of the solvent components. Additional tests employing internal irradiation of solvents with both simulants and SRS tank waste will be completed by the end of March, 2001 to provide confirmation of the results presented herein.

REFERENCE

¹ S. Beck, et al. "Bases, Assumptions, and Results of the Flowsheet Calculations for the Short List Salt Disposition Alternatives", WSRC-RP-98-00168, Rev. 1, October 29, 2000.

² C.L. Crawford, et al., "Radiation Stability of Calixarene Based Solvent System", WSRC-TR-98-00371, October 2, 1998.

³ (a) P. V. Bonnesen, L. H. Delmau, B. A. Moyer, and R. A. Leonard "A Robust Alkaline-Side CSEX Solvent Suitable for Removing Cesium from Savannah River High Level Waste," *Solvent Extr. Ion Exch.*, **18(6)**, 1079-1108 (2000).

⁴ G.D. Kerr and K.F. Eckerman, "Radiation Dosimetry for the CSSX Process", ORNL letter report, October 12, 2000.

⁵ R.A. Peterson, "Preparation of simulated waste solutions for solvent extraction testing," WSRC-RP-2000-361, May 1, 2000

APPROVALS

R. A. Peterson, Author Date

T.L. White, Author Date

S. Crump, Author Date

L.H. Delmau, Author Date

B.A. Moyer, Technical Review Date

L. N. Klatt, Technical Review Date

S. D. Fink, Manager, WPTS-LWP Date

J. T. Carter, Manager, HLW Process Engineering Date

K.J. Rueter, Salt Disposition Program, Director of Engineering Date

W. L. Tamosaitis, Manager, WPTS Date

Table A.1
Gradient reverse-phase HPLC method for Isopar L

Method	Conditions
Solvent system	Isopropanol-water
t_0 to t_1 = 10 min	70%/30%
t_2 = 12 min	95%/5%
t_3 = 27 min	95%/5%
t_4 = 29 min	70%/30%
Column	Dychrom Chemcosorb 5 ODS-UH 3.2x250 mm, 5 μ m pore size
Oven temperature	45°C
Flow-rate	0.25 mL
Stop time	33 min
UV	226 nm (modifier), 205 nm (calix)
injection volume	10 μ L
Retention time for 4-sec-butylphenol	7.25 min
Retention time for Cs-7SB	8.4 min
Retention time for calix	23.6 min
Linear calibration curve	
4-sec-butylphenol	1.0 mg/L to 70 mg/L, correlation = 0.998
Cs-7SB	1000 mg/L to 2000 mg/L, correlation = 0.999
calix	70 mg/L to 170 mg/L, correlation = 0.999

Table A.2
 Linearity of test compounds

Compound	Conc. range (mg/L)	Slope	y-Intercept	Correlation coefficient
4-sec-butylphenol	1.0-70	55.6	35	0.9983
Cs-7SB	1000- 2,000	30	3591	0.9996
calix[4]arene	70-170	143	917	0.9999
TOA (GCMS)	5.0-40	42951	101464	0.9989

Table A.3
 Resolution parameters for Isopar L

Compound	t_R	k'	R	N	T
4-sec-butylphenol	7.2	0.8		3287	1.00
Cs-7SB	8.3	1.1	1.8	1156	1.10
calix[4]arene	21.7	4.3	15.4	16384	1.00

t_R =Retention time; k' =capacity factor; R =resolution; N =number of plates
 T =peak symmetry factor

Table A.4
 GPC analyses

Method	Conditions
Solvent system	Chloroform
t_0 to t_1 = 10 min	
Column	Shodex GPC K-801 8x300 mm, 1500 exclusion limit
Flow-rate	1 mL
Stop time	10 min
UV (4-sec-butylphenol, 4-tert-octylphenol)	280 nm
ELSD (BOBCalixC6, Cs-7SB, and Cs-6)	0.8 SLM @ 60 psi @ 25 °C Evaporator Temp. = 85 °C Nebulizer Temp. = 40 °C Transfer line Temp. = 30 °C Time constant = 1
injection volume	20 μ L
Retention time for BOBCalixC6	5.7 min(ELSD)
Retention time for Cs-6	6.6 min(ELSD)
Retention time for Cs-7SB	6.8 min(ELSD)
Retention time for 4-tert-octylphenol	7.9 min(280 nm)
Retention time for 4-sec-butylphenol	8.5 min(280 nm)

November 20, 2000

Rev.0

Table A.5. Standards for GPC column.

Compound	MW, g/mole	Volume, mL	RT, min	Conc., mg/L
<i>GPC with ELSD analyses</i>				
Polystyrene	2340	5.218	5.218	224
Polystyrene	1180	5.623	5.623	231
calix[4]arene-bis(<i>t</i> -octylbenzo-crown-6)	1149.53	5.703	5.703	224
Polystyrene	979	5.786	5.786	248
1-(2,2,3,3-tetrafluoropropoxy)-3-(4- <i>sec</i> -butylphenoxy)-2-propanol	338.34	6.804	6.804	249
Calix[4]arene	424.5	7.218	7.218	199
Glycerol	92	8.649	8.649	~2000
Ethylene glycol	62	8.973	8.973	248
Polystyrene	484	3 peaks	3 peaks	
Polystyrene	266	no signal		
4- <i>sec</i> -butylphenol	150	no signal	no signal	254
Catechol	110			
<i>GPC with PDA analyses</i>				
Polystyrene	2340	5.122	5.122	224
Polystyrene	1180	5.514	5.514	231
calix[4]arene-bis(<i>t</i> -octylbenzo-crown-6)	1149.53	5.602	5.602	224
Polystyrene	979	5.679	5.679	248
1-(2,2,3,3-tetrafluoropropoxy)-3-(4- <i>sec</i> -butylphenoxy)-2-propanol	338.34	6.708	6.708	249
Calix[4]arene	424.5	7.12	7.12	199
Trioctylamine	353.68	5.9	5.9	
Polystyrene	266	7.092	7.092	189
Polystyrene	162	7.787	7.787	222
4- <i>sec</i> -butylphenol	150	8.582	8.582	254
catechol	110	9.978	9.978	~1000
Glycerol	92	8.524	8.524	~2000
Ethylene glycol	62	8.863	8.863	248
Polystyrene	484	3 peaks	3 peaks	

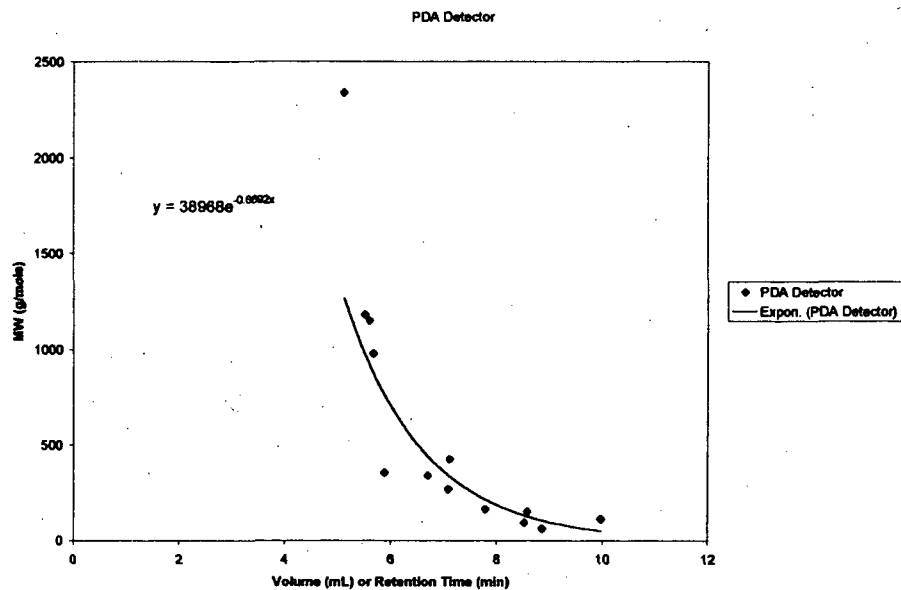


Figure A.1 Molecular weight as a function of volume through column (or retention time) for PDA.

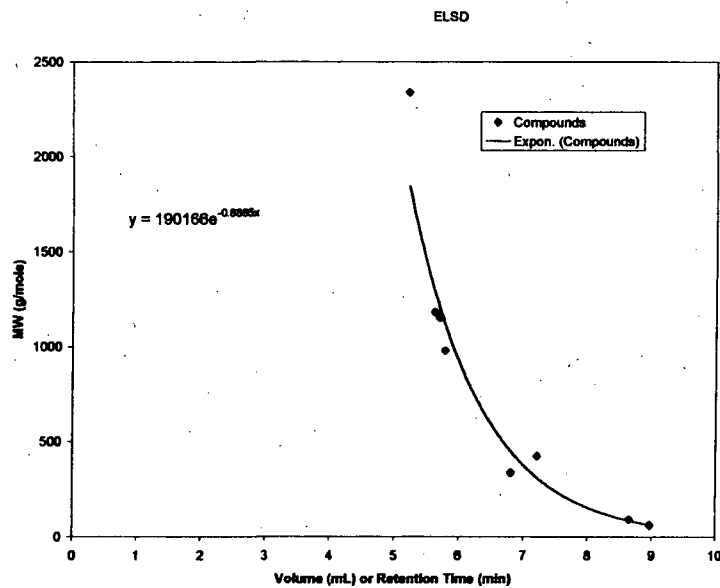


Figure A.2. Molecular weight as a function of volume through column (or retention time) for ELSD.

Appendix B.

Extraction – Scrub – Strip Protocol

Equipment

Glass vials (Kimble, part # 60910L-1)
Fixed volume pipetman pipetes (with tips)
Thermostated New Brunswick incubator shaker set for 25.0 C
Ambient temperature centrifuge

Chemicals

70% HNO₃ (Fisher)

Prepared 1 M Nitric acid (from dilution of stock concentrated nitric acid) with DDI water.
Prepare scrub and strip solution by dilution from the 1 M Nitric acid solution

1. Using a fixed volume pipetter, dispense the required volume of each solvent and aqueous phase into a 4 mL vial. These vials typically received 3 mL of solution.
2. The solutions were initially shaken by hand to achieve a distribution. Then the solutions were shaken for 1 hour at 200 rpm on a temperature controlled shaker table. Immediately after removal from the shaker table, the samples were again shaken vigorously by hand
3. The sample was then centrifuged for 1 minute at 8000 rpm

Phase Separation - simulant

1. Use a polyethylene disposable transfer pipette to remove approximately 80% of the organic layer off the top to a clean vial.
2. Obtain a 500 microL sample of the aqueous phase for analysis by ICP-MS.
2. 3. From the organic transfer vial, obtain a 500 microL sample for analysis by digestion/ICP-MS.

Calibration and Analysis

All analyses performed by SRTC analytical development section (ADS) (which performs calibrations and blanks during sample analysis).

Procurement Specification Cover Sheet

1. Title Monosodium Titanate (MST) Slurry		ENGINEERING DOC. CONTROL - SRS  00613723	
2. Specification No. X-SPP-S-00021	3. Revision 1	4. Page 1 of 14	
5. Functional Classification PS	6. Requester Department ARP/Salt Program	7. Requester Division LWDP/CBU	
8. Cognizant Technical Function Design Authority Engineering for ARP			
Name Satish (Sam) C. Shah <i>Sam Shah</i>		Date 3/4/03	
Title Principal Engineer			
Department ARP/Salt Program/LWDP/CBU			
9. Additional Reviewer J. T. Dahlstrom - Preparer / PCD - PESG <i>J. T. Dahlstrom</i>			
Name Mark D. Drumm <i>Mark D. Drumm</i>		Date 3/4/03	
Title Process Engineer			
Department ARP/Salt Program/LWDP/CBU			
10. Cognizant Quality Function			
Name H. J. Kunis, Jr. <i>Herman J. Kunis Jr.</i>		Date 3/5/03	
Title Pricpal Engineer			
Department DWPF/Quality			
11. Manager			
Name Michael R. Norton <i>Michael R. Norton</i>		Date 3/4/03	
Title Manager, ARP			
Department ARP/Salt Program/LWDP/CBU			
12. Other Approver			
Name David T. Hobbs <i>D.T. Hobbs</i>		Date 3/5/03	
Title Sr. Fellow Scientist			
Department SRTC			

TABLE OF CONTENTS

1.0	SCOPE	4
1.1	GENERAL DESCRIPTION OF ITEM.....	4
2.0	REFERENCES	4
2.1	DEFINITIONS.....	4
2.2	CODES, STANDARDS AND REGULATIONS.....	4
2.3	APPLICABLE DOCUMENTS.....	4
3.0	ITEM REQUIREMENTS	4
3.1	PERFORMANCE REQUIREMENTS.....	4
3.2	DESIGN REQUIREMENTS.....	6
3.3	SERVICE CONDITIONS.....	6
3.4	QUALITY REQUIREMENTS.....	6
3.5	WSRC FURNISHED MATERIAL, EQUIPMENT, SERVICES.....	6
3.6	SCHEDULE.....	6
3.7	PERSONNEL QUALIFICATIONS/CERTIFICATIONS.....	6
3.8	DELIVERABLES (INCLUDES SUBMITTALS).....	7
3.9	PACKING, HANDLING, SHIPPING, AND STORAGE.....	8
3.10	MARKING AND IDENTIFICATION.....	11
3.11	DEVIATIONS.....	12
4.0	ACCEPTANCE OF ITEM	12
4.1	EXAMINATION AND TESTING REQUIREMENTS.....	12
4.2	WSRC SURVEILLANCE AND AUDITS.....	13
4.3	PRE-SHIPMENT APPROVAL.....	13
4.4	FINAL ACCEPTANCE METHOD.....	13
5.0	ATTACHMENTS	14

Attachment 5.1

Monosodium Titanate (MST) Slurry
Chemical Composition and Physical Properties

<u>Property</u>	<u>Unit</u>	<u>Specification</u>
Monosodium Titanate (MST)	gm/L	150 – 200
Density	gm/L	Report as Found
pH	pH unit	10, Minimum
Sr DF (Strontium Decontamination Factor)	N/A	150 Minimum
→ Alcohol content	PPM	500, Maximum
Total Inorganic Carbon	PPM	100 Maximum
→ Total Organic Carbon	PPM	100 Maximum
Total Halides (F/Cl/Br)	PPM	100 Maximum
Particle Size: Less than 1 microns	% by Vol.	Less than 1%.
Particle Size: Greater than 35.5 microns	% by Vol.	Less than 1%

APPROVED for Release for
Unlimited (Release to Public)

5/3/2005

ENGINEERING DOC. CONTROL - SRS



00802749

OSR 45-244 (Rev 1-10-2000)

Calculation Cover Sheet

Project Actinide Removal Process (ARP) Facility		Calculation Number X-CLC-S-00113	Project Number W958	
Title Actinide Removal Process Material Balance Calculation with Low Curie Salt Feed		Functional Classification PS	Sheet 1 of 15	
<input checked="" type="checkbox"/> Preliminary <input type="checkbox"/> Confirmed				
Computer Program No.		<input checked="" type="checkbox"/> N/A	Version/Release No. N/A	
Purpose and Objective The calculation will capture all the flowsheet bases for the Actinide Removal Process Facility (512-S and 241-96H with 512-S) with Low Curie Salt Feed. This Preliminary Calculation provides information on the chemical process flows. Chemicals and radionuclides in the fresh waste feed are based on the Average Low Curie Salt feed vector (70% interstitial supernate removed with 600 mg/L sludge), High Cesium Case (Tank 36: 70% interstitial supernate removed with 600 mg/L sludge), and the Worst Dose Case (Tank 33: 70% interstitial supernate removed with 1200 mg/L sludge) in the Low Curie Feed Basis document (WSRC-TR-2001-00559).				
Summary of Conclusion The process flows for the ARP Facility with Low Curie Salt Feed are shown herein. Bases, assumptions and the resultant material balances for the 512-S and 241-96H with 512-S ARP Facility options (Reference 7) are presented in the accompanying text and appendices. The flowrates, batch sizes and cycle times presented herein are nominal values and may differ slightly from actual values based on current and future facility configurations for both 512-S and 241-96H. Additional material balance cases for 512-S and 241-96H with 512-S ARP Facility options are presented to show impacts of time-averaged filter flux for the 0.5 micron crossflow filter at 512-S, use of a 0.1 micron crossflow filter at 512-S and different MST strike times (0 to 24 hours) at 512-S and 241-96H.				
Revisions				
Rev No.	Revision Description			
D	Updating Material Balance to close open items and incorporate position paper (Reference 16) on material balance inputs (dilution of fresh decontamination factors, etc.)			
Sign Off				
Rev No.	Originator (Print) Sign/Date	Verification/ Checking Method	Verifier/Checker (Print) Sign/Date	Manager (Print) Sign/Date
D	S.G. Subazits S.G. Subazits 3/11/2004	Alternative (Hand) Cal.	Mark Hopkins Mark Hopkins 3/14/04	E.W.H. M.R. Nacton Mark Hopkins 3/12/04 S.J. Robertson S. Robert 3/23/04
Release to Outside Agency - Design Authority (Print)		Signature	Date	
NA		NA	NA	
Security Classification of the Calculation				
Unclassified				

Input:**512-S Only ARP Bases:**

- 0.01M NaOH is used for dilution of the salt waste feed in the LWPT to 5.6 M sodium (Ref 16). This dilution is necessary to increase the rate of alpha and strontium sorption, allowing a reasonable cycle time (Ref 1).
- • MST concentration used is 0.4 g of MST per liter of diluted feed in the LWPT (Ref 1).
- The filter cleaning cycle consists of seven steps: 0.02 M caustic (1), 0.02 M caustic (2), 0.02 M caustic (3), oxalic acid (4), 0.02 M caustic (5), 0.02 M caustic (6), 0.02 M caustic (7). Each wash step is 415 gallons (Ref 17).
- 0.5M oxalic acid used for filter cleaning (Ref 11)
- MST/sludge solids concentrated to approximately 5%_{wf} solids in the LWPT (Ref 1).
- Solids specific gravity = 1.8 (Ref 1)
- The amount of inhibited wash water required to wash the MST/sludge solids to a sodium concentration of 0.5 M (Ref 1) is determined to be ~1.57 gallons of washwater per gallon of salt solution. Using the following equation: Wash water = $\ln[\text{Na}(\text{initial})] - \ln[\text{Na}(\text{final})]$. This constant volume wash follows addition of 2000 gallons of inhibited wash water to raise the LWPT level to run the filter feed pump and dilute the LWPT heel sodium concentration. After the pump has been started, the LWPT will be pumped down to 1,600 gallons before the constant washing procedure begins.
- Based on 24-hour sorption reaction time, Strontium Decontamination Factor = 129.5 (Ref 2, 3, 16)
- Plutonium (Pu) Decontamination Factor = 12.9 (Ref 2, 3, 16)
- Uranium (U) Decontamination Factor = 1.2 (Ref 2, 3, 16)
- Neptunium (Np) Decontamination Factor = 3.7 (Ref 2, 3, 16)
- Americium (Am) Decontamination Factor = 1.7 (Ref 12)
- Curium (Cm) Decontamination Factor = 1.7 (Ref 12)
- Mixing of Caustic and Oxalic Acid from the spent cleaning solutions results in the following reaction: $\text{H}_2\text{C}_2\text{O}_4 + 2 \text{NaOH} \rightarrow \text{Na}_2\text{C}_2\text{O}_4 + 2\text{H}_2\text{O}$. For the cleaning protocol used in the mass balance calculations, the oxalic acid used consumes all the available NaOH in the spent cleaning solution and the solids washing heel of the LWPT. This results in a slightly acidic stream going forward to the Low Point Pump Pit Precipitate Tank and DWPF.
- The Cross-flow filter area is 230 ft² (Ref 6). The filter media are Mott 0.5 micron sintered metal tubes.
- The 512-S Only ARP Vessel and equipment configuration is based on the Case 2 option with the Option D MST sludge solids disposal path from the Actinide Removal Process Alternative Study and Selection document (Ref 7).
- The Henry's constants for methanol and isopropanol are 338 and 754 mmHg/mole fraction respectively (Ref 9).

APPROVED for Release for
Unlimited (Release to Public)
6/27/2005

**MEASUREMENTS OF FLAMMABLE GAS
GENERATION FROM SALTSTONE CONTAINING
SIMULATED TANK 48H WASTE (INTERIM
REPORT)**

A.D. Cozzi, D.A. Crowley, J.M. Duffey, R.E. Eibling, T.M. Jones, A.R.
Marinik, J.C. Marra, and J.R. Zamecnik

April 2005

Immobilization Technology Section
Savannah River National Laboratory
Aiken, SC 29808

Prepared for the U.S. Department of Energy Under Contract Number
DEAC09-96SR18500



SRNL
SAVANNAH RIVER NATIONAL LABORATORY

DISCLAIMER

This report was prepared by Westinghouse Savannah River Company (WSRC) for the United States Department of Energy under Contract No. DE-AC09-96SR18500 and is an account of work performed under that contract. Neither the United States Department of Energy, nor WSRC, nor any of their employees makes any warranty, expressed or implied, or assumes any legal liability or responsibility for the accuracy, completeness, or usefulness, of any information, apparatus, or product or process disclosed herein or represents that its use will not infringe privately owned rights. Reference herein to any specific commercial product, process, or service by trademark, name, manufacturer or otherwise does not necessarily constitute or imply endorsement, recommendation, or favoring of same by WSRC or by the United States Government or any agency thereof. The views and opinions of the authors expressed herein do not necessarily state or reflect those of the United States Government or any agency thereof.

Printed in the United States of America

**Prepared For
U.S. Department of Energy**

Key Words: Saltstone
Tetraphenylborate
Tank 48
Benzene

Retention: Permanent

MEASUREMENTS OF FLAMMABLE GAS GENERATION FROM SALTSTONE CONTAINING SIMULATED TANK 48H WASTE (INTERIM REPORT)

A.D. Cozzi, D.A. Crowley, J.M. Duffey, R.E. Eibling, T.M. Jones, A.R.
Marinik, J.C. Marra, and J.R. Zamecnik

April 2005

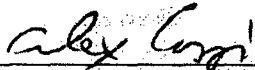
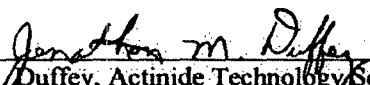
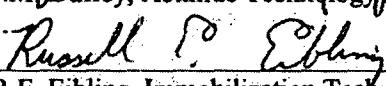
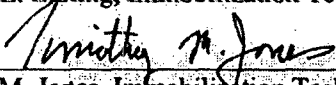
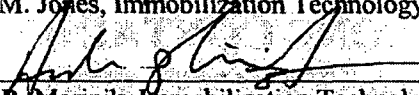
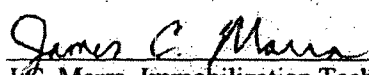
Immobilization Technology Section
Savannah River National Laboratory
Aiken, SC 29808

Prepared for the U.S. Department of Energy Under Contract Number
DEAC09-96SR18500



REVIEWS AND APPROVALS

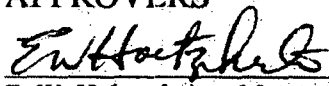
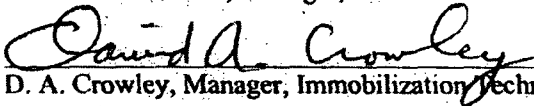
AUTHORS:

 A.D. Cozzi, Immobilization Technology Section	5/17/05 Date
 J.M. Duffey, Actinide Technology Section	5/17/05 Date
 R.E. Eibling, Immobilization Technology Section	5/17/05 Date
 T.M. Jones, Immobilization Technology Section	5/17/2005 Date
 A.R. Marinik, Immobilization Technology Section	5/17/2005 Date
 J.C. Marra, Immobilization Technology Section	5/17/05 Date
 J.R. Zamecnik, Immobilization Technology Section	5/17/05 Date

TECHNICAL REVIEWERS:

 M.J. Barnes, Waste Processing Technology Section	5/17/05 Date
 M.S. Hay, Waste Processing Technology Section	5/19/05 Date

APPROVERS

 E. W. Holtzschneider, Manager, Immobilization Technology Section	5/12/05 Date
 D. A. Crowley, Manager, Immobilization Technology & Business Development	5/19/05 Date
 J.E. Occhipinti, Manager, DWPF Process Engineering	5/24/05 Date

EXECUTIVE SUMMARY

The Savannah River National Laboratory was tasked with determining the benzene generation rates in Saltstone prepared with tetraphenylborate (TPB) concentrations ranging from 30 mg/L to 3000 mg/L in the salt fraction and with test temperatures ranging from ambient to 95 °C.¹ Defense Waste Processing Facility Engineering (DWPF-E) provided a rate of benzene evolution from saltstone of 2.5 µg/L /h saltstone (0.9 µg/kg saltstone/h) to use as a target rate of concern (TRC).²

The generation of benzene, toluene, and xylenes from saltstone containing a simulant of Tank 48H salt solution has been measured as a function of time at several temperatures and concentrations of TPB. The Tank 48H simulant contained potassium tetraphenylborate (KTPB), the decomposition products (phenol, biphenyl, and benzene), and diphenylmercury in addition to inorganic salts. The saltstone slurries were prepared from blends of the Tank 48H simulant and DWPF recycle simulant.

The purpose of this interim report is to provide DWPF-E with a brief description of the methodology and an indication of the trends of benzene evolution. The data presented are to be used by DWPF-E for preliminary calculations with the knowledge that more data are being collected and may alter the final results. A more complete description of the methods and materials will be included in the final report. The benzene evolution rates approximately follow an increasing trend with both increasing temperature and TPB concentration. The benzene generation rates at 95 °C from 1000 mg/L and 3000 mg/L TPB simulant exceeded the recovery-adjusted 0.9 µg/kg saltstone/h TRC (2.5 µg/L saltstone/h), while all other conditions resulted in benzene generation rates below this TRC (except for the initial rate from tests at 75 °C and 3000 mg/L). The toluene evolution rates for at least one sample at each temperature exceeded the TRC initially, but all dropped below the TRC within 2-5 days. The toluene emissions appear to be mainly dependent on the fly ash and are independent of the TPB level, indicating that toluene is not generated from TPB.

TABLE OF CONTENTS

1.0 EXECUTIVE SUMMARY v
2.0 INTRODUCTION AND BACKGROUND 1
3.0 APPROACH 2
 3.1 Salt Solution Simulants 2
 3.2 Saltstone Mixes 3
 3.3 Benzene Collection, Recovery and Analysis 5
 3.3.1 Collection 5
 3.3.2 Recovery 6
 3.3.3 Analysis 7
4.0 RESULTS 8
 4.1 Method Standards 8
 4.2 Recovery and Analysis 8
 4.2.1 Benzene 10
 4.2.2 Toluene 12
5.0 SUMMARY & CONCLUSIONS (TO DATE) 28
6.0 REFERENCES 29

LIST OF FIGURES

Figure 3-1. Geometry of test vessels.....	4
Figure 3-2. Filled vessels installed in oven.....	5
Figure 3-3. Schematic of benzene recovery methodology.....	6
Figure 3-4. Benzene collection configuration.....	6
Figure 3-5. Schematic of the methodology used for determining desorption efficiency from carbon tubes.....	7
Figure 4-1. Graphic representation of integrated (averaged) flow data.....	10
Figure 4-2. Benzene generation rates for simulants at 95 °C.....	13
Figure 4-3. Data from Figure 4-2 with a modified y-axis to clarify samples with lower benzene generation rates.....	14
Figure 4-4. Benzene generation rates for simulants at 75 °C.....	15
Figure 4-5. Benzene generation rates for simulants at 55 °C.....	15
Figure 4-6. Benzene generation rates for simulants at 25 °C.....	16
Figure 4-7. Benzene generation rates for blanks at 95 °C.....	16
Figure 4-8. Benzene generation rates for simulants at 75 °C (Figure 4-4) expanded to show detail.	17
Figure 4-9. Benzene generation rates for simulants at 55 °C (Figure 4-5) expanded to show detail.	17
Figure 4-10. Benzene generation rates for simulants at 25 °C (Figure 4-6) expanded to show detail.....	18
Figure 4-11. Mean values of benzene generation rates for all test conditions.....	18
Figure 4-12. Mean values of benzene generation rates at 95 °C.....	19
Figure 4-13. Mean values of benzene generation rates at 75 °C with 95L and blanks for reference.	19
Figure 4-14. Mean values of benzene generation rates at 55 °C with 75L and blanks for reference (Inset is data expanded to show detail).....	20
Figure 4-15. Mean values of benzene generation rates at 25 °C with 55L and blanks for reference (Inset is data expanded to show detail).....	20
Figure 4-16. Mean values of benzene generation rates in samples with 3000 mg/L TPB and blanks for reference (Inset is data expanded to show detail).....	21
Figure 4-17. Mean values of benzene generation rates in samples with 1000 mg/L TPB and blanks for reference (Inset is data expanded to show detail).....	21
Figure 4-18. Mean values of benzene generation rates in samples with 30 mg/L TPB and blanks for reference (Inset is data expanded to show detail).....	22
Figure 4-19. Toluene generation rates for simulants at 95 °C.....	22
Figure 4-20. Toluene generation rates for simulants at 75 °C.....	23
Figure 4-21. Toluene generation rates for simulants at 55 °C.....	23
Figure 4-22. Toluene generation rates for simulants at 25 °C.....	24
Figure 4-23. Data from Figure 4-19 with a modified y-axis to clarify samples with lower toluene generation rates.....	24
Figure 4-24. Toluene generation rates for blanks at 95 °C.....	25
Figure 4-25. Data from Figure 4-19 expanded to show detail.....	25
Figure 4-26. Data from Figure 4-20 expanded to show detail.....	26
Figure 4-27. Data from Figure 4-21 expanded to show detail.....	26
Figure 4-28. Data from Figure 4-22 expanded to show detail.....	27

LIST OF TABLES

Table 3-1. Composition of DWPF Recycle Simulant.	2
Table 3-2. Potential Sources of Benzene in Tank 48H Simulant.	2
Table 3-3. Calculated Composition and Properties of Salt Solutions.	3
Table 3-4. Premix Formulations for Processing.	3
Table 3-5. Matrix of Blend TPB Concentrations and Test Temperatures.	3

LIST OF ACRONYMS

ADS	Analytical Development Section
DWPF	Defense Waste Processing Facility
FID	Flame ionization detector
GC	gas chromatograph
GCMS	gas chromatograph – mass spectrometer
GGBFS	ground granulated blast furnace slag
ID	inner diameter
KTPB	Potassium tetrphenylborate
CLFL	Composite Lower Flammable Limit
NIOSH	National Institute for Occupational Safety and Health
SRNL	Savannah River National Laboratory
TPB	Tetraphenylborate
TRC	Target rate of concern

1. T.E. Chandler, "Determine Benzene Generation Rates from Saltstone at Elevated Temperatures," Task Technical Request SSF-TTR-2004-0005, (2004).
2. T.E. Chandler, Presentation at "Benzene Analysis Brainstorm Meeting," 11/1/2004.

1.0 INTRODUCTION AND BACKGROUND

The operating strategy for processing at Z-area Saltstone is projected to result in elevated temperatures in the Saltstone vaults over a period of months. This strategy resulted in a review of documentation for the production of benzene via the decomposition of potassium tetraphenylborate (KTPB) solids at elevated temperatures for an extended period of time. Initial review indicates that benzene and other flammable gases could accumulate in the vault vapor space with this proposed operating strategy. The current Z-Area (Saltstone) Safety Basis does not postulate an explosion in the vaults, and therefore, the Safety Basis does not restrict vault temperatures or tetraphenylborate (TPB) concentrations relative to a vault explosion.

An evaluation of prior Saltstone grout production confirmed that previous facility operation has not resulted in elevated grout temperatures for extended periods of time (maximum temperature observed 51°C and peak temperatures lasted for days rather than months). This review, combined with previous benzene measurements in the vault cells, provides the basis for the position that there is no imminent hazard.

The SRNL was tasked¹ with determining the benzene generation rates in Saltstone grout prepared with TPB concentrations ranging from 30 mg/L to 3000 mg/L in the salt fraction and test temperatures ranging from ambient to 95 °C. The request included determination of the effect of surface area to volume ratio on the benzene generation rate.

A literature review³ summarizing previous work on benzene generation and leach results provided the following conclusions.

- Data from past studies of benzene generation from saltstone samples containing TPB and TPB decomposition products should be used with caution due to the large uncertainty associated with the data.
- The average benzene generation rates, measured over the total duration of a test, span from <0.1 to 140 µg/hr per liter of saltstone in the reviewed studies. The peak rates, from individual measurement periods during the tests, range from <0.1 to 390 µg/hr per liter of saltstone. However, distinguishing what constitutes a statistically significant difference in rate proves difficult due to the high uncertainty present in the data.
- Results of past studies suggest the evolution of benzene from saltstone samples may show some temperature dependence with rates increasing with temperature. The change in benzene generation rate as a function of temperature cannot be quantified from the available data. The data also suggests that high peak rates may occur sooner when saltstone samples have been cured at higher temperature.

A multi-stage approach is being used to meet these objectives. In the first stage, several potential methodologies for the collection, recovery and analysis of benzene were evaluated. Stage II is ongoing and entails demonstrating the methodology selected in Stage I with surrogate materials. The data in Stage II is the information presented in this report. Testing of saltstone prepared with actual Tank 48H waste as the source of TPB is underway as Stage III and will be addressed in a separate interim report. Results of the surface area to volume (of saltstone) tests (generation vs. retention) will be discussed in the combined final report. Stage IV studies will investigate other volatile organics that may be emitted during curing and will be discussed in the combined final report.

2.0 APPROACH

The method to collect and analyze benzene selected from Stage I was to purge the head space of vessels containing saltstone and capture the benzene on a carbon bed. The benzene is subsequently desorbed and analyzed using a gas chromatograph (GC) with a flame ionization detector (FID). This method was also found to be applicable for the collection of toluene and xylene.

2.1 Salt Solution Simulants

The Defense Waste Processing Facility (DWPF) recycle simulant targeted the average sodium and the maximum anion and mercury content of the Tank 23H and Tank 24H samples taken 100 inches from the tank bottoms as reported by Swingle.⁴ Table 2-1 provides the composition of the DWPF recycle simulant based on the major components listed in Reference 4. The customer also requested a 2 mg/L spike of palladium into the salt solution.⁵ The Tank 48H simulant⁶ is based on samples of Tank 48H taken in 2003.⁷ Table 2-2 lists the potential sources of benzene from the Tank 48H simulant. Table 2-3 shows the physical properties of the two salt solution simulants and the calculated properties of the resulting blends used for this study. The different TBP concentrations are achieved via the aggregation of the Tank 48H simulant with the DWPF recycle simulant.

Table 2-1. Composition of DWPF Recycle Simulant.⁸

Compound	g/L	Component	M
NaNO ₂	21.734	Na	0.78
NaNO ₃	5.219	NO ₂ ⁻	0.32
NaOH	17.399	NO ₃ ⁻	0.06
Na ₂ CO ₃	7.419	OH ⁻	0.44
Hg(NO ₃) ₂ ·xH ₂ O	24.8 mg/L	CO ₃ ²⁻	0.07
Pd solution (15.27%) ^a	0.013	Hg	14.5 mg/L
Total	51.771		
Wt % solids	5.2%		

^aPd solution is palladium nitrate in nitric acid.

Table 2-2. Potential Sources of Benzene in Tank 48H Simulant.

Component	Compound	g/L
Sodium Tetrphenylborate ^a	(C ₆ H ₅) ₄ BNa	19.7
Diphenylmercury	(C ₆ H ₅) ₂ Hg	0.018
Phenol	C ₆ H ₅ OH	0.95
Biphenyl	(C ₆ H ₅) ₂	0.62
Benzene	C ₆ H ₆	0.055

^aAdded to simulant as sodium compound. Potassium compound precipitates during the simulant make up.

Table 2-3. Calculated Composition and Properties of Salt Solutions.

Material	TPB (mg/L)	Wt. % Solids		Density (g/mL)	Mercury (mg/L)
		Undissolved	Total		
Tank 48H7	18,800	2.18	18.42	1.144	10.3
DWPF Recycle simulant (s)	0	<1	5.09	1.039	14.54 (Tank 24H)
Tank 48H + DWPF Recycle	30	NM	5.1	1.04	14.5
	1000	NM	5.9	1.04	14.3
	3000	NM	7.4	1.06	13.8

NM-not measured

2.2 Saltstone Mixes

Saltstone grout was prepared using the salt solutions described previously and premix materials obtained from the Saltstone Processing Facility. Table 2-4 lists the premix composition and the water to premix ratios. The water to premix ratio is defined as the ratio of the mass of evaporable water from the waste (at ~110 °C) to the combined mass of cement, slag, and fly ash. For the purposes of processing, fixed concentrations (0.25 wt% of blended salt solution) of set retarder* and antifoam† were added. The dosage of set retarder and antifoam used are based on recommendations made in previous testing.⁹ Table 2-5 lists the test matrix for variables tested. This resulted in twelve TPB-temperature combinations investigated.

Table 2-4. Premix Formulations for Processing.

Premix	Water/Premix
45% Class F Fly Ash (FA) 45% GGBFS ^a (Slag) 10% Cement	0.63

^aGround granulated blast furnace slag

Table 2-5. Matrix of Blend TPB Concentrations and Test Temperatures.

TPB (mg/L)	Curing Temperature (°C)
30	Ambient
1000	55
3000	75
	95

To ensure that all of the TPB was incorporated into each batch, individual Tank 48H simulant samples were prepared for each saltstone mix. For example, to prepare the salt solution for the first replicate of the 3000 mg/L samples (one for each temperature), an 80 mL Tank 48H simulant was prepared and aggregated with 498 mL of DWPF recycle simulant. The Tank 48H simulant was blended with the appropriate amount of recycle simulant in a blender to make a salt solution with the desired TPB concentration. Premix was added and the mix was blended for one minute, visually inspected, and blended for an additional two minutes. The resulting saltstone slurry was poured into four vessels (~ 200 mL saltstone per ~ 325 mL vessel, one vessel for each temperature). Sketches of the "standard" vessel used for most of the tests and the high surface area vessels are shown in Figure 2-1. The other two vessel configurations are for testing of high

* W.R. Grace, Daratard 17

† Dow-Corning, Q2-3183A

surface area geometries that were initiated later. Results will be discussed in the final report. Each vessel was placed into an oven at the desired temperature. The vessel was then connected to a sampling tube. This process was repeated for each of the TPB concentrations. For each of the following two weeks, additional replicates were added by repeating the sample preparation method described above. Currently, triplicate samples are curing at each temperature to determine the effect of curing temperature on the flammable gas evolution rate. Each of the TPB levels (30, 1000, and 3000 mg/L referred to in the graphs as L, M, and H, respectively (low, medium, high)) was tested at each temperature in triplicate (replicates a, b, c). Triplicate blanks simulant saltstone which contains no TPB were also placed in the 95 °C oven. Two standard vessels that were periodically charged with a known amount of benzene standard were also placed in the 95 °C oven. The vessels were purged and the benzene recovered approximately once a week to help determine the effectiveness of the sampling technique. Figure 2-2 shows the vessels in place in the oven connected to the sampling tubes.

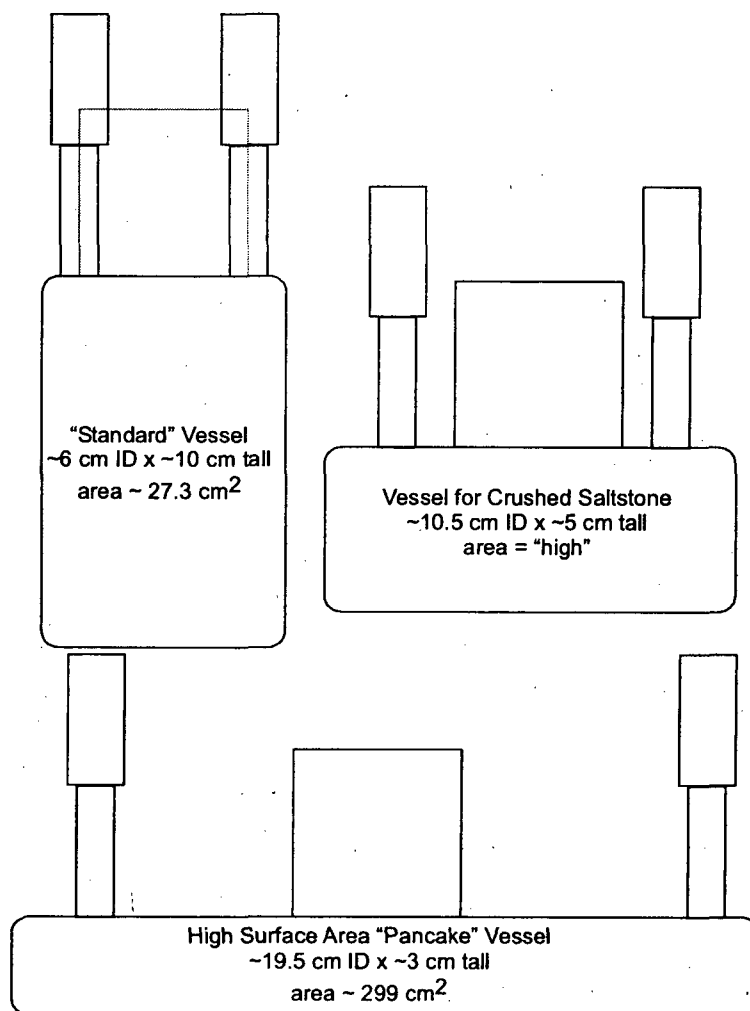


Figure 2-1. Geometry of test vessels.

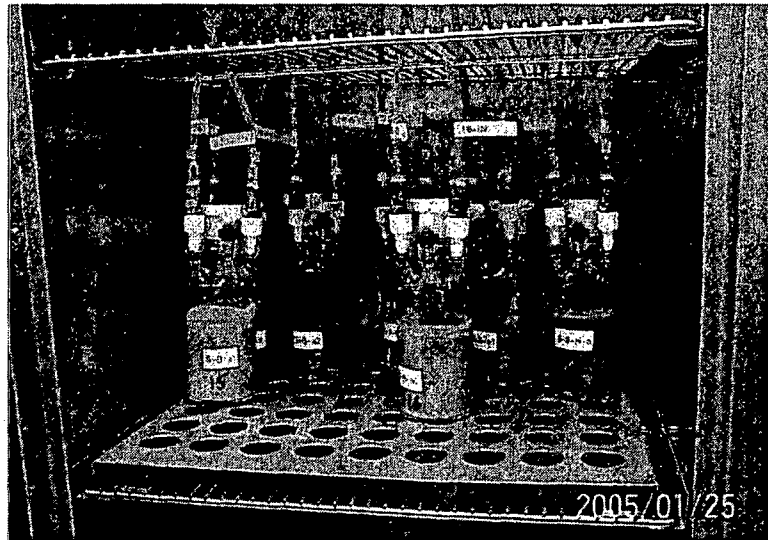


Figure 2-2. Filled vessels installed in oven.

2.3 Benzene Collection, Recovery and Analysis

2.3.1 Collection

The benzene collection method was based on National Institute for Occupational Safety and Health (NIOSH) method 1501 for benzene sampling.¹⁰ The curing saltstone samples are vented through a two-stage carbon bed sampling tube† fitted with an O-ring seal. The carbon bed sampling tube consists of two activated carbon beds separated by an inert filter. The first bed is intended to capture all of the benzene and the second bed is intended to confirm no breakthrough from the first bed occurred. This configuration ensures that any benzene released prior to active sampling will occur through the carbon bed. When the vessel is selected for sampling, bottled air, purified by a hydrocarbon trap, is introduced at approximately 100 mL/min. This rate is within the range of 10-200 mL/min recommended in Reference 10. Air is purged through the vessel for 7-10 minutes. This volume represents a minimum of five volume changes in the vessel headspace. After the purge is complete, the carbon tube is exchanged with a new carbon tube. A schematic of the collection method is shown in Figure 2-3. Recovery of benzene from the carbon sampling tubes was tested by adding a known amount of benzene standard (benzene in carbon disulfide [CS₂]) to the tube and then recovering and measuring the amount of benzene by the standard analytical method. Figure 2-4 is the configuration for introducing purge air and collecting benzene from saltstone samples curing in the 95 °C oven.

† SKC Anasorb® CSC Catalog# 226-01

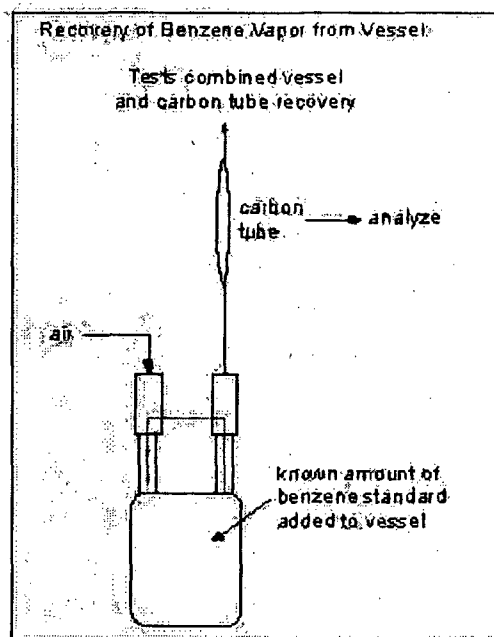


Figure 2-3. Schematic of benzene recovery methodology.

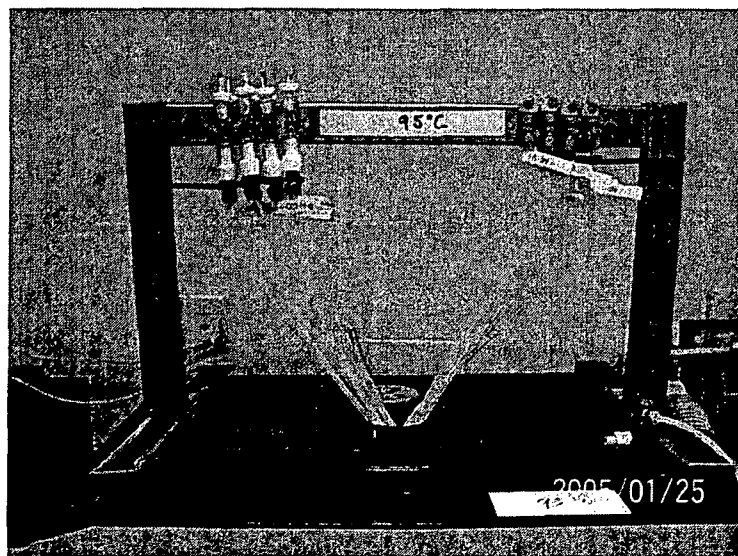


Figure 2-4. Benzene collection configuration.

2.3.2 Recovery

The method for recovery of the benzene from the carbon beds also parallels the method described in Reference 10. The collected sample tubes are opened and the two carbon beds are separated into individual vials. One milliliter of carbon disulfide is added to each vial as the eluent. The vial is capped, agitated and allowed to stand for at least 30 minutes before analysis. To determine desorption efficiency, an aliquot of benzene standard in carbon disulfide is also injected on a new carbon bed. The carbon bed is desorbed and the vial is processed as a sample. The desorption

efficiency is checked several times each week. A schematic of the methodology for determining desorption efficiency is shown in Figure 2-5.

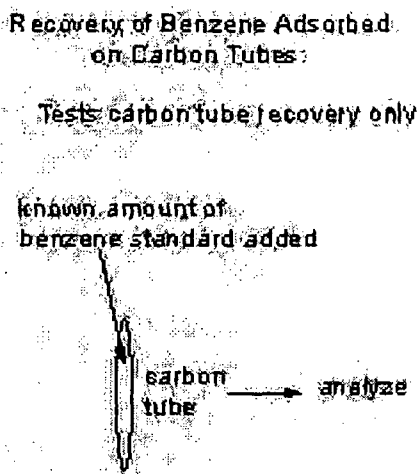


Figure 2-5. Schematic of the methodology used for determining desorption efficiency from carbon tubes.

2.3.3 Analysis

The analysis of the organic compounds recovered from the activated carbon tube uses a gas chromatograph equipped with a stainless steel capillary column and a flame ionization detector. The organic compounds are separated in the gas chromatograph using a capillary column with a polydimethylsiloxane stationary phase (Restek MXT@-1, 30 meters, 0.53 mm ID, 3.0 micron film thickness). Primary identification is based on retention time. Confirmation analysis was obtained (when needed) by gas chromatography-mass spectrometry (GCMS) using a different column (DB-5MS, 30 meter, 0.25 mm ID, 0.25 micron film thickness) using both retention time and the peak's mass spectrum. The GC is calibrated daily with standards consisting of benzene, toluene, and m,p,o-xylenes in carbon disulfide using the external standard technique. Three concentrations of benzene are used to develop the linear range of the GC. The detection limit of the gas chromatograph was approximately 1 ng/sample, which is roughly equivalent to 0.01 µg benzene/kg saltstone/h.

3.0 RESULTS

The release rates of benzene, toluene, and xylenes from saltstone containing a simulant of Tank 48H salt solution were measured as a function of time at several temperatures. Experiments were run at the four temperatures 95, 75, 55, and 25 °C. Each TPB level was tested at each temperature in triplicate.

3.1 Method standards

The recovery of benzene injected into empty vessels was measured. Two vessels were used, one vessel (S-S-a2) developed a plugged exit line due to the degradation of the check valve in the quick connect, so only 2 or 3 data points were considered to be valid. The other vessel (S-S-a1) was tested nine times. The average benzene recovery was about 60% with a standard deviation of about 20%. Based on this estimated recovery of 60%, the measured amounts of benzene recovered from the sample tubes for the actual test vessels should be divided by 60% (0.6), or multiplied by 1.67 to be more conservative. This recovery value should be considered preliminary since testing of carbon tube and vessel standards will continue through the completion of the tests to better quantify the recovery. A statistical analysis of the recovery also needs to be performed so that the conservativeness of the recovery factor can be determined. For this preliminary report, the 60% factor will be used, with the caveat that a lower recovery factor may be more appropriate, but that this determination will be deferred to the final report when more recovery data is available.

Recovery of benzene from the carbon sampling tubes was also tested as described in Section 2.3.2. The recovery of benzene from the sample tubes had a mean of 88% with a standard deviation of 19%. These sample tube recovery tests will also be continued, providing additional data on recovery for the final report.

3.2 Recovery and analysis

The sampling frequency for each vessel was adjusted so that measurable quantities of benzene would be collected on the carbon sampling tubes. In some cases, the amounts collected were much higher than anticipated, but not higher than the capacity of the sampling tube, as indicated by the absence of benzene (or any analyte) on the second bed. The presence of benzene on the second bed of the sampling tube indicates that the first section is saturated and can contain no more benzene. When this occurs, the total amount collected on both front and back is combined. Because there is benzene on the second bed, there is then the possibility that not all of the benzene has been collected. However, some samples may have been so concentrated, the analysis by GC resulted in saturating the detector such that the actual amount was higher than what was measured. These few samples will be reanalyzed with a greater dilution factor prior to the final report. (The samples referred to here are the ones with the highest benzene amounts, which were for some of the 3000 mg/L samples at 95 °C.) A few initial samples had benzene on the second bed due to water from the vessels being blown up through the sample line into the sampling tube. These samples will be flagged in the final report.

Results are reported in units of μg flammable gas/kg saltstone/h, where the flammable gas is either benzene (ϕ) or toluene. Analysis of xylene concentration data has not yet been done, but most values appear to be significantly lower than the benzene concentrations. To get the true flammability of a particular offgas mixture, the composite lower flammable limit (CLFL) of the mixture must be used, so the concentrations (generation rates) of all flammable species are needed unless they are negligible.

The customer has supplied a target rate of concern for flammable gas release of 2.5 $\mu\text{g/L}$ saltstone grout/h at which tentative calculations indicate that positive ventilation of the saltstone vaults would be required.² This release rate of 2.5 $\mu\text{g/L}$ saltstone/h is approximately equivalent to 1.5 $\mu\text{g/kg}$ saltstone/h given an approximate density of saltstone grout of 1.7 kg/L (estimated from a representative sample of saltstone). Since the density is estimated, the final values will be slightly different as the final densities will most likely be slightly different. The measured generation rates should be divided by the recovery factor to give a more conservative rate, but for this preliminary report, the TRC was instead decreased by the recovery factor, which accomplishes the same purpose. In the final report, the measured rates will be adjusted for the recovery factor rather than the TRC. Applying the 60% recovery factor to this rate gives a more conservative TRC of 0.9 $\mu\text{g/kg}$ saltstone/h. (Technically, the evolution rates should be divided by 60% rather than reducing the TRC, but the relative comparison will be the same. The rates will be adjusted properly in the final report.) Also, these rates are based on the as-cast mass of saltstone prior to curing since the final cured mass cannot be measured until the tests are complete. The final masses are expected to be less than the as-cast masses. Therefore, the generation rates may be higher than reported here.

The data reported in the following graphs show the mean values of the benzene generation rate over specific time intervals. The actual measurements made are the total amount of benzene generated during the time interval that the sampling tube is installed on the vessel. Therefore, the amount of benzene measured is the amount evolved integrated over the time interval. Because the sample is integrated, the resulting rate (amount collected / collection time interval) is the average rate over the time interval. Therefore, to properly display this information, this average rate should be plotted as a horizontal line over the time interval of the sample. An example of plotting like this is shown in Figure 3-1. Plotting as horizontal lines indicates that only the average generation rate over the time interval is known; the actual rate could have fluctuated significantly over the time interval, but only the average is known. Because it is very difficult to plot all of the data in this way (horizontal line averages), each generation rate average (over a time interval) was instead plotted as a single point at the average time of the interval. This way of plotting is compared to the horizontal line average plot in Figure 3-1.

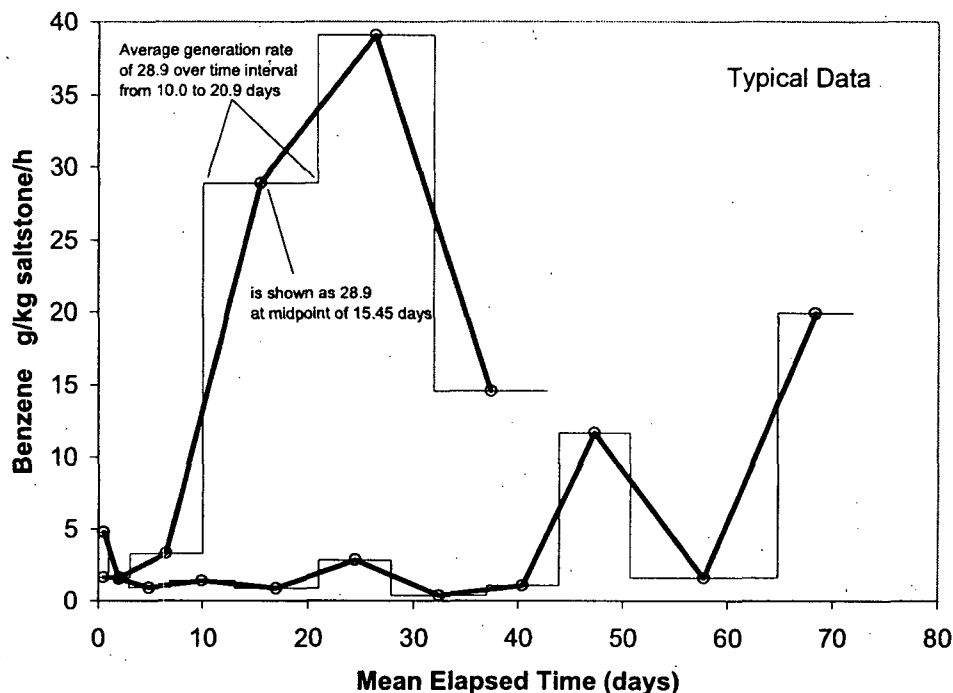


Figure 3-1. Graphic representation of integrated (averaged) generation rate data.

The experimental data are best described with a series of graphs comparing the benzene (and toluene) generation rates.

Note that all tentative conclusions given below are based on the assumption that sudden increases in benzene generation rate will not occur in the future.

3.2.1 Benzene

Figures 4-2 through 4-7 are plots of all of the data taken for benzene to date. Each plot shows data for the same temperature for the simulant tests; the blank vessel results at 95 °C are shown in Figure 3-7. Figure 3-2 shows the rates for the 95 °C simulant tests. Figure 3-3 shows this same data (30 and 1000 mg/L TPB only) plotted with a y-scale maximum of 1.6 µg/kg saltstone/h for comparison to Figures 4-4 through 4-7, which have the same y-scale. All data sets, except 1000 and 3000 mg/L at both 75 and 95 °C, display an initially high benzene generation rate that quickly drops off to somewhat of an asymptotic value. This initial release is presumed to be a release of the small amount of free benzene contained in the simulant. Several headspace gas samples that were taken from the blender during mixing of the 3000 mg/L saltstone and tested on the GCMS showed that significant amounts of benzene were released during the mixing. However, quantification of the amounts released was not possible.

The data in Figure 3-2 shows that at 1000 and 3000 mg/L TPB, the benzene generation rates all exceed the TRC value of 0.9 µg/kg saltstone/h, with 3000 mg/L exceeding this value by more than one order of magnitude. Figure 3-3 shows that the tests with 30 mg/L at 95 °C do not exceed the TRC. Figures 4-4 through 4-7 show that the TRC was not exceeded at any concentration at 25, 55, and 75 °C except for the initial point for 3000 mg/L and 75 °C. However, the 75 °C (a)

and (b) 3000 mg/L TPB replicates are showing a potential upward trend in the generation rate, so no conclusions can be drawn about these at this time. The TRC was also not exceeded by the blank at 95 °C. The blanks were found to contain highly variable amounts of toluene and also some benzene and xylenes, which most likely came from either the fly ash or the slag.

Most of the initial rates for the 25 °C samples exceeded the initial rates for the 55 and 75 °C samples, which was not expected. The initial rates are quite variable and the differences seen appear to be due to a combination of measurement uncertainty and possibly the way in which each saltstone preparation was handled from the start of mixing to pouring into the vessels. The “?-H-a” samples all have significantly higher initial benzene rates; these three saltstone samples were prepared in the same manner. These initial rates are greater than the approximate detection limit of 0.01 µg benzene/kg saltstone/h, but some of the 25, 55, and 75 °C data at longer times is on the order of this amount.

The benzene generation data for 75, 55, and 25 °C (except 75 °C and 3000 mg/L) are re-plotted in Figure 3-8 through Figure 3-10 with a y-scale maximum of 0.2 µg/kg saltstone/h so that the “steady-state” benzene rates can be compared. The mean values from each of the three replicates are shown in Figures 4-11 through 4-18. Because the replicate values do not all have the same time value (x-value), each data set was interpolated at regular intervals and the interpolated values were averaged. Figures in the Appendix show plots of each data set and the average values determined by interpolation.

All the mean data values except 1000 and 3000 mg/L at 95 °C, which were much higher, are shown on Figure 3-11. The mean data values at the four temperatures are plotted in Figures 4-12 through 4-15 along with the blank mean data values. These plots show that the 30 mg/L concentration at the next higher temperature falls approximately in between the 1000 and 3000 mg/L rates. The blank rates at 95 °C are greater than or equal to all the rates at 25 °C, and 55 °C, and greater than 75 °C and at 30 mg/L.

Figures 4-16 through 4-18 compare the mean benzene generation rates at constant TPB concentration. At all TPB levels, the 75 °C data always exceeds the lower temperature data, whereas the 25 °C and 55 °C data are approximately equal. As shown in other graphs, the 95 °C data always exceeds the 75 °C data at the same TPB concentration. The relative order of the benzene generation rates can be summarized with the following ranking:

Highest:	95H
∨	95M ≅ TRC
∨	75H
∨	95L ≅ 75H
∨	75M
∨	75L ≅ BLANK ≅ 55H
Lowest:	55M ≅ 55L ≅ 25H ≅ 25M ≅ 25L

3.2.2 Toluene

The evolution of toluene is shown in figures 3-19 through 3-28. For these, the evolution rate TRC for benzene is used as the approximate TRC for toluene. The recovery of similar species (toluene is very similar to benzene) should be about the same since the affinity of the carbon sample tubes for toluene is supposed to be essentially the same as for benzene. There is no reason why recovery of toluene from the standard vessels would be expected to be any different than the recovery of benzene. The LFL of toluene is 1.2-1.4 vol% compared to 1.1 vol% for benzene, so the equivalence assumption is conservative. (1.1 vol% benzene = 0.858 g/L; 0.858 g/L of toluene = 0.93 vol%, which is less than the LFL).

Figure 3-19 shows the toluene evolution rate from the 95 °C samples. For the first set of vessels (a), the initial rate was significantly higher (6-16 • g toluene/kg saltstone/h) than for the (b) and (c) replicates (<2 • g toluene/kg saltstone/h). Similar behavior was seen for the 25 °C, 55 °C, and 75 °C vessels (Figures 4-20 through 4-22). Toluene appears to be generated from either the fly ash or the slag, with fly ash likely the cause, because it contains some unburned carbonaceous compounds from coal. The (a) replicates may have been made up from a different source of fly ash, as there were several containers available. Unfortunately, the fly ash source was not recorded. (There were other researchers using the same raw materials.) Solvent extraction of fly ash and slag samples followed by GCMS analysis showed only small amounts of toluene. However, the fly ash source that may have been used for the (a) replicates was completely used up, so analysis was not possible. Another possible explanation of this difference is that the fly ash could have segregated in the container, with the more volatile carbonaceous compounds migrating to the top, where they would have been enriched in the (a) replicates relative to the other replicates.

Figure 3-23 shows the 95 °C data plotted on the same scale as the 25 °C, 55 °C, and 75 °C and blank data for comparison. It is apparent that the blank replicates (a1) and (a2), Figure 3-24 had the highest toluene emission rates, with rates exceeding the TRC even at 25 days. Blanks (a1) and (a2) were made with the same fly ash source as the (a) replicates, whereas the (a3) blank was probably made with the other fly ash source. Blank (a3) was made at about the same time as the (b) replicates.

Figures 4-25 through 4-28 show the toluene data plotted on a reduced scale (0-1 • g toluene/kg saltstone/h). The evolution rates at greater than 20 days are highest for the 75 °C (a) replicates, followed by the 95 °C (a) replicates, then the 25 °C (a) replicates. The 55 °C (a) replicates and all

the (b) and (c) replicates have evolution rates of less than $0.1 \text{ g toluene/kg saltstone/h}$, with the $25 \text{ }^\circ\text{C}$ and $55 \text{ }^\circ\text{C}$ samples having essentially no toluene emissions.

The results for toluene indicate that the source of fly ash may be the most significant factor affecting the emission rate. In all cases, the initial higher rate quickly diminishes within about 5 days. However, for some of the samples, the toluene emission rate did not decrease as much after the initial decline ($95 \text{ }^\circ\text{C}$ and $75 \text{ }^\circ\text{C}$, 1000 and 3000 mg/L (a) replicates). However, all were below the emission TRC. Toluene does not appear to be generated from decomposition of the TPB; if it were, there should be a TPB concentration dependence, and there was none.

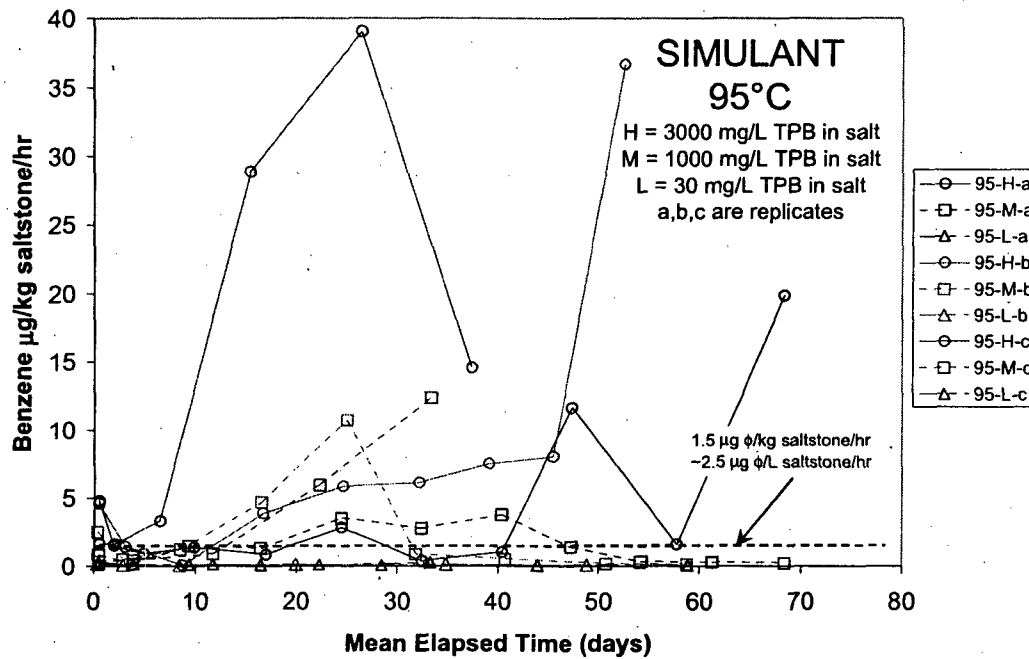


Figure 3-2. Benzene generation rates for simulants at 95 °C.

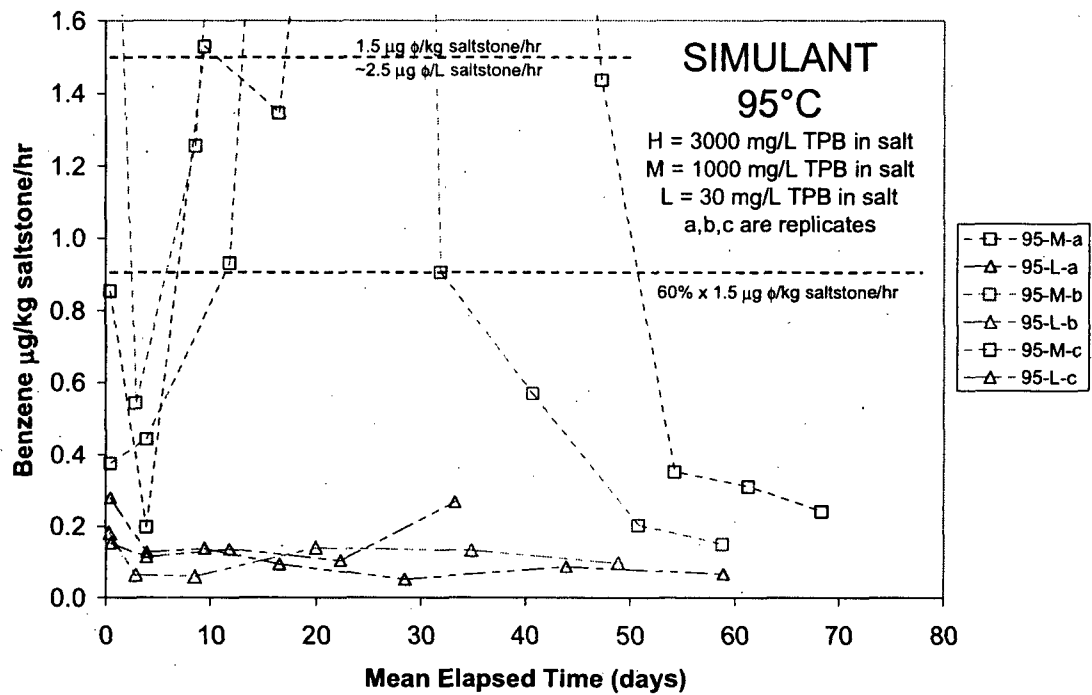


Figure 3-3. Data from Figure 4-2 with a modified y-axis to clarify samples with lower benzene generation rates.

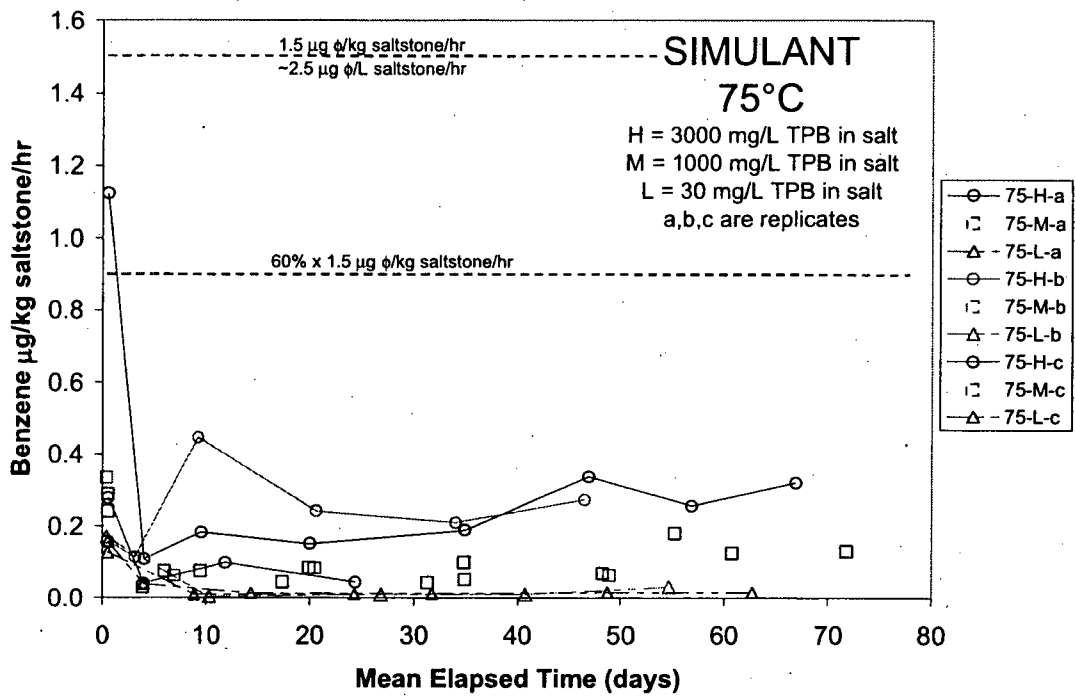


Figure 3-4. Benzene generation rates for simulants at 75 °C.

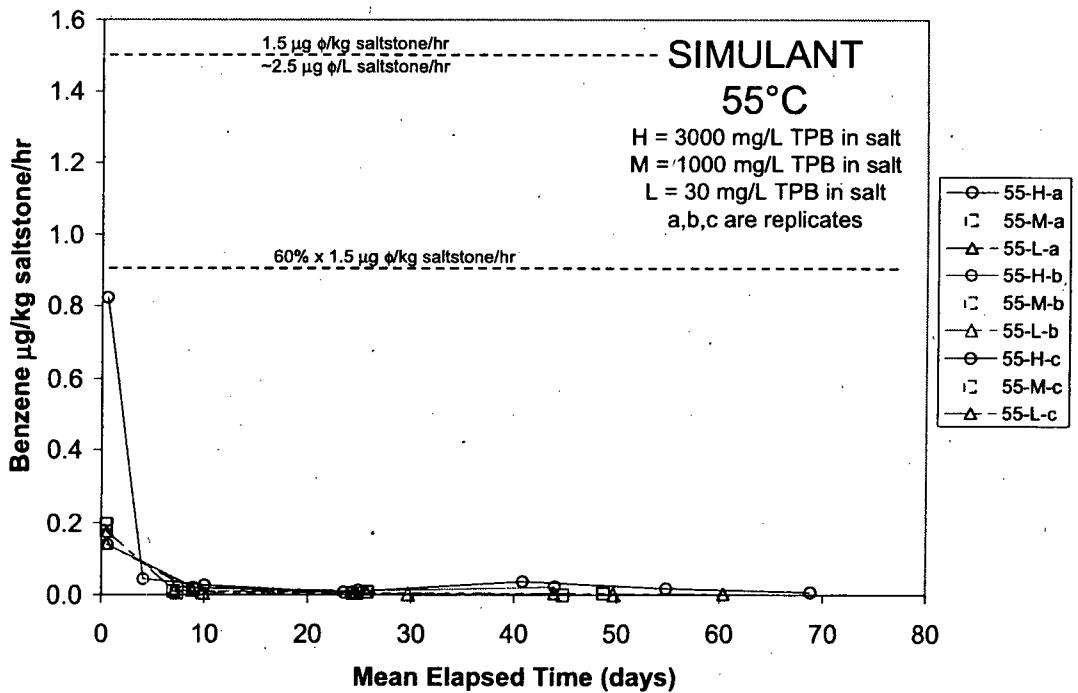


Figure 3-5. Benzene generation rates for simulants at 55 °C.

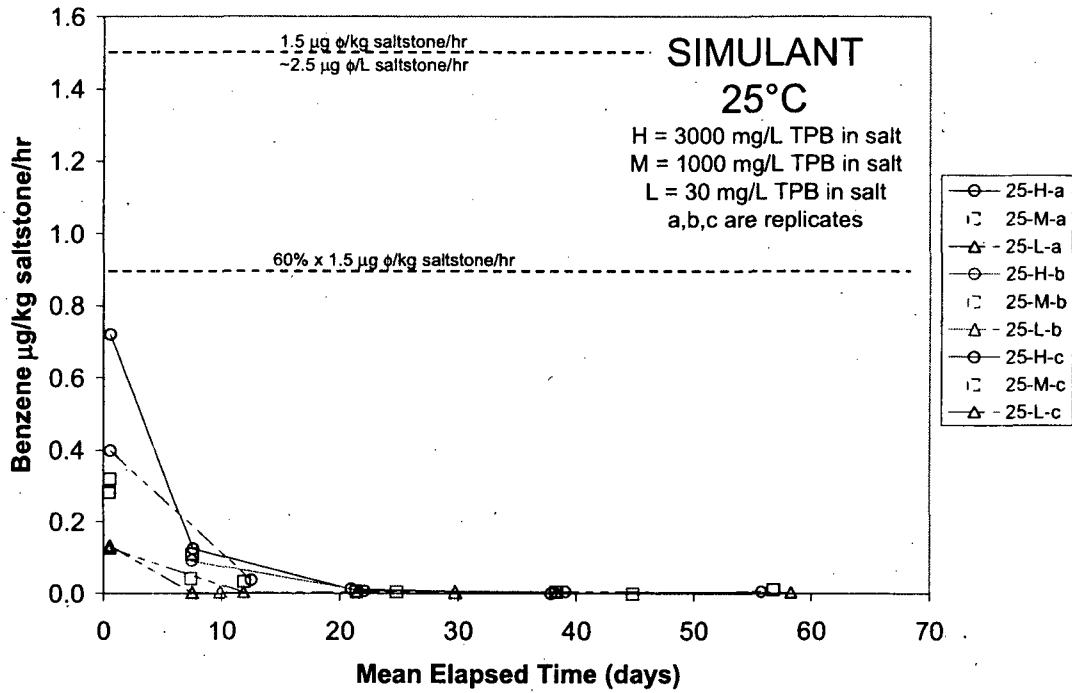


Figure 3-6. Benzene generation rates for simulants at 25 °C.

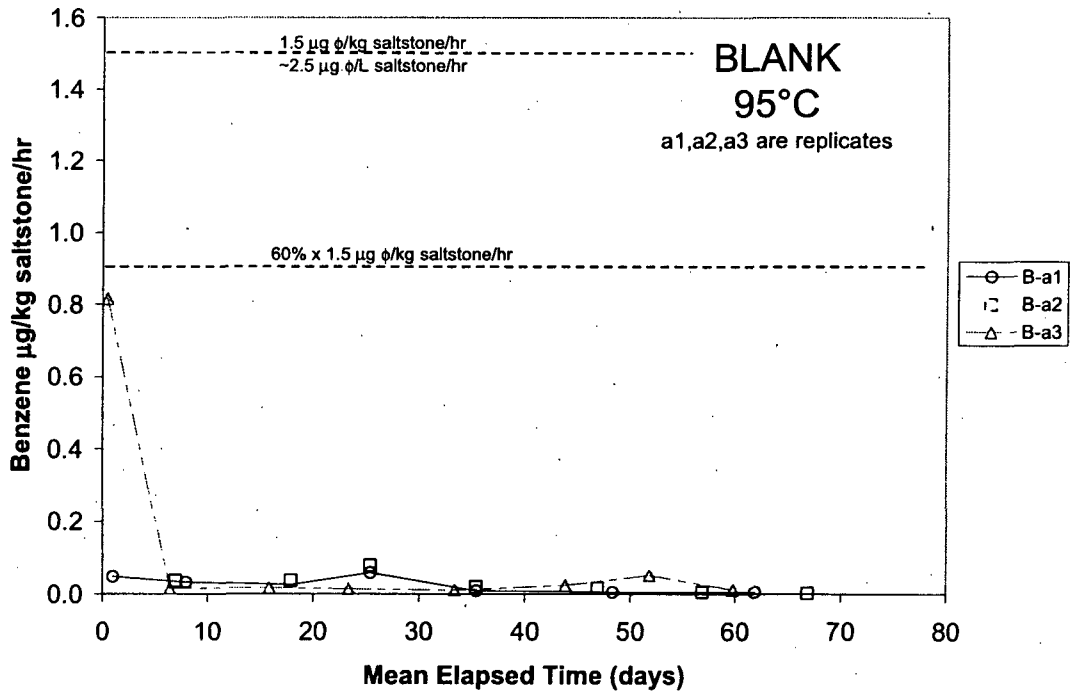
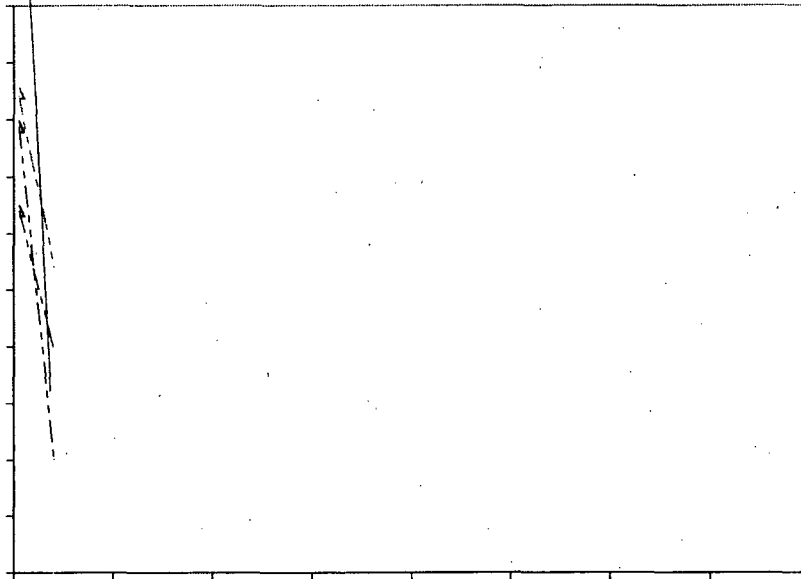
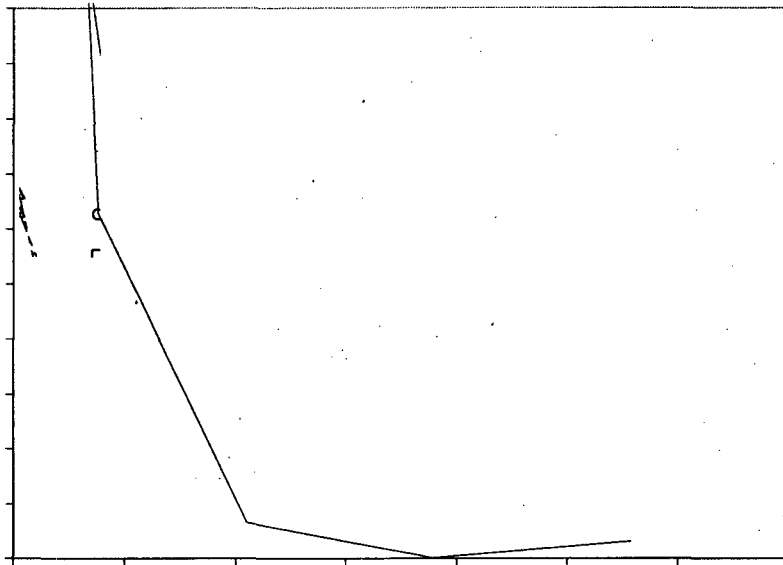


Figure 3-7. Benzene generation rates for blanks at 95 °C.





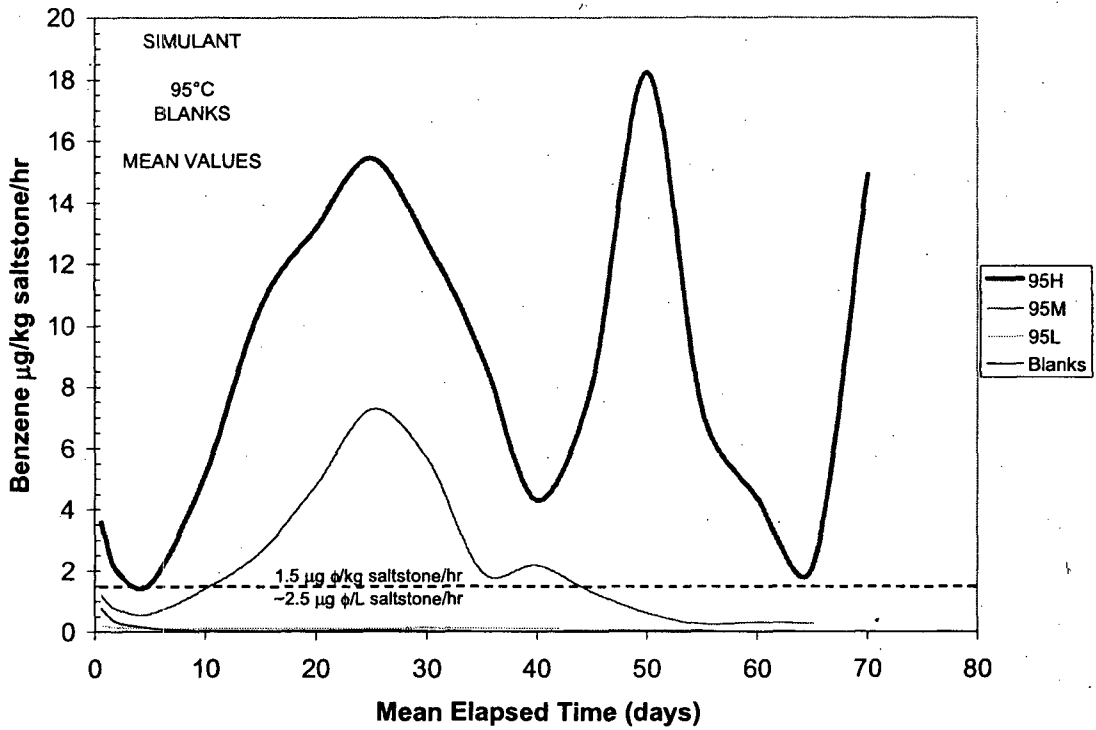


Figure 3-12. Mean values of benzene generation rates at 95 °C.

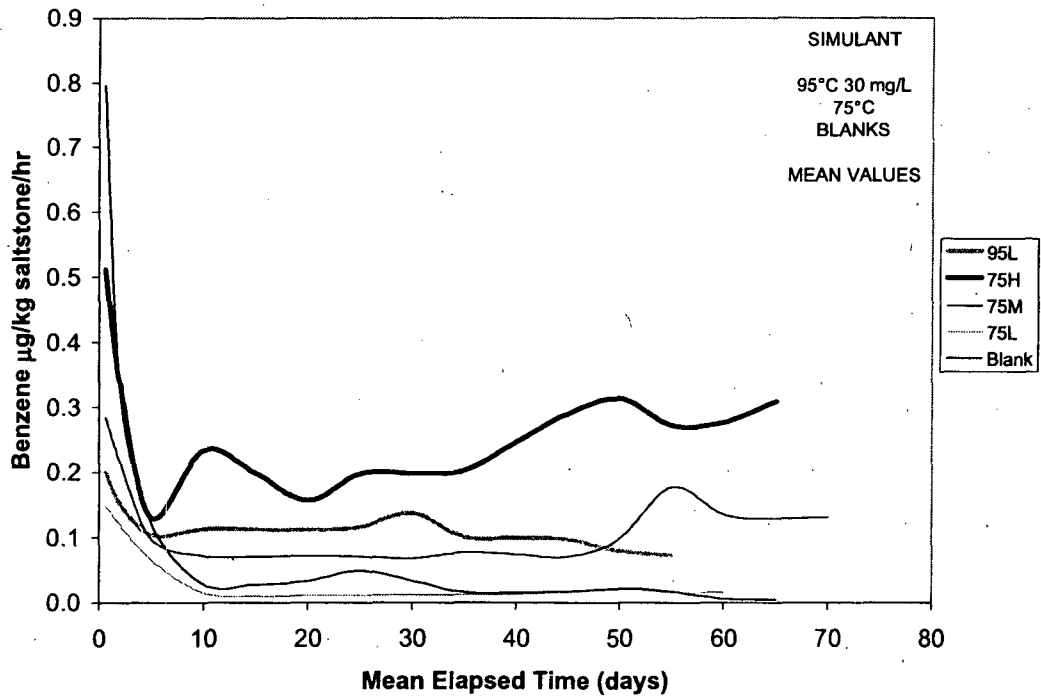


Figure 3-13. Mean values of benzene generation rates at 75 °C with 95L and blanks for reference.

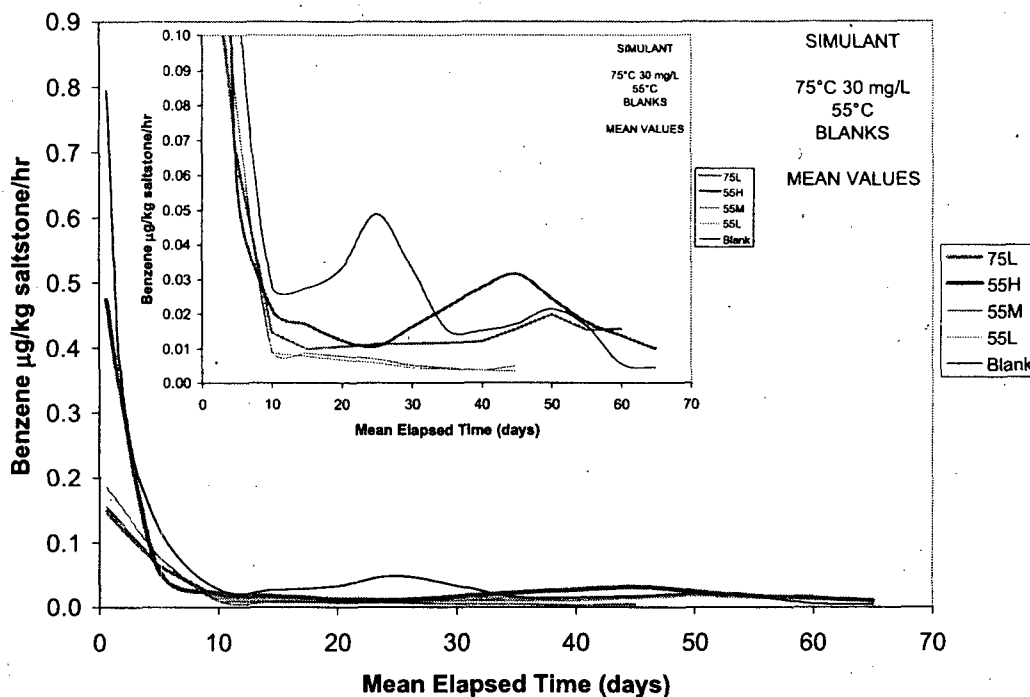


Figure 3-14. Mean values of benzene generation rates at 55 °C with 75L and blanks for reference (Inset is data expanded to show detail).

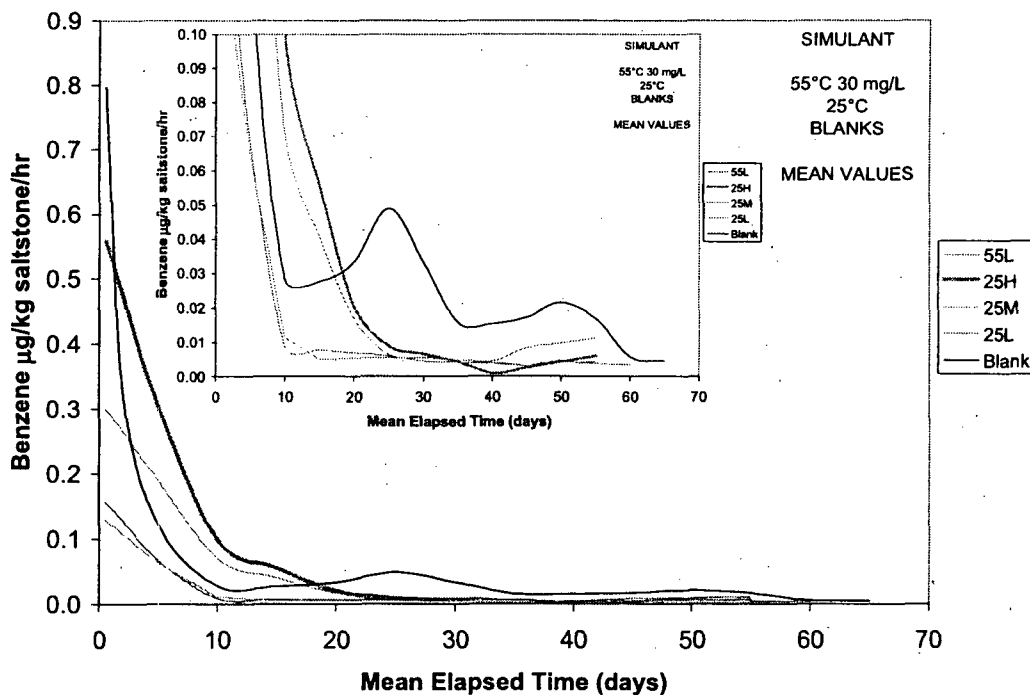


Figure 3-15. Mean values of benzene generation rates at 25 °C with 55L and blanks for reference (Inset is data expanded to show detail).

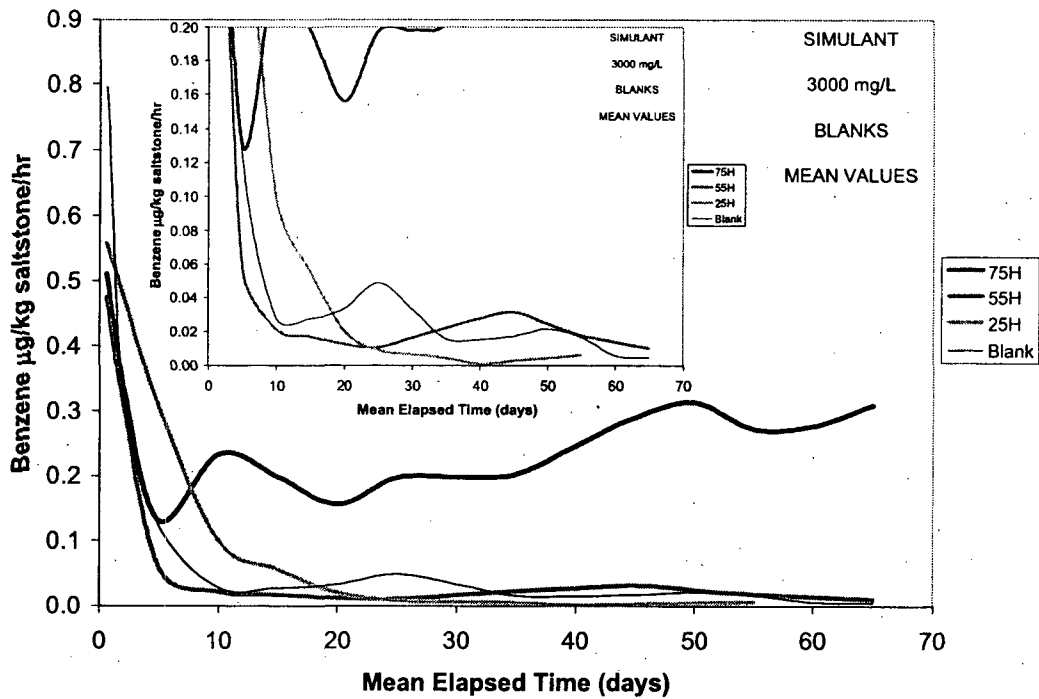


Figure 3-16. Mean values of benzene generation rates in samples with 3000 mg/L TPB and blanks for reference (Inset is data expanded to show detail).

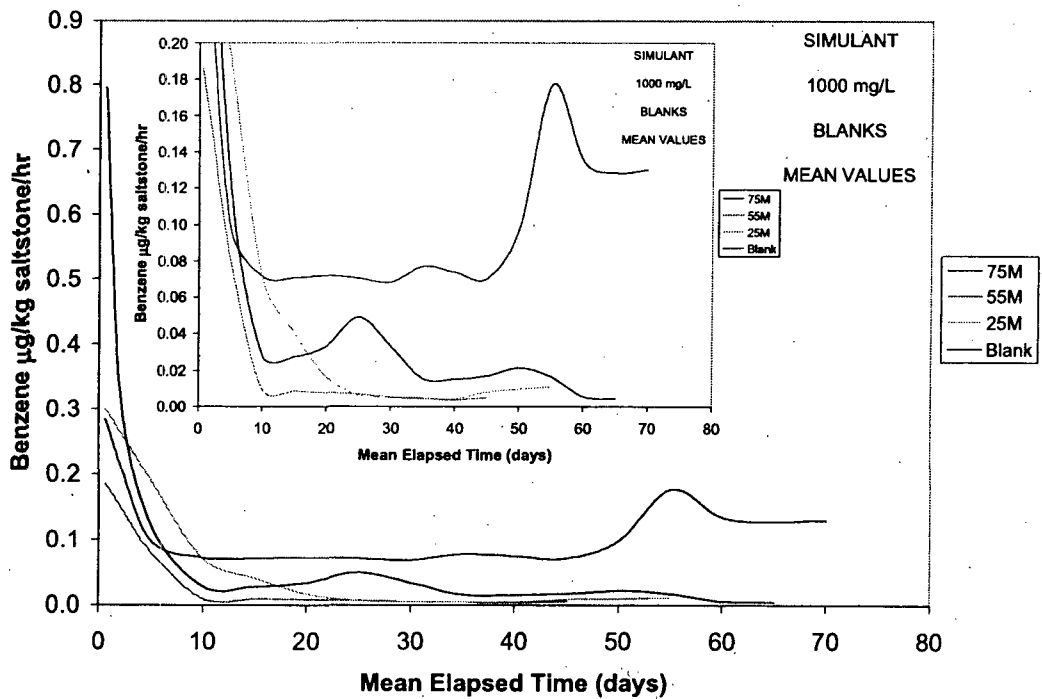


Figure 3-17. Mean values of benzene generation rates in samples with 1000 mg/L TPB and blanks for reference (Inset is data expanded to show detail).

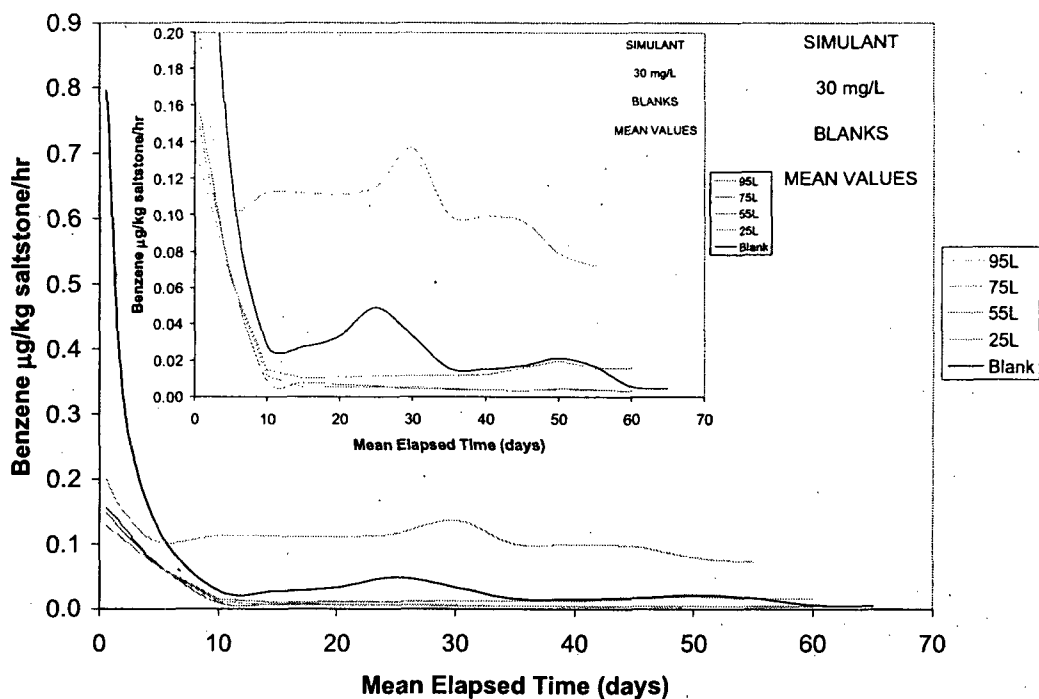


Figure 3-18. Mean values of benzene generation rates in samples with 30 mg/L TPB and blanks for reference (Inset is data expanded to show detail).

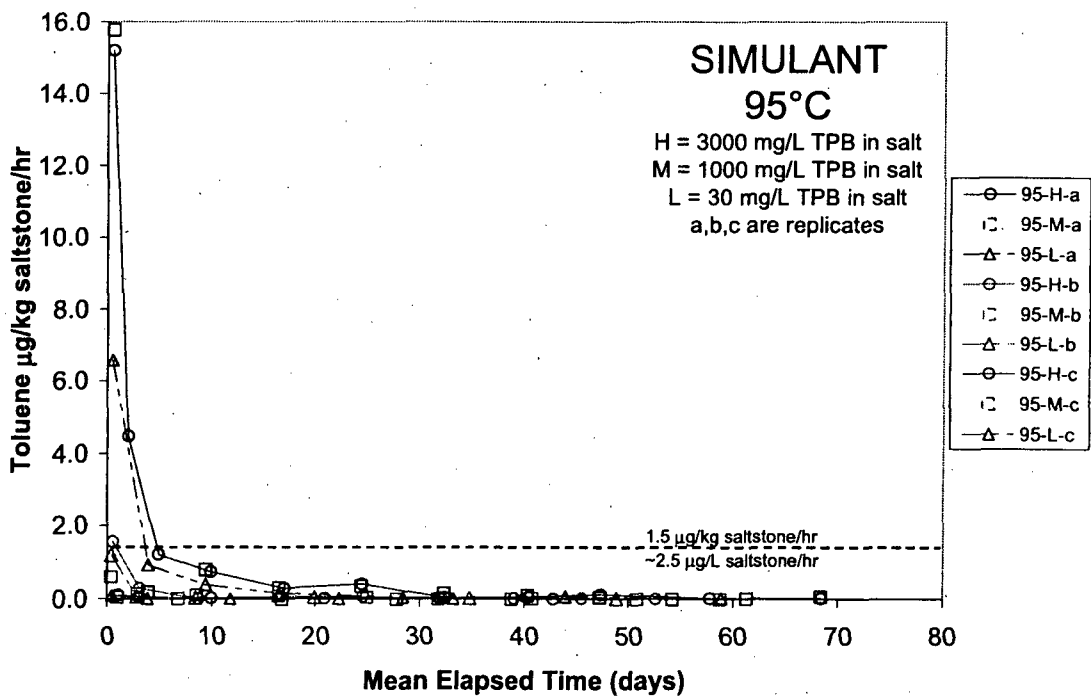
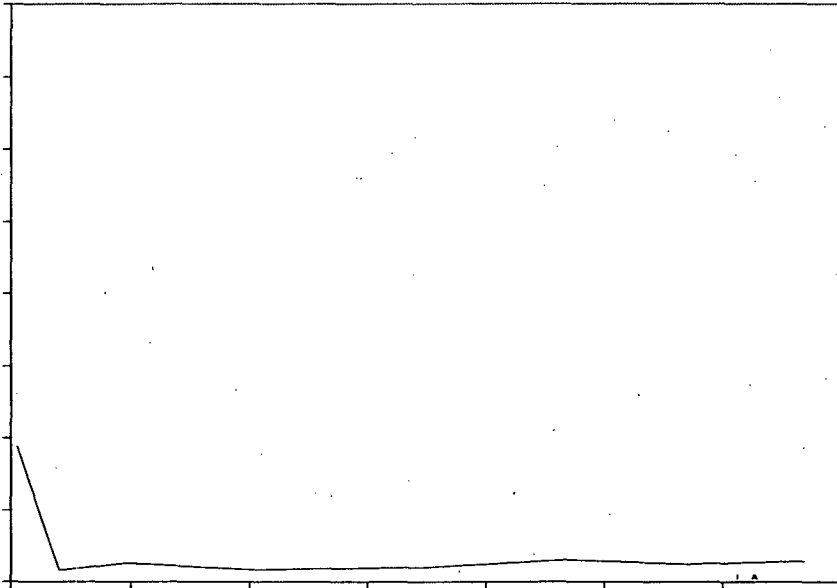


Figure 3-19. Toluene generation rates for simulants at 95 °C.



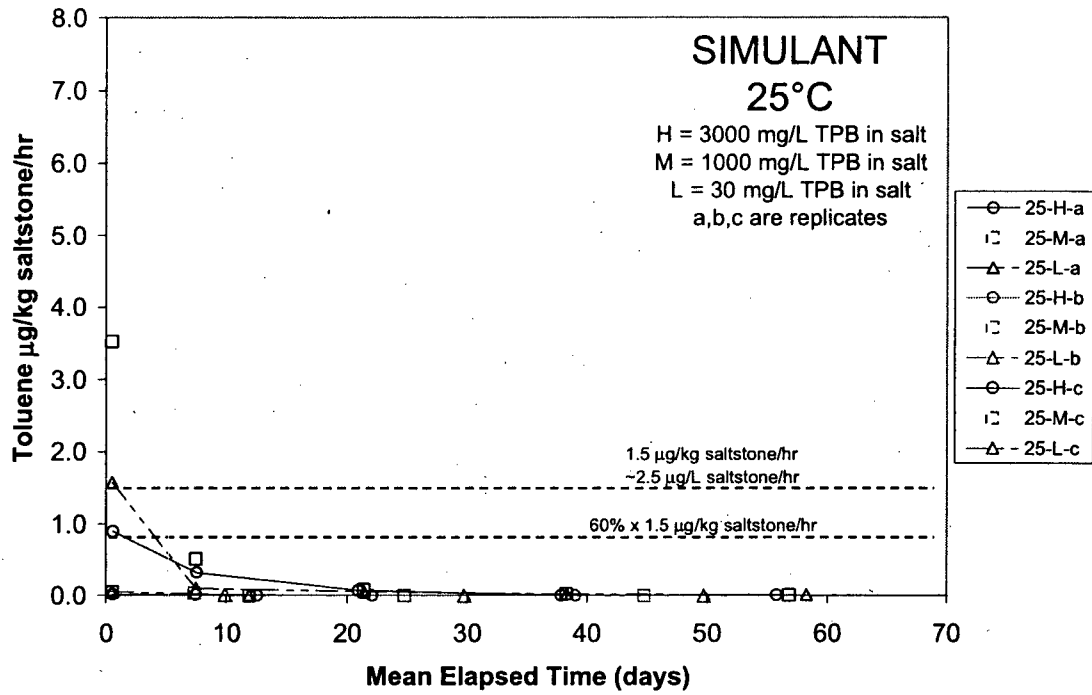
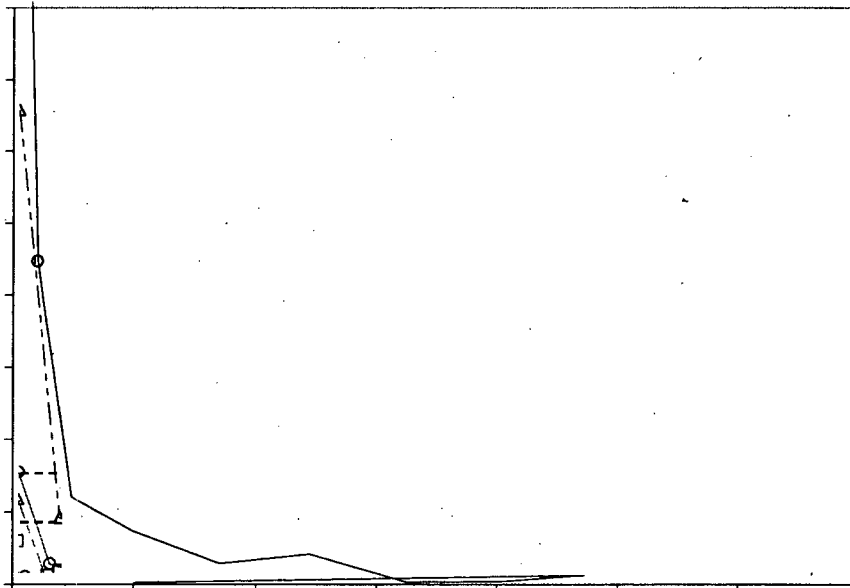


Figure 3-22. Toluene generation rates for simulants at 25 °C.



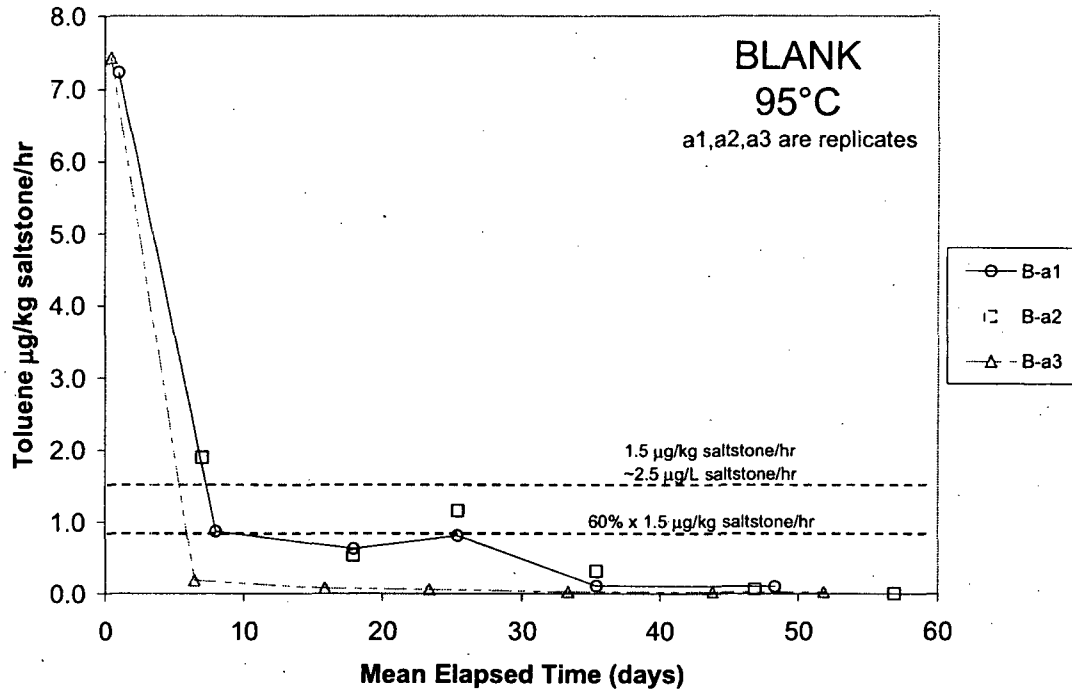
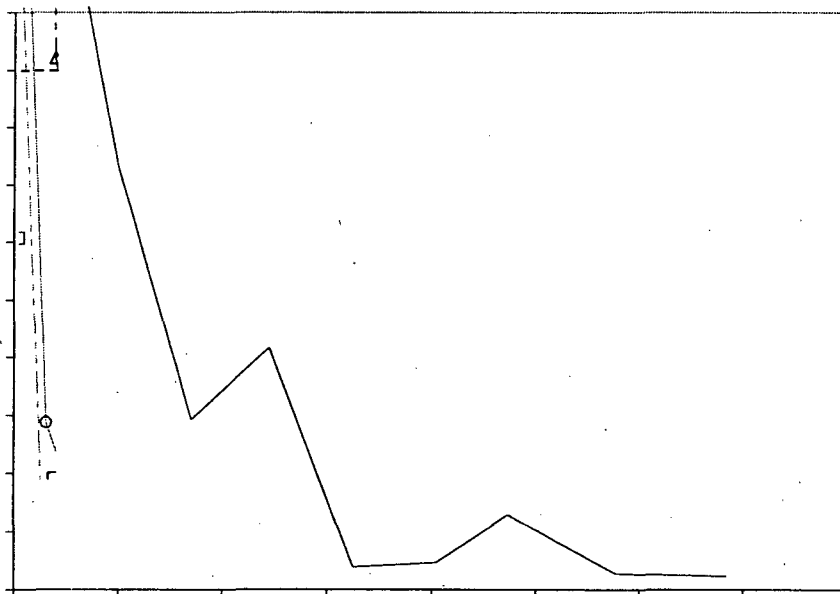
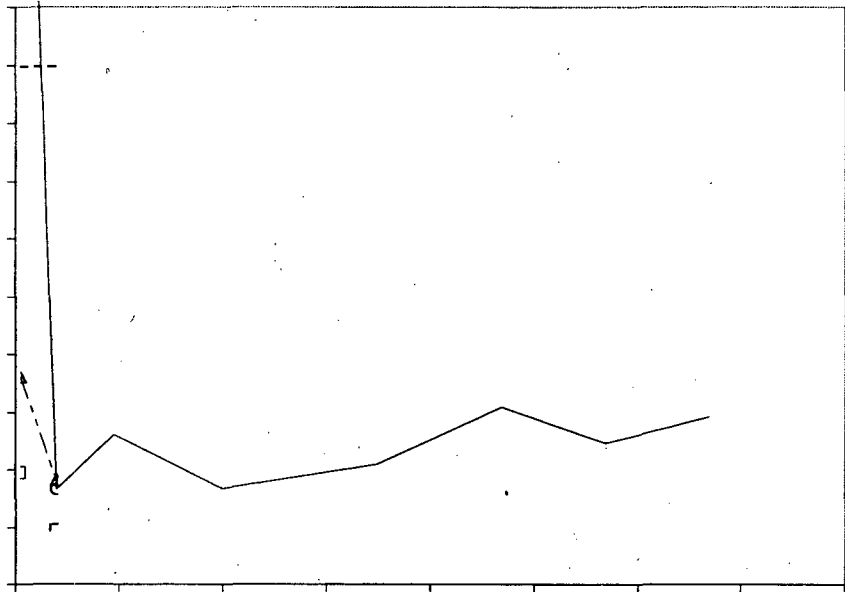
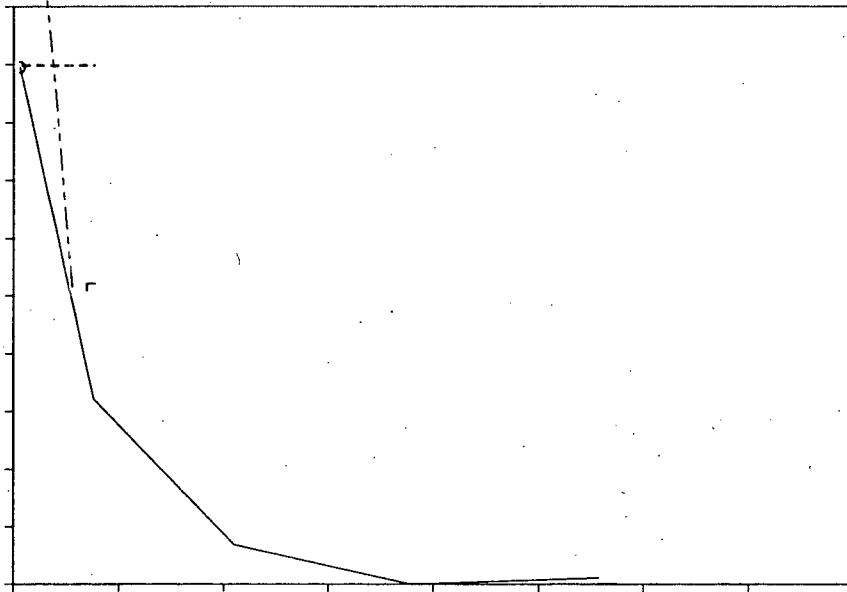


Figure 3-24. Toluene generation rates for blanks at 95 °C.







4.0 SUMMARY & CONCLUSIONS (TO DATE)

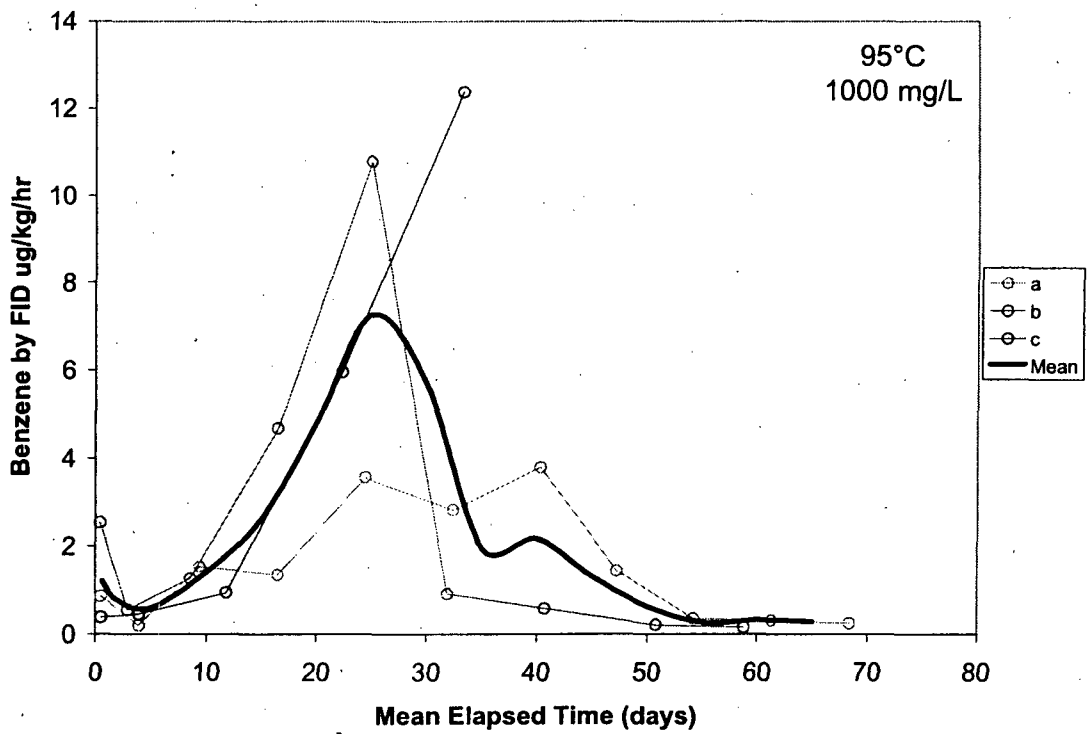
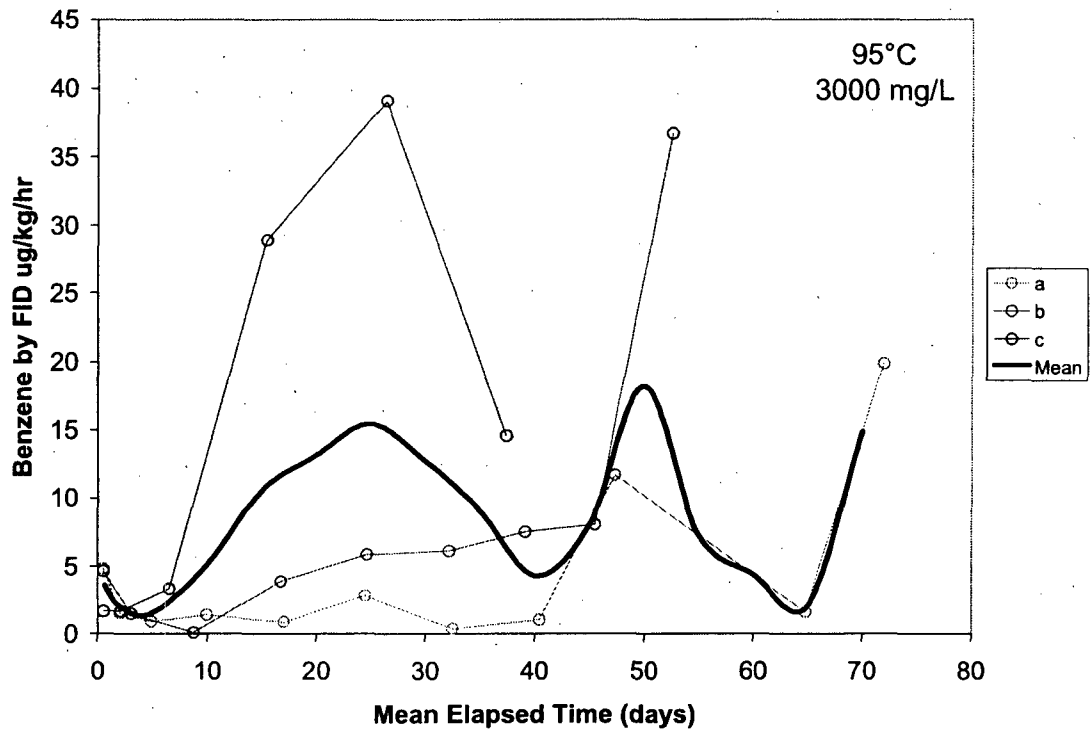
The benzene evolution rates approximated a trend directly proportional to both temperature and TPB concentration. The rates at 95 °C with 1000 and 3000 mg/L TPB exceeded the recovery-adjusted 0.9 µg/kg saltstone/h TRC, while all other conditions resulted in rates below this TRC (except for the very initial rate at 75 °C and 3000 mg/L). The toluene emission rates for at least one sample at each temperature exceeded the TRC initially, but all dropped below the TRC within 2-5 days. An exception is two of the blanks that barely exceeded the TRC until about 25 days. The toluene emissions appear to be mainly dependent on the fly ash and are independent of the TPB level, indicating that toluene is not generated from TPB.

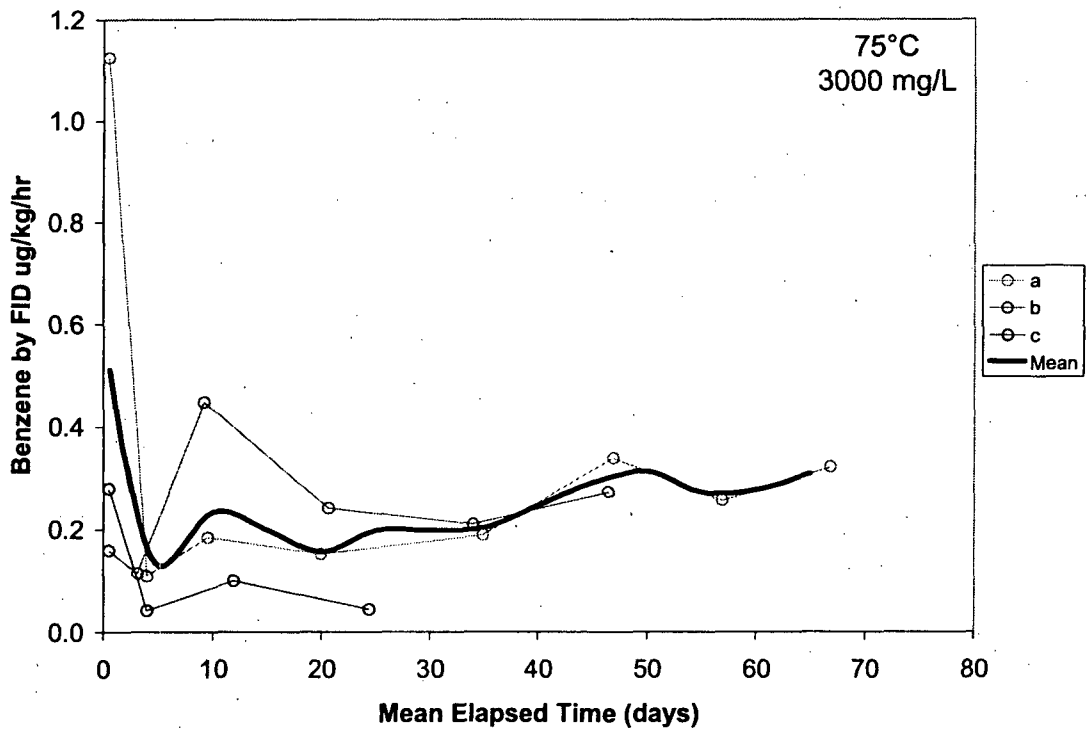
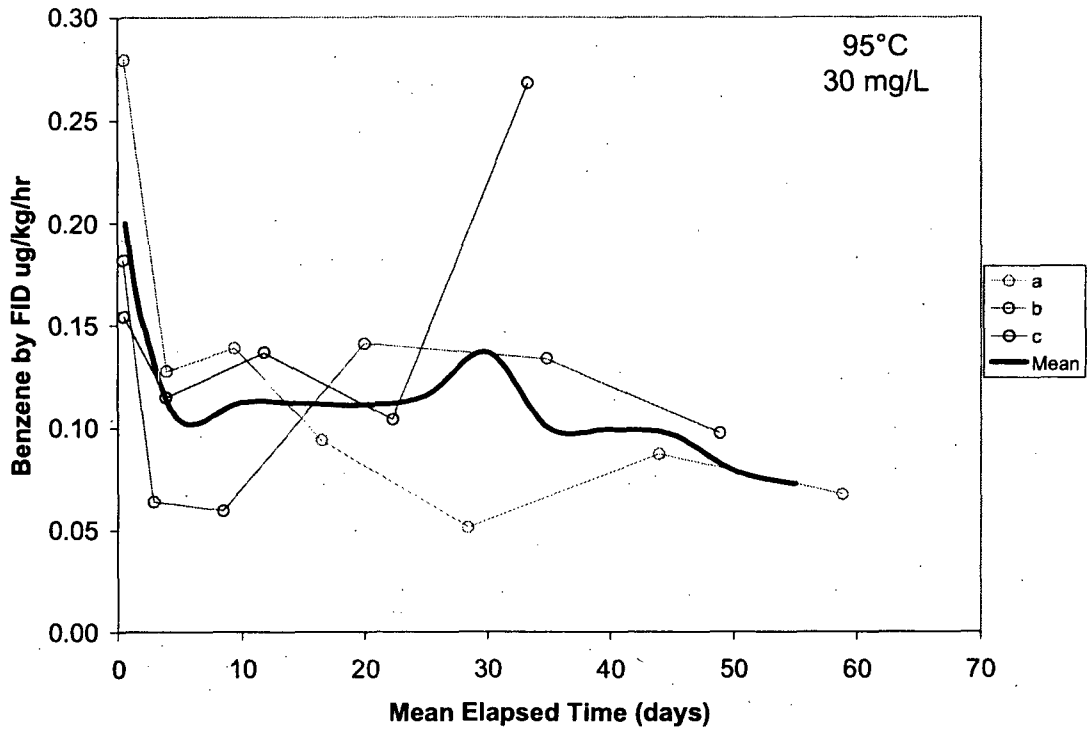
5.0 REFERENCES

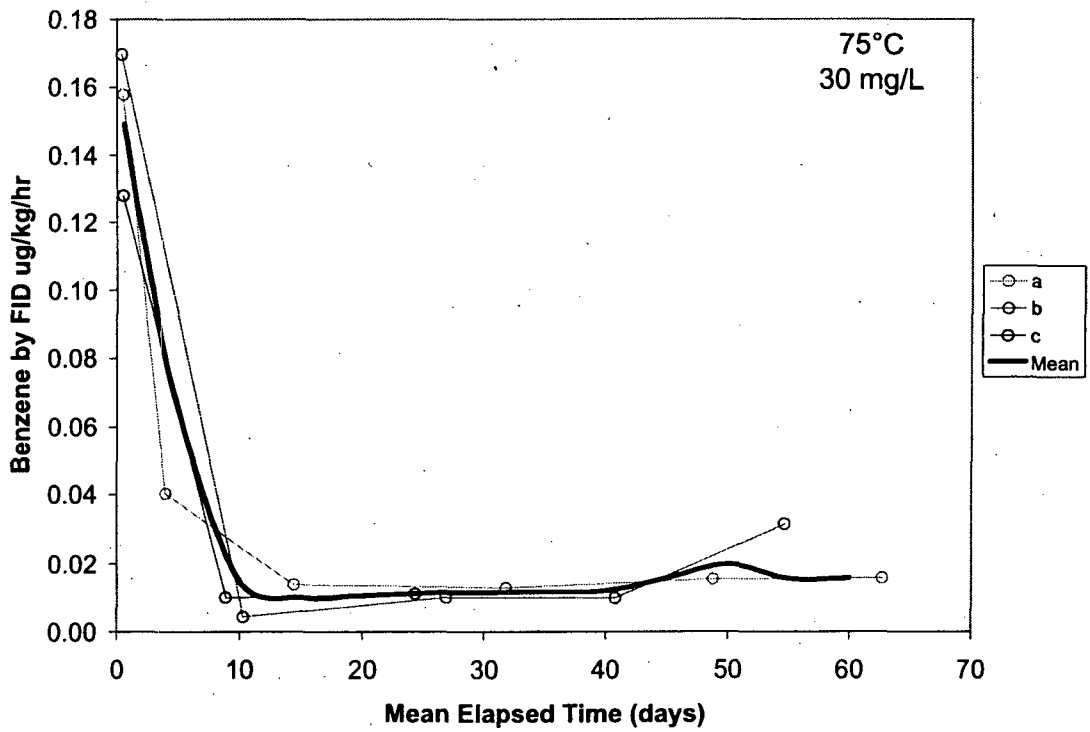
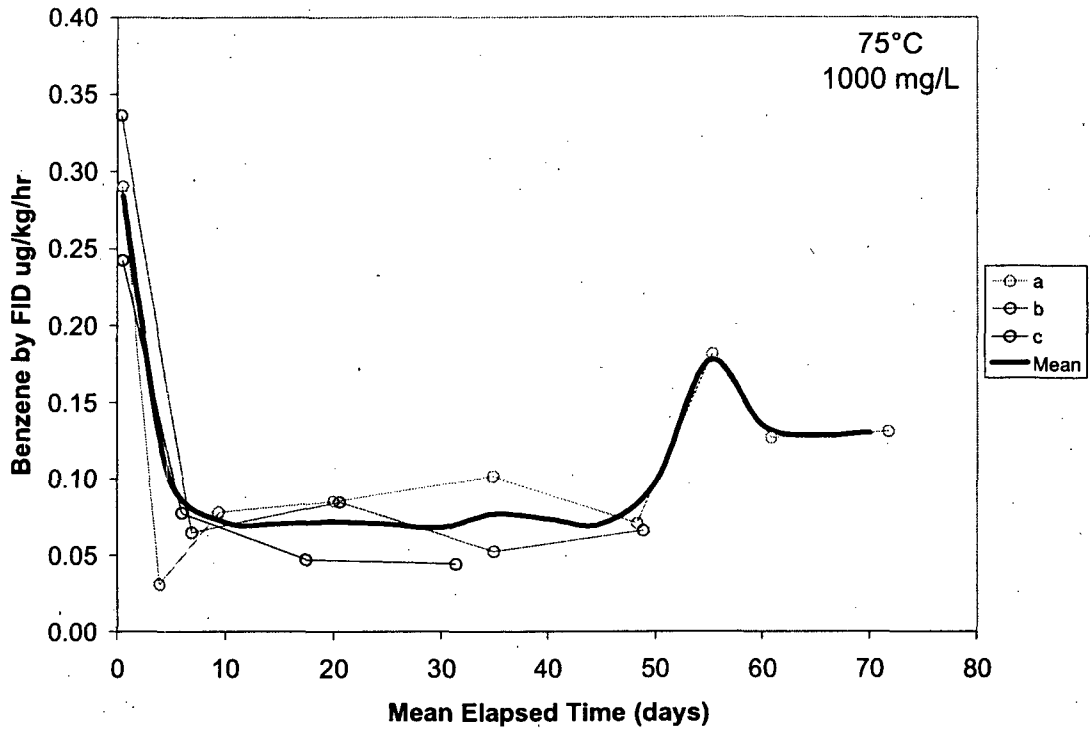
- 3.M.S. Hay, "Literature Review of the Effects of Tetraphenylborate on Saltstone Grout: Benzene Evolution and TCLP Performance,"WSRC-TR-2004-00383, (2004).
- 4.R.F. Swingle, "Results of Analyses of Tank 23H and 24H Saltstone WAC Samples HTK-521 – HTK-528," WSRC-TR-2003-00112, (2003).
- 5.A.D. Cozzi, E-mail to T.E. Chandler, 1/11/2005.
- 6.Lambert, D.P. "Tank 48H Simulant Validation", SRNL-LWP-2004-00009, (2004).
- 7.D.P. Lambert, T.B. Peters, M.E. Stallings, and S.D. Fink, "Analysis of Tank 48H Samples HTF-E-03-73 (June 03, 2003) and HTF-E-03-127 (September 17, 2003)," WSRC-TR-2003-00720, Revision 0 (2003).
- 8.A.D. Cozzi and J.R. Zamecnik, "Tetraphenylborate Decomposition in Saltstone," WSRC-RP-2004-00749, Revision 0 (2004).
9. A.D. Cozzi, "Formulation Development for Processing Tank 48H in Saltstone," WSRC-TR-2004-00477, Revision 0 (2004).
- 10.NIOSH method 1501, Issue 3, "Hydrocarbons, Aromatic" March 2003.

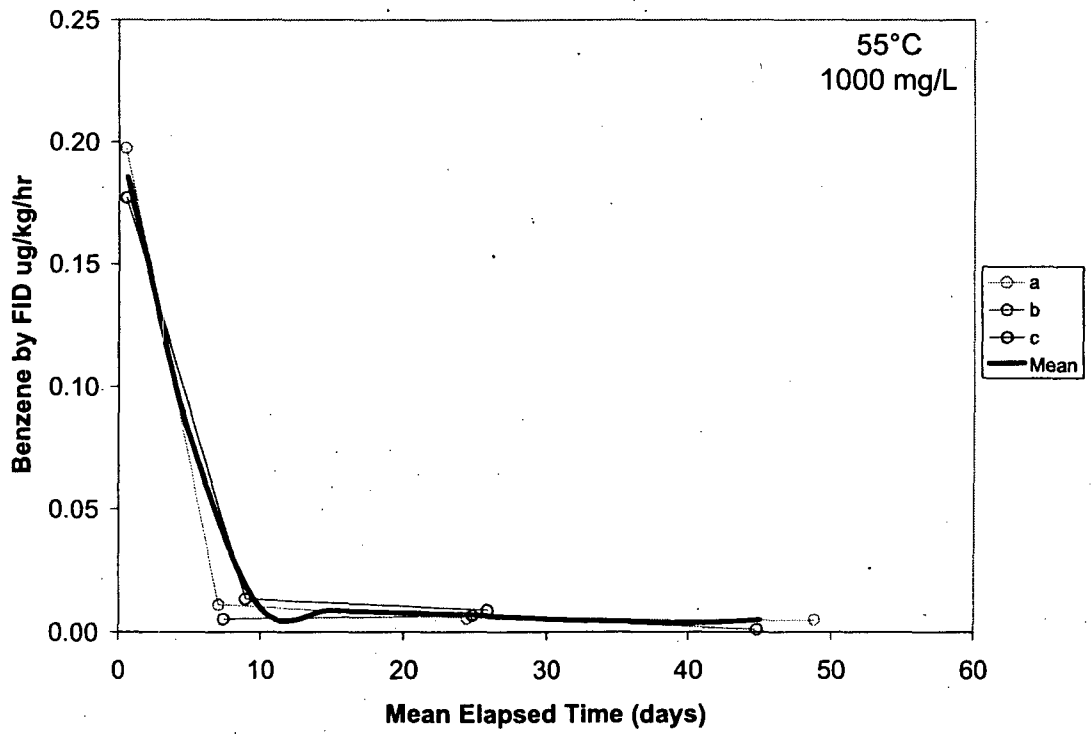
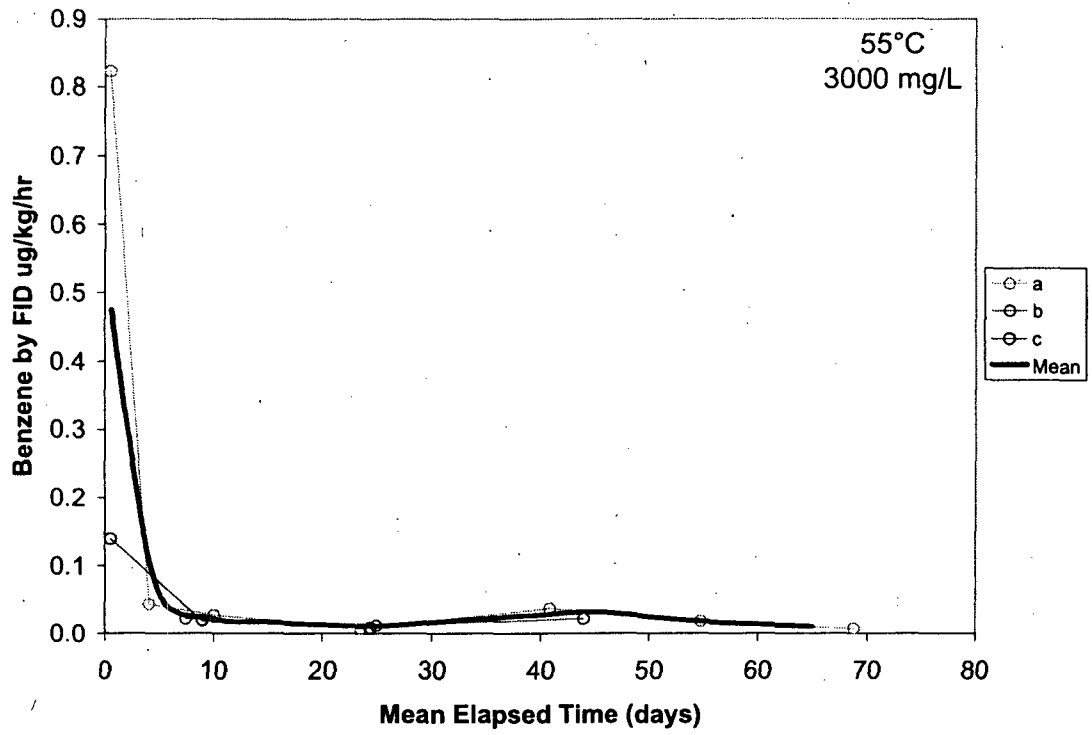
APPENDIX

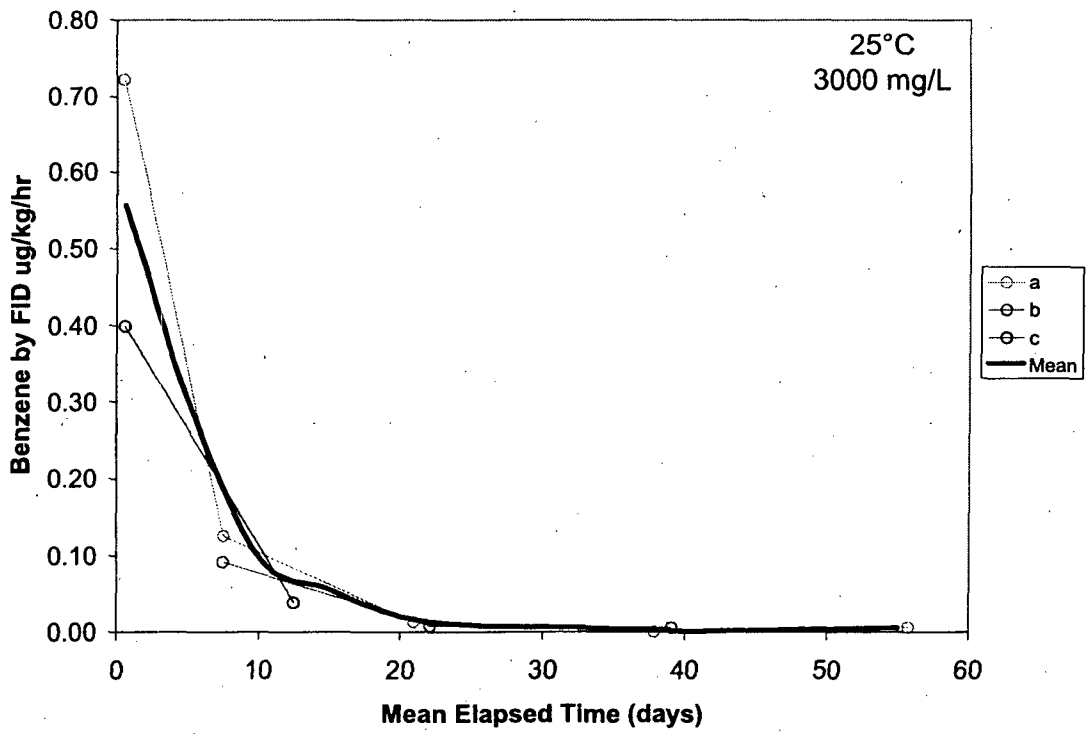
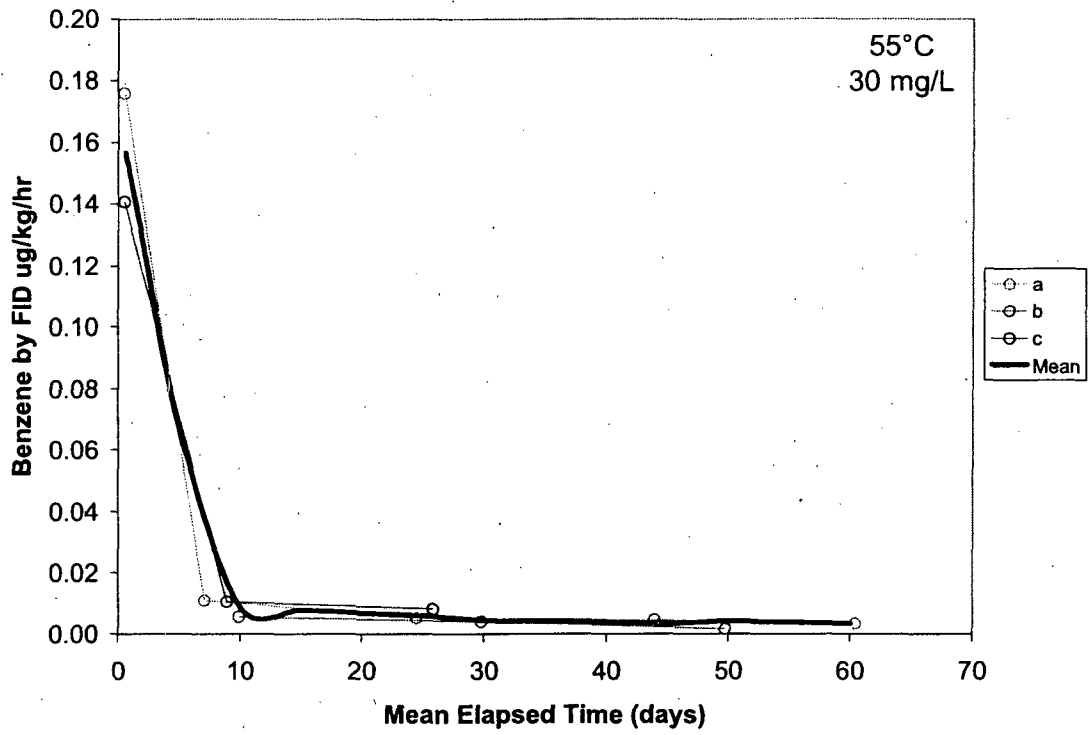
**GRAPHS OF MEAN BENZENE EVOLUTION RATE FOR REPLICATE
DATA SETS**

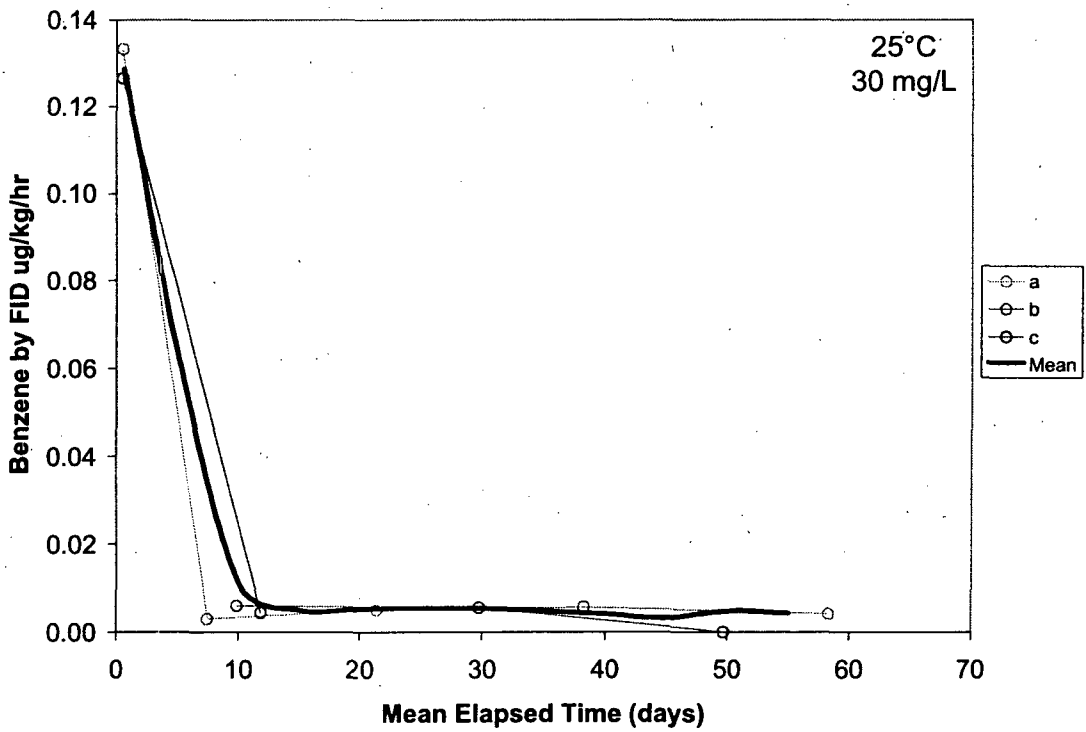
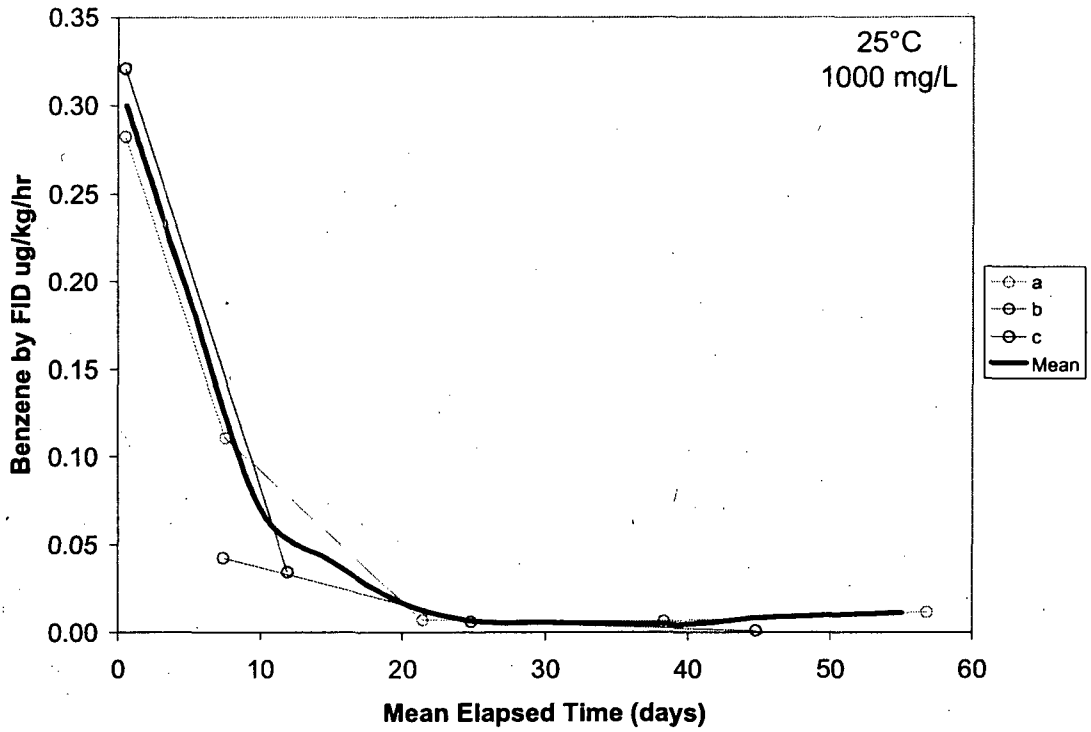


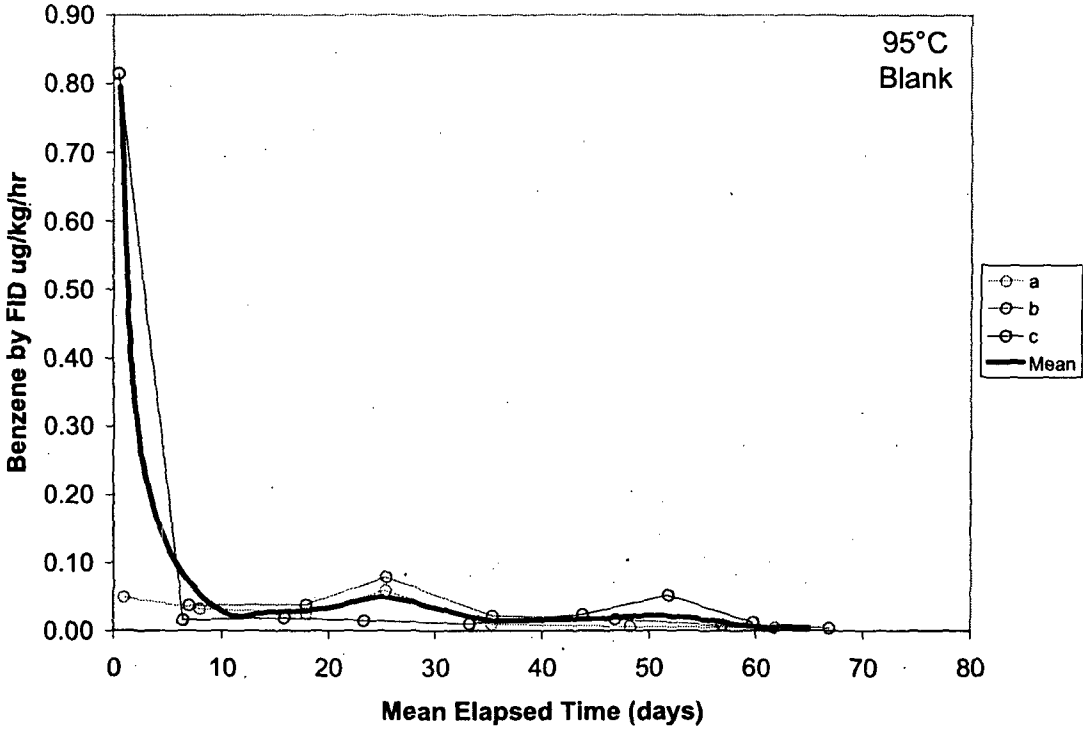












Task Title Tetraphenylborate Decomposition in Saltstone		TTR Number: SP-TTR-2004-0005	TTR Date: 11/17/2004
Task Leader A.D. Cozzi	Signature: <i>A.D. Cozzi</i>	Organization: SRNL/ITS	Date: 12/17/04
Task Leader J.R. Zamecnik	Signature: <i>J.R. Zamecnik</i>	Organization: SRNL/ITS	Date: 12/17/04
Technical Reviewer (if required): M.S. Hay	Signature: <i>M.S. Hay</i>	Organization: SRNL/WPT	Date: 1/4/05
Level 3 Manager (or designee): D.A. Crowley	Signature: <i>D.A. Crowley</i>	Organization: SRNL/ITS	Date: 1/4/05
Waste Solidification Engineering: J.R. Occhipinti	Signature: <i>J.R. Occhipinti</i>	Organization: CBU/WSE	Date: 1/11/05
ITS QA Coordinator: T.K. Snyder	Signature: <i>T.K. Snyder</i>	Organization: SRNL/ITS	Date: 1-3-05
SRNL QA Representative: J.P. Vaughan	Signature: <i>J.P. Vaughan</i>	Organization: SRNL-QA	Date: 1/3/05

Distribution:

T.E. Chandler,	704-Z	D. Maxwell,	766-H
D.T. Conrad,	766-H	J.E. Occhipinti,	704-S
A.D. Cozzi,	773-43A	L.M. Papouchado,	773-A
D.A. Crowley,	773-A	M.A. Rios-Armstrong,	766-H
W.B. Dean,	766-H	S.J. Robertson,	766-H
R.E. Eibling,	999-W	B.C. Rogers,	766-H
R. Dunn,	773-A	S.C. Shah,	766-H
S.D. Fink,	773-A	D.C. Sherburne,	704-S
R.C. Fowler,	703-H	J.A. Smith,	704-29S
J. Griffin,	773-A	T.K. Snyder,	999-W
J.R. Harbour,	773-42A	R.H. Spires,	766-H
M.S. Hay,	773-42A	A.V. Staub,	704-28S
E.W. Holtzscheiter,	773-A	P.C. Suggs,	766-H
D.P. Lambert,	773-A	D.G. Thompson,	704-Z
C.A. Langton,	773-43A	J.P. Vaughan,	773-41A
T.D. Lookabill,	704-Z	W.R. Wilmarth,	773-42A
S.L. Marra,	999-W	J.R. Zamecnik,	773-41A

Revision Number:	Page Number:	Date:	Revision:
0	All	12/15/04	Original Issue

I. INTRODUCTION

A. Task Definition

The operating strategy for processing at Saltstone is projected to result in elevated temperatures in the Saltstone vaults over a period of months. The review for this strategy resulted in a review of documentation for the production of benzene via the decomposition of potassium tetraphenylborate (KTPB) solids at elevated temperatures for an extended period of time. Initial results of this review indicate that benzene could potentially accumulate in the vault vapor space under the strategy. The current Z-Area Safety Basis does not postulate an explosion in the vaults, and therefore, the Safety Basis does not restrict vault temperatures or TPB concentrations relative to a vault explosion.

An evaluation of prior Saltstone production confirmed that previous facility operation has not resulted in elevated grout temperatures for extended periods of time (no temperature higher than 51°C and these peaks lasted for days rather than months). This review combined with previous sampling for benzene in vault cells provides the basis for the position that there is no imminent hazard at the vaults.

The Savannah River National Laboratory (SRNL) was requested to determine benzene generation rates in Saltstone prepared with TPB concentrations ranging from 30 mg/L to 3000 mg/L in the salt fraction and test temperatures ranging from ambient to 95°C¹. The request included determination of the effect of surface area to volume ratio on the benzene generation rate.

A three stage approach will be used to meet these objectives. In the first stage, testing will be performed to select one of several potential methodologies for the collection, recovery and analysis of benzene. The second stage will entail demonstrating the methodology selected in Stage I in testing with surrogate materials. Testing of saltstone prepared with actual Tank 48H waste as the source of TPB will take place in Stage III.

Materials and Mixes

The salt solutions to be tested in Stage II will consist of Tank 48H simulant (as the source of TPB) blended with a simulant of DWPF recycle material, inhibited water, or other salt solution specified by the customer and documented in the Laboratory Notebook*. Table 1 is the properties for the materials to be blended. The Tank 48H simulant² is based on samples of Tank 48H taken in 2003³. The DWPF recycle simulant will target the average sodium and the maximum anion and mercury content of the Tank 23 and Tank 24 samples taken 100 inches from the tank bottom as reported by Swingle⁴. Table 2 is the composition of the DWPF Recycle simulant based on the major components in Reference 4. Any additional constituents will be specified by the customer and documented in the Laboratory Notebook*. The salt solutions will target three TPB concentrations, 30 mg/L, the estimated concentration of TPB currently in Tank 50H, 1000 mg/L, the concentration limit of TPB in the Saltstone Processing Facility Documented Safety Analysis (SPF-DSA), and 3000 mg/L, the expected maximum or bounding TPB concentration in batches made with Tank 48H waste. Table 3 is the make up of each of the salt solutions.

Table 1. Composition and Properties of Materials for Simulant Makeup.

Material	TPB (mg/L)	Wt. % Solids		Density (g/ml)	Mercury (mg/L)
		Undissolved	Total [†]		
Tank 48H ³	18,800	2.18	18.42	1.144	10.3
DWPF Recycle simulant (s)	0	<1	5.09	1.039	14.5 ⁴ (Tank 24)
Inhibited Water (IW)	0	0	0.1	~1	0

[†] Total solids is used to determine the water:premix ratio used for Saltstone processing.

Table 2. Composition of DWPF Recycle Simulant.

* WSRC-NB-2004-00180 "Benzene Generation in Saltstone"

Compound	g/L	Component	M
NaNO ₂	21.734	Na	0.78
NaNO ₃	5.219	NO ₂ ⁻	0.32
NaOH	17.399	NO ₃ ⁻	0.06
Na ₂ CO ₃	7.419	OH ⁻	0.44
Hg(NO ₃) ₂ ·xH ₂ O	24.8 mg/L	CO ₃ ²⁻	0.07
Total	51.771	Hg	14.5 mg/L
Wt % solids	5.2%		

Table 3. Calculated Composition and Properties of Salt Solutions.

Material	TPB concentration (mg/L)	Wt. % Solids	Density (g/ml)	Mercury (mg/L)
Tank 48H + DWPF Recycle	30	5.1	1.04	14.5
	1000	5.9	1.04	14.3
	3000	7.4	1.06	13.8

Saltstone will be prepared using the salt solutions described previously and premix materials obtained from the Saltstone Processing Facility. Table 4 is the premix composition and the water to premix ratio. The water to premix ratio is the ratio of the mass of evaporable water from the waste (at ~110 °C) to the combined mass of the cement, slag, and fly ash. The values used are based on the recommendation made in previous testing⁵. Table 5 is the test matrix for the testing. Samples will be cured over a range of temperatures to determine the effect of curing temperature on the benzene generation rate. Results from the surrogate testing will be used to develop the matrix for the testing with radioactive materials in Stage III.

Table 4. Formulations for Processing.

Premix	Water/Premix
45% Class F Fly Ash (FA) 45% GGBFS ^a (Slag) 10% Cement	0.63

^aGround granulated blast furnace slag

Table 5. Matrix of Aggregates and Test Conditions.

	TPB (mg/L)	Curing Temperature (°C)
• Salt Solution	• 30 • 1000 • 3000	• Ambient • 55 • 75 • 95

Stage I. Develop Methodology for Sampling and Analysis of Benzene Evolved by the Decomposition of TPB during Saltstone Curing.

The assumption that the average generation rate of benzene will be approximately 1 µg/L salt/h was used to estimate the size of the samples for testing. A semi-batch method of generating benzene will be evaluated. This method will sample the same vessel numerous times throughout the experiment. This test method is divided into static and intermittent types. The static type uses no active purge, but replaces all of the headspace gas after each sample is taken. The intermittent type uses an air purge to collect the benzene in the headspace on a sorbent material. Table 6 defines the means of generating, collecting, and recovering the benzene that will be evaluated in this task. Standards will consist of Saltstone prepared with TPB-free salt solution. A known quantity of benzene will be added to the vessel immediately prior to sealing the sample. The purpose of the standard is to ensure that the benzene in the sample vessel is collected. Standards will be sampled two times during the duration of Stage I. The number and frequency of standards used in Stage II and Stage III will be determined from the results of Stage I testing. A single blank will be used in each of the sampling methods. The blank will consist of Saltstone prepared with TPB-free salt solution. All samples

will be analyzed using a gas chromatograph (GC) fitted with both a photo ionization detector (PID) and a flame ionization detector (FID). The PID is the preferred detector and will be used exclusively unless issues with water vapor in the samples affect the accuracy of the analysis. After a method has been selected, a second GC with the capabilities of supporting the selected methodology will be procured.

Table 6. Methods for Generating Benzene.

Test Method	Type	Purge	Sampling Method	Benzene Recovery
Semi- Batch	Static	No	Syringe	N/A
Semi- Batch	Static	No	Charcoal Buttons	Chemical Extraction
Semi- Batch	Intermittent	Yes	Charcoal Tubes	Chemical Extraction
Semi- Batch	Intermittent	Yes	Charcoal Tubes	Thermal Desorption

The results of the Stage I testing will be reviewed with the customer and a single method will be selected for the Stage II testing. Customer concurrence will be documented in the Laboratory Notebook*.

Stage II. Validate Methodology for Sampling and Analysis of Benzene Evolved by the Decomposition of TPB during Curing of Saltstone Prepared with Simulants.

Using the material blends in Table 3 and Table 4, and the test matrix in Table 5, the methodology evaluated in Stage I of the task will be validated. Samples prepared with salt solution from each of the specified TPB concentrations will be cured at each of the temperatures listed. The initial frequency for collection of samples for analysis is 1, 3, 7, and 14 days. Sampling frequency will be adjusted as necessary to reflect the actual benzene generation rates obtained. For one of the test conditions, two samples geometries (surface area to volume ratio) will be used to determine if sample geometry contributes to the benzene generation rate. Sampling at elevated temperatures will be terminated after approximately 100 days with customer concurrence. Sampling will continue on cooled samples for a time to be determined later and agreed upon by the customer. The duration of the extended sampling will be documented in the Laboratory Notebook.

Stage III. Determination of Benzene Evolved by the Decomposition of TPB during Saltstone Curing.

Salt solutions prepared as in Stage II (with actual Tank 48H waste used as the source of TPB) will be used to prepare Saltstone samples. The samples will be cured at ambient, 95°C, and a mid-point temperature determined from the Stage II testing. Initial sampling frequencies will be based upon the results of the Stage II testing. Samples will be cured for not less than 100 days and sampled with sufficient frequency to identify significant changes in benzene generation rate. Standards and blanks will be used based on the experience gained in Stage II testing.

B. Customer/Requester

Waste Solidification Engineering funds the work in this task. The scope of the work is established in Technical Task Request SP-TTR-2004-0005. The customer contact is J.E. Occhipinti.

This task consists of baseline R&D activities as determined by the Savannah River National Laboratory (SRNL) Procedure L1-7.10, "Control of Technical Work," Revision 4.

C. Task Responsibilities

SRNL/ITS: A.D. Cozzi and J.R. Zamecnik are responsible for the direction and completion of this task. This includes implementation of the SRNL Conduct of Research and Development⁶ prior to initiating lab work, adhering to this Task Technical and Quality Assurance Plan, and providing updates of progress to the customer.

* WSRC-NB-2004-00180 "Benzene Generation in Saltstone"

SRNL/ITS/WPT: R.E. Eibling and M.S. Hay are responsible for providing guidance for the development of experiments, providing guidance for sample and analytical control, and participating in interpretation of analytical results.

SPE: J.E. Occhipinti (or designee) is responsible for providing Waste Solidification Engineering (WSE) concurrence and facilitating interface, as necessary, with Planning, Integration and Technology.

SRNL/ITS: M.F. Williams and J.G. Wheeler (or designees) are responsible for sample preparation.

SRNL/SCO: C.M. Conley and W.D. Keel (or designees) are responsible for activities in and relating to the SRNL shielded cells.

SRNL/QA: J.P. Vaughan is responsible for reviewing and approving this Task Technical and Quality Assurance Plan and providing guidance and oversight for this work.

ITS QA Coordinator: T.K. Snyder is responsible for reviewing task plans related to this task, assisting in the preparation of records, coordinating surveillances associated with this task, and interfacing with SRNL/QA during overview activities and corrective actions.

D. Task Deliverables

1. Technical Task and Quality Assurance Plan (this document) outlining the objective of the tasks and the associated activities.
2. Interim results and updates as requested by WSE.
3. Technical report detailing results of the activities associated with these tasks.

II. TASK ACCEPTANCE CRITERIA

Acceptance testing is not an element of this task. Per the TTR, issuance and customer approval of the technical report will complete this task.

III. TASK ACTIVITIES

1. Prepare Task Technical and Quality Assurance Plan: Develop task plan, complete conduct of R&D.
2. Prepare Simulant: Simulants will be prepared to represent the waste streams to contain the requisite concentrations of TPB.
3. Prepare Saltstone: Saltstone will be prepared using Z-Area premix materials with a water to premix (w/c) ratio of 0.63⁵.
4. Stage I: Develop Test Methodology: A series of scoping tests will be performed to determine the best available methodology for measurement of benzene generated by the decomposition of TPB in saltstone curing under various conditions.
5. Stage II: Validate Methodology with Simulants: Saltstone samples prepared from simulated wastes will be cured at various temperatures to ensure that the test/analytical methodologies are valid and to provide testing parameters for experiments with radioactive wastes.
6. Shielded Cells Preparation: Two ovens will be modified for curing samples at the two high temperatures (95°C and the temperature selected from Stage II). Shielded Cells technicians identified by SCO management to support this task will become familiar with the process in mock-up.

7. Stage III: Determine Benzene Generation Rates: Saltstone samples prepared from actual and simulated wastes will be cured at two temperatures. The curing Saltstone will be sampled to calculate benzene generation rates.
8. Document Results: The results of the Task will be documented in a technically reviewed report, issued with WSE concurrence.

IV. TASK SCHEDULE

A detailed schedule of task activities and associated durations is located in the ITS Support Schedule of Activities. The schedule is updated weekly. Activities will be performed in parallel when applicable.

V. RESEARCH FACILITY PLANNING

1. **Products and By-Products.** Approved waste streams will dispose of all job control waste. By-products generated at the Aiken County Technical Laboratory will be disposed of in accordance with SRNL Manual L1 procedure 5.05 "ACTL Residue Management."
2. **Disposition of Test Equipment.** All of the equipment used in this study will be available for future use.
3. **Exposure of Personnel.** Some of the samples are radioactive and will be handled remotely in the Shielded Cells. Samples that have to be removed from the Shielded Cells for analyses will be prepared so that only a small portion of the radioactivity is removed from the cell. These radioactive samples are contact handled by Shielded Cells technicians and ITS technicians (in radioactive hoods and radiobenches). These samples will be controlled and comply with standing radiological work plans. If a sample is expected to exceed standing radiological work plan limits, a job specific radiological work plan will be written.

VI. PROGRAMMATIC RISK REVIEW

Risk	Impact	Mitigation
Benzene generation and collection method is unacceptable.	Cannot generate or measure benzene.	Evaluate several methods for generation and collection of benzene.
Simulant results are not correlated to results with actual waste.	Results from actual waste will be necessary for DSA revision.	Initiate testing with actual waste as early as practical.
Benzene measurements of standards are not precise.	Reported results will be less precise.	Evaluate several approaches to optimize precision.
Benzene not detectable in Stage I testing.	Cannot easily rank methodologies being evaluated.	Extend Stage I until benzene is detectable.
Gas chromatograph (GC) delivery delayed	Cannot initiate experiments. Schedule slips with delay.	Prepare for experiments. Make GC entry to service last activity for initiation of experiments
Gas chromatograph fails.	Inability to analyze samples.	Second GC will be procured after Stage I testing. SRNL-Analytical Development Section maintains a GC/mass spectrometer that may be used.
Loss of key personnel.	Activities are delayed and schedule is slipped.	Cross train current team members and increase team numbers.

Risk	Impact	Mitigation
Benzene collection methods have not been demonstrated at elevated temperatures.	High temperature data not reliable or available.	Use high temperature rated materials where available. Qualify materials not rated for temperature when possible.
Power interruptions during testing.	Samples could cool significantly altering the amount of cure time at temperature.	Simulant testing – Outage would be limited to 60 h. SCO testing – Outage limited to < 10 h.
Operations interruptions in SCO delay sampling. (Crane outage, stop work, other non-task related outage).	Samples unavailable for analysis.	Remove samples as generated. Use samplers with storage ratings > 7 days. Have coolant (dry ice) available for temporary refrigeration of samples.

VII. R&D HAZARDS SCREENING CHECKLIST

The hazards of this work were identified using the hazards screening checklist of the SRNL Conduct of Research and Development Manual⁶. Figure 3, the "R&D Hazards Screening Checklist," is on file with the Task Lead.

VIII. REFERENCES

1. T.E. Chandler, "Determine Benzene Generation Rates from Saltstone at Elevated Temperatures," Task Technical Request SSF-TTR-2004-0005, (2004).
2. Lambert, D.P. "Tank 48H Simulant Validation", SRNL-LWP-2004-00009, (2004).
3. D.P. Lambert, T.B. Peters, M.E. Stallings, and S.D. Fink, "Analysis of Tank 48H Samples HTF-E-03-73 (June 03, 2003) and HTF-E-03-127 (September 17, 2003)," WSRC-TR-2003-00720, Revision 0 (2003).
4. R.F. Swingle, "Results of Analyses of Tank 23H and 24H Saltstone WAC Samples HTK-521 – HTK-528," WSRC-TR-2003-00112, (2003).
5. A.D. Cozzi, "Formulation Development for Processing Tank 48H in Saltstone," WSRC-TR-2004-00477, Revision 0 (2004).
6. "SRNL Conduct of Research and Development," WSRC-IM-97-00024, Rev. 3, (2004).

IX. QA Plan Checklist

The following QA Procedures apply for this task (indicate Yes, No or "AR" - as required). Current revision of the procedure will be used. The QA controls are the procedures identified on the checklist. If the procedures on the matrix are changed, applicable procedures will be followed.

Yes	No	AR	
			1-0 ORGANIZATION
X			1Q, QAP 1-1, Organization
X			L1, 1.02, SRNL Organization
		X	1Q, QAP 1-2, Stop Work
			2-0 QUALITY ASSURANCE PROGRAM
X			1Q, QAP 2-1, Quality Assurance Program
X			L1, 8.02, SRNL QA Program Clarifications, Attachment 8.2-1
X			1Q, QAP 2-2, Personnel Training & Qualification
X			L1, 1.32, Read & Sign
X			1Q, QAP 2-3, Control of Research & Development Activities
X			L1, 8.02, SRNL QA Program Clarifications, Attachment 8.2-3
X			L1, 7.10, Control of Technical Work
X			L1, 7.16, Laboratory Notebooks & Logbooks
	X		1Q, 2-4 Auditor/Lead Auditor Qualification & Certification - does not apply to Immobilization Technology Section Tasks
	X		1Q, 2-5 Qualification & Certification of Independent Inspection Personnel – does not apply to Immobilization Technology Section Tasks
X			1Q, QAP 2-7, QA Program Requirements for Analytical Measurement Systems
			3.0 DESIGN CONTROL
	X		1Q, QAP 3-1, Design Control
	X		L1, 7.10, Control of Technical Work
			4-0 PROCUREMENT DOCUMENT CONTROL
		X	1Q, QAP 4-1, Procurement Document Control
		X	E7, 3.10, Determination of Quality Requirements for Procured Items
		X	7B, Procurement Management Manual (For Reference Only)
		X	3E, Procurement Specification Manual (For Reference Only)
			5-0 INSTRUCTIONS, PROCEDURES & DRAWINGS
X			1Q, QAP 5-1, Instructions, Procedures & Drawings
	X		E7, 2.30, Drawings
X			L1, 1.01, SRNL Procedure Administration
			6-0 DOCUMENT CONTROL
X			1Q, QAP 6-1, Document Control
X			1B, MRP 3.32, Document Control

Yes	No	AR	
			7-0 CONTROL OF PURCHASED ITEMS & SERVICES
		X	1Q, QAP 7-2, Control of Purchased Items & Services
		X	7B, Procurement Management Manual (for reference)
		X	3E, WSRC Procurement Specification Manual (for reference)
X			1Q, QAP 7-3, Commercial Grade Item Dedication
X			E7, 3.46, Replacement Item Evaluation/Commercial Grade Item Dedication
			8-0 IDENTIFICATION & CONTROL OF ITEMS
		X	1Q, QAP 8-1, Identification & Control of Items
		X	L1, 8.02, SRNL QA Program Clarifications, Attachment 8.8-1
	X		9-0 CONTROL OF PROCESSES - does not apply to Immobilization Technology Section Tasks
			10-0 INSPECTION & VERIFICATION
	X		1Q, QAP 10-1, Inspection & Verification
	X		L1, 8.10, Inspection
			11-1 TEST CONTROL
	X		1Q, QAP 11-1, Test Control
			12-1 CONTROL OF MEASURING & TEST EQUIPMENT
X			1Q, QAP 12-1, Control of Measuring & Test Equipment
	X		1Q, QAP 12-2, Control of Installed Process Instrumentation
	X		1Q, QAP 12-3 Control & Calibration of Radiation Monitoring Equipment - does not apply to Immobilization Technology Section Tasks
			13-0 PACKAGING, HANDLING, SHIPPING & STORAGE
		X	1Q, QAP 13-1, Packaging, Handling, Shipping & Storage
		X	L1, 8.02, SRNL QA Program Clarifications, Attachment 8.13-1
			14-0 INSPECTION, TEST & OPERATING STATUS
		X	1Q, QAP 14-1, Inspection, Test & Operating Status
		X	L1, 8.02, SRNL QA Program Clarifications, Attachment 8.14-1
			15-0 CONTROL OF NONCONFORMING ITEMS/ACTIVITIES
		X	1Q, QAP 15-1, Control of Nonconforming Items
		X	L1, 8.02, SRNL QA Program Clarifications, Attachment 8.15-1

Yes	No	AR	
		X	1B, MRP 4.23, Site Tracking Analysis and Reporting (STAR)
			16-0 CORRECTIVE ACTION SYSTEM
		X	1Q, QAP 16-3, Corrective Action Program
		X	1.01, MP 5.35, Corrective Action Program
		X	1B, MRP 4.23, Site Tracking Analysis and Reporting (STAR)
			17-0 QA RECORDS MANAGEMENT
X			1Q, QAP 17-1, QA Records Management
X			L1, 8.02, SRNL QA Program Clarifications, Attachment 8.17-1
X			L1, 7.16, Laboratory Notebooks & Logbooks
			18-0 AUDITS
		X	1Q, QAP 18-2, Quality Assurance Surveillance
		X	L1, 8.18.1, SRNL Surveillances
X			1Q, QAP 18-3, Quality Assurance External Audits
		X	1Q, QAP 18-4, Management Assessments
		X	12Q, Assessment Manual
		X	1Q, QAP 18-6, Quality Assurance Internal Audits
X			1Q, QAP 18-7, Quality Assurance Supplier Surveillance
			19-0 QUALITY IMPROVEMENT
		X	1Q, QAP 19-2, Quality Improvement
		X	L1, 8.02, SRNL QA Program Clarifications, Attachment 8.19-2
			20-0 SOFTWARE QUALITY ASSURANCE
X			1Q, QAP 20-1, Software Quality Assurance
X			L1, 8.20, Software Management & Quality Assurance
X			21-1 ENVIRONMENTAL QUALITY ASSURANCE - does not apply to Immobilization Technology Section Tasks
			In addition to procedures noted above, if RW-0333P requirements are invoked, the following procedures apply. These procedures may also apply at the discretion of the Task Leader to non-RW-0333P tasks.
X			L1, 8.21, Supplemental QA Requirements for DOE/RW-0333P
			Sample Control:
		X	L1, 7.15, Obtaining Analytical Support
			Scientific Investigation:

Yes	No	AR	
X			L1, 7.16, Laboratory Notebooks & Logbooks

X. Identify any exceptions or additions to the procedures listed in the QA Matrix:

DOE RW-0333P requirements do not apply to the work in this study.

WSRC-IM-2002-00011, "Technical Report Design Check Guidelines," will be used to help ensure the quality and consistency of the technical review process for technical reports produced by SRNL Waste Treatment Technology.

XI. Complete this part only if Section 20 procedures (software) are invoked. Identify who will act in each of the following capacities. If Section 20 is N/A, mark these N/A.

Owner: N/A
 Designer: N/A
 Maintainer: N/A
 Tester: N/A

XII. Document Approval:

Identify documents requiring management, customer or CQF approval

Document	Management		Customer		CQF	
	Yes	No	Yes	No	Yes	No
Task Technical & QA Plan	X		X		X	
Final Report (customer may review draft)	X		X			X

XIII. Anticipated Records:

The following records are anticipated from this task. Indicate Yes, No or AR (as required):

Yes	No	AR	Description
X			Task Technical & QA Plan
X			Technical Notebooks
X			Task Technical Reports
	X		Data Qualification Reports
		X	Supporting Documentation

XIV. ATTACHMENTS:

N/A

FORMULATION DEVELOPMENT FOR PROCESSING TANK 48H IN SALTSTONE

A.D. Cozzi

October 2004

SAVANNAH RIVER NATIONAL LABORATORY

UNCLASSIFIED
DOES NOT CONTAIN
UNCLASSIFIED CONTROLLED
NUCLEAR INFORMATION

ADC &
Reviewing
Official: *Earl Holtscheiter*
(Name and Title)
Section Manager
Date: *10-5-04*

APPROVED for Release for
Unlimited (Release to Public)

Immobilization Technology Section
Savannah River National Laboratory
Aiken, SC 29808

Prepared for the U.S. Department of Energy Under Contract Number
DEAC09-96SR18500



SRNL
SAVANNAH RIVER NATIONAL LABORATORY

DISCLAIMER

This report was prepared by Westinghouse Savannah River Company (WSRC) for the United States Department of Energy under Contract No. DE-AC09-96SR18500 and is an account of work performed under that contract. Neither the United States Department of Energy, nor WSRC, nor any of their employees makes any warranty, expressed or implied, or assumes any legal liability or responsibility for the accuracy, completeness, or usefulness, of any information, apparatus, or product or process disclosed herein or represents that its use will not infringe privately owned rights. Reference herein to any specific commercial product, process, or service by trademark, name, manufacturer or otherwise does not necessarily constitute or imply endorsement, recommendation, or favoring of same by WSRC or by the United States Government or any agency thereof. The views and opinions of the authors expressed herein do not necessarily state or reflect those of the United States Government or any agency thereof.

Printed in the United States of America

**Prepared For
U.S. Department of Energy**

Key Words:
Saltstone
Processing
TCLP

Retention: Permanent

Key References:
Technical Task Request: SP-TTR-2004-00004
Task Plan: WSRC-RP-2004-00270

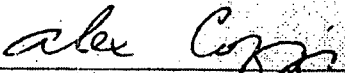
FORMULATION DEVELOPMENT FOR PROCESSING TANK 48H IN SALTSTONE

A.D. Cozzi

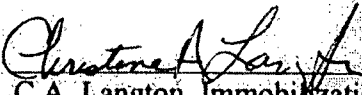
October 2004

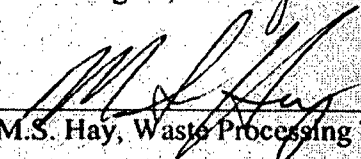
REVIEWS AND APPROVALS

AUTHOR:

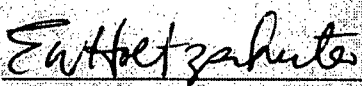

A.D. Cozzi, Immobilization Technology Section 10-5-04
Date

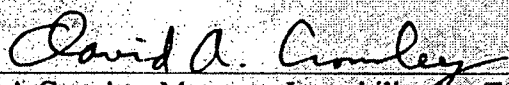
TECHNICAL REVIEWERS:

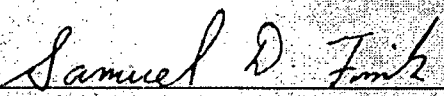

C.A. Langton, Immobilization Technology Section 10-5-04
Date

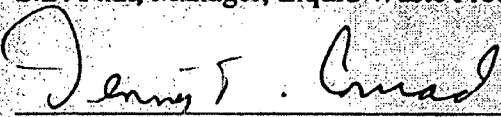

M.S. Hay, Waste Processing Technology Section 10-5-04
Date

APPROVERS

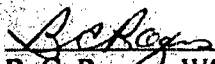

E. W. Holtzscheiter, Manager, Immobilization Technology Section 10-5-04
Date


D.A. Crowley, Manager, Immobilization Technology and Business Development 10/5/04
Date


S.D. Fink, Manager, Liquid Waste Processing 10-5-2004
Date


D. T. Conrad, Manager, Low Curie Salt Engineering 10-6-2004
Date


R. H. Spires, Manager, Salt Engineering 10-11-04
Date


B. C. Rogers, WSRC Project Manager, Tank 48H 10/11/04
Date

EXECUTIVE SUMMARY

Salt Program Engineering (SPE) requested research to help evaluate the Saltstone process as a disposition path for the contents of Tank 48H. The main objective of the task was to evaluate the processing and cured properties of Saltstone prepared with Tank 48H material aggregated with other Tank 50H inflows to determine the suitability of Saltstone as a disposition path for the contents of Tank 48H.

The Tank 48H waste was aggregated with inhibited water (IW) and a simulant of the recycle stream from the Defense Waste Processing Facility (DWPF). The aggregates targeted three tetraphenyl borate (TPB) concentrations: 1) 5500 mg/L, the aggregate determined from assumptions at the maximum reasonable limits, 2) 1500 mg/L, the aggregate containing the minimum proportion of Tank 48H material that is programmatically acceptable, and 3) 3500 mg/L, the average of the two endpoints. Saltstone prepared with Tank 48H waste aggregated with IW and a simulant of the recycle stream from the DWPF was produced in the Savannah River National Laboratory (SRNL) shielded cells. Processable Saltstone slurry formulations can be prepared with Tank 48H material and both DWPF recycle simulant and inhibited water with concentrations of 1500, 3500, and 5500 mg/L TPB. Toxic Characterization Leaching Procedure (TCLP) extractions were performed on the six aggregates. The extracts were analyzed for benzene, nitrobenzene and mercury. All of the samples passed TCLP.

Saltstone was also prepared with a Tank 48H simulant and DWPF recycle simulant. Testing of the fresh Saltstone slurry and cured Saltstone prepared with simulants indicate that neither the fresh nor cured Saltstone is hazardous for ignitability.

After transferring Tank 48H material to Tank 50H and prior to processing through the Saltstone Production Facility (SPF), Tank 50H should be sampled to verify processability.

This page intentionally left blank.

TABLE OF CONTENTS

EXECUTIVE SUMMARY	v
LIST OF TABLES	viii
LIST OF ACRONYMS	ix
1.0 INTRODUCTION AND BACKGROUND	1
2.0 APPROACH	3
2.1 Sample Preparation	4
2.2 Gel Time Determination	4
2.3 Bleed Water Determination	5
2.4 Set Time Determination	5
2.5 Toxic Characteristic Leaching Procedure	5
2.6 Ignitability Determination of Fresh Saltstone Slurry	7
2.7 Ignitability Determination of Cured Saltstone	7
3.0 RESULTS	9
3.1 Sample Preparation	9
3.2 1500 mg/L TPB with DWPF Recycle Simulant	9
3.3 1500 mg/L TPB with Inhibited Water	9
3.4 3500 mg/L TPB with Inhibited Water	10
3.5 3500 mg/L TPB with Recycle Simulant	10
3.6 3500 mg/L TPB with Inhibited Water (Second Iteration)	10
3.7 5500 mg/L TPB with Inhibited Water	11
3.8 5500 mg/L TPB with Recycle Simulant	11
3.9 5500 mg/L TPB with Inhibited Water (Second Iteration)	11
3.10 Additional Antifoam Tests with 3500 mg/L TPB with Inhibited Water	12
3.11 Toxic Characteristic Leaching Procedure	13
3.12 Ignitability Determination of Fresh Saltstone Slurry	14
3.13 Ignitability Determination of Cured Saltstone	15
4.0 CONCLUSIONS AND RECOMMENDATIONS	17
5.0 REFERENCES	19
6.0 ACKNOWLEDGEMENTS	21

LIST OF TABLES

Table 1-1. Process Terminology used in Study.....	1
Table 2-1. Composition of DWPF Recycle Simulant.....	3
Table 2-2. Concentration and Properties of Materials Used for Aggregation.....	3
Table 2-3. Calculated Compositions and Properties of Aggregates.....	3
Table 2-4. Premix Composition used in this Study.....	4
Table 2-5. EPA Regulatory Limits for Contaminants in TCLP Extracts.....	5
Table 2-6. Variance from EPA Method for TCLP Extraction.....	6
Table 3-1. Summary of Processing Properties of Saltstone Slurries.....	12
Table 3-2. Benzene Concentrations in TCLP Extracts.....	13
Table 3-3. Flash Point Results using a Closed Cup Tester.....	15
Table 4-1. Recommended Initial Processing Parameters for Tank 48H Aggregates.....	17

LIST OF ACRONYMS

ADS	Analytical Development Section
CVAA	Cold Vapor - Atomic Absorption
DWPF	Defense Waste Processing Facility
EPA	United States Environmental Protection Agency
FA	Fly Ash
GC	Gas Chromatography
GGBFS	Ground Granulated Blast Furnace Slag
ITP	In Tank Precipitation
IW	Inhibited Water
KTBP	Potassium Tetrphenylborate
MS	Mass Spectrometry
MST	Monosodium Titanate
SCS	Statistical Consulting Section
SPE	Salt Program Engineering
SPF	Saltstone Production Facility
SRNL	Savannah River National Laboratory
SVOA	Semi-Volatile Organic Analysis
SRS	Savannah River Site
TBP	Tri-n-butyl Phosphate
TCLP	Toxic Characteristic Leaching Procedure
TPB	Tetraphenyl borate
VOA	Volatile Organic Analysis
VOC	Volatile Organic Compound
ZHE	Zero-Headspace Extraction

This page intentionally left blank.

1.0 INTRODUCTION AND BACKGROUND

Tank 48H contains approximately 250,000 gallons of salt waste. The waste contains approximately 19,000 kg of organic material, primarily as potassium tetraphenyl borate (KTPB). The tetraphenyl borate, along with approximately 1450 kg monosodium titanate (MST), was added to Tank 48H during the demonstration and startup of the In-Tank Precipitation Facility (ITP). After the shutdown of the ITP process, no process existed for the destruction of the organic material in Tank 48H. Tank 48H is slated to serve as the feed tank for the Savannah River Site (SRS) Actinide Removal Process. Prior to this use, the current Tank 48H waste must be treated or removed.

Two options being considered for disposition of the contents of Tank 48H include¹:

1. Aggregation of the material with DWPF recycle stream and disposal in the Saltstone Processing Facility.
2. In-Situ Thermal Decomposition using heat in combination with pH reduction and catalyst addition.

Salt Program Engineering (SPE) requested research to help evaluate the Saltstone process (option #1 above) as a disposition path for the contents of Tank 48H. The main objective of the research was to evaluate the processing (gel time, set time and bleed water) and cured (leach) properties of Saltstone prepared with Tank 48H material aggregated with recycle from the DWPF or other tank contents to determine the suitability of Saltstone as a disposition path for the contents of Tank 48H. Table 1-1 is the designation of the processing terminology used in this study.

Table 1-1. Process Terminology used in Study.

Term	Designation
Gel Time	The time at which the Saltstone slurry does not flow due to gravity, i.e. readily pour from the casting cup. For this study, acceptable gel time is 30 min < gel time < 120 min.
Set Time*	The elapsed time from casting the Saltstone slurry until the mixture reaches rigidity as indicated by the Set Time Determination [†] (penetrometer penetration < 2.5 mm). Preferred set time is less than three days. However, set times up to six days are acceptable [‡] .
Bleed Water*	The autogenous emergence of water from Saltstone slurry caused by the settlement of solid materials. For this study, acceptable bleed water is 1% after 72 h [†] .

The Savannah River National Laboratory (SRNL) was requested to 1) confirm that Saltstone prepared with actual Tank 48H material can be processed into Saltstone and pass the Toxic Characteristic Leaching Procedure (TCLP) to be considered non-hazardous and 2) confirm that Saltstone mixes prepared with a Tank 48H simulant are not considered ignitable[‡].

* ASTM C 125-03 "Standard Terminology Relating to Concrete and Concrete Aggregates"

† Manual 704-Z Procedure 4400, "Saltstone Grout Lab Analysis (U), Rev. 11 (2002).

‡ Curing Saltstone passes the EPA manual SW-846 Methods 1010a "Pensky-Martens Closed-Cup Method for Determining Ignitability," Revision 1 (2002) and 1030 "Ignitability of Solids" Revision 0 (1996).

This page intentionally left blank.

2.0 APPROACH

The Tank 48H waste was aggregated with inhibited water (IW) and a simulant of the recycle stream from the DWPF. The DWPF recycle simulant targeted the average of the Tank 23 and Tank 24 samples taken 100 inches from the tank bottom as reported by Swingle². Table 2-1 is the composition of the DWPF Recycle simulant. The concentration of TPB in Tank 48H is 18,800 mg/L³. Table 2-2 is the components and properties of interest for the materials prior to aggregation. For the tests to determine ignitability, a simulant of the Tank 48H material was prepared to represent the material in Reference 3⁴.

Table 2-1. Composition of DWPF Recycle Simulant.

Component	g/L
NaNO ₂	21.734
NaNO ₃	5.219
NaOH	17.399
Na ₂ CO ₃	7.419
Hg(NO ₃) ₂	14.5 ppm
Total	51.771
Solids	5.2 wt %

Table 2-2. Concentration and Properties of Materials Used for Aggregation.

Material	TPB (mg/L)	Mercury (mg/L)	Cs activity ¹ (dpm/mL) (Ci/gal)	Alpha ³ (dpm/mL)	wt % Solids		Density (g/mL)
					Undissolved	Total [†]	
Tank 48H ³	18,800	10.3	1E+09 (1.72)	2.8E+05	2.18	18.42	1.144
DWPF Recycle simulant	0	14.5 ^{2†}	0	0	<1	5.2	1
Inhibited Water	0	0	0	0	0	0.1	1

[†]Total solids is used to determine the water:premix ratio used for Saltstone processing.

²Value from Tank 24.

The aggregates targeted three TPB concentrations: 5500 mg/L, the aggregate determined from assumptions at the maximum reasonable limits, 1500 mg/L, the aggregate containing the minimum proportion of Tank 48H material that is programmatically acceptable, and 3500 mg/L, the average of the two endpoints. This resulted in six aggregates for testing (i.e., three TPB levels with two simulants). These aggregates span the range of potential Saltstone compositions. Table 2-3 is the calculated make up of each of the aggregates.

Table 2-3. Calculated Compositions and Properties of Aggregates.

Material	TPB (mg/L)	Solids (wt %)	Density (g/ml)	Mercury (mg/L)	Cs activity (dpm/mL) (Ci/gal)	Alpha (dpm/mL)
Tank 48H/DWPF Recycle (s)	5500	8.0	1.04	13.3	3E+08 (0.50)	8.2E+04
	3500	6.2	1.03	13.7	2E+08 (0.32)	5.2E+04
	1500	4.4	1.01	14.2	8E+07 (0.14)	2.2E+04
Tank 48H/IW	5500	6.0	1.04	3.0	3E+08 (0.50)	8.2E+04
	3500	4.1	1.03	1.9	2E+08 (0.32)	5.2E+04
	1500	1.8	1.01	0.8	8E+07 (0.14)	2.2E+04

Together, the dry materials used to make the Saltstone slurry are called premix. The ratio of the premix materials was fixed for this study. Table 2-4 is the premix composition used throughout this study.

Table 2-4. Premix Composition used in this Study.

Premix by Weight
45% Class F Fly Ash (FA)
45% GGBFS* (Slag)
10% Cement

*Ground granulated blast furnace slag.

2.1 Sample Preparation

To prepare the aggregate, a portion of the Tank 48H material was transferred from a well-mixed bottle of the material from Reference 3 into a bottle and weighed. Using the measured mass of the Tank 48H material transferred and the data in Table 2-2, the amount of IW or DWPF recycle simulant required to achieve the desired TPB concentration in the aggregate was calculated. The data in Table 2-3 then was used to calculate the amount of premix to achieve the desired water to premix ratio.

To prepare the Saltstone slurry, the aggregated liquids were added to a one liter blender carafe. At this point, set retarder or antifoam was added to the aggregate, if appropriate. The calculated amount of premix was then added to the carafe. The materials were then agitated for one minute. The contents were inspected to ensure that the premix had dispersed. Any remaining premix that had not been dispersed was reintroduced to the slurry with a spatula. The slurry was then agitated for an additional two minutes.

For each mix, five 120-mL cups were marked at 50 milliliters. Two cups were designated for gel time, one cup was designated for set time, and the remaining two cups were reserved for bleed water determination. The Saltstone slurry was then cast into the five cups and capped. For each of the six unique aggregates, Saltstone slurry was cast into two Teflon[®] vessels suitable for elevated temperature and pressure engraved with permanent identifications. The vessels were filled to minimize head space. One sample of each aggregate cast in Teflon[®] (six vessels total) was set aside to cure at ambient temperature and the remaining samples were cured for 28 days at 90 °C for TCLP extractions. After curing was complete, the heated samples were cooled to ambient and placed with the unheated samples until sampling. The TCLP samples were collected randomly being handled one sample at a time to minimize exposure to atmosphere.

2.2 Gel Time Determination

There is not a formally documented range of gel times to designate Saltstone slurry as "acceptable". However, the range 30 min < gel time < 120 min is regarded as a conservative time frame where the formation of a gel structure in the slurry would be unlikely to cause difficulties pumping slurry to Saltstone Vaults and would not substantially increase the probability of the slurry settling. This range of gel times was applicable to the SPF prior to FY04 facility modifications and may not adequately meet the current needs of the SPF. The two samples designated for gel time determination were maintained undisturbed until a flowability test was performed. After an appropriate waiting period, the contents of one of the cups was poured into an empty cup and the flowability of the slurry was observed. Following a second waiting period, the contents of the second cup were poured into an empty cup and the flowability of the slurry was observed. This process was repeated until the slurry did not readily flow and was deemed gelled. The gel time was then recorded as the elapsed time between the casting of the sample and the unsuccessful pour that signified the conclusion of the test. For several of the aggregates it was necessary to add set retarder and antifoam to achieve an acceptable gel time. The set retarder used in these

experiments was Daratard 17^{*}. Two antifoams were used in these tests. The primary antifoam used in these tests was B52[†]. Previous testing indicates that B52 is effective in breaking down foam in aggregates containing TPB. An additional antifoam, tri-n-butyl phosphate (TBP), was also evaluated for effectiveness in mitigating foam formation.

2.3 Bleed Water Determination

The desired maximum bleed water is 1 vol %. The two cups designated for bleed water were inspected after 72 h. The mass of bleed water, if any, in the two cups is measured. By using 100 mL of Saltstone (two 50-mL samples), the volume percent bleed water is the mass of the water recovered from the two samples.

2.4 Set Time Determination

The desired maximum set time is three days. The time of set was determined using a Vicat needle modified for performance in shielded cells. The method of determination used instructions based on the Z-Area procedure[‡]. One day after casting into the cup in Section 2.1 designated for set time determination, the cup is placed under the Vicat needle and the zero distance mark is set with the needle at the surface of the sample. The needle is raised 50 mm and released. The penetration of the penetrometer into the sample is recorded from the gauge. This process is repeated daily until the penetration is <2.5 mm.

2.5 Toxic Characteristic Leaching Procedure

A solid waste exhibits the characteristic of toxicity if the concentration of the contaminants in the TCLP extract is greater than the regulatory levels[§]. The analysis of pure, unaggregated Tank 48H contents performed in Reference 3 reported the presence of hazardous concentrations of benzene as defined by the United States Environmental Protection Agency (EPA). The nitrobenzene content was below the detection limits, but greater than the EPA regulatory limit for toxicity. The mercury content of The Tank 48H was below the limits defined by the EPA as characteristic for toxicity. However, since mercury was part of the aggregates prepared with DWPF recycle simulant, and there was a potential for the formation of benzene and nitrobenzene during curing, a modified TCLP extraction based on the EPA method was used to determine the presence of these species in the TCLP extract[§]. Table 2-5 is the regulatory limit for the contaminants of concern in this study.

Table 2-5. EPA Regulatory Limits for Contaminants in TCLP Extracts.

Contaminant	Regulatory Level (mg/L)
Benzene	0.5
Nitrobenzene	2.0
Mercury	0.2

The EPA extraction method was adhered to as closely as possible as dictated by the test conditions (i.e. radioactive materials handled with manipulators in shielded cells). For example, in Section 7.2.5 of the method, a mass of at least 100 grams is specified. This was neither practical nor possible for the samples prepared in Section 2.1, as there was not sufficient Tank 48H material available to prepare sufficient Saltstone for all of the testing and perform TCLP extractions. Table 2-6 summarizes the deviations from

^{*} W.R. Grace Daratard 17

[†] Illinois Institute of Technology (IIT) B-52

[‡] Manual 704-Z: Procedure 4400, "Saltstone Grout Lab Analysis (U), Rev. 11 (2002).

[§] 40CFR261.24 Toxicity characteristic

the EPA method and provides explanations for the variance. To compensate for the deviation in extraction fluid to sample ratio in 7.2.11 of the EPA method, the analyses results are normalized to an extraction fluid to sample ratio of 15.

Table 2-6. Variance from EPA Method for TCLP Extraction.

Section	Action	Variance	Explanation
	Non-Volatiles		
7.2.5	Sample size Recommended > 100 g.	Used ~1 g samples.	Limited material available. Reference 6 precedence.
7.2.11	<ul style="list-style-type: none"> Extraction fluid volume 20x mass of sample. Rotate 30±2 rpm for 18±2 h @ 23±2 °C. 	<ul style="list-style-type: none"> Used fixed volume ~15x sample mass. T_{cell} not controlled, exceeded 25 °C. 	<ul style="list-style-type: none"> Used pre-measured extract for efficiency in shielded cell. Reduced ratio introduced conservatism. Test performed in summer. Air temperature of shielded cells not regulated.
7.2.12	Filter extract.	Settled solids and decanted extract.	During shakeout tests filters plugged, exposed extract to environment. Decant provides more conservative result.
7.2.14	Store extracts at 4 °C.	Extracts stored at ambient temperature in cells, refrigerated in ADS sample receiving.	To maintain 4 °C in shielded cells is costly. Samplers refrigerated in ADS sample receiving.
	Volatiles		
4.3.1	Use approved Zero-Headspace Extractor (ZHE) vessel.	Used glass vials with Teflon® lids filled to top.	Approved ZHE vessels for 25 g samples.
7.3.3	Sample size Recommended ~ 25 g.	Used ~1 g.	Limited material available. Reference 6 precedence.
7.3.15	Store extracts with minimal headspace at 4 °C.	Extracts stored with minimal headspace at ambient temperature. Samples refrigerated in ADS sample receiving.	To maintain 4 °C in shielded cells is costly. Samplers refrigerated in ADS sample receiving. Although samples are sealed with minimal head space, variance is non-conservative as benzene is a volatile compound.

2.5.1 Volatile Organic Compound (VOC) Extraction

After the samples prepared in Section 2.1 had cured for 28 days, samples were collected for extraction. Duplicate samples of approximately one gram each were retrieved from each vessel. The use of one gram of sample for extraction was explored previously⁶. Samples collected ranged from 0.773 to 1.015 grams. The samples were placed in 15 mL glass vials with Teflon® gaskets. To minimize exposure of the Saltstone to the environment, minimal effort was made to precisely collect one gram of material. A minimum of 0.75 grams was necessary to ensure that the extraction fluid to sample ratio was no more than 20. Extraction fluid 1⁷ was used to fill the vial to form a meniscus, and capped. The vials were

⁷ Extraction Fluid 1 is a pH 4.93 buffer made from acetic acid and sodium hydroxide.

placed in a rotator preset to 30 rpm and rotated for 18 h. After the vials were removed from the rotator, the samples were set aside to settle the solids. The extract was decanted into a sample vial and overfilled to minimize head space and limit volatility of volatile compounds. The vials then were removed from the shielded cells and submitted to the SRNL-Analytical Development Section (ADS) for volatile organic analysis (VOA) of benzene. The samples were analyzed by purge and trap Gas Chromatography / Mass Spectrometry (GC/MS). The method detection limit for this study was 0.005 mg/L for VOA. To determine the recovery of benzene during the analysis a matrix spiking experiment was performed. A 25 ppb spike of benzene was added to one of the samples and analyzed. It was determined that 83% of the benzene was recovered. This recovery rate is used to correct results for benzene losses during analysis.

2.5.2 Semi-Volatile Organic Compound (SVOC) and Metals Extraction

After the samples prepared in Section 2.1 had cured for 28 days, samples were collected for extraction. Approximately five additional grams of sample was collected to determine the appropriate extraction fluid for the TCLP⁶. Results determine that Extraction Fluid 2¹ be used for the SVOC and metals TCLP. Duplicate samples of approximately one gram each were retrieved from each vessel. The use of one gram of sample for extraction was explored previously⁶. Samples collected ranged from 0.967 to 1.025 grams. The samples were placed in 25 mL glass vials with Teflon[®] gaskets. A minimum of 0.75 grams was necessary to ensure that the extraction fluid to sample ratio was no more than 20. The vials were placed in a rotator preset to 30 rpm and rotated for 18 h. After the vials were removed from the rotator, the samples were set aside to settle the solids. The extract was decanted into two sample vials. The vials then were removed from the shielded cells and submitted to the SRNL-ADS for semi-volatile organic analysis (SVOA) of nitrobenzene and cold vapor atomic absorption (CV-AA) of mercury. The SVOC samples were extracted with methylene chloride, and the extract was analyzed by GC/MS. Gas Chromatography / Mass Spectrometry analysis was employed to identify organic compounds in the samples. The method detection limit for this study was 0.5 mg/L for nitrobenzene. The mercury is reduced to the elemental state and aerated from solution in a closed system. The mercury vapor passes through a cell positioned in the light path of an atomic absorption spectrophotometer. Absorbance (peak height) is measured as a function of mercury concentration. The method detection limit for this study was 0.11 mg/L for mercury.

2.6 Ignitability Determination of Fresh Saltstone Slurry

The presence of TPB in the Tank 48H material and the potential to form benzene in the Saltstone slurry is the basis for testing the Saltstone slurry for the characteristic of ignitability. A solid waste exhibits the characteristic of ignitability if the waste is a liquid and has a flash point of less than 60 °C (140 °F) as determined using a Pensky-Martens closed cup tester². Using a Tank 48H simulant⁷, an aggregate was made with DWPF recycle simulant to target a TPB concentration of 5500 mg/L. A water to premix ratio of 0.63 was used to prepare the Saltstone slurry. Four replicate samples were submitted to SRNL-ADS for flash point testing. Samples were tested using a flash point tester similar to the Pensky-Martens tester. Dodecane (flash point 71°C/160°F) was used as the standard material.

2.7 Ignitability Determination of Cured Saltstone

The potential for the TPB present in the Tank 48H material to create benzene during curing of the Saltstone dictates testing the cured Saltstone for the characteristic of ignitability. A solid waste exhibits the characteristic of ignitability if the waste is not a liquid and is capable of causing fire and, when ignited, burns so vigorously and persistently that it becomes a hazard³. Using a Tank 48H simulant⁷, an

⁶ ADS Manual L16.1, Procedure 2512, "Modified Toxicity Characteristic Leaching Process"

¹ Extraction Fluid 2 is a pH 2.88 solution made from acetic acid.

³ 40CFR261.21 Characteristic of Ignitability

aggregate was made with DWPF recycle simulant to target a TPB concentration of 5500 mg/L. The Saltstone sample was prepared using a water to premix ratio of 0.63. Two replicate samples were cast and tested for ignitability using the EPA method 1030 "Ignitability of Solids." A propane torch was used to produce an open flame of ~1050 °C. The flame was directed at one end of the sample for two minutes to determine if the sample was ignitable.

3.0 RESULTS

Saltstone prepared with Tank 48H waste aggregated with IW and a simulant of the recycle stream from the DWPF was produced in the SRNL shielded cells. Saltstone was also prepared with a Tank 48H simulant⁷ and DWPF recycle simulant. The processing (gel time, set time and bleed water) and cured (leach) properties of the Saltstone were determined for the samples prepared with Tank 48H material. The determination of whether the Saltstone slurry or cured Saltstone were characteristic for ignitability was determined with samples prepared with the Tank 48H simulant from Reference 7 and DWPF recycle simulant.

3.1 Sample Preparation

The Saltstone samples were prepared as described in Section 2.1. After the blender had mixed the Tank 48H aggregate with the premix materials it was noted during casting that air was entrained in slurry. The quantity of air entrained increased with increasing TPB concentration. Entrained air can enhance the gelation of the slurry by producing a structure in the slurry and necessitate the use of set retarders or antifoams. Additions of antifoam reduced the quantity of entrained air and the bubbles appeared to have coalesced into larger bubbles. The coalescing of the bubbles during antifoam addition may have helped reduce the quantity of air entrained in the sample.

3.2 1500 mg/L TPB with DWPF Recycle Simulant

3.2.1 Gel Time

The Saltstone slurry was prepared as described in Section 2.1 with a water to premix ratio of 0.6. When the slurry was inspected after the first minute of mixing, it appeared thicker than desired. Additional aggregate was added to reduce the consistency of the slurry and raise the water to premix ratio to 0.68. There did not appear to be any air entrainment in the form of frothing of the slurry. The first gel time pour was after 10 minutes and it was determined that the slurry had gelled.

3.2.2 Bleed Water

After 24 hours the two bleed water cups were inspected and no bleed water was detected.

3.2.3 Set Time

Set Time was determined to be one day.

3.3 1500 mg/L TPB with Inhibited Water

3.3.1 Gel Time

Based on the results of the previous test, the Saltstone slurry was prepared with a water to premix ratio of 0.66. In addition, a set retarder (Daratard 17) was added to the aggregate prior to mixing. The amount of set retarder added was equal to 0.12 wt % of the aggregate. The slurry appeared satisfactory as it did not exhibit frothing and was thin enough to pour. The first gel time pour was after 5 minutes and it was pourable. Gel time was declared on the fourth gel time pour after 35 minutes.

3.3.2 Bleed Water

After 48 hours the two bleed water cups were inspected the bleed water was determined to be 7.2 vol %.

3.3.3 Set Time

Set Time was not measured for this aggregate.

3.4 3500 mg/L TPB with Inhibited Water

Based on the results of the previous test, the water to premix ratio was reduced and the set retarder was increased. The Saltstone slurry was prepared with a water to premix ratio of 0.60. A 0.19 wt % addition of set retarder was made to the aggregate prior to mixing. The slurry exhibited noticeable frothing but was thin enough to pour. During casting, it was noted that significant quantities of fine bubbles were entrained in the slurry. The first gel time pour was after 11 minutes. The slurry was thick but pourable. Gel time was declared on the second gel time pour after 16 minutes.

3.4.1 Bleed Water

After 24 hours the two bleed water cups were inspected and no bleed water was detected.

3.4.2 Set Time

Set Time was not measured for this aggregate.

3.5 3500 mg/L TPB with Recycle Simulant

Based on the results of the previous test, the water to premix ratio was increased and the set retarder was increased. The Saltstone slurry was prepared with a water to premix ratio of 0.63. A 0.27 wt % addition of set retarder was made to the aggregate prior to mixing. Again, the slurry exhibited noticeable frothing but was thin enough to pour. The first gel time pour was after 12 minutes. The slurry was thick but pourable. Gel time was declared on the second gel time pour after 21 minutes.

3.5.1 Bleed Water

After 24 hours the two bleed water cups were inspected and no bleed water was detected.

3.5.2 Set Time

Set Time was not measured for this aggregate.

3.6 3500 mg/L TPB with Inhibited Water (Second Iteration)

Based on the results of the two previous tests, the need for antifoam was clear. Antifoam prepared for WSRC, IIT B52 was shown to act as both a defoamer and antifoam in material similar to the contents of Tank 48H⁸. The IIT B52 was too viscous to add precisely using manipulators. A predetermined blend of Daratard 17 and B52 of 2:1 was used. The water to premix ratio was increased, the set retarder was decreased and antifoam was introduced. The Saltstone slurry was prepared with a water to premix ratio of 0.66. The admixture addition consisted of 0.20 wt % of set retarder and 0.10 wt % of B52. The slurry exhibited minor frothing. During casting, it was noted that the fine bubbles present in previous tests had coalesced into larger, less numerous bubbles. The bubbles were still entrained in the slurry. The first gel time pour was after 5 minutes. The slurry was fluid and poured easily. The second gel time pour was after 15 minutes. The slurry was thick but pourable. Gel time was declared on the fourth gel time pour after 30 minutes.

3.6.1 Bleed Water

After 24 hours the two bleed water cups were inspected and no bleed water was detected.

3.6.2 Set Time

Set Time was determined to be two days.

3.7 5500 mg/L TPB with Inhibited Water

Based on the results of the previous test, the water to premix ratio and the admixtures (set retarder + antifoam) were left unchanged. The Saltstone slurry was prepared with a water to premix ratio of 0.65. The admixture addition consisted of 0.21 wt % of set retarder and 0.10 wt % of B52. The slurry exhibited greater frothing than the 3500 mg/L TPB aggregates, but was thin enough to pour. Again, it was noted during casting that significant quantities of large bubbles were entrained in the slurry. The first gel time pour was after 7 minutes. The slurry was thick but pourable. Gel time was declared on the second gel time pour after 15 minutes.

3.7.1 Bleed Water

After 24 hours the two bleed water cups were inspected and no bleed water was detected.

3.7.2 Set Time

Set Time was not measured for this aggregate.

3.8 5500 mg/L TPB with Recycle Simulant

Based on the results of the previous test, the water to premix ratio was maintained and the admixtures were increased. The Saltstone slurry was prepared with a water to premix ratio of 0.64. The admixture addition consisted of 0.31 wt % of set retarder and 0.15 wt % of B52. The quantity of the foam noted during casting was reduced from the previous test. The first gel time pour was after 10 minutes. The slurry poured easily. The second gel time pour was after 20 minutes. During the second pour, the potential for bleed water was detected. The test was halted after the fourth gel time pour after 40 minutes when it was determined that bleed water would be present.

3.8.1 Bleed Water

After 48 hours the two bleed water cups were inspected and 9 vol % bleed water was measured.

3.8.2 Set Time

Set Time was not measured for this aggregate.

3.9 5500 mg/L TPB with Inhibited Water (Second Iteration)

Based on the results of the two previous tests, the water to premix ratio was maintained and the admixtures were decreased. The Saltstone slurry was prepared with a water to premix ratio of 0.65. The admixture addition consisted of 0.26 wt % of set retarder and 0.13 wt % of B52. The slurry exhibited minor frothing. It was noted that the amount of bubbles was similar to the previous test. Bubbles were still entrained in the slurry during casting. The first gel time pour was after 10 minutes. The slurry was fluid and poured easily. The second gel time pour was after 20 minutes. The slurry was thick but pourable. Gel time was declared on the third gel time pour after 30 minutes.

3.9.1 Bleed Water

After 24 hours the two bleed water cups were inspected and no bleed water was detected.

3.9.2 Set Time

Set Time was not measured for this aggregate.

Table 3-1 is a summary of the processing properties of the aggregates tested. The "with adjustments" term was necessary as there was not sufficient Tank 48 material available to perform the necessary test iterations to definitively determine a formulation for each of the six aggregates. Therefore, by bounding the processing requirements, it was determined that there exists an acceptable formulation that could be achieved "with adjustments".

Table 3-1. Summary of Processing Properties of Saltstone Slurries.

Aggregate	Water/ Premix	Daratard 17 Admixture (Wt %)	IIT B52 Antifoam (Wt %)	Gel Time (min)	Set Time (d)	Bleed Water (Vol %)	Processable
1500 Recycle	0.68	0.00	None	10	1	0	with adjustments
1500 IW	0.66	0.12	None	35	--	7.2	with adjustments
3500 IW	0.60	0.19	None	16	--	0	with adjustments
3500 Recycle	0.63	0.27	None	21	--	0	with adjustments
3500 IW-2	0.66	0.2	0.1	30	2	0	YES
5500 IW	0.65	0.21	0.1	15	--	0	with adjustments
5500 Recycle	0.64	0.31	0.15	> 40	--	9	with adjustments
5500 IW-2	0.65	0.26	0.125	30	--	0	Probable*

*Set time was not measured but based on gel time and bleed water results, set is expected to be acceptable.

3.10 Additional Antifoam Tests with 3500 mg/L TPB with Inhibited Water

After the initial test results were analyzed, two additional tests were performed. Aggregate made with 3500 mg/L TBP and IW was selected to represent the most likely TBP concentration. Based on previous tests the water to premix ratio was targeted as 0.65. The admixture addition consisted of 0.2 wt % set retarder and 0.15 wt % antifoam. The only variable between the two tests was the antifoam. In the first test, B52 was used and in the second test, TBP was the antifoam. In both tests, the slurries exhibited minor frothing. During casting, the larger, less numerous bubbles noted in the earlier 3500 mg/L TPB were present. The bubbles were still entrained in the slurry. The slurries were fluid and poured easily. Gel time was declared after 25 minutes.

3.10.1 Bleed Water

After 24 hours the bleed water cups were inspected and no bleed water was detected in either test.

3.10.2 Set Time

The set time was tested after one day. Neither of the mixes were set. The set time was tested again after 3 days. Again, neither of the mixes were set, although the mix made with B52 had firmed considerably. The final test was performed at six days. The mix prepared with B52 was declared set. The mix prepared with TBP as the antifoam had not yet set.

3.11 Toxic Characteristic Leaching Procedure

TCLP extractions were performed in duplicate on samples cured at ambient temperature and at 90 °C for each unique aggregate.

3.11.1 Volatile Organic Compound (VOC) Extraction

TCLP extractions were performed and extracts were analyzed as described in Sections 2.5 and 2.5.1. One of the replicated of the 1500 mg/L TPB aggregate made with IW and cured at 90 °C was compromised during handling and was not removed from the shielded cells for analysis. A statistical analysis of the benzene results performed by SRNL-Statistical Consulting Section (SRNL-SCS) determined that the TPB concentration was the only statistically significant variable affecting the benzene concentration in the TCLP extracts. The curing temperature (90 °C vs. ambient) and aggregation material (DWPF recycle vs. IW) were statistically equivalent. Table 3-2 is the results of the benzene analysis. The measured benzene is corrected for the 83% recovery described in Section 2.5.1. The corrected value is then normalized for the variations in the sample mass to a mass of one gram. Figure 3-1 is the plot of the benzene concentration in the TCLP extracts as a function of the TPB concentration in the aggregate. The benzene limit for RCRA hazardous designation from Table 2-5 is 0.5 mg/L is also displayed for reference. All of the samples passed TCLP for benzene.

Table 3-2. Benzene Concentrations in TCLP Extracts.

TPB (mg/L)	Aggregate*	Cure Temperature (°C)	replicate	Sample Mass (g)	Measured Benzene (mg/L)	Corrected Benzene (mg/L)	Normalized Benzene (mg/L)
1500	IW	27	1	0.954	0.06	0.07	0.08
1500	IW	27	2	0.949	0.06	0.07	0.07
1500	IW	95	2	0.988	0.06	0.07	0.07
1500	RC	27	1	1.000	0.02	0.02	0.02
1500	RC	27	2	1.006	0.10	0.12	0.11
1500	RC	95	1	1.051	0.06	0.07	0.07
1500	RC	95	2	1.011	0.06	0.07	0.07
3500	IW	27	1	0.821	0.12	0.14	0.18
3500	IW	27	2	0.991	0.15	0.18	0.18
3500	IW	95	1	0.911	0.09	0.11	0.12
3500	IW	95	2	1.007	0.10	0.12	0.12
3500	RC	27	1	0.895	0.10	0.12	0.13
3500	RC	27	2	0.931	0.12	0.14	0.16
3500	RC	95	1	0.934	0.14	0.17	0.18
3500	RC	95	2	0.910	0.12	0.14	0.16
5500	IW	27	1	0.804	0.14	0.17	0.21
5500	IW	27	2	1.020	0.11	0.13	0.13
5500	IW	95	1	1.000	0.08	0.10	0.10
5500	IW	95	2	0.934	0.17	0.20	0.22
5500	RC	27	1	0.980	0.10	0.12	0.12
5500	RC	27	2	0.773	0.12	0.14	0.19
5500	RC	95	1	0.856	0.13	0.16	0.18
5500	RC	95	2	0.791	0.12	0.14	0.18

RC- DWPF Recycle Simulant; IW - Inhibited Water

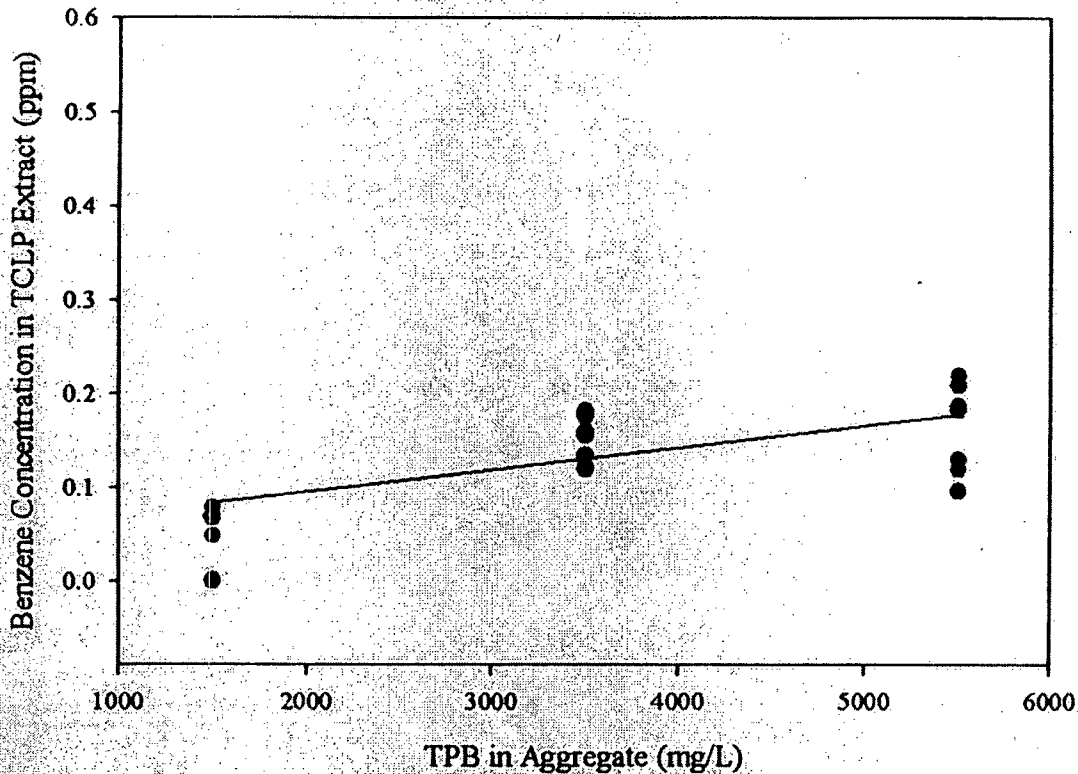


Figure 3-1. Benzene measured in the TCLP extracts for the TPB aggregates.

3.11.2 Semi-Volatile Organic Compound (SVOC) Analysis

TCLP extractions were performed and extracts were analyzed as described in Sections 2.5 and 2.5.2. The analysis for nitrobenzene for all of the samples was below the detection limits of the analytical method, 0.5 mg/L. The RCRA limit for nitrobenzene in TCLP extracts from Table 2-5 is 2.0 mg/L. Therefore all of the samples passed the TCLP for nitrobenzene.

3.11.3 Metals Analysis

TCLP extractions were performed and extracts were analyzed as described in Sections 2.5 and 2.5.2. The analysis for mercury (CV-AA) was performed only on samples that had the potential to be hazardous for mercury (i.e., Aggregates that were prepared with DWPF recycle simulant). Results for all of the samples analyzed were below the detection limits of the analytical method, 0.11 mg/L. The RCRA limit for mercury in TCLP extracts from Table 2-5 is 0.2 mg/L. Therefore all of the samples passed the TCLP for mercury.

3.12 Ignitability Determination of Fresh Saltstone Slurry

Four replicate samples submitted to SRNL-ADS for flash point testing were analyzed using a closed cup flash point tester. The Saltstone slurry made with the 5500 mg/L aggregate of Tank 48H simulant and DWPF recycle simulant was prepared and tested as described in Section 2.6 and sampled to make the four replicates. A dodecane standard (flash point 71 °C/160 °F) was analyzed prior to the first replicate and after the final replicate. Each replicate was tested a single time. The analysis of the Saltstone slurry began

approximately 20 minutes after the slurry was prepared and analysis continued for an additional 75 minutes. None of the four replicates exhibited a flash point below 100 °C, where the testing was terminated. Table 3-3 is the results of the flash point tests for the four replicates and two standards.

Table 3-3. Flash Point Results using a Closed Cup Tester.

Sample	Elapsed Time from Casting (min)	Flash Point (°C/°F)
Dodecane	10	79/174
5500 mg/L with DWPF Recycle-1	21	No Flash
5500 mg/L with DWPF Recycle-2	39	No Flash
5500 mg/L with DWPF Recycle-3	55	No Flash
5500 mg/L with DWPF Recycle-4	71	No Flash
Dodecane	86	81/178

3.13 Ignitability Determination of Cured Saltstone

The Saltstone slurry made with the 5500 mg/L aggregate of Tank 48H simulant and DWPF recycle simulant was prepared and tested as described in Section 2.7. The two replicate samples were exposed to an open flame for two minutes and it was determined that the samples were not ignitable, Figure 3-2.

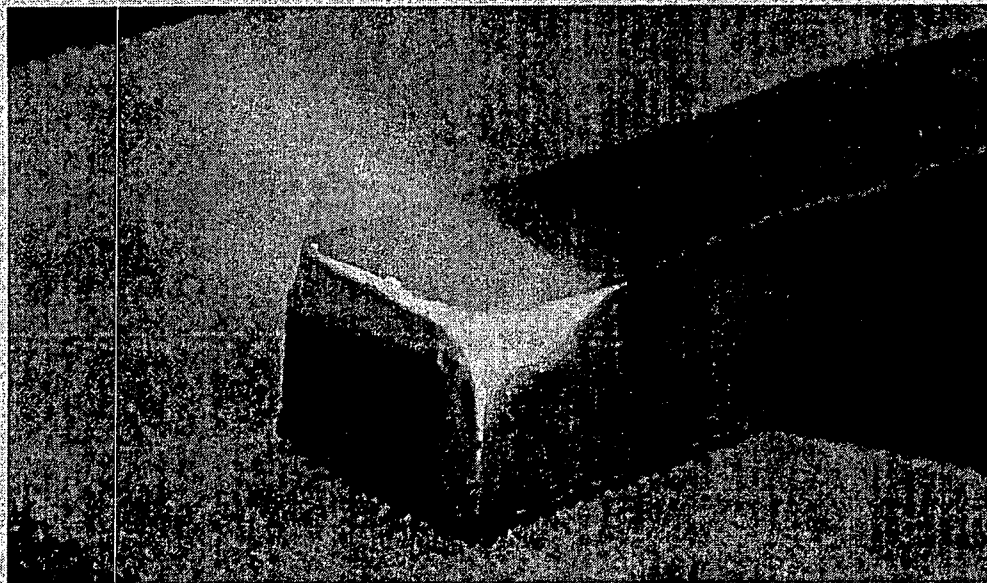


Figure 3-2. Ignitability test of cured Saltstone.

This page intentionally left blank.

4.0 CONCLUSIONS AND RECOMMENDATIONS

- Aggregates were prepared with Tank 48H material and either DWPF recycle simulant or inhibited water with concentrations of 1500, 3500, and 5500 mg/L TPB.
- Air entrainment caused by the mixing of the aggregate in the slurry preparation method used produced a stable structure that led to premature gelation of the slurries that required admixtures for remediation.
- Processable Saltstone slurry formulations were demonstrated with Tank 48H material and both DWPF recycle simulant and inhibited water with concentrations of 3500, and 5500 mg/L TPB. It is expected that acceptable formulation can be prepared with aggregates of 1500 mg/L TPB. Table 4-1 is the recommended initial processing parameters for the six aggregates tested.

Table 4-1. Recommended Initial Processing Parameters for Tank 48H Aggregates.

TPB (mg/L)	Water/Premix	Set Retarder (Wt %)	Antifoam (Wt %)
1500	0.60-0.63	0.1-0.2	0.1
3500	0.65	0.2	0.15
5500	0.65	0.30	0.15-0.2

- Analysis of the TCLP extracts of the Saltstone prepared from the six aggregates indicates that the resulting Saltstone is not hazardous for benzene, nitrobenzene, or mercury.
- Testing of the fresh Saltstone slurry and cured Saltstone prepared with simulants indicate that the neither the fresh nor cured Saltstone is hazardous for ignitability.
- After transferring Tank 48H material to Tank 50 and prior to processing through the SPF, Tank 50 should be sampled to verify processability with the recommended processing parameters in Table 4-1.

This page intentionally left blank.

5.0 REFERENCES

1. Maxwell, D., Barnes, M. J., and Lambert, D. P., *Tank 48H Disposition and Return to Service Research and Development Plan*, CBU-SPT-2004-00144, Rev. 0, (2004).
2. Swingle, R.F., *Results of Analyses of Tank 23H and 24H Saltstone WAC Samples HTK-521 – HTK-528*, SRT-LWP-2003-00008, January 2003.
3. Lambert, D.P., Peters, T.B., Stallings, M.E., and Fink, S.D., *Analysis of Tank 48H Samples HTF-E-03-73 (June 03, 2003) and HTF-E-03-127 (September 17, 2003)*, WSRC-TR-2003-00720, Revision 0 (2003).
4. Lambert, D.P., *Tank 48H Simulant Recipe Development and Documentation*, SRT-LWP-2004-00042, Rev. 1 June (2004)
5. EPA Manual SW-846 Method 1311, *Toxic Characteristic Leaching Procedure*, Rev. 0, (1992).
6. Ferrara, D.F., Cozzi, A.D., Langton, C.A., and Clark, J., *Tank 41H Saltstone Regulatory Analyses*, WSRC-TR-2004-00051, Rev. 0, (2004).
7. Lambert, D.P. *Tank 48H Simulant Validation*, SRNL-LWP-2004-00009, (2004).
8. Baich, M.A., Lambert, D.P. and Monson, P.R., *Laboratory Scale Antifoam Studies for the STTPB Process (U)*, WSRC-TR-2000-00261, Rev. 0, (2000).

This page intentionally left blank.

6.0 ACKNOWLEDGEMENTS

The author would like to thank: Chris Langton, Dan Lambert, Mark Barnes, and Mike Hay for technical guidance and review of the data; Maurice Lee, Phyllis Burkhalter and Dee Wheeler of the SRNL Shielded Cells for preparing the Saltstone slurries and performing the TCLP extractions; and Chuck Coleman, Steve Crump, and John Young of SRNL-ADS for taking an active interest in the sampling and analysis of the TCLP extracts.

**APPROVED for Release for
 Unlimited (Release to Public)
 6/23/2005**

Task Title Isopar L Release Rates from Saltstone		TTR Number: SSF-TTR-2005-0004 Rev.1	TTR Date: 5/24/2005
Task Leader A.D. Cozzi	Signature:	Organization: SRNL/ITS	Date:
Task Leader M.G. Bronikowski	Signature:	Organization: SRNL/ATS	Date:
Technical Reviewer (if required): M.S. Hay	Signature:	Organization: SRNL/WPT	Date:
Level 3 Manager (or designee): D.A. Crowley	Signature:	Organization: SRNL/ITS	Date:
Waste Solidification Engineering: J.E. Occhipinti	Signature:	Organization: CBU/WSE	Date:
ITS QA Coordinator: T.K. Snyder	Signature:	Organization: SRNL/ITS	Date:
SRNL QA Representative: J.P. Vaughan	Signature:	Organization: SRNL-QA	Date:

Distribution:

M.G. Bronikowski, 773-A	J.C. Marra, 773-42A
T.E. Chandler, 704-Z	J.E. Marra, 773-A
D.T. Conrad, 766-H	S.L. Marra, 999-W
A.D. Cozzi, 773-43A	D. Maxwell, 766-H
D.A. Crowley, 773-A	M.A. Norato, 704-S
W.B. Dean, 766-H	J.E. Occhipinti, 704-S
J.M. Duffey, 773-A	M.A. Rios-Armstrong, 766-H
R.W. Dunn, 773-A	S.J. Robertson, 766-H
R.E. Eibling, 999-W	B.C. Rogers, 766-H
S.D. Fink, 773-A	S.C. Shah, 766-H
F.F. Fondeur, 773-A	D.C. Sherburne, 704-S
R.C. Fowler, 703-H	J.A. Smith, 704-29S
J.C. Griffin, 773-A	T.K. Snyder, 999-W
J.R. Harbour, 773-42A	R.H. Spires, 766-H
M.S. Hay, 773-42A	A.V. Staub, 704-28S
E.W. Holtzscheiter, 773-A	P.C. Suggs, 766-H
T.M. Jones, 999-W	D.G. Thompson, 704-Z
D.P. Lambert, 773-A	J.P. Vaughan, 773-41A
C.A. Langton, 773-43A	W.R. Wilmarth, 773-42A
T.D. Lookabill, 704-27S	J.R. Zamecnik, 773-41A

Revision Number:	Page Number:	Date:	Revision:
0	All	5/27/05	Original Issue

I. INTRODUCTION

The Saltstone Production Facility (SPF) will receive the Decontaminated Salt Solution (DSS) stream from the Modular CSSX Unit (MCU) and the Salt Waste Processing Facility (SWPF). These streams are expected to contain entrained solvent. Recent information on the solvent droplet size in the DSS stream indicates that the drops will be smaller than assumed in the MCU decanter design basis. Therefore, the amount of expected carryover has increased. The higher solvent concentration in the MCU exit stream may cause flammability concerns in the SPF. The release rates of the volatile solvent components, Isopar L and Trioctylamine (TOA), are to be studied in saltstone in order to assess possible flammability issues in the saltstone vault.

NFPA 69 requires the flammable material concentration to be below 25% LFL in the vapor space of the vault if no safety interlocks are installed. If all of the Isopar L is released instantaneously into the vault vapor space when placing saltstone slurry, the allowable Isopar L concentration in the DSS is 4 ppm. If the release rate is not instantaneous, but slower due to TOA and grout interactions, the acceptable limit of entrained solvent could be significantly higher than 4 ppm. As the maximum expected Isopar L concentration in the DSS sent to SPF under normal process conditions was determined through small scale testing at the Savannah River National Laboratory (SRNL) to be 88 ppm,¹ determining the Isobar L release rate from saltstone is imperative.

SRNL was asked to determine the bounding Isopar L release rates from curing grout at various temperatures expected in the saltstone vault.² The release rates will be determined from saltstone prepared with a simulated DSS solution containing Isopar L concentrations ranging from 20 ppm to 200 ppm and the expected ratio of TOA to Isopar L to be used in the saltstone process. The rates are to be determined at 95 °C, 75 °C, and 25 °C.

A. Task Definition

Simulated DSS will be prepared as an "average salt solution" as described in WSRC-RP-2000-00361, Rev. 0 with minimal component omission. CsCl will not be added to the DSS as per the customer request.² The soluble metals and organic components may be removed from the recipe with customer concurrence. It may be useful to exclude Hg due to its small concentration and volatility. Excluding the organic components will theoretically increase the vapor pressure of the Isopar L and hence lead to a more conservative estimate. However, the organics may help with the mixing of the Isopar L/TOA solution with the simulated DSS and saltstone. Trimethylamine (TMA) could be excluded due to its small concentration, volatility, and low Threshold limit Value (TLV). Additionally, the TOA interaction with saltstone would be representative of the TMA interaction as it behaves in a chemically similar manner to TMA but has a lower volatility.

Saltstone will be prepared using the simulated DSS and premix materials obtained from the SPF. The premix composition and water to premix ratio to be used will be based on recommendations made in previous testing and are listed in Table 1. The water to premix ratio is the ratio of the mass of evaporable water from the waste (at -110 °C) to the combined mass of the cement, slag, and fly ash. The initial concentrations of Isopar L of 20 ppm, 50 ppm, 100 ppm, and 200 ppm will be tested. The 100 ppm concentration corresponds to the maximum expected amount in the DSS from MCU.¹ An initial scoping test at the 20 ppm and 50 ppm concentration will be used to determine the lowest Isopar L concentration to be studied. Three temperatures, 95 °C, 75 °C, and 25 °C will be investigated to cover the temperature variability in saltstone processing and curing.

Table 1. Formulations for Processing.³

Premix	Water/Premix
45% Class F Fly Ash (FA) 45% GGBFS* (Slag) 10% Cement	0.60

*Ground granulated blast furnace slag

Table 2. Test Conditions.

	Isopar L (mg/L)	Curing Temperature (°C)
• Salt Solution	• 20 or 50 • 90 • 200	• 25 • 75 • 95

Part I: Develop Methodology for Sampling and Analysis for Isopar L and TOA During Saltstone Curing.

The method developed for studying the benzene evolved during saltstone curing is expected to be used.⁵ The benzene method⁶ is to capture the offgas from a saltstone sample using a charcoal tube while the sample cures. The charcoal tube with the captured component will be stripped of the component with CS₂ and analyzed by GC-MS. A minor amount of work is expected in order to adapt and quantify this method for Isopar L and TOA. If TOA is not captured well enough a secondary collection tube with a different absorbent (i.e. a sulphuric acid treated carbon) may be added. Both Isopar L and TOA are less volatile than benzene. Thus, they are expected to offgas at a lesser rate than benzene. If the release rate is too slow another method with a lower detection limit will be determined.

The evaporation rate for Isopar/TOA will be determined prior to making saltstone samples. Evaporation rate tests with Isopar L, Isopar L/TOA, and Isopar L/TOA in salt simulant will be performed. The evaporation rate will be determined by weight loss and/or long path cell IR spectroscopy. With this information, a decision on the proper analytical method with a suitable lower limit of detection can be made.

Part II: Validate Methodology for Sampling and Analysis for Isopar during Curing of Saltstone with Simulants and determine Isopar L/TOA concentration.

Saltstone samples will be prepared with the materials given in Table 1, Isopar L and TOA, and the simulated DSS solution. The methodology developed in Part I for sampling and analysis will be validated for the saltstone samples. The saltstone produced will be cast into 2 inch diameter, 4 inch high vessels which have a large filling port and smaller input and output ports. The vessels are the similar to those used in the benzene study and can be purged with air continuously or closed for batch headspace sampling.

Saltstone samples will be cured at the three temperatures listed in Table 2 and the Isopar L and TOA offgas concentrations, as functions of time and temperature will be determined. The Isopar L and TOA from the headspace of the vessel will be collected and sampled at various intervals. The initial frequency for collection of samples for analysis is 1, 3, 7, and 14 days. Sample frequency will be adjusted as necessary to reflect the Isopar L generation rates found. Samples will be taken for at least 60 days at temperature. Sampling can continue on cooled samples for a time to be agreed upon by the customer.

B. Customer/Requester

Waste Solidification Engineering funds the work in this task. The scope of the work is established in Technical Task Request SSF-TTR-2005-0004 Rev.0. The customer contact is M.A. Norato.

This task consists of baseline R&D activities as determined by the Savannah River National Laboratory (SRNL) Procedure L1-7.10, "Control of Technical Work," Revision 4.

C. Task Responsibilities

SRNL/ITS/ATS: A.D. Cozzi and M.G. Bronikowski are responsible for the direction and completion of this task. This includes implementation of the SRNL Conduct of Research and Development¹ prior to initiating lab work, adhering to this Task Technical and Quality Assurance Plan, and providing updates of progress to the customer.

SRNL/ITS/WPT: R.E. Eibling, F.F. Fondeur, and M.S. Hay are responsible for providing guidance for the development of experiments, providing guidance for sample and analytical control, and participating in interpretation of analytical results.

WSE: J.E. Occhipinti (or designee) is responsible for providing Waste Solidification Engineering (WSE) concurrence and facilitating interface, as necessary, with Planning, Integration and Technology.

SRNL/ITS/ATS: M.F. Williams, J.G. Wheeler, and S.J. Emory (or designees) are responsible technician designation and for sample preparation.

SRNL/QA: J.P. Vaughan is responsible for reviewing and approving this Task Technical and Quality Assurance Plan and providing guidance and oversight for this work.

ITS QA Coordinator: T.K. Snyder is responsible for reviewing task plans related to this task, assisting in the preparation of records, coordinating surveillances associated with this task, and interfacing with SRNL/QA during overview activities and corrective actions.

D. Task Deliverables

1. Technical Task and Quality Assurance Plan (this document) outlining the objective of the tasks and the associated activities.
2. Interim results and updates as requested by WSE.
3. Technical report detailing results of the activities associated with these tasks.

II. TASK ACCEPTANCE CRITERIA

Acceptance testing is not an element of this task. Per the TTR, issuance and customer approval of the technical report will complete this task.

III. TASK ACTIVITIES

1. Prepare Task Technical and Quality Assurance Plan: Develop task plan, complete conduct of R&D.
2. Prepare DSS Simulant: Simulants will be prepared to represent the DSS streams to contain the requisite concentrations of Isopar L and TOA.
3. Prepare Saltstone: Saltstone will be prepared using Z-Area premix materials with a water to premix (w/c) ratio of 0.60³.

4. **Part I: Develop Test Methodology:** A series of scoping tests will be performed to determine if the benzene methodology can be used for measurement of Isopar L and TOA given off in saltstone curing under various conditions. The scoping tests will include an evaporation rate test of Isopar L and TOA.
5. **Part II: Validate Methodology with Simulants and Determine Isopar L Concentrations:** Saltstone samples prepared from simulated wastes will be cured at various temperatures to ensure that the test/analytical methodologies are valid with the saltstone present and to determine the concentration of the Isopar L and TOA given off while curing.
6. **Document Results:** The results of the task will be documented in a technically reviewed report and issued with WSE concurrence.

IV. TASK SCHEDULE

A detailed schedule of task activities and associated durations is located in the ITS Support Schedule of Activities. The schedule is updated weekly. Activities will be performed in parallel when applicable.

V. RESEARCH FACILITY PLANNING

1. **Products and By-Products.** Approved waste streams will dispose of all job control waste. By-products generated at:
 - the Aiken County Technical Laboratory will be disposed of in accordance with SRNL Manual L1 procedure 5.05 "ACTL Residue Management."
 - By-products generated at the SRNL will be disposed of in accordance with SRNL Manual L1, 6.0 waste disposition procedures.
2. **Disposition of Test Equipment.** All of the equipment procured for and used in this study will be available for future use.

VI. PROGRAMMATIC RISK REVIEW

Risk	Impact	Mitigation
Isopar L and TOA generation and collection method is unacceptable.	Cannot generate or measure Isopar L and TOA.	Evaluate several methods for generation and collection of Isopar L.
Isopar L and TOA measurements of standards are not precise.	Reported results will be less precise.	Evaluate several approaches to optimize precision.
Isopar L and TOA not detectable in Part II testing at lower temperatures.	Cannot estimate long term concentration of Isopar L or TOA or its possible buildup.	Extend Part II until Isopar L and TOA is detectable. 1) Raise lower temperature. 2) Estimate time by Arrhenius plot.
Isopar L and TOA not detectable in Part II testing.	Cannot generate or measure Isopar L and TOA.	Find a method with a lower limit of detection or increase concentration of Isopar L in saltstone.
IR spectrometer fails.	Cannot initiate experiments.	Two IR spectrometers are present for use.

Risk	Impact	Mitigation
Gas chromatograph fails.	Inability to analyze samples.	Second GC will be procured after Stage I testing. SRNL-Analytical Development Section maintains a GC/mass spectrometer that may be used.
Oven fails	Samples could cool significantly altering the amount of cure time at temperature.	Possible use of ovens at ACTL for short time duration while oven is being fixed.
Loss of key personnel.	Activities are delayed and schedule will slip.	Cross train current team members and increase team numbers.
Isopar L and TOA collection methods have not been demonstrated at elevated temperatures.	High temperature data not reliable or available.	Use high temperature rated materials where available. Teflon will be used and solvent interaction is noted for connectors. Qualify materials not rated for temperature when possible.
Power interruptions during testing.	Samples could cool significantly altering the amount of cure time at temperature.	Simulant testing – Outage would be limited to 60 h.
Operations interruptions delay sampling or shipping of samples to ACTL.	Samples unavailable for analysis.	Remove samples as generated. Use samplers with storage ratings > 7 days. Have coolant (dry ice) available for temporary refrigeration of samples.

VII. R&D HAZARDS SCREENING CHECKLIST

The hazards of this work were identified using the hazards screening checklist of the SRNL Conduct of Research and Development Manual.⁴ Figure 3, the "R&D Hazards Screening Checklist," is on file with the Task Lead.

VIII. REFERENCES

1. "Examination of Organic Carry over from 2-cm Contactors to Support the Modular CSSX Unit" C.A. Nash et al., WSRC-TR-2005-0018, Rev. 0, (2005).
2. "Determine Isopar L Release Rates from Saltstone," SSF-TTR-2005-0004, Rev. 0, (2005).
3. "Formulation Development for Processing Tank 48H in Saltstone," A.D. Cozzi, WSRC-TR-2004-00477, Revision 0 (2004).
4. "SRNL Conduct of Research and Development," WSRC-IM-97-00024, Rev. 3, (2004).
5. "Measurements of Flammable Gas Generation from Saltstone Containing Simulated Tank 48H Waste (Interim Report)" WSRC-TR-2005-00180, Revision 0, A.D. Cozzi, et al., April 2005.
6. "NIOSH Method 1501 issue 3, Aromatic Hydrocarbons", NIOSH Manual of Analytical Methods (NIMAM), 4th edition Mar. 15, 2003.

IX. QA Plan Checklist

The following QA Procedures apply for this task (indicate Yes, No or "AR" - as required). Current revision of the procedure will be used. The QA controls are the procedures identified on the checklist. If the procedures on the matrix are changed, applicable procedures will be followed.

Yes	No	AR	
			1-0 ORGANIZATION
X			1Q, QAP 1-1, Organization
X			L1, 1.02, SRNL Organization
		X	1Q, QAP 1-2, Stop Work
			2-0 QUALITY ASSURANCE PROGRAM
X			1Q, QAP 2-1, Quality Assurance Program
X			L1, 8.02, SRNL QA Program Clarifications, Attachment 8.2-1
X			1Q, QAP 2-2, Personnel Training & Qualification
X			L1, 1.32, Read & Sign
X			1Q, QAP 2-3, Control of Research & Development Activities
X			L1, 8.02, SRNL QA Program Clarifications, Attachment 8.2-3
X			L1, 7.10, Control of Technical Work
X			L1, 7.16, Laboratory Notebooks & Logbooks
	X		1Q, 2-4 Auditor/Lead Auditor Qualification & Certification - does not apply to Immobilization Technology Section Tasks
	X		1Q, 2-5 Qualification & Certification of Independent Inspection Personnel - does not apply to Immobilization Technology Section Tasks
X			1Q, QAP 2-7, QA Program Requirements for Analytical Measurement Systems
			3.0 DESIGN CONTROL
	X		1Q, QAP 3-1, Design Control
	X		L1, 7.10, Control of Technical Work
			4-0 PROCUREMENT DOCUMENT CONTROL
		X	1Q, QAP 4-1, Procurement Document Control
		X	E7, 3.10, Determination of Quality Requirements for Procured Items
		X	7B, Procurement Management Manual (For Reference Only)
		X	3E, Procurement Specification Manual (For Reference Only)
			5-0 INSTRUCTIONS, PROCEDURES & DRAWINGS
X			1Q, QAP 5-1, Instructions, Procedures & Drawings
	X		E7, 2.30, Drawings
X			L1, 1.01, SRNL Procedure Administration
			6-0 DOCUMENT CONTROL
X			1Q, QAP 6-1, Document Control
X			1B, MRP 3.32, Document Control

Yes	No	AR	
			7-0 CONTROL OF PURCHASED ITEMS & SERVICES
		X	1Q, QAP 7-2, Control of Purchased Items & Services
		X	7B, Procurement Management Manual (for reference)
		X	3E, WSRC Procurement Specification Manual (for reference)
X			1Q, QAP 7-3, Commercial Grade Item Dedication
X			E7, 3.46, Replacement Item Evaluation/Commercial Grade Item Dedication
			8-0 IDENTIFICATION & CONTROL OF ITEMS
		X	1Q, QAP 8-1, Identification & Control of Items
		X	L1, 8.02, SRNL QA Program Clarifications, Attachment 8.8-1
X			9-0 CONTROL OF PROCESSES - does not apply to Immobilization Technology Section Tasks
			10-0 INSPECTION & VERIFICATION
X			1Q, QAP 10-1, Inspection & Verification
X			L1, 8.10, Inspection
			11-1 TEST CONTROL
X			1Q, QAP 11-1, Test Control
			12-1 CONTROL OF MEASURING & TEST EQUIPMENT
X			1Q, QAP 12-1, Control of Measuring & Test Equipment
	X		1Q, QAP 12-2, Control of Installed Process Instrumentation
	X		1Q, QAP 12-3 Control & Calibration of Radiation Monitoring Equipment - does not apply to Immobilization Technology Section Tasks
			13-0 PACKAGING, HANDLING, SHIPPING & STORAGE
		X	1Q, QAP 13-1, Packaging, Handling, Shipping & Storage
		X	L1, 8.02, SRNL QA Program Clarifications, Attachment 8.13-1
			14-0 INSPECTION, TEST & OPERATING STATUS
		X	1Q, QAP 14-1, Inspection, Test & Operating Status
		X	L1, 8.02, SRNL QA Program Clarifications, Attachment 8.14-1
			15-0 CONTROL OF NONCONFORMING ITEMS/ACTIVITIES
		X	1Q, QAP 15-1, Control of Nonconforming Items
		X	L1, 8.02, SRNL QA Program Clarifications, Attachment 8.15-1

Yes	No	AR	
		X	1B, MRP 4.23, Site Tracking Analysis and Reporting (STAR)
			16-0 CORRECTIVE ACTION SYSTEM
		X	1Q, QAP 16-3, Corrective Action Program
		X	1.01, MP 5.35, Corrective Action Program
		X	1B, MRP 4.23, Site Tracking Analysis and Reporting (STAR)
			17-0 QA RECORDS MANAGEMENT
X			1Q, QAP 17-1, QA Records Management
X			L1, 8.02, SRNL QA Program Clarifications, Attachment 8.17-1
X			L1, 7.16, Laboratory Notebooks & Logbooks
			18-0 AUDITS
		X	1Q, QAP 18-2, Quality Assurance Surveillance
		X	L1, 8.18.1, SRNL Surveillances
	X		1Q, QAP 18-3, Quality Assurance External Audits
		X	1Q, QAP 18-4, Management Assessments
		X	12Q, Assessment Manual
		X	1Q, QAP 18-6, Quality Assurance Internal Audits
	X		1Q, QAP 18-7, Quality Assurance Supplier Surveillance
			19-0 QUALITY IMPROVEMENT
		X	1Q, QAP 19-2, Quality Improvement
		X	L1, 8.02, SRNL QA Program Clarifications, Attachment 8.19-2
			20-0 SOFTWARE QUALITY ASSURANCE
	X		1Q, QAP 20-1, Software Quality Assurance
	X		L1, 8.20, Software Management & Quality Assurance
	X		21-1 ENVIRONMENTAL QUALITY ASSURANCE - does not apply to Immobilization Technology Section Tasks
			In addition to procedures noted above, if RW-0333P requirements are invoked, the following procedures apply. These procedures may also apply at the discretion of the Task Leader to non-RW-0333P tasks.
	X		L1, 8.21, Supplemental QA Requirements for DOE/RW-0333P
			Sample Control:
		X	L1, 7.15, Obtaining Analytical Support
			Scientific Investigation:

Yes	No	AR	
X			L1, 7.16, Laboratory Notebooks & Logbooks

X. Identify any exceptions or additions to the procedures listed in the QA Matrix:

DOE RW-0333P requirements do not apply to the work in this study.

WSRC-IM-2002-00011, "Technical Report Design Check Guidelines," will be used to help ensure the quality and consistency of the technical review process for technical reports produced by SRNL Waste Treatment Technology.

XI. Complete this part only if Section 20 procedures (software) are invoked. Identify who will act in each of the following capacities. If Section 20 is N/A, mark these N/A.

Owner: N/A
 Designer: N/A
 Maintainer: N/A
 Tester: N/A

XII. Document Approval:

Identify documents requiring management, customer or CQF approval

Document	Management		Customer		CQF	
	Yes	No	Yes	No	Yes	No
Task Technical & QA Plan	X		X		X	
Final Report (customer may review draft)	X		X			X

XIII. Anticipated Records:

The following records are anticipated from this task. Indicate Yes, No or AR (as required):

Yes	No	AR	Description
X			Task Technical & QA Plan
X			Technical Notebooks
X			Task Technical Reports
	X		Data Qualification Reports
		X	Supporting Documentation

XIV. ATTACHMENTS:

N/A

CBU-PIT-2004-00012 ←
REVISION 0

KEYWORDS:
Tank 48, Salt Program
Saltstone

RETENTION: PERMANENT
CLASSIFICATION: U

Tank 48 Disposition Project Flowsheet for Aggregation Strategy 0.2 Ci/gal Cesium Max Feed

R. C. Fowler

APPROVED for Release for
Unlimited (Release to Public)
6/23/2005

Westinghouse Savannah River Company
Closure Business Unit
Planning Integration & Technology Department
Aiken, SC 29808

Prepared for U. S. Department of Energy Under Contract No. DE-AC09-96S

Summary

Tank 48 currently does not comply with the general Tank Farm safety requirements for organic content due to the presence of tetraphenylborate (TPB), and has been isolated from routine Tank Farm service since the shutdown of In-Tank Precipitation (ITP) process in late 1998. To restore Tank 48 to Tank Farm service, the TPB inventory must be removed or reduced to a level that meets the Tank Farm Documented Safety Analysis² (DSA) requirements. The Aggregation strategy consists of combining Tank 48 material with Defense Waste Processing Facility (DWPF) recycle material in both Tank 48 and Tank 50, with its final disposal in the Saltstone Facility as low level waste (LLW) in a grout waste form. The aggregated material in Tank 50 will meet the Saltstone Facility Waste Acceptance Criteria (WAC) prior to its transferring to the Saltstone Facility, including the maximum limits of 0.2 Ci/gal for Cesium-137 (Cs-137), 9.60E-04 Ci/gal^{6,7} for alpha concentration, and revised TPB concentration limit at the time of the aggregation processing. In addition, the free hydroxide concentration of the aggregated material will be maintained greater than 1.0 molar to minimize decomposition of TPB into benzene. This option also requires modification to the Saltstone Waste Acceptance Criteria to permit higher concentrations of tetraphenylborate (up to 3,000 mg/L from the current 30 mg/L).

Two cases were developed based on the current fill level of Tank 48. During the Tank 48 processing history the liquid reached a level of nearly 150 inches. This processing left residual film potentially containing TPB solids behind on the tank internal walls and components¹. To ensure that no significant residual TPB remains on the walls or tank internal structures, the tank level will be raised above 150 inches. In Case 1, the level in Tank 48 is raised above 150 inches a single time. In Case 2, the level is raised above 150 inches on two separate occasions (Batch 1 and Batch 4). While Case 2 requires more total batches to complete the TPB removal from Tank 50, it takes only 28 batches to reach the endpoint in Tank 48 versus the 31 batches needed in Case 1. Fluid totals for the two Aggregation cases are presented in Table 1.

Table 1 Material Volumes Used for Aggregation Flowsheet Cases

Streams (Kgal)	Case 1 (single rinse)	Case 2 (double rinse)
DWPF Recycle	3,405	4,099
NaOH (50 wt%)	162	195
ETP/HEU [†]	619	796
Total Addition Volumes	4,186	5,090

[†] The HEU and ETP project will transfer streams to Tank 50 and then Saltstone co-incident with the Aggregation process, but are independent of the Tank 48 Aggregation project.

APPROVED for Release for
Unlimited (Release to Public)

Caustic-Side Solvent Extraction: Chemical and Physical Properties of the Optimized Solvent

October 2002

Prepared by

Lætitia H. Delmau ←

Joseph F. Birdwell, Jr.

Peter V. Bonnesen

Linda J. Foote

Tamara J. Haverlock

Leon N. Klatt

Douglas D. Lee

Ralph A. Leonard

Tatiana G. Levitskaia

Michael P. Maskarinec

Bruce A. Moyer

Frederick V. Sloop, Jr.

Bruce A. Tomkins

DOCUMENT AVAILABILITY

Reports produced after January 1, 1996, are generally available free via the U.S. Department of Energy (DOE) Information Bridge:

Web site: <http://www.osti.gov/bridge>

Reports produced before January 1, 1996, may be purchased by members of the public from the following source:

National Technical Information Service
5285 Port Royal Road
Springfield, VA 22161
Telephone: 703-605-6000 (1-800-553-6847)
TDD: 703-487-4639
Fax: 703-605-6900
E-mail: info@ntis.fedworld.gov
Web site: <http://www.ntis.gov/support/ordernowabout.htm>

Reports are available to DOE employees, DOE contractors, Energy Technology Data Exchange (ETDE) representatives, and International Nuclear Information System (INIS) representatives from the following source:

Office of Scientific and Technical Information
P.O. Box 62
Oak Ridge, TN 37831
Telephone: 865-576-8401
Fax: 865-576-5728
E-mail: reports@adonis.osti.gov
Web site: <http://www.osti.gov/contact.html>

This report was prepared as an account of work sponsored by an agency of the United States Government. Neither the United States government nor any agency thereof, nor any of their employees, makes any warranty, express or implied, or assumes any legal liability or responsibility for the accuracy, completeness, or usefulness of any information, apparatus, product, or process disclosed, or represents that its use would not infringe privately owned rights. Reference herein to any specific commercial product, process, or service by trade name, trademark, manufacturer, or otherwise, does not necessarily constitute or imply its endorsement, recommendation, or favoring by the United States Government or any agency thereof. The views and opinions of authors expressed herein do not necessarily state or reflect those of the United States Government or any agency thereof.

**CAUSTIC-SIDE SOLVENT EXTRACTION :
CHEMICAL AND PHYSICAL PROPERTIES OF THE OPTIMIZED SOLVENT**

Lætitia H. Delmau, Joseph F. Birdwell, Jr., Peter V. Bonnesen, Linda J. Foote,
Tamara J. Haverlock, Leon N. Klatt, Douglas D. Lee, Ralph A. Leonard, Tatiana G. Levitskaia,
Michael P. Maskarinec, Bruce A. Moyer, Frederick V. Sloop, Jr., and Bruce A. Tomkins

Date Published: October 2002

Prepared by
OAK RIDGE NATIONAL LABORATORY
P.O. Box 2008
Oak Ridge, Tennessee 37831-6285
managed by
UT-Battelle, LLC
for the
U.S. DEPARTMENT OF ENERGY
under contract DE-AC05-00OR22725

CONTENTS

	Page
LIST OF FIGURES	vii
LIST OF TABLES	ix
EXECUTIVE SUMMARY	1
ABSTRACT	3
1. INTRODUCTION.....	3
2. CAUSTIC-SIDE SOLVENT EXTRACTION SOLVENT COMPOSITION RECOMMENDATION	5
2.1 BASIS FOR TASK AND SUMMARY RECOMMENDATION	5
2.2 EXPERIMENTAL APPROACHES	7
2.2.1 Solvent Test Samples.....	7
2.2.2 Experimental Procedures.....	8
2.2.2.1 BOBCalixC6 solubility studies.....	8
2.2.2.2 Extraction, scrub, and strip protocol.....	8
2.2.2.3 Third-phase determination	9
2.2.2.4 Dispersion-number measurement.....	9
2.2.2.5 Density.....	10
2.2.2.6 Viscosity	10
2.2.2.7 Surface tension and interfacial tension.....	11
2.3 EXPERIMENTAL RESULTS	12
2.3.1 BOBCalixC6 Solubility.....	12
2.3.2 Cesium Distribution Results.....	17
2.3.3 Flowsheet Robustness.....	19
2.3.4 Third-Phase Formation.....	21
2.3.5 Solvent Dispersion Numbers.....	22
2.3.6 Solvent Density.....	24
2.3.7 Solvent Viscosity.....	26
2.3.8 Solvent Interfacial Tension	29
2.4 SOLVENT-COMPOSITION RECOMMENDATION PROCESS	32
3. CESIUM DISTRIBUTION BEHAVIOR	35
3.1 INTRODUCTION.....	35
3.2 EXPERIMENTAL SECTION	35
3.3 RESULTS AND DISCUSSION	35
3.3.1 Extraction, Scrub, and Strip Performance.....	35
3.3.2 Temperature Variation.....	36
3.3.3 Multicycle Behavior.....	39
3.4 CONCLUSIONS	39
4. PARTITIONING OF SOLVENT COMPONENTS	41
4.1 INTRODUCTION.....	41
4.2 EXPERIMENTAL SECTION	41

4.2.1	Material and Contacting Method.....	41
4.2.2	Calixarene and Modifier Analyses.....	42
4.2.3	Tri- <i>n</i> -octylamine Analyses.....	43
4.3	RESULTS AND DISCUSSION.....	44
4.3.1	Calixarene Partitioning.....	44
4.3.2	Modifier Partitioning.....	44
4.3.3	Tri- <i>n</i> -octylamine Partitioning.....	45
4.4	CONCLUSIONS.....	46
5.	DISTRIBUTION OF MINOR ORGANIC AND INORGANIC COMPONENTS.....	49
5.1	INTRODUCTION.....	49
5.2	EXPERIMENTAL SECTION.....	49
5.3	RESULTS AND DISCUSSION.....	51
5.3.1	Distribution of Dibutylphosphate.....	51
5.3.2	Distribution of Other Metals and Selected Radionuclides.....	51
5.3.3	Effect of Organic Surfactants.....	54
5.4	CONCLUSIONS.....	55
6.	THERMAL STABILITY.....	57
6.1	INTRODUCTION.....	57
6.2	EXPERIMENTAL SECTION.....	57
6.2.1	Materials, Equipment, and Contacting Method.....	57
6.2.2	ESS Analyses of Phase-Stability Samples.....	58
6.2.3	HPLC Analyses of Phase-Stability Samples.....	59
6.3	RESULTS AND DISCUSSION.....	59
6.3.1	Phase Stability at Low Temperature.....	59
6.3.2	Chemical Stability at High Temperature.....	64
6.4	CONCLUSIONS.....	64
7.	PHYSICAL-PROPERTIES MEASUREMENTS.....	67
7.1	INTRODUCTION.....	67
7.2	EXPERIMENTAL PROCEDURES.....	67
7.2.1	Chemicals.....	67
7.2.2	Determination of Dispersion Number.....	68
7.2.3	Laboratory Dispersion-Number Procedures.....	69
7.3	DISPERSION-NUMBER DETERMINATIONS.....	70
7.3.1	Extraction Dispersion-Number Determinations.....	70
7.3.2	Scrubbing-Condition Dispersion-Number Determinations.....	71
7.3.3	Stripping-Condition Dispersion-Number Determinations.....	74
7.4	MEASUREMENT OF SOLVENT DENSITIES.....	78
7.5	MEASUREMENT OF SOLVENT VISCOSITIES.....	81
7.6	DISCUSSION AND CONCLUSIONS.....	84
7.6.1	Dispersion Numbers.....	84
7.6.2	Solvent Density.....	85
7.6.3	Solvent Viscosity.....	86
8.	CONCLUSIONS.....	87
8.1	OVERALL ASSESSMENT.....	87
8.2	EVALUATION OF RESULTS.....	87
8.3	RECOMMENDATIONS FOR FUTURE WORK.....	88
8.3.1	Summary Remarks.....	88

8.3.2	Solvent Composition.....	88
8.3.3	Actinide and Strontium Extraction.....	89
8.3.4	Radiation Stability.....	89
8.3.5	Thermal Stability.....	90
8.3.6	Solvent Cleanup.....	90
8.3.7	Minor Species.....	90
8.3.8	Fate of Trimethylamine.....	91
8.3.9	Role of Nitrite.....	91
8.3.10	Modeling.....	91
9.	REFERENCES.....	93
APPENDIX A. PREDICTED D_{Cs} VALUES USING THE log VERSUS log RELATIONSHIPS BETWEEN D_{Cs} VALUES AND BOBCALIXC6 AND Cs-7SB MODIFIER CONCENTRATIONS....		99

LIST OF FIGURES

Figure	Page
1 BOBCalixC6 solubility tests at 15 °C.....	13
2 BOBCalixC6 solubility tests at 25 °C.....	13
3 BOBCalixC6 solubility tests at 35 °C.....	14
4 Comparison of BOBCalixC6 solubility data	15
5 CSSX solvent dispersion numbers for extraction, scrub, and strip conditions at baseline O:A ratios	23
6 CSSX solvent dispersion numbers for solvent wash with dilute NaOH.....	23
7 CSSX solvent dispersion numbers for solvent washing as a function of NaOH concentration	24
8 CSSX solvent density as a function of Cs-7SB modifier concentration for 25.6 °C.....	25
9 Solvent viscosity as a function of temperature	26
10 Solvent shear stress as a function of temperature.....	27
11 Solvent and process solution surface tension	31
12 Solvent interfacial tension in extraction, scrub, and strip contacts.....	32
13 ESS tests at three different temperatures	38
14 ESS protocol for optimized solvent phase-stability test.....	58
15 Phase separation in the optimized solvent at 0 °C.....	60
16 Phase separation in the optimized solvent at -24 °C.....	61
17 Gel-like material formed during dispersion-number determinations.....	72
18 Graph of CSSX solvent extraction equilibration dispersion numbers.....	74
19 Graph of CSSX solvent scrub equilibration dispersion numbers	76
20 Graph of CSSX solvent strip equilibration dispersion numbers.....	77
21 Solvent density versus temperature.....	81
22 Solvent viscosity versus temperature.....	83
23 Solvent shear stress versus temperature.....	83

LIST OF TABLES

Table	Page
1 Summary of selection criteria and associated property.....	6
2 Test sample compositions.....	7
3 Validation data for the modified ESS protocol.....	9
4 BOBCalixC6 solubility data from FY 2001 study.....	15
5 BOBCalixC6 solubility data from FY 2000 study.....	16
6 ESS results obtained with constant TOA concentration.....	18
7 ESS results obtained with two selected solvents with variable TOA concentrations.....	19
8 Calculated robustness for various CSSX solvent compositions.....	20
9 Temperature range for third-phase appearance.....	21
10 Dispersion numbers for extraction, scrub, and stripping of CSSX solvents.....	22
11 Dispersion numbers for washing of CSSX solvents B001107-3-4 and B001107-3-5.....	24
12 Solvent-density determinations.....	25
13 Solvent-viscosity determinations.....	27
14 Surface-tension determinations.....	29
15 Interfacial tension versus simulant.....	30
16 Interfacial tension versus scrub solution.....	30
17 Interfacial tension versus strip solution.....	31
18 Cesium batch ESS performance for previous-baseline and optimized solvents.....	36
19 ESS results for three different temperatures.....	37
20 Apparent enthalpy changes for each ESS stage.....	38
21 Two-cycle ESS tests.....	39
22 Partition ratios for BOBCalixC6.....	45
23 Partition ratios for modifier Cs-7SB.....	46
24 Partitioning of dibutylphosphate.....	51
25 Detection limits of non-extractable metals.....	52

26	Concentrations of metals present in the solvent after extraction	52
27	Concentrations of anions present in the solvent at each stage	53
28	Concentrations of strontium in the aqueous phase at each stage	53
29	Distribution ratios of technetium obtained in ESS tests	54
30	Effect of dodecanoate on cesium extraction in ESS tests	55
31	Phase separation at 0 °C for the previous-baseline and the optimized solvents	60
32	Phase compositions at 0 °C for the previous-baseline and the optimized solvents	61
33	Phase separation at -24 °C for the previous-baseline and the optimized solvents	62
34	Phase compositions at -24 °C for the previous-baseline and the optimized solvents	62
35	Solvent compositions at 0 °C for the previous-baseline and the optimized solvents	62
36	Solvent compositions at -24 °C for the previous-baseline and the optimized solvents	63
37	ESS tests at 25 °C using the low temperature-conditioned previous baseline solvent	63
38	ESS tests at 25 °C using the low temperature-conditioned optimized solvent	64
39	ESS tests at 25 °C using the high temperature-stressed optimized solvent	65
40	Simulant composition (major components)	68
41	Materials for full simulant (added trace metals and organic species)	69
42	Dispersion numbers for extraction with optimized CSSX solvent	73
43	Dispersion numbers for scrub with optimized CSSX solvent	75
44	Dispersion numbers for strip with optimized CSSX solvent	78
45	Water-density determinations	79
46	Optimized-solvent density determinations	80
47	Solvent-viscosity determinations	82
48	Dispersion numbers for CSSX solvent extraction, scrub, and stripping	84
49	Comparison of CSSX solvent densities	85
50	Comparison of solvent viscosities	86
A-1	Predicted D_{Cs} values	97

EXECUTIVE SUMMARY

The present work was undertaken to optimize the solvent used in the Caustic Side Solvent Extraction (CSSX) process and to measure key chemical and physical properties related to its performance. The CSSX process was selected by the USDOE in FY 2001 as the preferred technology for removal of cesium from the alkaline high-level salt waste stored in tanks at the Savannah River Site. This decision had been made with the understanding that the component concentrations of the baseline solvent employed till then would have to be adjusted to avoid supersaturation with respect to the extractant. Taking into consideration bounding requirements, an optimization of the solvent composition was performed, resulting in the following recommended component concentrations in Isopar[®] L diluent: 0.007 M calix[4]arene-bis(*tert*-octylbenzo-crown-6) (BOBCalixC6) extractant, 0.75 M 1-(2,2,3,3-tetrafluoropropoxy)-3-(4-*sec*-butylphenoxy)-2-propanol (Cs-7SB) phase modifier, and 0.003 M tri-*n*-octylamine (TOA) stripping aid. Criteria for this selection included BOBCalixC6 solubility, batch cesium distribution ratios (D_{Cs}), calculated flowsheet robustness, third-phase formation, dispersion numbers, and density. Although some minor compromises within acceptable limits were made in flowsheet robustness and solvent density, significant benefits from solvent optimization were gained in lower risk of third-phase formation (operation to as low as 11 °C at high cesium and potassium loading versus 20 °C using the previous solvent) and lower solvent cost. The solubility of BOBCalixC6 in Isopar[®] L containing 0.5–1.0 M Cs-7SB at 15–35 °C was examined by monitoring the concentration of BOBCalixC6 as it precipitated from supersaturated solutions over a period of approximately 9 months. Its solubility at 0.75 M Cs-7SB was found to be 7.7 mM at 25 °C. Extract/scrub/strip (ESS) tests showed that the optimized solvent performs acceptably; the extraction strength from baseline waste simulant is lower by 20%, but this is compensated partially by 5–14% improved stripping. When the optimized solvent was washed with an aqueous solution of 10 mM sodium hydroxide following an ESS test, identical D_{Cs} values were obtained on a second ESS test with fresh aqueous phases. The temperature dependence of D_{Cs} values in ESS testing was found to be similar to that of the former baseline solvent, and parameters are reported for the estimation of D_{Cs} values for ESS contacts in the range 15–35 °C. Measurements of the partition ratios of BOBCalixC6, Cs-7SB, and TOA between the optimized solvent and aqueous process solutions indicate that the losses of these solvent components by partitioning to the aqueous process solutions will be negligible to minor. Respective fractional replacements of the three components due solely to partitioning losses over the course of one year are estimated to be 4%, 27%, and 9% respectively. The partitioning behavior of selected organic anions examined in studies of the previous baseline solvent were repeated with the optimized solvent with no change in behavior found. For example, dibutylphosphate, present in the waste in trace amounts, will partition weakly into the solvent on extraction, and the fraction that is extracted will remain in the solvent to be washed out efficiently by the NaOH wash stage. Similarly, trace metal distribution was not significantly changed. Trace Ag, Cr, Cu, Hg, Mn, Mo, Pb, Pd, Rh, Ru, Sn, and Zn were not extracted; traces of Al, Ca, Sr, and Fe were detected in the optimized solvent after extraction but are scrubbed out. The bulk metals Na and K are also extracted as expected, and these are also scrubbed out. Technetium in the form of pertechnetate anion is extracted very weakly from the simulant ($D_{Tc} = 0.038$ or 1% extracted) and, like dibutylphosphate, remains in the solvent in the acidic scrub and strip stages, subsequently to be washed out in the NaOH wash stage. On storage at or below 0 °C, both the previous and optimized solvents exhibit phase splitting in which the more dense of two phases is concentrated in BOBCalixC6 and Cs-7SB. On warming to room temperature and remixing, the solvents are restored to their original composition and ESS performance. A 43-day test of the solvent stability to elevated temperatures, 35 and 60 °C, showed no evidence of degraded ESS performance. The physical properties density, viscosity, and dispersion number for the solvent against full simulant, scrub, and strip solutions at 15–35 °C were measured and found to be adequate for contactor operation. Dispersion numbers (N_{Di}) under all conditions met the criterion $N_{Di} > 4 \times 10^{-4}$; the solvent density and viscosity at 25 °C were respectively 0.8516 ± 0.0001 and 3.51 ± 0.1 cP. Overall, optimization and testing of the CSSX solvent has reduced the technical risk of the CSSX process by resolving previously identified issues and raising no new issues.

ABSTRACT

This work was undertaken to optimize the solvent used in the Caustic Side Solvent Extraction (CSSX) process and to measure key chemical and physical properties related to its performance in the removal of cesium from the alkaline high-level salt waste stored in tanks at the Savannah River Site. The need to adjust the solvent composition arose from the prior discovery that the previous baseline solvent was supersaturated with respect to the calixarene extractant. The following solvent-component concentrations in Isopar[®] L diluent are recommended: 0.007 M calix[4]arene-bis(*tert*-octylbenzo-crown-6) (BOBCalixC6) extractant, 0.75 M 1-(2,2,3,3-tetrafluoropropoxy)-3-(4-*sec*-butylphenoxy)-2-propanol (Cs-7SB) phase modifier, and 0.003 M tri-*n*-octylamine (TOA) stripping aid. Criteria for this selection included BOBCalixC6 solubility, batch cesium distribution ratios (D_{Cs}), calculated flowsheet robustness, third-phase formation, coalescence rate (dispersion numbers), and solvent density. Although minor compromises within acceptable limits were made in flowsheet robustness and solvent density, significant benefits were gained in lower risk of third-phase formation and lower solvent cost. Data are also reported for the optimized solvent regarding the temperature dependence of D_{Cs} in extraction, scrubbing, and stripping (ESS); ESS performance on recycle; partitioning of BOBCalixC6, Cs-7SB, and TOA to aqueous process solutions; partitioning of organic anions; distribution of metals; solvent phase separation at low temperatures; solvent stability to elevated temperatures; and solvent density and viscosity. Overall, the technical risk of the CSSX process has been reduced by resolving previously identified issues and raising no new issues.

1. INTRODUCTION

The Caustic-Side Solvent-Extraction (CSSX) process [1,2] for cesium removal from alkaline high-level waste has been developed for application at the United States Department of Energy (USDOE) Savannah River Site (SRS) [3]. In 2001 the USDOE selected the CSSX process flowsheet as the preferred technology for this application [4,5] following an evaluation of alternative technologies [6–10]. This selection was largely founded on extensive testing and demonstration data that successfully addressed four high technology risks, including chemical stability [11], radiation stability [11–15], proof-of-concept demonstration with waste simulant [15], and demonstration with actual SRS high-level waste [16]. All criteria were met or even exceeded. The contactor tests using simulated- and actual-waste feeds met their goals for decontamination factor ($DF \geq 40,000$) and concentration factor ($CF \geq 15$) [15,16]. The stability of solvent to chemical, thermal, and radiation stresses was shown to be high, indicating a solvent lifetime significantly greater than one year [11–15]. Extensive data characterizing the distribution behavior of major and minor system components in extraction, scrubbing, and stripping (ESS) were collected, and effective means for solvent cleanup were described [11]. As work for technology selection drew to a close in April 2001, issues for continued research and development (R&D) were identified [7,11], ultimately leading to renewed effort through the end of FY 2002 [18]. The most important issue regarding chemical and physical properties was the probable supersaturation of the solvent. Namely, the solubility of the calixarene in the solvent comprising the modifier and tri-*n*-octylamine in Isopar[®] L

appeared to be lower than the 10 mM used in the baseline solvent. Since the calixarene solubility increased with increasing concentration of modifier, the issue of supersaturation was apparently resolvable with little risk by an adjustment of the concentrations of the solvent components. Hence, technology selection proceeded with the understanding that such an adjustment would be necessary early in the subsequent R&D phase.

Following the selection of the CSSX technology, systematic measurements were performed in late FY 2001 and early FY 2002 toward selection of the new optimized concentrations of the three solvent components. In addition to BOBCalixC6 solubility, the dependence of cesium ESS behavior, flowsheet robustness, coalescence, third-phase formation, and solvent density also were factored into the optimization. The conclusions of this initial phase of the work reported herein form the basis of the selection of the optimum solvent composition described in Chapter 2. In the course of the solvent-optimization effort and subsequent experiments, the flowsheet and its requirements were assumed to be unchanged. Hence, the compositions of the aqueous waste simulant, scrub solution, and strip solution remained the same. The reader is referred to a prior report for a complete description of the baseline simulant [11]; its composition may be found in Chapter 7 of the present report.

The changed solvent composition necessitated further characterization of the properties of the optimized solvent, as reflected in program plans [18]. Since rather minor changes were expected in the behavior of the optimized solvent as compared with the previous baseline solvent, a less ambitious testing regimen was undertaken. Chapter 3 describes the cesium distribution behavior in batch ESS tests, its temperature dependence, and a confirmation of the recyclability of the solvent. Chapter 4 re-examines the question of partitioning of the solvent components between the solvent and aqueous process solutions, affording an opportunity to reduce the uncertainties in evaluating loss rates of the solvent components. Chapter 5 focuses on how other system constituents, including both organic and inorganic species, distribute under process conditions. Chapter 6 confirms the chemical and thermal stability of the solvent under process conditions. Finally, Chapter 7 provides data on solvent density and viscosity, as well as its dispersion numbers in contact with process solutions. Overall, the experiments conducted on the optimized solvent were intended to reduce the risk that the changed composition would lead to an unacceptable change in process performance. In reporting results toward reducing this risk, this document not only establishes the properties of the optimized solvent, but it also serves as a companion to the previous inclusive report on the previous baseline solvent [11].

2. CAUSTIC-SIDE SOLVENT EXTRACTION SOLVENT-COMPOSITION RECOMMENDATION

2.1. BASIS FOR TASK AND SUMMARY RECOMMENDATION

The purpose of this chapter is to provide the experimental information that forms the basis for a recommended change in the baseline composition of the caustic-side solvent extraction (CSSX) solvent. In the year and a half prior to technology selection in May 2001, the baseline CSSX solvent composition was 0.010 M calix[4]arene-bis(*tert*-octylbenzo-crown-6), known as BOBCalixC6; 0.5 M 1-(2,2,3,3-tetrafluoropropoxy)-3-(4-*sec*-butylphenoxy)-2-propanol, known as Cs-7SB modifier; and 0.001 M tri-*n*-octylamine (TOA) in the diluent Isopar[®] L [3]. Data for the solubility of BOBCalixC6 acquired and reported for the Salt Processing Program (SPP) alternative technology down-select decision showed the above composition is supersaturated with respect to BOBCalixC6 [11]. Although samples of the baseline solvent have been observed for approximately one year without any solids formation, the CSSX technical team recommended a solvent-composition optimization task be undertaken to address the BOBCalixC6 solubility and other issues [19] such as third-phase formation, as a function of the plant operating temperature.

To accomplish the task of recommending a new baseline solvent composition, the CSSX technical team, the Tanks Focus Area (TFA), and SPP management team, in cooperation with the U.S. Department of Energy-Savannah River, developed an experimental program designed to provide the required information. Part of this effort included the development of the solvent-composition selection criteria [20].

The recommendation for the new solvent composition is a consensus opinion of the CSSX technical team. Based on the results to follow in this chapter, the recommended composition is as follows:

0.007 M BOBCalixC6 extractant,
0.75 M Cs-7SB modifier,
0.003 M TOA stripping aid (sometimes referred to as a suppressor), and
Isopar[®] L diluent.

Table 1 contains a summary of the bounding and goal-selection criteria and the value of the experimental property for the respective criterion for the recommended solvent composition.

Table 1. Summary of selection criteria and associated properties

Criterion	Bounding condition	Goal condition	Value of property
BOBCalixC6 solubility	Thermodynamically stable	Thermodynamically stable	≥ 7.55 mM @ 25 °C
D_{Cs} values	Extraction $D_{Cs} > 8$ Scrub $D_{Cs} > 0.6$ Strip $D_{Cs} < 0.16$	Extraction $D_{Cs} > 17.8$ Scrub $D_{Cs} > 1.6$ Strip $D_{Cs} < 0.15$	Extraction $D_{Cs} = 14.1$ Scrub $D_{Cs} = 1.3$ Strip $D_{Cs} = 0.10$
Flowsheet robustness	1.0	3.0	> 8.0
Third-phase formation	$15 \leq T \leq 35$ °C at $[K^+] = 0.05$ M	$15 \leq T \leq 35$ °C at $[K^+] = 0.05$ M	< 10 °C at $[K^+] = 0.05$ M
Dispersion number against simulant, scrub, and strip solutions	$> 4.0 \times 10^{-4}$	$> 4.0 \times 10^{-4}$	$> 5.0 \times 10^{-4}$
Dispersion number against NaOH wash solution	$> 4.0 \times 10^{-4}$	$> 4.0 \times 10^{-4}$	$> 4.5 \times 10^{-4}$ at 0.3 M NaOH
Solvent density	≤ 0.90 g/mL at 25 °C	≤ 0.86 g/mL at 25 °C	0.85 g/mL at 25.6 °C

It should be noted that the criteria dealing with the change in the cesium distribution ratio D_{Cs} values as a function of solvent composition (i.e., solvent robustness) and the cost of solvent components did not enter into the decision process. These two criteria were intended to be used if the other criteria identified multiple acceptable compositions.

The results presented in the chapter were first documented in a report [21] of limited availability for use by the CSSX technical team in planning and initiating tasks in FY 2002. This document was later converted to an Oak Ridge National Laboratory (ORNL) report whose format is prescribed by the USDOE Office of Scientific and Technical Information (OSTI) [22]. In that the results are, for practical purposes, inseparable from the other results presented herein, the information is again reported in the form of the present chapter. In addition to minor editing, the only technical change of significance made in duplicating this material is the inclusion of the BOBCalixC6 solubility data collected at longer times. Hence, the present report represents the most comprehensive source of information to date on CSSX chemical and physical properties.

2.2 EXPERIMENTAL APPROACHES

2.2.1 Solvent Test Samples

A total of 13 test samples of solvent were prepared for this study. The compositions of these samples are given in Table 2. A sample of the baseline solvent was included for reference purposes. Single lots of modifier (Lot No. PVB B000894-48P) and BOBCalixC6 (Lot No. IBC 000714HMKC-0004) were used to prepare all of the test samples. Solvents containing 3 and 10 mM TOA were prepared by adding a measured amount of 0.2 M TOA in Isopar[®] L to the solvents originally prepared with 1 mM TOA. All solvents were washed twice with 0.1 M NaOH, twice with 0.05 M HNO₃, three times with deionized water, and allowed to stand overnight before being decanted into clean containers. Scrub (0.05 M HNO₃) and strip (0.001 M HNO₃) solutions were prepared by diluting commercially available stock solutions with deionized water. Sodium hydroxide solutions were prepared by diluting a commercially available standard solution. Savannah River Site (SRS) waste supernatant simulant was formulated according to the SRS procedure [23]. The nominal cesium concentration in all simulant batches used in the testing was 0.00014 M. Aliquots of the solvent were transferred to the Nuclear Sciences and Technology Division (NSTD) at Oak Ridge National Laboratory (ORNL) for measurements of dispersion number, viscosity, density, surface tension, and interfacial tension. Other measurements, plus the initial solvent preparation, were carried out in the ORNL Chemical Sciences Division (CSD).

Table 2. Test sample compositions

Solvent identification	Test no.	[BOBCalixC6] (mM)	[Cs-7SB] (M)	[TOA] (mM)
Previous baseline		10	0.50	1
B001107-3-1	1	10	0.65	1
B001107-3-2	2	8	0.65	1
B001107-3-3	3	10	0.75	1
B001107-3-4	4	8	0.75	1
B001107-3-5	5	6	0.75	1
B001107-3-6	6	8	0.85	1
B001107-3-7	7	6	0.85	1
B001107-3-8	8	8	1.00	1
B001107-3-9	9	6	1.00	1
B001107-3-2A	10	8	0.65	3
B001107-3-2B	11	8	0.65	10
B001107-3-4C	12	8	0.75	3
B001107-3-4D	13	8	0.75	10

2.2.2 Experimental Procedures

2.2.2.1 BOBCalixC6 solubility studies

A series of solvents were prepared from five different pristine nonwashed solutions of Cs-7SB modifier in Isopar[®] L (0.5, 0.65, 0.75, 0.85, and 1.0 M) containing 1 mM TOA as follows. Three and one-half grams of BOBCalixC6 (Lot 000714 HMKC-0004) was dissolved in 50 mL of modifier solution in Isopar[®] L by applying sonication and heating to about 50 °C, cooling to room temperature, and then seeding with about 2 mg of recrystallized BOBCalixC6. BOBCalixC6 was used as received from IBC Advanced Technologies, Inc. The modifier solutions in Isopar[®] L were washed following the standard washing protocol. The samples were then shaken and divided into six samples of equal volume. Samples in duplicate were placed in a water bath at 15 °C, an air box at 25 °C, and an incubator at 35 °C. Agitation was effected by shaking in the water bath and wheel rotation in the air box and incubator. The initial concentration of BOBCalixC6 in each sample was 59 mM. After a given time interval, the samples were allowed to settle for 30 to 60 min, whereupon an aliquot of the supernatant solution was withdrawn, filtered through No. 40 filter paper, diluted with chloroform, and submitted for high-performance liquid chromatography (HPLC) analysis. Samples archived from the solubility study initiated approximately 1 year ago [11] were also analyzed. A new calibration curve was prepared with fresh calixarene solutions for each analysis series.

2.2.2.2 Extraction, scrub and strip protocol

Extraction, scrub, and strip (ESS) tests were performed on all of the samples listed in Table 2. The experiments were conducted following the protocol defined in Ref. 11 using organic:aqueous (O:A) volume ratios of 1:3 on extraction and 5:1 on scrubs and strips. An extra scrub step was added to the previous protocol [11] to more realistically approximate the flowsheet. It should be noted that the solvent weakly extracts sodium and potassium, and the second scrub step more completely removes these metals from the solvent prior to stripping. With only one scrub, the first strip step is expected to exhibit slightly higher values of D_{Cs} , because the incomplete scrubbing of sodium and potassium results in these metal nitrates reporting to the aqueous phase of the first strip step, thereby increasing the aqueous-phase nitrate concentration. The data validating the modified ESS protocol are given in Table 3. The data confirm that addition of the second scrub improves stripping performance as expected. The D_{Cs} values are slightly dependent on the O:A ratios employed, with better performance occurring when the strip O:A ratio is lower. All stripping D_{Cs} values converge to the same value upon successive stripping. In the solvent-optimization tests, an increase in modifier concentration is expected to increase sodium and potassium extraction [11]. However, the consequent negative impact on stripping is expected to be essentially eliminated by the second scrub and thus appropriately rendered an insignificant factor in solvent selection.

2.2.2.3 Third-phase determination

Third-phase formation experiments involved the 10 solvents containing 1 mM of TOA and three different simulants: baseline simulant ($[Cs^+] = 0.14$ mM, $[K^+] = 0.02$ M), high-potassium simulant ($[Cs^+] = 0.14$ mM, $[K^+] = 0.05$ M); and high-potassium, high-cesium simulant ($[Cs^+] = 0.44$ mM, $[K^+] = 0.05$ M). These conditions encompass those that could be potentially encountered with real wastes [3]. After two repeated contacts with the simulants (O:A = 1:3) at 25 °C, the solvent samples were cooled in a water bath and shaken periodically. The presence or absence of a third phase was determined by independent visual examination by two researchers.

Table 3. Validation data for the modified ESS protocol

Step	Value of D_{Cs} by O:A ratios ^a			
	1:3 (E)	1:5 (E)	1:3 (E)	1:5 (E)
	5:1 (SS)	3:1 (SS)	5:1 (SS)	3:1 (SS)
Extraction	17.6	17.1	16.6	17.3
Scrub no. 1	1.55	1.57	1.56	1.57
Scrub no. 2	NA	NA	1.56	1.57
Strip no. 1	0.137	0.130	0.120	0.116
Strip no. 2	0.080	0.075	0.078	0.071
Strip no. 3	0.064	0.064	0.062	0.062
Strip no. 4	0.052	0.054	0.052	0.054

^aThe letter "E" denotes O:A ratio for extraction; "SS" denotes O:A ratio for scrub and strip. NA denotes "not applicable," as the second scrub was intentionally omitted in the corresponding sequence.

2.2.2.4 Dispersion-number measurement

Dispersion numbers were determined under extraction, scrubbing, and stripping conditions in the presence of cesium. Prior to use, all new or previously used glassware and plastic vessels were washed by rinsing with tap water three times, rinsing with deionized water three times, rinsing with ethanol two times, and rinsing with acetone two times. The equipment was allowed to air dry or was dried with a stream of dry nitrogen or argon before use. In all tests, phase volumes proportional to the flow rates of the solvent, scrub, and strip solutions in the CSSX baseline flowsheet were placed into a 100-mL graduated Pyrex[®] cylinder. The position of the interface was recorded. The cylinder was capped with a ground-glass stopper, the solutions were agitated at ambient laboratory temperature for 20 s. Agitation was suspended for 10 s and then resumed for an additional 20 s. At the end of the second agitation, a stopwatch was started and the time required for the interface to return to its original position was

recorded. In these tests, the “original” position was assumed to be that within 1–2 mm of the interface prior to the agitation and when all indications of dispersed phases at the interface had disappeared. The total height of the dispersion within the cylinder was measured. Each determination was repeated three times. Dimensionless dispersion numbers were calculated according to the expression [24]:

$$N_{Di} = \frac{1}{t_b} \sqrt{\frac{z}{g_c}} \quad (1)$$

where t_b is the break time in seconds, z is the dispersion band height in centimeters, and g_c is the gravitational force of 981 cm/s².

2.2.2.5 Density

The solvent densities were measured using procedures based on ASTM D891 [25] and ASTM D1429, [25] using new 50-mL class A borosilicate glass volumetric flasks with ground-glass stoppers. Calibration of the volumetric flasks for density measurements was performed based on ASTM E542 [27]. A Mettler AE260 analytical balance (S/N J19097) capable of measuring to 0.1 mg was used to weigh the flasks. National Institute of Standards and Technology (NIST)–based test weights were used to check the balance calibration. A thermometer accurate to 0.1 °C (LaPine 398-12-53) was used to measure the temperature of the liquid in the flasks. The flasks were cleaned and dried before each use as described above, using tap water, deionized water, ethanol, and acetone, followed by drying with argon gas. Each flask was filled using a 10-mL transfer pipette to just below the line and then adjusted to the line with a small transfer pipette. The actual volume of each flask was calculated from the weight of the water contained.

2.2.2.6 Viscosity

The viscosities of each of the nine candidate solvents and the previous baseline solvent were measured at 20, 25, 30, 35, and 40 °C using procedures adapted from ASTM D2196 [28] and the Brookfield viscometer operating instructions [29]. The determinations were made using a Brookfield rotational viscometer model LVTDV-II, serial number D15869, with a UL adapter. The water jacket on the UL adapter was heated and cooled by a VWR model 13270-615 circulation bath, with 190-Ws cooling, and operated at a coolant recirculation rate of ~2 L/min. It contained a 50/50 mixture of ethylene glycol and water, which was circulated by the water bath circulation pump. The thermometer used, the LaPine 398-12-53, was immersed in the water bath for the temperature measurement. (There is no room in the UL adapter for a thermometer.) The spindle speed was set to give a torque percent reading in the middle or upper portion of the scale. The UL adapter (a large-diameter spindle in a cylindrical container just slightly larger in diameter than the spindle) is used for measuring low-viscosity liquids (liquids with viscosities between 1 and 20 cP). The UL adapter with spindle holds 16 mL of sample for measurement.

Each test was begun by adding the test solvent to the UL adapter, installing it on the viscometer, starting the spindle rotation at 60 rpm, and then setting the temperature bath to 20 °C. After the temperature had stabilized for several minutes, the viscosity of the sample was measured. The temperature bath was then adjusted to the next temperature and the system temperature allowed to stabilize before the next reading was taken.

2.2.2.7 Surface tension and interfacial tension

The surface tension of each of the nine candidate solvents, the previous baseline solvent, simulant, strip solution, and scrub solution were measured at ~25 °C using a CSC Du Nouy tensiometer (serial no. 013457) with a 6-cm-circumference ring. The experimental procedures were adapted from ASTM D971 [30] and ASTM D1331 [31]. The tensiometer was calibrated against known weights and its zero point adjusted according to the procedure of the manufacturer. Interfacial tension was determined by measuring the force necessary to detach a planar ring of platinum wire from the surface of the liquid of higher surface tension, that is, upward from the aqueous-organic interface. To calculate the interfacial tension, the force so measured was corrected by an empirically determined factor that depends upon the force applied, the densities of both organic and aqueous layers, and the dimensions of the ring. Measurements are made under rigidly standardized nonequilibrium conditions in which the measurement is completed within 60 s after formation of the interface. The surface tension of deionized water was measured to determine that the apparatus was functioning correctly. A value of 71–73 dyn/cm must be obtained; the literature value at 25 °C is 72.0 dyn/cm [32].

A Teflon[®] sample container having a minimum diameter of 45 mm was used. The container was cleaned as described above (with tap water, deionized water, ethanol, and acetone) between each solvent/aqueous determination. The ring was then flamed in a blue gas flame, using spinning to obtain rapid, uniform heating. The ring should barely glow orange and should be heated for no more than 5 s.

Interfacial tension measurements were made by carefully placing a layer of the organic on the surface of the aqueous layer (the aqueous layer was placed in the container first and the ring submerged in this layer) until a depth of at least 10 mm was reached using a pipette. This procedure was used to ensure that minimum mixing occurred and that the organic did not touch the surface of the submerged ring. The organic-aqueous interface was allowed to age for 30 ± 1 s after the last of the organic had been layered onto the water. The platform was lowered and the value at rupture recorded. The measurement was timed so that, as nearly as possible, 30 s were required to draw the ring through the interface. The entire operation, from the time of pouring the organic onto the aqueous until the interface ruptured, was completed in about 60 ± 10 s. Each solvent was tested in duplicate, with the cup and the ring cleaned between the two readings.

The interfacial tension of the sample was calculated by means of the following equation:

$$\text{Interfacial tension, dyn/cm} = P_{\text{interface}} \times F \quad (2)$$

where $P_{\text{interface}}$ is the scale reading when the film ruptures (in dynes per centimeter) and F is the factor converting the scale reading (in dynes per centimeter) to interfacial tension, as obtained from Eq. (3). The value of the diameter ratio, R/r , for the ring, as specified by the manufacturer, is 53.6. The value of F is obtained as follows:

$$F = 0.7250 + [0.01452P_{\text{interface}}/C^2 (\rho_{\text{aq}} - \rho_{\text{org}}) + 0.04534 - 1.679/(r_{\text{ring}}/r_{\text{wire}})]^{1/2} \quad (3)$$

where C is the circumference of the ring (5.992 cm), ρ_{aq} is the density of the aqueous layer at 25 °C, in grams per milliliter; ρ_{org} is the density of the organic layer for interfacial testing at 25 °C, in grams per milliliter; r_{ring} is the radius of the ring, in centimeters; and r_{wire} is the radius of the wire of the ring, in centimeters.

2.3 EXPERIMENTAL RESULTS

2.3.1 BOBCalixC6 Solubility

The data on the BOBCalixC6 are a combination of information acquired from the experiments conducted in the latter portion of FY 2001 (see Experimental Section) and from the previous experiments [11]. This summary of the experimental results is necessary because of the long periods of time required for the BOBCalixC6 to achieve the solubility equilibrium condition. Table 4 summarizes the data obtained from the most recent solubility study.

The time-trend analysis of the data shows that after eight weeks, solubility equilibrium has not been achieved. Nevertheless, the data imply the supersaturation of the baseline solvent. After 36 weeks, the change in the calixarene content is fairly minor, as can be seen in Figs. 1–3, where the temperatures were chosen to represent respectively the minimum, medium, and maximum temperatures encountered in the process. (Note that the results after 36 weeks were not available when the composition of the optimized solvent was chosen [21]).

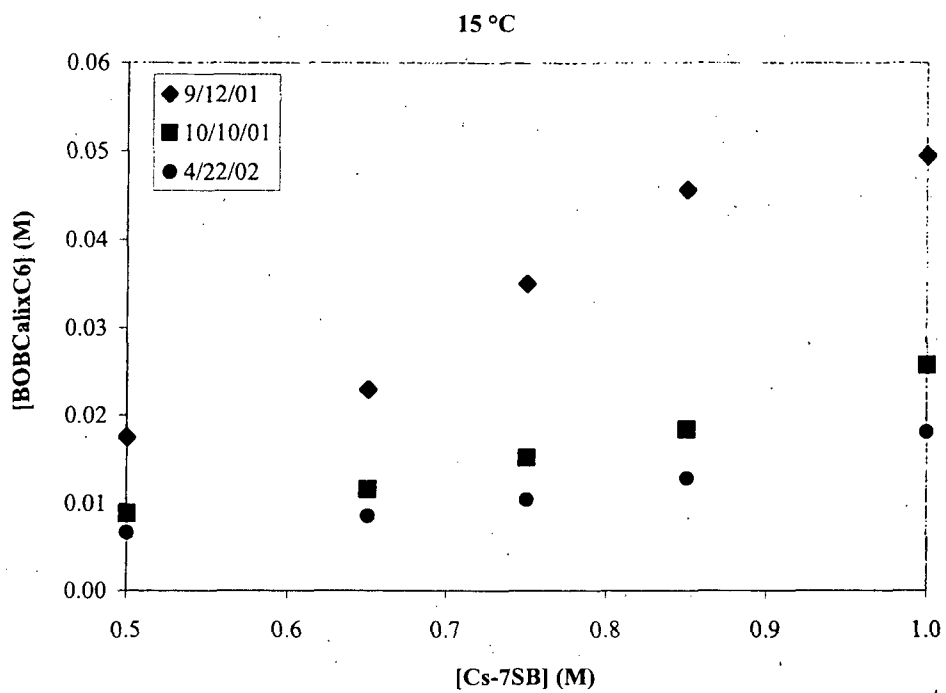


Fig. 1. BOBCalixC6 solubility tests at 15 °C.

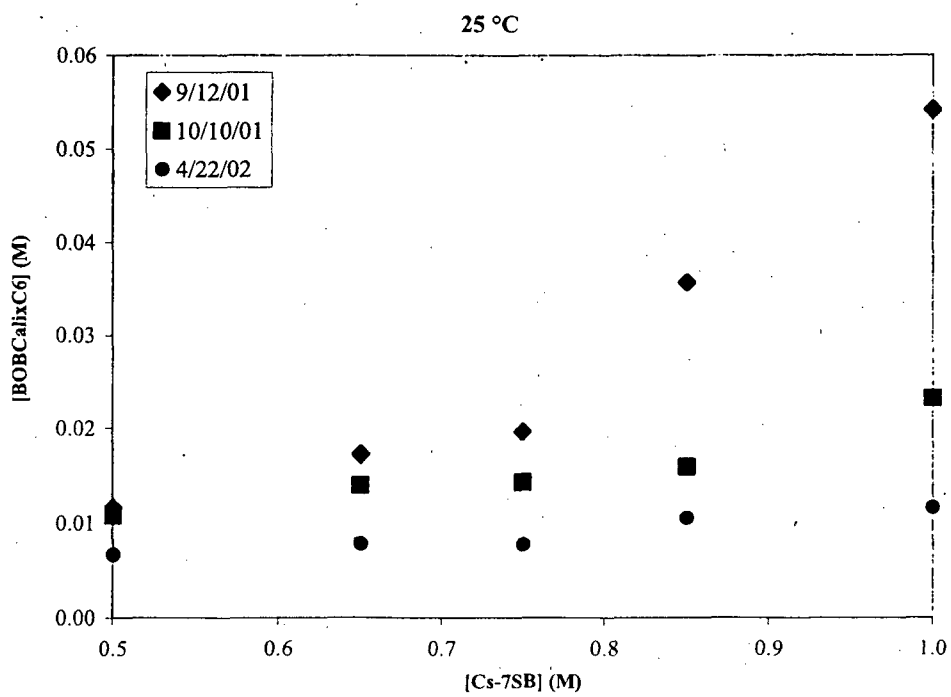


Fig. 2. BOBCalixC6 solubility tests at 25 °C.

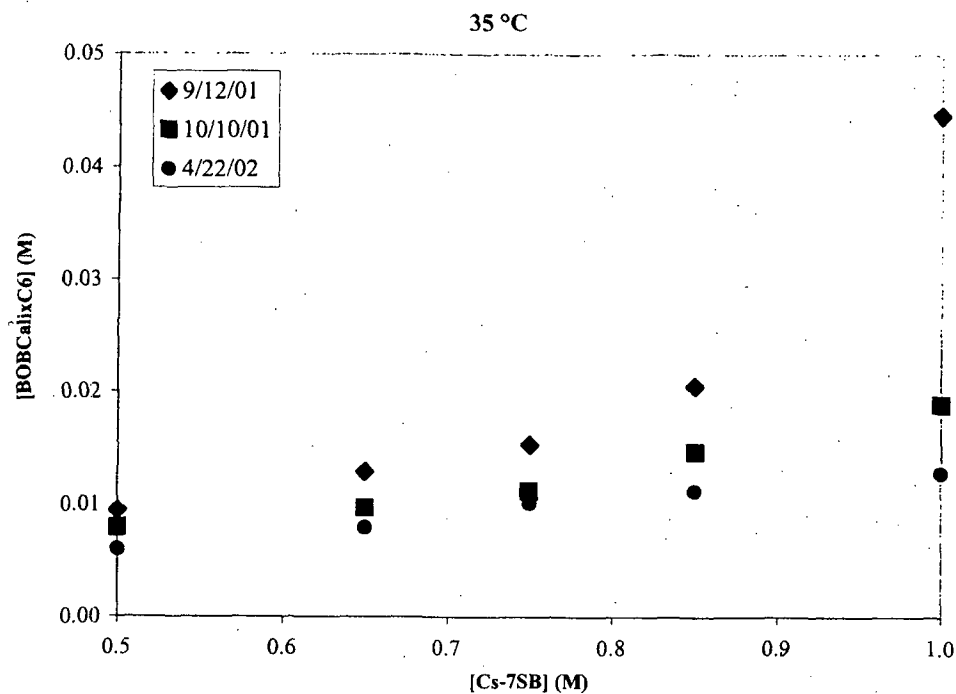


Fig. 3. BOBCalixC6 solubility tests at 35 °C.

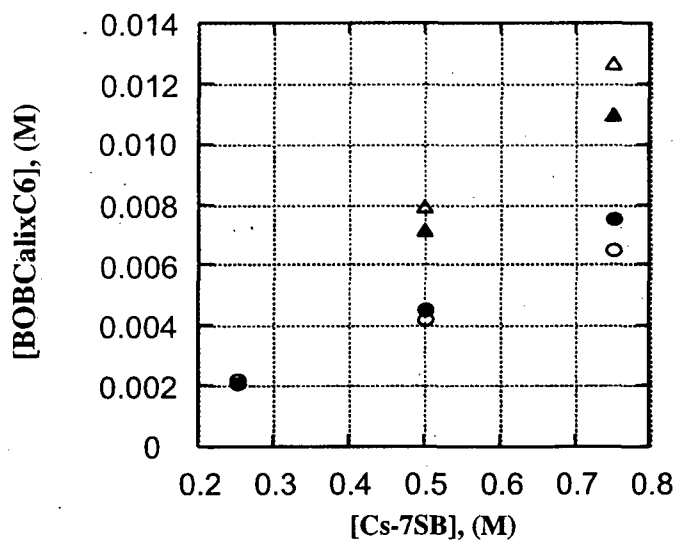
The experiment carried out at 35 °C indicates that the solubility of calixarene in a solvent containing the chosen concentration of modifier for the optimized solvent (0.75 M) varied minimally in 6 months, and the concentration of soluble calixarene is still greater than 7 mM. For the two other temperatures, the gap between the measurements performed in October 2001 and in April 2002 is larger, but BOBCalixC6 is still at a concentration greater than 7 mM in both cases for a concentration of modifier of 0.75 M.

A conservative estimate of the lower bound of the BOBCalixC6 solubility at 25 °C was obtained by reanalysis of samples from the solubility study that was initiated approximately 1 year ago [11]. These samples had been stored at the original experimental temperatures with intermittent agitation. Selected results are summarized in Fig. 4. As indicated in the legend, data are shown for both as-received and recrystallized BOBCalixC6 and for equilibrium approached from the direction of both dissolution (solid BOBCalixC6 present at start) and precipitation (starting with supersaturated BOBCalixC6 upon sonication and then seeding). In each case, no TOA or water is present in the solvent; that is, solid BOBCalixC6 is suspended in Cs-7SB at the indicated concentration in Isopar® L only. A tabulation of the data after 1 year, including systems containing TOA and water, is given in Table 5. Except for the single data point at 0.25 M Cs-7SB, which shows a deviation of $\pm 26\%$, the average analytical deviation among duplicate samples is $\pm 3.5\%$. The data show that TOA and water have little or no effect on BOBCalixC6 solubility.

Table 4. BOBCalixC6 solubility data from FY 2001 study^a

[Cs-7SB] (M)	[BOBCalixC6] (mM)									
	Initial	15 °C			25 °C			35 °C		
		4 wks	8 wks	36 wks	4 wks	8 wks	36 wks	4 wks	8 wks	36 wks
0.50	59	17.5	8.80	6.70	11.7	10.7	6.59	9.50	7.94	6.04
0.65	59	22.9	11.5	8.54	17.3	14.0	7.72	12.9	9.72	7.98
0.75	59	35.0	15.2	10.4	19.7	13.1	7.69	15.4	11.2	10.1
0.85	59	45.6	18.3	12.9	35.7	15.9	10.5	20.5	14.7	11.3
1.0	59	49.5	25.7	18.1	54.1	23.1	11.6	44.7	19.0	12.9

^aEach value is the average of an analysis of each of duplicate solubility samples.



- Recrystallized BOBCalixC6, dissolution, equilibrated for 52 days
- Recrystallized BOBCalixC6, dissolution, equilibrated for 410 days
- △ As-received BOBCalixC6, precipitation, equilibrated for 38 days
- ▲ As-received BOBCalixC6, precipitation, equilibrated for 395 days

Fig. 4. Comparison of BOBCalixC6 solubility data. The circles correspond to solubility tests performed by dissolution with recrystallized calixarene; the triangles correspond to solubility tests performed by precipitation with calixarene used as-received.

Conservatively, the lower bound of the BOBCalixC6 thermodynamic solubility corresponds to the recrystallized BOBCalixC6 that had been dissolving over the course of 13 months. At 0.75 M Cs-7SB, the lower bound at 25 °C is 7.55 mM. Although the solubility of BOBCalixC6 generally increases with increasing Cs-7SB concentration, a gap exists between the data for the recrystallized BOBCalixC6 that is dissolving and the as-received BOBCalixC6 that is precipitating.

Table 5. BOBCalixC6 solubility data from FY 2000 study^a

Sample no.	[Cs-7SB] (M)	[TOA] (mM)	Solvent washed?	Dissolution method	[BOBCalixC6] purification	[BOBCalixC6] (mM)	[BOBCalixC6] average (mM)
					Recrystallized		
5-A	0.25	0	No	Dissolve		2.62	
5-B	0.25	0	No	Dissolve	Recrystallized	1.55	2.08
6-A	0.50	0	No	Dissolve	Recrystallized	4.31	
6-B	0.50	0	No	Dissolve	Recrystallized	4.76	4.54
7-A	0.75	0	No	Dissolve	Recrystallized	6.98	
7-B	0.75	0	No	Dissolve	Recrystallized	8.12	7.55
8-A	0.50	1	No	Dissolve	Recrystallized	4.38	
8-B	0.50	1	No	Dissolve	Recrystallized	4.48	4.43
9-A	0.50	1	Yes	Dissolve	Recrystallized	4.26	
9-B	0.50	1	Yes	Dissolve	Recrystallized	4.64	4.45
10-A	0.50	1	No	Precipitate	Recrystallized	6.18	
10-B	0.50	1	No	Precipitate	Recrystallized	6.68	6.43
11-A	0.50	0	No	Precipitate	As Received	7.26	
11-B	0.50	0	No	Precipitate	As Received	7.05	7.15
12-A	0.75	0	No	Precipitate	As Received	11.1	
12-B	0.75	0	No	Precipitate	As Received	10.8	10.95
13-A	0.50	0	Yes	Precipitate	As Received	5.11	
13-B	0.50	0	Yes	Precipitate	As Received		

^aHPLC analysis of samples held at 25 °C for approximately 13 months.

From the data shown in Fig. 1, one may conclude that the true solubility of BOBCalixC6 in Isopar® L that contains only Cs-7SB at 25 °C lies within this gap. Both sets of data show a very slow convergence over the course of the past year. The increases in solubility upon dissolution were 8.4% and 16.5% for 0.5 and 0.75 M Cs-7SB, respectively. The comparable decreases upon precipitation were 9.7% and 13.4% for 0.5 and 0.75 M Cs-7SB, respectively. At this time, it is impossible to determine conclusively whether the upper set differs from the lower set because of the purity of BOBCalixC6 or because of the direction from which equilibrium is being approached. However, we believe that the latter cause is more probable, because the high concentration of Cs-7SB likely negates any effects on solubility of minor impurities in the as-received BOBCalixC6. As discussed earlier [11], these impurities apparently have an effect on the rate of dissolution of BOBCalixC6. Whereas recrystallized BOBCalixC6 can be dissolved very slowly (even with prolonged sonication and warming), the as-received material, nominally 97% pure, quickly dissolves to concentrations as high as 50 mM. For this reason, it has been impractical to experimentally approach equilibrium by precipitation of recrystallized BOBCalixC6. It is clear, then, that the lower bound of 7.55 mM BOBCalixC6 at 0.75 M Cs-7SB is a conservative estimate for the BOBCalixC6 solubility. Not only is the final plateau concentration of BOBCalixC6 likely to be higher, but the most realistic condition in a plant environment is for equilibrium to be approached by precipitation of the as-received material.

2.3.2 Cesium Distribution Results

The cesium distribution data obtained with the ESS tests are summarized in Tables 6 and 7. The data in Table 6 are for the series of test samples containing 1 mM TOA, and the results in Table 7 are for the series of test samples containing varying amounts of TOA and modifier with fixed BOBCalixC6 concentration.

Table 6. ESS results obtained with constant TOA concentration^a

[BOBCalixC6] (mM)	[Cs-7SB] (M)	D_{Cs}						
		Extract	Scrub # 1	Scrub # 2	Strip # 1	Strip # 2	Strip # 3	Strip # 4
10	0.50	17.2	1.52	1.52	0.114	0.070	0.055	0.051
10	0.65	19.6	1.75	1.79	0.136	0.084	0.066	0.057
10	0.75	20.7	1.91	1.91	0.152	0.092	0.072	0.062
8	0.65	15.4	1.38	1.44	0.109	0.066	0.053	0.045
8	0.75	16.1	1.52	1.54	0.120	0.075	0.056	0.050
8	0.85	17.2	1.68	1.66	0.134	0.077	0.062	0.053
8	1.00	17.7	1.87	1.78	0.145	0.086	0.069	0.060
6	0.75	12.2	1.12	1.16	0.089	0.051	0.042	0.036
6	0.85	12.3	1.23	1.25	0.095	0.055	0.044	0.040
6	1.00	13.6	1.39	1.39	0.112	0.065	0.051	0.046

^aTemperature = 25 °C. [TOA] = 1 mM.

Interest in increasing the TOA concentration is twofold. First, as the TOA concentration increases, the CSSX process becomes more resistant to anionic impurities. Second, thermal [11] and radiolytic [12,14] stability test results showed that TOA is the solvent component most susceptible to decomposition. However, the concentration cannot be increased excessively, because the organic-phase concentration of nitrate in the scrub stage will increase by the protonation of TOA. This extracted nitrate will be partially released in the first strip stage, causing the value of D_{Cs} for the first strip stage to increase, which could ultimately limit stripping efficiency. Assuming an O:A ratio of 5:1 in the strip section, stripping becomes ineffective (because of "pinching") when the first strip D_{Cs} value becomes equal to or greater than 0.2. The data show that stripping will not be so affected at TOA concentrations as high as 10 mM.

The results show that values of D_{Cs} for the two scrubs decrease as the concentration of TOA increases. This behavior is expected, because more nitrate is extracted, which both decreases the aqueous nitrate concentration and decreases the effective concentration of modifier, as more modifier molecules are tied up in solvating the nitrate. The D_{Cs} values in the initial strip stages also increase. Again, this result is expected, because greater nitrate extraction in scrubbing implies greater release of nitrate from the solvent into the strip aqueous phase. As a result of this higher nitrate concentration in the first strip stage and resultant higher D_{Cs} , more stages are required for the D_{Cs} value to converge to the limiting value. This limiting value should, in principle, be the same for all TOA concentrations. It also appears that the extraction D_{Cs} values decrease with increasing TOA concentrations. Assuming this slight decrease is real, it may reflect more modifier molecules being tied up in solvating the TOA.

Table 7. ESS results obtained with two selected solvents with variable TOA concentrations^a

[TOA], (mM)	D_{Cs}						
	Extract	Scrub no. 1	Scrub no. 2	Strip no. 1	Strip no. 2	Strip no. 3	Strip no. 4
[BOBCalixC6] = 8 mM, [Cs-7SB] = 0.65 M							
1	15.4	1.38	1.44	0.109	0.066	0.053	0.045
3	14.9	1.08	1.39	0.116	0.081	0.069	0.056
10	14.7	1.00	0.76	0.134	0.104	0.090	0.076
[BOBCalixC6] = 8 mM, [Cs-7SB] = 0.75 M							
1	16.4	1.54	1.55	0.121	0.073	0.059	0.052
3	15.5	1.26	1.49	0.124	0.083	0.075	0.059
10	15.2	1.20	0.70	0.137	0.101	0.091	0.078

^aTemperature = 25 °C.

Based on the cesium distribution ratio (D_{Cs}) data contained in Tables 6 and 7, all of the tested solvent compositions meet the D_{Cs} acceptance criterion. The D_{Cs} values in Tables 6 and 7, when analyzed as $\log D_{Cs}$ versus $\log(\text{BOBCalixC6 concentration})$ and $\log D_{Cs}$ versus $\log(\text{Cs-7SB modifier concentration})$, are linear with slopes approximately equal to one. Using these relationships, a simple set of equations can be used to predict the D_{Cs} values as a function of the BOBCalixC6 and Cs-7SB modifier concentrations. The results of the prediction for BOBCalixC6 and modifier concentrations about the recommended solvent composition are given in Appendix A, Table A.1.

2.3.3 Flowsheet Robustness

A series of Spreadsheet Algorithms for Stagewise Solvent Extraction (SASSE) [33] calculations were performed using the D_{Cs} values contained in Tables 6 and 7. The assumptions used in these calculations include the following: (1) the extraction and scrub D_{Cs} values are proportional to the concentration of free BOBCalixC6 in the organic phase; (2) the BOBCalixC6 is loaded with only one cesium ion; (3) the D_{Cs} value for the strip is proportional to the concentration of nitrate in the aqueous phase; (4) the total cesium concentration of the waste feed is 0.00014 M; (5) the temperature of the entire contactor cascade is 25 °C; (6) the stage efficiency is 80%; (7) 0.1% other-phase carryover occurs between stages; (8) there are 15 extraction stages, 2 scrub stages, and 15 strip stages; (9) there are 20.1 gal/min of waste feed and 1.33 gal/min of strip feed, and (10) the O:A in the scrub section is 5.0.

The results of the calculations are given in Table 8. The robustness number (Rb) is defined as the ratio of the decontamination factor for a given set of flowsheet conditions to the process-required bounding decontamination factor of 40,000. The baseline flowsheet specifies a solvent flow rate of

6.6 gal/min [3]. The maximum robustness was obtained by varying the solvent flow rate, which is shown in the fourth column of Table 8.

All of the solvent compositions tested meet the bounding criterion for robustness at the baseline solvent flow rate; however, the two solvent compositions containing 10 mM TOA do not meet the “goal” (i.e., the target criterion) for robustness. When the solvent flow rate is adjusted to achieve the maximum robustness, all of the solvent compositions meet the goal for robustness.

Table 8. Calculated robustness for various CSSX solvent compositions

Solvent identification ^a	Rb at 6.6 gal/min		Optimum flow rate
	waste feed	Rb _{max}	(Flow rate at Rb _{max} , gal/min)
Previous baseline	21.9	25.3	6.1
B001107-3-1	11.9	26.4	5.3
B001107-3-2	25.0	25.3	6.7
B001107-3-3	6.6	23.6	4.9
B001107-3-4	19.3	20.7	6.2
B001107-3-5	8.8	24.3	8.5
B001107-3-6	15.7	21.2	5.8
B001107-3-7	9.1	17.8	8.0
B001107-3-8	7.3	15.4	5.4
B001107-3-9	14.3	15.6	7.0
B001107-3-2A	8.8	10.1	6.1
B001107-3-2B	1.1	3.0	5.3
B001107-3-4C	6.9	9.7	5.8
B001107-3-4D	1.0	3.2	5.1

^aSee Table 2 for the composition of the specified solvent.

It should be noted that the SASSE calculations are considered to be conservative, since they assume a constant process temperature and a stage efficiency of 80%. In the actual process, the extraction section will be kept cooler than the scrub section, thereby improving the process robustness. For example, if the extraction section were at 25 °C, the scrub section at 29 °C, and the strip section at 33 °C, the robustness for the baseline solvent at a flow rate of 6.6 gal/min increases from 21.9 to 80.7. Thus, process robustness can be increased substantially by means of temperature control.

At the time the calculations were performed, it was believed that while a stage efficiency of 80% was assumed for the centrifugal contactor, the expected efficiency will be greater than 90% [34,35]. Assuming a 90% stage efficiency in the SASSE calculations at 25 °C, the robustness for the baseline

solvent at a flow rate of 6.6 gal/min would increase from 21.9 to 599. Higher stage efficiency, which can be expected with the plant-scale contactors, would increase process robustness. Since then, experiments carried out at INEEL with the baseline solvent in 5.5 cm contactors (ORNL design) showed a lower efficiency (72–75% on extraction, 36–60% on stripping). However, it is expected that process chemistry was not the cause, that an optimized contactor design could solve the low efficiency issue and that the assumptions considered for the SASSE calculations were still valid [36].

2.3.4 Third-Phase Formation

One of the major criteria the solvent must meet is the absence of third-phase formation for the expected maximum loading of the solvent at 15 °C, which occurs at the high cesium and potassium concentrations. This requirement was determined in FY 2001 at the time the process temperature range was established [3]. The results of the third-phase evaluations for solvents containing 1 mM TOA are presented in Table 9. Results of these experiments indicate that the use of any solvent containing 10 mM BOBCalixC6 is not recommended at a Cs-7SB modifier concentration less than 0.75 M.

Table 9. Temperature range for third-phase appearance

[BOBCalixC6] (mM)	[Cs-7SB] (M)	Temperature range (°C)		
		Full SRS simulant	High-potassium simulant	High-cesium and high- potassium simulant
10	0.50	15.0–16.5	17.5–20.0	17.5–20.0
10	0.65	12.0–13.0	15.0–16.5	15.0–16.5
10	0.75	10.0–11.0	12.0–13.0	12.0–13.0
8	0.65	10.0–11.0	12.0–13.0	12.0–13.0
8	0.75	8.5–9.0	10.0–11.0	10.0–11.0
8	0.85	7.5–8.0	8.5–9.0	8.5–9.0
8	1.00	6.5–7.0	6.5–7.0	6.5–7.0
6	0.75	6.5–7.0	8.0–8.5	8.5–9.0
6	0.85	5.0–6.5	7.0–7.5	7.0–7.5
6	1.00	F ^a	F ^a	F ^a

^aThe letter “F” denotes that the solvent did not exhibit a third-phase at 5 °C. However, because of the high concentration of modifier, the solvent viscosity had increased significantly at that temperature, making observation of a third-phase difficult.

2.3.5 Solvent Dispersion Numbers

The results for the dispersion-number determinations are given in Table 10 and shown graphically in Fig. 5. The subset of the solvent test samples contained 1 mM TOA. The data for the baseline solvent are taken from earlier testing [34]. The results show that all nine compositions meet the dispersion-number criterion for extraction, scrub, and strip conditions (cf. Table 1).

Dispersion-number determinations for a selected subset of the samples against 10-mM NaOH wash solutions are shown in Fig. 6. None of the solvent samples met the NaOH solvent-wash solution criterion. The 10-mM NaOH concentration was used during the FY 2001 flowsheet tests at Argonne National Laboratory [16], which used simulant as the feed, and tests at Savannah River Technology Center [17], which used real waste as the feed. During these tests, minor emulsion formation was observed. Solvent samples B001107-3-4 and B001107-3-5 were determined to have the most desirable characteristics when compared against all of the selection criteria. These two solvents were selected for dispersion-number determinations as a function of NaOH concentrations. The results of these tests are given in Table 11 and shown graphically in Fig. 7. When the NaOH concentration was 300 mM, these two solvent compositions met the dispersion-number criterion for solvent washing.

Table 10. Dispersion numbers for extraction, scrub, and stripping of CSSX solvents

Solvent description ^a	Dispersion number			Wash/solvent 0.01 M NaOH (O:A = 5:1)
	Simulant/solvent	Scrub/solvent	Strip/solvent	
Previous baseline	0.00149	0.00096	0.00115	–
B001107-3-1	0.00075	0.00102	0.00091	–
B001107-3-2	0.00056	0.00070	0.00078	0.00022
B001107-3-3	0.00102	0.00052	0.00088	–
B001107-3-4	0.00102	0.00053	0.00094	0.00034
B001107-3-5	0.00118	0.00050	0.00088	0.00024
B001107-3-6	0.00105	0.00059	0.00075	0.00016
B001107-3-7	0.00125	0.00058	0.00085	0.00016
B001107-3-8	0.00120	0.00062	0.00054	–
B001107-3-9	0.00141	0.00041	0.00051	–

^aSee Table 2 for the composition of the specified solvent.

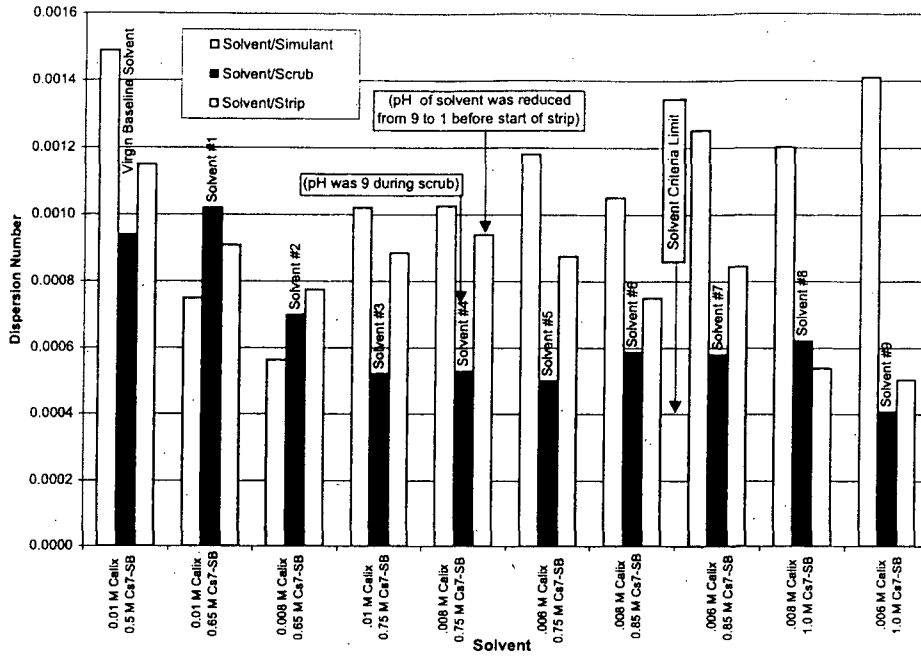


Fig. 5. CSSX solvent dispersion numbers for extraction, scrub, and strip conditions at baseline O:A ratios.

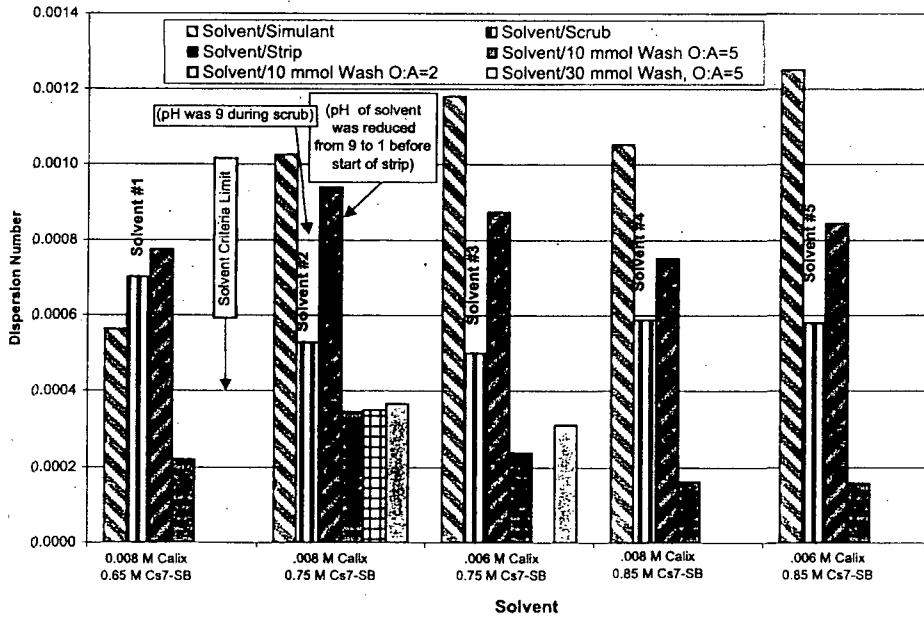


Fig. 6. CSSX solvent dispersion numbers for solvent wash with dilute NaOH.

Table 11. Dispersion numbers for washing of CSSX solvents B001107-3-4 and B001107-3-5

Solvent descriptor ^a	Solvent/wash dispersion number			
	0.01 M NaOH wash	0.03 M NaOH wash	0.1 M NaOH wash	0.3 M NaOH wash
B001107-3-4	0.00035	0.00037	0.00037	0.00049
B001107-3-5	0.00024	0.00031	0.00024	0.00045

^aSee Table 2 for the composition of the specified solvent.

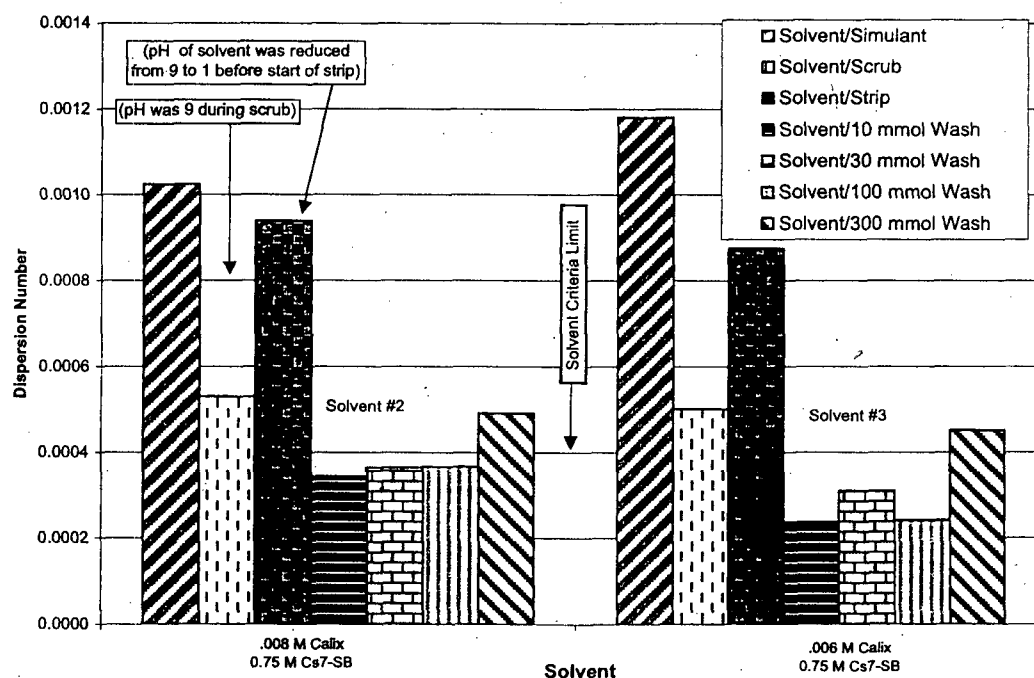


Fig. 7. CSSX solvent dispersion numbers for solvent washing as a function of NaOH concentration.

2.3.6 Solvent Density

The results of the density determinations are presented in Table 12. As expected, solvent density is primarily dependent on the modifier concentration. The relationship between density and modifier concentration is shown in Fig. 8. All the solvent samples that were tested met the bounding criterion for density (cf. Table 1); however, the solvent samples with modifier concentrations equal to or greater than 0.85 M did not meet the goal for density.

Table 12. Solvent-density determinations

Solvent identification ^a	Mass of solvent (g)	Density ^b (g/cm ³)	[Calix] (M)	[Modifier] (M)	Corrected volume (mL)	Mass of water (g)	Specific gravity	50-mL vol. flask
Baseline ^c		0.810						
B001107-3-1	41.9085	0.8395	0.010	0.65	49.9202	49.7819	0.99723	1
B001107-3-2	41.9230	0.8395	0.008	0.65	49.9362	49.7979	0.99723	2
B001107-3-3	42.5920	0.8531	0.010	0.75	49.9242	49.7859	0.99723	3
B001107-3-4	42.5149	0.8525	0.008	0.75	49.8703	49.7322	0.99723	5
B001107-3-5	42.4714	0.8516	0.006	0.75	49.8703	49.7322	0.99723	5
B001107-3-6	43.0887	0.8644	0.008	0.85	49.8480	49.7099	0.99723	6
B001107-3-7	43.1036	0.8632	0.006	0.85	49.9362	49.7979	0.99723	2
B001107-3-8	44.0269	0.8819	0.008	1.00	49.9242	49.7859	0.99723	3
B001107-3-9	44.6565	0.8951	0.006	1.00	49.8925	49.7543	0.99723	4

^aSee Table 2 for the composition of the specified solvent.

^bTemperature was 25.6 °C.

^cMeasured previously on previous-baseline pristine solvent.

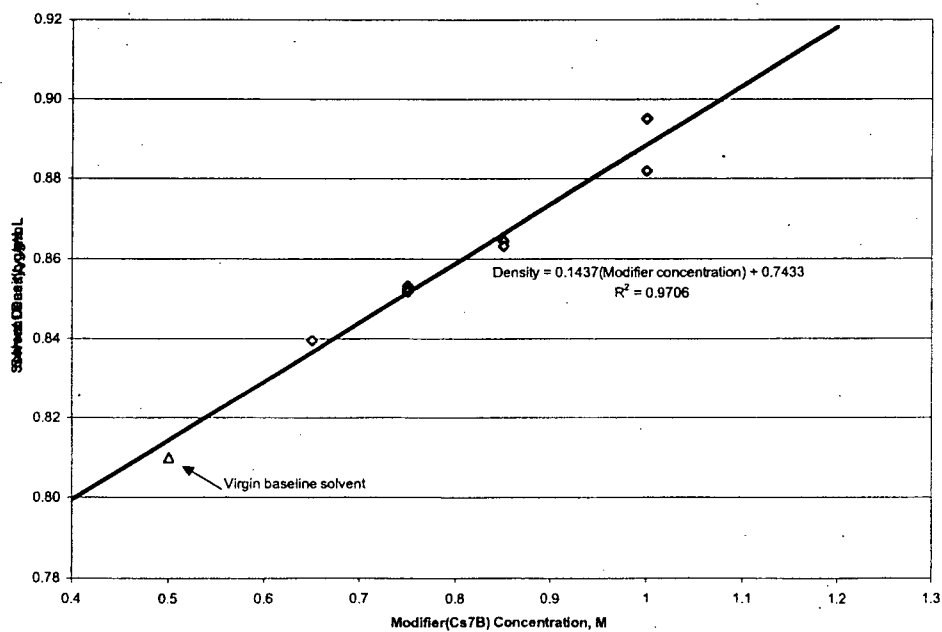


Fig. 8. CSSX solvent density as a function of Cs-7SB modifier concentration for 25.6 °C.

2.3.7 Solvent Viscosity

The results of the solvent-viscosity measurements are shown in Fig. 9, and Fig. 10 shows the shear stress as a function of temperature. The data are presented in tabular form in Table 13. The solvents with the lowest concentration of the Cs-7SB modifier have the lowest viscosity. The BOBCalixC6 concentration has only a minor effect on the viscosity decrease, because its concentration decreases at a given Cs-7SB concentration. The viscosity of all solvent samples decreases with increasing temperature, as expected for this type of liquid.

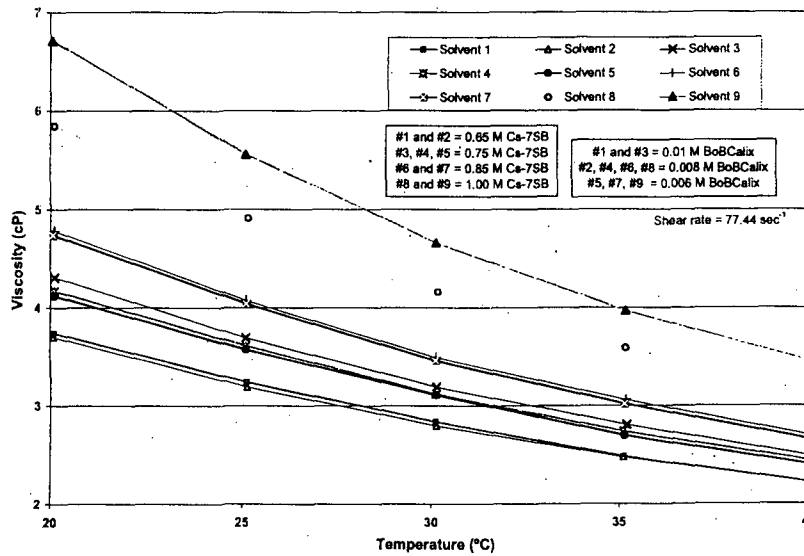


Fig. 9. Solvent viscosity as a function of temperature. The numbers in the legend are the test numbers from Table 2.

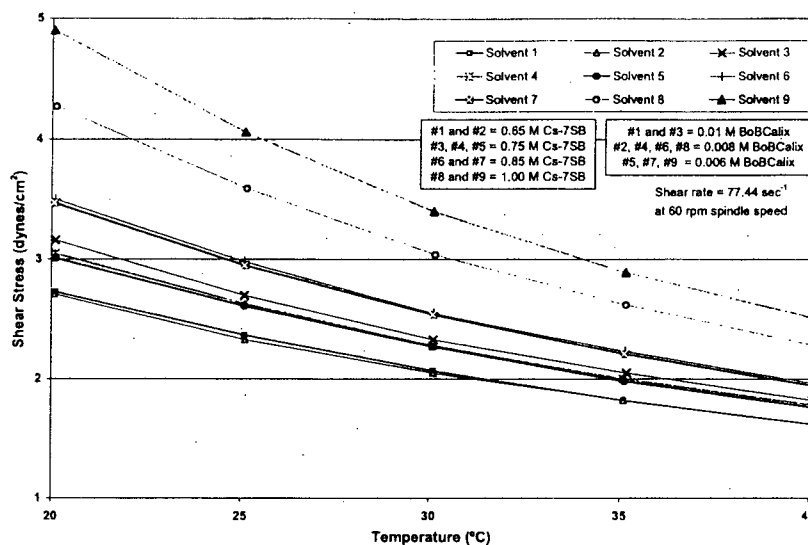


Fig. 10. Solvent shear stress as a function of temperature. The solvent numbers in the legend are the test numbers from Table 2.

Table 13. Solvent-viscosity determinations^a

Solvent ^b	Temperature (°C)	Torque (%)	Viscosity ^c (cP)	Shear stress (dyn/cm ²)
B001107-3-1	20.00	37.3	3.74	2.73
	25.00	32.3	3.24	2.37
	30.00	28.2	2.84	2.07
	35.00	24.9	2.49	1.82
	40.00	22.2	2.22	1.62
B001107-3-2	19.98	36.9	3.70	2.71
	25.02	31.9	3.19	2.33
	30.02	28.0	2.80	2.05
	35.00	24.8	2.48	1.82
	40.00	22.2	2.22	1.62
B001107-3-3	20.00	43.2	4.31	3.16
	25.00	36.9	3.69	2.70
	30.02	31.9	3.19	2.33
	35.08	28.0	2.81	2.05
	40.00	24.8	2.49	1.82

Table 13 - continuation. Solvent-viscosity determinations^a

Solvent ^b	Temperature (°C)	Torque (%)	Viscosity ^c (cP)	Shear stress (dyn/cm ²)
B001107-3-4	20.00	41.8	4.17	3.05
	25.00	36.0	3.61	2.63
	25.00	36.0	3.61	2.63
	30.00	31.2	3.12	2.28
	35.00	27.4	2.74	2.00
	40.02	24.4	2.44	1.78
B001107-3-5	20.00	41.3	4.12	3.01
	25.00	35.7	3.57	2.61
	30.00	31.0	3.11	2.27
	35.02	27.1	2.70	1.98
	40.02	24.0	2.40	1.76
B001107-3-6	20.00	47.8	4.78	3.50
	25.00	40.7	4.07	2.98
	30.03	34.9	3.49	2.55
	35.05	30.5	3.06	2.23
	40.05	26.8	2.69	1.96
B001107-3-7	19.96	47.3	4.74	3.47
	25.00	40.3	4.04	2.95
	30.00	34.6	3.46	2.54
	35.02	30.2	3.02	2.21
	40.06	26.6	2.65	1.94
B001107-3-8	20.00	58.5	5.85	4.27
	25.05	49.0	4.91	3.59
	30.06	41.6	4.16	3.04
	35.06	35.8	3.59	2.62
	40.06	31.3	3.12	2.28
B001107-3-9	19.95	67.1	6.71	4.90
	25.00	55.4	5.56	4.06
	30.02	46.5	4.66	3.40
	35.05	39.7	3.97	2.89
	40.05	34.3	3.44	2.51

^aBrookfield LVTDV-II (Serial Number D15869) UL Adapter with heating jacket.

^bSee Table 2 for the composition of the specified solvent.

^cStandard deviation is estimated to be ± 0.1 centipoise (cP).

2.3.8 Solvent Interfacial Tension

The results of the measurements are given in Tables 14–17 and are shown graphically in Figs. 11 and 12. The tables contain the data for the four series of tests. Figure 11 shows the surface tension of the solvents and also contains the surface tensions of the aqueous simulant, scrub solution, and strip solution. Figure 12 shows the interfacial tension of the solvents versus simulant, scrub, and strip solutions. The results reveal nothing unusual, and the individual solvents behave similarly with the three aqueous solutions tested.

Table 14. Surface-tension determinations

Solution identification ^a	Density (g/cm ³)	Indicated surface tension (dyn/cm)		Instrument reading, average ($P_{\text{interface}}$)	Correction factor (F) from Eq. 3	Actual surface tension (dyn/cm)
		Trial 1	Trial 2			
B001107-3-1	0.8395	26.9	26.8	26.9	0.8896	23.9
B001107-3-2	0.8395	26.8	26.8	26.8	0.8895	23.8
B001107-3-3	0.8531	26.8	26.7	26.8	0.8888	23.8
B001107-3-4	0.8525	26.8	26.9	26.9	0.8890	23.9
B001107-3-5	0.8516	27.0	27.1	27.1	0.8893	24.1
B001107-3-6	0.8644	27.0	26.9	27.0	0.8886	23.9
B001107-3-7	0.8632	26.9	27.0	27.0	0.8886	23.9
B001107-3-8	0.8819	27.0	27.1	27.1	0.8879	24.0
B001107-3-9	0.8951	27.1	27.0	27.1	0.8874	24.0
Strip solution	0.9974	41.0	40.0	40.5	0.8999	36.4
Scrub solution	0.9984	48.3	48.1	48.2	0.9085	43.8
Simulant	1.2536	64.6	64.8	64.7	0.9122	59.0

^aSee Table 2 for the composition of the specified solvent.

Table 15. Interfacial tension versus simulant

Solvent identification ^a	Density (g/cm ³)	Indicated interfacial tension (dyn/cm)		Instrument reading, average ($P_{interface}$)	Correction factor from Eq. 3	Actual interfacial tension (dyn/cm)
		Trial 1	Trial 2			
		B001107-3-1	0.8395			
B001107-3-2	0.8395	20.8	20.7	20.8	0.9106	18.9
B001107-3-3	0.8531	20.9	20.8	20.9	0.9127	19.0
B001107-3-4	0.8525	20.7	20.5	20.6	0.9119	18.8
B001107-3-5	0.8516	20.7	20.6	20.7	0.9119	18.8
B001107-3-6	0.8644	20.3	20.4	20.4	0.9129	18.6
B001107-3-7	0.8632	20.2	20.4	20.3	0.9126	18.5
B001107-3-8	0.8819	20.5	20.5	20.5	0.9160	18.8
B001107-3-9	0.8951	20.1	20.3	20.2	0.9172	18.5

^aSee Table 2 for the composition of the specified solvent.

Table 16. Interfacial tension versus scrub solution

Solvent identification ^a	Density (g/cm ³)	Indicated interfacial tension (dyn/cm)		Instrument reading, average ($P_{interface}$)	Correction factor from Eq. 3	Actual interfacial tension (dyn/cm)
		Trial 1	Trial 2			
		B001107-3-1	0.8395			
B001107-3-2	0.8395	16.8	16.9	16.9	0.9640	16.2
B001107-3-3	0.8531	16.5	16.6	16.6	0.9706	16.1
B001107-3-4	0.8525	16.7	16.5	16.6	0.9704	16.1
B001107-3-5	0.8516	16.6	16.5	16.6	0.9696	16.0
B001107-3-6	0.8644	16.4	16.3	16.4	0.9772	16.0
B001107-3-7	0.8632	16.1	16.1	16.1	0.9748	15.7
B001107-3-8	0.8819	16.0	16.0	16.0	0.9892	15.8
B001107-3-9	0.8951	16.0	15.8	15.9	1.0016	15.9

^aSee Table 2 for the composition of the specified solvent.

Table 17. Interfacial tension versus strip solution

Solvent identification ^a	Density (g/cm ³)	Indicated interfacial tension (dyn/cm)		Instrument reading, average ($P_{interface}$)	Correction factor from Eq. 3	Actual interfacial tension (dyn/cm)
		Trial 1	Trial 2			
B001107-3-1	0.8395	16.0	16.0	16.0	0.9599	15.4
B001107-3-2	0.8395	16.0	15.9	16.0	0.9596	15.3
B001107-3-3	0.8531	15.2	15.8	15.5	0.9651	15.0
B001107-3-4	0.8525	16.0	15.8	15.9	0.9670	15.4
B001107-3-5	0.8516	15.2	15.7	15.5	0.9639	14.9
B001107-3-6	0.8644	15.7	15.6	15.7	0.9736	15.2
B001107-3-7	0.8632	15.7	15.6	15.7	0.9727	15.2
B001107-3-8	0.8819	15.6	15.8	15.7	0.9880	15.5
B001107-3-9	0.8951	16.0	15.5	15.8	1.0015	15.8

^aSee Table 2 for the composition of the specified solvent.

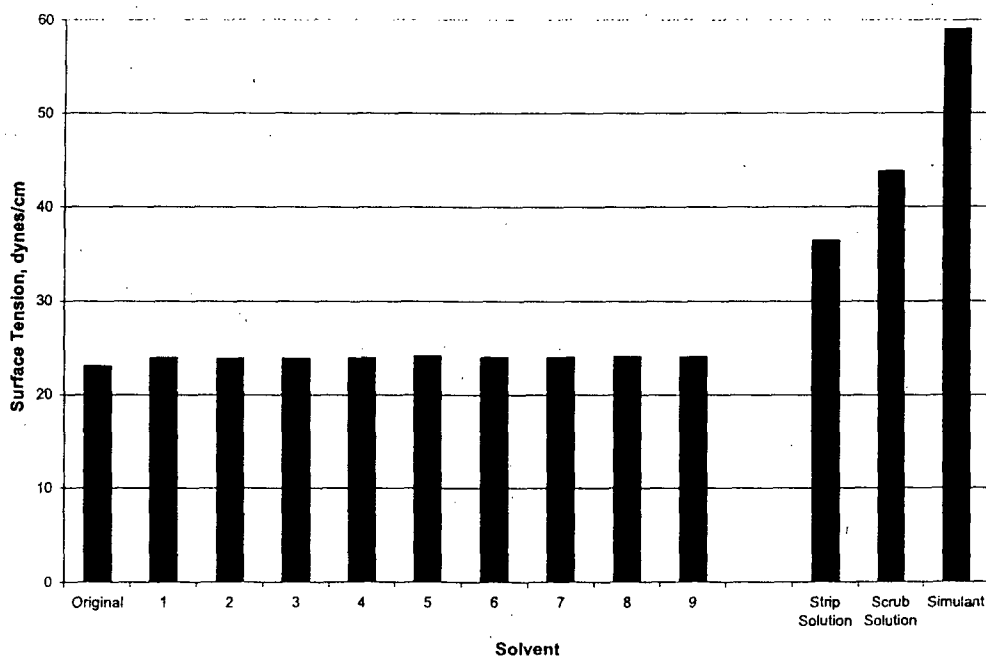


Fig. 11. Solvent and process solution surface tension. The numbers on the abscissa are the test numbers from Table 2.

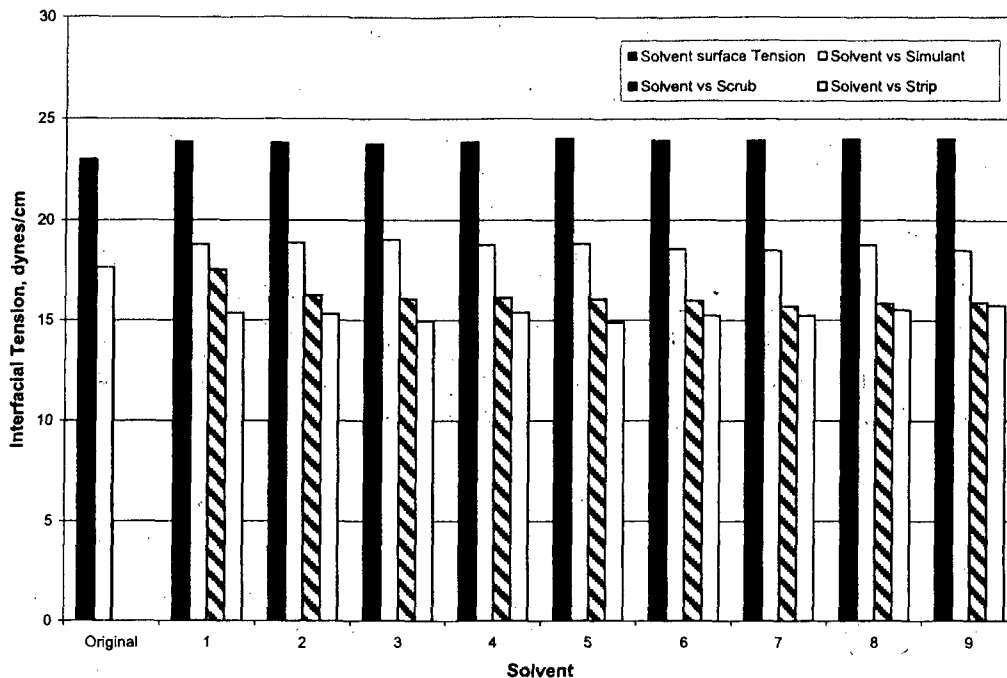


Fig. 12. Solvent interfacial tension in extraction, scrub, and strip contacts. The numbers on the abscissa are the test numbers from Table 2.

2.4 SOLVENT-COMPOSITION RECOMMENDATION PROCESS

The process used by the CSSX team to arrive at the solvent-composition recommendation involved several actions. First, the experimental data described in this report were distributed to the team members. Second, two conference calls were held. During the first call, the methods of data acquisition and the significance of the data relative to the selection criteria were discussed [20]. The action item from this discussion was for each participant to make a recommendation concerning the solvent composition and forward this to all of the participants. A compilation of the individual recommendations was distributed prior to the second conference call. The second call focused on the individual recommendations. Between the two calls, a technical presentation was given during the weekly TFA program status review [37]. The recommended composition was a consensus opinion of the CSSX technical team. The rationale used by the CSSX team in arriving at the recommended solvent composition is described in Ref. 20.

The primary criterion involved the selection of a composition that is thermodynamically stable with respect to the crystallization of BOBCalixC6. The fact that BOBCalixC6 has a solubility limit of 7.55 mM (for a concentration of Cs-7SB of 0.75 M) suggests that the concentration should be less than 7.5 mM to accommodate variations in solvent preparation without exceeding this limit. The solubility data also indicate that the thermodynamic solubility value for BOBCalixC6 is linked to the Cs-7SB modifier

concentration. For example, if the BOBCalixC6 concentration is 7 mM, the Cs-7SB modifier concentration should be approximately 100 times higher. The data on third-phase formation also suggest the need for a solvent composition with a BOBCalixC6 concentration of 8 mM or less and a Cs-7SB modifier concentration of at least 0.65 M. The density criterion suggests compositions with the Cs-7SB modifier concentration equal to or less than 0.85 M. Contactor throughput and phase separation are dependent on the density difference of the two phases; that is, for a given contactor size, throughput is larger and the phase separation performance generally improves as the density difference increases.

Although all of the candidate compositions met the bounding criterion for the D_{Cs} values, only the previous baseline composition meets the goal. Thus, a composition with D_{Cs} values close to the goal is preferred because it would provide the ability to process waste blends that have properties that are modestly different from those of the waste simulant composition. The flowsheet robustness calculations suggest a BOBCalixC6 concentration between 6 and 8 mM and a modifier concentration between 0.65 and 0.85 M.

The combination of BOBCalixC6 solubility, D_{Cs} values, and high flowsheet robustness, as well as the desire to have a low density, establishes the basis for the 7 mM BOBCalixC6 and 0.75 M Cs-7SB modifier concentration recommendation.

The recommended TOA concentration increase from 1 mM to 3 mM is based on three considerations. First, the flowsheet robustness calculations indicate that 10 mM TOA will require a major alteration of the solvent flow rate to achieve process performance above the bounding condition. Second, since TOA is the solvent component most susceptible to thermal and radiolytic decomposition, selecting a TOA concentration higher than the 1 mM baseline value will provide the CSSX process more resistance to the variations in anionic impurity content that are certain to be encountered with the different waste blends. Third, a TOA concentration greater than 1 mM will also provide greater flexibility in solvent preparation and process control.

The solvent dispersion numbers for all the solvent compositions tested against the waste simulant, scrub, and strip solutions met the selection criterion and consequently did not provide a means to differentiate between different solvent compositions. However, comparison of solvent dispersion numbers against the 0.01 M NaOH solvent wash solution indicates the need to re-evaluate the NaOH concentration used for solvent washing. This need was in fact addressed in contactor tests with the optimized solvent [38], showing that the 10 mM NaOH wash performs satisfactorily.

Although the viscosity, surface tension, and interfacial tension were not explicitly identified in any of the selection criteria, these physical properties can impact the dispersion number. Therefore, experimental determination of these properties was included in the study to verify that no unexpected behavior occurred. The experimental results did not reveal any such behavior.

3. CESIUM DISTRIBUTION BEHAVIOR

3.1 INTRODUCTION

This chapter describes batch cesium distribution behavior of the optimized CSSX solvent. Since the solvent was in fact not explicitly among those tested, but rather an intermediate composition, it was first necessary to determine its extraction, scrub, and strip (ESS) behavior. Second, parameters are needed for estimation of cesium distribution ratios within the range of expected operating temperatures 15–35 °C. Finally, it was desirable to demonstrate recycle of the solvent by showing that results obtained during a second ESS cycle are within experimental error identical to those obtained with the pristine solvent. It may be recalled that D_{Cs} values on the second and subsequent cycles were found to be higher, especially on stripping, when the previous baseline solvent was employed [11]. This behavior was mainly linked to the presence of the lipophilic anion dibutylphosphate, which is readily removed upon washing the solvent with NaOH, thereby restoring normal function on subsequent cycles. Thus, it was of interest here to observe whether the increased TOA concentration of the optimized solvent suppressed this effect, with or without a NaOH wash.

3.2 EXPERIMENTAL SECTION

The optimized CSSX solvent was employed (Chapter 2), as recommended previously [21,22]. The standard ESS protocol (one extraction at O:A = 0.33, two scrubs at O:A = 5, and four strips at O:A = 5) was followed. Contacts were performed in 50-mL Teflon[®] fluorinated ethylene propylene (FEP) tubes for the extraction step and 15-mL capacity polypropylene tubes for scrubs and strips. The contacting was carried out for 30 minutes using end-over-end rotation in a 25.0 ± 0.5 °C constant-temperature air box. ESS tests at low (15 °C) and high (35 °C) temperatures were carried out respectively in a thermostated water bath and in an incubator. Agitation was effected by orbital shaking in the water bath and wheel rotation in the incubator.

3.3 RESULTS AND DISCUSSION

3.3.1 Extraction, Scrub, and Strip Performance

Experiments involving the determination of cesium distribution ratios with the optimized solvent were carried out in triplicate and compared to the values obtained with the previous baseline solvent. Table 18 presents the results obtained with the optimized solvent where the extraction is performed using the full simulant, the scrub using nitric acid 50 mM, and the strip using nitric acid 1 mM. The results are very close to the predicted values presented in the Table A1 in Appendix A. The values, calculated from a

double interpolation of the distribution ratios found for different concentrations of calixarene and modifier, are acceptable for process development. Additional tests were performed using strip solutions mimicking off-normal conditions in which some of the acid is neutralized.

Table 18. Cesium batch ESS performance for previous-baseline and optimized solvents

Conditions ^a	D_{Cs}						
	Extact	Scrub #1	Scrub #2	Strip #1	Strip #2	Strip #3	Strip #4
Standard ESS	14.05	1.14	1.35	0.115	0.076	0.117	0.053
Standard ESS	14.14	1.14	1.35	0.118	0.081	0.093	0.052
Standard ESS	14.30	1.13	1.34	0.113	0.080	0.063	0.053
NaNO ₃ 1mM	13.53	1.13	1.35	0.119	0.125	0.078	0.066
NaNO ₃ 1mM	14.33	1.14	1.34	0.128	0.223	0.078	0.066
NaNO ₃ 1mM/HNO ₃ 0.05 mM	14.24	1.13	1.33	0.123	0.087	0.078	0.064
NaNO ₃ 1mM/HNO ₃ 0.05 mM	14.14	1.12	1.35	0.120	0.091	0.079	0.064
Previous-baseline solvent	17.56	1.60	1.60	0.133	0.083	0.065	0.059

^aExcept where indicated (last line), the optimized solvent was used for each experiment. "NaNO₃ 1 mM" indicates that the four strips were carried out using a neutral solution of 1 mM sodium nitrate. "NaNO₃ 1 mM/HNO₃ 0.05 mM" indicates that the four strips were carried out using a mildly acidic solution of 1 mM sodium nitrate and 0.05 mM nitric acid.

Even with mildly acidic or even neutral stripping solutions, the cesium distribution ratios remain acceptable. Of course, the whole range of altered stripping solutions potentially encountered in the system was not tested. It is important to point out that these conditions include an acidic scrub, which is probably sufficient to ensure enough TOA protonation, therefore a good stripping. Poorer results could have been expected in the event that the two scrubs are alkaline due to entrained carryover of waste simulant from extraction.

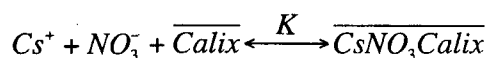
3.3.2 Temperature Variation

Temperature-variation experiments were carried out at three different temperatures encompassing those temperatures that would potentially be encountered during the CSSX process. This experiment permits calculation of an apparent enthalpy change associated with each stage, thereby providing an approximate correction factor for any given temperature. It should be noted that the mechanism of extraction is complex [39], and thus, only an *apparent* enthalpy change is given as an empirical parameter for estimation purposes. Results are presented in Table 19.

Table 19. ESS results for three different temperatures

T (°C)	1000/T (K ⁻¹)	D _{Cs}						
		Extraction	Scrub #1	Scrub #2	Strip #1	Strip #2	Strip #3	Strip #4
15	3.4704	27.41	4.37	3.73	0.330	0.242	0.197	0.171
15	3.4704	24.86	4.14	3.60	0.364	0.276	0.221	0.192
25	3.3540	12.83	0.99	1.20	0.099	0.065	0.051	0.045
25	3.3540	12.89	0.98	1.19	0.098	0.064	0.051	0.045
35	3.2451	7.07	0.41	0.50	0.040	0.027	0.022	0.021
35	3.2451	7.18	0.41	0.49	0.041	0.028	0.023	0.021

Assuming that only a single equilibrium is involved in the cesium extraction, scrub, or strip steps, it may be shown that there is a direct relationship between the cesium distribution ratio and the formation constant of the considered equilibrium. For example, let's consider the simplest system:



$$D = \frac{[\overline{Cs^+}]}{[Cs^+]} = \frac{[\overline{CsNO_3Calix}]}{[Cs^+]} = K[NO_3^-][\overline{Calix}]$$

where overbars indicate organic-phase species. As long as the organic-phase cesium complex is mononuclear and neutral, such a proportionality between D and K should hold for different extraction mechanisms. Assuming that the temperature variation does not impact the loading of the calixarene or the total concentration of nitrate in the aqueous phase, one then may write:

$$\ln D = A + \ln K$$

$$\ln K = -\frac{\Delta G_{app}}{RT}, \quad \ln K = -\frac{\Delta H_{app}}{RT} + \frac{\Delta S_{app}}{R}$$

$$\ln D = B - \frac{\Delta H_{app}}{RT}$$

where T is expressed in degrees Kelvin; A and B are constants; and B includes A and $\Delta S_{app}/R$. The slope of the line $\ln D$ versus $1000/T$ should give the value of the apparent (app) enthalpies associated with the different stages of the process. The linearity of the different plots is confirmed as seen in Fig. 13. All results per stage are shown in Table 20.

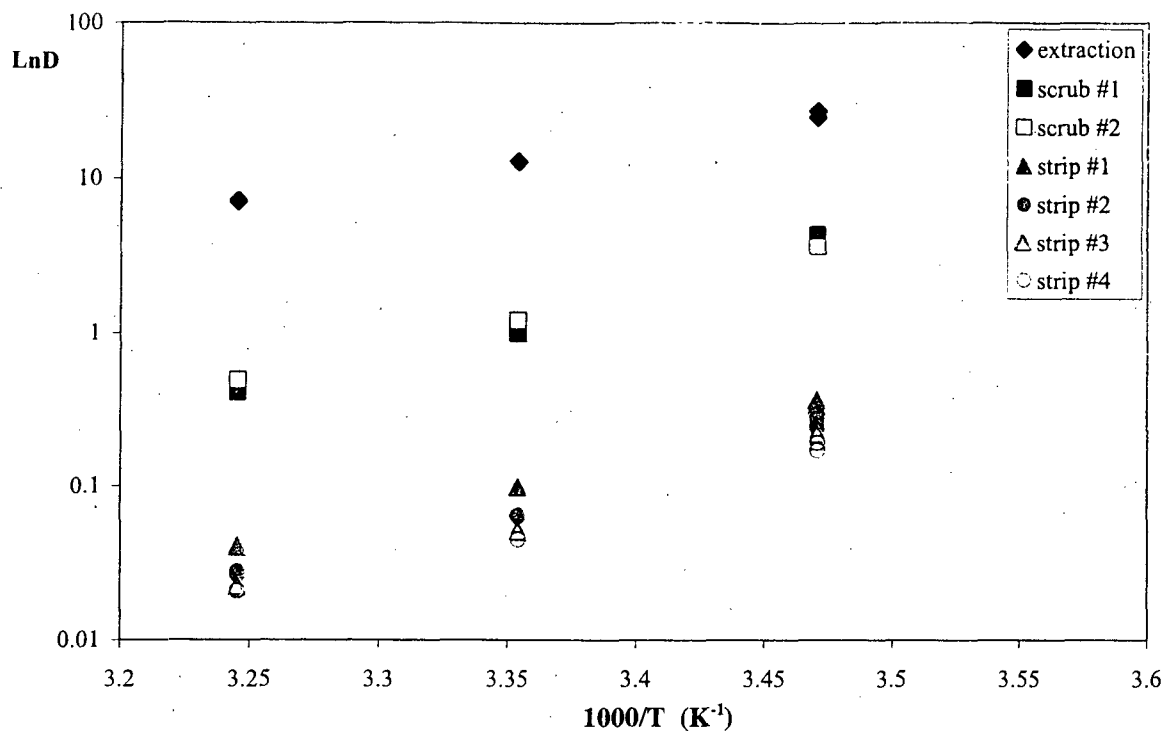


Fig. 13. ESS test at three different temperatures.

Table 20. Apparent enthalpy changes for each ESS stage

Stage	ΔH_{app} (kJ/mol)
Extraction	-47.95
Scrub #1	-86.82
Scrub #2	-74.24
Strip #1	-79.36
Strip #2	-82.94
Strip #3	-82.49
Strip #4	-79.71

The apparent enthalpy values are close to those obtained with the previous baseline solvent. Less scattering is observed here for the four strip values, probably because of the greater reliability of the data obtained at 15 °C. As observed before [11], the extraction step is the least sensitive to temperature variation, most likely because of the higher loading of BOBCalixC6 with potassium as the temperature decreases. This loading corresponds to a lower concentration of free BOBCalixC6, therefore lower D_C values, which in turn give a less steep apparent slope.

3.3.3 Multicycle Behavior

This test reproduces in part the multicycle tests performed in FY 2001. Based on the satisfactory results obtained with the previous baseline solvent, only two cycles were included in this test with the optimized solvent. After the first cycle, one sample was washed with sodium hydroxide 10 mM (O:A = 1:1) before going on to the extraction of the second cycle, while the other one was not. Results are summarized in Table 21.

Table 21. Two-cycle ESS tests

Test	D_{Cs}						
	Extraction	Scrub #1	Scrub #2	Strip #1	Strip #2	Strip #3	Strip #4
1 st cycle	13.88	1.110	1.267	0.1236	0.0721	0.0540	0.0478
1 st cycle duplicate	13.34	1.165	1.177	0.1107	0.0730	0.0532	0.0482
2 nd cycle	13.84	1.180	1.268	0.1356	0.0699	0.0540	0.0508
2 nd cycle with wash	13.79	1.107	1.261	0.1297	0.0724	0.0552	0.0492

A small increase in D_{Cs} is noticeable for the first and fourth strips on the second cycle, but this increase is close to, or within, the experimental error for ESS tests, approximately $\pm 7\%$ [11]. The caustic wash seems to improve slightly the overall behavior.

3.4 CONCLUSIONS

The cesium extraction behavior of the optimized solvent is similar to the behavior obtained in FY 2000 and FY 2001 with the previous baseline solvent [11]. As expected, cesium distribution ratios are lower due to the decrease in the calixarene concentration, but the decrease in extraction is somewhat counterbalanced by the decrease in the cesium stripping values. As a result, the decrease in the ratio of D_{Cs} on extraction to that on stripping is not large, which corresponds to the observation in Chapter 2 that the flowsheet robustness is not unacceptably compromised. Apparent thermodynamic parameters for each stage are also very similar to those obtained with the previous baseline solvent. The results are consistent with the results of other studies showing that the formation constants associated with extraction equilibria did not vary much upon changing the solvent [41]. Finally, batch cesium extraction performance is not altered upon a second cycle, which can be taken as an indication of the effectiveness of the increased TOA concentration in the optimized solvent.

4. PARTITIONING OF SOLVENT COMPONENTS

4.1 INTRODUCTION

Partitioning ratios of solvent components are critical parameters of the CSSX process. Loss of any component (particularly of the calixarene extractant) can translate into loss of extraction performance and costs for replenishing the solvent to its original composition. Solvent components can be lost to the aqueous phase through two different mechanisms: partitioning and entrainment. Although BOBCalixC6, Cs-7SB, and TOA are each highly lipophilic, they possess small, finite tendencies to partition into the aqueous process solutions. Among these aqueous phases, the waste feed is the most important, because its flow will be much larger (15-fold in the current flowsheet) than the flow of the strip or wash solutions. Since the solvent will be recycled several thousand times in the course of a year's operation, it is clear that the partition ratios must be sufficiently high to avoid problems. For less than 10% loss of a reagent per year, the minimum partition ratio is approximately 10^5 (more exactly, assuming 2800 cycles, $P > 88,600$ for O:A = 1:3). Measurement of such high P values, however, represents a considerable analytical challenge [11]. For the critical, expensive reagent, BOBCalixC6, it was thought likely that the condition of $P > 10^5$ was met, although only a lower limit ($P_{\text{BOBCalixC6}} > 12,500$) could be reported in the case of the previous baseline solvent in contact with waste simulant, strip solution, or wash solution [11]. Partition ratios for Cs-7SB and TOA were high and on the borderline of reliable measurement in that same study. For example, for partitioning into the waste simulant from the previous baseline solvent, these two reagents were found to have partition ratios of respectively $>50,000$ and $38,000\text{--}200,000$. For TOA, loss to the acidic strip solution would be more significant, since it was found that $P = 14,000\text{--}55,000$ [11]. Overall, it thus appears likely that partitioning is not a significant issue. However, in view of both the acceptance of an optimized solvent composition and the uncertainty in the previous measurements, especially those for BOBCalixC6, it was judged desirable to address the partitioning issue again with the intent to improve upon analytical technique. Provided that partitioning losses of reagents could be more confidently shown to be small, it would then be possible elsewhere to approach the question of solvent losses in terms of entrainment, namely, the physical loss of solvent to the aqueous phase due to incomplete coalescence of fine droplets.

4.2 EXPERIMENTAL SECTION

4.2.1 Materials and Contacting Method

Solvent Lot No. PVB B000894-87W (87W) was used for all experiments. This batch of washed solvent has the following composition: 0.007 M BOBCalixC6 (Lot #000714HMKC-0004), 0.750M Cs-7SB modifier (Lot #B000894-64DM), 0.003 M tri-*n*-octylamine (Lot #B000894-186), and Isopar[®] L (Lot #03081001-6-2). Full Simulant, draw #5 with Cs added to 1.4×10^{-4} M, was obtained in FY 2000.

Sodium hydroxide pellets (Lot # 41171126) used to prepare all caustic solutions were obtained from EM Science. Nitric acid was ultrapure Ultrex II (J. T. Baker, Lot #T19541). Dichloromethane (EM Science, Lot 38301846) was used as received.

Solvent 87W was contacted with various aqueous phases using O:A ratio of 1:100. The contacts were done by handshaking the two phases in 1 L Teflon[®] separatory funnels. The aqueous layers were then drained into 250-mL Teflon[®] centrifuge bottles and centrifuged for 20 min at 3000 rpm. The aqueous phases were carefully siphoned into clean bottles using small Tygon[®] capillary tubing to avoid organic-phase contamination. Known volumes of the aqueous phases (approx. 200 mL) were then back-extracted two times using a small volume (~10–15 mL) of fresh dichloromethane each time. The dichloromethane was taken to dryness by evaporation or nitrogen blow-down, and the resultant residue prepared for analysis.

4.2.2 Calixarene and Modifier Analyses

Sample Preparation

All samples were originally presented as dichloromethane extracts (approximately 10 mL each) in 20-mL vials. The solvent was removed using a stream of dry flowing nitrogen while heating the bottom of each vial to 34 °C. The residues were then redissolved in 1 mL isopropanol and submitted for HPLC analysis.

HPLC Analysis

All samples were analyzed with a Hewlett-Packard Model 1090 high-pressure liquid chromatograph equipped with an automatic sampler (maximum 100 individual samples; maximum injection volume 250 mL), ternary solvent gradient capability, and a diode array detector (wavelength range 190–600 nm). A PRP-1 (polystyrene divinylbenzene) reversed-phase column (150 × 4.1 mm), packed with 10 μm diameter particles (100 Å porosity), a product of the Hamilton Co. (Reno, NV), was used for all determinations. The analytes were eluted isocratically from the column using a 60/40 (v/v) mixture of isopropanol/acetonitrile at a flow rate of 1.00 mL/min. The sample analysis time was 5 minutes per sample; each was analyzed in duplicate. Both the analytical column and the solvent were heated to 40 °C using the internal column oven.

Because there was a difference of up to four orders of magnitude in the concentrations of BOBCalixC6 and Cs-7SB modifier, each sample was analyzed using two independent HPLC methods. In the first (used for low-level BOBCalixC6), the injection volume was 25 μL; in the second (used for high-level Cs-7SBT modifier), the injection volume was 10 μL. More significant differences between the two methods are described under “Quantitation” below.

Quantitation

The quantitation of BOBCalixC6 was performed using the 25-μL injection volume described above and a measuring wavelength of 210 nm. The calibration procedure employed seven independently-prepared standards of BOBCalixC6, ranging in concentration between 0.001 and 0.1 mM, using

isopropanol as the diluent. Each standard was analyzed twice. The calibration data was fit to a least-squares calibration line, where the coefficient of determination, r^2 , exceeded 0.9995. The detection limit was taken as the concentration that would produce the peak with the smallest integration, here 0.001 mM (i.e., 10^{-6} M).

The quantitation of Cs-7SB modifier was performed using the 10- μ L injection volume described above and a measuring wavelength of 254 nm. The calibration procedure employed seven independently-prepared standards of Cs-7SB modifier, ranging in concentration between 1 and 100 mM, using isopropanol as the diluent. Each standard was analyzed twice. The calibration data was fit to a least-squares calibration line, where the coefficient of determination, r^2 , exceeded 0.998.

4.2.3 Tri-*n*-octylamine Analyses

Sample Preparation

The samples, which were originally prepared in an unspecified volume of dichloromethane, were initially taken to dryness at room temperature, then reconstituted in 1.0 mL dichloromethane. These rediluted samples were then transferred to 2-mL capacity automatic sampler vials for gas chromatographic analysis.

Gas Chromatographic Analysis

Gas chromatography was performed on a Hewlett Packard HP6850 series GC system using an HP-5MS (crosslinked 5% phenyl methyl siloxane) fused silica capillary column (Agilent Technologies catalog number 190915-433E) of length 30 meters, column internal diameter of 0.25 mm, phase ratio 250, and film thickness of 0.25 μ m. The carrier gas was helium (purity > 99.999%) flowing at 1 mL/min. The sample injection volume was 1 μ L, with a split ratio of 1/100. The column oven temperature was programmed from 50 °C to 280 °C at 10 °C/min, with a hold at 280 °C for 10 min. A flame ionization detector (FID) was used to detect the presence of TOA. The flows of the FID gases (i.e., air, hydrogen, and carrier) were set to factory-recommended values. All injections were performed using an Agilent Model 7683 automatic sampler.

Calibration

The response of the FID was calibrated using six independently-prepared standards ranging in concentration between 0.05 and 2 mM TOA in dichloromethane. The responses were fit to a linear least-squares calibration line, whose coefficient of determination, r^2 , exceeded 0.9999. The detection limit of the FID was taken to be the standard concentration that produced the peak with the smallest integration, here 0.05 mM, corresponding to 177 pg actually injected on column.

4.3 RESULTS AND DISCUSSION

In all cases, the partitioning of the three solvent components was measured not only using the aqueous phases encountered in the different stages of the process (simulant, scrub, and strip solutions), but also using several concentrations of nitric acid (to assess the influence on tri-*n*-octylamine) and sodium hydroxide (being the candidate of choice for solvent washes in the process). All organic concentrations presented in the tables were determined by subtracting the measured aqueous concentration from the initial organic concentration. In order to be in the best possible conditions to obtain measurable amounts of organic compounds in the aqueous phases, an O:A ratio of 1:100 was used.

4.3.1 Calixarene Partitioning

Precision in calixarene detection was greatly improved compared to results obtained in FY 2000 and FY 2001. Results reported for similar experiments using the previous baseline solvent indicated that all partition ratios were greater than 12,500 based on the detection limit of the method [11]. Table 22 reflects the improved precision, as partition ratios are now at least 10 times greater than reported earlier, confirming the extremely low affinity of BOBCalixC6 for the aqueous phase.

In all cases, the amount of calixarene lost due to the contact with the aqueous phase is negligible. No real trend can be discerned from these experiments. Moreover, the method used to limit the potential contamination of that aqueous phase with the organic phase (siphoning) was the best available, but could not guarantee a complete contamination-free transfer. A mere contamination of 5–10 μL of the aqueous phase with the organic phase is sufficient to mask any potential trend.

4.3.2 Modifier Partitioning

The modifier Cs-7SB is more soluble in the aqueous phase than the calixarene based on the partition ratios obtained with the previous baseline solvent. Moreover, its greater initial concentration in the optimized solvent (50% greater than the previous baseline solvent) makes it easier to detect in the aqueous phase after contact. Results are presented in Table 23.

Quantities of modifier solubilized in the aqueous phases are again found to be much greater than those of calixarene, which is at first not surprising in that the original amount of modifier is 100 times greater. However, that ratio is no longer maintained, which is a good indication that the technique used for subsampling the aqueous phase was adequate to minimize entrainment. Based on these experiments, it is difficult to assess with precision whether the presence of these organic components in the aqueous phase is due to true partitioning. More lengthy experiments would have been needed to add that detail. However, it can be said that if there is some entrainment contributing to the presence of solvent components in the aqueous phases, while its contribution to the calixarene partitioning is unknown, its contribution to modifier partitioning is negligible. One could assume in an extreme case that all the calixarene present in the aqueous phases is due to entrainment. By implication, this would still leave about 90% of soluble modifier that ought to be accounted for through true partitioning.

Table 22. Partition ratios for BOBCalixC6^a

Aqueous phase	Organic concentration ^b (M)	Aqueous concentration (M)	Partition ratio
Full simulant	7.00E-03	3.31E-08	2.12E+05
Full simulant	7.00E-03	3.15E-08	2.22E+05
Scrub solution	7.00E-03	4.69E-08	1.49E+05
Scrub solution	7.00E-03	4.80E-08	1.46E+05
Strip solution	7.00E-03	1.09E-08	6.41E+05
Strip solution	7.00E-03	1.34E-08	5.22E+05
1 M NaOH	7.00E-03	2.59E-08	2.70E+05
1 M NaOH	7.00E-03	2.56E-08	2.74E+05
0.1 M NaOH	7.00E-03	4.73E-08	1.48E+05
0.1 M NaOH	7.00E-03	4.56E-08	1.53E+05
0.01 M NaOH	7.00E-03	1.23E-08	5.68E+05
0.01 M NaOH	7.00E-03	1.54E-08	4.54E+05
0.001 M NaOH	6.99E-03	5.61E-08	1.25E+05
0.001 M NaOH	6.99E-03	5.54E-08	1.26E+05
1 M nitric acid	7.00E-03	1.00E-08	6.97E+05
1 M nitric acid	7.00E-03	1.18E-08	5.93E+05
0.1 M nitric acid	7.00E-03	9.35E-09	7.49E+05
0.1 M nitric acid	7.00E-03	6.64E-09	1.05E+06
0.01 M nitric acid	7.00E-03	1.77E-08	3.96E+05
0.01 M nitric acid	7.00E-03	2.20E-08	3.18E+05

^aThe numeric notation used in this table and some subsequent tables in this report is the normal scientific notation, where 7.00E-03 represents 7.00×10^{-3} . Both notations are used interchangeably.

^bNot measured. Values are calculated from the mass balance between the initial concentration of BOBCalixC6 in the solvent (0.007 M) and that measured in the aqueous phase at an O:A of 1:100.

4.3.3 Tri-*n*-octylamine Partitioning

Results for tri-*n*-octylamine partitioning were relatively satisfactory, but inconclusive. Tri-*n*-octylamine was probably present in amounts that were too low to be detected by the method designed to analyze the samples. A complete calibration curve was obtained, with the smallest integrable peak corresponding to 5×10^{-5} M. All analyzed samples fell well below the detection limit (not even a hint of peak was noticeable), corresponding to a lower limit for the partition ratio of 6000. However, based on these observations and previous results [11], it is reasonable to propose that the partitioning of TOA is not an issue for the process.

Table 23. Partition ratios for modifier Cs-7SB

Aqueous phase	Organic concentration ^a (M)	Aqueous concentration ^b (M)	Partition ratio
Full simulant	7.50E-01	BDL	>3.50E+04
Full simulant	7.50E-01	BDL	>3.50E+04
Scrub solution	7.44E-01	6.41E-05	1.16E+04
Scrub solution	7.44E-01	6.40E-05	1.16E+04
Strip solution	7.47E-01	3.49E-05	2.14E+04
Strip solution	7.46E-01	3.52E-05	2.12E+04
1 M NaOH	7.47E-01	3.35E-05	2.23E+04
1 M NaOH	7.47E-01	3.37E-05	2.21E+04
0.1 M NaOH	7.45E-01	5.48E-05	1.36E+04
0.1 M NaOH	7.45E-01	5.36E-05	1.39E+04
0.01 M NaOH	7.45E-01	5.31E-05	1.40E+04
0.01 M NaOH	7.45E-01	5.31E-05	1.40E+04
0.001 M NaOH	7.45E-01	5.07E-05	1.47E+04
0.001 M NaOH	7.45E-01	5.09E-05	1.46E+04
1 M nitric acid	7.38E-01	1.17E-04	6.29E+03
1 M nitric acid	7.39E-01	1.11E-04	6.68E+03
0.1 M nitric acid	7.44E-01	6.09E-05	1.22E+04
0.1 M nitric acid	7.44E-01	6.06E-05	1.23E+04
0.01 M nitric acid	7.44E-01	6.39E-05	1.16E+04
0.01 M nitric acid	7.44E-01	6.39E-05	1.16E+04

^aNot measured. Values were calculated from the mass balance between the initial concentration of modifier in the solvent (0.75 M) and that measured in the aqueous phase at an O:A of 1:100.

^bBDL denotes below detection limit.

4.4 CONCLUSIONS

Partition ratios for BOBCalixC6 and Cs-7SB have been obtained with improved precision, leading to confidence that partitioning losses of these costly solvent components are small with respect to a goal of less than one solvent replacement per year. In the case of BOBCalixC6, partitioning losses to the aqueous raffinate are expected to amount to less than 4.2% per year, based on 2800 solvent cycles at O:A = 1:3 and $P_{\text{BOBCalixC6}} = 2.2 \times 10^5$. Taking $P_{\text{Cs-7SB}} = 3.5 \times 10^4$, corresponding losses of Cs-7SB are expected to be 27% per year. The partitioning of TOA to the aqueous phase was below the detection limit of the gas-chromatographic technique employed, giving $P_{\text{TOA}} > 6000$. No conclusion is therefore possible for TOA, but in view of results on the previous baseline solvent [11], the value of P_{TOA} is likely more than an order of magnitude larger than 6000. Based on chemical reasoning, it may be expected that loss of TOA will be more significant to the strip solution, and if one takes $P_{\text{TOA}} > 6000$ for 2800 solvent cycles at O:A = 5:1, the implied loss of TOA will be less than 9.3%. Given that TOA is critical for good stripping, it is

recommended that more definite measurements of TOA partitioning be sought. It may be noted that commercially available trialkylamines having a higher molecular weight, such as tridecyl- or tridodecylamine, can be substituted for TOA to obtain greater lipophilicity and lower partitioning losses, if desired. On the other hand, recalling that the major breakdown product of TOA is dioctylamine, which is expected to be washed out by the strip solution [11], the analogous breakdown products of more lipophilic trialkylamines will be more difficult to wash out, making solvent cleanup possibly more difficult over extended cycling.

One of the questions asked regarding the present results is whether partitioning and entrainment can be distinguished. Based on the data obtained, it can be deduced that the predominant portion of the modifier present in the aqueous phase is due to solubility, not entrainment. It is less certain that this is the case for BOBCalixC6, since minute traces of entrainment or other artifacts (e.g., suspended dust) can mask its true partition ratio. It is again worth noting that the theoretically expected partition ratio for BOBCalixC6 is astronomical [11]. While the data obtained overall imply small partitioning losses of the solvent components, the expected gradual losses of Cs-7SB and possibly TOA likely necessitate periodic replenishment throughout the course of a year.

5. DISTRIBUTION OF MINOR ORGANIC AND INORGANIC COMPONENTS

5.1 INTRODUCTION

Besides understanding how the element of interest, cesium, and the solvent components distribute in the CSSX flowsheet, it is necessary to understand the fate of key minor inorganic and organic components. These may be introduced into the system from the waste feed or by degradation of the solvent components. Studies in FY 2001 with the previous baseline solvent showed that the strip effluent contained almost exclusively cesium nitrate in 1 mM nitric acid [11]. All other inorganic constituents of the simulant were either not detectably extracted or scrubbed out readily. Certain minor organic species extractable as anions or as neutral weak acids were found to impair stripping if present in sufficient concentration, but washing with dilute aqueous sodium hydroxide was effective in removing them and restoring solvent performance. Such organic species included dibutylphosphate, found in the waste as a breakdown product of tributylphosphate, phenol derivatives formed by degradation of Cs-7SB, or surfactants having 12 carbon atoms or less. Among the different tests run in FY 2001 with the previous baseline solvent, three experiments in which the distribution of minor organic or inorganic components may be impacted due to the change in solvent composition were chosen for repetition with the optimized solvent. Inorganic species included the competing alkali metals Na and K, radioactive metals Tc (as pertechnetate) and Sr, certain transition metals (e.g., Mn and Fe), noble metals, other metals (Ca and Al), and anions (nitrate, nitrite, and sulfate). Organic species included dibutylphosphate and the surfactant dodecanoate. Actinides were previously indicated to be negligibly extracted in simulant tests [11], as was confirmed on tests with real waste [40], and therefore actinides were not included in the present study.

5.2 EXPERIMENTAL SECTION

Phosphorus-31 Nuclear Magnetic Resonance spectra were obtained on a Bruker Avance 400 wide-bore spectrometer as described in Chapter 2. Chemical shifts were referenced against phosphoric acid, set to 0.0 ppm by way of a separate standard sample (sealed tube from Bruker). Preliminary contacts between the solvent 87W and the scrub, strip, or sodium hydroxide at different concentrations were performed in 15-mL polypropylene tubes at 25 °C with an O:A ratio of 1:1. Two types of experiments were performed; simulant compositions were described previously [11]. Either the full simulant (5th draw) was placed in contact with the solvent with an O:A ratio of 1:3, or the "salts+metals" simulant was used at an O:A ratio of 1:3 with the solvent in which a spike corresponding to 75 ppm of dibutylphosphate was added. The "salts+metals" simulant was the same as the full simulant but lacked the minor organic components [11]. The distribution of dibutylphosphate between the solvent 87W and the simulant, scrub, strip, or NaOH solutions were carried out as follows: solvent samples were analyzed directly with no dilution or addition of reagents for integration standards. Aliquots of solvent or simulant were placed directly into 10-mm quartz tubes. A quartz insert containing tributylphosphate (TBP) at 1

mM in deuteriochloroform was placed inside the 10-mm tube, and this solution external to the sample was used as the deuterium lock and integration standard. The insert permitted solvent or simulant samples to be run neat without the need to dilute or mix with a standard solution. Before running sample unknowns, spectra of the empty external tube with the insert and of the solvent containing 1 mM dibutylphosphate (210 ppm) were acquired. For unknown samples, an overnight acquisition (10k–12k scans) was performed to ensure that a reasonable signal/noise ratio was achieved. Data point files for each spectrum were converted to ASCII files and treated under MS Excel for deconvolution. Each peak was considered as a pure Lorentzian and approximated this way. This manipulation allowed more precise determination of the peak areas. The procedure was similar to that used earlier, and further details can be found in that document [11].

Tests involving the distribution of inorganic components (simulant components) were carried out through the regular ESS protocol [11]. The scrub and strip acidic phases were analyzed directly by inductively coupled argon plasma atomic emission spectrometry (ICAP-AES). Solvent samples were analyzed by first adding an equal volume of 1,3-diisopropylbenzene, stripping with an equal volume of deionized water, and analysis of the water layer by ICAP-AES. Strontium and technetium were added separately to the full simulant (originally prepared by Roger Spence, August 2000, filtered draw #5). Technetium was obtained from ORNL Isotope Sales as the ammonium pertechnetate form. A stock solution of 3×10^{-3} M was used, and a spike of 0.15 mL was added to 45 mL of simulant to obtain a final Tc concentration of 10^{-5} M. Strontium nitrate was obtained from J. T. Baker. An aliquot of a 0.01 M $\text{Sr}(\text{NO}_3)_2$ solution was used to spike the simulant.

The surfactant tested was lauric acid (dodecanoic acid), 99%, Emery Industries, Inc., Downey, CA. The surfactant was tested in the optimized solvent at 2×10^{-5} M. A 5-mM stock solution of dodecanoate was made by dissolving via sonication 10.1 mg of dodecanoic acid in 10 mL of Isopar[®] L (Exxon, Lot #0306 10967). A 48- μL volume of 5 mM dodecanoate was added to 12 mL of Cs-7SB solvent, making an effective concentration of 2×10^{-5} M dodecanoate in the solvent. To wash out the surfactant, an equal volume of 10 mM NaOH was contacted with the dodecanoate-containing Cs-7SB solvent by end-over-end rotation inside a 25 °C constant-temperature air box for 30 minutes. The tube was then centrifuged and the solvent layer isolated. Three samples were subjected to the ESS protocol. Solvent designated 87P was pristine solvent; 87SS was solvent containing 2×10^{-5} M dodecanoate; 87WSS was dodecanoate-containing solvent that was subsequently subjected to the 10-mM NaOH wash procedure. The standard ESS protocol (extraction, two scrubs, and four strips) was followed. Contacts were performed in 50-mL Teflon[®] FEP tubes for the extraction step and 17-mL capacity polypropylene tubes for scrubs and strips. Contacts lasted 30 minutes using end-over-end rotation in a 25 °C air box.

5.3 RESULTS AND DISCUSSION

5.3.1 Distribution of Dibutylphosphate

The distribution of dibutylphosphate between the optimized solvent and various aqueous phases could differ from the values obtained in FY 2001 because of the variation in the solvent composition. However, the differences were found to be relatively minor. The same deconvolution technique was used to measure as precisely as possible the area of the peaks. As observed previously, dibutylphosphate partitions quantitatively to the aqueous phase when using a sodium hydroxide wash. The slight increase in the distribution value for larger concentrations of sodium hydroxide is actually due to the necessity of adding more dibutylphosphate to the system; that component was added in its acid form, and consequently some of the hydroxide was consumed.

The moderate partitioning of dibutylphosphate into the solvent was confirmed by using either the full simulant (containing the organic species) or the salts+metals simulant and a spike of dibutylphosphate to the solvent. In both cases, the partition ratios are identical. All results are summarized in Table 24.

Table 24. Partitioning of dibutylphosphate

	O:A	Initial concentration (ppm)	Concentration in the organic phase after contact (ppm)	Partition ratios
Simulant	1:3	25 ^a	43	4.1
Simulant	1:3	75 ^b	43	4.1
HNO ₃ 0.05 M	1	500	60	0.12
HNO ₃ 0.001 M	1	500	64	0.13
NaOH 0.001 M	1	500	1.5	3.0×10^{-3}
NaOH 0.01 M	1	500	BDL ^c	$<5 \times 10^{-4}$
NaOH 0.1 M	1	3750	6	1.6×10^{-3}
NaOH 1M	1	6660	120	1.8×10^{-2}

^aDibutylphosphate is originally in the simulant. Pristine simulant was used.

^bThe solvent was spiked. The simulant used in this case was the Salts+Metals simulant.

^cBelow detection limit.

5.3.2 Distribution of Other Metals and Selected Radionuclides

The extraction of metals originally present in the waste simulant can be influenced by the change in solvent composition. It was determined in FY 2001 that the number of elements and their concentration in stages past the first scrub was negligible compared to the amount of cesium nitrate and nitric acid eventually present in the strip effluent. Two radionuclides potentially found in the actual waste (but not present in the baseline simulant composition [11]), strontium and technetium, were included in this study.

Concentrations presented in the three tables below were determined by stripping the organic phase, to which an equal volume of 1,3-diisopropyl benzene was added, with water. Elements presented in Table 25 along with their detection limits were not extracted by the optimized solvent. This is consistent with the results obtained with the previous baseline solvent.

Table 25. Detection limits of non-extractable metals

	Detection limits	
	(mg/L)	(M)
Ag	0.54	5.0E-06
Cr	0.021	4.1E-07
Cu	0.0027	4.2E-08
Hg	0.098	4.9E-07
Mn	0.0006	1.1E-08
Mo	0.014	1.5E-07
Pb	0.40	2.0E-06
Pd	0.010	9.6E-08
Rh	0.11	1.1E-06
Ru	0.094	9.3E-07
Sn	0.047	4.0E-07
Zn	0.0048	7.3E-08

Elements present in the simulant and their concentrations actually detected in one of the process stages are summarized in Table 26.

Table 26. Concentrations of metals present in the solvent after extraction^a

Stage	Concentrations (M)				
	Al	Ca	Fe	K	Na
Extraction	6.60E-06	7.29E-07	1.17E-05	5.50E-03	3.82E-03
Scrub #1	BDL	5.52E-06	5.20E-06	1.49E-04	1.83E-05
Scrub #2	BDL	BDL	BDL	1.20E-05	4.03E-05
Strip #1	BDL	BDL	BDL	BDL	3.24E-05

^aBDL = below detection limit. Detection limits are respectively 4.2×10^{-6} M for Al, 3.0×10^{-8} M for Ca, 7.0×10^{-8} M for Fe, 3.9×10^{-6} M for K, and 4.3×10^{-6} M for Na.

As expected, potassium and sodium are fairly well extracted and remain in the system following the cesium pattern. Except for sodium, all elements are scrubbed from the solvent by the second scrub stage. The analysis involved also the major anions present in the system. Results for nitrite, nitrate, and sulfate are shown in Table 27.

Table 27. Concentrations of anions present in the solvent at each stage^a

	NO ₂ ⁻	NO ₃ ⁻	SO ₄ ²⁻
Extraction	3.79E-04	1.06E-03	2.10E-05
Scrub #1	BDL	4.72E-03	1.12E-05
Scrub #2	BDL	9.54E-03	5.12E-06
Strip #1	BDL	1.56E-03	BDL

^aBDL = below detection limit. Detection limits are respectively 2.2×10^{-6} M for NO₂⁻, 8.1×10^{-6} M for NO₃⁻, and 2.0×10^{-6} M for SO₄²⁻.

As expected, only nitrate remains after the second scrub. Its concentration increases in the two scrub stages because of the protonation of tri-*n*-octylamine. Two other anions were taken under consideration, but their concentrations fell below the detection limit, respectively 7.0×10^{-6} M for Cl⁻ and 1.0×10^{-6} M for PO₄³⁻. Chloride and phosphate did not appear in any of the phases analyzed above.

Based on the direct aqueous measurements (first part of Table 28) and the washes (indirect measurements of the organic phase), it is reasonable to say that strontium is very poorly extracted and is readily scrubbed from the solvent.

Table 28. Concentrations of strontium in the aqueous phase at each stage^a

Stage	Aqueous [Sr] (M)
Scrub #1	3.99E-08
Scrub #2	BDL
Strip	7.99E-09
Extraction wash	6.85E-09
Scrub #1 wash	BDL
Scrub #2 wash	BDL
Strip wash	BDL

^aWashes were performed by adding to the organic phase an equal volume of 1,3-diisopropyl benzene and contacting that phase with deionized water. BDL denotes analysis was below detection limit, which is 15 ppb or 1.71×10^{-9} M for strontium.

On the contrary, it was found that, while technetium is poorly extracted, it remains in the solvent as long as the aqueous phase in contact is acidic. However, its build-up in the solvent is not a concern in that a sodium hydroxide wash (concentrations 10–300 mM) is sufficient to remove it quantitatively from the solvent. Table 29 presents the results obtained at each stage and also for a water wash done on solvent after each contact.

Table 29. Distribution ratios of technetium obtained in ESS tests

Stage	D_{Tc}	D_{Tc} upon stripping the organic phase with water
Extraction	3.78E-02	2.61E-02
Scrub #1	9.35E-01	5.27E+00
Scrub #2	6.77E-01	4.21E+00
Strip #1	9.03E+00	4.61E+00
Strip #2	9.73E+00	
Strip #3	1.31E+01	
Wash of strip #3 with 0.01M NaOH	2.85E-02	
Wash of strip #3 with 0.3 M NaOH	1.21E-02	

All inorganic elements identified to be potentially in the actual wastes have been determined to be of no impact on the extraction system. The change in solvent composition does not affect the previous conclusions regarding the partition of inorganic components and confirms the robustness of the solvent found in FY 2001.

5.3.3 Effect of Organic Surfactants

Distribution of organic surfactants has been considered to be of major interest [11], particularly after anticaking agents present in salts used to prepare waste simulants were found to create stripping problems [41]. This aspect of the process chemistry had been extensively investigated with the previous baseline solvent, and a remedy was found in every case, the best one being the TOA already present in the solvent. A repeat experiment involving solely sodium dodecanoate has been performed in the present work using the regular ESS test, with and without a wash of the solvent using sodium hydroxide. The results are presented in Table 30.

From the data, it may be observed that dodecanoate-containing solvent (at 2×10^{-5} M) performed almost no differently than the pristine or NaOH-washed solvent. The higher level of TOA chosen for the optimized solvent apparently offsets effects of the surfactant at this low concentration.

Table 30. Effect of dodecanoate on cesium extraction in ESS tests

Test	D_{Cs}						
	Extraction	Scrub #1	Scrub #2	Strip #1	Strip #2	Strip #3	Strip #4
87P ^a	13.36	0.9765	1.235	0.0923	0.0594	0.0494	0.0430
87SS ^b	13.50	0.9428	1.195	0.0917	0.0596	0.0472	0.0445
87WSS ^c	13.83	0.9569	1.139	0.0912	0.0600	0.0479	0.0424

^a87P indicates pristine solvent.

^b87SS indicates solvent initially containing dodecanoate at an initial concentration of 2×10^{-5} M.

^c87WSS indicates solvent initially containing dodecanoate at an initial concentration of 2×10^{-5} M that was, prior to the ESS test, washed with 10 mM NaOH at a 1:1 ratio by end-over-end rotation for 30 minutes on a Glas-Col Rugged Rotator in a 25 °C airbox.

5.4 CONCLUSIONS

The distribution of the solvent constituents and of the trace organic and inorganic components was characterized. The major difference noticed between the results [11] involving the previous baseline solvent and the present results involving the optimized solvent is the demonstration of the ineffective stripping of technetium (as the pertechnetate anion form) from acidic solutions and the need to have a caustic wash following the last strip. All other components behaved as expected based on the results obtained earlier with the previous baseline solvent.

6. THERMAL STABILITY

6.1 INTRODUCTION

Experiments conducted in FY 2001 involved a series of extraction, scrub, and strip steps where the solvent was allowed to remain in contact with one of the corresponding aqueous phases for an extended period of time at 35 °C or 60 °C. The ultimate conclusion was that chemical and thermal stability of the previous baseline solvent significantly exceeds requirements. Logically, the optimized solvent is not expected to differ in this regard in that its chemical constituents are the same, and the work described in this chapter was accordingly intended to provide experimental support for this expectation [11]. In addition to a repeat of the ESS experiments run at the two temperatures 35 °C and 60 °C, experiments at two low temperatures were added, simulating conditions potentially encountered by the solvent upon shipping during winter months. Since only the solvent would be subject to such temperature stress, no contact with aqueous phases was performed before warming the solvent back to room temperature. Performance of the optimized solvent having been subjected to the different thermal and chemical conditions was assessed by ESS experiments uniformly performed at 25 °C.

6.2 EXPERIMENTAL SECTION

6.2.1 Materials, Equipment, and Contacting Method

Three different solvents were used for these tests: two different batches of the previous baseline solvent and the optimized solvent. Batches PVB B000718-156W and B000718-124W of the previous baseline solvent are composed of 0.010 M BOBCalixC6 (IBC Advanced Technologies, Lot No. B000718-100CP), 0.50 M Cs-7SB modifier (Lot No. PVB B000718-10DMP), 0.001 M tri-*n*-octylamine (Lot No. PVB B000718-105L) in Isopar[®] L (ExxonMobil, Lot No. 0306 10967A). The optimized solvent (Batch PVB B000894-87W) is composed of 0.007 M BOBCalixC6 (IBC Advanced Technologies, Lot No. 000714HMKC-004), 0.75 M Cs-7SB modifier (Lot No. B000894-64DM), 0.003 M tri-*n*-octylamine (Lot No. PVB B000894-86) in Isopar[®] L (ExxonMobil, Lot No. 03081001-6-2).

Low-temperature experiments involving the solvents were carried out in a VWR laboratory refrigerator (0 °C) and in the freezer section of VWR combination refrigerator-freezer (-24 °C). Calibrated thermometers were used to determine the temperatures in the freezer and the refrigerator.

Experiments conducted at 35 ± 0.5 °C (35 °C) and 60 ± 0.5 °C (60 °C) were performed in Labline Imperial III (Model 305PI) incubators. The samples were agitated by end-over-end rotation on Glas-Col rugged rotators placed inside the incubators. Manipulations of the solvent and aqueous phases were performed using calibrated Eppendorf pipettes. ESS performance tests were run in standard order beginning with the solvent phase that had undergone thermal exposure over a 43-day contacting period.

6.2.2 ESS Analyses of Phase-Stability Samples

In order to remix the phases that had separated at low temperature, the test samples were agitated by end-over-end rotation on a Glas-Col rugged rotator located in an air box under a constant temperature of 25 °C. The optimized-solvent (-87W) samples were placed on the wheel first, and the -156W baseline samples followed two days later.

The ESS testing was performed on the -87W samples after 7 days on the wheel in the 25 °C airbox and involved an extraction step (O:A = 1:3), two scrub steps (O:A = 5:1), and four strips (O:A = 5:1). Waste simulant (SRS full simulant, draw #5 with 1.4×10^{-4} M Cs added) was spiked with $^{137}\text{CsCl}$ at an activity of 0.30 $\mu\text{Ci/mL}$ (56.25 μL of 80 $\mu\text{Ci/mL}$ into 15 mL of simulant using a calibrated Eppendorf pipette). In order to have sufficient counts for the third and fourth strips, a second spike (5 μL of 88 $\mu\text{Ci/mL}$ $^{137}\text{CsNO}_3$, affording a ^{137}Cs activity of 0.629 $\mu\text{Ci/mL}$, in the aqueous phase) was added to the third strip.

Teflon[®] FEP tubes (50 mL) were used for extraction, whereas 17-mL capacity polypropylene tubes were used in scrubs and strips. All tubes were washed prior to use according to the standard tube-washing protocol [11]. Individual tubes were shaken 10 times before being rotated on the wheel for 35 minutes. Phase separation was accomplished by centrifuging for 3 minutes at 2910 rpm in a refrigerated tabletop centrifuge (set point of 25 °C). A 0.250-mL sample was removed from each phase for ^{137}Cs gamma counting using a Packard Cobra Quantum Model 5003 gamma counter equipped with a 3-inch NaI(Tl) crystal through-hole detector. A count time of 10-minutes duration was used with a window setting of 580–750 keV (^{137m}Ba) for determining ^{137}Cs activity. The protocol is represented in Fig. 14.

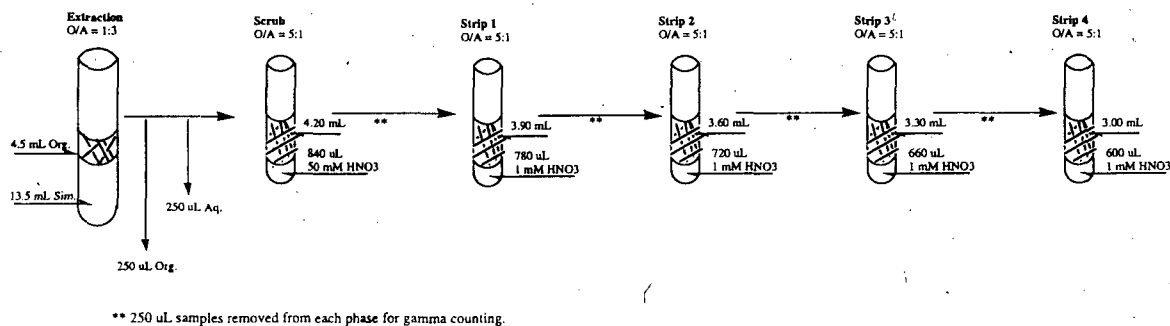


Fig. 14. ESS protocol for optimized solvent phase-stability test.

6.2.3 HPLC Analyses of Phase-Stability Samples

In the cases where solvent samples displayed stratification (separation into different layers) upon cooling in the refrigerator and freezer, aliquots of each layer were submitted for compositional analysis by HPLC. Samples were prepared for HPLC analysis by diluting 100 μL of the solvent with 2-propanol to a final volume of 1 mL. All samples were analyzed according to the method described in section 5.2.2.

Quantitation

The analytes, BOBCalixC6 and Cs-7SB modifier, were quantitated using the wavelengths 226 nm and 254 nm, respectively, set using the diode array detector. Each analyte was calibrated using seven independent standards prepared in isopropanol/Isopar[®] L, each analyzed in duplicate. The calibration ranges for BOBCalixC6 and Cs-7SB modifier were 0.02 to 2 mM and 1 to 100 mM, respectively. The measured integrated peak areas were fit to a linear least-squares line, where the coefficient of determination, r^2 , exceeded 0.999.

6.3 RESULTS AND DISCUSSION

Experiments involving the temperatures of $-24\text{ }^{\circ}\text{C}$ and $0\text{ }^{\circ}\text{C}$ are presented below in section 6.3.1. Experiments in which the solvent was contacted for an extended period of time with simulant, scrub, or strip solutions at $35\text{ }^{\circ}\text{C}$ or $60\text{ }^{\circ}\text{C}$ are described in section 6.3.2.

6.3.1 Phase Stability at Low Temperature

Samples of the pristine previous-baseline and optimized solvents that were stored in the refrigerator at $0\text{ }^{\circ}\text{C}$ in 10-mL volumetric flasks overnight were observed to have split into two phases (Figure 15). As the density of the modifier (1.197 g/mL at $25\text{ }^{\circ}\text{C}$) is substantially more than the Isopar[®] L diluent (0.76 g/mL at $20\text{ }^{\circ}\text{C}$), the lower, heavier phase was presumed to be enriched in modifier relative to the upper, lighter phase. The thickness of the heavier layer was observed to increase with storage time over the course of 4 days (Table 31), after which the phase thickness was essentially unchanged. The composition of lower and upper layers for both solvents was determined by HPLC analysis (Table 32).

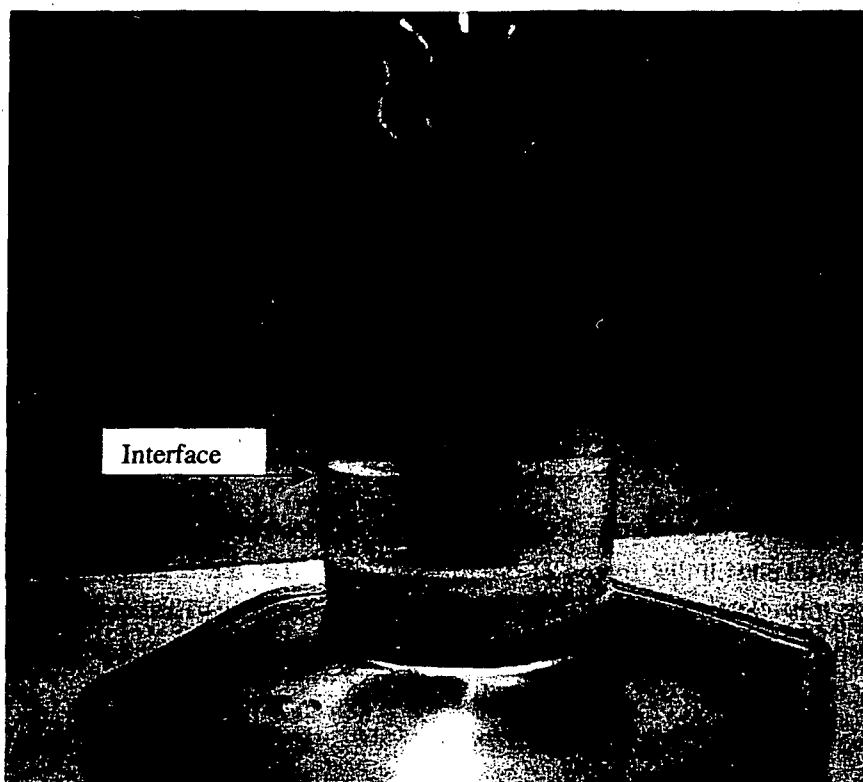


Fig. 15. Phase separation in the optimized solvent at 0 °C.

Table 31. Phase separation at 0 °C for the previous-baseline and the optimized solvents

Phase	Optimized solvent -87W			Original solvent -156W		
	Phase mass (g)	Phase density (g/mL)	Calculated volume (mL)	Phase mass (g)	Phase density (g/mL)	Calculated volume (mL)
Top	5.9115	0.826	7.157	7.517	0.825	9.111
Bottom	2.2776	0.969	2.350	0.6777	0.985	0.688
TOTAL	8.1891		9.51	8.1947		9.80

Table 32. Phase compositions at 0 °C for the previous-baseline and the optimized solvents

		Optimized solvent		Original solvent	
		Repeats (mM)	Avg. (mM)	Repeats (mM)	Avg. (mM)
Top layer	BOBCalixC6	2.81	2.85	7.05	7.04
		2.88		7.02	
	Cs-7SB	412.7	417.8	409.7	408.6
		422.9		407.5	
Bottom	BOBCalixC6	18.9	17.9	40.5	40.5
		16.9		40.5	
	Cs-7SB	1665.0	1611.6	1557.1	1555.8
		1558.3		1554.4	

A similar experiment was performed by placing 10-mL volumetric flasks filled with the optimized and previous baseline solvents in the freezer at $-24\text{ }^{\circ}\text{C}$ overnight. The result is shown in Fig. 16, where, in spite of the frost, it is clearly evident that a white phase had separated. That heavier phase also seems to be frozen, likely due to the water contained in the solvent from the solvent-washing operation.



Fig. 16. Phase separation in the optimized solvent at $-24\text{ }^{\circ}\text{C}$.

Table 33. Phase separation at -24 °C for the previous-baseline and the optimized solvents

Phase	Optimized solvent -87W			Original solvent -156W		
	Phase mass (g)	Phase density (g/mL)	Calculated volume (mL)	Phase mass (g)	Phase density (g/mL)	Calculated volume (mL)
Top	5.1245	0.803	6.382	6.1929	0.788	7.859
Bottom	3.0263	1.006	3.008	1.9418	1.036	1.874
TOTAL	8.1508		9.39	8.1347		9.73

Table 34. Phase compositions at -24 °C for the previous-baseline and the optimized solvents

		Optimized solvent		Original solvent	
		Repeats (mM)	Avg. (mM)	Repeats (mM)	Avg. (mM)
Top layer	BOBCalixC6	0.49	0.49	0.87	0.88
		0.48		0.89	
	Cs-7SB	119.5	117.9	93.6	93.7
		116.4		93.8	
Bottom	BOBCalixC6	20.0	20.0	43.0	43.0
		20.0			
	Cs-7SB	1913.9	1916.2	2012.5	2012.5
		1918.6			

When the refrigerator-cooled samples were allowed to stand at room temperature for about four hours, the interface or boundary separating the two layers was no longer visible. However, when the samples were shaken gently, schlieren effects ("swirls" in the solvent) were visible suggesting that the solvent was not yet homogeneous (a density gradient still remained). Subsamples at the very top and very bottom of the flasks were taken, and the composition of these phases were again determined by HPLC. Note that the concepts of "very top" and "very bottom" are subjective. Results are presented in Table 35.

Table 35. Solvent compositions at 0 °C for the previous-baseline and the optimized solvents

		Optimized Solvent		Original Solvent	
		Repeats (mM)	Avg. (mM)	Repeats (mM)	Avg. (mM)
Top Surface	BOBCalixC6	3.35	3.36	9.78	9.77
		3.37		9.75	
	Cs-7SB	458.5	459.7	475.9	474.9
		461.0		473.9	
Very Bottom	BOBCalixC6	14.7	14.8	9.6	9.70
		14.9		9.7	
	Cs-7SB	1347.5	1355.5	481.9	483.6
		1363.5		485.2	

Similarly, the freezer-cooled samples were allowed to stand at room temperature to see how long it would take for the interface between the layers to be no longer visible. After a couple of days at room temperature, the interface was gone, and the “very top” and “very bottom” portions of the solvent in the flasks were again analyzed by HPLC (Table 36). It is noteworthy that, despite there being no visible sign of a phase separation, there remained a density gradient in the static samples. Of course, mixing the solvent results in homogenization.

Table 36. Solvent compositions at -24 °C for the previous-baseline and the optimized solvents

		Optimized solvent		Original solvent	
		Repeats (mM)	Avg. (mM)	Repeats (mM)	Avg. (mM)
Top surface	BOBCalixC6	0.65	0.67	1.06	1.06
		0.68		1.06	
	Cs-7SB	156.1	157.7	125.6	126.1
		159.4		126.5	
Very bottom	BOBCalixC6	18.8	19.0	34.6	34.2
		19.1		33.8	
	Cs-7SB	1883.5	1889.0	1594.2	1574.3
		1894.5		1554.5	

It is apparent and not surprising that the miscibility of the nonpolar aliphatic diluent Isopar[®] L and the polar fluorinated alcohol modifier is not infinite at all temperatures. Thus, static storage of the wet solvent at temperatures at or below freezing can result in phase separation, in which the concentrations of the solvent components in each layer are quite different. The phase separation is presumed to be fully reversible upon mixing and warming, but to verify that this is the case, the cesium-distribution behavior of the solvent following remixing was determined. After a 1-week equilibration at room temperature, solvents were subjected to ESS testing. Experiments were run in duplicate, and a pristine-solvent control was added to the series. These tests were done for both previous-baseline and optimized solvents. Results are summarized in Tables 37 and 38.

Table 37. ESS tests at 25 °C using the low temperature-conditioned previous baseline solvent

Conditions	D_{Cs}					
	Extraction	Scrub #1	Strip #1	Strip #2	Strip #3	Strip #4
0 °C	17.03	1.521	0.133	0.074	0.055	0.052
0 °C	17.41	1.542	0.135	0.076	0.056	0.053
-24 °C	17.03	1.487	0.138	0.081	0.061	0.055
-24 °C	16.87	1.482	0.136	0.078	0.058	0.050
Control	17.54	1.537	0.140	0.075	0.057	0.048

Table 38. ESS tests at 25 °C using the low temperature-conditioned optimized solvent

Conditions	D_{Cs}						
	Extraction	Scrub #1	Scrub #2	Strip #1	Strip #2	Strip #3	Strip #4
0 °C	13.39	1.03	1.15	0.103	0.066	0.054	0.048
0 °C	13.57	1.01	1.24	0.102	0.066	0.052	0.047
-24 °C	13.34	1.03	1.25	0.107	0.068	0.055	0.048
-24 °C	13.46	1.05	1.23	0.102	0.065	0.053	0.046
Control	13.29	1.04	1.23	0.098	0.064	0.052	0.048

The results indicate that cold conditions did not impair the performance of the solvents, previous-baseline or optimized, and that the phase separation is a fully reversible phenomenon. The cesium distribution behavior of the “cold-conditioned” solvents is comparable to their corresponding controls.

6.3.2 Chemical Stability at High Temperature

Stability tests at elevated temperatures (35 °C and 60 °C) were similar to those carried out in FY 2001. Solvent samples were carried partially through an ESS procedure and allowed to remain in prolonged contact with one of the aqueous solutions used in the sequence: the waste simulant, scrub solution, or strip solution. For example, to test the stability of the solvent to prolonged contact with strip solution, the solvent sample would undergo an extraction and two scrubs before being placed in prolonged contact with the strip solution. The experiments were carried out for 43 days. Cesium extraction performance of the thermally treated solvent samples was assessed by running ESS tests at 25 °C. Results are summarized in Table 39. Explanations for the entry nomenclature are given in the footnotes to the table, where the numbers in the sample codes indicate the temperature of the prolonged contact, either 35 or 60 °C.

In all cases, the solvents behaved similarly to the controls and furthermore gave ESS results remarkably close to those obtained in Chapter 3 with pristine solvent. Over a 43-day treatment, performance remained essentially unchanged for both 35 °C and 60 °C samples. In only one case, TS60SCB (treatment over scrub solution at 60 °C), did the D_{Cs} value seem high on stripping, but only for the second strip. This thermal-stability study thus yielded results comparable to those obtained in FY 2001.

6.4 CONCLUSIONS

The results validate the expectation that the optimized solvent would possess adequate thermal stability. It was clear from the thermal-stability tests on the previous baseline solvent [11] that the solvent undergoes degradation only when in contact with the acidic scrub and strip solutions, owing to

Table 39. ESS tests at 25 °C using the high temperature-stressed optimized solvent

Test	D_{Cs}									
	Extract	Scrub #1	Scrub #2	Strip #1	Strip #2	Strip #3	Strip #4	Extract	Scrub #1	Scrub #2
TS35P ^a	14.69	1.096	1.276	0.1065	0.0647	0.0513	0.0486			
TS60P ^a	13.90	1.101	1.298	0.1164	0.0718	0.0547	0.0485			
TS35S ^b	13.88	1.110	1.267	0.1344	0.0673	0.0516	0.0472			
TS60S ^b	13.34	1.165	1.177	0.1109	0.0693	0.0544	0.0475			
TS35SCB ^c		1.063	1.273	0.1018	0.0696	0.0539	0.0483	13.89		
TS60SCB ^c		1.165	1.305	0.1240	0.0971	0.0602	0.0484	13.90		
TS35ST ^d				0.1156	0.0699	0.0540	0.0478	13.84	1.180	1.268
TS60ST ^d				0.1397	0.0724	0.0552	0.0482	13.79	1.107	1.261

^aTS35P or TS60P indicates use of pristine solvent, no contact with aqueous phases over the course of 43 days at either 35 °C or 60 °C.

^bTS35S or TS60S indicates use of solvent that was in contact with simulant at O:A = 1:3 (draw #5 to which was added 1.4×10^{-4} M Cs) via end-over-end rotation for 43 days at either 35 °C or 60 °C.

^cTS35SCB or TS60SCB indicates use of solvent that was contacted with simulant for 30 minutes at 25 °C via end-over-end rotation; the solvent phase was then contacted at O:A = 5:1 with scrub solution via end-over-end rotation for 43 days at either 35 °C or 60 °C.

^dTS35ST or TS60ST indicates use of solvent that was contacted with simulant for 30 minutes at 25 °C via end-over-end rotation; the solvent phase was then contacted at O:A = 5:1 with scrub solution for 30 minutes at 25 °C via end-over-end rotation; the solvent phase then contacted at O:A = 5:1 with strip solution for 43 days via end-over-end rotation at either 35 °C or 60 °C.

degradation of the TOA. This effect was only detectable for the elevated-temperature samples (61 °C) held for 46 days or more. Pristine solvent held for 235 days at 61 °C underwent no noticeable degradation in performance, which was also true of solvent contacted with the waste simulant for 235 days at 61 °C. The present study reflects almost the same behavior, though the duration of the test (43 days) was insufficient to detect any impact to performance at either temperature. Making the assumption that only 4.4% of the solvent inventory resides in the scrub and strip sections of the flowsheet at any given time and that negligible degradation occurs outside of these sections [11], 43 days at the maximum normal operating temperature of 35 °C corresponds to a minimum of 977 days of solvent lifetime. Thus, it can be reasonably said that thermal stress should not have a significant impact on the performance of the optimized solvent.

It also was informative to examine the behavior of the optimized solvent under low-temperature conditions, which may be encountered during storage or shipping in winter months. The phase separation that occurs at low temperature does not impair the solvent performance upon warming and remixing. ESS experiments proved that the cesium extraction performance of the previous-baseline and optimized solvents is not altered by a cold-temperature conditioning resulting in a phase separation, possibly even a freezing of these phases. It is clear that solvent stored or shipped under cold conditions should be remixed at room temperature to ensure good quality results.

7. PHYSICAL-PROPERTIES MEASUREMENTS

7.1 INTRODUCTION

Laboratory-scale physical-property evaluations of the optimized Caustic-Side Solvent Extraction (CSSX) formulation have been completed to help determine the operating characteristics for design of the centrifugal contactors used in cesium removal at the Savannah River Site [20]. The properties measured in these tests were solvent density, viscosity, and dispersion numbers for the solvent against full simulant, scrub, and strip solutions at temperatures between 15 and 35 °C.

The evaluations included determination of phase separation by gravity settling under conditions present in the extraction, scrubbing, and stripping sections of the CSSX cascade, measurement of solvent density, measurements of solvent viscosity at several temperatures, and measurements of solvent surface tension and the interfacial tension of each solvent/simulant, solvent scrub, and solvent/strip combination. Results of these tests show that all of the formulations will perform the required separations and will perform satisfactorily in the contactors.

7.2 EXPERIMENTAL PROCEDURES

7.2.1 Chemicals

The CSSX solvent is a blend of the organic materials listed above. Scrub (0.05 M HNO₃) and strip (0.001 M HNO₃) aqueous solutions were formulated using 1.0 M HNO₃, procured from J. T. Baker Co. and diluted with water that had been deionized using a Barnstead Nanopure B filtration system. Sodium hydroxide solutions used to wash the solvent were formulated using a standard 0.1 M sodium hydroxide solution (ACS reagent grade, procured from the J. T. Baker Co.). SRS waste supernatant simulant was formulated according to SRS procedure [23], but the composition listed in that document for "average" SRS supernatant simulant was adjusted slightly as shown in Table 1 to match the new average simulant. The cesium concentration in the simulant batch used in testing was 0.000143 M. The simulant was prepared by first combining the ingredients shown below except for the cesium and silica. These were added along with the metals and organic components shown in Table 2 to make the complete simulant. After the materials in Tables 40 and 41 were all combined and allowed to age over a three-day period, the simulant was filtered through a 0.45- μ m Gelman polypropylene groundwater filter to remove any precipitates formed. The simulant remained clear after filtration during all remaining testing.

7.2.2 Determination of Dispersion Number

The purpose of these tests was to determine phase-separation performance of the optimized CSSX solvent under conditions approximating those present in the extraction, scrubbing, and stripping sections of the CSSX cascade. Phase-separation performance was quantified in terms of dimensionless dispersion numbers, determined at temperatures ranging from 15 °C to 35 °C. Prior to phase-separation determinations, the solvent was equilibrated according to the test condition. Extraction-condition test solvent was equilibrated under extraction conditions.

Table 40. Simulant composition (major components)

Component	Avg. SRS ^a simulant (M)	New Avg. SRS ^b waste diluted with H ₂ O (M)	Compound used	Mol. Wt.	Mass for new avg. (g/L)
Na ⁺	5.6	5.6			
Cs ⁺	0.00014	0.000143	CsCl	168.37	0.024077
K ⁺	0.015	0.0146	KNO ₃	101.10	1.47606
OH ⁻	1.91	2.086	NaOH	40.00	81.56
NO ₃ ⁻	2.14	2.039	NaNO ₃	84.99	173.295
NO ₂ ⁻	0.52	0.494	NaNO ₂	69.00	34.086
AlO ₂ ⁻	0.31	0.289	Al(NO ₃) ₃ ·9H ₂ O	375.14	108.415
CO ₃ ²⁻	0.16	0.147	Na ₂ CO ₃ ·H ₂ O	124.01	18.2295
SO ₄ ²⁻	0.15	0.137	Na ₂ SO ₄	142.04	19.4595
Cl ⁻	0.025	0.025	NaCl	58.44	1.4610
F ⁻	0.032	0.030	NaF	41.99	1.2597
PO ₄ ³⁻	0.010	0.007	Na ₂ HPO ₄ ·7H ₂ O	268.09	1.8766
C ₂ O ₄ ²⁻	0.008	0.018	Na ₂ C ₂ O ₄ (Sodium Oxalate)	134.00	2.412
SiO ₃ ²⁻	0.004	0.003	Na ₂ SiO ₃ ·9H ₂ O	284.20	0.8526
MoO ₄ ²⁻	0.0002	0.0002	Na ₂ MoO ₄ ·2H ₂ O	241.95	0.04839

^aWSRC-RP-98-00168, Rev. 1.

^bWSRC-RP-99-00006, Rev. 3.

Table 41. Materials for full simulant (added trace metals and organic species)

Component	Concentration in simulant (M)	Compound used	Molecular weight	Mass (g/L)
Cu ²⁺	2.27 × 10 ⁻⁵	CuSO ₄ ·5H ₂ O	249.68	0.00566
Cr ⁶⁺	1.44 × 10 ⁻³	Na ₂ CrO ₄	161.97	0.2336
Zn ²⁺	1.22 × 10 ⁻⁴	Zn(NO ₃) ₂ ·6H ₂ O	297.47	0.0364
Pb ²⁺	1.01 × 10 ⁻⁵	Pb(NO ₃) ₂	331.20	0.00336
Fe ³⁺	2.58 × 10 ⁻⁵	Fe(NO ₃) ₃ ·9H ₂ O	404.00	0.01042
Sn ²⁺	2.02 × 10 ⁻⁵	SnCl ₂ ·2H ₂ O	225.63	0.00456
Hg ²⁺	2.49 × 10 ⁻⁷	Hg(NO ₃) ₂ ·H ₂ O	342.61	0.0000854
Rh ³⁺	2.04 × 10 ⁻⁶	Rh(NO ₃) ₃ ·2H ₂ O	324.95	0.000663
Pd ²⁺	3.85 × 10 ⁻⁶	Pd(NO ₃) ₂	230.43	0.000888
Ag ⁺	9.27 × 10 ⁻⁸	AgNO ₃	169.87	0.0000157
Ru ³⁺	8.11 × 10 ⁻⁶	RuCl ₃	207.43	0.00168
TPB	1.88 × 10 ⁻⁶	Tributylphosphate	266.32	0.0005
DBP	1.19 × 10 ⁻⁴	Dibutylphosphate	210.21	0.025
MBP	1.62 × 10 ⁻⁴	Monobutylphosphate	154.10	0.025
<i>n</i> -Butanol	2.70 × 10 ⁻⁵	C ₄ H ₉ OH	74.12	0.002
CHO ₂ ⁻	3.33 × 10 ⁻²	NaCHO ₂ (sodium formate)	68.01	1.5
TMA	1.69 × 10 ⁻⁴	Trimethylamine	59.11	0.01

Scrub-conditioned solvent was obtained from extraction-equilibrated solvent and was batch equilibrated with scrub solution prior to testing. Strip-conditioned solvent was obtained from extraction- and scrub-equilibrated solvent, and was equilibrated with strip solution prior to testing. Single-batch pre-equilibrations were used to mitigate errors that might be introduced due to variations in technique that could affect split-batch operations. Dispersion numbers were determined as described in Chapter 2.

7.2.3 Laboratory Dispersion-Number Procedures

The procedure above was used with the solvent for each extraction, scrub, and strip contact at each temperature from 15 to 35 °C at 5 °C increments simulating the operations in each step of the CSSX process. A total of 300 mL of optimized solvent, 1500 mL of simulated SRS waste supernatant (full recipe), 200 mL of CSSX scrub solution (0.05 M HNO₃), and 100 mL of CSSX strip solution (0.001 M HNO₃) were required for the tests. Glass graduated cylinders (100 mL) with ground glass stoppers, an electronic stopwatch, a thermometer (LaPine 398-12-53), a refrigerated water bath (VWR model 13270-615 circulation bath, with 190 watts cooling and operated at about 5 L/min coolant recirculation rate and filled with distilled water), and a millimeter scale rule were used. Prior to use, all new or previously used

glassware and plastic vessels were washed by rinsing with tap water three times, rinsing with demineralized water three times, rinsing with ethanol two times, and rinsing with acetone two times. The equipment was allowed to air dry or dried with a stream of dry nitrogen or argon before use.

To pre-equilibrate the solvent to extraction conditions, 300 mL of solvent was combined with 936 mL of supernatant simulant and 60 mL of scrub solution in a 2-L flask at room temperature (24.5 °C). The flask was shaken vigorously for 20 s, held for 10 s, agitated for 20 s, held for 10 s, and agitated for 20 s again. The dispersion was allowed to separate, the solvent phase was collected, and the aqueous simulant solution was discarded.

7.3 DISPERSION-NUMBER DETERMINATIONS

7.3.1 Extraction Dispersion-Number Determinations

Extraction dispersion-number determinations were made using the full SRS simulant containing salts, metals, and organics and with non-radioactive cesium at a cesium concentration of 0.000143 M as shown in Tables 40 and 41. The tests were begun by placing 17.66 mL of solvent, 3.53 mL of scrub solution, and 53.81 mL of simulant in each graduated cylinder using Rainin EDP electronic 1 and 10-mL digital pipettes. The position of the stable interface between organic and aqueous phases and the height of the liquid column were measured. The cylinders were then placed in the temperature bath. After reaching the desired test temperature, the solution temperature was measured and each stoppered cylinder was removed from the bath and manually agitated for 20 s, held still for 10 s, and agitated for another for another 20 s, and then placed back into the water bath. The time elapsed between cessation of agitation and the return of the interface to its original position (i.e., the collapse of the dispersion) was recorded. The total height of the dispersion column in the graduate at the beginning of the settling period was also recorded. (If agitated correctly, the dispersion column height should be the height of the liquid column inside the graduate.) This was repeated two more times, and after the third time, the temperature of the solution in the graduate was measured again. This procedure was then repeated for 20, 25, 30, and 35 °C temperatures.

An additional extraction dispersion-number determination was made, again using the full simulant. The solvent (40 mL) was again pre-equilibrated with simulant (124.9 mL) and 8 mL of scrub solution as described above. The 17.66 mL of solvent, 3.53 mL of scrub solution, and 53.81 mL of simulant was added to each of the graduates and the extraction contacts were completed at 15, 20, 25, 30, and 35 °C.

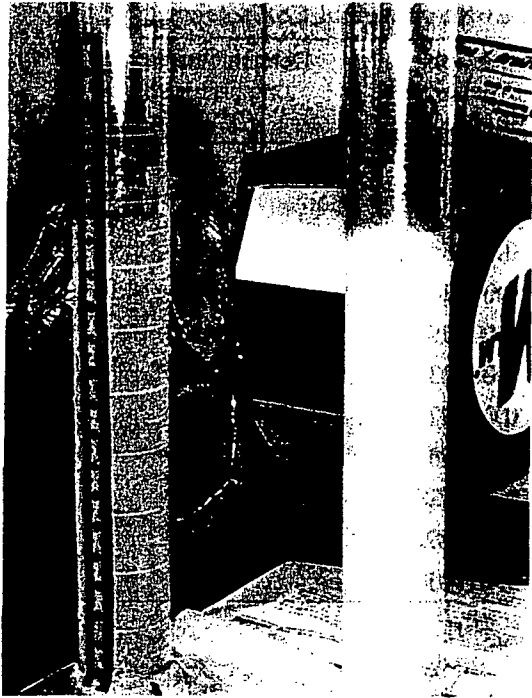
A separate experiment following a similar procedure as that described above was completed using solvent that was not pre-equilibrated with simulant. The first time this was attempted, at 15 °C, one of the two graduates, when shaken, had the look of a gel for the dispersion and this took longer to separate. At 20 °C, the other one had the gel-like look and took longer to separate. That graduate continued to have the gel-look when shaken at the rest of the temperatures and the gel-like dispersion took longer to separate than the other. When it was separated, though, there was no visual difference between the two graduates except that in the one that had the gel-like formation, both organic and aqueous were clear as

soon as the break was achieved. When the normal shake and break occurred, the tube had foam after shaking and both phases were slightly cloudy for 30 min to 2 h after break. No data was taken for break time during this trial. The gel-like formation is shown in the photos in Fig. 17 at various stages of phase separation.

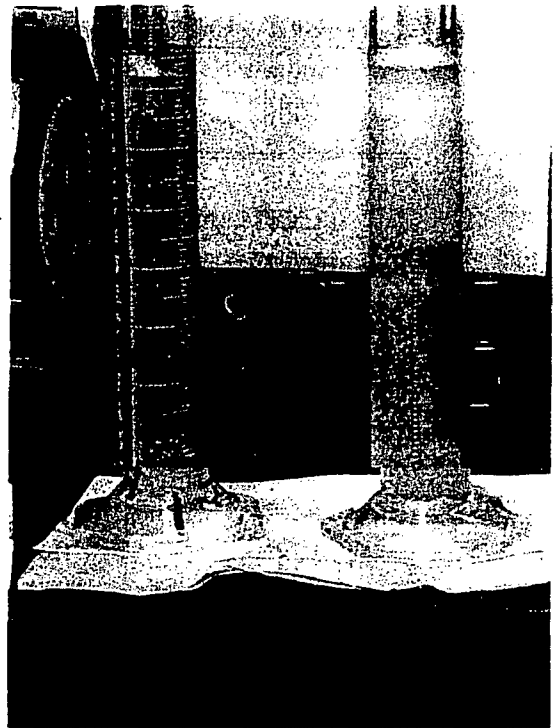
The graduates were left as they were, and after five days in the graduates, the shakeouts were repeated. This time, both tubes were clear the first two shakes at 15 °C, but on the third shake, the gel-like formation returned in the second tube, and it took about a minute to separate. At 20 °C, no gel appeared in either tube. Then the temperature was increased to 35 °C, and shakeouts continued. On the second shake, gel-like formation occurred in the second tube. It took slightly longer to separate, but then on the third shake, both were normal again. At 30 and 25 °C, neither tube had the gel like formations on any shakeouts. The trigger for the gel-like formation is not known. Sometimes it occurred in one tube, then the other, and most times not at all. It could not be predicted when or at what temperature the material would behave this way and if it did, whether it would continue. All data are shown in Table 42 and Fig. 18.

7.3.2 Scrubbing-Condition Dispersion-Number Determinations

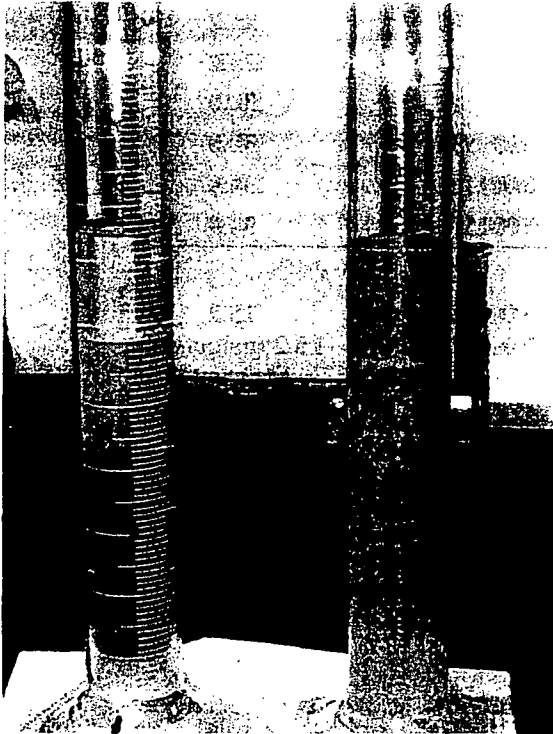
Solvent for the stripping dispersion number determinations was recovered from the single-batch extraction-condition equilibration and was determined to be 261.6 mL. It was placed into a clean 500-mL separatory funnel and a volume of scrub solution equal to one-fifth the solvent volume was added (52.32 mL). The funnel was agitated vigorously for 20 s, held for 10 s, agitated for 20 s, held for 10 s, and agitated for 20 s again. The temperature of the dispersion was determined (24.5 °C) and the dispersion was allowed to separate. The solvent phase was collected and the aqueous solution was discarded.



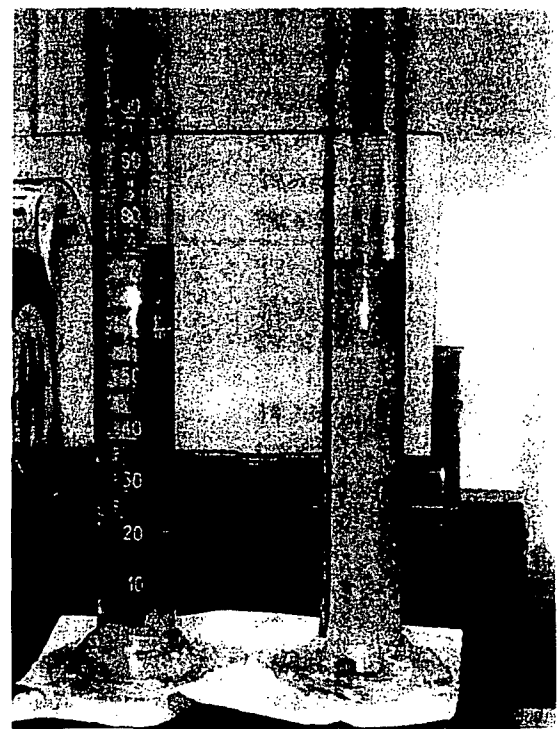
At the start of settling (gel on left)



After about 1 minute



About 90% complete settling.



Completion of settling.

Fig. 17. Gel-like material formed during dispersion-number determinations.

Table 42. Dispersion numbers for extraction with optimized CSSX solvent

Solvent sample	Dispersion height (cm)	Simulant/solvent dispersion number	Determination temperature (°C)
Trial 1			
15C#1	13.3	0.001013	15.6
15C#2	13.75	0.000864	15.6
20C#1	13.3	0.001243	20.6
20C#2	13.75	0.001070	20.6
25C#1	13.3	0.001431	25.2
25C#2	13.75	0.001371	25.2
30C#1	13.3	0.001581	30.0
30C#2	13.75	0.001629	30.0
35C#1	13.3	0.001782	34.8
35C#2	13.75	0.001909	34.8
Trial 2			
15C#1	14.0	0.000623	15.3
15C#2	13.2	0.000680	15.3
20C#1	14.0	0.000872	20.2
20C#2	13.2	0.000893	20.2
25C#1	14.0	0.001001	25.2
25C#2	13.2	0.001212	25.2
30C#1	14.0	0.001107	30.0
30C#2	13.2	0.001338	30.0
35C#1	14.0	0.001226	34.9
35C#2	13.2	0.001591	34.9
Trial 3			
15C#1	14.2	0.000451	15.2
15C#2	14.6	0.000436	15.2 (gel on one shakeout)
20C#1	14.2	0.000424	20.1
20C#2	14.6	0.000438	20.1
25C#1	14.2	0.000516	25.2
25C#2	14.6	0.000485	25.2
30C#1	14.2	0.000632	30.0
30C#2	14.6	0.000569	30.0
35C#1	14.2	0.000813	35.0
35C#2	16.7	0.000664	35.0 (gel on one shakeout)

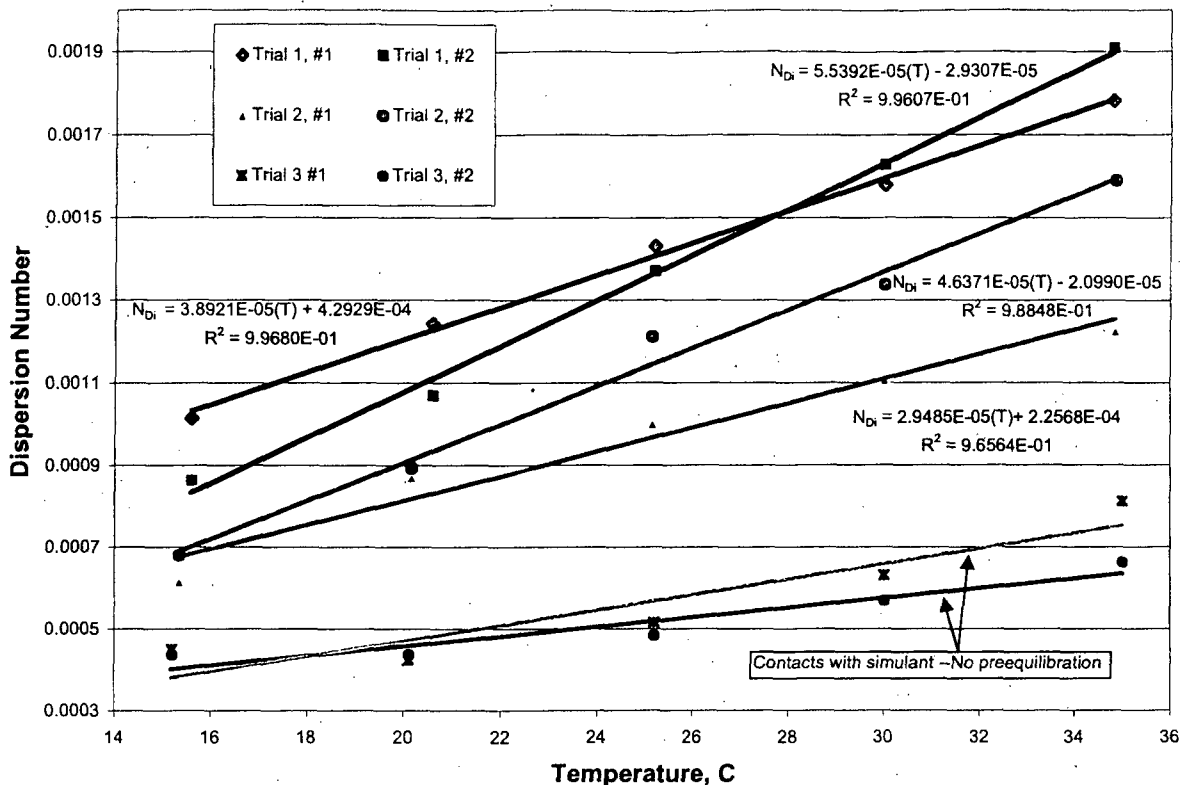


Fig. 18. Graph of CSSX solvent extraction equilibration dispersion numbers.

Then, 62.5 mL of recovered solvent was placed into each of two clean, 100 mL graduated cylinders and 12.5 mL of scrub solution (0.05 M HNO₃) was added to each cylinder. The position of the stable interface between organic and aqueous phases and the height of the liquid column were measured. They were then placed in the water bath and equilibrated to the test temperature. After reaching the desired test temperature, the solution temperature was measured and each stoppered cylinder was removed from the bath and manually agitated for 20 s, held still for 10 s, agitated for another 20 s, and then placed back into the water bath. The time from the cessation of agitation to the reestablishment of the interface was measured as the breaktime. Each equilibration was repeated two times, and then the temperature of the solution in the graduate was measured after the third equilibration. The temperature of the bath was then adjusted to the next test temperature and the equilibration process was repeated at 20, 25, 30, and 35 °C. The scrub-condition, dispersion numbers results are shown in Fig. 19 and in Table 43.

7.3.3 Stripping-Condition Dispersion-Number Determinations

Solvent for the stripping determinations was recovered from the single-batch scrub-condition equilibration. A total of 130 mL solvent was placed into a clean 500-mL separatory funnel. A volume of

strip solution equal to one-fifth the solvent volume (26 mL) was added. The funnel was agitated vigorously for 20 s, held for 10 s, agitated for 20 s, held for 10 s, and agitated for 20 s again. The temperature of the dispersion was determined (24.5 °C) and the dispersion was allowed to separate. The solvent phase was collected and the aqueous solution was discarded.

Then, 62.5 mL of the recovered solvent was placed into each of two clean, 100-mL graduated cylinders and 12.5 mL of strip solution (0.001 M HNO₃) was added to each cylinder. The position of the stable interface between organic and aqueous phases and the height of the liquid column was measured. The cylinders were then placed in the water bath and equilibrated to the test temperature. After reaching the desired test temperature, the solution temperature was measured and each stoppered cylinder was removed from the bath and manually agitated for 20 s, held still for 10 s, agitated for another 20 s, and then placed back into the water bath. The time from the cessation of agitation to the reestablishment of the interface was measured as the breaktime. Each equilibration was repeated two times, and then the temperature of the solution in the graduate was measured after the third equilibration. The temperature of the bath was then adjusted to the next test temperature and the equilibration process was repeated at 20, 25, 30, and 35 °C. The stripping dispersion number results are shown in Fig. 20 and in Table 44.

Table 43. Dispersion numbers for scrub with optimized CSSX solvent

Solvent sample	Dispersion height (cm)	Scrub/solvent Dispersion number	Determination temperature (°C)
15C#1	14.5	0.000602	15.6
15C#2	14.3	0.000623	15.6
20C#1	14.4	0.000856	20.4
20C#2	14.4	0.000828	20.4
25C#1	14.6	0.001070	25.2
25C#2	14.5	0.001045	25.2
30C#1	14.6	0.001289	29.75
30C#2	14.5	0.001254	29.75
35C#1	14.6	0.001506	34.55
35C#2	14.5	0.001453	34.55

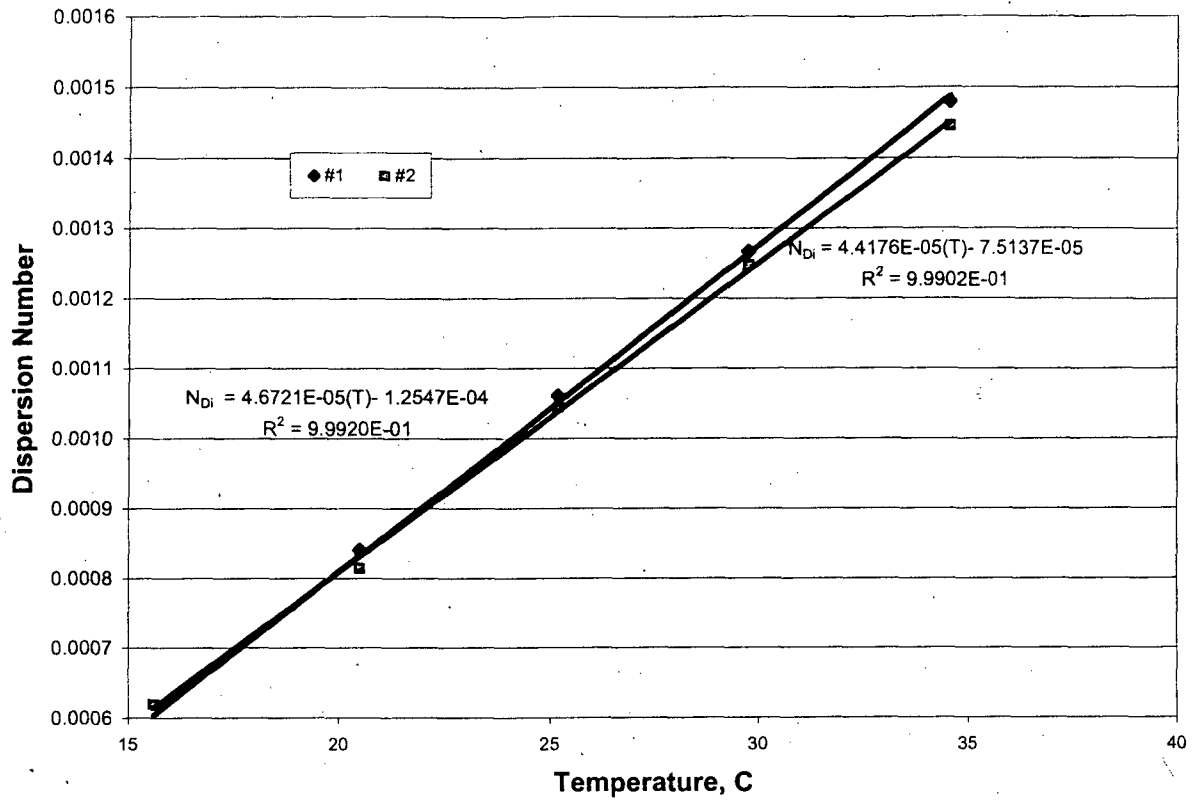


Fig. 19. Graph of CSSX solvent scrub equilibration dispersion numbers.

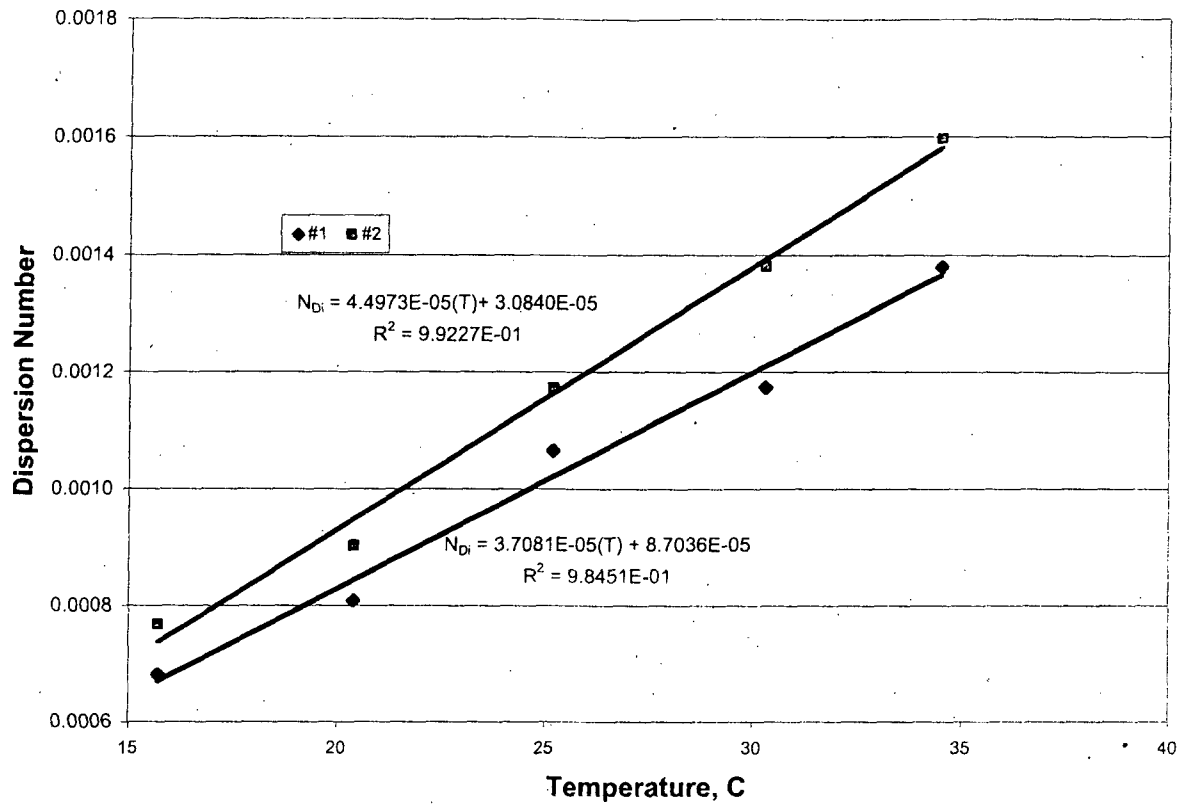


Fig. 20. Graph of CSSX solvent strip equilibration dispersion numbers.

Table 44. Dispersion numbers for strip with optimized CSSX solvent

Solvent sample	Dispersion height (cm)	Scrub/solvent dispersion number	Determination temperature (°C)
15C#1	14.0	0.000686	15.7
15C#2	14.9	0.000779	15.7
20C#1	14.0	0.000813	20.4
20C#2	14.9	0.000915	20.4
25C#1	14.1	0.001080	25.2
25C#2	14.8	0.001190	25.2
30C#1	14.15	0.001189	30.3
30C#2	14.9	0.001400	30.3
35C#1	14.2	0.001398	34.5
35C#2	14.95	0.001620	34.5

7.4 MEASUREMENT OF SOLVENT DENSITIES

The solvent densities were measured using procedures described in Chapter 2. Each flask was filled using a 500-mL separatory funnel to just below the line and then adjusted to the line with a small transfer pipette after coming to temperature in the water bath. The actual volume of each flask was calculated from the weight of the water contained at 20 °C, and the volume at the other test temperatures was calculated according to ASTM E542. The density of water at each temperature was measured and then compared to the published data for water density at those temperatures. The calculated volume was used in subsequent density determinations of the solvent at each temperature. The results for the flask volume determinations are shown in Table 45.

For the solvent densities, the same volumetric flasks were emptied and rinsed twice with ethanol, twice with acetone, and allowed to air dry over night. They were weighed and then filled to the line with solvent using a separatory funnel. They were then placed in the water bath at 15 °C and allowed to come to bath temperature. After reaching bath temperature, the levels in each flask were adjusted by adding or removing (at higher temperatures) solvent using a small pipette. After adjustment of the levels, they remained in the bath for ten more minutes, then removed and the levels checked again and adjusted if needed. They were then dried and weighed. After weighing, they were returned to the bath and the temperature of the bath adjusted to the next test temperature. The results of the solvent density determinations are shown in Table 46 and Fig. 21.

Table 45. Water-density determinations

Temperature (°C)		Flask 1	Flask 2	Flask 3	Actual water density at temperature (g/cm ³)
24.4	Tare wt.	60.1097	62.3954	61.1582	
	Gr. Wt.	159.6757	161.9962	160.7973	0.997197
	Net Wt.	99.5660	99.6008	99.6391	
	density	0.9966	0.9970	0.9968	
	deviation	0.00059	0.00018	0.00036	
	Flask Vol _{24.4} =	99.9046	99.8991	99.9548	
15.10	Gr. Wt.	159.9030	162.2013	161.0086	0.999099
	Net Wt.	99.7933	99.8059	99.8504	
	density	0.9990	0.9992	0.9990	
	deviation	0.00012	-6.1E-05	5.1E-05	
		Flask Vol ₁₅ =	99.8953	99.8898	99.9455
20.00	Gr. Wt.	159.8188	162.0990	160.9174	
	Net Wt.	99.7091	99.7036	99.7592	0.998204
	density	0.9981	0.9981	0.9981	
	deviation	0.00012	0.00012	0.00012	
		Flask Vol ₂₀ =	99.9002	99.8947	99.9504
30.00	Gr. Wt.	159.5551	161.8550	160.6975	0.995647
	Net Wt.	99.4454	99.4595	99.5392	
	density	0.9953	0.9955	0.9958	
	deviation	0.00030	0.00010	-0.00014	
		Flask Vol ₃₀ =	99.9102	99.9047	99.9604
35.10	Gr. Wt.	159.4301	161.6880	160.5176	0.993997
	Net Wt.	99.3204	99.2926	99.3594	
	density	0.9940	0.9938	0.9939	
	deviation	-4.9E-05	0.00017	6.0E-05	
		Flask Vol ₃₅ =	99.9153	99.9097	99.9655
40.15	Gr. Wt.	159.2345	161.5226	160.3544	0.992158
	Net Wt.	99.1248	99.1272	99.1962	
	density	0.9920	0.9921	0.9923	
	deviation	0.00012	4.1E-05	-9.6E-05	
		Flask Vol ₄₀ =	99.9204	99.9148	99.9705

Table 46. Optimized-solvent density determinations^a

Temperature (°C)		Flask 1	Flask 2	Flask 3	Average density	Standard deviation	Variance
15.00	Tare wt.	60.1097	62.3954	61.1582			
	Gr. Wt.	145.9414	148.2582	147.0724			
	Net Wt.	85.8317	85.8628	85.9142			
	density	0.8592	0.8596	0.8596	0.8595	0.0002	4.7E-08
	Vol ₁₅ =	99.8952	99.8897	99.9454			
20.05	Gr. Wt.	145.5436	147.8496	146.6507			
	Net Wt.	85.4339	85.4542	85.4925			
	density	0.8552	0.8554	0.8553	0.8553	0.0001	1.6E-08
	Vol ₂₀ =	99.9002	99.8947	99.9504			
25.00	Gr. Wt.	145.1693	147.4782	146.2873			
	Net Wt.	85.0596	85.0828	85.1291			
	density	0.8514	0.8517	0.8517	0.8516	0.00028	2.5E-08
	Vol ₂₅ =	99.9052	99.8997	99.9554			
30.00	Gr. Wt.	144.7731	147.0728	145.893			
	Net Wt.	84.6634	84.6774	84.7348			
	density	0.8474	0.8476	0.8477	0.8476	0.0001	2.1E-08
	Vol ₃₀ =	99.9102	99.9047	99.9604			
35.00	Gr. Wt.	144.366	146.6559	145.496			
	Net Wt.	84.2563	84.2605	84.3378			
	density	0.8433	0.8434	0.8437	0.8434	0.0002	4.2E-08
	Vol ₃₅ =	99.9152	99.9096	99.9654			
40.15	Gr. Wt.	143.9722	146.2631	145.0803			
	Net Wt.	83.8625	83.8677	83.9221			
	density	0.8393	0.8394	0.8395	0.8394	0.0001	7.7E-09
	Vol ₄₀ =	99.9204	99.9148	99.9705			

^aDensity results are bolded for easier reading.

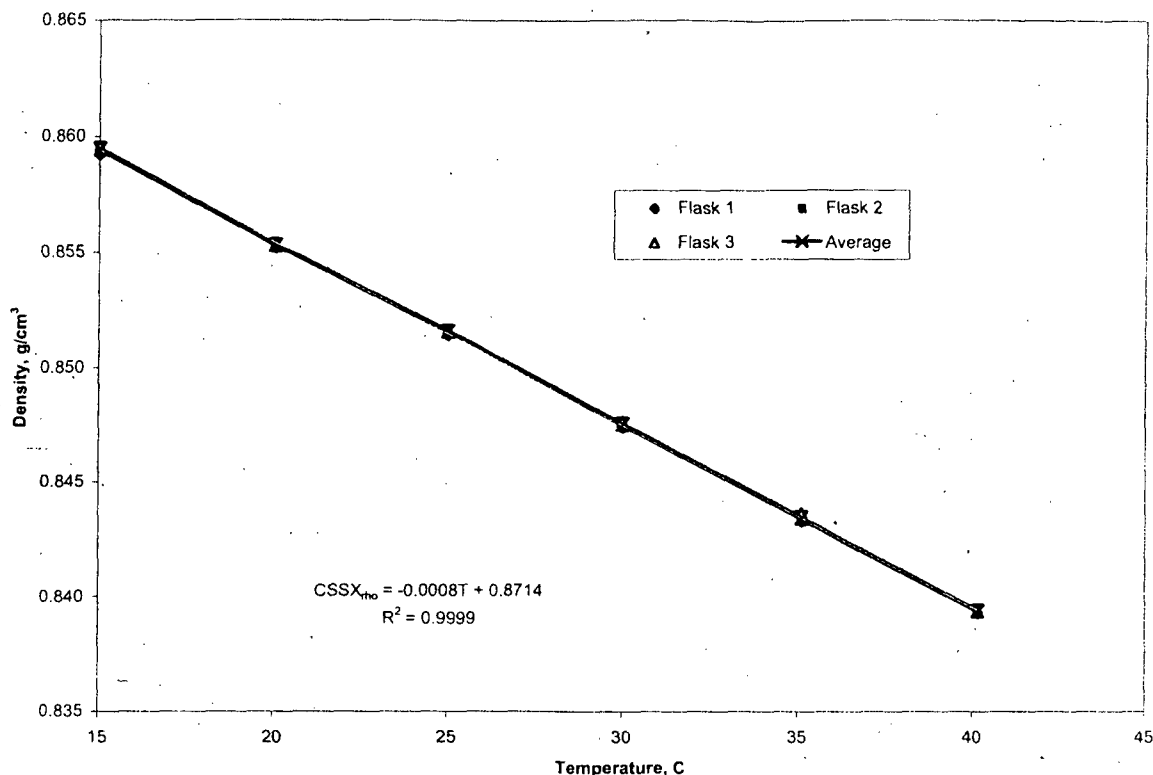


Fig. 21. Solvent density versus temperature.

7.5 MEASUREMENT OF SOLVENT VISCOSITIES

The viscosity of the new formulation of solvents was measured as described in Chapter 2. Each test was begun by adding 16 mL of the solvent to the UL adaptor, installing it on the viscometer, starting the spindle rotation at 60 rpm, and then setting the temperature bath to 15 °C. After the temperature had stabilized for several minutes, the viscosity of the sample was measured. The temperature bath was then adjusted to the next temperature and the system temperature allowed to stabilize before the next reading. The set of viscosity determinations were made three times. The second set was completed with fresh solvent, and the third set repeated the tests in reverse order with the same solvent after 30 min at 40 °C. The results of three determinations of the solvent viscosity measurements are shown in Table 47. The results are given for the percent torque, the viscosity, and the shear rate at each temperature. The results are also presented graphically in Figs. 22 and 23. Figure 22 is a plot of the viscosity versus temperature and Fig. 23 is a plot of the shear stress versus the temperature. The solvent's viscosity decreases with increasing temperature as expected for this type of liquid.

Table 47. Solvent-viscosity determinations^a

Solvent	Temperature (°C)	Torque (%)	Viscosity (cP)	Shear Stress (dyn/cm ²)
Optimized solvent	15.05	48.2	4.83	3.53
	20.10	40.9	4.09	2.99
	25.00	35.1	3.51	2.57
	30.00	30.5	3.07	2.23
	35.10	26.8	2.69	1.96
	40.10	23.8	2.38	1.73
<hr/>				
Repeat fresh solvent	15.05	48.6	4.86	3.55
	20.10	41.2	4.12	3.01
	25.08	35.3	3.54	2.59
	30.05	30.6	3.07	2.24
	35.02	26.9	2.69	1.96
	40.10	24.0	2.39	1.74
<hr/>				
Repeat same solvent starting at 40 °C	40.10	23.9	2.39	1.74
	35.08	26.9	2.70	1.98
	30.04	30.6	3.07	2.24
	25.10	35.1	3.52	2.57
	20.10	40.8	4.07	2.99
	15.05	48.4	4.84	3.54

^aBrookfield LVTDV-II (Serial Number D15869) UL Adapter with heating jacket was used. Precision of viscosity measurement is ± 0.1 cP.

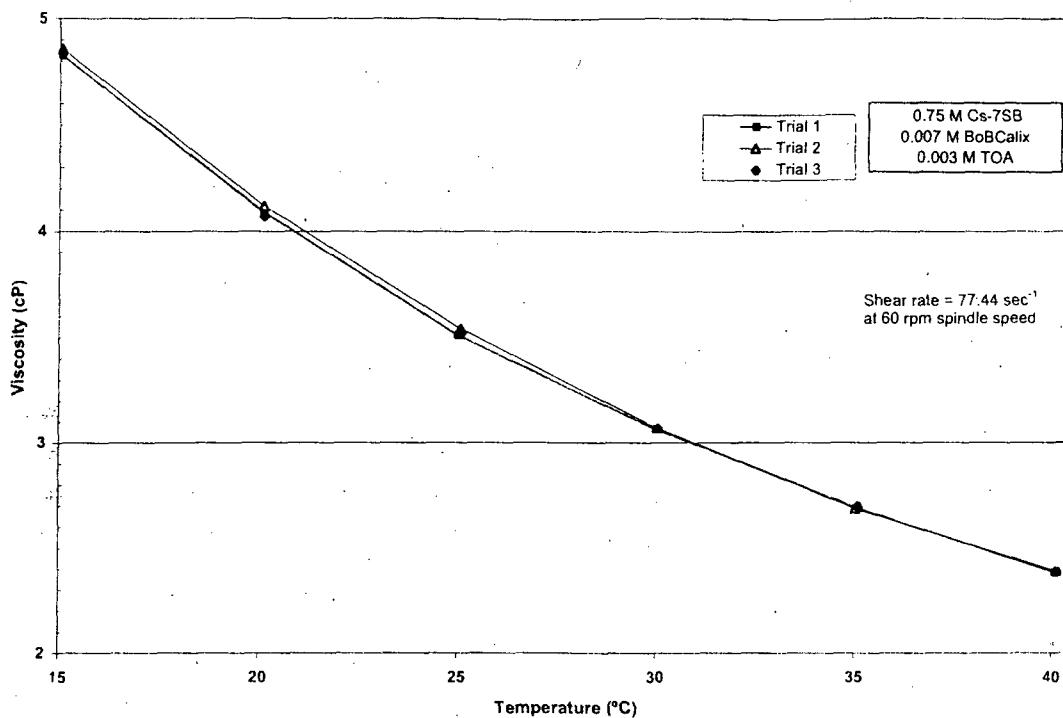


Fig. 22. Solvent viscosity versus temperature.

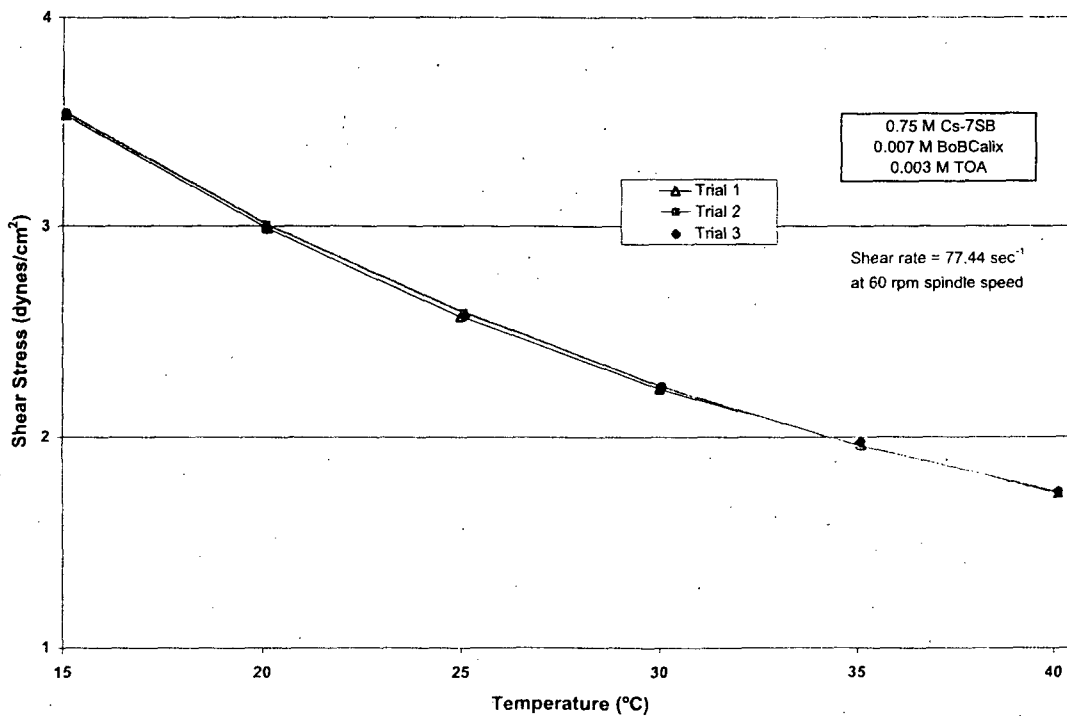


Fig 23. Solvent shear stress versus temperature.

7.6 DISCUSSION AND CONCLUSIONS

7.6.1 Dispersion Numbers

The phase-coalescence behavior of the optimized CSSX solvent in contact with aqueous process solutions was characterized by dispersion numbers, as needed for centrifugal-contactors design. The criteria required the solvent dispersion number be greater than or equal to 4×10^{-4} when contacted with the waste simulant, scrub, and strip solutions at the baseline flowsheet O:A ratios [20]. Table 48 summarizes the dispersion numbers obtained for optimized solvent contacted with waste simulant and scrub and strip solutions at 25 °C. It may be seen that these values all meet the criteria. Within the usual wide variability of such results, the values also compare favorably with the dispersion numbers obtained for the previous test solvents (portion of the table below the dashed line) taken at ambient laboratory temperature for solvent selection (see Chapter 2). For extraction contacts, the dispersion numbers covered the range of dispersion numbers obtained for all of the previous test solvents but were in the range of acceptability defined in the composition criteria. For the scrub and strip contacts, the optimized

Table 48. Dispersion numbers for CSSX solvent extraction, scrub, and stripping

Solvent ^a	Simulant/solvent dispersion number	Scrub/solvent dispersion number	Strip/solvent dispersion number
Optimized solvent trial 1 (#1)	0.00143	0.00107	0.00108
Optimized solvent trial 1 (#2)	0.00137	0.00104	0.00119
Optimized solvent trial 2 (#1)	0.00100		
Optimized solvent trial 2 (#2)	0.00121		
Optimized solvent trial 3 (#1)	0.00052		
Optimized solvent trial 3 (#2)	0.00048		
Previous baseline solvent	0.00149	0.00096	0.00115
B001107-3-1	0.00075	0.00102	0.00091
B001107-3-2	0.00056	0.00070	0.00078
B001107-3-3	0.00102	0.00052	0.00088
B001107-3-4	0.00102	0.00053	0.00094
B001107-3-5	0.00118	0.00050	0.00088
B001107-3-6	0.00105	0.00059	0.00075
B001107-3-7	0.00125	0.00058	0.00085
B001107-3-8	0.00120	0.00062	0.00054
B001107-3-9	0.00141	0.00041	0.00051

^aOptimized solvent was run at 25 °C. Data below the dashed line were collected at ambient laboratory temperature, as taken from Chapter 2 (Table 10).

solvent gave comparable, if not better, dispersion numbers.

Earlier, a gel-like formation was described that occurred during the extraction contacts using the optimized solvent. The formation of the gel-like material was not predictable, and it occurred at least once at each test temperature and in either or both of the two tubes used. Attempts to cause the occurrence of the gel-like material were inconclusive; no specific triggering event or required condition was found.

7.6.2 Solvent Density

The density of the optimized solvent is 0.8516 g/cm³ at 25 °C which is comparable to the density at 25.6 °C for the solvent compositions measured previously that are close in composition to the optimized solvent as shown below in Table 49. The Cs-7SB contributes the most to the changes in total solvent density among the different formulations and the three formulations with 0.75 M Cs-7SB have densities very close to the optimized solvent, as expected.

Table 49. Comparison of CSSX solvent densities

Solvent	[BOBCalixC6] (M)	[Cs-7SB] (M)	[TOA] (M)	Density at 25 °C (g/cm ³)
Optimized solvent	0.007	0.75	0.003	0.8516
Original solvent	0.010	0.50	0.001	0.8100
B001107-3-1	0.010	0.65	0.001	0.8395
B001107-3-2	0.008	0.65	0.001	0.8395
B001107-3-3	0.010	0.75	0.001	0.8531
B001107-3-4	0.008	0.75	0.001	0.8525
B001107-3-5	0.006	0.75	0.001	0.8516
B001107-3-6	0.008	0.85	0.001	0.8644
B001107-3-7	0.006	0.85	0.001	0.8632
B001107-3-8	0.008	1.00	0.001	0.8819
B001107-3-9	0.006	1.00	0.001	0.8951

7.6.3 Solvent Viscosity

The optimized solvent viscosity also compares well with the viscosities measured for the same test solvents listed above with similar Cs-7SB content as shown in Table 50.

Table 50. Comparison of CSSX solvent viscosities

Solvent	Temperature (°C)	Viscosity (cP)
Optimized solvent	15.05	4.83
	20.10	4.09
	25.00	3.51
	30.00	3.07
	35.10	2.69
B001107-3-3	40.10	2.38
	20.00	4.31
	25.00	3.69
	30.02	3.19
	35.08	2.81
B001107-3-4	40.00	2.49
	20.00	4.17
	25.00	3.61
	30.00	3.12
	35.00	2.74
B001107-3-5	40.02	2.44
	20.00	4.12
	25.00	3.57
	30.00	3.11
	35.02	2.70
	40.02	2.40

8. CONCLUSIONS

8.1 OVERALL ASSESSMENT

As necessitated by the supersaturation of the previous CSSX baseline solvent by the calixarene extractant, the purpose of this investigation was to optimize the solvent composition and to measure key chemical and physical properties related to its performance. This purpose has been fulfilled. Overall, it may be said that the optimization of the solvent composition has reduced the overall technical risk in meeting processing requirements using the CSSX process. Experimental results indicate that the changed solvent composition shifted various process performance measures incrementally, some with minor compromise and some with real improvement. A greater understanding of solvent properties and process performance has been obtained, and the precision with which performance can be predicted has been increased.

8.2 EVALUATION OF RESULTS

The optimization of the solvent composition specifically reduced technical risk by ensuring the integrity of the solvent with regard to crystallization of BOBCalixC6, to third-phase formation, and to the effects of impurities. Based on an established set of criteria [20], a matrix of trial concentrations of the baseline solvent components was examined toward the objective of a new, optimum solvent composition. No new constituents were added to the solvent; only the component concentrations were changed. The results led to a straightforward recommendation of a new baseline solvent having the following component concentrations in Isopar[®] L diluent: 0.007 M BOBCalixC6 extractant, 0.75 M Cs-7SB modifier, and 0.003 M TOA stripping aid. This composition met all of the criteria with regard to BOBCalixC6 solubility, third-phase formation, cesium batch distribution ratios, calculated flowsheet robustness, coalescence rate, and solvent density. Acceptable compromises were made in flowsheet robustness and solvent density, with no impact on process goals. Improved resistance to third-phase formation allows the process to operate at lower temperatures (as low as 11 °C) compared with the previous baseline solvent (20 °C), a significant advantage. In addition, the reduction of the concentration of the expensive BOBCalixC6 extractant implies a reduction in the total materials cost of the solvent by approximately 16%. Finally, the higher TOA concentration decreases the risk that buildup of minor anionic species in the solvent could impact stripping performance.

Further data were collected to characterize the performance of the optimized solvent more thoroughly and to ensure that the optimization procedure did not unexpectedly produce unacceptable changes in process performance. Experiments specifically dealt with the temperature dependence of D_{Cs} in extraction, scrubbing, and stripping (ESS); ESS performance on recycle; partitioning of BOBCalixC6, Cs-7SB, and TOA to aqueous process solutions; partitioning of organic anions; distribution of metals; solvent phase separation at low temperatures; solvent stability to elevated temperatures; and solvent

density and viscosity. In general, these system properties were changed only incrementally by solvent optimization, as judged from data presented earlier [11]. The temperature dependence of cesium distribution was found to exhibit approximately the same tendency toward decreasing extraction strength with increasing temperature as the former baseline solvent. This property may be used to advantage to increase extraction efficiency by cooling the extraction section and to increase stripping efficiency by warming the stripping section. New parameters were measured for quantifying the temperature dependence of cesium distribution in extraction, scrubbing, and stripping stages. Better measurements of the partitioning of the solvent components now allow a more confident assertion to be made that the solubility losses of solvent components to the aqueous phase are acceptable within the goal of a maximum of one solvent replacement per year. Some uncertainty remains with regard to the exact loss rate of the modifier, but loss of the expensive calixarene was shown to be definitely negligible. Thus, this conclusion has impact on methods for solvent recovery in that the major expected loss pathway is entrainment, which may be dealt with by mechanical methods. No changes in qualitative conclusions regarding the impacts of minor organic or metallic components on process performance have been found for the optimized solvent. Limited thermal-stability experiments again confirm earlier conclusions concerning the high stability of the solvent. A thermal-chemical stability of the solvent of more than 977 days at the maximum normal operating temperature of 35 °C is indicated by the data. A more focused examination of phase stability at low temperatures was necessitated by observation of unusual ESS behavior on batches of optimized CSSX solvent shipped to other laboratories. It was confirmed from earlier indications [11] that the solvent splits into two phases on storage at low temperatures, conditions expected during shipment or outside storage in the winter, necessitating warming to room temperature and remixing before use. Overall, solvent performance was found to be similar to that of the former baseline solvent, with no issues raised concerning unexpected phenomena.

8.3 RECOMMENDATIONS FOR FUTURE WORK

8.3.1 Summary Remarks

From the perspective of a year and a half since the previous assessment of needs for research and development in the area of CSSX chemistry [11], it is instructive to examine current needs. In particular, Chapter 9 of the previous report enumerated nine areas of possible investigation. These areas were listed under nine secondary headings similar to those given below. Additional information on potential needs may be found in FY 2002 program planning [18] and in documentation issued in connection with the solicitation for design, construction, and commissioning of the SRS Salt Waste Processing Facility [42].

8.3.2 Solvent Composition

The first need identified was for solvent optimization [11], which has now been fulfilled. Nevertheless, it may still be worthwhile to pursue additional measurements on BOBCalixC6 solubility

with resolve to continue tests until true equilibrium is reached. The needed measurement time is perhaps a year or more. In addition, it would be valuable to understand if the solubility is impacted by variables such as TOA and aqueous-phase composition. Given the rate of diluent evaporation recently measured [43], possible questions on the environmental acceptability of hydrocarbon emissions or on the ease of process control could motivate consideration of the use of less volatile diluents. Finally, alternative calixarenes are being developed that behave similarly to BOBCalixC6 but have improved solubility [44]. A particularly promising example is calix[4]arene-bis(2-ethylhexylbenzo-crown-6), which has the same framework structure as BOBCalixC6, but with alternative alkyl groups.

8.3.3 Actinide and Strontium Extraction

It would be an obvious advantage toward an overall footprint reduction in the Salt Processing Facility if the CSSX process could also remove the traces of actinides and strontium from the waste. Based on current data, actinides are not significantly extracted by the CSSX solvent [11,40]. A project is under way to examine whether new solvent-extraction chemistry may be developed to remove actinides and strontium from alkaline high-level waste such as that stored at the SRS [45]. This might be accomplished by developing a new solvent and corresponding flowsheet to operate in tandem with the CSSX process. Or possibly the CSSX solvent chemistry may be augmented in a way that enables it to extract cesium, actinides, and strontium simultaneously.

8.3.4 Radiation Stability

Testing in FY 2001 on the previous baseline solvent indicated no significant technical risks due to radiation-induced degradation of the CSSX solvent components [11-14]. In support of this conclusion, an encouraging review of the literature [46] recently suggested that the rate of degradation of the solvent components should be no higher than 1% per year. Although these studies reduce the urgency for further examination of this issue, it remains desirable to pursue unanswered questions. That same literature review [46] also suggested that the aging of the solvent under process conditions should yield a complex mixture of possible organic degradation products that might not wash out. Only two key degradation products have so far been identified, dioctylamine and 4-*sec*-butylphenol [11-14], and these were fairly predictable. There remain the questions of how these products may further react and whether other, less obvious, products are also formed. An open issue exists as to the impact of slow degradation processes that occur after an initial irradiation period [11]. A further question pertains to whether the effects of irradiation differ between static batch tests and the dynamic flowsheet in which the solvent cycles between alkaline and acid conditions. The present report has provided no new data on radiation degradation, and little new data have become available in the past year. Although the risk from radiolysis effects appears low, further radiation experiments to provide data on the optimized solvent would be helpful, especially from the point of view of solvent aging and possible impurity buildup (see section 8.3.7 below).

8.3.5 Thermal Stability

Static tests continue to show the high chemical and thermal stability of the CSSX, as verified herein and elsewhere [47] for the optimized solvent. As pointed out above, a recent review [46] suggests the solvent should have adequate chemical stability in terms of the rate of breakdown of the solvent components. Nevertheless, the same general questions remain as were identified above in the case of radiation stability. Such questions pertain to the reactions of dioctylamine and 4-*sec*-butylphenol, the formation of other as-yet unidentified degradation products, the difference between static and dynamic behavior, and the effects of solvent aging. In particular, it continues to be desirable to understand TOA degradation, particularly under acidic conditions. Earlier work showed that TOA is the most easily degraded solvent component, with deleterious consequences for stripping [11].

8.3.6 Solvent Cleanup

As previously recommended [11], it would be prudent to prepare for the possibility (see below) that strongly lipophilic anions accumulate in the solvent and eventually overcome the ability of TOA to suppress their harmful effect on stripping. In the work reported herein, limited data were collected to show that the effect of small amounts of dibutylphosphate and dodecanoate was negligible, as expected. Whereas dibutylphosphate is expected to be removed easily by a sodium hydroxide wash step, surfactants having more than 12 carbons are sufficiently lipophilic that their removal will be incomplete by washing [11]. Hence, alternative solvent cleanup methods, such as anion exchange, should be further developed as a ready solution to potential difficulties.

8.3.7 Minor Species

In simple batch contacting, it was found herein that minor organic and inorganic species pose no particular recognizable risks based on current knowledge of the waste composition, solvent breakdown products, the distribution behavior of minor species, and available solvent-cleanup methods. This limited conclusion agrees with the results of more extensive testing with the previous baseline solvent, including results from batch tests with waste simulant [11] and from contactor tests with simulant [16,48] and with real waste [17,49] over a relatively small number of cycles. On the other hand, experience in solvent-extraction hydrometallurgy shows that long-term operation generally leads to buildup of species that can eventually impact the performance of a process [50]. Fortunately, the types of problems that may be encountered (e.g., poor phase disengagement, interfacial crud, or loss of extraction and stripping performance) generally yield to acceptable technical solutions. It may be expected that the impact to schedule and facility cost will decrease the earlier the problems are recognized and dealt with. Thus, the more that is known regarding the behavior of minor species prior to facility design, the lower the technical risk will be. Accordingly, contactor tests with long run times using real waste are especially recommended. Given that the solvent will be cycled approximately 3000 times in a year, tests running at least 300 cycles would start to be fruitful in revealing potential problems that may be encountered over

the course of operating a plant for a full year. Thus far, flowsheet tests with real waste have been carried out for only ~1% of the number of annual cycles. In addition, analysis of the wastes for lipophilic organic species should continue, as should study of the fate of surfactant species in the flowsheet. Certain metals such as technetium should be further studied to understand observed behavior in contactor testing. As pointed out above, it does not appear that actinides [40] nor any metals other than the alkali metals are extracted to a significant degree by the pristine CSSX solvent [11]. An unanswered question, though, is how minor waste components distribute when the solvent is aged from extended use and presumably accumulates organic species that do not wash out. For example, do degradation products or surfactant species that build up over a year begin to extract other metals? Such questions suggest the need for tests designed to simulate aging and to reveal how the aged solvent behaves, particularly with regard to the buildup of minor components and their effects.

8.3.8 Fate of Trimethylamine

Trimethylamine is a minor component expected at low concentrations in the waste feed. Its origin is thought to be the breakdown of strong-base anion-exchange resins in the waste. In previous tests, trimethylamine was shown to have the potential to build up in a loop between the extraction and scrub sections [11]. Although this species was not observed to cause any particular difficulties in batch tests, more evaluation is needed to definitely establish its fate in the flowsheet and its impacts on process performance.

8.3.9 Role of Nitrite

It has been recently established that impaired stripping associated with high nitrite concentrations in certain simulant testing [11] was caused by a surfactant added to the reagent sodium nitrite used to make the simulants [41]. The presence of nitrite as nitrous acid was also shown not to increase the already low risk of nitration of solvent components in scrubbing [47]. Hence, the effects of nitrite appear reasonably minimal. It should be noted, however, that nitrous acid is generated from co-extracted nitrite as the solvent moves from the extraction section into the scrubbing section. As nitrite is a reactive species [46,47], its continuous generation in the flowsheet could contribute to more rapid solvent aging effects than static tests indicate, as nitrous acid quickly dissipates in a static test [47].

8.3.10 Modeling

Progress has been made in modeling the CSSX process using the optimized solvent system, where it has been possible to predict with reasonable accuracy the cesium distribution ratios on variable aqueous-feed composition [39]. It is now desirable to factor in the effect of certain minor components, variation of the concentration of solvent components, and temperature variation. Data on the partitioning of Cs-7SB and TOA presented in this report together with data on diluent evaporation [42] reveal that variation of both the relative and absolute concentrations of the solvent components may be expected in normal process operation. It would therefore be helpful if the effects of such variation were easily predicted.

Acid extraction by TOA needs to be studied and incorporated into the model, as this phenomenon affects how the cesium distribution ratio changes from stage to stage in scrubbing and stripping. In terms of making the model more accessible, a convenient user interface is needed, and the equilibrium model must be incorporated into a flowsheet model.

9. REFERENCES

1. P. V. Bonnesen, L. H. Delmau, B. A. Moyer, and R. A. Leonard, "A Robust Alkaline-Side CSEX Solvent Suitable for Removing Cesium from Savannah River High Level Waste," *Solvent Extr. Ion Exch.* **18** (6), 1079-1107 (2000).
2. B. A. Moyer, P. V. Bonnesen, R. A. Sachleben, and D. J. Presley, "Solvent and Process for Extracting Cesium from Alkaline Waste Solutions," U.S. Patent 6,174,503, January 16, 2001.
3. R. A. Dimenna et al., *Bases, Assumptions, and Results of the Flow Sheet Calculations for the Decision Phase Salt Disposition Alternatives*, WSRC-RP-99-00006, Rev. 3, Westinghouse Savannah River Company, Aiken, South Carolina, May 2001.
4. *Savannah River Site Salt Processing Alternatives Final Supplemental Environmental Impact Statement (EIS)*, DOE/EIS-0082-S2D, U.S. Department of Energy, Aiken, South Carolina, July 20, 2001.
5. *Federal Register*, **66** (201), 52752-52756, October 17, 2001.
6. National Research Council, Committee on Radionuclide Separation Processes for High-Level Waste at the Savannah River Site, *Research and Development on a Salt Processing Alternative for High-Level Waste at the Savannah River Site*, National Academy Press, Washington, D.C., 2001.
7. H. Harmon, S. Schlahta, D. Wester, J. Walker, S. Fink, and M. Thompson, *Tanks Focus Area Savannah River Site Salt Processing Project Research and Development Summary Report*, TFA-0105, Pacific Northwest National Laboratory, Richland, Washington, May 2001.
8. J. T. Case, J. G. Burritt, J. L. Kovach, R. W. Kupp, R. P. Palluzi, L. L. Tavlarides, and R. F. Vance, *Evaluation of Alternatives for Salt Waste Processing at the Savannah River Site*, TAT Report, Rev. H., Savannah River Salt Processing Project Technical Advisory Team, U.S. Department of Energy, May 31, 2001.
9. K. Lang, W. F. Spader, K. Picha, and K. Gerdes, *Final Report on the Salt Processing Project Technology Selection, Technical Working Group*, U.S. Department of Energy, June 2001.
10. M. Frei, L. Erickson, B. Smith, C. Hansen, and T. Fryberger, *Salt Processing Project Management Review Board Summary Report*, U.S. Department of Energy, May 24, 2001.
11. B. A. Moyer, S. D. Alexandratos, P. V. Bonnesen, G. M. Brown, J. E. Caton, Jr., L. H. Delmau, C. R. Duchemin, T. J. Haverlock, T. G. Levitskaia, M. P. Maskarinec, F. V. Sloop, Jr., and C. L. Stine, "Caustic-Side Solvent Extraction Chemical and Physical Properties: Progress in FY 2000 and FY 2001." Report ORNL/TM-2001/285, Oak Ridge National Laboratory, Oak Ridge, Tennessee, February 2002.

12. R. A. Peterson, T. L. White, S. Crump, and L. H. Delmau, *Solvent Extraction External Radiation Stability Testing*, WSRC-TR-2000-00413, Rev. 0, Westinghouse Savannah River Company, Aiken, South Carolina, November 20, 2000.
13. R. A. Peterson, T. L. White, and N. E. Gregory, *Solvent Extraction External Irradiation Update*, SRT-LWP-2000-00101, Westinghouse Savannah River Company, Aiken, South Carolina, June 16, 2000.
14. R. D. Spence, L. N. Klatt, L. H. Delmau, F. V. Sloop, Jr., P. V. Bonnesen, and B. A. Moyer, *Batch-Equilibrium Hot-Cell Tests of Caustic-Side Solvent Extraction (CSSX) with SRS Simulant Waste and Internal ¹³⁷Cs Irradiation*, ORNL/TM-2001/49, Oak Ridge National Laboratory, Oak Ridge, Tennessee, September 2001.
15. J. F. Birdwell, Jr., and R. L. Cummings, *Irradiation Effects on Phase-Separation Performance Using a Centrifugal Contactor in a Caustic-Side Solvent Extraction Process*, ORNL/TM-2001/91, Oak Ridge National Laboratory, Oak Ridge, Tennessee, August 2001.
16. R. A. Leonard, S. B. Aase, H. A. Arafat, D. B. Chamberlain, C. Conner, M. C. Regalbuto, and G. F. Vandegrift, *Multi-day Test of the Caustic-Side Solvent Extraction Flowsheet for Cesium Removal from a Simulated SRS Tank Waste*, ANL-02/11, Argonne National Laboratory, Argonne, Illinois, January 15, 2002.
17. S. G. Campbell, M. W. Geeting, C. W. Kennell, J. D. Law, R. A. Leonard, M. A. Norato, R. A. Pierce, T. A. Todd, D. D. Walker, and W. R. Wilmarth, *Demonstration of Caustic-Side Solvent Extraction with Savannah River Site-High-Level Waste*, WSRC-TR-2001-00223, Rev. 0, Westinghouse Savannah River Company, Aiken, South Carolina, April 19, 2001.
18. H. Harmon, R. Leugemors, S. Schlahta, S. Fink, M. Thompson, and D. Walker, *Savannah River Site Salt Processing Project: FY 2002 Research and Development Program Plan*, PNNL-13707, Rev. 1, Pacific Northwest National Laboratory, Richland, Washington, December 2001.
19. H. Harmon, S. Schlahta, J. Walker, D. Wester, K. Rueter, and S. Fink, *Tanks Focus Area, Savannah River Site Salt Processing Project, Research and Development Program Plan*, PNNL-13253, Rev. 1, Pacific Northwest National Laboratory, Richland, Washington, November 2000.
20. L. N. Klatt, *Criteria for Optimum Composition of the Caustic-Side Solvent Extraction (CSSX) Solvent*, CERS/SR/SX/025, Rev. 0, Nuclear Science and Technology Division, Oak Ridge National Laboratory, Oak Ridge, Tennessee, August 2001.

21. L. N. Klatt, J. F. Birdwell, Jr., P. V. Bonnesen, L. H. Delmau, L. J. Foote, D. D. Lee, R. A. Leonard, T. G. Leviskaia, M. P. Maskarinec, and B. A. Moyer, *Caustic-Side Solvent Extraction Solvent-Composition Recommendation*, CERS/SR/SX/026, Rev. 0, Nuclear Science and Technology Division, Oak Ridge National Laboratory, Oak Ridge, Tennessee, November 8, 2001.

22. L. N. Klatt, J. F. Birdwell, Jr., P. V. Bonnesen, L. H. Delmau, L. J. Foote, D. D. Lee, R. A. Leonard, T. G. Leviskaia, M. P. Maskarinec, and B. A. Moyer, *Caustic-Side Solvent Extraction Solvent-Composition Recommendation*, ORNL/TM-2001/258, Oak Ridge National Laboratory, Oak Ridge, Tennessee, January 2001.

23. R. A. Peterson, *Preparation of Simulated Waste Solutions for Solvent Extraction Testing*, WSRC-RP-2000-00361, Rev. 0, Westinghouse Savannah River Company, Aiken, South Carolina, May 2000.

24. R. A. Leonard, "Solvent Characterization Using The Dispersion Number," *Sep. Sci. Technol.* **30** (7-9), 1103-1122 (1995).

25. ASTM Standard D 891-95, "Standard Test Method for Specific Gravity, Apparent, of Liquid Industrial Chemicals," American Society for Testing and Materials, Philadelphia, 2000.

26. ASTM Standard D 1429-95, "Standard Test Methods for Specific Gravity of Water and Brine," American Society for Testing and Materials, Philadelphia, 2000.

27. ASTM Standard E 542-00, "Standard Practice for Calibration of Laboratory Volumetric Apparatus," American Society for Testing and Materials, Philadelphia, 2000.

28. ASTM Standard D 2196-99, "Standard Test Method for Rheological Properties of Non-Newtonian Materials by Rotational (Brookfield type) Viscometer," American Society for Testing and Materials, Philadelphia, 1999.

29. "The Brookfield Digital Viscometer Model DV-II Operating Instructions," Manual No. M/85-160-F, Brookfield Engineering Laboratories, Inc., Stoughton, Massachusetts, 1985.

30. ASTM Standard D 971-99a, "Standard Test Method for Interfacial Tension of Oil Against water by the Ring Method," American Society for Testing and Materials, Philadelphia, 1999.

31. ASTM Standard D 1331-89, "Standard Test Method for Surface and Interfacial Tension of Solutions of Surface-Active Agents," American Society for Testing and Materials, Philadelphia, 1989.

32. *CRC Handbook of Chemistry and Physics*, 66th ed., CRC Press, Boca Raton, Florida, 1985, p. F-32.
33. R. A. Leonard and M. C. Regalbuto, "A Spreadsheet Algorithm for Stagewise Solvent Extraction," *Solvent Extr. Ion Exch.* **12** (5), 909-930 (1994).
34. J. F. Birdwell, Jr., and K. K. Anderson, *Evaluation of 5-cm Centrifugal Contactor Hydraulic and Mass Transfer Performance for Caustic-Side Solvent Extraction of Cesium*, ORNL/TM-2001/137, Oak Ridge National Laboratory, Oak Ridge, Tennessee, August 2001.
35. J. F. Birdwell, Jr., "Throughput Performance of a Fully-Pumping 5-cm Centrifugal Contactor with Vane Modifications," Tanks Focus Area (TFA) Plan of the Week (POW) Technical Discussion, Oak Ridge National Laboratory, Oak Ridge, Tennessee, November 5, 2001.
36. J. D. Law, R. D. Tillotson, and T. A. Todd, "Evaluation of the Hydraulic Performance and Mass Transfer Efficiency of the CSSX Process with the Optimized Solvent in a Single Stage of 5.5-cm Diameter Centrifugal Contactor," INEEL/EXT-02-01109, Idaho National Engineering and Environmental Laboratory, Idaho Falls, Idaho, September 2002.
37. L. H. Delmau, L. J. Foote, P. V. Bonnesen, H. Jennings, T. G. Levitskaia, M. P. Maskarinec, B. A. Moyer, D. D. Lee, K. K. Anderson, and L. N. Klatt, "Solvent Optimization," TFA POW Technical Discussion, Oak Ridge National Laboratory, Oak Ridge, Tennessee, October 29, 2001.
38. J. F. Birdwell, Jr., K. K. Anderson, and D. E. Hobson, *Investigation of Emulsion Formation in Solvent Washing in the Caustic-Side Solvent Extraction (CSSX) Process*, ORNL/TM-2002/126, Oak Ridge National Laboratory, Oak Ridge, Tennessee, June 2002.
39. L. H. Delmau, D. A. Bostick, T. J. Haverlock, and B. A. Moyer, *Caustic-Side Solvent Extraction: Extended Equilibrium Modeling of Cesium and Potassium Distribution Behavior*, ORNL/TM-2002/116, Oak Ridge National Laboratory, Oak Ridge, Tennessee, May 2002.
40. W. R. Wilmarth, V. H. Dukes, J. T. Mills, C. C. DiPrete, and D. P. DiPrete, *Solvent Composition Impacts on the Extraction of Uranium and Plutonium in the Caustic Side Solvent Extraction Process*, WSRC-TR-2002-00060, Westinghouse Savannah River Company, Aiken, South Carolina, January 18, 2002.
41. L. H. Delmau, T. J. Haverlock, and B. A. Moyer, *Caustic-Side Solvent Extraction: Anti-Caking Surfactants Found to Be Cause of Apparent Effect of High Nitrite Concentration on Cesium Stripping*, ORNL/TM-2002/104, Oak Ridge National Laboratory, Oak Ridge, Tennessee, May 2002.

42. *Design, Construction, and Commissioning of a Salt Waste Processing Facility*, Request for Proposal No. DE-RP09-02SR22210, Amendment 002, U. S. Department of Energy, Savannah River Operations Office, Aiken, South Carolina, January 9, 2002.

43. D. D. Lee, J. F. Birdwell, Jr., P. V. Bonnesen, and B. A. Tomkins, *Density Changes in the Optimized CSSX Solvent System*, ORNL/TM-2002/204, Oak Ridge National Laboratory, Oak Ridge, Tennessee, October 2002.

44. B. A. Moyer, P. V. Bonnesen, J. C. Bryan, N. L. Engle, T. J. Keever, T. G. Levitskaia, R. A. Sachleben, R. A. Bartsch, V. S. Talanov, H. W. Gibson, J. W. Jones, and B. P. Hay, *Next Generation Extractants for Cesium Separation from High-Level Waste: From Fundamental Concepts to Site Implementation*, FY 2002 Annual Report, Environmental Management Science Program, August, 2002; posted on the EMSP web site <http://emsp.em.doe.gov/>.

45. L. H. Delmau, K. N. Raymond, and D. T. Hobbs, *Combined Extraction of Cesium, Strontium, and Actinides from Alkaline Media: An Extension of the Caustic-Side Solvent Extraction (CSSX) Process Technology*, FY 2002 Annual Report, Environmental Management Science Program, June, 2002; posted on the EMSP web site <http://emsp.em.doe.gov/>.

46. L. M. Stock, D. M. Camaioni, D. W. Wester, and C. D. Gutsche, *Decomposition Pathways for the Savannah River Site Caustic-Side Solvent Extraction System*, PNNL-13935, Pacific Northwest National Laboratory, Richland, Washington, July 2002.

47. P. V. Bonnesen, F. V. Sloop, Jr., and N. L. Engle, *Stability of the Caustic-Side Solvent Extraction (CSSX) Process Solvent: Effect of High Nitrite on Solvent Nitration*, ORNL/TM-2002/115, Oak Ridge National Laboratory, Oak Ridge, Tennessee, July 2002.

48. M. P. Maskarinec, *Analysis of a Sample of the Solvent Used in the Argonne National Laboratory Multiday Flowsheet Test*, CERS/SR/SX/027, Rev. 0, Chemical Sciences Division and Nuclear Science and Technology Division, Oak Ridge National Laboratory, Oak Ridge, Tennessee, February 19, 2002.

49. S. L. Crump, M. A. Norato, R. A. Pierce, R. J. Ray, D. D. Walker, and T. L. White, *Demonstration of Caustic-Side Solvent Extraction with Savannah River Site High-Level Waste: Results of Organic and Trace Component Analyses*, WSRC-TR-2001-00372, Rev. 0, Westinghouse Savannah River Company, Aiken, South Carolina, December 7, 2001.

50. B. Grinbaum and L. Kogan, "Verification of a Process in a Demonstration Plant: How Long Does it Take to Find All the Problems?" Proc. Internat. Solvent Extraction Conf. (ISEC 2002), Cape Town, South Africa, Mar. 17-21, 2002, K. C. Sole P. M. Cole, J. S. Preston, D. J. Robinson, Eds., Chris van Rensburg Publications, Melville, South Africa, 2002; Vol. 2, pp. 1408-1413.

Appendix A

PREDICTED D_{Cs} VALUES USING THE log VERSUS log RELATIONSHIPS BETWEEN D_{Cs} VALUES AND BOBCalixC6 AND Cs-7SB MODIFIER CONCENTRATIONS

Table A.1. Predicted D_{Cs} values

Process step	D_{Cs}		
	[Cs-7SB] = 0.70 M	[Cs-7SB] = 0.75 M	[Cs-7SB] = 0.80 M
[BOBCalixC6] = 6.5 mM			
Extraction	12.76	13.08	13.40
Scrub no. 1	1.16	1.22	1.28
Scrub no. 2	1.21	1.26	1.31
Strip no. 1	0.91	0.096	0.101
Strip no. 2	0.054	0.057	0.059
Strip no. 3	0.043	0.045	0.047
Strip no. 4	0.037	0.039	0.041
[BOBCalixC6] = 7.0 mM			
Extraction	13.77	14.13	14.48
Scrub no. 1	1.26	1.32	1.38
Scrub no. 2	1.30	1.35	1.40
Strip no. 1	0.099	0.104	0.109
Strip no. 2	0.059	0.062	0.065
Strip no. 3	0.047	0.049	0.051
Strip no. 4	0.040	0.043	0.045
[BOBCalixC6] = 7.5 mM			
Extraction	14.78	15.18	15.56
Scrub no. 1	1.35	1.42	1.49
Scrub no. 2	1.39	1.45	1.50
Strip no. 1	0.106	0.112	0.117
Strip no. 2	0.060	0.070	0.070
Strip no. 3	0.051	0.053	0.055
Strip no. 4	0.044	0.046	0.048

INTERNAL DISTRIBUTION

1. J. F. Birdwell, Jr.
2. P. V. Bonnesen
3. J. L. Collins
4. R. L. Cummins
- 5-7. L. H. Delmau
8. R. D. Hunt
- 9-10. T. J. Keever
11. D. D. Lee
12. M. P. Maskarinec
13. A. J. Mattus
14. C. P. McGinnis
- 15-16. B. A. Moyer
17. F. V. Sloop, Jr.
18. R. D. Spence
19. J. F. Walker, Jr.
20. J. S. Watson
21. ORNL Central Research Library
22. Laboratory Records, RC
23. Laboratory Records, OSTI

EXTERNAL DISTRIBUTION

24. J. T. Carter, Westinghouse Savannah River Company, P.O. Box 616, Building 766-H, Aiken, SC 29808
25. D. Chamberlain, Argonne National Laboratory, Building 205, 9700 South Cass Avenue, Argonne, IL 60439
26. N. F. Chapman, Westinghouse Savannah River Company, P.O. Box 616, Building 704-3N, Aiken, SC 29808
27. W. D. Clark, U.S. Department of Energy, Savannah River Operations Office, Bldg. 704-3N, Aiken, SC 29808
28. C. Conner, Argonne National Laboratory, Building 205, 9700 South Cass Avenue, Argonne, IL 60439

29. R. G. Edwards, Westinghouse Savannah River Company, P.O. Box 616, Building 704-3N, Aiken, SC 29808
30. S. D. Fink, Westinghouse Savannah River Company, P.O. Box 616, Building 773-A, Aiken, SC 29808
31. H. D. Harmon, Tank Focus Area Salt Processing Program, P.O. Box 616, Building 704-3N, Aiken, SC 29808
32. R. T. Jones, Westinghouse Savannah River Company, P.O. Box 616, Building 704-3N, Aiken, SC 29808
33. L. N. Klatt, 111 Carnegie Drive, Oak Ridge, TN 37830
34. R. A. Leonard, 224 Franklin Ave, River Forest, IL 60305
35. T. G. Levitskaia, Pacific Northwest National Laboratory, P.O. Box 999; MSIN P7-22, Richland, WA 99352
36. J. R. Noble-Dial, U.S. Department of Energy, Oak Ridge Operations Office, P.O. Box 2001, Oak Ridge, TN 37831-8620
37. M. Norato, Westinghouse Savannah River Company, P.O. Box 616, Building 773-A, Aiken, SC 29808
38. R. Pierce, Westinghouse Savannah River Company, P.O. Box 616, Building 773-A, Aiken, SC 29808
39. S. N. Schlahta, Battelle, Pacific Northwest National Lab, P.O. Box 999 / MS K9-14 Richland, WA 99352
40. P. C. Suggs, U.S. Department of Energy, Savannah River Operations Office, P.O. Box A, Building 704-3N, Aiken, SC 29808
41. W. L. Tamosaitis, Westinghouse Savannah River Company, P.O. Box 616, Building 773-A, Aiken, SC 29808
42. M. C. Thompson, Westinghouse Savannah River Company, P.O. Box 616, Building 773-A, Aiken, SC 29808

43. T. A. Todd, Idaho National Engineering & Environmental Laboratory, Building 637, MS-5218, Idaho Falls, ID 834415-5218
44. G. F. Vandegrift, Argonne National Laboratory, Building 205, 9700 South Cass Avenue, Argonne, IL 60439
45. D. D. Walker, Westinghouse Savannah River Company, P.O. Box 616, Building 773-A, Aiken, SC 29808
46. D. Wester, Battelle, Pacific Northwest National Lab, P.O. Box 999 / MS K8-93 Richland, WA 99352
47. Vickie Wheeler, U.S. Department of Energy, Savannah River Operations Office, P.O. Box A, Building 776-H, Aiken, SC 29808
48. W. R. Wilmarth, Westinghouse Savannah River Company, P.O. Box 616, Building 773-A, Aiken, SC 29808
49. Tanks Focus Area Technical Team, c/o B. J. Williams, Pacific Northwest National Laboratory, P.O. Box 999, MSIN K9-69, Richland, WA 99352
50. Tanks Focus Area Field Lead, c/o T. P. Pietrok, U.S. Department of Energy, Richland Operations Office, P.O. Box 550, K8-50, Richland, WA 99352
51. Tanks Focus Area Headquarters Program Manager, c/o K. D. Gerdes, DOE Office of Science and Technology, 19901 Germantown Rd., 1154 Cloverleaf Building, Germantown, MD 20874-1290
49. Nicole Simon and Jean-François Dozol, CEA Cadarache, DESD/SEP/LPTE, Bat.326, 13108 St Paul lez Durance Cedex, France
50. Charles Madic, CEA Valrhô-Marcoule, DCC, BP 171, 30207 Bagnols s/Seze Cedex, France

**RESPONSE TO RAI COMMENT 58
ROADMAP TO REFERENCES**

REFERENCED DOCUMENT	*EXCERPT LOCATION	REMARK
Bradbury and Sarott 1995	Excerpt included in response.	
Cook et al. 2005 – Section A.2.5 and Table A-8.	Excerpt included in response.	
Hoeffner 1984a	Excerpt included in response.	
Hoeffner 1984b	Excerpt included in response.	
Hoeffner 1985	Excerpt included in response.	
Kaplan 2004	Excerpt included in response.	
Kaplan et al. 1998	Excerpt included in response.	
McIntyre 1988	Excerpt included in response.	
NCRP 1996	Excerpt included in response.	
Serzik and Johnson 1994	Excerpt included in response.	
Sheppard and Thibault 1990	Excerpt included in response.	

*Excerpt Locations:

1. Excerpt included in response: The excerpt is included within the text of the response or is appended to the response.
2. Excerpt enclosed following response: The excerpt is enclosed on a separate sheet or sheets following the response.
3. Representative excerpt(s) enclosed following response: Representative excerpts from a document that is wholly or largely applicable are enclosed following the response.
4. Other

**APPROVED for Release for
Unlimited (Release to Public)**

7/15/2005

**RESPONSE TO RAI COMMENT 59
ROADMAP TO REFERENCES**

REFERENCED DOCUMENT	*EXCERPT LOCATION	REMARK
Cook 1981 Figure 1	Excerpt included in response.	
MMES 1992	Excerpt enclosed following response.	Appendix D Section D.4.2

***Excerpt Locations:**

1. Excerpt included in response: The excerpt is included within the text of the response or is appended to the response.
2. Excerpt enclosed following response: The excerpt is enclosed on a separate sheet or sheets following the response.
3. Representative excerpt(s) enclosed following response: Representative excerpts from a document that is wholly or largely applicable are enclosed following the response.
4. Other

APPROVED for Release for
Unlimited (Release to Public)

7/15/2005

4/10/98

APPROVED for Release for
Unlimited (Release to Public)
6/23/2005

WSRC-RP-92-1360 ←

**RADIOLOGICAL
PERFORMANCE ASSESSMENT FOR THE Z-AREA
SALTSTONE DISPOSAL FACILITY (U)**

RC
2/14/93

Prepared for the
WESTINGHOUSE SAVANNAH RIVER COMPANY
Aiken, South Carolina

by

**MARTIN MARIETTA ENERGY SYSTEMS, INC.
EG&G IDAHO, INC.
WESTINGHOUSE HANFORD COMPANY
WESTINGHOUSE SAVANNAH RIVER COMPANY**

December 18, 1992

Rev. 0

Results from the final solutions using the steps outlined above are shown below.

→ **D.4.2 Interactions with the Sediment**

The composition of the pore fluid in equilibrium with the grout phases, as described in Sect. D.3, was reacted with mineral phases in the unsaturated zone. Reaction of the evolved pore solution (Table D.3-3) with CO_2 in the unsaturated zone reduces the pH from 13.78 to 7.32.

The pore fluid changed very little after reacting with the soil minerals. A small amount of diaspore was precipitated, reducing the aluminum concentration in the interstitial fluid. Presence of an iron oxide or iron hydroxide phase has very little effect on the precipitated phases or intensive parameters (i.e., pH, Eh). Further, the specific composition of the iron phase did not substantially change the composition of the reacted solution or the composition or quantity of the precipitated minerals. A small amount of the iron phase dissolved, adding iron to the reacted solution. This is present almost totally as ferric iron. The amount of dissolved iron varies according to what iron phase is chosen.

The composition of the pore solution after reacting with unsaturated zone minerals and CO_2 is presented in Table D.4-1, along with the amount of the precipitated phase. Speciation of the pore solution is presented in Table D.4-2.

In summary, reaction with iron minerals increased the concentration of iron in solution from nearly zero to 3 ppb. The concentration of the three primary pollutants, ^{99}Tc , tritium, and nitrate do not substantially change in the interstitial fluid during communication with the unsaturated zone minerals. The precipitation of diaspore ($\text{AlO}\cdot\text{OH}$), would attenuate tritium to a small degree, but the amount is insignificant. The concentration of all three pollutants will decrease in the interstitial fluid due to the dilution by naturally occurring water present in the vadose zone.

**RESPONSE TO RAI COMMENT 60
ROADMAP TO REFERENCES**

REFERENCED DOCUMENT	*EXCERPT LOCATION	REMARK
Cook et al. 2005 Page A-24	Excerpt enclosed following response.	Tc-99 – $K_d = 1000$ mL/g for reducing saltstone.
1992 PA Page D-9	Excerpt enclosed following response.	
1992 PA Page D-10	Excerpt enclosed following response.	
Bradbury & Sarott Page 39	Excerpt enclosed following response.	Section 5.2.10 - Technetium

***Excerpt Locations:**

1. Excerpt included in response: The excerpt is included within the text of the response or is appended to the response.
2. Excerpt enclosed following response: The excerpt is enclosed on a separate sheet or sheets following the response.
3. Representative excerpt(s) enclosed following response: Representative excerpts from a document that is wholly or largely applicable are enclosed following the response.
4. Other

APPROVED for Release for
Unlimited (Release to Public)

7/14/2005

APPROVED for Release for
Unlimited (Release to Public)
6/6/2005

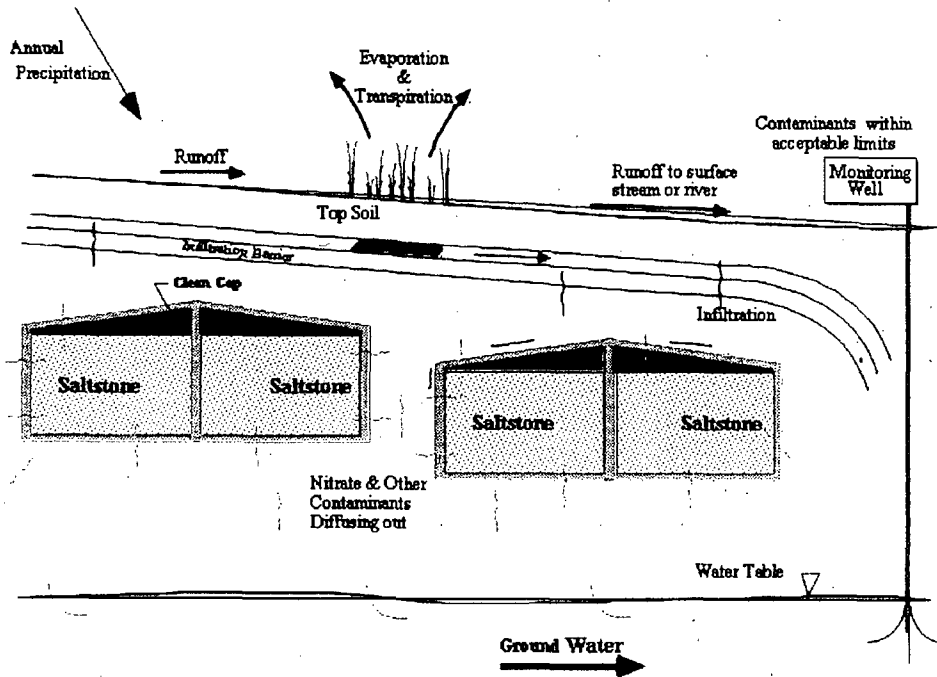
WSRC-TR-2005-00074
Revision 0

KEY WORDS: Performance Assessment
Low-level Radioactive Waste Disposal

**SPECIAL ANALYSIS:
REVISION OF SALTSTONE VAULT 4 DISPOSAL LIMITS (U)**

**PREPARED BY:
James R. Cook
Elmer L. Wilhite
Robert A. Hiergesell
Gregory P. Flach**

MAY 26, 2005



Westinghouse Savannah River Company
Savannah River Site
Aiken, SC 29808

Prepared for the U.S. Department of Energy Under
Contract Number DE-AC09-96SR18500



Pu5-242	1.50E+01	1.50E+01	5.00E+01	5.00E+03	5.00E+03
U-238	8.00E+02	8.00E+02	1.60E+03	2.00E+03	2.00E+03
Pu-244	3.70E+02	3.70E+02	6.50E+03	5.00E+03	5.00E+03
Pu5-244	1.50E+01	1.50E+01	5.00E+01	5.00E+03	5.00E+03
Ra-226	5.00E+02	5.00E+02	9.10E+03	5.00E+01	5.00E+01
Rb-87	5.50E+01	5.50E+01	2.70E+02	5.50E+01	5.50E+01
Se-79	3.60E+01	3.60E+01	7.60E+01	1.00E-01	1.00E-01
Sn-126	1.30E+02	1.30E+02	6.70E+02	1.00E+03	1.00E+03
Sr-90	1.00E+01	1.00E+01	1.10E+02	1.00E+00	1.00E+00
Tc-99	1.00E-01	1.00E-01	1.00E-01	1.00E+03	1.00E+03
Th-228	3.20E+03	3.20E+03	5.80E+03	5.00E+03	5.00E+03
Ra-224	5.00E+02	5.00E+02	9.10E+03	5.00E+01	5.00E+01
Th-229	3.20E+03	3.20E+03	5.80E+03	5.00E+03	5.00E+03
Ra-225	5.00E+02	5.00E+02	9.10E+03	5.00E+01	5.00E+01
Ac-225	4.50E+02	4.50E+02	2.40E+03	5.00E+03	5.00E+03
Th-230	3.20E+03	3.20E+03	5.80E+03	5.00E+03	5.00E+03
Ra-226	5.00E+02	5.00E+02	9.10E+03	5.00E+01	5.00E+01
Pb-210	2.70E+02	2.70E+02	5.50E+02	5.00E+02	5.00E+02
Po-210	1.50E+02	1.50E+02	3.00E+03	5.00E+02	5.00E+02
Th-232	3.20E+03	3.20E+03	5.80E+03	5.00E+03	5.00E+03
Ra-228	5.00E+02	5.00E+02	9.10E+03	5.00E+01	5.00E+01
Th-228	3.20E+03	3.20E+03	5.80E+03	5.00E+03	5.00E+03
Ra-224	5.00E+02	5.00E+02	9.10E+03	5.00E+01	5.00E+01
U-232	8.00E+02	8.00E+02	1.60E+03	2.00E+03	2.00E+03
Th-228	3.20E+03	3.20E+03	5.80E+03	5.00E+03	5.00E+03
Ra-224	5.00E+02	5.00E+02	9.10E+03	5.00E+01	5.00E+01
U-233	8.00E+02	8.00E+02	1.60E+03	2.00E+03	2.00E+03
Th-229	3.20E+03	3.20E+03	5.80E+03	5.00E+03	5.00E+03
Ra-225	5.00E+02	5.00E+02	9.10E+03	5.00E+01	5.00E+01
U-234	8.00E+02	8.00E+02	1.60E+03	2.00E+03	2.00E+03
Th-230	3.20E+03	3.20E+03	5.80E+03	5.00E+03	5.00E+03
Ra-226	5.00E+02	5.00E+02	9.10E+03	5.00E+01	5.00E+01
Pb-210	2.70E+02	2.70E+02	5.50E+02	5.00E+02	5.00E+02
Po-210	1.50E+02	1.50E+02	3.00E+03	5.00E+02	5.00E+02
U-235	8.00E+02	8.00E+02	1.60E+03	2.00E+03	2.00E+03
Pa-231	5.50E+02	5.50E+02	2.70E+03	5.00E+03	5.00E+03
Ac-227	4.50E+02	4.50E+02	2.40E+03	5.00E+03	5.00E+03
Th-227	3.20E+03	3.20E+03	5.80E+03	5.00E+03	5.00E+03
Ra-223	5.00E+02	5.00E+02	9.10E+03	5.00E+01	5.00E+01
U-236	8.00E+02	8.00E+02	1.60E+03	2.00E+03	2.00E+03
U-238	8.00E+02	8.00E+02	1.60E+03	2.00E+03	2.00E+03
Th-234	3.20E+03	3.20E+03	5.80E+03	5.00E+03	5.00E+03
U-234	8.00E+02	8.00E+02	1.60E+03	2.00E+03	2.00E+03
Zr-93	6.00E+02	6.00E+02	3.30E+03	5.00E+03	5.00E+03
Nb-93m	1.60E+02	1.60E+02	9.00E+02	5.00E+02	5.00E+02
Zr-95	6.00E+02	6.00E+02	3.30E+03	5.00E+03	5.00E+03
Nb-95	1.60E+02	1.60E+02	9.00E+02	5.00E+02	5.00E+02



APPROVED for Release for
Unlimited (Release to Public)
6/23/2005

4/10980
WSRC-RP-92-1360 ←

**RADIOLOGICAL
PERFORMANCE ASSESSMENT FOR THE Z-AREA
SALTSTONE DISPOSAL FACILITY (U)**

JRC
2/4/93

Prepared for the
WESTINGHOUSE SAVANNAH RIVER COMPANY
Aiken, South Carolina

by

**MARTIN MARIETTA ENERGY SYSTEMS, INC.
EG&G IDAHO, INC.
WESTINGHOUSE HANFORD COMPANY
WESTINGHOUSE SAVANNAH RIVER COMPANY**

December 18, 1992

Rev. 0

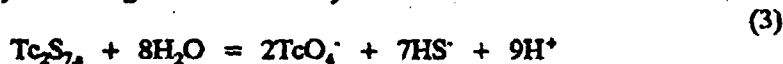
Table D.3-3. Calculated saltstone pore fluid composition using MINTeq, the results of the hydration calculations and equilibrium with calcite, C_3AH_6 , C-S-H gel, and C_3FH_6 . ^{99}Tc is calculated by assuming equilibrium with Tc_2S_7 , as described in the text

Species	mg/L	HS (mg/L)	^{99}Tc (pCi/L)
Na ⁺	139,000		
CO ₃ ²⁻	12,800		
SO ₄ ²⁻	15,000		
NO ₂ ⁻	36,800		
NO ₃ ⁻	159,000		
OH ⁻	32,900		
Ca ²⁺	1		
SiO _{2(aq)}	1		
Al ³⁺	11		
K ⁺	9,800		
NH ₄ ⁺	400		
pH	13.97		
Total N as NO ₃ ⁻	209,000		
Density	1.26		
High sulfide		10	2.4×10^{-8} ←
Stoichiometric		0.003	46,300

The Tc_2S_7 phase is very insoluble, limiting the TcO_4^- concentration in pore fluids to very low concentrations. To calculate the concentration of TcO_4^- in the pore fluid, the concentration of HS^- is needed. Angus and Glasser (1985) report aqueous sulfide concentration for slag cement ore fluids of up to 1100 mg/L for a mixture containing 97.5% slag. For a mixture containing 50% slag (similar to the saltstone mix) 12 mg/L sulfide was reported (Angus and Glasser 1985). This value was used in conjunction with the pore fluid to calculate concentrations of technetium. Additionally, a technetium concentration was calculated by assuming that technetium and sulfide occurred in solution in stoichiometric proportions (i.e., 2:7). The second concentration of technetium is higher, and the total sulfide concentration is much lower. The resulting concentrations of sulfide and technetium are presented in Table D.3-3.

Using the higher TcO_4^- concentration from Table D.3-3, K_d values for technetium can be calculated. The total loading of ^{99}Tc in saltstone is 25,000 pCi/g. From the hydration calculations the volume of pore fluid per gram of saltstone is 0.306 mL (57.8 mL/188.7 g). A total of 14 pCi ($46,000 \text{ pCi/L} \times 0.000306 \text{ L}$) of technetium occurs in the 0.306 mL of pore fluid. The remaining 24,986 pCi occurs in the 0.614 g of the solid matrix, with a concentration of 40,700 pCi/g. Although the technetium concentration is limited by the solubility of Tc_2S_7 , the solid and aqueous concentration can be used to estimate a K_d of 880 mL/g $[(40,700 \text{ pCi/g})/(46.3 \text{ pCi/mL})]$ for ^{99}Tc in saltstone.

Technetium concentrations are insensitive to the variations in the total salt concentration or to the selection of solid cement phases used in the equilibrium calculations. The sensitivity of technetium concentration to pH and sulfide concentration can be evaluated by examining the stoichiometry of the dissolution reaction



$$\log [\text{TcO}_4^-] = 0.5 \log Q - 3.5 \log [\text{HS}^-] + 4.5 \text{ pH} \quad (4)$$

where $\log Q$ is a conditional equilibrium quotient (constant at constant ionic strength) and brackets denote molal concentration. Examination of the coefficients in equation (4) indicates that the concentration of TcO_4^- decreases by a factor of 3,200 for each 10 fold increase in HS^- concentration. An increase of pH by 1 unit results in an increase in TcO_4^- concentration by a factor of 32,000.

For the case in which technetium and sulfur are related by stoichiometry, $\log [\text{TcO}_4^-]$ is directly proportional to pH. Because the aqueous concentration of TcO_4^- is proportional to pH, the value of K_d for ^{99}Tc in saltstone calculated above will also be dependent on pH. The dependency is calculated using this proportional relationship and the K_d of 880 in mL/g and is given by:

$$\log K_d = 16.94 - \text{pH} \quad (5)$$



Labor für Entsorgung

**Sorption Databases for the
Cementitious Near-Field of a
L/ILW Repository for
Performance Assessment**

Michael H. Bradbury and Flurin-Andry Sarott

that the same solid phase in each case was ultimately determining the solubility limit. Sn solubilities were not affected by the range of redox conditions examined. Solubility results presented in a later paper (BAYLISS et al. 1991) suggest that cassiterite (SnO_2) may be the solubility limiting phase with a solubility limit in the range 10^{-9} to 10^{-6} M, i.e. a different, and lower solubility limit than in their earlier paper.

It appears from this work that tetravalent Sn is stable under repository conditions. By analogy with the tetravalent actinides and Zr, plus the tendency of Sn^{4+} to form very strong hydroxy complexes, significant sorption for Sn on cementitious materials is to be expected. On this basis and the measurements of BAYLISS et al. (1989), we have selected a conservative $R_d(\text{Sn})$ of $1 \text{ m}^3 \text{ kg}^{-1}$ for regions I and II falling to $10^{-1} \text{ m}^3 \text{ kg}^{-1}$ in region III (see section 5.1) with no redox dependency.

5.2.10 Technetium

Sorption data for Tc on cementitious materials are sparse. Under oxidising conditions, distribution ratios of TcO_4^- in the range 10^{-3} to $10^{-2} \text{ m}^3 \text{ kg}^{-1}$ have been reported (see for example ALLARD et al. 1985). We have selected a value of $10^{-3} \text{ m}^3 \text{ kg}^{-1}$ for regions I and II and zero for region III.

Under "reducing" conditions technetium is present as hydrolysed Tc (IV) species and the solubility limit over technetium dioxide has been measured to be $\sim 10^{-7}$ M (PILKINGTON 1990). In some recent work, using Tc (IV) at trace levels ($< 10^{-11}$ M) and sodium dithionite as reducing agent, distribution ratios of $\sim 5 \text{ m}^3 \text{ kg}^{-1}$ have been reported (BAYLISS et al. 1991). For similar reasons as those given for Sn, Tc might be expected to sorb strongly under reducing conditions at high pH. As a conservative value we select a distribution ratio under reducing conditions of $1 \text{ m}^3 \text{ kg}^{-1}$ for region I and II, falling to $10^{-1} \text{ m}^3 \text{ kg}^{-1}$ in region III (see section 5.1).

5.2.11 Selenium, Palladium and Molybdenum

No sorption data at all could be found for Se, Pd and Mo in cement systems.

Under the redox and pH range appropriate to the repository Se and Mo are likely to exist predominantly as anionic species ($\text{SeO}_4^{2-}/\text{SeO}_3^{2-}/\text{HSe}^-$ and

**RESPONSE TO RAI COMMENT 61
ROADMAP TO REFERENCES**

REFERENCED DOCUMENT	*EXCERPT LOCATION	REMARK
This Response has no associated references.		

***Excerpt Locations:**

1. Excerpt included in response: The excerpt is included within the text of the response or is appended to the response.
2. Excerpt enclosed following response: The excerpt is enclosed on a separate sheet or sheets following the response.
3. Representative excerpt(s) enclosed following response: Representative excerpts from a document that is wholly or largely applicable are enclosed following the response.
4. Other

APPROVED for Release for
Unlimited (Release to Public)

7/14/2005

**RESPONSE TO RAI COMMENT 62
ROADMAP TO REFERENCES**

REFERENCED DOCUMENT	*EXCERPT LOCATION	REMARK
Cook et al. 2002	Other	Referenced as a document that did not include dose from use of contaminated groundwater.
Cook et al. 2005: Figure 2-1	Excerpt included in response as Figure 62-1.	
Table A-11	Excerpt included in response as Table A-11.	
Section A.3.3.1	Excerpt enclosed following response	Section A.3.3.1
d'Entremont & Drumm 2005	Excerpt included in response as Table 62-1.	
Rosenberger et al. 2005	Excerpt included in response as Table 62.3. Additional Excerpt enclosed following response	Included Section 8.3.3 of the PODD to show the sensitivity scenario in its entirety.
MMES 1992	Other	Referenced as a document that did not include dose from use of contaminated groundwater.
Simpkins 2004 – LADTAP XL program	Other	An SRS implementation of the NRC computer code.

***Excerpt Locations:**

1. Excerpt included in response: The excerpt is included within the text of the response or is appended to the response.
2. Excerpt enclosed following response: The excerpt is enclosed on a separate sheet or sheets following the response.
3. Representative excerpt(s) enclosed following response: Representative excerpts from a document that is wholly or largely applicable are enclosed following the response.
4. Other

7/15/2005

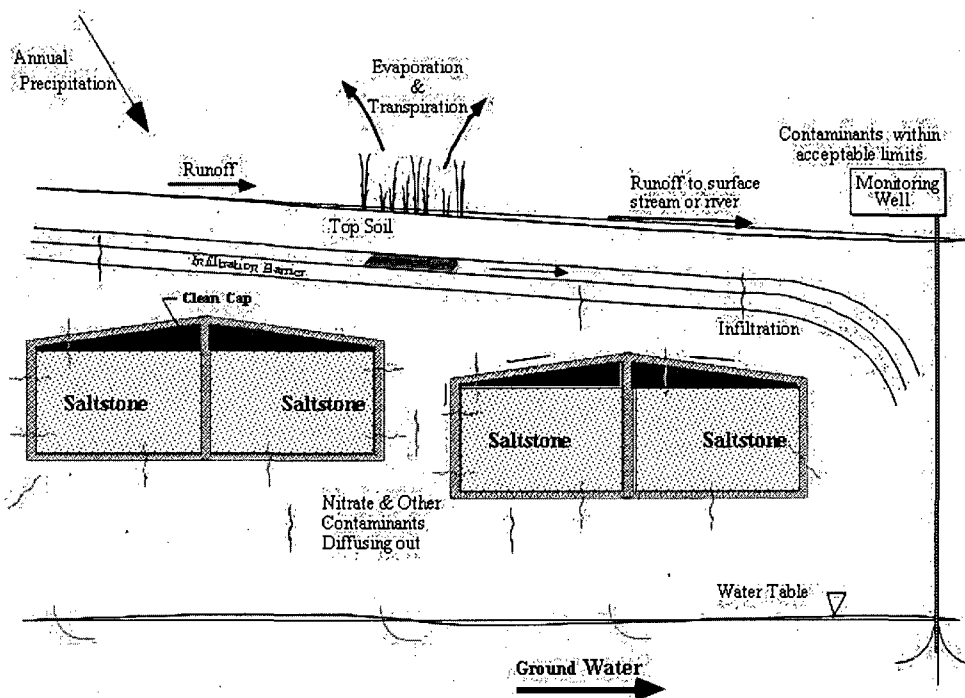
APPROVED for Release for
Unlimited (Release to Public)

KEY WORDS: Performance Assessment
Low-level Radioactive Waste Disposal

**SPECIAL ANALYSIS:
REVISION OF SALTSTONE VAULT 4 DISPOSAL LIMITS (U)**

PREPARED BY:
James R. Cook
Elmer L. Wilhite
Robert A. Hiergesell
Gregory P. Flach

MAY 26, 2005



Westinghouse Savannah River Company
Savannah River Site
Aiken, SC 29808

Prepared for the U.S. Department of Energy Under
Contract Number DE-AC09-96SR18500



A.3.3 Transport Model

A.3.3.1 Source Terms

For each of the contaminants and all daughters, the source terms are expressed as the fractional release to the water table calculated by the unsaturated-zone modeling. The fractional release has the unit of mole/year/mole of parent. The time history of each component is used as the source term. The amount released is assumed to be evenly distributed to the total volume of the 12 source cells listed in Table A-12. Based on the grid coordinates, the volumes of all these cells are calculated (Table A-13). The total volume is $6.1215 \times 10^5 \text{ ft}^3$.

Table A-13
Source Node Locations and Volumes

I	J	K	XC	YC	ZC	VOL
13	13	14	21350.0	11750.0	230.110	5.1200E+04
13	14	14	21350.0	11850.0	230.650	5.0900E+04
13	15	14	21350.0	11950.0	231.306	5.0525E+04
14	12	14	21450.0	11650.0	229.997	5.1250E+04
14	13	14	21450.0	11750.0	230.353	5.1100E+04
14	14	14	21450.0	11850.0	230.822	5.0850E+04
14	15	14	21450.0	11950.0	231.405	5.0500E+04
15	10	14	21550.0	11450.0	229.486	5.1525E+04
15	11	14	21550.0	11550.0	229.935	5.1250E+04
15	12	14	21550.0	11650.0	230.340	5.1050E+04
15	13	14	21550.0	11750.0	230.699	5.0925E+04
16	11	14	21650.0	11550.0	230.306	5.1075E+04
					TOTAL	6.1215E+05

The fractional release is divided by the total volume to obtain the concentration increments in the source nodes in mole/ft³/mole parent. However, because fractional release is often a very small number, within PORFLOW we multiply it by $10^{12}/6.1215 \times 10^5 \text{ ft}^3 = 1.6336 \times 10^6$. The concentration unit in PORFLOW saturated-zone computation is, therefore, pico-mole/ft³/mole parent. This multiplication factor is the same for every contaminant. PORFLOW has a "SCALE" command so that users can apply it to each fractional release time history. In PORFLOW 5.97.0, the scaling is performed by the code if a user enters "TOTAL VOLUME" in the SOURCE command. The source terms are read by a PORFLOW input file.

The flux terms exiting the bottom of the unsaturated zone model was processed using a Fortran program to truncate the fluxes less than 10^{-20} times the peak flux such that only the significant part of the output flux profile was utilized to generate the input source terms for the saturated zone model.

CBU-PIT-2005-00146
Revision 0

SALTSTONE
PERFORMANCE OBJECTIVE DEMONSTRATION DOCUMENT
(U)

PREPARED BY:
Kent H. Rosenberger
Bernice C. Rogers
R. Kim Cauthen

JUNE 2005

APPROVED for Release for
Unlimited (Release to Public)

Westinghouse Savannah River Company
Savannah River Site
Aiken, SC 29808

Prepared for the U.S. Department of Energy Under
Contract Number DE-AC09-96SR18500



8.3.3 Potential Water Usage Inside the 100 meter Buffer Zone Sensitivity

8.3.3.1 Potential Water Usage Inside the 100 meter Buffer Zone Sensitivity Scenario Description

The intruder analyses in the 1992 PA and subsequent 2002 SA and 2005 SA did not include dose from use of contaminated groundwater. Additionally, the intruder analyses argued that the physical integrity of a Saltstone vault would prevent drilling through it for 10,000 years. To determine the dose to a hypothetical inadvertent intruder who is presumed to drill a well near, but not through, a Saltstone vault, and use the water for a variety of purposes (e.g., drinking, irrigating a garden), the following analysis was conducted.

The groundwater modeling in the Vault 4 SA (Cook et al., 2005) did not monitor groundwater concentrations at points nearer than 100 feet from a vault. Therefore, groundwater concentrations immediately under a vault were estimated by assuming that the maximum radionuclide flux leaving the vadose zone in a year was contained in the volume of water in the first layer of the model nodes in the saturated zone below the vault. This is conservative because the groundwater concentrations are from the water directly below the vaults, does not account for concentration dilution within the water table, and uses all of the activity released in a year in that volume of water. Figure 4.2 presents the upper portion of the model (i.e. the vadose zone). The flux to the water table is the amount of contaminant crossing into the water table indicated at the 0 foot elevation in Figure 4-2. These groundwater concentrations were used to calculate, for each radionuclide, the all-pathways dose from use of the water.

The peak radionuclide flux over 10,000 years was obtained from Table A-11 of Cook et al., 2005 (The tables and pertinent text from Cook et al., 2005 are reproduced in Appendix E.). The volume of the first layer of groundwater model nodes below Vault 4 is $1.73E7$ L. Since the porosity of the soil is 0.42, the volume of water in the first layer of groundwater model nodes below Vault 4 is $7.27E6$ L.

The radionuclide composition of salt waste for disposal in the Saltstone Disposal Facility has recently been revised (d'Entremont and Drumm, 2005). The revised projected inventory of radionuclides in Vault 4 is shown in Table 8-6.

Table 8-7 shows the peak fractional radionuclide flux from the vadose zone, the peak fractional radionuclide concentration, the revised projected inventory in Vault 4, and the estimated maximum concentration in groundwater under Vault 4 using the radionuclide inventory in Table 8-6.

Table 8-6 Projected Vault 4 Radionuclide Inventory

Radionuclide	Curies	Radionuclide	Curies	Radionuclide	Curies
H-3	2.43E+03	Cs-137	1.20E+06	Np-237	5.76E-01
C-14	6.88E+01	Ba-137m	1.13E+06	Pu-238	3.69E+03
Na-22	2.59E+02	Ce-144	3.46E-01	Pu-239	3.36E+01
Al-26	1.03E+00	Pr-144	3.46E-01	Pu-240	8.39E+00
Ni-59	3.46E-01	Pm-147	2.93E+02	Pu-241	1.72E+02
Co-60	4.46E+01	Sm-151	3.04E+02	Pu-242	9.32E-03
Ni-63	8.77E+01	Eu-152	1.48E+00	Am-241	1.44E+01
Se-79	1.96E+00	Eu-154	8.10E+01	Am-242m	7.52E-03
Sr-90	5.29E+03	Eu-155	1.72E+01	Pu-244	9.38E-06
Y-90	5.29E+03	Ra-226	2.44E-01	Am-243	6.22E-03
Nb-94	1.02E-03	Ra-228	6.41E-06	Cm-242	6.21E-03
Tc-99	7.16E+02	Ac-227	1.37E-06	Cm-243	2.88E-03
Ru-106	4.82E+01	Th-229	2.79E-03	Cm-244	3.16E+00
Rh-106	4.82E+01	Th-230	1.49E-03	Cm-245	3.03E-04
Sb-125	2.05E+02	Pa-231	3.80E-06	Cm-247	5.55E-13
Te-125m	4.98E+01	Th-232	6.41E-06	Cm-248	5.79E-13
Sn-126	9.56E+00	U-232	9.52E-03	Bk-249	4.23E-20
Sb-126	1.33E+00	U-233	9.82E-01	Cf-249	3.21E-12
Sb-126m	9.50E+00	U-234	6.59E+00	Cf-251	2.47E-01
I-129	4.40E-01	U-235	7.41E-02	Cf-252	3.56E-15
Cs-134	2.40E+03	U-236	1.42E-01		
Cs-135	4.14E+00	U-238	1.61E-01		

Nuclide	Daughter	Peak Fractional Flux Ci/yr/Ci ^a	Peak Fractional Concentration pCi/L/Ci	Projected Inventory Ci/Vault 4	Estimated Peak Concentration, pCi/L
Am-243		1.43E-32	1.96E-27	6.22E-03	1.22E-29
	Np-239	4.53E-36	6.22E-31		3.87E-33
	Pu-239	4.53E-27	6.22E-22		3.87E-24
	Pu-5-239	1.65E-30	2.27E-25		1.41E-27
C-14		3.44E-24	4.73E-19	6.88E+01	3.25E-17
Cm-245		1.24E-38	1.70E-33	3.03E-04	5.15E-37
	Pu-241	4.48E-40	6.15E-35		1.86E-38
	Pu5-241	1.75E-43	2.40E-38		7.27E-42
	Am-241	2.32E-37	3.19E-32		9.67E-36
	Np-237	3.96E-24	5.44E-19		1.65E-22
Cs-135		1.10E-14	1.51E-09	4.14E+00	6.25E-09
Cs-137		1.42E-41	1.95E-36	1.20E+06	2.34E-30
H-3		4.03E-13	5.54E-08	2.43E+03	1.35E-04
I-129		1.29E-07	1.77E-02	4.40E-01	7.79E-03
Nb-94		3.33E-21	4.57E-16	1.02E-03	4.67E-19
Ni-59		2.37E-18	3.26E-13	3.46E-01	1.13E-13
Np-237		7.25E-24	9.96E-19	5.76E-01	5.74E-19
Pu-238		5.59E-42	7.68E-37	3.69E+03	2.83E-33
	Pu5-238	2.07E-45	2.84E-40		1.05E-36
	U-234	4.13E-26	5.67E-21		2.09E-17
Pu-239		7.75E-27	1.06E-21	3.36E+01	3.56E-20
	Pu5-239	2.81E-30	3.86E-25		1.30E-23
	U-235	1.83E-27	2.51E-22		8.43E-21
Pu-240		3.59E-27	4.93E-22	8.39E+00	4.14E-21
	Pu5-240	1.30E-30	1.79E-25		1.50E-24
	U-236	5.85E-27	8.04E-22		6.75E-21
Pu-241		3.93E-68	5.40E-63	1.72E+02	9.28E-61
	Pu5-241	1.64E-71	2.25E-66		3.87E-64
	Am-241	4.00E-39	5.49E-34		9.45E-32
	Np-237	7.25E-24	9.96E-19		1.71E-16
Pu-242		1.01E-26	1.39E-21	9.32E-03	1.29E-23
	Pu5-242	3.68E-30	5.05E-25		4.71E-27
	U-238	1.26E-28	1.73E-23		1.61E-25
Se-79		7.11E-07	9.77E-02	1.96E+00	1.91E-01
Sn-126		2.03E-22	2.79E-17	9.56E+00	2.67E-16
Sr-90		4.32E-19	5.93E-14	5.29E+03	3.14E-10
Tc-99		5.61E-20	7.71E-15	7.16E+02	5.52E-12
Th-232		3.13E-36	4.30E-31	6.41E-06	2.76E-36
	Ra-228	9.13E-45	1.25E-39		8.04E-45
	Th-228	4.74E-46	6.51E-41		4.17E-46

Nuclide	Daughter	Peak Fractional Flux Ci/yr/Ci*	Peak Fractional Concentration pCi/L/Ci	Projected Inventory Ci/Vault 4	Estimated Peak Concentration, pCi/L
	Ra-224	1.59E-47	2.18E-42		1.40E-47
U-232		2.38E-48	3.27E-43	9.52E-03	3.11E-45
	Th-228	1.66E-50	2.28E-45		2.17E-47
	Ra-224	5.58E-52	7.66E-47		7.30E-49
U-233		4.45E-26	6.11E-21	9.82E-01	6.00E-21
	Th-229	5.04E-29	6.92E-24		6.80E-24
	Ra-225	1.79E-33	2.46E-28		2.42E-28
U-234		4.52E-26	6.21E-21	6.59E+00	4.09E-20
	Th-230	3.58E-29	4.92E-24		3.24E-23
	Ra-226	2.86E-23	3.93E-18		2.59E-17
	Pb-210	7.72E-25	1.06E-19		6.99E-19
	Po-210	2.36E-26	3.24E-21		2.14E-20
U-235		4.65E-26	6.39E-21	7.41E-02	4.73E-22
	Pa-321	1.09E-30	1.50E-25		1.11E-26
	Ac-227	8.86E-34	1.22E-28		9.02E-30
	Th-227	2.93E-37	4.02E-32		2.98E-33
	Ra-223	1.15E-36	1.58E-31		1.17E-32
U-236		4.65E-26	6.39E-21	1.42E-01	9.07E-22
U-238		4.65E-26	6.39E-21	1.61E-01	1.03E-21
	Th-234	1.72E-37	2.36E-32		3.80E-33
	U-234	7.12E-32	9.78E-27		1.57E-27

8.3.3.2 Results From Potential Water Usage Inside the 100 meter Buffer Zone Sensitivity

The dose from all-exposure pathways (e.g., drinking water, eating crops irrigated by groundwater) from the use of groundwater under Saltstone Vault 4 is shown in Table 8-8. The dose was calculated from the peak groundwater concentrations using the LADTAP XL program (Simpkins 2004b), which is an SRS implementation of the NRC code. The total dose is calculated to be 0.27 mrem/year. This total dose is very conservative in that it assumes that the peak groundwater concentrations for each radionuclide are coincident in time.

Table 8-8. Peak All-Pathways Dose from Use of Groundwater Below Saltstone Vault 4

Nuclide	Peak All-Pathways Dose, mrem/year
H-3	1.17E-08
C-14	3.45E-17
Ni-59	1.50E-16
Se-79	2.56E-01
Sr-90	1.66E-10
Nb-94	1.43E-18
Tc-99	6.44E-13
Sn-126	2.86E-16
I-129	1.05E-02
Cs-135	2.73E-09
Cs-137	7.24E-30
Th-232	2.78E-35
U-232	2.84E-45
U-233	5.02E-21
U-234	1.92E-16
U-235	3.65E-22
U-236	6.90E-22
U-238	7.21E-22
Np-237	7.04E-18
Pu-238	1.66E-17
Pu-239	4.54E-19
Pu-240	5.72E-20
Pu-241	2.10E-15
Pu-242	1.55E-22
Am-243	4.88E-23
Cm-245	2.02E-21
Total	2.67E-01 ←

**RESPONSE TO RAI COMMENT 63
ROADMAP TO REFERENCES**

REFERENCED DOCUMENT	*EXCERPT LOCATION	REMARK
Cook et al. 2002	Excerpt included in response.	Referenced as a document that did not consider disruption of engineered barriers or natural features of the disposal site by a hypothetical inadvertent intruder.
Cook et al. 2005	Excerpt included in response	Referenced as a document that did not consider disruption of engineered barriers or natural features of the disposal site by a hypothetical inadvertent intruder.
MMES 1992	Excerpt included in response	Referenced as a document that did not consider disruption of engineered barriers or natural features of the disposal site by a hypothetical inadvertent intruder.
Phifer and Nelson 2003	Excerpt included in response.	Section 5.0 "Closure Cap Degradation" from Phifer and Nelson 2003. Section 6.0 "Closure Cap Infiltration" from Phifer and Nelson 2003.
Rosenberger et al. 2005 - PODD	Excerpt enclosed following response.	
USNRC 2000 – NUREG-1573, 6/2000	Excerpt enclosed following response.	
Wood et al. 1994	Excerpt included in response.	Section 2.19 "The Intruder and the All-Pathways Analyses" from Wood et al. 1994.

***Excerpt Locations:**

1. Excerpt included in response: The excerpt is included within the text of the response or is appended to the response.
2. Excerpt enclosed following response: The excerpt is enclosed on a separate sheet or sheets following the response.
3. Representative excerpt(s) enclosed following response: Representative excerpts from a document that is wholly or largely applicable are enclosed following the response.
4. Other

7/15/2005

APPROVED for Release for
Unlimited (Release to Public)

CBU-PIT-2005-00146
Revision 0

SALTSTONE
PERFORMANCE OBJECTIVE DEMONSTRATION DOCUMENT
(U)

PREPARED BY:
Kent H. Rosenberger
Bernice C. Rogers
R. Kim Cauthen

JUNE 2005

APPROVED for Release for
Unlimited (Release to Public)

Westinghouse Savannah River Company
Savannah River Site
Aiken, SC 29808

Prepared for the U.S. Department of Energy Under
Contract Number DE-AC09-96SR18500



8.0 Sensitivity Analysis and Uncertainty Analysis

The objective of the performance assessment calculations is to quantitatively estimate the system performance for comparison to the performance objectives of 10 CFR 61, Subpart C. The sensitivity analyses identify the assumptions and parameters that affect the quantitative estimate of performance by evaluating the effects of changing the values of input variables or changing model structures. The uncertainty analysis provides a tool for understanding, in quantitative terms, the effect of parameter and model uncertainties. These uncertainties are described by considering a reasonable range of conditions, processes, or events to test the robustness of the SDF in comparison to the performance objectives.

The sensitivity and uncertainty analysis has been expanded for the current radiological composition of the waste to demonstrate that compliance with the performance objectives of 10 CFR 61, Subpart C can be reasonably assured.

8.1 Sensitivity of Groundwater Model Parameters

The result of the all-pathways analysis in this PODD is dose (mrem/yr). Therefore, factors that affect the estimation of dose are the focus of the sensitivity and uncertainty analysis discussed in this section. These factors include those that influence the transportation of radionuclides through saturated and unsaturated media (soil, concrete, saltstone, etc).

A series of Saltstone Vault 4 sensitivity calculations were performed using PORFLOW (ACRI, 2002) to quantify the impact of key model parameter settings on groundwater contaminant concentrations and dose at the 100 meter compliance hypothetical well using a time frame at the conclusion of institution control (IC) through 10,000 years. Four radionuclides, H-3, C-14, Se-79, and I-129; were chosen as the limiting cases for this sensitivity analysis because the 2005 SA shows that these radionuclides are the major contributor to the dose when all pathways are considered. Parameters for the scenarios are identified in Tables 8-1 and 8-2 and are described in detail in the following sections.

8.1.1 Key Model Parameters

8.1.1.1 Infiltration rates through the upper geosynthetic clay liner

The changes in infiltration rates through the upper GCL are reflected by different land use scenarios. Three land use scenarios were modeled. The nominal case assumes the land use scenario of a 100 year institutional control (IC) period, which is bamboo cover, followed by development of a pine forest cover. The second land use scenario is a continuous bamboo cover. The third land use scenario is a 100 year institutional control followed by farming and eventually development of a pine forest cover. These different

land use scenarios impact the effectiveness and longevity of the Vault 4 closure cap, identified as the infiltration rate. The different infiltration rates also impact the hydraulic properties of the lower drainage layer and the vault base drainage layer due to transport and accumulation of silt in the drainage layers. Base case (nominal), lower and upper bounding infiltration through the upper GCL is provided by Phifer (2005). Higher infiltration rate through the upper GCL results in higher transport rates of silt through the drainage layers and more rapid accumulation of silt.

8.1.1.2 Saltstone Waste Form and the Vault Concrete Parameters

The fundamental concept of the SDF is the controlled radionuclide release. Due to the low hydraulic conductivity and low molecular diffusion in cementitious materials, contaminant leaching from the SDF is very slow. The hydraulic conductivities represent the ease through which the water will pass through the material. There are two parts to the hydraulic conductivity, the initial saturated hydraulic conductivity and the hydraulic conductivity rate. The hydraulic conductivity rates are expressed in terms of a degradation rate constant (α). The rates at which the hydraulic conductivities of the Saltstone waste form and the Saltstone vault concrete increase over time were varied around the values used in the 2005 SA (the 2005 SA value is considered the nominal value). The higher the hydraulic conductivity, the higher the degradation rate constant, and the faster the degradation of the material occurs.

The initial saturated hydraulic conductivity of the material used in the 2005 SA is identified as K_{sat} . For the Saltstone waste form the K_{sat} is 10^{-12} cm/sec. For the vault concrete K_{sat} is 10^{-11} cm/sec. For the sensitivity analysis, the K_{sat} 's were varied by an order of magnitude about these values.

For the purposes of this sensitivity analysis, the relative permeability was set to unity thus forcing the vault and saltstone grout to be saturated through the analysis period.

For the purposes of this sensitivity analysis, the molecular diffusion coefficients were varied by an order of magnitude about the values used in the 2005 SA.

For the purposes of this sensitivity analysis, the distribution coefficients (K_d) were set to zero for these species in the vadose and aquifer transport simulations. (H-3 is zero in the base case.)

8.1.2 Scenario Description and Input Parameters

Table 8-1 summarizes the scenario runs and the corresponding sensitivity setting of each key modeling parameter. Scenario run 1 represents the nominal or base case for each contaminant species. The nominal designation shown in Tables 8-1 and 8-2 refer to the value of the model parameter setting used in the 2005 SA. The sensitivity runs include scenario runs 2 through 19. The paragraphs following the tables discuss what the different scenario runs represent and a basis for selection of the parameter setting.

Table 8-1. Sensitivity Scenarios and Settings for Infiltration, Vadose Zone Concrete and Saltstone Hydraulic Conductivity.

Run	Infiltration	Vadose Zone Concrete Hydraulic Conductivity	Vadose Zone Saltstone Hydraulic Conductivity	Distribution Coefficient	Vadose Zone Concrete Diffusion Coefficient (D_M)	Vadose Zone Saltstone Diffusion Coefficient (D_M)
1	IC to Pine Forest	Nominal	Nominal	Nominal	Nominal	Nominal
2	Continuous Bamboo Cover	Nominal	Nominal	Nominal	Nominal	Nominal
3	IC to Farm to Pine Forest	Nominal	Nominal	Nominal	Nominal	Nominal
4	IC to Pine Forest	$\alpha = 1.0$	Nominal	Nominal	Nominal	Nominal
5	IC to Pine Forest	$\alpha = 2.0$	Nominal	Nominal	Nominal	Nominal
6	IC to Pine Forest	$0.1 \times K_{sat}$	Nominal	Nominal	Nominal	Nominal
7	IC to Pine Forest	$10 \times K_{sat}$	Nominal	Nominal	Nominal	Nominal
8	IC to Pine Forest	Nominal	$\alpha = 0.5$	Nominal	Nominal	Nominal
9	IC to Pine Forest	Nominal	$\alpha = 1.5$	Nominal	Nominal	Nominal
10	IC to Pine Forest	Nominal	$0.1 \times K_{sat}$	Nominal	Nominal	Nominal
11	IC to Pine Forest	Nominal	$10 \times K_{sat}$	Nominal	Nominal	Nominal
12	IC to Farm to Pine Forest	$\alpha = 2.0$	$\alpha = 1.5$	Nominal	Nominal	Nominal
13	IC to Pine Forest	$k_r = 1$	$k_r = 1$	Nominal	Nominal	Nominal
14	IC to Pine Forest	Nominal	Nominal	Nominal	$0.1 \times D_M$	Nominal
15	IC to Pine Forest	Nominal	Nominal	Nominal	$10 \times D_M$	Nominal
16	IC to Pine Forest	Nominal	Nominal	Nominal	Nominal	$0.1 \times D_M$
17	IC to Pine Forest	Nominal	Nominal	Nominal	Nominal	$10 \times D_M$
18	IC to Pine Forest	Nominal	Nominal	Nominal	$10 \times D_M$	$10 \times D_M$
19	IC to Pine Forest	Nominal	Nominal	0	Nominal	Nominal

IC – Institutional Control
 α = degradation rate constant
 k_r = relative permeability

The sensitivity of the all-pathways dose to land use and closure cover degradation is captured in Sensitivity Scenario Runs 2 and 3. The sensitivity to different land use scenarios above the Vault 4 is captured by Sensitivity Scenario Runs 2 and 3. The nominal case (Sensitivity Scenario Run 1) assumes a 100 year institutional control (bamboo cover) period followed by development of a pine forest cover. Sensitivity Scenario Run 2 is a land use scenario with a continuous bamboo cover. Sensitivity Scenario Run 3 is a land use scenario with a 100 year institutional control followed by farming and eventually development of a pine forest cover. Figure C-1 in Appendix C shows the infiltration rate through the upper GCL for the three different land use scenarios. The different infiltration rates also impact the hydraulic properties of the lower drainage layer and the vault base drainage layer due to transport and accumulation of silt in the drainage layers. Higher infiltration rate through the upper GCL results in higher transport rates of silt through the drainage layers and more rapid accumulation of silt. The variation over time of the saturated horizontal conductivity of the lower drainage layer and the vault base drainage layer is shown in Appendix C, Figures C-2 and C-4, respectively. Similarly, the variation over time of the saturated vertical conductivity of the lower drainage layer and the vault base drainage layer is shown in Appendix C, Figures C-3 and C-5, respectively. In both cases, there is a substantial reduction in the performance of the horizontal drainage layers over time due to the accumulation of silt.

The sensitivity of the all-pathways dose to the degradation of the concrete vault is captured in Sensitivity Scenario Runs 4, 5, 6, and 7. Sensitivity Scenario Runs 4 and 5 address the rate at which the concrete vault saturated hydraulic conductivity increases with time due to degradation of the concrete as the result of chemical attack or cracking. The nominal variation over time for the saturated hydraulic conductivity of the concrete vault is assumed to increase by three orders of magnitude after the 100 year IC period through 10,000 years as shown in Appendix C, Figure C-6. The functional form for the increase in conductivity over time is documented in the 2005 SA and is based on engineering judgment. Sensitivity Scenario Runs 4 and 5 increase the concrete vault conductivity by two and four orders of magnitude, respectively. In Sensitivity Scenario Runs 6 and 7, the concrete vault saturated hydraulic conductivity sensitivity is addressed. The increase in concrete vault saturated hydraulic conductivity over time, due to degradation, is taken from the 2005 SA and is used as the nominal rate. For the Sensitivity Scenario runs, the concrete vault saturated hydraulic conductivity is varied by an order of magnitude about the nominal value over the entire simulation period. Appendix C, Figure C-7 shows the nominal condition and the sensitivity values.

The sensitivity of the all-pathways dose to the degradation of the Saltstone waste form is captured in Sensitivity Scenario Runs 8, 9, 10, and 11. Sensitivity Scenario Runs 8 and 9 address the rate at which the Saltstone saturated hydraulic conductivity increases with time due to degradation of the Saltstone waste form as the result of chemical attack or cracking. The nominal variation over time for the Saltstone waste form is assumed to increase by two orders of magnitude after the 100 year IC period through 10,000 years, as is shown in Appendix C, Figure C-8. Sensitivity Scenario Runs 7 and 8 increase the

conductivity by one and three orders of magnitude, respectively. In Sensitivity Scenario Runs 10 and 11, the Saltstone waste form saturated hydraulic conductivity is varied by an order of magnitude about the nominal value over the entire simulation period. The nominal rate of increase in conductivity, due to degradation over time, is used. Appendix C, Figure C-9 shows the nominal condition and the sensitivity values.

The sensitivity of the all-pathways dose to combination effect of high filtrations with degraded horizontal drain performance is captured in Sensitivity Scenario Run 12. Sensitivity Scenario Run 12 is a combined sensitivity based on Sensitivity Scenario Runs 3, 5 and 9. A high infiltration rate with degraded horizontal drain performance (Sensitivity Scenario Run 3) is combined with highest rate increase in saturated hydraulic conductivity of the concrete vault and Saltstone over time.

The sensitivity of the all-pathways dose to uncertainties in the water retention curves for the concrete vault and Saltstone is captured in Sensitivity Scenario Run 13. The relative permeability (k_r) of the concrete vault and the Saltstone waste form was set to unity in Sensitivity Scenario Run 13. This was done to address uncertainties in the water retention curves for the concrete vault and Saltstone.

The sensitivity of the all-pathways dose to uncertainties in the diffusion coefficient for each radionuclide as they pass through the Saltstone waste form and the concrete vault are captured in Sensitivity Scenario Runs 14, 15, 16, 17, 18, and 19. The nominal values of the molecular diffusion coefficients for each species in the concrete vault are shown in Table A-9 of the 2005 SA (Cook et al., 2005). The molecular diffusion coefficients for each species in the concrete vault were varied an order of magnitude about their nominal values for Sensitivity Scenario Runs 14 and 15. The molecular diffusion coefficients for each species in the Saltstone waste form were varied an order of magnitude about their nominal values shown in Table A-9 of the 2005 SA (Coo et al, 2005). Sensitivity Scenario Runs 16 and 17 address this sensitivity. Sensitivity Scenario Run 18 is a combined sensitivity run of Sensitivity Scenario Runs 15 and 17. The molecular diffusion coefficients for each species are an order of magnitude higher than nominal for both the concrete vault and the Saltstone waste form in this scenario.

A distribution coefficient of zero was used through out the vadose and aquifer zone transport simulations for C-14, I-129 and Se-79 for Scenario 19. This case is not considered credible, but it does show the importance of the distribution coefficient in the model calculations.

8.1.3 Sensitivity Results

The predicted peak fractional fluxes to the water table and peak concentrations for C-14, H-3, I-129 and Se-79 are shown in Appendix C, Tables C-1 to C-4, respectively. All the radionuclides except H-3 appear to show the logical trend of lower/higher peak concentration with lower/higher sensitivity setting for a given parameter.

In Appendix C, Table C-2, the nominal case (scenario 1) for H-3 has a higher peak concentration than scenario 3 as a result of a higher infiltration rate over the first 800 years.

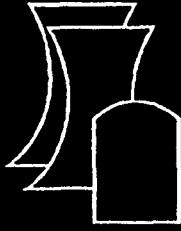
The H-3 peak concentration appears to be insensitive to changes in the concrete vault and Saltstone saturated hydraulic conductivity over the ranges assumed in the sensitivity analysis.

8.1.3.1 Sensitivity Results Expressed as Dose from All Pathways

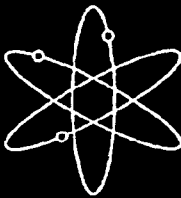
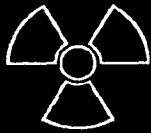
The peak fractional concentrations and the revised inventory of radionuclides in Vault 4 were used to calculate peak radionuclide concentrations over 10,000 years. The peak concentrations were input to the LADTAP program (Simpkins, 2004a) to calculate the all pathways dose for each of the scenarios. The resulting doses are shown in Table 8-2. The doses range from 0.02 mrem/year for scenario 2 (decreased infiltration due to continuous bamboo cover) to 38 mrem/year for scenario 19 (an incredible case in which all radionuclide distribution coefficients set to zero).

Table 8-2. All-Pathways Doses from the Sensitivity Scenarios.

Scenario Run	Dose (mrem/year)
1	5.12E-02
2	2.12E-02
3	2.81E-01
4	3.31E-02
5	5.42E-02
6	3.36E-02
7	5.39E-02
8	3.97E-02
9	2.47E-01
10	4.00E-02
11	2.57E-01
12	4.18E+00
13	1.87E-01
14	3.66E-02
15	1.83E-01
16	4.16E-02
17	6.74E-02
18	7.15E-01
19	3.78E+01



A Performance Assessment Methodology for Low-Level Radioactive Waste Disposal Facilities



Recommendations of NRC's Performance
Assessment Working Group



U.S. Nuclear Regulatory Commission
Office of Nuclear Material Safety and Safeguards
Washington, DC 20555-0001



ML00-77

considered in terms of the indefinite future and evaluated for at least a 500-year timeframe. The 500-year timeframe corresponds to the period when the hazard from moderately high-activity, short- and intermediate-lived radionuclides contained in Classes B and C waste is greatest, and when the ensuing need for achieving long-term stability of engineered features, such as multi-layered covers, concrete vaults, high-integrity waste containers (HICs), stabilized waste forms, and intruder barriers to Class C waste is greatest. The main design function of these engineered features is to limit infiltration of water into the waste so as to minimize leaching of radionuclides into the environment, and to provide protection to an inadvertent intruder. Part 61 requires stability lifetimes on the order of 300 to 500 years for B/C Class waste forms, HICs, and intruder barriers. The timeframe previously recommended for considering design bases, natural events, or phenomena for engineered barrier performance was 500 years (NRC, 1982). As discussed in Section 3.2.2 ("Role of Engineered Barriers"), service lives for engineered barriers, on the order of a few hundred years, are still considered credible, if justified by adequate technical analyses and data.

Beyond the specified service life for engineered barriers,¹⁰ and into "the indefinite future," the focus of performance is on the continued isolation of long-lived radionuclides in the waste. At this time, the performance of the "physical" constituents of the engineered barriers can no longer be assumed and reliance must be placed primarily on the engineered barrier's "chemical characteristics" as well as the site's natural (geologic) qualities to continue to limit environmental releases of long-lived radionuclides. In evaluating site suitability, the PAWG suggests refraining from excessive speculation about the extremely distant future, and recommends limiting evaluations of the natural site's geologic evolution to the next 10,000 years. This 10,000-year timeframe is the time period of regulatory concern recommended by the PAWG (see Section 3.2.3, "Timeframe for LLW Performance Assessment Analyses"). All significant conditions, processes, and events that are of concern to the ability of the engineered disposal system and natural site to meet the performance objectives need to be considered. However, it is not necessary to demonstrate that the stability of natural site features, including those primarily intended for achieving stability of engineered barriers, will continue to be met beyond 500 years.¹¹

3.2.1.2 Site Conditions in Performance Assessment Models

At the time scale appropriate to assessing LLW disposal, natural site conditions may range from being relatively static to highly dynamic, depending on the influence of processes that are driven by the forces of tectonics and climate. Natural events occurring at a site, which at times may be catastrophic, are tangible manifestations of these active processes. However, as stated above, Part 61 emphasizes selecting sites based on geologic stability, waste isolation, long-term performance, and defensible modeling. Therefore, it should be possible to develop a set of reasonably anticipated natural conditions, processes, and events to be represented in site

¹⁰ As determined by the LLW disposal facility developer, with adequate technical justification.

¹¹ 10 CFR 61.7(a)(2) requires that in selecting a disposal site, "...site characteristics should be considered in terms of the indefinite future and evaluated for at least a 500-year timeframe...."

conceptual models (e.g., distribution of infiltration to account for variation in rainfall, and a service life for concrete that bounds the impact of degradation processes). The overall intent is to discourage excessive speculation about future events and the PAWG does not intend for analysts to model long-term transient or dynamic site conditions, or to assign probabilities to natural occurrences.¹² In developing this "reference natural setting," changes in vegetation, cycles of drought and precipitation, and erosional and depositional processes should be considered; future events should include those that are known to occur periodically at the site (e.g., storms, floods, and earthquakes). It must be emphasized that the goal of the analysis is not to accurately predict the future, but to test the robustness of the disposal facility against a reasonable range of potential outcomes. Accordingly, the parameter ranges and model assumptions selected for the LLW performance assessment should be sufficient to capture the variability in natural conditions, processes, and events.

Consistent with the above, consideration given to the issue of evaluating site conditions that may arise from changes in climate or the influences of human behavior should be limited so as to avoid unnecessary speculation. It is possible that, within some disposal site regions, glaciation or an interglacial rise in sea level could occur in response to changes in global climate. These events are envisaged as broadly disrupting the disposal site region to the extent that the human population would leave affected areas as the ice sheet or shoreline advances. Accordingly, an appropriate assumption under these conditions would be that no individual is living close enough to the facility to receive a meaningful dose. In addition, the hazard from the inventory remaining in typical LLW after about 500 years is expected to be relatively low. The PAWG believes that an applicant could use similar reasoning to explain how potential effects of glaciation will not render a disposal site unacceptable. Therefore, the PAWG recommends that new site conditions that may arise directly from significant changes to existing natural conditions, processes, and events do not need to be quantified in LLW performance assessment modeling.

For disposal sites where the impacts of global climate change consist primarily of changes from present-day meteorologic patterns, ascertaining the nature, timing, and magnitude of related meteorological processes and events (i.e., regional consequences) and their effects on disposal site performance is highly uncertain. However, a key aspect of an LLW performance assessment is determining how variations in precipitation result in varying rates of percolation into disposal units and of recharge to the water table. The PAWG recommends using historical and current weather data, and other site information (e.g., field tests) to establish a broad range of infiltration

¹² By virtue of the siting guidelines found at Section 61.50, developers need to site LLW disposal facilities in geologic settings that are essentially stable (quiescent) or, alternatively, in areas in which active features, events, and processes will not significantly affect the ability of the site and design to meet the Subpart C performance objectives. In practical terms, the effect the Section 61.50 requirements have on the LLW performance assessment scenario selection methodology is that, after site characterization, the candidate site be defined in terms of its expected geologic evolution, where all likely scenarios are accounted for in the performance assessment model and treated equally, with a probability of (1). If the results of site characterization conclude that, geologically, there is the potential for low-probability scenarios – say on the order of 10^{-4} per year, in frequency of occurrence, or lower – they can be considered unimportant and thus screened out of the site model (and the subsequent analysis). In this fashion, uncertainty in the future system state of the disposal system is accounted for in the analysis.

rates that may be used to simulate both wetter and drier conditions than the current average. Sensitivity analyses performed as part of the LLW performance assessment will provide some insight into the effects that such variations could have on the dose calculations. The PAWG believes that the treatment of infiltration in this manner will allow an analyst to consider the effects of broad variations in weather, without the need for speculating on how climate might change.

Given the uncertainty in projecting the site's biological environment beyond relatively short periods of a few hundred years, it is sufficient to assume that current biological trends remain unchanged throughout the period of analyzed performance. Similarly, consideration of societal changes would result in unnecessary speculation and should not be included in performance assessments. With respect to human behavior, it may be assumed that current local land-use practices and other human behaviors continue unchanged throughout the duration of the analysis. For instance, it is reasonable to assume that current local well-drilling techniques and/or water use practices will be followed at all times in the future. Finally, the disruptive actions of an inadvertent intruder do not need to be considered when assessing releases of radioactivity off-site. ←

Assurance about site performance into the far future is also provided by limiting the amounts of long-lived radionuclides that may be disposed of at an LLW disposal facility, including those shown by analysis to be significant only after tens of thousands of years have passed. The effect of placing inventory limits on long-lived radionuclides is to mitigate, given what is foreseeable today, the potential consequences of waste disposal to generations in the distant future. See Section 3.2.3 for a discussion of timeframes for dose calculations in LLW performance assessments and inventory limits on long-lived radionuclides.

3.2.2 Role of Engineered Barriers

The term engineered barrier as defined in Section 61.2 means "... a man-made structure or device that is intended to improve the land disposal facility's ability to meet the performance objectives in Subpart C...." As such, engineered barriers are usually designed to inhibit water from contacting waste, limit release of radionuclides from disposal units, or mitigate doses to potential human intruders. Materials composing the "physical" constituents of the engineered barriers may range from purely (geo)synthetic membranes to natural soils to concrete vaults that are reconfigured to impart some characteristic or property enabling it to perform as an engineered barrier. Examples of physical engineered barriers are surface drainage systems and cover systems, concrete vaults, HICs, backfills, infills, etc. Engineered barriers improve LLW disposal facility performance by physically limiting the amount of water that can contact disposed-of waste and/or chemically retarding the release of radionuclides to the environment. Specific features to include as engineered barriers, and how they should be designed are site-specific decisions left to the discretion of the disposal facility developer. Although engineered barriers may be used to improve facility performance, it is nonetheless expected that the disposal characteristics of the site itself will meet the suitability requirements of 10 CFR 61.50.

**RESPONSE TO RAI COMMENT 64
ROADMAP TO REFERENCES**

REFERENCED DOCUMENT	*EXCERPT LOCATION	REMARK
Cook et al. 2005	Section 7.5.3	Excerpt enclosed following response.
	Section 7.5.4	Excerpt enclosed following response.
	Table 7-9	Excerpt enclosed following response.
	Table 7-10	Excerpt enclosed following response.
	Table B-5	Excerpt enclosed following response.
Weber 1998	Table XIX	Excerpt enclosed following response.

***Excerpt Locations:**

1. Excerpt included in response: The excerpt is included within the text of the response or is appended to the response.
2. Excerpt enclosed following response: The excerpt is enclosed on a separate sheet or sheets following the response.
3. Representative excerpt(s) enclosed following response: Representative excerpts from a document that is wholly or largely applicable are enclosed following the response.
4. Other

APPROVED for Release for
Unlimited (Release to Public)

7/14/2005

APPROVED for Release for
Unlimited (Release to Public)
6/6/2005

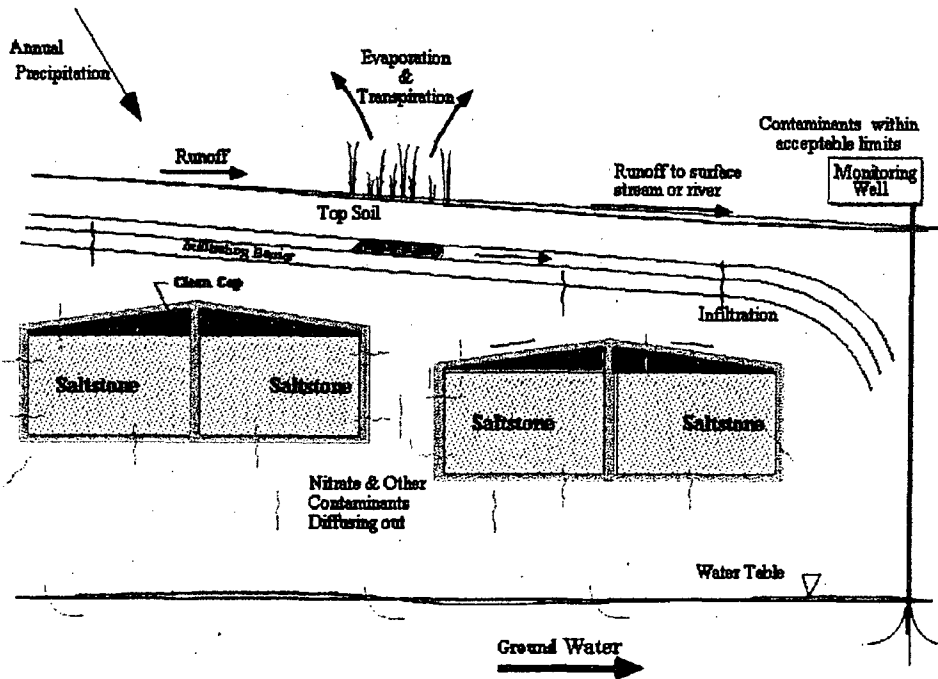
WSRC-TR-2005-00074
Revision 0

KEY WORDS: Performance Assessment
Low-level Radioactive Waste Disposal

**SPECIAL ANALYSIS:
REVISION OF SALTSTONE VAULT 4 DISPOSAL LIMITS (U)**

**PREPARED BY:
James R. Cook
Elmer L. Wilhite
Robert A. Hiergesell
Gregory P. Flach**

MAY 26, 2005



Westinghouse Savannah River Company
Savannah River Site
Aiken, SC 29808

Prepared for the U.S. Department of Energy Under
Contract Number DE-AC09-96SR18500



The conclusion of this quick study is that there is no impact of plume interaction from Vault 1 for nitrate beyond the 100-ft point of assessment and the 1,000-year time of assessment. There appears to be an impact beyond the 100-m perimeter of Vault 4. However, the interaction only increases nitrate concentrations by about 25%. The Sum-of-Fractions of the 10,000-year groundwater limits is only 0.004. Applying a 25% reduction factor to all 10,000-year groundwater limits would only increase the Sum-of-Fractions to 0.005. The potential for plume interaction will be quantified in the upcoming Saltstone PA revision and will be included, as appropriate, in limits determined therein.

7.5.2 Peak Fractional Contaminant Flux of I-129 to the Water Table

The fractional contaminant flux of I-129 to the water table at 10,000 years is 1.29E-07 mole/yr/mole as shown in Table A-11. The flux is predominantly the diffusive component of the total flux and quickly rising beyond 10,000 years (Figure 7-16). To capture the peak of the flux, the simulation run time was extended to 70,000 years. As shown in Figure 7-17, the flux curve has an inflection point before 30,000 years and approaches a peak at 70,000 years. The peak fractional contaminant flux of I-129 to the water table at 70,000 years is 3.83E-06 mole/yr/mole which is a factor of 30 greater than the value at 10,000 years. This result is helpful in understanding the behavior of the SDF over extremely long times but results calculated over such time frames are not appropriate for establishing disposal limits. However, even if the 10,000-year disposal limit for ¹²⁹I based on the groundwater pathway were decreased by a factor of 30 (i.e., to 7.3 Ci), the projected Vault 4 inventory of ¹²⁹I would be only about 10% of that limit.

→ 7.5.3 Inadvertent Intruder Post-Drilling Scenario

In the inadvertent intruder analysis, which is presented in Section 3 and Appendix B, the long-term durability of the Saltstone waste form and the concrete vault are assumed to prevent drilling a well through a disposal vault. To explore the sensitivity of the analysis results to this assumption, an alternate scenario, termed the post-drilling scenario, was assessed.

The post-drilling scenario is based on the assumption that a person could drill a well through a disposal vault. For this sensitivity analysis, the assumption is that drilling through a vault first becomes credible at 1,000 years after closure. The post-drilling scenario is assessed from 1,000 years after closure to 10,000 years after closure. In the post-drilling scenario, the subsurface material exhumed during drilling includes some of the Saltstone waste. This material is assumed to be mixed with soil in a garden and the intruder is exposed to the waste through a variety of pathways (e.g. direct radiation, ingesting food stuffs grown in the garden). The limits derived from the post-drilling analysis are presented in Table B-5.

The post-drilling limits are generally smaller (i.e., more restrictive) than the resident limits, which are presented in Table 3-2. If the post-drilling scenario were to be considered credible, the sum-of-fractions of the 10,000-year limits would increase from 0.22 to 0.31.

7.5.4 Agricultural Scenario Following Failure of Erosion Barrier

In the inadvertent intruder analysis, which is presented in Section 3 and Appendix B, the long-term persistence of the erosion barrier is assumed to preclude the Agricultural Scenario by maintaining a distance greater than that required to excavate a basement (10 ft.). To explore the sensitivity of the analysis results to this assumption, an alternate scenario in which the erosion barrier was assumed to erode at the same rate as the other cover material was assessed. The disposal limits derived from this study for a 10,000-year assessment period are shown in Table 7-9. Table 7-10 shows a comparison of these limits with the projected Vault 4 inventory.

The Sum-of-Fractions for these limits is 1.49, which, if the scenario were considered credible, would indicate non-compliance with the intruder performance measure. However, the erosion barrier is constructed of material sized to remain in place during a rainfall event with a 10,000-year recurrence interval calculated using an extreme-value distribution (i.e., 3.3 inches of rain in a 15 minute time span, [Weber 1998]). Thus, the scenario is not credible.

Table 7-9. Intruder-Based Radionuclide Disposal Limits for Vault 4 – Agriculture Scenario Following Failure of Erosion Barrier with Transient Calculation for 100 – 10,000 Years

Radionuclide	Time of Limit (Years)	Concentration Limit ($\mu\text{Ci}/\text{m}^3$)	Inventory Limit (Ci/Unit)
C-14	3275	1.64E+04	1.30E+03
Al-26	3275	4.37E+01	3.44E+00
Cl-36	3275	1.43E+02	1.13E+01
Ar-39	1132	1.63E+07	1.29E+06
K-40	3275	5.84E+02	4.60E+01
Ca-41	3275	6.90E+04	5.44E+03
Ni-59	3275	2.43E+06	1.91E+05
Ni-63	1280	8.72E+10	6.87E+09
Se-79	3275	1.33E+05	1.05E+04
Rb-87	3275	8.50E+04	6.70E+03
Sr-90	1132	2.11E+16	1.66E+15
Zr-93	3275	2.61E+06	2.06E+05
Nb-94	1132	8.18E+01	6.45E+00
Mo-93	1720	1.31E+06	1.03E+05
Tc-99	3275	1.39E+04	1.09E+03
Pd-107	3275	4.89E+06	3.85E+05
Ag-108m	1132	5.17E+02	4.07E+01
Sn-121m	1132	5.67E+11	4.47E+10
Sn-126	1132	6.48E+01	5.11E+00
I-129	3275	2.07E+03	1.63E+02
Cs-135	3275	1.37E+05	1.08E+04
Cs-137	1132	4.82E+13	3.79E+12
Sm-151	1132	9.51E+11	7.50E+10
Eu-152	3275	4.12E+17	3.25E+16
Pb-210	1150	---	9.56E+18
Bi-207	1132	5.15E+12	4.06E+11

→ **Table 7-9. Intruder-Based Radionuclide Disposal Limits for Vault 4 – Agriculture Scenario Following Failure of Erosion Barrier with Transient Calculation for 100 – 10,000 Years**

Radionuclide	Time of Limit (Years)	Concentration Limit (uCi/m³)	Inventory Limit (Ci/Unit)
Ra-226	1132	1.11E+02	8.76E+00
Ac-227	1132	1.18E+18	9.32E+16
Th-229	1132	4.51E+02	3.55E+01
Th-230	9080	6.25E+01	4.92E+00
Th-232	3275	4.39E+01	3.46E+00
Pa-231	3275	1.87E+02	1.48E+01
U-232	1132	6.34E+06	5.00E+05
U-233	10000	5.70E+02	4.49E+01
U-234	10000	8.03E+02	6.33E+01
U-235	10000	4.64E+02	3.66E+01
U-236	3275	1.50E+04	1.18E+03
U-238	10000	4.01E+03	3.16E+02
Np-237	10000	3.13E+02	2.47E+01
Pu-238	10000	2.28E+06	1.80E+05
Pu-239	3275	5.65E+03	4.45E+02
Pu-240	3275	7.28E+03	5.73E+02
Pu-241	1132	1.33E+06	1.05E+05
Pu-242	3275	5.44E+03	4.28E+02
Pu-244	10000	3.37E+02	2.65E+01
Am-241	1132	4.55E+04	3.58E+03
Am-242m	1132	8.32E+05	6.56E+04
Am-243	1132	8.88E+02	7.00E+01
Cm-242	10000	4.49E+08	3.53E+07
Cm-243	3275	4.48E+06	3.53E+05
Cm-244	3275	2.63E+06	2.07E+05
Cm-245	3275	1.37E+03	1.08E+02
Cm-246	3275	8.01E+03	6.31E+02
Cm-247	10000	2.85E+02	2.24E+01
Cm-248	3275	1.37E+03	1.08E+02
Bk-249	1132	1.33E+06	1.05E+05
Cf-249	1132	3.43E+03	2.70E+02
Cf-250	3275	2.91E+06	2.29E+05
Cf-251	1132	3.02E+03	2.38E+02
Cf-252	3275	1.87E+08	1.47E+07

→ **Table 7-10. Comparison of 10,000-Year Agriculture Scenario Limits with Projected Inventory**

Radionuclide	Limit, Ci	Estimated Inventory, Ci	Fraction of Limit
Am-241	3.58E+03	4.93E+02	1.38E-01
Am-242m	6.56E+04	3.31E+02	5.05E-03
Am-243	7.00E+01	1.30E-03	1.86E-05
C-14	1.30E+03	4.44E+00	3.43E-03
Cf-251	2.38E+02	2.47E-01	1.04E-03
Cm-243	3.53E+05	8.06E-02	2.28E-07
Cm-244	2.07E+05	4.19E+02	2.02E-03
Cm-245	1.08E+02	7.91E-02	7.33E-04
Cs-135	1.08E+04	2.29E-02	2.12E-06
Cs-137	3.79E+12	1.25E+06	3.29E-07
Eu-152	3.25E+16	5.14E-03	1.58E-19
I-129	1.63E+02	8.09E-01	4.96E-03
Nb-94	6.45E+00	9.91E-04	1.54E-04
Ni-59	1.91E+05	3.35E+00	1.75E-05
Ni-63	6.87E+09	4.23E+00	6.15E-10
Np-237	2.47E+01	7.23E-01	2.93E-02
Pu-238	1.80E+05	3.33E+03	1.85E-02
Pu-239	4.45E+02	4.20E+01	9.43E-02
Pu-240	5.73E+02	7.74E+01	1.35E-01
Pu-241	1.05E+05	1.55E+03	1.48E-02
Pu-242	4.28E+02	1.56E-01	3.64E-04
Se-79	1.05E+04	1.99E+00	1.89E-04
Sm-151	7.50E+10	9.29E-04	1.24E-14
Sn-126	5.11E+00	2.65E+00	5.19E-01
Sr-90	1.66E+15	1.24E+05	7.47E-11
Tc-99	1.09E+03	9.82E+01	8.98E-02
Th-232	3.46E+00	3.62E-03	1.05E-03
U-232	5.00E+05	9.46E+00	1.89E-05
U-233	4.49E+01	1.46E+01	3.25E-01
U-234	6.33E+01	6.53E+00	1.03E-01
U-235	3.66E+01	7.91E-02	2.16E-03
U-236	1.18E+03	1.85E-01	1.57E-04
U-238	3.16E+02	3.61E-01	1.14E-03
		Sum-of-Fractions	1.49E+00

→ **Table B-5. Intruder-Based Radionuclide Disposal Limits for Vault 4 –
Post-Drilling Scenario with Transient Calculation for 1000 - 10000 Years**

Radionuclide	Time of Limit (Years)	Concentration Limit ($\mu\text{Ci}/\text{m}^3$)	Inventory Limit (Ci/Unit)
Ac-227	1000	3.93E+17	3.10E+16
Th-228	1000	---	---
Th-229	1000	1.85E+04	1.46E+03
Th-230	9090	2.46E+03	1.94E+02
Th-232	1000	5.03E+03	3.96E+02
Pa-231	1000	4.21E+03	3.32E+02
U-232	1000	2.73E+08	2.15E+07
U-233	10000	2.32E+04	1.83E+03
U-234	10000	2.67E+04	2.10E+03
U-235	10000	1.83E+04	1.45E+03
U-236	1000	1.33E+05	1.05E+04
U-238	10000	1.26E+05	9.95E+03
Np-237	10000	3.69E+03	2.91E+02
Pu-238	10000	7.55E+07	5.95E+06
Pu-239	1000	5.12E+04	4.04E+03
Pu-240	1000	5.53E+04	4.36E+03
Pu-241	1000	5.81E+06	4.58E+05
Pu-242	1000	5.25E+04	4.14E+03
Pu-244	10000	2.92E+04	2.30E+03
Am-241	1000	1.98E+05	1.56E+04
Am-242m	1000	2.16E+06	1.70E+05
Am-243	1000	4.14E+04	3.26E+03
Cm-242	10000	1.49E+10	1.17E+09
Cm-243	1000	4.21E+07	3.32E+06
Cm-244	1000	2.00E+07	1.58E+06
Cm-245	1600	2.51E+04	1.98E+03
Cm-246	1000	5.67E+04	4.46E+03
Cm-247	10000	2.59E+04	2.04E+03
Cm-248	1000	1.34E+04	1.05E+03
Bk-249	1000	7.51E+07	5.92E+06
Cf-249	1000	1.94E+05	1.53E+04
Cf-250	1000	2.06E+07	1.62E+06
Cf-251	1000	7.91E+04	6.23E+03
Cf-252	1000	1.82E+09	1.43E+08

Tornado, Maximum Wind Gust, and Extreme Rainfall Event Recurrence Frequencies at the Savannah River Site

by
A. H. Weber
Westinghouse Savannah River Company
Savannah River Site
Aiken, South Carolina 29808

RECORDS ADMINISTRATION



R0097008

APPROVED for Release for
Unlimited (Release to Public)
6/21/2005

DOE Contract No. DE-AC09-96SR18500

This paper was prepared in connection with work done under the above contract number with the U. S. Department of Energy. By acceptance of this paper, the publisher and/or recipient acknowledges the U. S. Government's right to retain a nonexclusive, royalty-free license in and to any copyright covering this paper, along with the right to reproduce and to authorize others to reproduce all or part of the copyrighted paper.

Table XIX. Extreme Rainfall Estimates by Accumulation Period

Return Period (yrs)	Frequency (per year)	Accumulation Period				
		15 min	1 hour	3 hours	6 hours	24 hours
10	1×10^{-2}	1.5	2.7	3.3	3.7	5.0
25	4×10^{-3}	1.8	3.2	4.0	4.4	6.1
50	2×10^{-2}	2.0	3.5	4.6	5.0	6.9
100	1×10^{-2}	2.1	3.9	5.1	5.7	7.8
200	5×10^{-3}	2.3	4.2	5.8	6.4	8.8
500	2×10^{-3}	2.6	4.7	6.7	7.4	10.3
1000	1×10^{-3}	2.7	5.0	7.4	8.3	11.5
2000	5×10^{-4}	2.9	5.4	8.2	9.2	12.8
5000	2×10^{-4}	3.2	5.8	9.4	10.7	14.7
10000	1×10^{-4}	3.3	6.2	10.3	11.8	16.3
50000	2×10^{-5}	3.7	7.0	12.8	15.1	20.6
100000	1×10^{-5}	3.9	7.4	14.1	16.7	22.7



**RESPONSE TO RAI COMMENT 65
ROADMAP TO REFERENCES**

REFERENCED DOCUMENT	*EXCERPT LOCATION	REMARK
Cook et al. 2005	Excerpt included in response.	Table 7-2
Cook et al. 2005	Excerpt enclosed following response.	Table B-2
d'Entremont & Drumm 2005	Excerpt enclosed following response.	Table A-8. Add batches 0-7 and about 50% of 8 to generate Table 65-1 of this response.
d'Entremont & Drumm 2005	Excerpt enclosed following response.	Table A-9. Used to generate Batches 0-5 of Table 65-2 of this response.
d'Entremont & Drumm 2005	Excerpt enclosed following response.	Table A-12 Used to generate Batches 6-9 and SWPF Average of Table 65-2 of this response.
Rosenberger et al. 2005	Excerpt enclosed following response.	Table 5-4 calculates the total dose (approximately 22 mrem/yr)

***Excerpt Locations:**

1. Excerpt included in response: The excerpt is included within the text of the response or is appended to the response.
2. Excerpt enclosed following response: The excerpt is enclosed on a separate sheet or sheets following the response.
3. Representative excerpt(s) enclosed following response: Representative excerpts from a document that is wholly or largely applicable are enclosed following the response.
4. Other

**APPROVED for Release for
Unlimited (Release to Public)**

7/15/2005

APPROVED for Release for
Unlimited (Release to Public)
6/6/2005

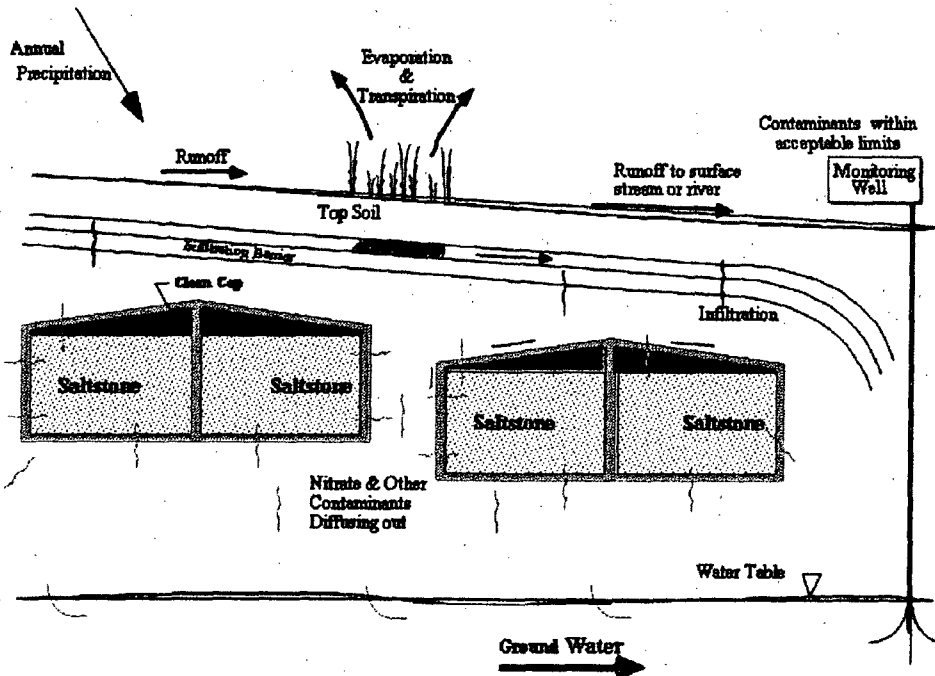
WSRC-TR-2005-00074
Revision 0

KEY WORDS: Performance Assessment
Low-level Radioactive Waste Disposal

**SPECIAL ANALYSIS:
REVISION OF SALTSTONE VAULT 4 DISPOSAL LIMITS (U)**

PREPARED BY:
James R. Cook
Elmer L. Wilhite
Robert A. Hiergesell
Gregory P. Flach

MAY 26, 2005



Westinghouse Savannah River Company
Savannah River Site
Aiken, SC 29808

Prepared for the U.S. Department of Energy Under
Contract Number DE-AC09-96SR18500



B.4 LIMIT CALCULATIONS

After the radionuclide- and scenario-specific dose coefficients have been determined, the concentration limit for each radionuclide based on each scenario can be calculated by:

$$DL_i = \frac{H}{DC_{is}} \tag{Eq. B-10}$$

where

DL_i = the disposal limit for radionuclide i (μCi /cm³)

H = Effective dose equivalent (0.1 rem/year), and

DC_{is} = radionuclide- and scenario- specific dose coefficient (rem*cm³/μCi*year).

The concentration limits can be converted to disposal unit limits in curies using appropriate unit conversions to express the limit in units of Ci/m³ (in this case, (μCi /cm³ is equivalent to Ci/m³) and then multiplying by the volume of the disposal unit (78,800 m³ for Vault 4).

B.5 RESULTS

The parameters specific to Vault 4 used in the intruder analysis are given in Table B-2.

Table B-2. Intruder Parameters for Vault 4

Resident Geometry Factor	0.6	Cook et al. 2002		
Post-Drilling Geometry Factor	1	Cook et al. 2002		
Waste Volume (m ³)	78800	Cook et al. 2002		
Resident Analysis Start Time (yr)	100			
Post-Drilling Analysis Start Time (yr)	1000			
Resident Shielding Thickness (cm)	100			
Transient Layer Model (Surface to Top of Waste) (Phifer and Nelson 2004)				
Layer	Thickness (m)	Description	Erosion Rate (mm/yr)	Degradation Time (yr)
1	0.9144	Soil cover (36")	1.4	0
2	0.3048	Erosion barrier (12")	1.00E-10	0
3	2.7178	Soil backfill (107")	1.4	0
4	0.5080	Concrete/Grout Min (20")	1.4	1000

The results of the analysis of the resident scenario for the period 100 to 1,000 years and 100 to 10,000 years are presented in Tables B-3 and B-4, respectively. Table B-5 gives the results for the post-drilling scenario for the period 1,000 to 10,000 years. In Tables B-3 through B-5 the entry “--” in the Time of Limit column means that the dose calculation is always zero so there is no limit. For cases where there is a time given, there may be an entry “---” in one or both of the limit columns. In this case the entry “---” indicates a limit value greater than or equal to the threshold value of 1E+20.

CBU-PIT-2005-00013

REVISION: 3

June 21, 2005

KEYWORDS:

Tank Farm, Salt Program,
Waste Solidification, Class C,
Permit, Saltstone

RETENTION: PERMANENT

CLASSIFICATION: U

Does not contain UCNI

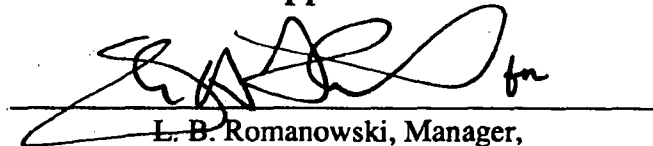
Paul D. d'Entremont
6/21/05 ADC/RO

Radionuclide Concentrations in Saltstone

P. D. d'Entremont, 766-H

M.D. Drumm, 766-H

Approval:



L. B. Romanowski, Manager,
CBU Salt Disposition Planning

APPROVED for Release for
Unlimited (Release to Public)

Westinghouse Savannah River Company
Closure Business Unit
Planning Integration & Technology Department
Aiken, SC 29808

Table A- 8: Interim Strategy Saltstone Batches Total Activity

Ci	Batch 0	Batch 1	Batch 2	Batch 3	Batch 4	Batch 5	Batch 6	Batch 7	Batch 8	Batch 9
H-3	1.00E+01	3.48E+02	2.82E+02	7.38E+02	2.69E+02	2.70E+02	1.77E+02	1.03E+02	3.99E+02	1.48E+02
C-14	3.01E-02	9.59E+00	4.96E+00	1.30E+01	8.85E+00	8.80E+00	1.02E+01	9.67E+00	7.02E+00	9.72E+00
Co-60	1.50E-02	1.01E+01	2.90E+00	7.60E+00	7.48E+00	7.41E+00	1.82E+00	5.30E+00	4.11E+00	5.36E+00
Ni-59	4.04E-07	3.30E-02	3.31E-03	5.43E-03	6.15E-02	6.05E-02	2.14E-02	1.46E-01	1.17E-02	1.35E-01
Ni-63	4.66E-02	1.14E+01	7.04E+00	1.84E+01	1.23E+01	1.22E+01	4.41E+00	1.68E+01	9.97E+00	1.66E+01
Se-79	1.50E-05	2.03E-01	1.22E-01	2.01E-01	1.84E-01	1.81E-01	7.91E-01	2.78E-02	4.35E-01	1.12E-01
Sr-90	4.69E-03	1.64E+03	1.13E+02	1.85E+02	1.13E+03	1.12E+03	2.48E+02	7.86E+02	1.36E+02	7.39E+02
Y-90	4.69E-03	1.64E+03	1.13E+02	1.85E+02	1.13E+03	1.12E+03	2.48E+02	7.86E+02	1.36E+02	7.39E+02
Nb-94	1.18E-10	5.34E-06	9.63E-07	1.58E-06	5.27E-06	5.19E-06	6.22E-06	6.53E-06	3.42E-06	6.60E-06
Tc-99	5.55E-03	6.77E+01	4.54E+01	7.46E+01	6.27E+01	6.17E+01	2.93E+02	6.05E+00	1.61E+02	3.78E+01
Ru-106	3.83E-04	4.64E+00	3.13E+00	5.15E+00	4.39E+00	4.32E+00	2.02E+01	7.03E-01	1.11E+01	2.86E+00
Rh-106	3.83E-04	4.64E+00	3.13E+00	5.15E+00	4.39E+00	4.32E+00	2.02E+01	7.03E-01	1.11E+01	2.86E+00
Sb-125	1.55E-03	1.97E+01	1.27E+01	2.09E+01	1.96E+01	1.93E+01	8.20E+01	7.29E+00	4.51E+01	1.56E+01
Sn-126	7.57E-05	9.37E-01	6.19E-01	1.02E+00	8.68E-01	8.54E-01	4.00E+00	1.02E-01	2.20E+00	5.33E-01
I-129	6.10E-03	3.66E-02	2.60E-02	4.44E-02	3.42E-02	3.37E-02	1.59E-01	3.76E-03	2.91E-02	2.11E-02
Cs-134	1.83E-02	4.64E+02	3.13E+02	5.15E+02	4.30E+02	4.23E+02	1.69E+02	4.03E+01	9.27E+01	2.59E+02
Cs-135	6.22E-02	7.88E-01	5.32E-01	8.74E-01	7.31E-01	7.19E-01	2.86E-01	6.85E-02	1.57E-01	4.40E-01
Cs-137	1.91E+01	2.31E+05	1.56E+05	2.56E+05	2.14E+05	2.11E+05	8.40E+04	2.01E+04	4.62E+04	1.29E+05
Ba-137m	1.80E+01	2.19E+05	1.48E+05	2.43E+05	2.03E+05	2.00E+05	7.95E+04	1.90E+04	4.37E+04	1.22E+05
Ce-144	9.97E-07	1.21E-02	8.16E-03	1.34E-02	5.17E-02	5.08E-02	5.27E-02	1.42E-01	2.90E-02	1.35E-01
Pr-144	9.97E-07	1.21E-02	8.16E-03	1.34E-02	5.17E-02	5.08E-02	5.27E-02	1.42E-01	2.90E-02	1.35E-01
Pm-147	6.45E-04	3.29E+01	5.28E+00	8.68E+00	5.01E+01	4.93E+01	3.41E+01	1.03E+02	1.88E+01	9.72E+01
Eu-154	1.53E-04	2.78E+01	1.25E+00	2.06E+00	1.72E+01	1.69E+01	8.09E+00	5.36E+00	4.45E+00	5.75E+00
Th-232	1.24E-06	8.44E-07	6.65E-07	1.83E-06	6.50E-07	6.53E-07	2.26E-07	2.72E-07	5.40E-08	3.69E-07
U-232	1.43E-10	No Data	No Data	No Data	1.15E-05	1.13E-05	1.10E-09	4.01E-05	4.49E-09	3.64E-05
U-233	1.10E-07	2.66E-02	3.32E-01	5.66E-01	2.05E-02	2.06E-02	7.14E-03	8.58E-03	1.70E-03	1.16E-02
U-234	1.56E-08	6.83E-02	1.09E+00	1.81E+00	4.34E-02	4.32E-02	7.62E-03	9.16E-03	1.82E-03	1.24E-02
U-235	2.05E-04	9.12E-04	1.07E-03	2.15E-03	6.30E-04	6.27E-04	1.21E-04	2.61E-04	2.89E-05	3.02E-04
U-236	2.56E-04	1.67E-02	3.67E-02	6.48E-02	1.02E-02	1.01E-02	1.40E-03	1.70E-03	3.34E-04	2.29E-03
U-238	1.09E-02	2.70E-03	2.81E-03	6.96E-03	6.03E-03	5.98E-03	7.16E-04	1.47E-02	1.72E-04	1.37E-02
Np-237	4.01E-08	1.43E-01	8.66E-02	1.63E-01	8.25E-02	8.16E-02	6.32E-03	7.64E-03	1.51E-03	1.03E-02
Pu-238	2.87E-02	7.93E+02	6.27E+02	1.15E+03	4.82E+02	4.77E+02	3.80E+01	1.19E+02	9.07E+00	1.29E+02

Ci	Batch 0	Batch 1	Batch 2	Batch 3	Batch 4	Batch 5	Batch 6	Batch 7	Batch 8	Batch 9
Pu-239	1.82E-01	2.08E+00	2.57E+00	6.05E+00	4.91E+00	4.86E+00	5.58E-01	1.22E+01	1.35E-01	1.14E+01
Pu-240	1.97E-03	7.08E-01	5.59E-01	1.54E+00	1.28E+00	1.28E+00	1.90E-01	2.81E+00	4.56E-02	2.65E+00
Pu-241	2.89E-05	1.24E+01	9.81E+00	2.70E+01	2.70E+01	2.67E+01	3.34E+00	6.48E+01	8.03E-01	6.05E+01
Pu-242	1.09E-09	7.93E-05	6.26E-05	1.72E-04	2.08E-04	2.06E-04	2.13E-05	5.40E-04	5.14E-06	5.01E-04
Am-241	1.16E-02	1.98E+00	5.00E-01	8.22E-01	2.10E+00	2.07E+00	3.23E+00	2.67E+00	1.78E+00	2.78E+00
Am-242m	3.52E-08	1.94E-03	2.88E-04	4.74E-04	1.21E-03	1.19E-03	1.86E-03	3.71E-05	1.02E-03	2.39E-04
Cm-244	1.34E-03	3.12E-01	2.00E-01	3.29E-01	2.84E-01	2.79E-01	1.29E+00	2.65E-02	7.11E-01	1.66E-01
Cm-245	2.41E-09	3.05E-05	1.97E-05	3.24E-05	2.78E-05	2.74E-05	1.27E-04	2.54E-06	7.01E-05	1.63E-05
Na-22	3.40E-04	3.24E+01	2.78E+00	4.58E+00	3.74E+01	3.68E+01	7.56E+01	6.45E+01	9.89E+00	6.04E+01
Al-26	2.18E-06	1.25E-01	1.78E-02	2.93E-02	1.42E-01	1.40E-01	3.16E-01	2.27E-01	6.33E-02	2.18E-01
Te-125m	3.79E-04	4.82E+00	3.10E+00	5.10E+00	4.78E+00	4.70E+00	2.00E+01	1.78E+00	1.10E+01	3.82E+00
Sb-126	1.06E-05	1.31E-01	8.67E-02	1.43E-01	1.22E-01	1.20E-01	5.60E-01	1.43E-02	3.08E-01	7.46E-02
Sb-126m	7.57E-05	9.37E-01	6.19E-01	1.02E+00	8.68E-01	8.54E-01	4.00E+00	1.02E-01	2.20E+00	5.33E-01
Sm-151	7.23E-04	7.91E+01	5.92E+00	9.73E+00	5.87E+01	5.77E+01	3.82E+01	4.46E+01	2.10E+01	4.46E+01
Eu-152	3.50E-06	3.82E-01	2.86E-02	4.71E-02	2.84E-01	2.79E-01	1.85E-01	2.16E-01	1.02E-01	2.16E-01
Eu-155	4.09E-05	4.47E+00	3.34E-01	5.50E-01	3.32E+00	3.26E+00	2.16E+00	2.52E+00	1.19E+00	2.52E+00
Ra-226	3.51E-14	1.18E-01	2.45E-06	4.07E-06	6.37E-02	6.27E-02	1.72E-08	2.07E-08	4.10E-09	2.80E-08
Ra-228	1.24E-06	8.44E-07	6.65E-07	1.83E-06	6.50E-07	6.53E-07	2.26E-07	2.72E-07	5.40E-08	3.69E-07
Ac-227	4.67E-08	2.08E-07	2.44E-07	4.91E-07	1.44E-07	1.43E-07	2.76E-08	5.95E-08	6.59E-09	6.88E-08
Th-229	3.14E-10	7.57E-05	9.43E-04	1.61E-03	5.84E-05	5.86E-05	2.03E-05	2.44E-05	4.85E-06	3.31E-05
Th-230	4.30E-12	3.30E-04	3.00E-04	4.98E-04	1.80E-04	1.77E-04	2.10E-06	2.53E-06	5.02E-07	3.43E-06
Pa-231	1.30E-07	5.78E-07	6.79E-07	1.36E-06	3.99E-07	3.97E-07	7.66E-08	1.65E-07	1.83E-08	1.91E-07
Pu-244	3.47E-06	3.63E-07	2.86E-07	7.88E-07	9.52E-07	9.43E-07	9.73E-08	2.47E-06	2.35E-08	2.29E-06
Am-243	1.17E-08	1.28E-03	9.57E-05	1.57E-04	9.48E-04	9.33E-04	6.18E-04	7.21E-04	3.40E-04	7.21E-04
Cm-242	2.89E-08	1.61E-03	2.36E-04	3.88E-04	1.01E-03	9.90E-04	1.53E-03	3.04E-05	8.40E-04	1.96E-04
Cm-243	6.84E-09	7.48E-04	5.60E-05	9.21E-05	5.55E-04	5.46E-04	3.62E-04	4.22E-04	1.99E-04	4.22E-04
Cm-247	1.32E-18	1.44E-13	1.08E-14	1.77E-14	1.07E-13	1.05E-13	6.97E-14	8.13E-14	3.83E-14	8.14E-14
Cm-248	1.37E-18	1.50E-13	1.12E-14	1.85E-14	1.11E-13	1.10E-13	7.26E-14	8.48E-14	4.00E-14	8.48E-14
Bk-249	1.00E-25	1.10E-20	8.22E-22	1.35E-21	8.14E-21	8.01E-21	5.31E-21	6.19E-21	2.92E-21	6.20E-21
Cf-249	7.62E-18	8.33E-13	6.23E-14	1.02E-13	6.18E-13	6.08E-13	4.03E-13	4.70E-13	2.22E-13	4.70E-13
Cf-251	2.61E-19	2.85E-14	2.13E-15	3.51E-15	2.11E-14	2.08E-14	1.38E-14	1.61E-14	7.58E-15	1.61E-14
Cf-252	8.46E-21	9.25E-16	6.92E-17	1.14E-16	6.86E-16	6.75E-16	4.47E-16	5.22E-16	2.46E-16	5.22E-16

Table A-9: Interim Strategy Saltstone Batches Concentrations

Ci/gal	Batch 0	Batch 1	Batch 2	Batch 3	Batch 4	Batch 5	Batch 6	Batch 7	Batch 8	Batch 9
H-3	1.34E-05	2.79E-04	3.63E-04	4.10E-04	2.36E-04	2.38E-04	1.23E-04	8.41E-05	2.85E-04	1.20E-04
C-14	4.01E-08	7.67E-06	6.40E-06	7.21E-06	7.77E-06	7.75E-06	7.06E-06	7.89E-06	5.01E-06	7.90E-06
Co-60	2.00E-08	8.04E-06	3.74E-06	4.22E-06	6.56E-06	6.53E-06	1.26E-06	4.32E-06	2.93E-06	4.36E-06
Ni-59	5.39E-13	2.64E-08	4.27E-09	3.02E-09	5.39E-08	5.33E-08	1.48E-08	1.20E-07	8.39E-09	1.10E-07
Ni-63	6.21E-08	9.10E-06	9.09E-06	1.02E-05	1.07E-05	1.07E-05	3.07E-06	1.37E-05	7.12E-06	1.35E-05
Se-79	2.00E-11	1.63E-07	1.58E-07	1.12E-07	1.61E-07	1.59E-07	5.50E-07	2.27E-08	3.11E-07	9.13E-08
Sr-90	6.25E-09	1.31E-03	1.46E-04	1.03E-04	9.94E-04	9.83E-04	1.72E-04	6.42E-04	9.74E-05	6.01E-04
Y-90	6.25E-09	1.31E-03	1.46E-04	1.03E-04	9.94E-04	9.83E-04	1.72E-04	6.42E-04	9.74E-05	6.01E-04
Nb-94	1.57E-16	4.27E-12	1.24E-12	8.80E-13	4.62E-12	4.57E-12	4.32E-12	5.33E-12	2.44E-12	5.37E-12
Tc-99	7.40E-09	5.41E-05	5.86E-05	4.15E-05	5.50E-05	5.43E-05	2.04E-04	4.94E-06	1.15E-04	3.07E-05
Ru-106	5.10E-10	3.71E-06	4.04E-06	2.86E-06	3.85E-06	3.81E-06	1.41E-05	5.74E-07	7.95E-06	2.33E-06
Rh-106	5.10E-10	3.71E-06	4.04E-06	2.86E-06	3.85E-06	3.81E-06	1.41E-05	5.74E-07	7.95E-06	2.33E-06
Sb-125	2.07E-09	1.58E-05	1.64E-05	1.16E-05	1.72E-05	1.70E-05	5.70E-05	5.95E-06	3.22E-05	1.27E-05
Sn-126	1.01E-10	7.50E-07	7.99E-07	5.66E-07	7.62E-07	7.53E-07	2.78E-06	8.34E-08	1.57E-06	4.33E-07
I-129	8.14E-09	2.93E-08	3.35E-08	2.46E-08	3.00E-08	2.97E-08	1.10E-07	3.07E-09	2.08E-08	1.72E-08
Cs-134	2.45E-08	3.71E-04	4.04E-04	2.86E-04	3.77E-04	3.73E-04	1.17E-04	3.29E-05	6.62E-05	2.11E-04
Cs-135	8.29E-08	6.31E-07	6.86E-07	4.86E-07	6.41E-07	6.34E-07	1.99E-07	5.60E-08	1.12E-07	3.58E-07
Cs-137	2.54E-05	1.85E-01	2.01E-01	1.42E-01	1.88E-01	1.86E-01	5.83E-02	1.64E-02	3.30E-02	1.05E-01
Ba-137m	2.40E-05	1.75E-01	1.90E-01	1.35E-01	1.78E-01	1.76E-01	5.52E-02	1.55E-02	3.12E-02	9.93E-02
Ce-144	1.33E-12	9.72E-09	1.05E-08	7.45E-09	4.53E-08	4.48E-08	3.66E-08	1.16E-07	2.07E-08	1.10E-07
Pr-144	1.33E-12	9.72E-09	1.05E-08	7.45E-09	4.53E-08	4.48E-08	3.66E-08	1.16E-07	2.07E-08	1.10E-07
Pm-147	8.60E-10	2.64E-05	6.81E-06	4.82E-06	4.40E-05	4.35E-05	2.37E-05	8.42E-05	1.34E-05	7.90E-05
Eu-154	2.04E-10	2.22E-05	1.62E-06	1.14E-06	1.51E-05	1.49E-05	5.62E-06	4.38E-06	3.18E-06	4.68E-06
Th-232	1.65E-12	6.75E-13	8.58E-13	1.02E-12	5.70E-13	5.75E-13	1.57E-13	2.22E-13	3.86E-14	3.00E-13
U-232	1.91E-16	No Data	No Data	No Data	1.01E-11	9.95E-12	7.63E-16	3.28E-11	3.21E-15	2.96E-11
U-233	1.47E-13	2.13E-08	4.28E-07	3.15E-07	1.80E-08	1.82E-08	4.96E-09	7.01E-09	1.22E-09	9.46E-09
U-234	2.08E-14	5.46E-08	1.40E-06	1.00E-06	3.81E-08	3.81E-08	5.29E-09	7.48E-09	1.30E-09	1.01E-08
U-235	2.73E-10	7.30E-10	1.38E-09	1.20E-09	5.52E-10	5.52E-10	8.39E-11	2.13E-10	2.06E-11	2.45E-10
U-236	3.41E-10	1.33E-08	4.74E-08	3.60E-08	8.95E-09	8.92E-09	9.70E-10	1.38E-09	2.38E-10	1.86E-09
U-238	1.45E-08	2.16E-09	3.63E-09	3.86E-09	5.29E-09	5.27E-09	4.97E-10	1.20E-08	1.23E-10	1.11E-08
Np-237	5.34E-14	1.14E-07	1.12E-07	9.03E-08	7.24E-08	7.19E-08	4.39E-09	6.24E-09	1.08E-09	8.41E-09
Pu-238	3.82E-08	6.35E-04	8.08E-04	6.39E-04	4.23E-04	4.20E-04	2.64E-05	9.75E-05	6.48E-06	1.05E-04

Ci/gal	Batch 0	Batch 1	Batch 2	Batch 3	Batch 4	Batch 5	Batch 6	Batch 7	Batch 8	Batch 9
Pu-239	2.42E-07	1.67E-06	3.32E-06	3.36E-06	4.31E-06	4.29E-06	3.88E-07	9.98E-06	9.61E-08	9.25E-06
Pu-240	2.63E-09	5.67E-07	7.21E-07	8.56E-07	1.13E-06	1.12E-06	1.32E-07	2.30E-06	3.26E-08	2.15E-06
Pu-241	3.85E-11	9.95E-06	1.27E-05	1.50E-05	2.37E-05	2.36E-05	2.32E-06	5.29E-05	5.73E-07	4.92E-05
Pu-242	1.45E-15	6.35E-11	8.07E-11	9.58E-11	1.83E-10	1.82E-10	1.48E-11	4.41E-10	3.67E-12	4.07E-10
Am-241	1.54E-08	1.59E-06	6.45E-07	4.57E-07	1.85E-06	1.82E-06	2.24E-06	2.18E-06	1.27E-06	2.26E-06
Am-242m	4.70E-14	1.55E-09	3.72E-10	2.63E-10	1.06E-09	1.05E-09	1.29E-09	3.03E-11	7.32E-10	1.94E-10
Cm-244	1.78E-09	2.50E-07	2.58E-07	1.83E-07	2.49E-07	2.46E-07	8.98E-07	2.16E-08	5.08E-07	1.35E-07
Cm-245	3.21E-15	2.44E-11	2.54E-11	1.80E-11	2.44E-11	2.41E-11	8.85E-11	2.07E-12	5.00E-11	1.33E-11
Na-22	4.53E-10	2.59E-05	3.59E-06	2.54E-06	3.28E-05	3.24E-05	5.25E-05	5.26E-05	7.06E-06	4.91E-05
Al-26	2.90E-12	1.00E-07	2.30E-08	1.63E-08	1.25E-07	1.23E-07	2.20E-07	1.85E-07	4.52E-08	1.77E-07
Te-125m	5.05E-10	3.85E-06	4.00E-06	2.83E-06	4.19E-06	4.14E-06	1.39E-05	1.45E-06	7.87E-06	3.10E-06
Sb-126	1.41E-11	1.05E-07	1.12E-07	7.92E-08	1.07E-07	1.05E-07	3.89E-07	1.17E-08	2.20E-07	6.07E-08
Sb-126m	1.01E-10	7.50E-07	7.99E-07	5.66E-07	7.62E-07	7.53E-07	2.78E-06	8.34E-08	1.57E-06	4.33E-07
Sm-151	9.64E-10	6.33E-05	7.64E-06	5.40E-06	5.15E-05	5.09E-05	2.66E-05	3.64E-05	1.50E-05	3.63E-05
Eu-152	4.66E-12	3.06E-07	3.69E-08	2.61E-08	2.49E-07	2.46E-07	1.28E-07	1.76E-07	7.26E-08	1.76E-07
Eu-155	5.45E-11	3.57E-06	4.32E-07	3.05E-07	2.91E-06	2.87E-06	1.50E-06	2.06E-06	8.49E-07	2.05E-06
Ra-226	4.68E-20	9.43E-08	3.16E-12	2.26E-12	5.59E-08	5.52E-08	1.19E-14	1.69E-14	2.93E-15	2.28E-14
Ra-228	1.65E-12	6.75E-13	8.58E-13	1.02E-12	5.70E-13	5.75E-13	1.57E-13	2.22E-13	3.86E-14	3.00E-13
Ac-227	6.23E-14	1.67E-13	3.15E-13	2.73E-13	1.26E-13	1.26E-13	1.92E-14	4.86E-14	4.71E-15	5.60E-14
Th-229	4.19E-16	6.06E-11	1.22E-09	8.95E-10	5.12E-11	5.17E-11	1.41E-11	1.99E-11	3.46E-12	2.69E-11
Th-230	5.73E-18	2.64E-10	3.87E-10	2.77E-10	1.58E-10	1.56E-10	1.46E-12	2.06E-12	3.58E-13	2.79E-12
Pa-231	1.73E-13	4.63E-13	8.76E-13	7.57E-13	3.50E-13	3.50E-13	5.32E-14	1.35E-13	1.31E-14	1.55E-13
Pu-244	4.62E-12	2.90E-13	3.69E-13	4.38E-13	8.35E-13	8.31E-13	6.76E-14	2.02E-12	1.68E-14	1.86E-12
Am-243	1.56E-14	1.02E-09	1.23E-10	8.73E-11	8.32E-10	8.22E-10	4.29E-10	5.89E-10	2.43E-10	5.86E-10
Cm-242	3.85E-14	1.29E-09	3.05E-10	2.16E-10	8.82E-10	8.72E-10	1.06E-09	2.48E-11	6.00E-10	1.59E-10
Cm-243	9.13E-15	5.99E-10	7.23E-11	5.11E-11	4.87E-10	4.81E-10	2.51E-10	3.45E-10	1.42E-10	3.43E-10
Cm-247	1.76E-24	1.15E-19	1.39E-20	9.85E-21	9.38E-20	9.27E-20	4.84E-20	6.64E-20	2.74E-20	6.62E-20
Cm-248	1.83E-24	1.20E-19	1.45E-20	1.03E-20	9.78E-20	9.66E-20	5.05E-20	6.92E-20	2.85E-20	6.89E-20
Bk-249	1.34E-31	8.78E-27	1.06E-27	7.50E-28	7.14E-27	7.06E-27	3.69E-27	5.06E-27	2.09E-27	5.04E-27
Cf-249	1.02E-23	6.66E-19	8.04E-20	5.69E-20	5.42E-19	5.36E-19	2.80E-19	3.84E-19	1.58E-19	3.82E-19
Cf-251	3.48E-25	2.28E-20	2.75E-21	1.95E-21	1.85E-20	1.83E-20	9.57E-21	1.31E-20	5.41E-21	1.31E-20
Cf-252	1.13E-26	7.40E-22	8.93E-23	6.32E-23	6.02E-22	5.95E-22	3.11E-22	4.26E-22	1.76E-22	4.24E-22
Vol (kgal)	750	1,250	775	1,800	1,140	1,135	1,440	1,225	1,400	1,230

Ci	DDA	ARP/MCU	SWPF	Total
Sb-126	6.91E-01	8.68E-01	6.15E+01	6.30E+01
Sb-126m	4.93E+00	6.20E+00	4.39E+02	4.50E+02
Sm-151	3.00E+02	5.93E+01	4.19E+03	4.55E+03
Eu-152	1.45E+00	2.87E-01	2.03E+01	2.20E+01
Eu-155	1.70E+01	3.35E+00	2.37E+02	2.57E+02
Ra-226	2.44E-01	2.13E-08	1.27E+01	1.30E+01
Ra-228	6.52E-06	2.80E-07	1.04E-01	1.04E-01
Ac-227	1.40E-06	3.42E-08	1.77E-05	1.91E-05
Th-229	2.80E-03	2.52E-05	4.70E-03	7.53E-03
Th-230	1.49E-03	2.60E-06	3.38E-02	3.53E-02
Pa-231	3.90E-06	9.49E-08	4.92E-05	5.32E-05
Pu-244	1.16E-05	1.21E-07	7.85E-04	7.96E-04
Am-243	4.85E-03	9.58E-04	1.47E-02	2.05E-02
Cm-242	4.46E-03	2.37E-03	9.85E-02	1.05E-01
Cm-243	2.84E-03	5.61E-04	2.33E-02	2.67E-02
Cm-247	5.48E-13	1.08E-13	4.49E-12	5.15E-12
Cm-248	5.71E-13	1.13E-13	4.68E-12	5.36E-12
Bk-249	4.17E-20	8.23E-21	5.81E-19	6.31E-19
Cf-249	3.16E-12	6.24E-13	4.41E-11	4.79E-11
Cf-251	1.08E-13	2.14E-14	1.51E-12	1.64E-12
Cf-252	3.51E-15	6.93E-16	4.90E-14	5.32E-14

Table A- 12: Concentrations Sent to Saltstone

Ci/gal	DDA	ARP/MCU	SWPF	Total
H-3	2.33E-04	2.03E-04	6.91E-05	8.68E-05
C-14	6.94E-06	6.05E-06	4.56E-06	4.80E-06
Co-60	4.96E-06	2.09E-06	6.00E-07	1.01E-06
Ni-59	4.78E-08	1.17E-08	2.44E-08	2.61E-08
Ni-63	1.02E-05	5.06E-06	1.47E-06	2.31E-06
Se-79	1.11E-07	4.32E-07	9.06E-07	8.25E-07
Sr-90	6.14E-04	1.35E-04	1.39E-05	6.88E-05
Y-90	6.14E-04	1.35E-04	1.39E-05	6.88E-05
Nb-94	3.38E-12	3.40E-12	7.12E-12	6.70E-12
Tc-99	3.82E-05	1.60E-04	3.36E-04	3.06E-04
Ru-106	2.71E-06	1.10E-05	2.32E-05	2.11E-05
Rh-106	2.71E-06	1.10E-05	2.32E-05	2.11E-05
Sb-125	1.24E-05	4.48E-05	9.39E-05	8.56E-05
Sn-126	5.30E-07	2.18E-06	4.58E-06	4.17E-06
I-129	2.21E-08	6.62E-08	1.81E-07	1.65E-07
Cs-134	2.63E-04	9.20E-05	5.79E-08	2.51E-05
Cs-135	4.53E-07	1.56E-07	9.84E-11	4.33E-08
Cs-137	1.31E-01	4.58E-02	2.89E-05	1.25E-02
Ba-137m	1.24E-01	4.34E-02	2.73E-05	1.18E-02
Ce-144	4.44E-08	2.88E-08	6.03E-08	5.81E-08

Ci/gal	DDA	ARP/MCU	SWPF	Total
Pr-144	4.44E-08	2.88E-08	6.03E-08	5.81E-08
Pm-147	3.73E-05	1.86E-05	3.90E-05	3.83E-05
Eu-154	8.21E-06	4.41E-06	9.24E-06	9.03E-06
Th-232	7.01E-13	9.87E-14	1.08E-09	9.63E-10
U-232	1.07E-11	1.97E-15	2.22E-10	1.98E-10
U-233	1.06E-07	3.11E-09	1.28E-08	2.06E-08
U-234	3.30E-07	3.32E-09	8.70E-09	3.62E-08
U-235	6.62E-10	5.27E-11	6.00E-10	5.91E-10
U-236	1.53E-08	6.09E-10	1.65E-09	2.80E-09
U-238	6.85E-09	3.13E-10	5.22E-08	4.70E-08
Np-237	6.17E-08	2.76E-09	1.59E-08	1.95E-08
Pu-238	4.06E-04	1.66E-05	1.02E-04	1.26E-04
Pu-239	4.76E-06	2.44E-07	6.36E-06	6.06E-06
Pu-240	1.16E-06	8.3E-08	1.71E-06	1.62E-06
Pu-241	2.45E-05	1.46E-06	7.1E-05	6.51E-05
Pu-242	1.9E-10	9.3E-12	1.78E-09	1.6E-09
Am-241	1.39E-06	1.76E-06	8.04E-07	8.8E-07
Am-242m	5.79E-10	1.02E-09	4.63E-10	4.88E-10
Cm-244	1.72E-07	7.06E-07	8.71E-07	8.07E-07
Cm-245	1.68E-11	6.95E-11	8.58E-11	7.94E-11
Na-22	2.57E-05	3.01E-05	4.93E-05	4.68E-05
Al-26	9.66E-08	1.34E-07	2.32E-07	2.18E-07
Te-125m	3.02E-06	1.09E-05	2.29E-05	2.09E-05
Sb-126	7.42E-08	3.06E-07	6.41E-07	5.84E-07
Sb-126m	5.3E-07	2.18E-06	4.58E-06	4.17E-06
Sm-151	3.23E-05	2.09E-05	4.37E-05	4.21E-05
Eu-152	1.56E-07	1.01E-07	2.11E-07	2.04E-07
Eu-155	1.82E-06	1.18E-06	2.47E-06	2.38E-06
Ra-226	2.63E-08	7.49E-15	1.33E-07	1.2E-07
Ra-228	7.01E-13	9.87E-14	1.08E-09	9.63E-10
Ac-227	1.51E-13	1.2E-14	1.85E-13	1.77E-13
Th-229	3.01E-10	8.86E-12	4.91E-11	6.98E-11
Th-230	1.6E-10	9.16E-13	3.53E-10	3.27E-10
Pa-231	4.19E-13	3.34E-14	5.13E-13	4.92E-13
Pu-244	1.24E-12	4.25E-14	8.19E-12	7.38E-12
Am-243	5.22E-10	3.37E-10	1.54E-10	1.9E-10
Cm-242	4.79E-10	8.33E-10	1.03E-09	9.76E-10
Cm-243	3.06E-10	1.98E-10	2.43E-10	2.48E-10
Cm-247	5.89E-20	3.8E-20	4.69E-20	4.77E-20
Cm-248	6.13E-20	3.96E-20	4.89E-20	4.97E-20
Bk-249	4.48E-27	2.9E-27	6.07E-27	5.85E-27
Cf-249	3.4E-19	2.2E-19	4.61E-19	4.44E-19
Cf-251	1.16E-20	7.52E-21	1.58E-20	1.52E-20
Cf-252	3.78E-22	2.44E-22	5.11E-22	4.93E-22
Vol (kgal)	9,305	2,840	95,800	107,945

CBU-PIT-2005-00146
Revision 0

SALTSTONE
PERFORMANCE OBJECTIVE DEMONSTRATION DOCUMENT
(U)

PREPARED BY:
Kent H. Rosenberger
Bernice C. Rogers
R. Kim Cauthen

JUNE 2005

APPROVED for Release for
Unlimited (Release to Public)

Westinghouse Savannah River Company
Savannah River Site
Aiken, SC 29808

Prepared for the U.S. Department of Energy Under
Contract Number DE-AC09-96SR18500



5.6 Intruder Performance Objective Demonstration

These limits for the intruder pathway are compared with limits derived for the other pathways and with the projected Vault 4 inventory in Table 3.2. For the projected Vault 4 inventory, only Cs-137 produces a significantly large fraction of the intruder limit.

For the projected Vault 4 inventory, the dose to the inadvertent intruder presented in Table 5-4 from the resident scenario, which is the only credible scenario within the 10,000-year time frame, is 21.7 mrem/year (Cook et al., 2005), which is 4% of the NRC performance objective of 500 mrem/year (USNRC, 1982).

Since the highest Cs-137 concentration per vault is from DDA material in Vault 4 and any other nuclide with a lower inventory limit, such as Sn-126, is spread out among future vaults and thus is not concentrated in any individual vault, the intruder dose for Vault 4 bounds future operations.

Table 5-4. Evaluation of Inadvertent Intruder Doses (Cook et al., 2005)

Radionuclide	10,000-Year Disposal Limit (Ci/Vault 4)*	Vault 4 Projected Inventory (Ci)**	Fraction of 10,000-Year Disposal Limit	Dose (mrem/yr)
Na-22	7.80E+15	2.59E+02	3.32E-14	3.32E-12
Al-26	1.61E+02	1.03E+00	6.40E-03	6.40E-01
Co-60	5.75E+09	4.46E+01	7.76E-09	7.76E-07
Nb-94	1.01E+03	1.02E-03	1.01E-06	1.01E-04
Tc-99	3.66E+13	7.16E+02	1.95E-11	1.95E-09
Sn-126	1.17E+03	9.56E+00	8.17E-03	8.17E-01
Sb-125	1.41E+17	2.05E+02	1.45E-15	1.45E-13
Cs-134	4.12E+19	2.40E+03	5.83E-17	5.83E-15
Cs-137	5.99E+06	1.20E+06	2.00E-01	2.00E+01
Eu-152	6.42E+06	1.48E+00	2.30E-07	2.30E-05
Eu-154	1.15E+08	8.10E+01	7.04E-07	7.04E-05
Eu-155	1.12E+19	1.72E+01	1.54E-18	1.54E-16
Ra-226	4.21E+02	2.44E-01	5.80E-04	5.80E-02
Ra-228	3.72E+08	6.41E-06	1.72E-14	1.72E-12
Ac-227	8.78E+07	1.37E-06	1.56E-14	1.56E-12
Th-229	8.61E+03	2.79E-03	3.24E-07	3.24E-05
Th-230	3.29E+02	1.49E-03	4.53E-06	4.53E-04
Th-232	1.56E+02	6.41E-06	4.11E-08	4.11E-06
Pa-231	2.15E+04	3.80E-06	1.77E-10	1.77E-08

Radionuclide	10,000-Year Disposal Limit (Ci/Vault 4)*	Vault 4 Projected Inventory (Ci)**	Fraction of 10,000-Year Disposal Limit	Dose (mrem/yr)
U-232	9.00E+03	9.52E-03	1.06E-06	1.06E-04
U-233	1.35E+04	9.82E-01	7.27E-05	7.27E-03
U-234	4.48E+03	6.59E+00	1.47E-03	1.47E-01
U-235	1.03E+05	7.41E-02	7.19E-07	7.19E-05
U-236	3.17E+08	1.42E-01	4.48E-10	4.48E-08
U-238	6.60E+04	1.61E-01	2.44E-06	2.44E-04
Np-237	6.73E+04	5.76E-01	8.56E-06	8.56E-04
Pu-238	1.27E+07	3.69E+03	2.91E-04	2.91E-02
Pu-239	1.37E+10	3.36E+01	2.45E-09	2.45E-07
Pu-240	2.96E+12	8.39E+00	2.83E-12	2.83E-10
Pu-241	1.02E+10	1.72E+02	1.69E-08	1.69E-06
Pu-242	4.91E+10	9.32E-03	1.90E-13	1.90E-11
Pu-244	3.65E+03	9.38E-06	2.57E-09	2.57E-07
Am-241	3.38E+08	1.44E+01	4.25E-08	4.25E-06
Am-242m	9.83E+06	7.25E-03	7.38E-10	7.38E-08
Am-243	2.96E+05	6.22E-03	2.10E-08	2.10E-06
Cm-242	2.51E+09	6.21E-03	2.47E-12	2.47E-10
Cm-243	7.00E+09	2.88E-03	4.11E-13	4.11E-11
Cm-244	1.08E+15	3.16E+00	2.93E-15	2.93E-13
Cm-245	8.42E+06	3.03E-04	3.60E-11	3.60E-09
Cm-247	2.45E+04	5.55E-13	2.27E-17	2.27E-15
Cm-248	4.64E+07	5.79E-13	1.25E-20	1.25E-18
Bk-249	4.92E+07	4.23E-20	8.60E-28	8.60E-26
Cf-249	1.27E+05	3.21E-12	2.53E-17	2.53E-15
Cf-251	1.83E+06	2.47E-01	1.35E-07	1.35E-05
Cf-252	6.31E+12	3.56E-15	5.64E-28	5.64E-26
Totals			2.17E-01	2.17E+01

* Vault 4 inventory limits from Table 3-2 of Cook et al., (2005) based upon intruder dose limit of 100 mrem/yr

** Projected inventory from d'Entremont and Drumm (2005)

**RESPONSE TO RAI COMMENT 66
ROADMAP TO REFERENCES**

REFERENCED DOCUMENT	*EXCERPT LOCATION	REMARK
Beres 1990		General reference, no excerpt enclosed with this response..
Cook et al. 2005	Excerpt enclosed following response.	Section 6.
Simpkins 2004		Abstract included for this spreadsheet program used to analyze the exposure pathways involving transport by water that were used in the Vault 4 SA (Cook et al. 2005).

***Excerpt Locations:**

1. Excerpt included in response: The excerpt is included within the text of the response or is appended to the response.
2. Excerpt enclosed following response: The excerpt is enclosed on a separate sheet or sheets following the response.
3. Representative excerpt(s) enclosed following response: Representative excerpts from a document that is wholly or largely applicable are enclosed following the response.
4. Other

APPROVED for Release for
Unlimited (Release to Public)

7/15/2005

THE CLEAN AIR ACT ASSESSMENT PACKAGE-1988
(CAP-88)
A DOSE AND RISK ASSESSMENT METHODOLOGY
FOR RADIONUCLIDE EMISSIONS TO AIR

VOLUME 1

USER'S MANUAL

Prepared By:

Deborah A. Beres
SC&A, Inc.
1311 Dolley Madison Blvd.
McLean, VA 22101

Contract No. 68-D9-0170
Work Assignment 1-28

Prepared For:

U.S. Environmental Protection Agency
Office of Radiation Programs
401 M Street, S.W.
Washington, D.C. 20460

Larry Gray
Work Assignment Manager

October 1990

APPROVED for Release for
Unlimited (Release to Public)
6/6/2005

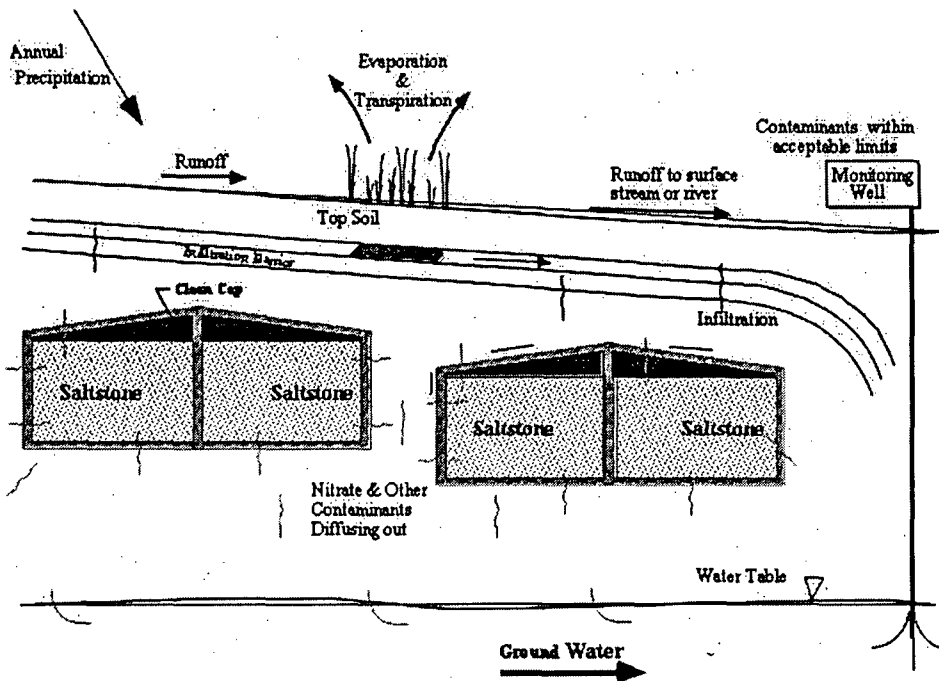
WSRC-TR-2005-00074
Revision 0

KEY WORDS: Performance Assessment
Low-level Radioactive Waste Disposal

**SPECIAL ANALYSIS:
REVISION OF SALTSTONE VAULT 4 DISPOSAL LIMITS (U)**

PREPARED BY:
James R. Cook
Elmer L. Wilhite
Robert A. Hiergesell
Gregory P. Flach

MAY 26, 2005



Westinghouse Savannah River Company
Savannah River Site
Aiken, SC 29808

Prepared for the U.S. Department of Energy Under
Contract Number DE-AC09-96SR18500



6.0 ALL-PATHWAYS ANALYSIS

One of the USDOE performance objectives is DOE 435.1.IV.P (1) (a):

Dose to representative members of the public shall not exceed 25 mrem (0.25 mSv) in a year total effective dose equivalent from all exposure pathways, excluding the dose from radon and its progeny in air.

In this SA, exposures from all pathways are calculated using the peak groundwater concentrations derived in the groundwater analysis (Section 2) and the peak air doses derived in the air analysis (Section 4).

6.1 Methodology

For radionuclides transported by the groundwater, the maximum groundwater concentration of each radionuclide within the time frame of interest (i.e., 1,000 years or 10,000 years) calculated in Section 2 is input to the LADTAP XL© program (Jannik 2005), which is the model used at SRS for demonstrating water pathway dose compliance (Simpkins 2004). The maximum groundwater concentrations are calculated for a unit curie inventory of each radionuclide.

It is conservatively assumed that a future resident farmer uses the contaminated groundwater at the 100-meter well as a source of 1) drinking water, 2) pond water (in which fish are raised and recreational activities occur), and 3) irrigation water used for raising vegetables, meat, and milk.

LADTAP XL© contains two worksheets: LADTAP and IRRIDOSE. The LADTAP worksheet estimates dose from environmental pathways including external exposure resulting from recreational activities (swimming, boating, and shoreline use) and from ingestion of water and fish. IRRIDOSE estimates dose from food crops irrigated with contaminated water. It is conservatively assumed that all of the food consumed by the resident farmer was irrigated with contaminated groundwater.

The air pathway doses calculated in Section 4 include not only direct radiation and inhalation from the airborne plume but also doses from consumption of vegetables, meat, and milk contaminated from the airborne plume. The air pathway dose is also calculated for a unit curie inventory of each radionuclide.

The all-pathways dose from the groundwater pathway and the all-pathways dose from the air pathway are summed to obtain the total all-pathways dose. The total all-pathways dose per curie is ratioed with the all-pathways performance objective of 25 mrem/year to obtain the all-pathways limit for each radionuclide.

6.2 Results

Table 6-1 presents the all-pathways limits for both the 1,000-year and 10,000-year time frames.

These limits for the all pathways are compared with limits derived for the other pathways and with the projected Vault 4 inventory in Section 7. For the projected Vault 4 inventory, none of the radionuclides produces a significantly large fraction of the all-pathways limit.

Table 6-1. All-Pathways Disposal Limits for Saltstone Disposal Vault 4

Radionuclide	1,000-Year Disposal Limit (Ci/Vault 4)	10,000-Year Disposal Limit (Ci/Vault 4)
H-3	1.30E+12	1.30E+12
C-14	1.10E+08	1.10E+08
Al-26	4.86E+18	2.31E+10
Cl-36	3.67E+19	5.15E+18
K-40	1.10E+09	1.31E+04
Ni-59		1.58E+19
Se-79	9.85E+06	1.02E+03
Rb-87		5.12E+09
Sr-90	1.42E+17	1.42E+17
Nb-93m	8.99E+08	1.46E+05
Nb-94		6.98E+17
Mo-93	3.46E+09	6.17E+05
Tc-99		1.07E+17
Pd-107		1.84E+17
Sn-126		2.92E+19
I-129	3.27E+08	4.03E+03
Ra-226		3.84E+16
Np-237		8.93E+18

LADTAP XL©: A SPREADSHEET FOR ESTIMATING DOSE RESULTING FROM AQUEOUS RELEASES

Ali A. Simpkins

APPROVED for Release for
Unlimited (Release to Public)
5/4/2004

Technical Reviewer

February 2004

Westinghouse Savannah River Company
Savannah River Site
Aiken, SC 29808



SAVANNAH RIVER SITE

LADTAP XL©: A SPREADSHEET FOR ESTIMATING DOSE RESULTING FROM AQUEOUS RELEASES

By A. A. Simpkins

**Westinghouse Savannah River Company
Savannah River Site
Aiken, SC 29808**

1. INTRODUCTION

LADTAP XL© is an EXCEL© spreadsheet used at the Savannah River Site (SRS) to estimate dose to offsite individuals and populations resulting from routine releases of radioactive materials to the Savannah River. LADTAP XL© contains two worksheets: LADTAP and IRRIDOSE. The LADTAP worksheet estimates dose for environmental pathways including external exposure resulting from recreational activities on the Savannah River and ingestion of water, fish, and invertebrates of Savannah River origin. IRRIDOSE estimates offsite dose to individuals and populations from irrigation of food crops with contaminated water from the Savannah River.

LADTAP XL© was previously verified prior to adding the IRRIDOSE methods (Hamby 1991a). IRRIDOSE was developed as an independent worksheet in 1993 (Hamby 1993) with methods taken from LADTAP II (Streng 1986) which resides on the IBM Mainframe at SRS. LADTAP XL© version 4.0 includes improvements to the LADTAP worksheet as well as the addition of the IRRIDOSE methods. Since changes were extensive, a complete verification is being performed in accordance with Savannah River Technology Center (SRTC) Quality Assurance (QA) Procedures (SRTC 2001). This document includes model description, verification of methods, and a user's manual.

2. METHODOLOGY

Since methods for irrigation and non-irrigation pathways are contained within two separate worksheets within the LADTAP XL© spreadsheet, they are discussed separately here. LADTAP XL© refers to the entire spreadsheet containing both LADTAP and IRRIDOSE spreadsheets. LADTAP methods refer to all methods except those involving irrigation pathways.

2.1. LADTAP Methods

The LADTAP transport model estimates river concentrations assuming a continuous and constant release of a period of one year. Nuclide concentrations are determined by simple volumetric dilution without taking into account nuclide depletion except through radioactive

decay. Additional dilution in the Savannah River estuary is further accounted for by use of a dilution factor.

2.1.1. Determination of Nuclide Concentrations

LADTAP worksheet implements the liquid-release dose models of USNRC (1977b). These dose models involve a complex series of physical, chemical, and biological processes. Some of these processes involve dilution, while others involve physical or biological reconcentration followed by transfer through various pathways to man.

The environmental effects of radioactive releases to surface waters are evaluated through a variety of pathways: 1) water ingestion, 2) aquatic food consumption, and 3) recreational use of water bodies and shores. The relative importance of the three main liquid pathways generally depends on the radionuclides of concern and their release amounts. However, for routine SRS liquid releases to the Savannah River, the exposure pathways involving the consumption of river water and aquatic foods have been demonstrated to be the most significant (Jannik 1997).

All individual and population doses are based on the assumption that liquids discharged from an SRS facility are completely mixed in the river before reaching the potentially exposed individuals. This assumption is supported by annual tritium mass-balance measurements indicating that complete mixing occurs in the river prior to reaching River Mile 118.8 (U.S. Highway 301 bridge), which is the assumed location of the maximally exposed individual (Jannik 1997). The dose calculations also are based on the conservative assumption that sediment adsorption does not occur and radionuclides are not depleted during transport (with the exception of radiological decay), even though limited data on cesium-137 indicates that there is a significant reduction in cesium concentration via deposition (Hayes 1983a; 1983b) (ranging from 48% in the river water to 98% in the finished water).

For annual routine releases, offsite dose varies each year with the amount of radioactivity released and the amount of dilution (flow rate) in the Savannah River. Although daily flow rates are measured at gauging stations at the SRS Boat Dock and at River Mile 118.8, these data are not used directly in dose calculations. This is because daily river flow rates fluctuate widely (i.e., short-term dilution varies from day to day). Instead, "effective" flow rates, which are based on annual-average measured concentrations of tritium and the total quantity of aqueous tritium released from the site during the year, are used and are calculated by:

$$F_{\text{eff}} = \frac{Q_i \cdot CF}{C_i} \quad (1)$$

where:

F_{eff} "effective" flow rate (cfs)

Q_i annual amount of aqueous tritium released from SRS and Plant Vogtle (Ci/yr)

CF conversion factor (1.1198 yr ft³ pCi / sec mL Ci)

\overline{C}_i the annual average tritium concentration measured in river water (River Mile 118.8 concentration for MEI dose, raw water concentration from down river treatment plants for population dose) (pCi/mL)

For prospective dose assessments, historical flow rates are utilized to determine daily and annual average flows (Hayes and Marter 1991). Recommended flow rates for prospective studies are shown in Table 1.

Table 1 Savannah River Flow Rates for Prospective Dose Assessments

Assessment (flow average)	Flow Rate (cfs) at Specified Location	
	River Mile 118.8	Water Treatment Plants
Routine (annual average)	10,500	13,000
Minimal Flow (annual average)	5,300	6,600
Accident (daily average)	3,900	4,900

* from Hayes and Marter (1991)

The analytical methods used for estimating radiation exposure to man from the various liquid pathways are described in the following sections. For the maximally exposed individual, the doses from all pathways are summed to determine the total dose. Dose to the population is calculated by summing average doses to the following receptors:

- drinking water users at the Beaufort-Jasper and Port Wentworth treatment plants
- recreational users of the Savannah River
- consumers of fish from the Savannah River
- consumers of invertebrates from the Savannah River estuary

2.1.2. Water Ingestion

The dose to the maximally exposed individual (MEI) from drinking river water is estimated assuming the river water has not been treated. Predictions of population dose, however, are made with the assumption that the water has been processed through one of the down river water treatment facilities at Beaufort/Jasper or Port Wentworth, although removal of radionuclides during the treatment process is not considered. The annual average concentration of radionuclide *i* in the Savannah River is estimated by volumetric dilution. The river concentration at the receptor location is given by:

$$\bar{C}_i = \frac{Q_i \cdot CF}{F_{\text{eff}}} \quad (2)$$

where

\bar{C}_i annual average concentration of radionuclide i in river water (pCi/mL)

Q_i annual amount of radionuclide i released (Ci/yr)

CF conversion factor (1.1198yr ft³ pCi / sec mL Ci)

F_{eff} "effective" flow rate (from equation 1) (cfs)

The annual MEI internal dose from consumption of river water is then calculated by:

$$D_w^{\text{ing}} = U_w \cdot \sum_i \bar{C}_i \cdot DF_i \cdot e^{-\lambda_i \cdot t} \quad (3)$$

where

D_w^{ing} annual effective dose equivalent (EDE) to MEI from consumption of river water (mrem)

U_w annual maximum water consumption rate (for MEI, assumed to be 730 L, or 730,000 mL) (USNRC 1977a)

\bar{C}_i annual average concentration of radionuclide i in river water at River Mile 118.8 (from equation 2) (pCi/mL)

DF_i ingestion dose factor for radionuclide i (mrem/pCi) (USDOE 1988b)

λ_i radioactive decay constant of radionuclide i (d)

t elapsed time between release of the radionuclide and ingestion of water, (assumed to be 1.5 d for MEI and 4 d for water treatment plant consumers) (Hamby 1991a)

The exponential expression in equation 3 yields the concentration of radionuclide i at the time the water is consumed. Again, no credit is taken for possible radionuclide removal by water treatment purification processes. Water ingestion population doses are estimated for Beaufort-Jasper and Port Wentworth treatment plant consumers by multiplying the consumer population times the average individual drinking water dose:

$$D_{w\text{-pop}}^{\text{ing}} = \frac{U_w \cdot N}{1000} \cdot \sum_i \bar{C}_i \cdot DF_i \cdot e^{-\lambda_i \cdot t} \quad (4)$$

where

- D_w^{ing} annual population EDE at Beaufort-Jasper or Port Wentworth, from consumption of treated river water (person-rem)
- U_w annual average water consumption rate (assumed to be 370 L or 370,000 mL) (Hamby 1991a)
- N the applicable consumer population (112,000 persons at Beaufort-Jasper or 11,000 persons at Port Wentworth) (Mamatey 2003)
- 1000 conversion factor (mrem/rem)
- \bar{C}_i annual average concentration of radionuclide i in river water at Beaufort-Jasper or Port Wentworth, (from equation 2) (pCi/mL)
- DF_i ingestion dose factor for radionuclide i (mrem/pCi) (USDOE 1988b)
- λ_i radioactive decay constant of radionuclide i (d)
- t elapsed time between release of the radionuclide and ingestion of water, (assumed to be 4 d for water treatment plant consumers) (Hamby 1991b)

2.1.3. Aquatic Food Consumption

The concentrations of radionuclides in aquatic foods are assumed to be directly related to the concentrations of the radionuclides in the river water. With the exception of a site-specific factor of 3,000 L/kg for cesium accumulation in freshwater fish (Jannik 2003), the aquatic animal bioaccumulation factors, which are the equilibrium ratios between concentration in aquatic foods and concentration in water, can be found in Thompson (1972).

The dose to the maximally exposed individual from aquatic food consumption is estimated assuming the consumption of 19 kg/yr of fish harvested from the River Mile 118.8 location (Hamby 1991b). Because the Savannah River is closed indefinitely to shellfish harvesting, the consumption of fresh water invertebrates is not considered for the MEI or the population dose estimates (Hamby 1994). The population dose is determined assuming that the total harvest is consumed by the 80-km population. The annual average consumption rate of aquatic foods (9 kg/yr of fish and 2 kg/yr of saltwater invertebrates) is a prorated amount of aquatic foods harvested (Hamby 1991b). In the case of a small population or large annual harvest, some of the harvested seafood is assumed to be exported from the 80-km region. Only the aquatic foods needed to support the 80-km population are assumed to be consumed.

The annual MEI internal dose from consumption of aquatic foods is determined by:

$$D_{af}^{ing} = U_{af} \cdot 1,000 \cdot \sum_i \bar{C}_i \cdot BF_i \cdot DF_i \cdot e^{-\lambda_i \cdot t} \quad (5)$$

where

D_{af}^{ing} annual EDE to MEI from consumption of aquatic foods (mrem)

U_{af} annual maximum aquatic food consumption rate (for MEI, assumed to be 19 kg) (Hamby 1991b)

1,000 conversion factor mL/L

\bar{C}_i annual average concentration of radionuclide i in river water at River Mile 118.8 (from equation 2) (pCi/mL)

BF_i bioaccumulation factor for radionuclide i (L/kg) (Thompson 1972)

DF_i ingestion dose factor for radionuclide i (mrem/pCi) (USDOE 1988b)

λ_i radioactive decay constant of radionuclide i (d)

t elapsed time between harvest and consumption of fish, (assumed to be 2 d for MEI) (Hamby 1991b)

2.1.4. Population Dose Estimates

Population dose from the consumption of aquatic foods is estimated by adding the dose from the sport fish harvest, the commercial fish harvest, and the saltwater invertebrate harvest. The population dose is determined by adding the dose from equations 6 through 8.

In LADTAP, it is conservatively assumed that all fish and invertebrates harvested commercially from the Savannah River are consumed by the population within 80 km of SRS. Because of the lack of age-specific dose conversion factors, the populations within 80-km of SRS, and the downstream water consumers, are assumed to be adults.

2.1.5. Sport Fish

The population dose from ingestion of sport fish is estimated by the following equation:

$$D_{sf-pop}^{ing} = HARVEST_{sf} \cdot \sum_i \bar{C}_i \cdot BF_i \cdot DF_i \cdot e^{-\lambda_i \cdot t} \quad (6)$$

where

D_{sf-pop}^{ing} annual population EDE from consumption of sport fish (person-rem)

$HARVEST_{sf}$ the lesser amount of the actual sport fish harvested by the 80 km population during the year (35,000 kg-person, from Hamby 1991b) and the total 80-km population fish consumption for the year (assumed to be 9 kg x 714,000 persons or 6,400,000 kg-person,) (kg-person)

\bar{C}_i annual average concentration of radionuclide i in river water at River Mile 118.8, (from equation 2) (pCi/mL)

BF_i bioaccumulation factor for radionuclide i (L/kg) (Thompson 1972)

DF_i ingestion dose factor for radionuclide i (mrem/pCi) (USDOE 1988b)

λ_i radioactive decay constant of radionuclide i (d)

t elapsed time between harvest and consumption of sport fish, (assumed to be 10 d for MEI) (Hamby 1991b)

2.1.6. Commercial Fish

The population dose for ingestion of commercial fish is estimated by the following equation:

$$D_{cf-pop}^{ing} = HARVEST_{cf} \cdot \sum_i \bar{C}_i \cdot BF_i \cdot DF_i \cdot e^{-\lambda_i \cdot t} \quad (7)$$

where

D_{cf-pop}^{ing} annual population EDE from consumption of commercial fish (person-rem)

$HARVEST_{cf}$ the lesser amount of the actual commercial fish harvested by the 80 km population during the year (2,700 kg-person, from Hamby 1991b) and the difference between the total 80-km population fish consumption for the year (assumed to be 9 kg x 714,000 persons or 6,400,000 kg-person) and the total 80-km sport fish harvest (kg-person)

\bar{C}_i annual average concentration of radionuclide i in river water at River Mile 118.8, (from equation 2) (pCi/mL)

BF_i bioaccumulation factor for radionuclide i (L/kg) (Thompson 1972)

DF_i ingestion dose factor for radionuclide i (mrem/pCi) (USDOE 1988b)

- λ_i radioactive decay constant of radionuclide i (d)
- t elapsed time between harvest and consumption of commercial fish, (assumed to be 13 d for MEI) (Hamby 1991a)

2.1.7. Saltwater Invertebrates

The population dose from the ingestion of saltwater invertebrates is estimated by the following equation:

$$D_{\text{swi-pop}}^{\text{ing}} = \text{HARVEST}_{\text{swi}} \cdot \sum_i \frac{\bar{C}_i}{3} \cdot \text{BF}_i \cdot \text{DF}_i \cdot e^{-\lambda_i \cdot t} \quad (8)$$

where:

- $D_{\text{swi-pop}}^{\text{ing}}$ annual population EDE from consumption of saltwater invertebrates (person-rem)
- $\text{HARVEST}_{\text{swi}}$ the lesser amount of the actual saltwater invertebrates harvested by the 80 km population during the year (390,000 kg-person, from Hamby 1991b) and the total 80-km population invertebrate consumption for the year (assumed to be 2 kg x 714,000 persons or 1,400,000 kg-person, from Hamby 1991b) (kg-person)
- \bar{C}_i annual average concentration of radionuclide i in river water from the Savannah River estuary, (from equation 2) (pCi/mL)
- 3 factor to account for tidal dilution (Hamby 1991a)
- BF_i bioaccumulation factor for radionuclide i in saltwater invertebrates (L/kg) (Thompson 1972)
- DF_i ingestion dose factor for radionuclide i (mrem/pCi) (USDOE 1988b)
- λ_i radioactive decay constant of radionuclide i (d)
- t elapsed time between harvest and consumption of saltwater invertebrates, (assumed to be 13 d for MEI) (Hamby 1991a)

2.1.8. Recreational Use of the Savannah River

LADTAP considers four exposure modes when estimating individual and population external dose during recreational use of the Savannah River; (1) exposure to radionuclide deposits on the shoreline, (2) exposure to suspended nuclides while swimming, (3) exposure to suspended nuclides while boating, and (4) absorption of tritium through the skin while swimming.

2.1.8.1. Shoreline

The calculation of dose from shoreline deposits is complex because it involves estimations of sediment load, transport, and concentrations of radionuclides associated with suspended and deposited materials (Soldat 1974). However, the following equation simplifies the estimation of radiation dose to the MEI from exposure to shoreline sediments:

$$D_{SH}^{ext} = T_{w-s} \cdot U_{SH} \cdot W_{SH} \cdot 1000 \cdot \sum_i \bar{C}_i \cdot \tau_i \cdot DF_i^{gs} \cdot [e^{-\lambda_i \cdot t_p}] [1 - e^{-\lambda_i \cdot t_b}] \quad (9)$$

where:

- D_{SH}^{ext} annual EDE to the MEI from shoreline deposits (mrem)
- T_{w-s} water-to-sediment transfer coefficient (100 L/m²-d) (Simpson 1980)
- U_{SH} annual shoreline usage factor specifying the time of exposure to shoreline sediments (assumed to be 23 hr for the MEI)
- W_{SH} shoreline width factor, dimensionless (0.2 for river shoreline) (Simpson 1980)
- 1,000 conversion factor (mL/L)
- \bar{C}_i annual average concentration of radionuclide *i* in river water at River Mile 118.8, (from equation 2) (pCi/mL)
- τ_i half life of radionuclide *i* (d)
- DF_i^{gs} ground shine dose factor for radionuclide *i* (mrem-m²/pCi-hr) (USDOE 1988a)
- λ_i decay constant of radionuclide *i* (d⁻¹)
- t_p elapsed time between release of the radionuclide and the point of exposure (assumed to be 1 d for MEI and population) (Hamby 1991b)
- t_b period of time for which sediment or soil is exposed to the contaminated water (40 yr) (Hamby 1991a) (d)

The population dose estimate from shoreline exposure is determined by substituting into equation 9 the assumed population exposure time of 960,000 person-hrs (Hamby 1991a) for the individual shoreline exposure time (U_{SH}). It is assumed that the buildup and decay of radionuclides (based on the current year's release) in the Savannah River shoreline sediments has occurred for the past 50 years, which is the approximate operating period of SRS facilities.

2.1.8.2. Swimming and Boating

Predictions of external dose while swimming in the Savannah River are determined assuming uniform nuclide concentrations and complete submersion (4π geometry). Boating doses are estimated assuming a 2π geometry with no shielding considerations. The same water submersion dose factors (USDOE 1988a) are used for both swimming and boating estimates. Shielding provided by the boat's hull is not considered. The external dose received by the MEI from swimming or boating is estimated by:

$$D_{S/B}^{ext} = G_{S/B} \cdot U_{S/B} \cdot 114.2 \cdot \sum_i \bar{C}_i \cdot DF_i^{sub} \cdot e^{-\lambda_i \cdot t_p} \quad (10)$$

where:

$D_{S/B}^{ext}$ annual EDE to the MEI from swimming and boating (mrem)

$G_{S/B}$ geometry factor (1 for swimming and 0.5 for boating) (Hamby 1991a)

$U_{S/B}$ annual MEI usage factor (8.9 hrs for swimming and 21 hrs for boating) (Hamby 1991b)

114.2 conversion factor (mL-yr/m³-hrs)

\bar{C}_i annual average concentration of radionuclide i in river water at River Mile 118.8, (from equation 2) (pCi/mL)

DF_i^{sub} submersion dose factor for radionuclide i (mrem-m³/pCi-hr) (USDOE 1988a)

λ_i decay constant of radionuclide i (d⁻¹)

t_p elapsed time between release of the radionuclide and the point of exposure (assumed to be 1 d for MEI and population) (Hamby 1991b)

The population dose estimates from swimming and boating exposure are performed by substituting into equation 10 the assumed population usage times of 160,000 person-hrs for swimming and 1,100,000 person-hrs for boating (Hamby 1991a) for the individual swimming and boating usage times ($U_{S/B}$).

Because tritium concentrations in the Savannah River are potentially high enough to cause a significant dose from skin absorption (relative to the external dose from swimming and boating), LADTAP was written to consider the tritium dose via skin absorption while swimming (Hamby 1991a). The dose from skin absorption while swimming is estimated by:

$$D_S^{abs} = U_S \cdot \bar{C}_T \cdot DF_T^{int} \cdot I^{abs} \quad (11)$$

where:

- D_S^{abs} annual EDE to the MEI from skin absorption of tritium while swimming (mrem)
- U_S annual MEI usage factor (8.9 hrs for swimming) (Hamby 1991b)
- \bar{C}_T annual average concentration of tritium in measured river water at River Mile 118.8, (pCi/mL)
- DF_T^{int} tritium internal dose factor (mrem-m³/pCi-hr) (USDOE 1988b)
- I^{abs} water absorption rate for total body submersion (35 mL/hr) (Hamby 1991a)

Because of its relatively long half-life, radioactive decay of tritium is not considered. The population dose from the absorption of tritium while swimming is determined by substituting into equation 11 the assumed population usage time of 160,000 person-hrs for swimming for the individual swimming usage time (U_S).

Water from the Savannah River is processed for consumption at two facilities approximately 100 river miles downstream of the SRS. The Beaufort-Jasper Water Treatment Plant, a facility supplying Beaufort and Jasper Counties in South Carolina, utilizes river water for service to water consumers. Several miles further downstream, the City of Savannah Industrial and Domestic Water Supply Plant (formally Cherokee Hill Water Treatment Plant), located near Port Wentworth, GA, withdraws water from the river to supply a business-industrial complex near Savannah, Georgia.

The total population dose resulting from a routine SRS release is the sum of four contributing categories: 1) Beaufort-Jasper water consumers, 2) Port Wentworth water consumers, 3) consumption of fish and invertebrates of Savannah River origin, and 4) recreational activities on the Savannah River.

For 2003, the Beaufort-Jasper water treatment authority estimates that its consumer population was approximately 112,000. The Port Wentworth commercial and industrial consumers of Savannah River water are estimated to be 11,000. These estimates are subject to change and should be verified annually. The transit time from the Savannah River at Steel Creek to the water treatment river intakes is approximately 72 hours. The raw river water is assumed to have an average system retention time of 24 hours before distribution to water consumers. Therefore, a total holdup time of 96 hours is used in the calculation of drinking water dose to the downstream population. This holdup time is only significant for nuclides with very short half-lives.

The 80-km population receives no river water downstream of SRS for domestic purposes. However, this population is assumed to use the river for the harvesting of fish and invertebrates and for recreational purposes. Dose from the consumption of aquatic foods is

calculated assuming the concentrations of radionuclides in edible tissues are under equilibrium or steady-state conditions with that in the surrounding water.

2.2. IRRIDOSE Methods

IRRIDOSE is the second worksheet within the LADTAP XL© spreadsheet and dose is estimated using a three-stage process: 1) concentrations in the irrigation water are determined, 2) concentrations in foodstuffs are determined, and 3) potential doses to an MEI and the population are estimated.

2.2.1. Nuclide Concentrations in Water Used for Irrigation

Concentrations of nuclides in the Savannah River released from SRS facilities are determined using a simple dilution model. Releases are assumed to occur at a constant rate throughout the release period (one year) and are diluted instantaneously by the Savannah River. Complete mixing and dilution is assumed to have occurred by the time the contaminated water is used for irrigation. Rainfall dilution is not considered. Estimates of nuclide concentrations in the Savannah River are given by:

$$C_{iw} = \frac{cRe^{-\lambda_t t_t}}{F} \quad (12)$$

where:

C_{iw} concentration of nuclide I in river water (pCi/L)

c conversion factor (1.12E-09 ft³/yr/L s)

R activity release rate (pCi/yr)

λ_t radiological decay constant (1/d)

t_t transport time down river (d)

F effective flow rate (ft³/s)

2.2.2. Nuclide Concentration in Vegetable Crops and Fodder

Nuclide concentration in vegetation are calculated assuming that two uptake paths exist; 1) via direct deposition on plant surfaces, and 2) via uptake through the plants root system. The following equation is used to estimate concentrations of nuclides in both vegetation and fodder.

$$C_{iv} = C_{iw} \cdot I \cdot (\text{leaf} + \text{root}) \cdot e^{-\lambda_t t_h} \quad (13)$$

where:

$$\text{leaf} = \frac{r(1 - e^{-\lambda_e t_e})}{Y_v \lambda_e} \quad (14)$$

$$\text{root} = \frac{B_{iv}(1 - e^{-\lambda_e t_b})}{P \lambda_e} \quad (15)$$

- C_{iv} concentration of nuclide I in vegetation (pCi/kg)
 C_{iw} concentration of nuclide I in river water (pCi/L)
 I irrigation rate (L/m²d)
 t_h vegetable hold-up time
 r retention of radionuclide on plant surface (unitless)
 λ_e weathering and radiological decay constant (1/d)
 t_e vegetation exposure/irrigation duration (d)
 Y_v vegetation production yield (kg/m²)
 B_{iv} plant-to-soil ratio (unitless)
 t_b buildup time of radionuclides in soil (d)
 P surface soil density (kg/m²)

All other terms have been previously defined.

Plant to soil ratios were taken from USNRC (1977a) where possible and for those not available in the regulatory guide Yu et. al (2001) and Baes et al. (1984) were used.

The 'leaf' and 'root' equations shown above account for the uptake pathways described above. Changes in the parameter values of vegetation holdup time, vegetation exposure duration, and vegetation production yield are required for calculating concentrations in vegetables grown for human consumption and fodder (Bermuda grass). The vegetation holdup time for estimated fodder concentration is normally zero indicating that cattle consume grass directly from grazing while the holdup time for vegetable concentration estimates varies, indicating the time between harvest and consumption. For individual dose calculations, holdup times are assumed to be relatively short since the maximally exposed individual is someone with a backyard garden.

All concentrations of nuclides in vegetation are determined using the method described above and equation 13 with the exception of tritium which is discussed next

2.2.3. Tritium concentration in Vegetation

The model for estimating tritium concentration in vegetation following irrigation is based on a very simple concept; the concentration of tritium in plant water, C_{sv} , is assumed to be equal to the concentration of tritium in the water used for irrigation, C_{iw} .

Radiological decay is not considered since the half-life of tritium is very long relative to vegetation transport times. Fodder, produce, and leafy vegetables all are assumed to have the same tritium concentrations dependent on the tritium concentrations of the water. This assumption is very conservative in that dilution by rainfall is not considered.

2.2.4. Nuclide Concentration in Meat and Milk

Concentrations of nuclides in the beef and milk of cattle grazing on irrigated pasture grass are determined as follows:

$$C_{ib} = F_{ib} [f_f C_{if} Q_f + f_w C_{iw} Q_w] e^{-\lambda_i t_b} \quad (16)$$

$$C_{im} = F_{im} [f_f C_{if} Q_f + f_w C_{iw} Q_w] e^{-\lambda_i t_m} \quad (17)$$

where:

C_{ib} concentration of nuclide I in beef (pCi/kg)

C_{im} concentration of nuclide I in milk (pCi/L)

F_{ib} transfer fraction from fodder to beef (d/kg)

F_{im} transfer fraction from fodder to milk (d/L)

F_f fraction of fodder taken from irrigated pasture (unitless)

C_{if} concentration of nuclide I in fodder (pCi/kg)

Q_f cattle consumption rate of fodder (kg/d)

f_w fraction of water taken from Savannah River

Q_w cattle consumption rate of water (l/d)

t_b harvest to consumption time for beef (d)

t_m harvest to consumption time for milk (d)

The model allows the user to consider ingestion of both water and fodder contaminated from the release of radioactivity to the Savannah River, however, pasture grass is generally not irrigated and water is probably supplied by surface ponds or groundwater surfaces.

2.2.5. Individual Ingestion Dose

The dose to an individual who consumes vegetables, meat and milk produced on land irrigated with contaminated water is calculated by the following equations

$$D_i^{veg} = DF_i \cdot C_{iv} (U_v + U_l) \quad (18)$$

where:

D_i^{veg} individual dose from irrigation (mrem/y)

DF_i ingestion dose factor for nuclide I (mrem/pCi)

U_v vegetable consumption rate (kg/y)

U_l leafy vegetable consumption rate (kg/y)

C_{iv} concentration of nuclide I in vegetation (pCi/kg)

$$D_i^b = DF_i \cdot C_{ib} \cdot U_b \quad (19)$$

where:

U_b beef consumption rate (kg/y)

C_{ib} concentration of nuclide I in beef (pCi/kg)

$$D_i^m = DF_i \cdot C_{im} \cdot U_m \quad (20)$$

where:

U_m milk consumption rate (L/y)

C_{im} concentration of nuclide I in milk (pCi/L)

Dose to the individual from irrigation is not a function of the land area irrigated. Ingestion dose factors are calculated following the ICRP 26 methodology (ICRP 1977) as implemented in ICRP 30(1979). Specifically the dose factors are those specified by the Department of Energy (USDOE 1988). The total dose to the MEI is the sum of the above three pathways.

2.2.6. Population Ingestion Dose

Dose to a population of individuals consuming irrigated foodstuffs can be calculated by one of two methods: the irrigated land area method or the population count method. The two methods are provided so that population dose can be calculated if the analysis calls for the irrigation of a given area of land or the irrigation of crops necessary to support a family farm. The irrigated land area method is typically used, but the population count method is included as an option.

2.2.6.1. Irrigated Land Area Method

The irrigated land area method is used to estimate the population dose resulting from the irrigation of a particular size farm or garden. The land area is assumed to produce, simultaneously, the foodstuffs of each food ingestion pathways discussed above. Beef and milk cattle are assumed to graze on the irrigated land with production yields equal to the average productions yields within 50 miles of the SRS. The total production for the land area entered is used to estimate the population dose using the following equation for each pathway:

$$D_i^{\text{pop}} = DF_i \cdot C_{ik} \cdot TP_k \cdot 10^{-3} \frac{\text{rem}}{\text{mrem}} \quad (21)$$

where:

D_{ik} population dose for foodstuff k (person-rem/yr)

C_{ik} concentration of foodstuff k (pCi/kg)

TP_k total production of foodstuff k in area of interest (kg-person)

2.2.6.2. Population Count Method

Population dose also can be estimated by assuming that the consumption of vegetables, beef, and milk by a given number of people is supported by a family farm irrigated with the Savannah River water. The population count methods estimates dose using the following equation for each pathway:

$$D_i^{\text{pop}} = DF_i \cdot C_{ik} \cdot N \cdot \bar{U}_k \cdot 10^{-3} \frac{\text{rem}}{\text{mrem}} \quad (22)$$

where:

N number of individuals consuming foodstuff from the irrigated area

U_k average consumption rate of foodstuff k (kg/yr)

3. VERIFICATION OF MODELS

**RESPONSE TO RAI COMMENT 67
ROADMAP TO REFERENCES**

REFERENCED DOCUMENT	*EXCERPT LOCATION	REMARK
Phifer and Nelson 2003 Section 4.0	Excerpt enclosed following response.	
Figure 4.7-1	Excerpt included in response.	
Table 5.4-1	Excerpt included in response.	

***Excerpt Locations:**

1. Excerpt included in response: The excerpt is included within the text of the response or is appended to the response.
2. Excerpt enclosed following response: The excerpt is enclosed on a separate sheet or sheets following the response.
3. Representative excerpt(s) enclosed following response: Representative excerpts from a document that is wholly or largely applicable are enclosed following the response.
4. Other

APPROVED for Release for
Unlimited (Release to Public)

7/14/2005

APPROVED for Release for
Unlimited (Release to Public)
3/19/2004

WSRC-TR-2003-00436 ←

Revision 0

KEY WORDS:
Saltstone Disposal Facility
Performance Assessment
Closure Cap

**SALTSTONE DISPOSAL FACILITY
CLOSURE CAP CONFIGURATION AND DEGRADATION
BASE CASE:
INSTITUTIONAL CONTROL TO PINE FOREST SCENARIO (U)**

SEPTEMBER 22, 2003

PREPARED BY:

Mark A. Phifer^a

Eric A. Nelson^a

Westinghouse Savannah River Company LLC^a

**Westinghouse Savannah River Company LLC
Savannah River Site
Aiken, SC 29808**



Prepared for the U.S. Department of Energy under Contract No. DE-AC09-96SR18500

→ 4.0 CLOSURE CAP CONFIGURATION

Sections 4.1 through 4.6 provide a progressive reevaluation of the closure cap configuration previously presented in Section 2.0. The changes made in a previous section are carried over into the evaluation of subsequent sections, until all changes have been discussed and made. The final revised closure cap configuration is summarized in Section 4.7, Figure 4.7-1 and Table 4.7-1.

4.1 Hydraulic Barrier

As outlined in section 2.0, the current SDF PA (MMES 1992) and closure plan (Cook et al. 2000) assume that controlled compacted kaolin is utilized as the closure cap hydraulic barrier layer. However the previously planned controlled compacted kaolin layer for the E-Area Low-Level Waste Facility closure cap was replaced with a geosynthetic clay liner (GCL) as the hydraulic barrier layer within revision 2 of the 'Closure Plan for the E-Area Low-Level Waste Facility' (Cook et al. 2002b). The applicability of also replacing the kaolin layers in the SDF closure cap with GCLs is investigated herein. The acceptability of this change in the hydraulic barrier layer for E-Area was documented within 'Unreviewed Disposal Question Evaluation: Closure Cap Design Change from Compacted Kaolin to Geosynthetic Clay Liner' (Jones and Phifer 2003). An overview of the reasoning for the E-Area change is presented below (Cook et al. 2002a; Cook et al. 2003; Jones and Phifer 2003).

A GCL consists of "bentonite sandwiched between two geotextiles" (USEPA 2001). Bentonite, the hydraulically functional portion of a GCL, is the general term given to a swelling-type montmorillonite clay which formed as the stable alteration product of volcanic ash (Worrall 1975; Jones and Phifer 2003). Therefore bentonite is expected to remain mineralogically and chemically stable. The following is the definition of a Geotextile GCL as defined by the Environmental Protection Agency (USEPA 2001):

A Geotextile GCL "is a relatively thin layer of processed" bentonite ... "fixed between two sheets of geotextile. ... A geotextile is a woven or nonwoven sheet material ... resistant to penetration." ... "Adhesives, stitchbonding, needlepunching, or a combination of the three" are used to affix the bentonite to the geotextile. "Although stitchbonding and needlepunching create small holes in the geotextile, these holes are sealed when the installed GCL's clay layer hydrates."

The following are some of the typical advantages of a Geotextile GCL over compacted clay layers, which led to the replacement of the compacted kaolin with a GCL:

- A GCL has a lower hydraulic conductivity than compacted kaolin (i.e. $< 5.0 \times 10^{-9}$ cm/s for a GCL versus $< 1.0 \times 10^{-7}$ cm/s for a compacted kaolin layer) (Phifer 1991; USEPA 2001; GSE 2002)
- Infiltration through a GCL closure cap is generally lower than infiltration through a compacted kaolin closure cap (Cook et al. 2002a; Jones and Phifer 2003).
- A GCL is faster and easier to install than an equivalent compacted kaolin layer (USEPA 2001). Installation of a GCL essentially consists of unrolling the dry GCL like a carpet, overlapping adjacent GCL panels, and covering the GCL with at least a foot of soil. Whereas compacted kaolin must be installed wet of optimum to tight moisture and density controls in multiple lifts with heavy equipment. (Jones and Phifer 2003)
- The bulk of the required Quality Assurance / Quality Control (QA/QC) associated with a GCL is factory based whereas that of compacted kaolin is entirely field based. Factory based QA/QC generally provides a higher degree of QA/QC, and it is included in the cost of the material. (Phifer 1991; GSE 2002; Jones and Phifer 2003)
- Installation of a GCL hydraulic barrier generally costs less than installation of an equivalent compacted kaolin layer (USEPA 2001; Jones and Phifer 2003).

- Installation of a GCL is generally safer than installation of an equivalent compacted kaolin layer, since less heavy equipment use is required (Jones and Phifer 2003).
- A GCL has the ability to self-heal rips or holes, whereas compacted kaolin does not. Additionally a GCL can undergo repeated cycles of dehydration and hydrate without negative impacts to the GCL's saturated hydraulic conductivity, whereas compacted kaolin may irreversibly shrink, crack, and incur increases in its saturated hydraulic conductivity (Phifer 1991; Phifer et al. 1995; Rumer and Ryan 1995; USEPA 2001).
- A GCL incurs less negative impact "due to differential settlement, freezing-thawing cycles, and wetting-drying cycles" than a compacted kaolin layer (Rumer and Mitchell 1995).
- A GCL is not as thick as a compacted kaolin layer (USEPA 2001).
- Hydraulic barriers consisting of compacted clay are 1970's and 1980's technology whereas GCLs are 1990's technology (Jones and Phifer 2003).

The same reasoning for the E-Area change is applicable to the SDF. In order to confirm that replacement of the SDF closure cap compacted kaolin hydraulic barrier with a GCL is appropriate, HELP modeling has been performed. The modeling has been performed to demonstrate that a GCL closure cap is equivalent to or better than the current kaolin closure cap in terms of percolation through the cap and out the facility bottom. Table 4.1-1 provides a comparison of the two configurations from top to bottom. Both configurations consist of 119 inches of material from the top of the upper gravel drainage layer to the bottom of the clean grout on top of the concrete vault roof as required by the PA resident scenario intruder analysis.

Table 4.1-1. Closure Cap Configuration Comparison

Current Kaolin Closure Cap		Replacement GCL Closure Cap	
Layer	Thickness (inches)	Layer	Thickness (inches)
Topsoil	6	Topsoil	6
Backfill	30	Backfill	30
Gravel Drainage	12	Drainage Layer	12
Kaolin	30	GCL	0.2
Backfill	12	Backfill	61.28
Gravel Drainage	6	Drainage Layer	6
Kaolin	19.68	GCL	0.2
Clean Grout	39.37 (1 m)	Clean Grout	39.37 (1 m)
Concrete Vault Roof	4	Concrete Vault Roof	4
Clean Grout	16	Clean Grout	16
Saltstone	288	Saltstone	288
Concrete Vault Floor	30	Concrete Vault Floor	30

Several required HELP model input parameters are common to both configurations. Table 4.1-2 provides a listing of these generic input parameters (i.e., HELP model query) and the associated values selected. Use of selected fixed values for these HELP model queries provides compatibility between the different HELP model runs. The landfill area is based upon the length (600 feet) and width (200 feet) of vault 4, which results in a surface area of 120,000 feet squared or 2.75 acres. It has been assumed that the final covers are appropriately sloped so that 100 percent of the covers allow runoff to occur (i.e., there are no depressions). A yes response has been provided to the HELP model

query, which asks, "Do you want to specify initial moisture storage? (Y/N)." The amount of water or snow on the surface of the covers was assumed to be zero as the initial model condition.

Table 4.1-2. Generic Input Parameter Values

Input Parameter (HELP Model Query)	Generic Input Parameter Value
Landfill area =	2.75 acres
Percent of area where runoff is possible =	100%
Do you want to specify initial moisture storage? (Y/N)	Y
Amount of water or snow on surface =	0 in.

As stated the initial moisture storage has been specified for all soil layers. While the initial moisture storage is not a fixed value for all runs, a fixed method of selecting the initial moisture storage value has been utilized for consistency. The initial, soil moisture storage value has been selected as follows:

- The initial moisture storage of soil layers designated as either a vertical percolation layer or a lateral drainage layer was set at the field capacity of the soil.
- The initial moisture storage of soil layers designated as a barrier soil liner was set at the porosity of the soil.

The Soil Conservation Service (SCS) runoff curve number (CN) is another required HELP model input parameter that has been made consistent. The HELP model provides three options to specify the CN. The option that produces a HELP model computed curve number, based on surface slope and slope length, soil texture of the top layer, and vegetation, was utilized. Table 4.1-3 provides the input values of surface slope and slope length, soil texture of the top layer, and vegetation that were utilized to produce the HELP model computed curve number. The 3 percent slope is that specified for the top surface of the Saltstone final cover within the Saltstone closure plan (Cook et al. 2000). The 600-foot slope length is the length of an individual Saltstone vault (Cook et al. 2000). The soil texture selected as an input for calculation of the CN is a loamy fine sand per the United States Department of Agriculture (USDA) and a silty sand per Unified Soil Classification System (USCS), since it closely represents the typical vegetative soil layers utilized at SRS. The corresponding number in the HELP default soil texture list is 5. Based upon these input parameter values the HELP model computed a CN of 53.40.

Table 4.1-3. Input Parameters for HELP Model Computed Curve Number

CN Input Parameter (HELP Model Query)	CN Input Parameter Value
Slope =	3%
Slope length =	600 ft
Soil Texture =	5 (HELP model default soil texture)
Vegetation =	4 (i.e., a good stand of grass)
HELP Model Computed Curve Number = 53.40	

Table 4.1-4 provides a comparison of the HELP model results for both configurations. The HELP model estimate for the average annual percolation through the upper kaolin hydraulic barrier layer was approximately 0.90 inches/year, while that through the upper GCL hydraulic barrier layer was approximately 0.47 inches/year, approximately half that through the kaolin. The HELP model estimate for the average annual percolation through the lower kaolin hydraulic barrier layer was approximately 0.84 inches/year, while that through the lower GCL hydraulic barrier layer was

approximately 0.055 inches/year, approximately fifteen times less than that through the kaolin. For both configurations the average annual percolation through the vault floor was estimated to be 0.00001 inches/year, however this percolation is controlled by the very low saturated hydraulic conductivity of the vault roof and floor (see Table 3.0-2) rather than by the closure cap hydraulic barrier layers. The results clearly show that replacement of the kaolin layers with GCLs produces a closure cap that is equivalent to or better than the current kaolin closure cap in terms of percolation. See the following appendices for the detailed HELP model input data and output files for both configurations:

- Appendix E, Current Kaolin Closure Cap: HELP Model Input Data and Output File (output file name: ZKAOout.OUT)
- Appendix F, Replacement GCL Closure Cap: HELP Model Input Data and Output File (output file name: ZGCLout.OUT)

Table 4.1-4. Comparison of Closure Cap Configurations HELP Model Results

HELP Model Output Parameter	Current Kaolin Closure Cap	Replacement GCL Closure Cap	Replacement GCL Closure Cap w/o Vault
Percolation through upper hydraulic barrier layer	0.90 inches/year	0.47 inches/year	0.47 inches/year
Percolation through lower hydraulic barrier layer	0.84 inches/year	0.055 inches/year	0.055 inches/year
Percolation out vault floor	0.00001 inches/year	0.00001 inches/year	Not applicable

A separate HELP model run was made for the GCL closure cap without inclusion of the vault layers (i.e. the last four layers in Table 4.1-1). This was done to determine whether or not inclusion of the vault layers was necessary to determine the percolation rate through the upper GCL-hydraulic barrier. Percolation through the upper GCL hydraulic barrier is to be utilized as input to the subsequent PORFLOW vadose zone flow and contaminant transport modeling. The PORFLOW model will be utilized to model flow and contaminant transport through the vault. The vault is assumed to degrade over time, particularly through settlement- and earthquake-induced cracking. The HELP model can not take into account such cracking degradation directly. The cracking would have to be converted into an equivalent saturated hydraulic conductivity for use in the HELP model. Therefore, if inclusion of the vault layers is not necessary, the HELP modeling could be significantly simplified by their exclusion. As indicated by Table 4.1-4 elimination of the vault layer from the replacement GCL closure cap configuration HELP modeling did not affect the estimated percolation through the upper GCL, therefore these layer will be deleted from further HELP modeling associated with this evaluation. See the following appendix for the detailed HELP model input data and output file:

- Appendix G, Replacement GCL Closure Cap without Vault Layers: HELP Model Input Data and Output File (output file name: ZGCLAout.OUT)

4.2 Drainage System Configuration

Three conceptual SDF closure cap drainage system configurations have been evaluated versus percolation through the upper GCL, soil fill volume, ditch length, and relative long-term maintenance requirements. The relationship of each of these parameters to configuration preference is as follows:

- The configuration with the least amount of percolation through the upper GCL is preferable in order to minimize contaminant transport. The configuration determines the maximum slope length over a vault, which in turn impacts the quantity of percolation.
- The configuration that requires the least amount of soil fill volume is preferable in order to minimize construction costs.
- The configuration that requires the least ditch length is preferable in order to minimize construction costs and long-term maintenance. The ditches must be specialized ditches that not only accommodate surface runoff but also intersect and accommodate flow from the subsurface drainage layers. These ditches are expensive to construct and will require substantial long-term maintenance in order to maintain their functionality.

Vaults 1 through 12 are considered representative of all the vaults, therefore vaults 13 through 15 are not considered specifically here (see Figure 2.0-1). The 600-foot slope length configuration shown in Figure 4.2-1 is essentially the configuration presented in the current Performance Assessment (MMES 1992) and Closure Plan (Cook et al. 2000). The closure cap crest is between the two rows of vaults (i.e. between vaults 1 through 6 and vaults 7 through 12) and drainage is directed to the perimeter of the entire disposal area in this configuration. The 300-foot slope length configuration shown in Figure 4.2-2 has a crest down the centerline of each row of vaults and drainage is directed to the perimeter of the entire disposal area and between the two rows of vaults. The 100-foot slope length configuration shown in Figure 4.2-3 has a separate crest down the centerline of each individual vault and drainage is directed between vaults and then to the perimeter of the entire disposal facility.

Table 4.2-1 provides a comparison of the percolation, soil fill volume, ditch length, and relative long-term maintenance requirements relative to the three drainage system configurations. The percolation through the upper GCL associated with the Figure 4.2-1 drainage configuration is the same as that presented in Table 4.1-4 for the GCL closure cap without vault layers. See the following appendices for the detailed HELP model input data and output files associated with the Figures 4.2-2 and 4.2-3 drainage system configurations, respectively:

- Appendix H, Replacement GCL Closure Cap with 300-foot Slope Lengths: HELP Model Input Data and Output File (output file name: ZGCLBout.OUT)
- Appendix I, Replacement GCL Closure Cap with 100-foot Slope Lengths: HELP Model Input Data and Output File (output file name: ZGCLCout.OUT)

See Appendix J for the calculations associated with the fill volume and ditch lengths associated with each drainage system configuration.

Based upon this evaluation the 300-foot, slope length drainage system configuration (Figure 4.2-2) has been selected. It substantially reduces percolation through the upper GCL and required soil fill volume over the current PA (MMES 1992) and closure plan (Cook et al. 2000) configuration, while minimizing the increase in ditch lengths and resultant relative long-term maintenance over the 100-foot, slope length drainage system configuration.

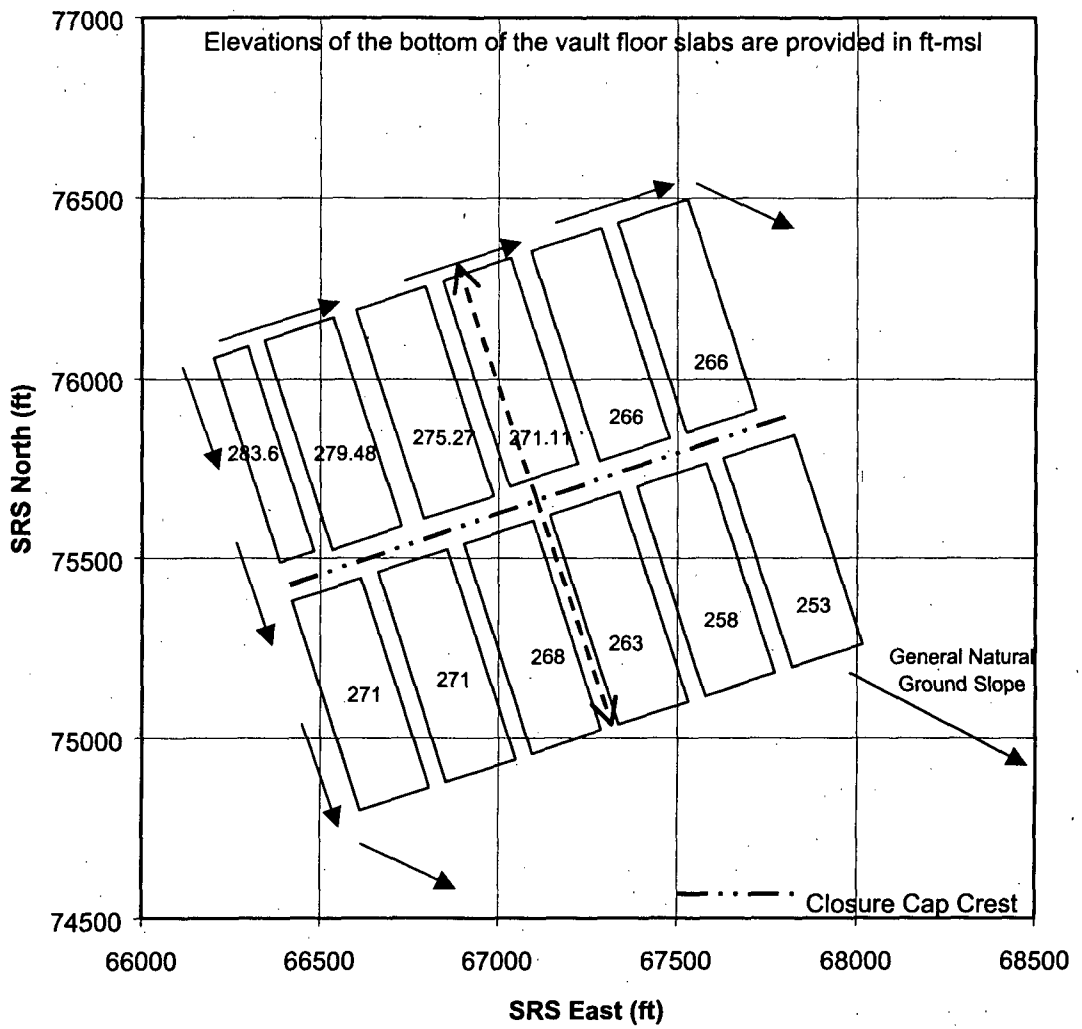


Figure 4.2-1. Current PA and Closure Plan 600-foot Slope Length Drainage System Configuration

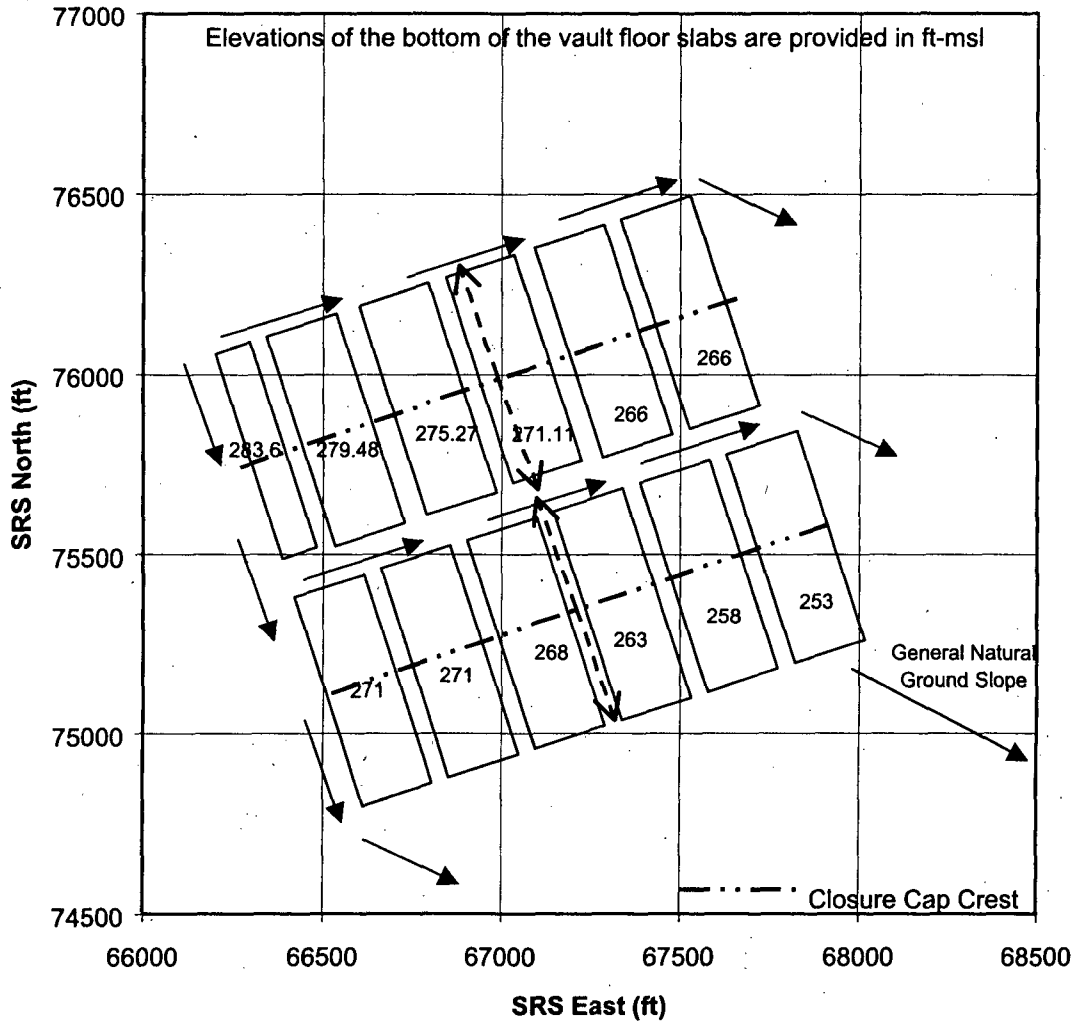


Figure 4.2-2. 300-Foot Slope Length Drainage System Configuration

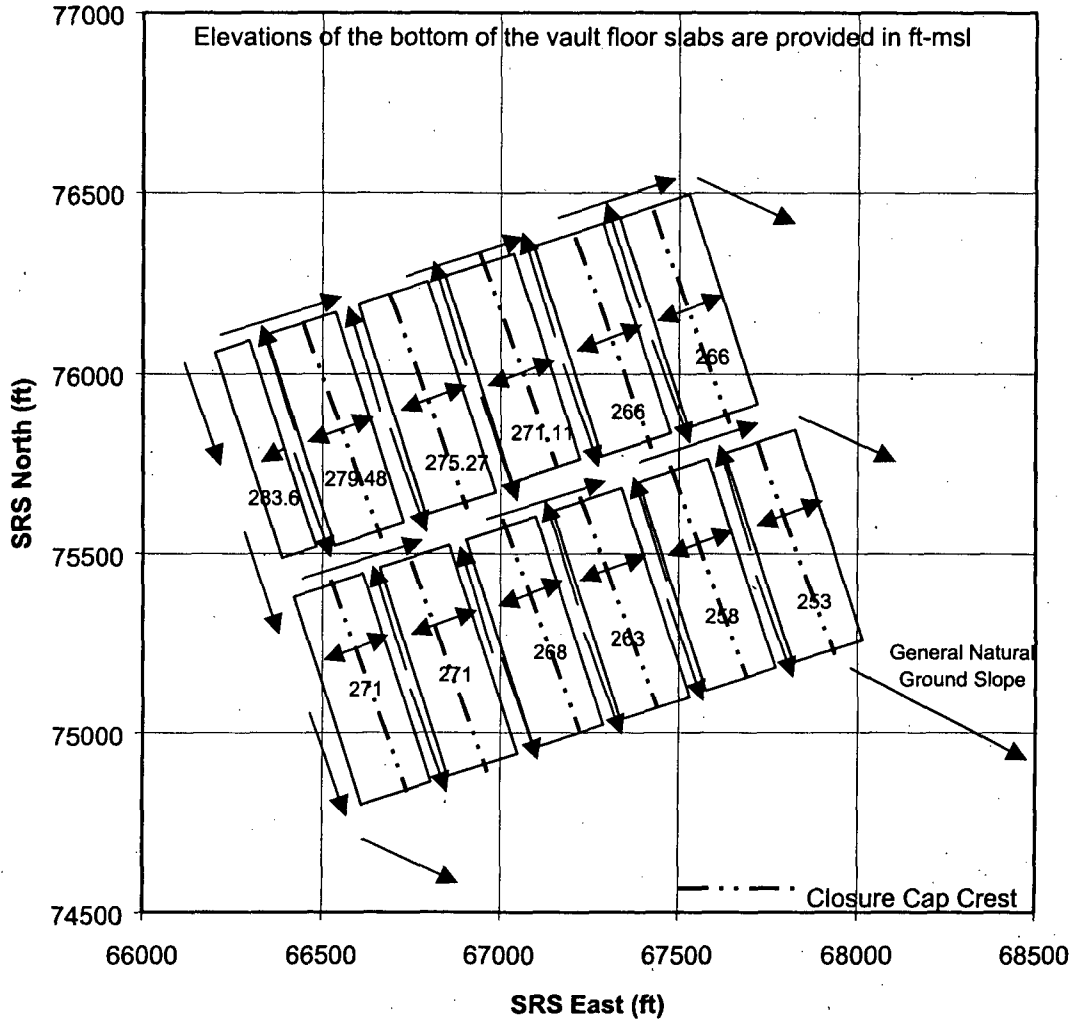


Figure 4.2-3. 100-Foot Slope Length Drainage System Configuration

Table 4.2-1. Drainage System Configuration Comparison

Parameter	Drainage System Configuration		
	Figure 4.2-1 ¹	Figure 4.2-2 ²	Figure 4.2-3 ³
Maximum Slope Length over a Vault, ft	600	300	100
Percent Slope Length Reduction		50%	83%
Percolation through Upper GCL, in/yr	0.467	0.254	0.110
Percent Percolation Reduction		46%	76%
Soil Fill Volume, cu yd	1,588,300	1,197,600	987,600
Percent Fill Reduction		25%	38%
Ditch Lengths, ft	4,200	5,650	13,450
Percent Ditch Increase		134%	320%
Relative Long-term Maintenance Requirements	Least	Slightly More	Significantly More

¹ Current PA (MMES 1992) and closure plan (Cook et al. 2000) 600-foot slope length drainage system configuration.

² 300-foot slope length drainage system configuration

³ 100-foot slope length drainage system configuration

4.3 Erosion Barrier And Upper Drainage Layer

To produce acceptable exposure results associated with the resident scenario intruder analysis, the current PA and closure plan assume that the upper gravel drainage layer functions as both a drainage layer and an erosion barrier to maintain the required material thickness of 3 meters (119 inches) above the vault roof. To function as a drainage layer the grain size of the material needs to be balanced between the need for a fairly high saturated hydraulic conductivity and the need to minimize the infiltration of overlying fines. Such an infiltration of fines would negatively impact the saturated hydraulic conductivity. To function as an erosion barrier the grain size of the material needs to be large enough to prevent material transport by erosion. These two functions can not be readily reconciled therefore an erosion control barrier separate from and overlying the drainage layer will be utilized.

The erosion barrier has been sized based upon the maximum precipitation event for a 10,000-year return period. The maximum precipitation event for a 10,000-year return period is 3.3 inches over a 15-minute accumulation period (Table XIX from Weber et al. 1998). Based upon this precipitation event a one foot thick layer of 2-inch to 6-inch granite stone with a d_{50} (i.e. median size) of 4 inches has been selected for use as the erosion barrier (sizing based upon Logan 1977; Goldman et al. 1986; NCSU 1991). See Appendix K for the calculations associated with this selection.

In order to prevent the loss of overlying material into the erosion barrier and to reduce the saturated hydraulic conductivity of the erosion barrier layer, the granite stone will be filled with a Controlled Low Strength Material (CLSM) or Flowable Fill. This results in a combined material with the soil properties listed in Table 4.3-1. See Appendix K for the calculations associated with the soil properties for this combined material.

Table 4.3-1. Erosion Barrier Combined Material Soil Properties

Property	Property Value
Saturated hydraulic conductivity	3.97E-04 cm/s
Porosity	0.06
Field Capacity	0.056
Wilting Point	0.052

4.4 Erosion Impact upon Evapotranspiration Zone

Table 4.4-1 presents the revised GCL closure cap configuration based upon the changes outlined in Sections 4.1 through 4.3. HELP modeling of this configuration with and without the layers above the erosion barrier (i.e. topsoil and underlying backfill layers) has been performed to evaluate the potential impact of complete erosion of these layers on the hydraulic performance. See the following appendices for the detailed HELP model input data and output files associated with the configurations with and without the layers above the erosion barrier, respectively:

- Appendix L, Replacement GCL Closure Cap with Erosion Barrier: HELP Model Input Data and Output File (output file name: ZGCLDout.OUT)
- Appendix M, Replacement GCL Closure Cap with Erosion Barrier without Overlying Layers: HELP Model Input Data and Output File (output file name: ZGCLEout.OUT)

Table 4.4-1. Replacement GCL Closure Cap Configuration

Layer	Thickness (inches)
Topsoil	6
Upper Backfill	30
Erosion Barrier	12
Geotextile Filter Fabric ¹	-
Upper Drainage Layer	12
Upper GCL	0.2
Lower Backfill	49.28
Geotextile Filter Fabric ¹	-
Lower Drainage Layer	6
Lower GCL	0.2
Clean Grout	39.37 (1 m)

¹ It is assumed that a geotextile filter fabric will be placed above the drainage layers to minimize the infiltration of fines from the overlying layers into the drainage layer. However it is not necessary to include the filter fabric in the HELP models.

Table 4.4-2 presents a comparison of the pertinent HELP model results for this configuration with and without the layers above the erosion barrier. As seen in Table 4.4-2 elimination of the layer above the erosion barrier result in significantly less evapotranspiration and significantly more water flux into the upper drainage layer. This increased water flux to the upper drainage layer would require the drainage system to handle additional water volumes and would result in increased infiltration through the upper GCL particularly with any degradation of the GCL. The decrease in evapotranspiration is due the intersection of the evapotranspiration zone with the drainage layer. The evapotranspiration

zone is assumed to extend 22 inches deep from the ground surface (USEPA 1994a; USEPA 1994b). It intersects the top 10 inches of the upper drainage layer with elimination of the layers above the erosion barrier. The drainage layer does not provide effective water storage for evapotranspiration but quickly removes water from the evapotranspiration zone, and therefore decreases the overall evapotranspiration. In order to increase evapotranspiration for the case where the soil layers above the erosion barrier have eroded away, a twelve-inch backfill layer will be placed between the erosion barrier and the upper drainage layer. HELP modeling of this configuration without the layers above the erosion barrier but with the backfill layer between the erosion barrier and upper drainage layer has been performed. See the following appendix for the detailed HELP model input data and output file associated with this configuration:

- Appendix N, Replacement GCL Closure Cap with Erosion Barrier without Overlying Layers Plus Middle Backfill Layer: HELP Model Input Data and Output File (output file name: ZGCLFout.OUT)

A comparison of the HELP model results for this configuration with the other two is also provided in Table 4.4-2. As seen the addition of this backfill layer between the erosion barrier and upper drainage layer, the evapotranspiration greatly improves.

Table 4.4-2. HELP Model Results for Replacement GCL Closure Cap Configurations with and without Upper Topsoil and Backfill Layers

HELP Model Output Parameter	Configuration with Upper Topsoil and Backfill Layers	Configuration without Upper Topsoil and Backfill Layers	Deviation	Configuration without Upper Topsoil and Backfill Layers Plus Middle Backfill Layer
Runoff, inches/year	0.16	0.19	Increase of 0.03	0.24
Evapotranspiration, inches/year	34.6	23.7	Decrease of 10.9	29.7
Lateral Drainage from Upper Drainage Layer, inches/year	13.8	24.5	Increase of 10.7	18.6
Percolation / Leakage through Upper GCL, inches/year	0.25	0.43	Increase of 0.18	0.33

4.5 Grout Layer over Vault Roof

The 2002 Saltstone Intruder Special Analysis (Cook et al. 2002a) assumed in the resident scenario intruder analysis that the resident excavates 3 meters deep for construction of a basement. This led to the requirement for 3 meters of material between the vault top and the top of the erosion barrier in order to prevent the resident from excavating into the Saltstone waste itself. In the Special Analysis, a 1-meter-thick grout layer above the vault roof was added to achieve the requirement for 3 meters of material. According to the Special Analysis the only reason for adding the grout layer was to increase the material thickness between the vault top and the top of the erosion barrier. Typical soil materials would perform the required function as well as grout. Therefore the 1-meter-thick grout layer will be replaced with 1 meter of soil materials.

4.6 Lower Drainage Layer

Previous undocumented PORFLOW modeling has indicated that water could build up on top of the vault, due to the low permeability of the vault roof and the inadequate thickness of the overlying drainage layer particularly as the drainage layer silts-in over time (see Section 5.3). Such a build up increases the hydraulic head, which is the driving force for flow of water through the vault. To minimize build up of water on top of the vault the following changes to the closure cap configuration were made:

- The lower drainage layer thickness was increased from 6 inches to 2 feet,
- A 3-foot wide vertical drainage layer was added along the sides of the vaults, and
- A 5-foot-thick by 10-foot-long drainage layer was added at the base of the vaults.

All three of these layers are interconnected in order to route water off the vault top along the vault sides to the soil layer below the vaults.

4.7 Closure Cap Configuration Summary and Intact Infiltration

The following are the changes that have been made to the closure cap configuration from that described within the current PA, Closure Plan, and PA Intruder Special Analysis (MMES 1992; Cook et al. 2000; Cook et al. 2002a) as outlined in Section 2.0:

- The kaolin hydraulic barriers have been replaced with GCLs (see Section 4.1).
- The drainage system configuration has been revised from that depicted in Figure 4.2-1 to that of Figure 4.2-2. This decreases the slope lengths from a maximum of 600 feet to 300 feet over the vaults. The Figure 4.2-2 configuration has a crest down the centerline of each row of vaults and drainage is directed to the perimeter of the entire disposal area and between the two rows of vaults. (see Section 4.2)
- An erosion barrier separate from and above the upper drainage layer has been added. The erosion barrier is one-foot thick and consists of 2-inch to 6-inch granite stone with a d_{50} (i.e. median size) of 4 inches. (see Section 4.3)
- A twelve-inch-thick backfill layer has been added between the erosion barrier and the upper drainage layer.
- The 3-meter-thick grout layer has been replaced with 3 meters of soil materials.
- The lower drainage layer thickness has been increased from 6 inches to 2 feet, a 3-foot wide vertical drainage layer has been added along the sides of the vaults, and a 5-foot-thick by 10-foot-long drainage layer has been added at the base of the vaults.

Figure 4.7-1 and Table 4.7-1 present the resulting SDF GCL closure cap configuration. Table 4.7-1 also includes the associated HELP Model soil input data. Additional HELP model input change from the previous modeling include:

- The landfill area modeled has been modified to conform to the Figure 4.2-2 drainage layer configuration as shown in Figure 4.7-1. The area modeled has been changed 350-foot by 250-foot, which results in a surface area of 87,500 feet squared or 2.009 acres.
- The surface slope length has been changed to 350 feet as shown in Figure 4.7-1. This change results in a HELP model computed curve number of 55.20.
- The slope length of the upper drainage layer has been changed to 350 feet.
- The slope length of the lower drainage layer has been changed to 250 feet.

The initial moisture storage has been specified as done in Section 4.1.

HELP modeling of the Table 4.7-1 intact SDF GCL closure cap configuration has been performed as outlined above. Based upon this modeling the infiltration through the upper GCL has been estimated to be 0.29 inches per year for intact conditions. The following appendix provides the detailed HELP model, input data and output file for the intact condition:

- Appendix O, Intact SDF GCL Closure Cap (0 Years): HELP Model Input Data and Output File (output file name: ZGCLiout.OUT)

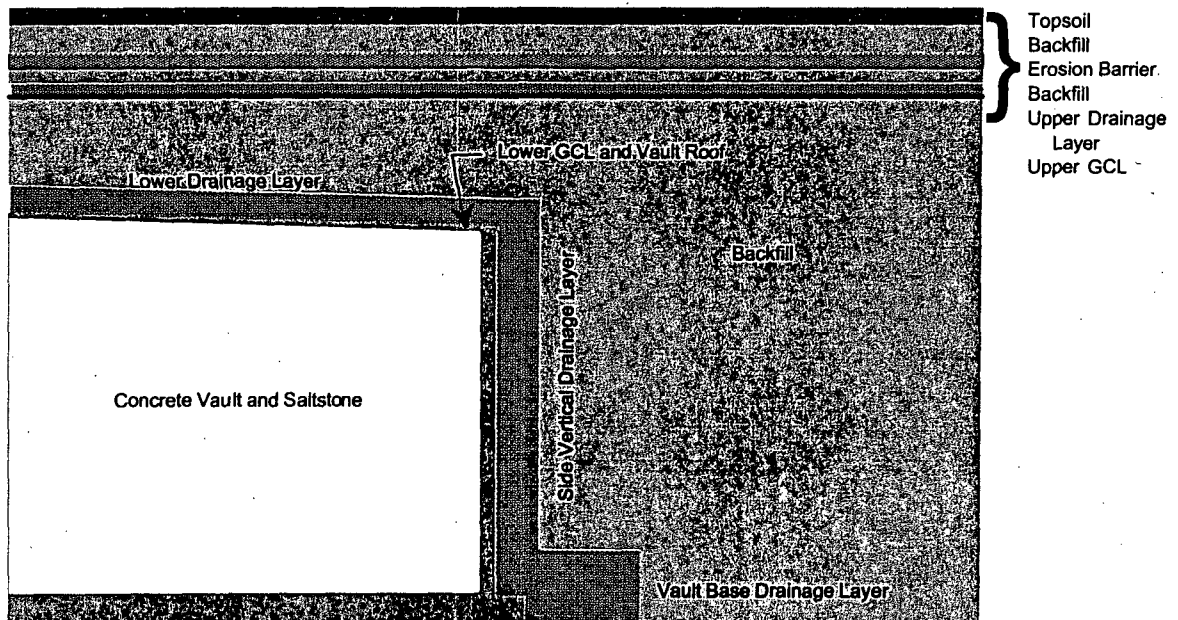
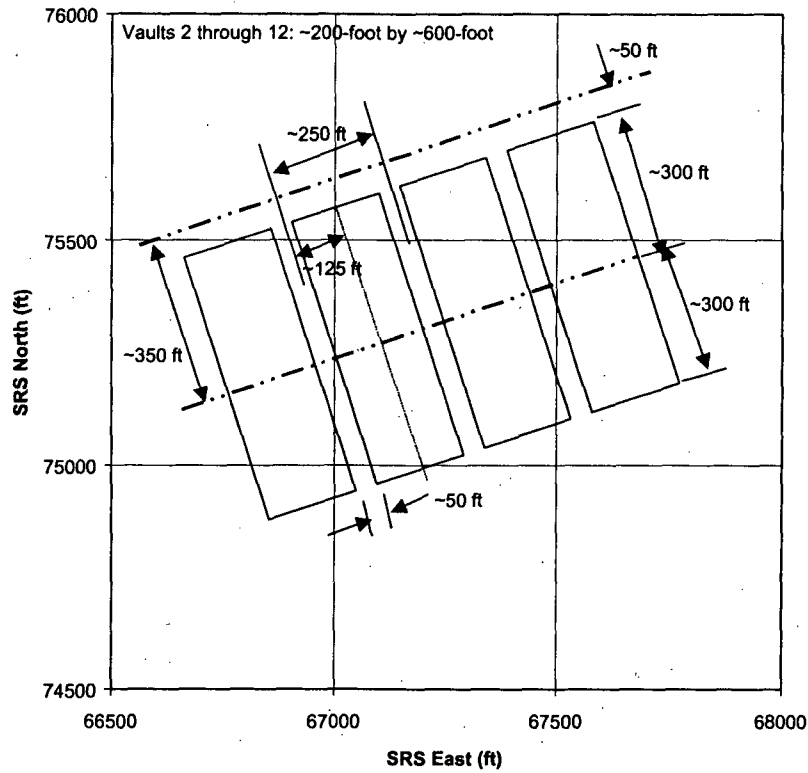


Figure 4.7-1. SDF GCL Closure Cap Configuration

Table 4.7-1. Intact SDF GCL Closure Cap Configuration and HELP Model Required Soil Property Data

Layer	Thickness (inches)	Saturated Hydraulic Conductivity (cm/sec)	Total Porosity (Vol/Vol)	Field Capacity (Vol/Vol)	Wilting Point (Vol/Vol)
Topsoil ¹	6	1.00E-03	0.4	0.11	0.058
Upper Backfill ¹	30	1.00E-04	0.37	0.24	0.136
Erosion Barrier ²	12	3.97E-04	0.06	0.056	0.052
Middle Backfill ¹	12 ⁶	1.00E-04	0.37	0.24	0.136
Geotextile Filter Fabric ⁵	-	-	-	-	-
Upper Drainage Layer ¹	12	1.00E-01	0.38	0.08	0.013
Upper GCL	0.2	5.00E-09 ³	0.75 ⁴	0.747 ⁴	0.40 ⁴
Lower Backfill ¹	58.65 ⁶	1.00E-04	0.37	0.24	0.136
Geotextile Filter Fabric ⁵	-	-	-	-	-
Lower Drainage Layer ¹	24 ⁶	1.00E-01	0.38	0.08	0.013
Lower GCL	0.2	5.00E-09 ²	0.75 ³	0.747 ³	0.40 ³

¹ WSRC 2002

² See Section 4.3

³ GSE 2002

⁴ USEPA 1994a and USEPA 1994b

⁵ It is assumed that a geotextile filter fabric will be placed above the drainage layers to minimize the infiltration of fines from the overlying layers into the drainage layer. However it is not necessary to include the filter fabric in the HELP models.

⁶ The 39.37 inches (1 m) of clean grout immediately above the vault roof was replaced with 12 inches of Middle Backfill, 9.37 inches of Lower Backfill, and 18 inches of lower drainage layer.

**RESPONSE TO RAI COMMENT 68
ROADMAP TO REFERENCES**

REFERENCED DOCUMENT	*EXCERPT LOCATION	REMARK
Chaki 2002 – CAP88-PC, Version 3.0	Introduction included as an excerpt enclosed following response.	Clean Air Act Assessment computer model.
Cook et al. 2005		Generically referenced, no specific reference included in response.
Hamby 1991	Representative excerpts enclosed following response.	References used to generate Table 68-1 of this response.
Jannik 2003	Excerpt enclosed following response.	
Simpkins 2004		Abstract included for this spreadsheet program used to analyze the exposure pathways involving transport by water that were used in the Vault 4 SA (Cook et al. 2005).

***Excerpt Locations:**

1. Excerpt included in response: The excerpt is included within the text of the response or is appended to the response.
2. Excerpt enclosed following response: The excerpt is enclosed on a separate sheet or sheets following the response.
3. Representative excerpt(s) enclosed following response: Representative excerpts from a document that is wholly or largely applicable are enclosed following the response.
4. Other

APPROVED for Release for
Unlimited (Release to Public)

7/14/2005

CAP88-PC Version 3.0 User Guide

Draft Revision 1

Produced in Response to Work Assignment 14
Contract 68-D-00-210
Sanjib Chaki, EPA Work Assignment Manager
Office of Radiation and Indoor Air
Ariel Rios Building
1200 Pennsylvania Avenue, NW
Washington, DC 20460

By

Trinity Engineering Associates, Inc.
8832 Falmouth Dr.
Cincinnati, OH 45231-5011

August, 2002

Table of Contents

1. INTRODUCTION	1
1.1 Background.....	1
1.2 Purpose.....	1
1.3 Model Summary.....	2
1.4 Validation.....	3
1.5 Limitations.....	3
1.6 Summary of Version 2.1 Changes from Version 2.0.....	4
1.7 Summary of Version 3 Changes from Version 2.1.....	5
2. GETTING STARTED.....	6
2.1. Installation of Version 3.0.....	6
2.2 Installation Notes:.....	6
2.2.1 Installation Procedure.....	7
2.3. Running Version 3.0.....	8
2.3.1 Initial Post-Installation Running of Version 3.0.....	8
2.3.2 Building an Example Data Set.....	8
2.4 Uninstall CAP88-PC Version 2.1.....	20
3. FILE MENU.....	21
3.1 New Dataset.....	21
3.2 Open Dataset.....	21
3.3 Close Dataset.....	21
3.4 Save Dataset.....	21
3.5 Save Dataset As.....	21
3.6 Print Setup.....	21
3.7 Print Preview.....	21
3.8 Maintenance.....	22
3.9 File Maintenance.....	22
3.10 List Maintenance.....	22
3.11 Convert SCR File.....	22
3.12 Create INPUT.DAT File.....	22
3.13 Exit.....	22
4. RUN MENU.....	23
4.1 Execute.....	23
4.2 Scan Population File Format.....	23
4.3 Population File Editor.....	24
4.4 Population File Library.....	24
4.5 Scan Wind File Format.....	24
4.6 Wind File Library.....	24
4.7 Stability Array/Wind File Generator.....	25
5. NEW DATASET INFORMATION.....	26
5.1 New Dataset Information Form.....	26
6. SELECT DATASET INFORMATION.....	27
6.1 Select Dataset Form.....	27
7. PRINT/VIEW.....	28
7.1 Print/View.....	28
8. MAINTENANCE OPERATIONS.....	29
8.1 File Maintenance Operations Form.....	29
8.2 Select File.....	30
8.3 Save File As Form.....	30
8.4 Change List Information Form.....	31
9. DATASET DATA.....	33
9.1 Facility Data.....	33
9.2 Run Options.....	34
9.3 Meteorological Data.....	36
9.4 Source Data.....	37

9.5	Agricultural Data	38
9.6	Nuclide Data	39
10	41
10.1	Purpose Of Default Value	41
10.1.1	User Changeable Defaults	41
10.1.2	Permanent Defaults	41
10.2	Changeable Defaults	41
10.2.1	Variable Names and Descriptions.....	41
10.2.2	Changing Default Values	44
10.2.3	Restoring DEFAULT.DAT Values.....	46
10.2.4	Alternative DEFAULT.DAT Files.....	46
10.3	PERMANENT DEFAULTS.....	47
11	CONVERTING WEATHER DATA WITH GETWIND.....	48
11.1	Purpose.....	48
11.2	Program Input.....	48
11.3	Program Output.....	48
11.4	Running GETWIND	48
11.5	Error Messages.....	49
12	MATHEMATICAL MODELS	51
12.1	Environmental Transport.....	51
12.1.1	Plume Rise.....	51
12.1.2	Plume Dispersion	53
12.1.3	Dry Deposition.....	55
12.1.4	Precipitation Scavenging.....	56
12.1.5	Plume Depletion	56
12.1.6	Dispersion Coefficients.....	59
12.1.7	Area Sources	60
12.1.8	Carbon-14 and Tritium.....	60
12.1.9	Rn-222 Working Levels	60
12.1.10	Ground Surface Concentrations.....	61
12.2	Dose and Risk Estimates	61
12.2.1	Air Immersion	62
12.2.2	Surface Exposure.....	62
12.2.3	Ingestion and Inhalation.....	63
12.2.4	Maximally-Exposed Individual	63
12.2.5	Collective Population	63
13	REFERENCES	64

Appendix A: Valid Radionuclides

Appendix B: STAR File Format

Appendix C: State Agricultural Productivities

Appendix D: Weather Data Library

Appendix E: Differences With Mainframe Versions of AIRDOS-EPA/DARTAB

Appendix F: Population File Format

Appendix G: Outputs from MODTEST Sample Case File

1. INTRODUCTION

1.1 Background

On October 31, 1989 the Environmental Protection Agency (EPA) issued final rules for radionuclide emissions to air under 40 CFR 61, National Emission Standards for Hazardous Air Pollutants (NESHAPS). Emission monitoring and compliance procedures for Department of Energy (DOE) facilities (40 CFR 61.93 (a)) require the use of CAP-88 or AIRDOS-PC computer models, or other approved procedures, to calculate effective dose equivalents to members of the public.

The CAP88 (which stands for Clean Air Act Assessment Package - 1988) computer model is a set of computer programs, databases and associated utility programs for estimation of dose and risk from radionuclide emissions to air. CAP88 is composed of modified versions of AIRDOS-EPA (Mo79) and DARTAB (ORNL5692). The original CAP88 model is written in FORTRAN77 and has been compiled and run on an IBM 3090 under OS/VS2, using the IBM FORTRAN compiler, at the EPA National Computer Center in Research Triangle Park, NC.

1.2 Purpose

The original CAP88-PC software package, version 1.0, allowed users to perform full-featured dose and risk assessments in a DOS environment for the purpose of demonstrating compliance with 40 CFR 61.93 (a). CAP88-PC provides the CAP-88 methodology for assessments of both collective populations and maximally-exposed individuals. The complete set of dose and risk factors used in CAP88 is provided. CAP88-PC differs from the dose assessment software AIRDOS-PC in that it estimates risk as well as dose, offers a wider selection of radionuclide and meteorological data, provides the capability for collective population assessments, and allows users greater freedom to alter values of environmental transport variables. CAP88-PC version 1.0 was approved for demonstrating compliance with 40 CFR 61.93 (a) in February 1992.

CAP88-PC version 2.0 provided a framework for developing inputs to perform full-featured dose and risk assessments in a Windows environment for the purpose of demonstrating compliance with 40 CFR 61.93 (a). Version 2.1 included some additional changes compared to the DOS version and the previous Windows version, 2.0. The changes included the addition of more decay chains, improvements in the Windows code error handling, and a modified nuclide data input form. Section 1.6 provides a summary of the changes incorporated into Version 2.1 relative to Version 2.0.

CAP88-PC Version 3.0 is a significant update to the version 2 system. Version 3 incorporates dose and risk factors from Federal Guidance Report 13 (FGR 13, EPA99) in place of the RADRISK data that was used in previous versions. The FGR 13 factors are based on the methods in Publication 72 of the International Commission on Radiological Protection (ICRP72). . In addition, the CAP88-PC database, the user interface, input files, and output files, were modified to accommodate the FGR 13

data formats and nomenclature. Section 1.7 describes the modifications incorporated into Version 3 relative to Version 2.1.

1.3 Model Summary

CAP-88 PC uses a modified Gaussian plume equation to estimate the average dispersion of radionuclides released from up to six emitting sources. The sources may be either elevated stacks, such as a smokestack, or uniform area sources, such as a pile of uranium mill tailings. Plume rise can be calculated assuming either a momentum or buoyant-driven plume. Assessments are done for a circular grid of distances and directions for a radius of up to 80 kilometers (50 miles) around the facility. The Gaussian plume model produces results that agree with experimental data as well as any model, is fairly easy to work with, and is consistent with the random nature of turbulence.

There are a few differences between CAP88-PC and earlier mainframe versions of AIRDOS, PREPAR and DARTAB. In particular, population assessments are easier to perform in CAP88-PC. When performing population assessments, population arrays must always be supplied to the program as a file, using the same format as the mainframe version of CAP88. Sample population files are supplied with CAP88-PC, which the user should modify to reflect their own population distributions. Population files for the mainframe version of CAP88 may be downloaded in ASCII format and used with CAP88-PC. When performing population dose assessments, CAP88-PC uses the distances in the population array to determine the sector midpoint distances where the code calculates concentrations. Note that CAP88-PC only uses circular grids. When an individual assessment is run, the sector midpoint distances are input by the user on the Run Option tab form. Direct user input of radionuclide concentrations is not an option in CAP88-PC.

CAP88-PC has the capability to vary equilibrium fractions; previously they were set to a constant of 0.7. The new method varies the equilibrium fractions depending on the distance from the source. Linear interpolation is used to determine the equilibrium fractions for distances that do not match the set distances given.

Agricultural arrays of milk cattle, beef cattle and agricultural crop area are generated automatically, requiring the user to supply only the State name or agricultural productivity values. When a population assessment is performed, the arrays are generated to match the distances used in the population arrays supplied to the code, and use State-specific or user-supplied agricultural productivity values. The state name (standard two letter abbreviation) must be provided on the Facility Data tab form. Users are given the option to override the default agricultural productivity values by entering the data directly on the Agricultural Data tab form. If Alaska, Hawaii, or Washington, D.C. is selected, agricultural productivity values are set to zero and must be provided by the user.

CAP88-PC is also modified to do either "Radon-only" or "Non-Radon" runs, to conform to the format of the 1988 Clean Air Act NESHAPS Rulemaking. "Radon-only" assessments, which only have Rn-222 in the source term, automatically include working level calculations; any other source term ignores working levels. Synopsis reports customized to both formats are automatically generated. Assessments for Radon-222 now automatically include Working Level calculations

when only a single source term of Rn-222 may be used in this option. Input of any additional radionuclides, even Rn-220, will cause CAP88-PC to omit working level calculations. Version 3 has not changed the "Radon Only" methodology relative to the previous versions 2.0 and 2.1.

The calculation of deposition velocity and the default scavenging coefficient is defined by current EPA policy. Deposition velocity is set to $3.5e-2$ m/sec for Iodine, $1.8e-3$ m/sec for Particulate, and 0.0 m/sec for Gas. The default scavenging coefficient is calculated as a function of annual precipitation, which is input on the Meteorological Data tab form. Version 3 has not modified these calculations.

Organs and weighting factors have been modified in Version 3 to follow the FGR 13 method. In accordance with the FGR 13 dose model, the code now calculates dose for 23 internal organs, rather than the 7 organs used in earlier versions. A '24th' organ is also calculated, which is the total effective dose equivalent. The code now reports cancer risk for the 15 target cancer sites used in FGR 13. As was the case in version 2, changing the organs and weights will invalidate the results.

1.4 Validation

The CAP88-PC programs represent one of the best available validated codes for the purpose of making comprehensive dose and risk assessments. The Gaussian plume model used in CAP88-PC to estimate dispersion of radionuclides in air is one of the most commonly used models in Government guidebooks. It produces results that agree with experimental data as well as any model, is fairly easy to work with, and is consistent with the random nature of turbulence. Version 3 has not modified the basic Gaussian plume algorithm used by the AIRDOS module of CAP88-PC, and comparison cases between version 2 and 3 have shown no significant changes in the dispersion calculations.

The Office of Radiation and Indoor Air has made comparisons between the predictions of annual-average ground-level concentration to actual environmental measurements, and found very good agreement. In the paper "Comparison of AIRDOS-EPA Prediction of Ground-Level Airborne Radionuclide Concentrations to Measured Values" (Be86), environmental monitoring data at five Department of Energy (DOE) sites were compared to AIRDOS-EPA predictions. EPA concluded that as often as not, AIRDOS-EPA predictions are within a factor of 2 of actual concentrations.

1.5 Limitations

Like all models, there are some limitations in the CAP88-PC system.

While up to six stack or area sources can be modeled, all the sources are modeled as if located at the same point; that is, stacks cannot be located in different areas of a facility. The same plume rise mechanism (buoyant or momentum) is used for each source. Also, area sources are treated as uniform. Variation in radionuclide concentrations due to complex terrain cannot be modeled.

Errors arising from these assumptions will have a negligible effect for assessments where the distance to exposed individuals is large compared to the stack height, area or facility size.

WSRC-RP-91-17

**LAND AND WATER USE CHARACTERISTICS IN THE
VICINITY OF THE SAVANNAH RIVER SITE (U)**

March 1991

**APPROVED for Release for
Unlimited (Release to Public)
6/12/2003**

**Westinghouse Savannah River Company
Savannah River Site
Aiken, SC 29808**



PREPARED FOR THE U.S. DEPARTMENT OF ENERGY UNDER CONTRACT NO. DE-AC09-89SR18035

Table 1. NRC Default Values for Land Usage and Individual Consumption

	NRC Default	Units	NRC Ref.
<u>Land Usage Statistics</u>			
Beef-cow forage consumption (wet)	50	kg/day	2
Milk-cow forage consumption (wet)	50	kg/day	2
Pasture-grass exposure time	30	days	2,30
Transport time (feed-milk-man)	4	days	sp
Holdup time (pasture grass, forage)	0	days	sp
Holdup time (stored feed)	90	days	sp
Fraction of time milk-cow on pasture	0.75	-	31
Fraction of time beef-cow on pasture	0.75	-	31
Time from slaughter to consumption	20	days	sp
Crop exposure time	60	days	2,30
Fraction of leafy vegetables from garden	1.0	-	sp
Fraction of other vegetables from garden	0.76	-	sp
Transport time (leafy veg, produce; pop)	14	days	sp
Transport time (leafy veg.; MI)	1	days	sp
Transport time (produce; MI)	60	days	sp
Agricultural productivity (pasture grass)	0.7	kg/sq m	32
Agricultural productivity (produce/veg.)	2.0	kg/sq m	9
Vegetable garden productivity	2.0	kg/sq m	9
<u>Average Individual Usage</u>			
Other vegetable consumption	190	kg/yr	2,33
Meat consumption	95	kg/yr	2,33
Milk consumption	110	L/yr	2,33
Water consumption	370	L/yr	2
Invertebrate consumption	1.0	kg/yr	2,33
<u>Maximum Individual Usage</u>			
Leafy vegetable consumption	64	kg/yr	2,33
Other vegetable consumption	520	kg/yr	2,33
Meat consumption	110	kg/yr	2,33
Milk consumption	310	L/yr	2,33
Water consumption	730	L/yr	2
Fish consumption	21	kg/yr	2
Invertebrate consumption	5	kg/yr	2,33
Recreational shoreline usage	12	hr/yr	2

sp=NRC staff position

Table 2. SRS-Specific Parameter Values for Dose Estimates

	Units	NRC Default	1979-83 Survey	This Survey	Ref.
Land Usage Statistics					
Beef-cow forage consumption (wet)	kg/day	50	50	36(a)	10
Milk-cow forage consumption (wet)	kg/day	50	50	52(a)	10
Pasture-grass exposure time	days	30	30	30	10,11
Agricultural productivity (pasture grass)	kg/sqm	0.7	0.501	1.8	10
Transport time (feed-milk-man)	days	4	4	3	12
Holdup time (pasture grass, forage)	days	0	0	0	1
Holdup time (stored feed)	days	90	90	90	1
Fraction of time milk-cow on pasture	-	0.75(b)	0.58	1.0	10
Fraction of time beef-cow on pasture	-	0.75(b)	0.79	1.0	10
Fraction of intake from pasture (milk cow)	-	1(b)	0.45	0.56	10
Fraction of intake from pasture (beef-cow)	-	1(b)	0.85	0.75	10
Time from slaughter to consumption	days	20	20	6	10
Fraction of leafy vegetables from garden	-	1.0	0.75	1.0	1
Fraction of other vegetables from garden	-	0.76	0.76	0.76	1
Transport time (leafy veg, produce;pop)	days	14	14	14	1
Transport time (leafy veg; MI)	days	1	1	1	1
Transport time (produce; MI)	days	60	60	60	1
Agricultural productivity (produce/veg.)	kg/sq m	2.0	0.894	0.7	**
Vegetable garden productivity	kg/sq m	2.0	0.632	0.7	**
Crop exposure time	days	60	60	70	14
Water Usage Statistics					
Edible sport fish harvest (d)	kg/yr	-	9.1E+04*	3.5E+04	19
Edible commercial fish harvest (c)	kg/yr	-	3.2E+04*	2.7E+03	20,21
Edible commercial invertebrate harvest	kg/yr	-	3.0E+05*	3.9E+05	10,21
Edible fraction of harvest: Fish(whole)	-	-	0.50	0.50	22
Crab (whole)	-	-	-	0.14	24
Shrimp(headless)	-	-	-	0.90	23
Oysters(meat)	-	-	-	1.00	23
Clams(meat only)	-	-	-	1.00	23
Population shoreline usage	per-hrs	-	1.1E+05	9.6E+05	25
Population swimming usage	per-hrs	-	8.5E+03	1.6E+05	25
Population boating usage	per-hrs	-	2.3E+05	1.1E+06	25
Drinking Water					
Effective population - Beaufort/Jasper	persons	-	5.1E+04	5.0E+04	17
Effective population - Port Wentworth	persons	-	2.0E+04	1.5E+04	15
Transit time from discharge to river	hours	-	24	24	18
Transit time, river entry to treatment facility	hours	-	72	72	18

* Values are for total harvest (not only edible portion).

** Values obtained from questionnaire.

(a) dry weight converted to wet weight assuming 75% of plant mass is water.

(b) not specifically given in Reg. Guide 1.109 but obtained from GASPAR manual, NUREG-0597.

(c) approximately 96% of 1989 harvest was American shad(not full time residents of Savannah River and not included here).

(d) sport invertebrate harvest not included due to closure of Savannah River to invertebrate fishing.

Table 3. Beef Production Grid (kg/yr)

Sector	10-20 Mi	20-30 Mi	30-40 Mi	40-50 Mi
N	5.3E+04	8.8E+04	2.5E+05	9.8E+05
NNE	5.3E+04	8.8E+04	2.0E+05	4.1E+05
NE	7.1E+04	1.7E+05	3.5E+05	4.5E+05
ENE	8.3E+04	2.0E+05	4.6E+05	5.7E+05
E	8.3E+04	1.9E+05	3.4E+05	5.1E+05
ESE	8.3E+04	1.9E+05	2.2E+05	2.5E+05
SE	1.2E+05	2.1E+05	2.6E+05	3.0E+05
SSE	1.1E+05	1.9E+05	2.6E+05	2.9E+05
S	9.4E+04	1.5E+05	2.0E+05	2.7E+05
SSW	9.5E+04	1.8E+05	2.9E+05	3.9E+05
SW	9.5E+04	1.7E+05	2.7E+05	3.2E+05
WSW	9.5E+04	1.6E+05	2.3E+05	4.0E+05
W	5.8E+04	1.0E+05	2.1E+05	4.1E+05
WNW	4.8E+04	6.2E+05	1.3E+05	2.9E+05
NW	5.8E+04	8.0E+04	2.8E+05	2.7E+05
NNW	5.3E+04	8.8E+04	3.3E+05	6.2E+05

Table 4. Milk Production Grid (L/yr)

Sector	10-20 MI	20-30 Mi	30-40 Mi	40-50 Mi
N	4.2E+04	6.9E+04	1.0E+06	5.3E+06
NNE	4.2E+04	6.9E+04	2.1E+05	5.0E+05
NE	3.2E+04	1.0E+06	2.7E+06	2.0E+06
ENE	2.5E+04	1.2E+06	4.4E+06	5.2E+06
E	2.5E+04	1.4E+06	3.9E+06	4.9E+06
ESE	2.5E+04	5.6E+05	3.0E+04	4.9E+05
SE	2.5E+03	0.0E+00	0.0E+00	0.0E+00
SSE	4.8E+05	8.6E+05	1.2E+06	1.2E+06
S	1.0E+06	2.1E+06	3.0E+06	3.5E+06
SSW	9.9E+05	3.8E+06	7.4E+06	7.6E+06
SW	9.9E+05	2.2E+06	5.8E+06	4.8E+06
WSW	9.9E+05	1.7E+06	2.4E+06	3.5E+06
W	6.7E+05	1.3E+06	2.2E+06	3.6E+06
WNW	2.3E+05	1.1E+06	1.2E+06	2.0E+06
NW	4.2E+04	3.8E+05	1.4E+06	1.0E+06
NNW	4.2E+04	6.0E+04	1.7E+06	3.4E+06

Table 5 Vegetable Production Grid (kg/yr)

Sector	10-20 Mi	20-30 Mi	30-40 Mi	40-50 Mi
N	3.4E+05	5.7E+05	8.0E+05	8.3E+05
NNE	3.4E+05	5.7E+05	4.8E+05	2.9E+03
NE	3.4E+05	6.5E+05	9.4E+05	4.5E+05
ENE	3.4E+05	6.2E+05	1.1E+06	1.3E+06
E	3.4E+05	5.7E+05	8.4E+05	1.3E+06
ESE	3.4E+05	2.1E+06	1.8E+06	1.0E+06
SE	2.3E+06	4.3E+06	2.9E+06	1.0E+06
SSE	1.6E+06	2.8E+06	3.4E+06	1.0E+06
S	6.9E+04	5.2E+05	8.0E+05	9.3E+05
SSW	2.5E+02	1.2E+05	2.4E+05	1.0E+05
SW	2.5E+02	5.1E+02	1.2E+03	3.1E+05
WSW	2.5E+02	4.2E+02	7.7E+03	2.6E+03
W	4.4E+04	2.3E+04	1.7E+04	2.1E+03
WNW	2.5E+05	3.8E+04	4.3E+04	1.0E+06
NW	3.4E+05	4.1E+05	8.0E+05	1.0E+06
NNW	3.4E+05	5.7E+05	8.0E+05	1.0E+06

Table 6. Leafy-Vegetable Production Grid (kg/yr)

SECTOR	10-20 Mi	20-30 Mi	30-40 Mi	40-50 Mi
N	1.7E+04	2.8E+04	3.9E+04	4.0E+04
NNE	1.7E+04	2.8E+04	2.4E+04	3.4E+04
NE	1.7E+04	4.3E+04	7.9E+04	4.6E+04
ENE	1.7E+04	3.3E+04	1.0E+05	1.3E+05
E	1.7E+04	1.4E+04	1.2E+04	9.2E+04
ESE	1.7E+04	9.7E+04	9.1E+04	4.5E+04
SE	1.2E+05	2.1E+05	1.4E+05	5.0E+04
SSE	8.2E+04	1.4E+05	1.7E+05	5.0E+04
S	3.4E+03	2.5E+04	3.9E+04	4.5E+04
SSW	9.5E+01	6.1E+03	1.3E+04	6.3E+03
SW	9.5E+01	2.7E+02	9.9E+02	1.3E+03
WSW	9.5E+01	1.6E+02	2.2E+02	3.0E+02
W	1.7E+03	1.4E+02	2.2E+02	5.0E+04
WNW	1.2E+04	1.4E+02	1.9E+04	5.0E+04
NW	1.7E+04	1.9E+04	3.9E+04	5.0E+04
NNW	1.7E+04	2.8E+04	3.9E+04	5.0E+04

Table 7. Suggested Age-Specific Consumption Rates for Offsite Dosimetry at the SRS

Average Individual Consumption					
	Units	Adult	Teen	Child	Infant
Land Usage Statistics					
Leafy vegetable consumption	kg/yr	21(ns)	14(ns)	8.5(ns)	-
Other vegetable consumption	kg/yr	163(190)	205(240)	171(200)	-
Meat consumption*	kg/yr	43(95)	27(59)	17(37)	-
Milk consumption	L/yr	120(110)	218(200)	186(170)	186(170)
Water Usage Statistics					
Water consumption	L/yr	370(370)	260(260)	260(260)	260(260)
Invertebrate consumption	kg/yr	2.0(1.0)	1.5(0.75)	0.7(0.33)	-
Fish consumption	kg/yr	9.0(6.9)	6.8(5.2)	2.9(2.2)	-

Maximum Individual Consumption**					
	Units	Adult	Teen	Child	Infant
Land Usage Statistics					
Leafy vegetable consumption	kg/yr	43(64)	28(42)	17(26)	-
Other vegetable consumption	kg/yr	276(520)	334(630)	276(520)	-
Meat consumption*	kg/yr	81(110)	48(65)	30(41)	-
Milk Consumption	L/yr	230(310)	297(400)	244(330)	244(330)
Water Usage Statistics					
Water consumption	L/yr	730(730)	510(510)	510(510)	330(330)
Fish consumption	kg/yr	19(21)	14(16)	6(6.9)	-
Invertebrate consumption	kg/yr	8.0(5)	6.1(3.8)	2.7(1.7)	-
Recreational shoreline usage	hr/yr	23(12)	128(67)	27(14)	-
Swimming usage	hr/yr	8.9(ns)	50(ns)	10(ns)	-
Boating usage	hr/yr	21(ns)	117(ns)	25(ns)	-

Values in parentheses are NRC defaults (ns - not specified).

* Consumption rates from this report do not include the consumption of pork or poultry

**Teen, child, and infant consumption values are determined using the age-specific ratios of NRC defaults.

Table 8. Comparison of Consumption Rates for Adult Average and Maximum Individuals

Adult Average Individual					
	Units	NRC Default	1979-83 Survey	This Survey	Ref
<u>Land Usage Statistics</u>					
Leafy vegetable consumption	kg/yr	ns	30	21	8
Other vegetable consumption	kg/yr	190	190	163	8
Meat consumption	kg/yr	95	95	43	8
Milk consumption	L/yr	110	110	120	8
<u>Water Usage Statistics</u>					
Water consumption	L/yr	370	370	370	1
Invertebrate consumption	kg/yr	1.0	1.0	2.0	8
Fish consumption	kg/yr	6.9	11.3	9.0	8
Adult Maximum Individual					
	Units	NRC Default	1980 Survey	This Survey	Ref
<u>Land Usage Statistics</u>					
Leafy vegetable consumption	kg/yr	64	64	43	8
Other vegetable consumption	kg/yr	520	520	276	8
Meat consumption	kg/yr	110	110	81	8
Milk consumption	L/yr	310	310	230	8
<u>Water Usage Statistics</u>					
Water consumption	L/yr	730	730	730	1
Fish consumption	kg/yr	21	34	19	8
Invertebrate consumption	kg/yr	5	5	8	8
Recreational shoreline usage	hr/yr	12	20	23	8

Figure 1 Beef Production by County

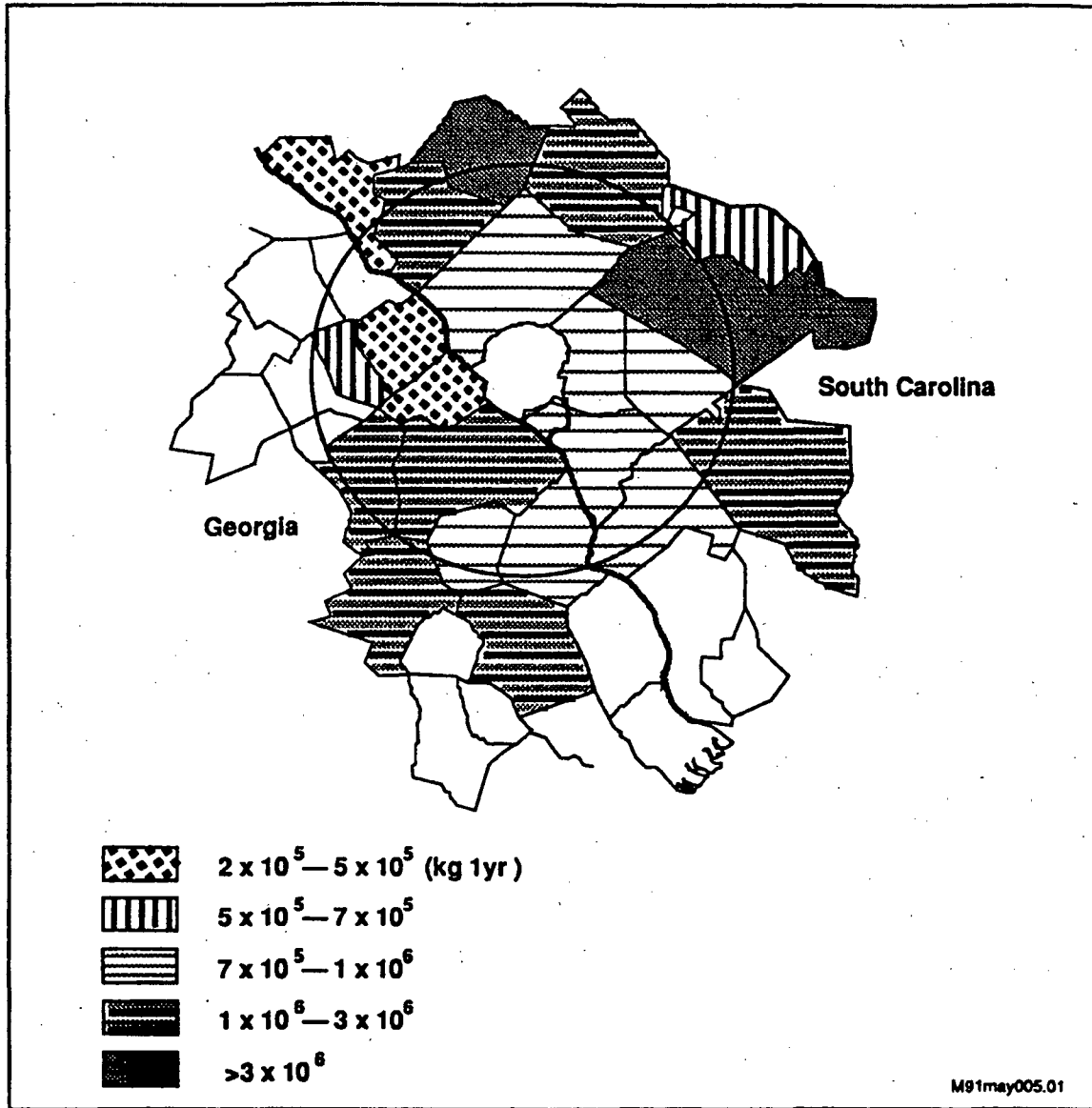


Figure 2 Milk Production by County

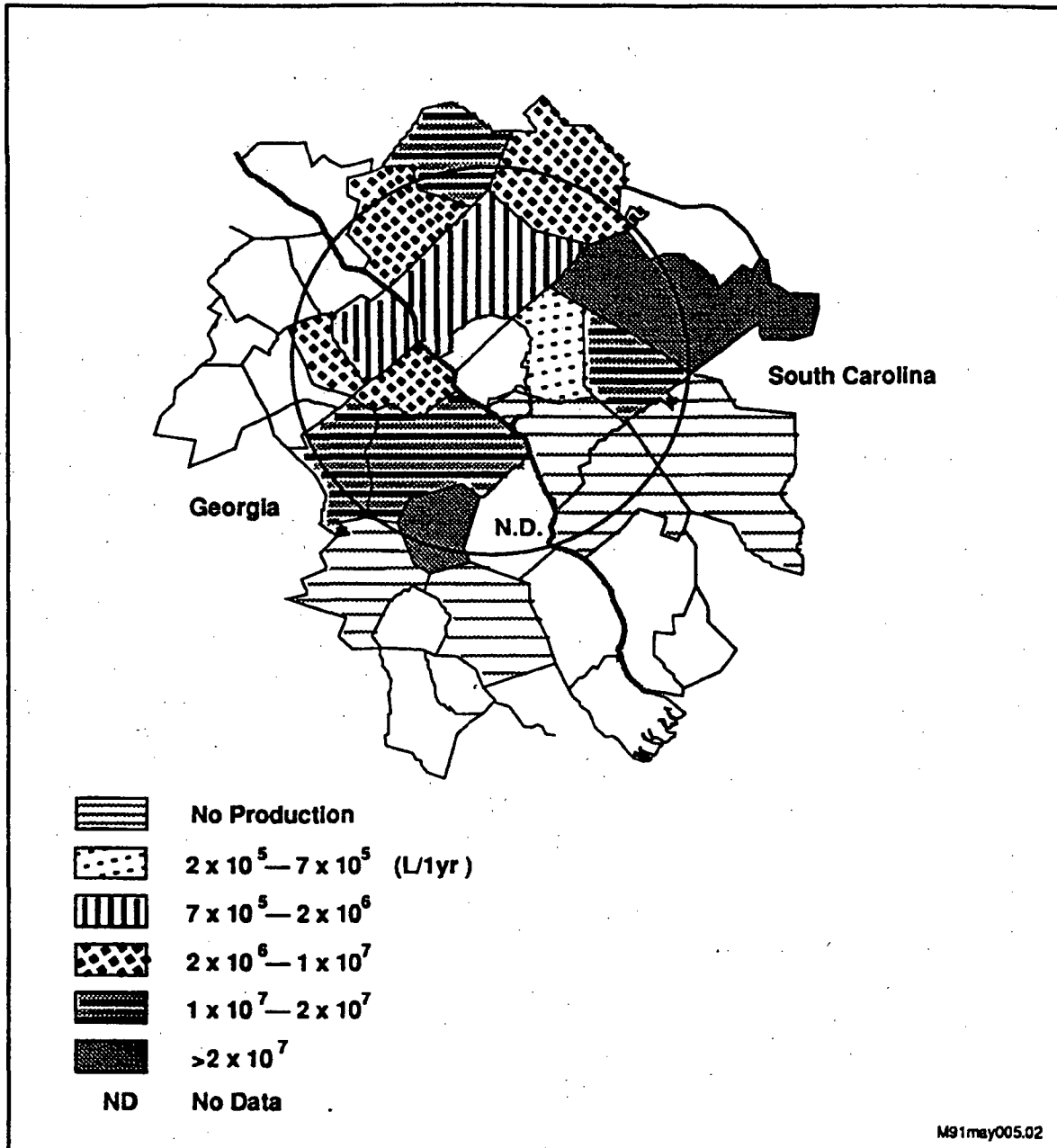
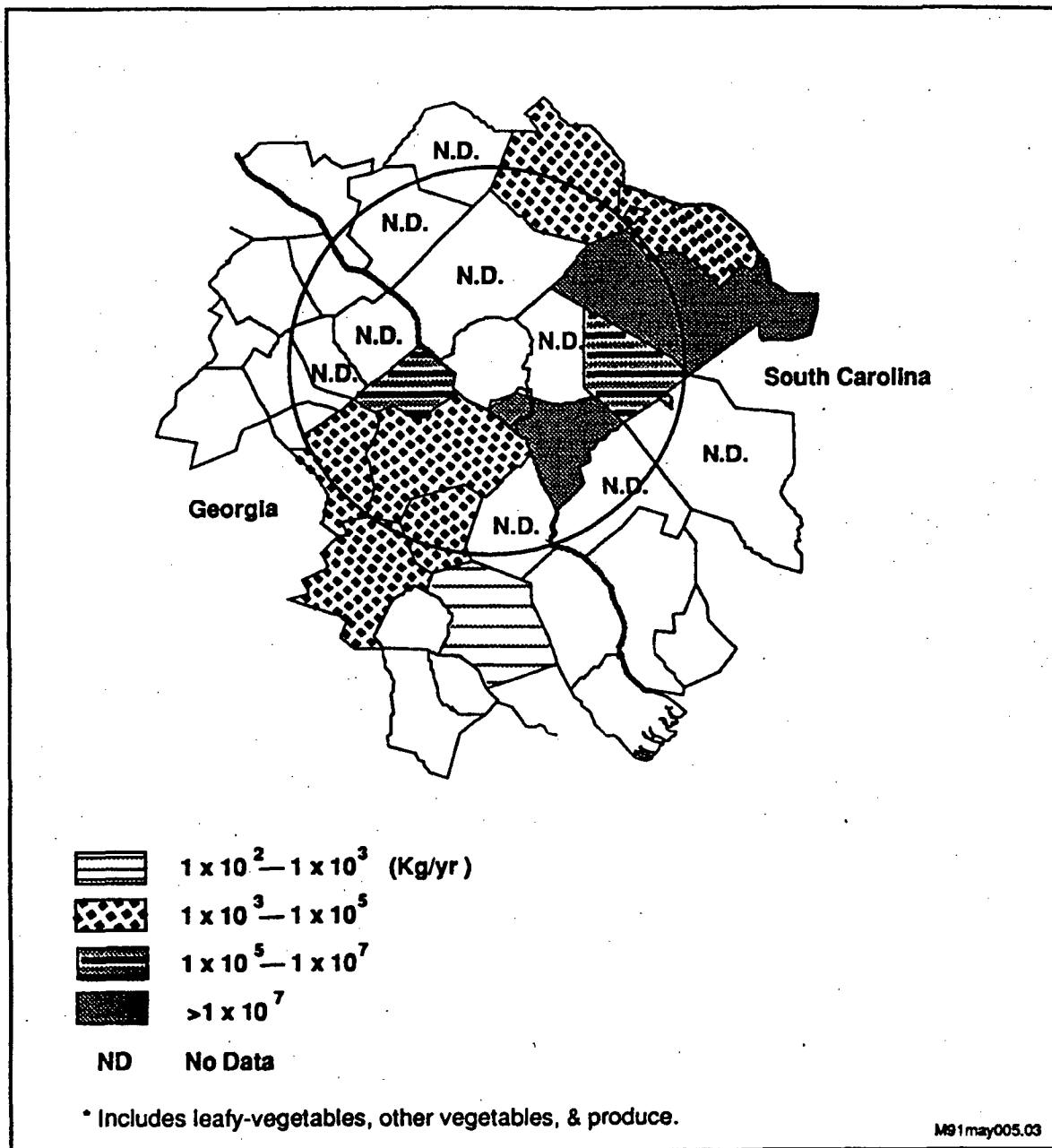


Figure 3 Vegetable Production by County



WESTINGHOUSE SAVANNAH RIVER COMPANY
INTER-OFFICE MEMORANDUM

SRT-EST-2003-00134

July 15, 2003

Technical Review

TO: Environmental Dosimetry Files

FROM: G.T. Jannik, 773-42A

Cesium-137 Bioconcentration Factor for Freshwater Fish in the SRS Environment

This memo serves to document the justification for the continuing use of a Savannah River Site (SRS) site-specific bioconcentration factor of 3,000 for cesium-137 in freshwater fish.

The Nuclear Regulatory Commission (NRC) default bioconcentration factor for cesium in fish is 2,000 (NRC, 1977). This value is taken from Thompson, et al. (1972).

It is documented in Cummins (1994) that SRS determined values ranged between 600 and 39,000 (in fish muscle). Cummins further documented that non-SRS values ranged between 400 and 14,000 (Blaylock, 1982; Coughtrey and Thorne, 1985; Jorgensen et al. 1991, Till and Meyer, 1983; Vanderploeg et al. 1975).

The original justification for the use of a cesium-137 bioconcentration factor of 3,000 for SRS fish was documented in Gladden (1982). Because this memorandum does not have a site document number, it is attached to this report.

→ In Jannik (1995), it is documented that in 1994, the weighted average concentration of cesium-137 in fish flesh harvested from near Savannah River Mile 120 was 0.07 pCi/g. This was approximately 3,000 times more than the 0.000023 pCi/mL concentration of cesium-137 measured (using ultra-low level techniques) in water sampled from near River Mile 120 during 1994.

In review of some other related literature (Rowan and Rasmussen, 1994; Mohler, et al., 1997; and Whicker, et al., 1990) it is shown that the bioconcentration factor for cesium-137 in fish varies greatly depending upon the 1) amount of dissolved potassium in the water, 2) amount of suspended solids in the water, 3) temperature of the water, 4) trophic

level of the fish (piscivores bioconcentrate cesium-137 much more than insectivores and benthivores), and 5) length of the food chain.

In light of all this information, it appears that no single bioconcentration factor is ideal, but the factor of 3,000 for cesium-137 in generic fish from the SRS is consistent with site data and is conservative in comparison to the NRC default value. Therefore, it should continue to be used as the site-specific factor in all applicable environmental dosimetry calculations at SRS.

References:

- Blaylock, B.G., 1982, *Radionuclide Data Bases Available for Bioaccumulation Factors for Freshwater Biota*, Nuclear Safety, Vol. 23, No 4 pp 427-438.
- Coughtrey, P.J. and M.C. Thorne, 1985, *Radionuclide Distribution and Transport in Terrestrial and Aquatic Ecosystems*, A.A. Balkema Publication, Boston MA.
- Cummins, C.L., 1994, *Radiological Bioconcentration Factors for Aquatic, Terrestrial, and Wetland Ecosystems at the Savannah River Site*, Savannah River Technology Center, Aiken, SC.
- Gladden, J.B., memorandum to M.H. Smith, 1982, *Cs-137 Concentration Factor for Savannah River Fish*, Savannah River Ecology Laboratory, Aiken, SC.
- Jannik, G.T., 1995, *Radiological Impact of 1994 Operations at the Savannah River Site*, SRT-ETS-950087, Savannah River Technology Center, Aiken, SC.
- Jorgensen, S.E., S.N. Nielson, and L.A. Jorgensen, 1991, *Handbook of Ecological Parameters and Ecotoxicology*, pp 843-848, Elsevier, New York, NY.
- Mohler, H.J., F.W. Whicker, and T.G. Hinton, 1997, *Temporal trends of Cs-137 in an Abandoned Reactor Cooling Reservoir*, J. Environ. Radioactivity, Vol 37, No. 3, pp 251-268, Great Britain.
- Rowan, D.J., and J.B. Rasmussen, 1994, *Bioaccumulation of Radiocesium by Fish: the Influence of Physicochemical Factors and Trophic Structure*, Canadian Journal of Fisheries and Aquatic Sciences, Vol. 51, Number 11, pp 2388-2410.
- Thompson, S.E., C.A. Burton, D.J. Quinn, and Y.C. Ng, 1972, *Concentration Factors of Chemical Elements in Edible Aquatic Organisms*, TID-4500, UC-48, URCL450564, Revision 1, Lawrence Livermore Laboratory, Livermore, CA.
- Till, J.E., and H.R. Meyer, 1983, *Radiological Assessment, A Textbook on Environmental Dose Analysis*, U.S. NRC, NUREG/CR-3332, Washington, D.C.
- U.S. Nuclear Regulatory Commission, 1977, "Calculations of Annual Dose to Man from Routine Releases of Reactor Effluents for the Purpose of Evaluation Compliance with 10CFR Part 50, Appendix I, *Regulatory Guide 1.109*, Revision 1. Washington, D.C.
- Vanderploeg, H.A., D.C. Parzyck, W.H., W.H. Wilcox, J.R. Kercher, and S.V. Kaye, 1975, *Bioaccumulation Factors for Radionuclides in Freshwater Biota*, ORNL-5002, ESD Publication 783, Oak Ridge National Laboratory, Oak Ridge, TN.
- Whicker, F.W., J.E. Pinder, J.W. Bowling, J.J. Alberts, and I.L. Brisban, *Distribution of Long-Lived Radionuclides in an Abandoned Reactor Cooling Reservoir*, Ecological Monographs, 60(4), pp 471-496, Ecological Society of America.

SRT-EST-2003-00134 .
July 15, 2003

cc: J.B. Gladden, 773-42A
A.A. Simpkins, 773-42A
P.L. Lee, 773-42A
P.D. Fledderman, 735-B
Dosimetry Files (2)
J.M. Malanowski, 773-42A

LADTAP XL©: A SPREADSHEET FOR ESTIMATING DOSE RESULTING FROM AQUEOUS RELEASES

Ali A. Simpkins

APPROVED for Release for
Unlimited (Release to Public)
5/4/2004

Technical Reviewer

February 2004

Westinghouse Savannah River Company
Savannah River Site
Aiken, SC 29808



SAVANNAH RIVER SITE

PREPARED FOR THE U.S. DEPARTMENT OF ENERGY UNDER CONTRACT NO. DE-AC09-96 SR18500

DISCLAIMER

This report was prepared as an account of work sponsored by an agency of the United States Government. Neither the United States Government nor any agency thereof, nor any of their employees, makes any warranty, express or implied, or assumes any legal liability or responsibility for the accuracy, completeness, or usefulness of any information, apparatus, product, or process disclosed, or represents that its use would not infringe privately owned rights. Reference herein to any specific commercial product, process, or service by trade name, trademark, manufacturer, or otherwise does not necessarily constitute or imply endorsement, recommendation, or favoring by the United States Government or any agency thereof. The views and opinions of authors expressed herein do not necessarily state or reflect those of the United States Government or any agency thereof.

Key Words Dose Determination
 Aqueous Releases

Retention: Lifetime

LADTAP XL[®]: A SPREADSHEET FOR ESTIMATING DOSE RESULTING FROM AQUEOUS RELEASES

A. A. Simpkins

Issued: February 2004

SRTC

**SAVANNAH RIVER TECHNOLOGY CENTER
AIKEN, SC 29808
Westinghouse Savannah River Company
Savannah River Site
Aiken, SC 29808**

**PREPARED FOR THE U.S. DEPARTMENT OF ENERGY UNDER CONTRACT NO.
DE-AC09-96SR18500**

ABSTRACT

LADTAP XL© is an EXCEL© spreadsheet used to estimate dose to offsite individuals and populations resulting from routine releases of radioactive materials to the Savannah River. LADTAP XL© contains two worksheets: LADTAP and IRRIDOSE. The LADTAP worksheet estimates dose for environmental pathways including external exposure resulting from recreational activities on the Savannah River and ingestion of water, fish, and invertebrates of Savannah River origin. IRRIDOSE estimates offsite dose to individuals and populations from irrigation of food crops with contaminated water from the Savannah River. Minimal input is required to run the models and site-specific parameters are used when possible. A complete code description, verification of models, and user's manual have been included.

**RESPONSE TO RAI EDITORIAL COMMENTS
ROADMAP TO REFERENCES**

REFERENCED DOCUMENT	*EXCERPT LOCATION	REMARK
Cook et al. 2005		Reference to 2005 Saltstone Special Analysis generally

***Excerpt Locations:**

1. Excerpt included within response: The excerpt is included within the text of the response or is appended to the response.
2. Excerpt enclosed following response: The excerpt is enclosed on a separate sheet or sheets following the response.
3. Representative excerpt(s) enclosed following response: Representative excerpts from a document that is wholly or largely applicable are enclosed following the response.
4. Other

7/14/2005